



Indicators of Climate Change in California



Lauren Zeise, Ph.D.
Director, Office of Environmental
Health Hazard Assessment



Edmund G. Brown Jr.
Governor



Matthew Rodriguez
Secretary for
Environmental Protection



INDICATORS OF CLIMATE CHANGE IN CALIFORNIA

May 2018

Prepared by:

Carmen Milanes, Tamara Kadir, Bennett Lock, Laurie Monserrat,
Nathalie Pham, Karen Randles
Integrated Risk Assessment and Research Section
Office of Environmental Health Hazard Assessment
California Environmental Protection Agency

Reviewed by:

John B. Faust, David M. Siegel, Allan Hirsch, Lauren Zeise
Office of Environmental Health Hazard Assessment

Ashley Conrad-Saydah, John Blue
Office of the Secretary, California Environmental Protection Agency

Suggested citation:

Office of Environmental Health Hazard Assessment, California Environmental Protection Agency (2018). *Indicators of Climate Change in California*.

Page intentionally blank

CONTRIBUTORS

Heather Amato, California Department of Public Health
Michael L. Anderson, California Department of Water Resources
Dennis Baldocchi, UC Berkeley
Christopher Barker, UC Davis
Hassan J. Basagic, Portland State University
Rupa Basu, California Office of Environmental Health Hazard Assessment
Steven R. Beissinger, UC Berkeley
Russel W. Bradley, Point Blue Conservation Science
Rachel Broadwin, California Office of Environmental Health Hazard Assessment
Thomas J. Conway, National Oceanic and Atmospheric Administration
Carolyn Cook, California Department of Food and Agriculture
Michael Dettinger, Scripps Institution of Oceanography
Edward J. Dlugokencky, National Oceanic and Atmospheric Administration
Christopher Dolanc, Mercyhurst University
Paul English, California Department of Public Health
Jennifer Fisher, Oregon State University
Marc L. Fischer, Lawrence Berkeley National Laboratory
Matthew L. Forister, University of Nevada Reno
Andrew G. Fountain, Portland State University
Guido Franco, California Energy Commission
Brian Gaylord, UC Davis
Frank Gehrke, California Department of Water Resources
Jeffrey Goddard, UC Santa Barbara
Ellyn Gray, UC Berkeley
Amrith Gunasekara, California Department of Food and Agriculture
Benjamin Hatchett, Western Regional Climate Center
Elise Hellwig, UC Davis
Robert Hijmans, UC Davis
Tessa M. Hill, UC Davis
Allan Hollander, UC Davis
Anny Huang, California Air Resources Board
Diana Humple, Point Blue Conservation Science
Kym Jacobson, National Oceanic and Atmospheric Administration
Jaime Jahncke, Point Blue Conservation Science
Katherine Jarvis-Shean, UC Cooperative Extension
Ralph Keeling, Scripps Institution of Oceanography
Chris Keithley, California Department of Forestry and Fire Protection
Anne E. Kelly, UC Irvine
Anne Kjemtrup, California Department of Public Health
Vicki Kramer, California Department of Public Health
Toshihiro Kuwayama, California Air Resources Board
John Largier, UC Davis
Alyssa Louie, California Department of Food and Agriculture
Regina Linville, California Office of Environmental Health Hazard Assessment
Dan McEvoy, Western Regional Climate Center
Patrick J. McIntyre, NatureServe

Sharon Melin, National Oceanic and Atmospheric Administration
Nicole Michel, National Audubon Society
Tadashi Moody, California Department of Forestry and Fire Protection
Nehzat Motallebi, California Air Resources Board
Sarah Myhre, University of Washington
Nadav Nur, Point Blue Conservation Science
Nina Oakley, Western Regional Climate Center
David Passovoy, California Department of Forestry and Fire Protection
Stephen Piper, Scripps Institution of Oceanography
William Reisen, UC Davis
Emily Rivest, College of William and Mary
Maurice Roos, California Department of Water Resources
Mark Rosenberg, California Department of Forestry and Fire Protection
Eric Sanford, UC Davis
Leo Salas, Point Blue Conservation Science
David Sapsis, California Department of Forestry and Fire Protection
Arthur Shapiro, UC Davis
S. Geoffrey Schladow, UC Davis
Rebecca Stanton, California Office of Environmental Health Hazard Assessment
Pieter Tans, National Oceanic and Atmospheric Administration
Alicia Torregrosa, US Geological Survey
James Thorne, UC Davis
Abhilash Vijayan, California Air Resources Board
Rich Walker, California Department of Forestry and Fire Protection
Shohei Watanabe, UC Davis
Brian Wells, National Oceanic and Atmospheric Administration
Anthony L. Westerling, UC Merced

OEHHA thanks the following for their technical assistance:

Simone Alin, Steve Bograd, Toby Garfield (National Oceanic and Atmospheric Administration)
Bev Anderson-Abbs, Jarma Bennett, Greg Gearheart, Rafael Maestu (State Water Resources Control Board)
Dan Cayan (UC San Diego/Scripps Institution of Oceanography)
Marisol Garcia-Reyes (Farallon Institute)
Vanessa Gusman (California Department of Fish and Wildlife)
Mike Kolian (US Environmental Protection Agency)
Peter Coombe, Elissa Lynn (California Department of Water Resources)

OEHHA staff (current and former) who assisted with the preparation of this report:

Linda Mazur, Elisa Fernandes-McDade, Kelsey Craig, Carolyn Flowers, Katie Fong, Julian Leichty, Sofia Mitchell, Amanda Palumbo, Anna Smith, Barbara Washburn

Graphics: Brandon Lee Design

Editorial consultant: Krystyna von Henneberg, Ph.D., Creative Language Works

Cover photos: Nudibranch sea slug — Jeffrey Goddard/UC Santa Barbara; vineyard and Los Angeles cityscape — California Department of Water Resources

FROM THE SECRETARY

While California is a national leader in environmental protection, it continues to face serious challenges in ensuring a healthy and sustainable future for its children. None of these challenges are more formidable than the need to respond to the significant and increasingly stark impacts of climate change on the state.



Climate change is not just a theory. It is a real, immediate, and growing threat to California's future. This report presents 36 indicators that document some of the many ways in which climate change is already occurring in California and its effects on the state's weather, environment and wildlife. By measuring and tracking the changes occurring in California's physical environment and ecosystems, the report provides an essential scientific foundation to inform the state's efforts to respond to climate change through a combination of mitigation, adaptation, research and joint action.

The extreme weather events of the last several years are not isolated incidents. They are suggestive of the significant and increasingly discernible impacts of climate change in California. The most dramatic impacts include wildfires that are larger and more frequent, and the most severe drought since recordkeeping began. Underlying these events is a long-term warming trend that has accelerated since the mid-1970s. In addition, spring snowmelt runoff is decreasing, sea levels are rising, glaciers are shrinking, lakes and ocean waters are warming, and plants and animals are migrating. These impacts are similar to those that are occurring globally.

Fortunately, there is some good news. Our state's pioneering efforts to curb emissions of greenhouse gases are working. Concentrations of the short-lived climate pollutant black carbon have dropped by more than 90 percent over the last fifty years. We are on a course to meet our target of reducing greenhouse gas emissions to 1990 levels by 2020, and California's integrated plan for addressing climate change, outlined in our 2017 [Climate Change Scoping Plan](#), calls for reducing these emissions an additional 40 percent by 2030. In September 2018, leaders from around the world will join us in San Francisco for a Global Climate Action Summit to encourage greater international efforts to reduce emissions of greenhouse gases.

By providing information on climate change impacts that are already occurring in California, this report underscores the importance of our continued efforts to fight climate change. It is also intended to be a valuable resource for leaders and policymakers undertaking the critical work of climate adaptation and mitigation. We invite you to join us in this important work.

Matthew Rodriguez, Secretary
California Environmental Protection Agency

Page intentionally blank



SUMMARY

From record temperatures to proliferating wildfires and rising seas, climate change poses an immediate and escalating threat to California’s environment, public health, and economic vitality. Recent climate-related events – such as the devastating 2017 wildfires and the record-setting 2012-16 drought – have highlighted the challenges that confront the state as its climate continues to evolve.

California has been a pioneer in addressing climate change. This report helps support policy decisions and facilitates communication about climate change by providing, in a single document, indicators characterizing its multiple aspects in California.

Indicators are scientifically-based measurements that track trends in various aspects of climate change. Many indicators reveal discernable evidence that climate change is occurring in California and is having significant, measurable impacts in the state.

The report’s 36 indicators are grouped into four categories, as listed below. The report discusses what these indicators show, why they are important, and the factors that may be influencing them.

- Human-influenced (anthropogenic) drivers of climate change, such as greenhouse gas emissions
- Changes in the state’s climate
- Impacts of climate change on physical systems, such as oceans, lakes and snowpack
- Impacts of climate change on biological systems – humans, vegetation and wildlife

The following pages summarize and highlight the report findings.



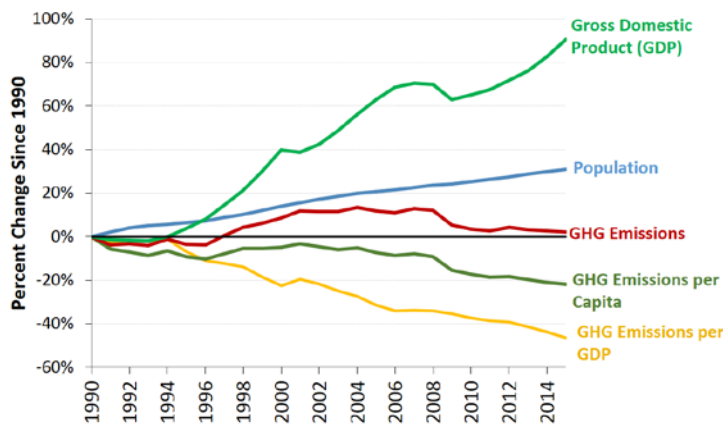
Climate Change Drivers

The Earth's climate is warming, mostly due to human activities such as changes in land cover and emissions of certain pollutants. Greenhouse gases are the major human-influenced drivers of climate change. These gases warm the Earth's surface by trapping heat in the atmosphere.

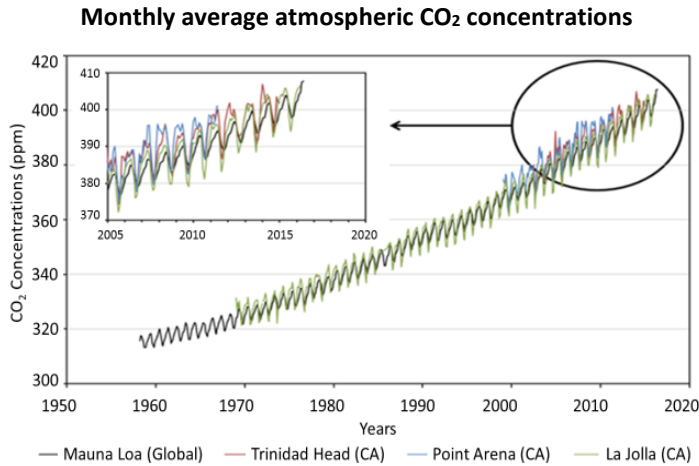
International climate agreements aim to stabilize atmospheric greenhouse gas concentrations at a level that would prevent "dangerous anthropogenic interference with the climate system." The 2015 Paris Agreement calls for keeping the rise in the global average temperature to well below 2 degrees Celsius (°C) above pre-industrial levels. The Agreement also commits to pursue efforts to further limit the increase to 1.5°C. These efforts would significantly reduce the risks and impacts of climate change.

California's **greenhouse gas emissions** show promising downward trends, with emissions per capita and per dollar of its gross domestic product declining since 1990. These trends are the result of California's pioneering efforts to curb greenhouse gas emissions, and are occurring despite an increase in the state's population and economic output. Greenhouse gases are emitted from fossil fuel combustion for transportation and energy, landfills, wastewater treatment facilities, and livestock. The major greenhouse gases are carbon dioxide (CO₂), methane, nitrous oxide, and fluorinated gases. CO₂ accounts for 85 percent of greenhouse gas emissions in the state, and transportation is its largest source, accounting for over a third of the total emissions in 2015.

Trends in California's population, economy, and greenhouse gas (GHG) emissions since 1990

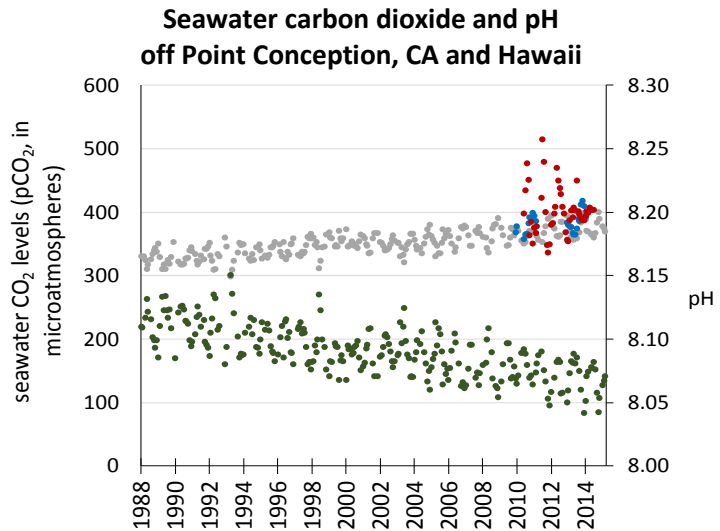


Concentrations of black carbon in California’s air have dropped by more than 90 percent over the past 50 years despite a seven-fold increase in statewide diesel fuel consumption — its largest anthropogenic source. This is largely due to tailpipe emission standards, diesel fuel regulations and biomass burning restrictions. Black carbon is a “short-lived climate pollutant.” Unlike CO₂, it does not persist for long in the atmosphere. It is also a powerful global warming agent. Black carbon is the second most important contributor to global warming after CO₂.

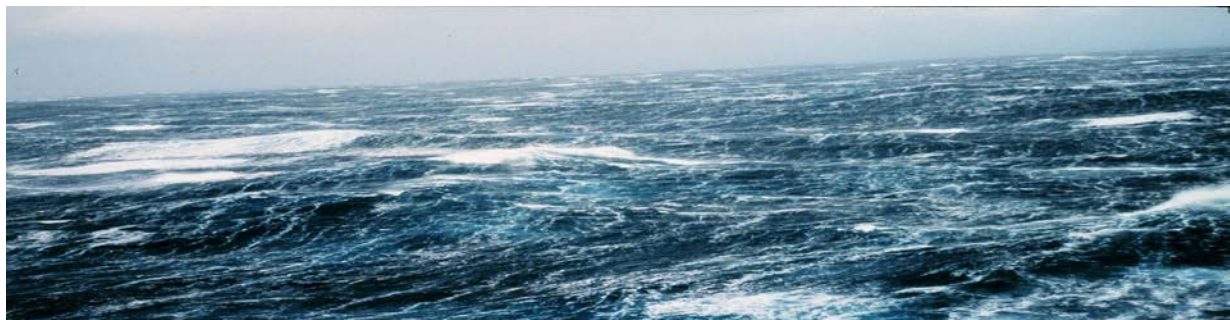


Atmospheric concentrations of CO₂ continue to increase. Measurements at California coastal sites are consistent with those at Mauna Loa, Hawaii, where the first and longest continuous measurements of global atmospheric CO₂ concentrations have been taken. In less than six decades, concentrations of CO₂ have increased from 315 parts per million (ppm) to over 400 ppm in 2015. Since CO₂ persists in the atmosphere for centuries, its levels are expected to remain above 400 ppm for many generations.

As atmospheric concentrations of CO₂ increase, so do levels in the ocean, leading to **ocean acidification**. The ocean absorbs approximately 30 percent of the CO₂ released into the atmosphere each year. Monitoring off Hawaii from 1988 to 2015 shows CO₂ levels in seawater are increasing at a steady rate. The longest-running publicly available data in California from Point Conception, near Santa Barbara, began in 2010. While not measured long enough to discern a trend for California waters, values are similar to those measured at Hawaii at similar times.



pCO₂, Aloha Station, HI
 pCO₂, 140 miles off Point Conception
 pH (calculated), Aloha Station, HI
 pCO₂, 20 miles off Point Conception

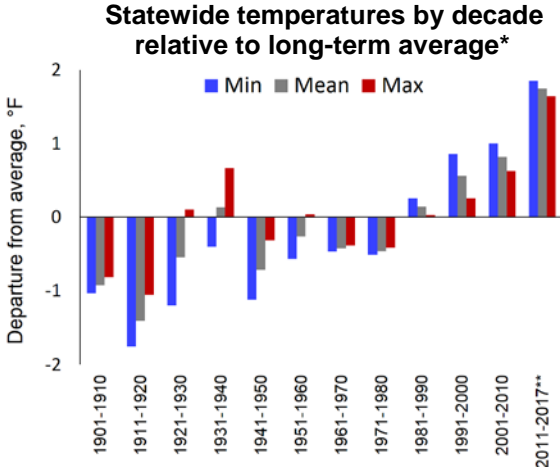
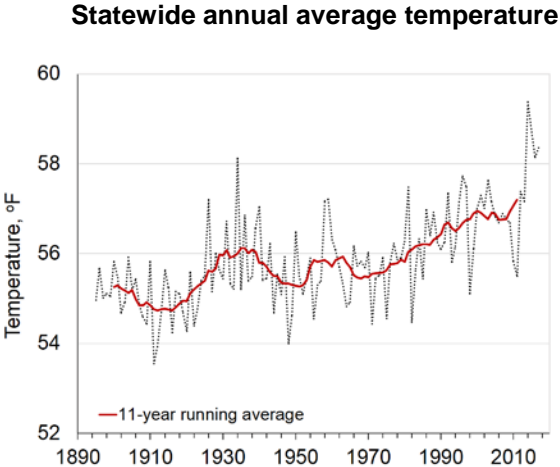




Changes in Climate

Climate is generally defined as “average weather,” usually described in terms of the mean and variability of temperature, precipitation and wind over a period of time. The evidence that the climate system is warming is unequivocal. In California, consistent with global observations, each of the last three decades has been successively warmer than any preceding decade.

Since 1895, **annual average air temperatures** have increased throughout the state, with temperatures rising at a faster rate beginning in the 1980s. The last four years were notably warm, with 2014 being the warmest on record, followed by 2015, 2017, and 2016. Temperatures at night have increased more than during the day: minimum temperatures (which generally occur at night) increased at a rate of 2.3 degrees Fahrenheit (°F) per century, compared to 1.3°F per century for maximum temperatures.



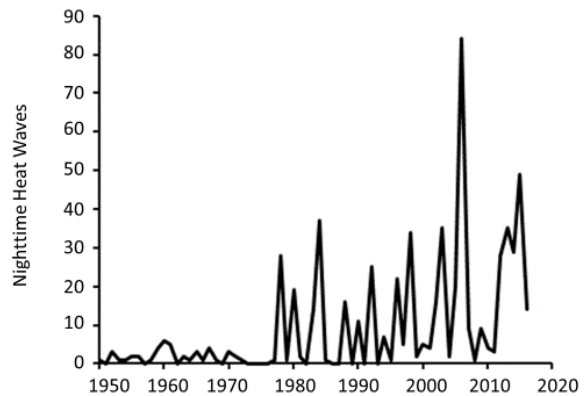
* 1949-2005 base period
 ** Partial decade

Temperature is a basic physical factor that affects many natural processes and human activities. Warmer air temperatures alter precipitation and runoff patterns, affecting the availability of freshwater supplies. Temperature changes can also increase the risk of severe weather events such as heat waves and intense storms. A wide range of impacts on ecosystems and on human health and well-being are associated with increased temperatures.

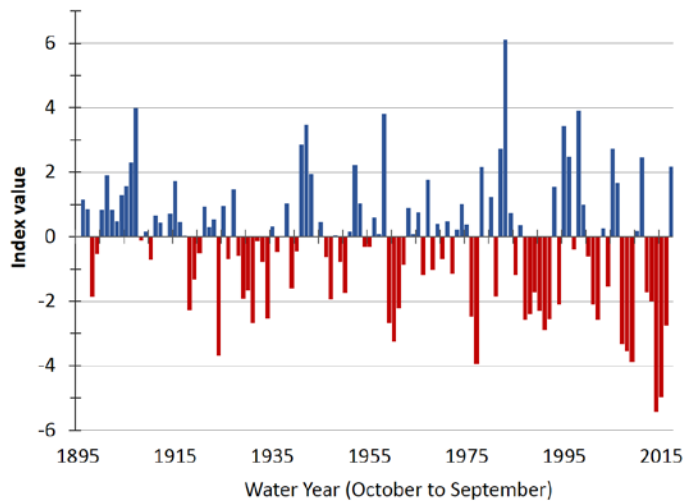


Extremely hot days and nights — that is, when temperatures are at or above the highest 2 percent of maximum and minimum daily temperatures, respectively — have become more frequent since 1950. Both extreme heat days and nights have increased at a faster rate in the past 30 years. Heat waves, defined as five or more consecutive extreme heat days or nights, are also increasing, especially at night. Nighttime heat waves, which were infrequent until the mid-1970s, have increased markedly over the past 40 years.

Nighttime heat waves (April to October)



Palmer Drought Severity Index



A universally used indicator of **drought** — the Palmer Drought Severity Index — shows that California has become drier over time. Five of the eight years of severe to extreme drought (when index values fell below -3) occurred between 2007 and 2016, with unprecedented dry years in 2014 and 2015. The record warmth from 2012 to 2016 coincided with consecutive dry years, including a year of record low snowpack, leading to the most extreme drought since instrumental records began in 1895.

Other indicators of changes in climate show that:

- **Winter chill** has been declining in certain areas of the Central Valley. This is the period of cold temperatures above freezing but below a threshold temperature needed by fruit and nut trees to become and remain dormant, bloom, and subsequently bear fruit. When tracked using “chill hours,” a metric used since the 1940s, more than half the sites studied showed declining trends; with the more recently developed “chill portions” metric, fewer sites showed declines.
- With warmer temperatures, the energy needed to cool buildings during warm weather — measured by “**cooling degree days**” — has increased, while the energy needed to heat buildings during cold weather — measured by “**heating degree days**” — has decreased.
- Statewide **precipitation** has become increasingly variable from year to year. In seven of the last ten years, statewide precipitation has been below the statewide average (22.9 inches). In fact, California’s driest consecutive four-year period occurred from 2012 to 2015. In recent years, the fraction of precipitation that falls as rain (rather than snow) over the watersheds that provide most of California’s water supply has been increasing — another indication of warming temperatures.





Impacts on Physical Systems

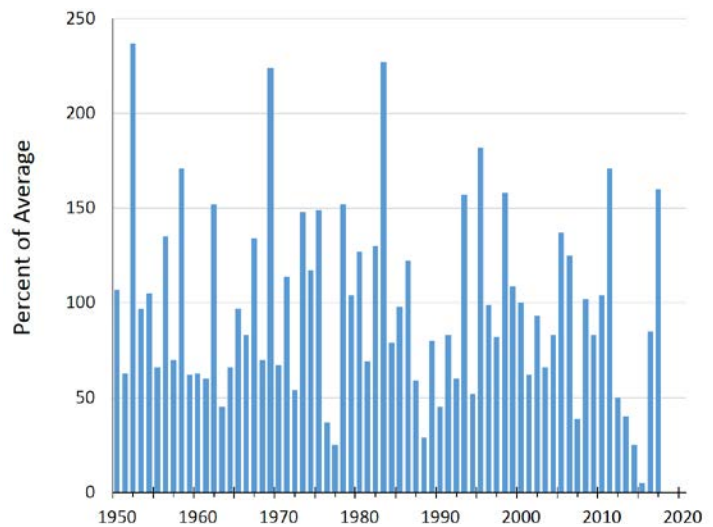
Warming temperatures and changing precipitation patterns have altered California’s “physical systems” — the ocean, lakes, rivers and snowpack — upon which the state depends. Winter snowpack and spring snowmelt runoff from the Sierra Nevada and southern Cascade Mountains provide approximately one-third of the state’s annual water supply.

The amount of water stored in the state’s snowpack — referred to as **snow-water content** — is highly variable from year to year, ranging from a high in 1952 of about 240 percent of the long-term average to a record low of 5 percent in 2015. Less snowpack accumulates when winter temperatures are warmer because more precipitation falls as rain instead of snow.

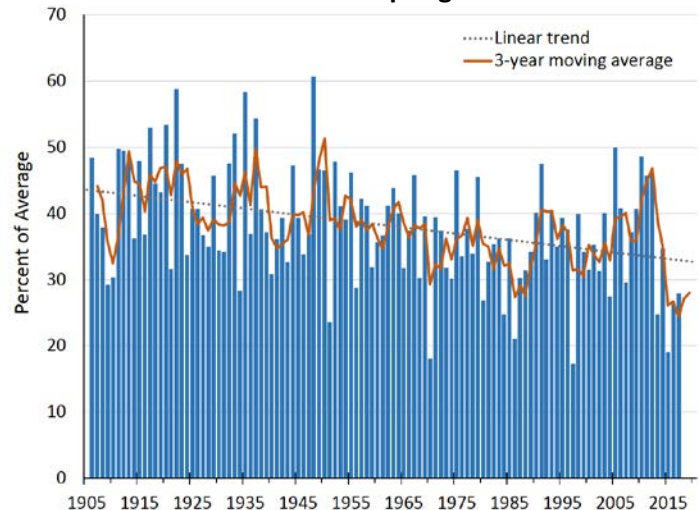
The fraction of **snowmelt runoff** reaching the Sacramento River between April and July has decreased by about 9 percent since 1906. This reduction is influenced by earlier spring warming and more winter precipitation falling as rain. With less spring runoff, less water is available during summer months to meet the state’s domestic and agricultural water demands. These reductions also affect the generation of hydroelectricity, impair cold-water habitat for certain fishes, and stress forest vegetation. The latter has consequences for wildfire risk and long-term forest health.



Snow-water content, as a percentage of average



Sacramento River spring* runoff



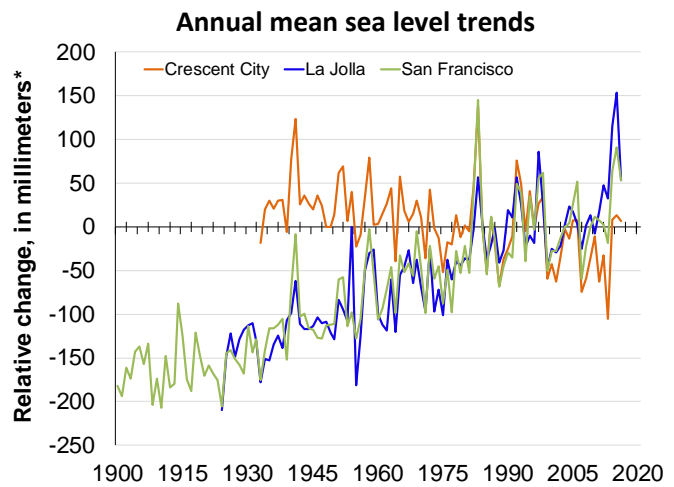
*April to July as a percent of total year runoff



From the beginning of the 20th century to 2014, some of the largest **glaciers** in the Sierra Nevada have lost an average of about 70 percent of their area. Reductions ranged from about 50 to 85 percent of each glacier's area in 1903. Glaciers are important indicators of climate change: winter snowfall nourishes the glaciers, and spring/summer temperatures melt ice and snow. Winter air temperature determines whether precipitation falls as rain or snow, affecting glacier mass gain; summer air temperature affects glacier loss. Glacier shrinkage worldwide is an important contributor to global sea level rise.



Along the California coast, **sea levels** have generally risen. Since 1900, mean sea level has increased by about 180 millimeters (7 inches) at San Francisco and by about 150 millimeters (6 inches) since 1924 at La Jolla. In contrast, sea level at Crescent City has declined by about 70 millimeters (3 inches) since 1933 due to an uplift of the land surface from the movement of the Earth's plates. Sea level rise threatens existing or planned infrastructure, development, and ecosystems along California's coast.



* Relative to tidal datum (reference point set by the NOAA)

Other indicators of the impacts of climate change on physical systems show that:

- Average **lake water temperatures** at Lake Tahoe have increased by nearly 1°F since 1970, at an average rate of 0.02°F per year. During the last four years, warming accelerated about 10 times faster than the long-term rate. The lake surface warmed faster — almost 0.04°F per year. The warming of Lake Tahoe's waters can disrupt the lake's ecosystem by affecting key physical and biological processes.
- **Coastal ocean temperatures** at three sites in California have warmed over the past century. Over 90 percent of the Earth's observed warming over the past 50 years has occurred in the ocean. Warming sea surface temperatures can alter the distribution and abundance of many marine organisms, including commercially important species. Ocean warming accounts for about half of the sea level rise that has occurred globally over the past century.
- **Oxygen concentrations** at three water depths offshore of San Diego indicate overall decreases as well as low-oxygen events. Declining oxygen concentrations can lead to significant ecological changes in marine ecosystems, including wide-ranging impacts on species diversity, abundance, and marine food webs. Changing ocean chemistry, in concert with changes in temperature, may lead to even greater and more widespread impacts on coastal marine ecosystems.





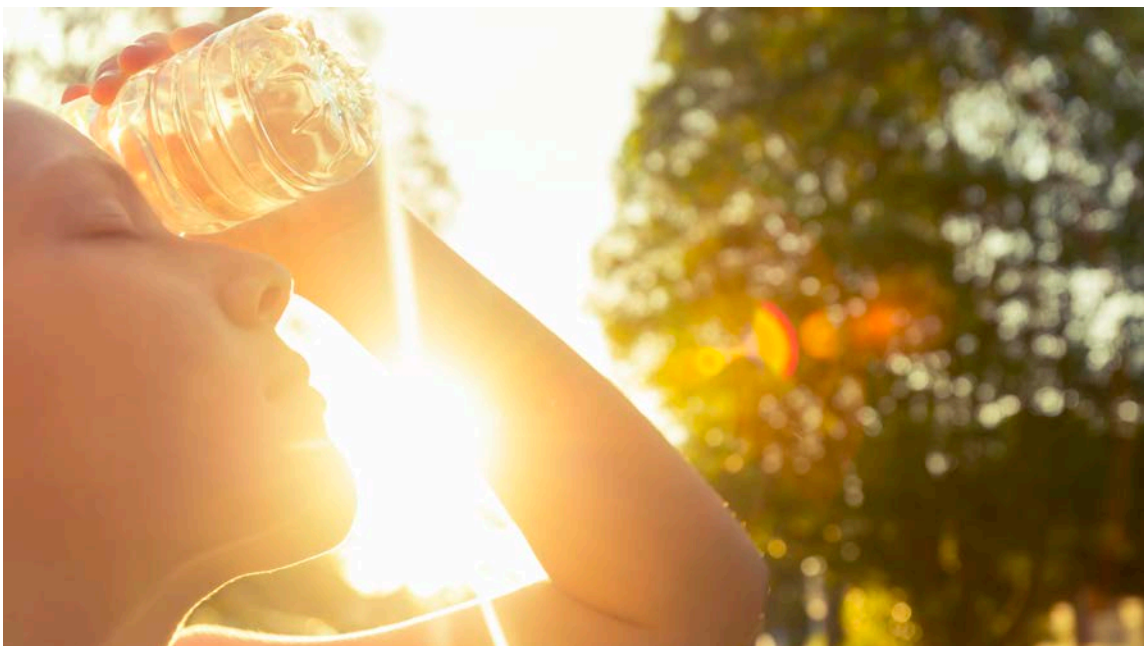
Impacts on Biological Systems

Climate change impacts on terrestrial, marine and freshwater ecosystems have been observed in California. As with global observations, species responses include those consistent with warming: elevational or latitudinal shifts in range; changes in the timing of key plant and animal life cycle events (known as “phenology”); and changes in the abundance of species and in community composition. With continued climate change, many species may be unable to adapt or to migrate to suitable climates, particularly given the influence of other factors such as land use, habitat alteration, and emissions of pollutants.

HUMANS

Humans are better able to adapt to a changing climate than plants and animals in natural ecosystems. Nevertheless, climate change poses a threat to public health. While it is difficult to track its influence using indicators, climate change can impact human well-being in many ways. Examples include injuries and fatalities from extreme events and respiratory stress from poor air quality. Indicators of the impacts of climate change on human health show that:

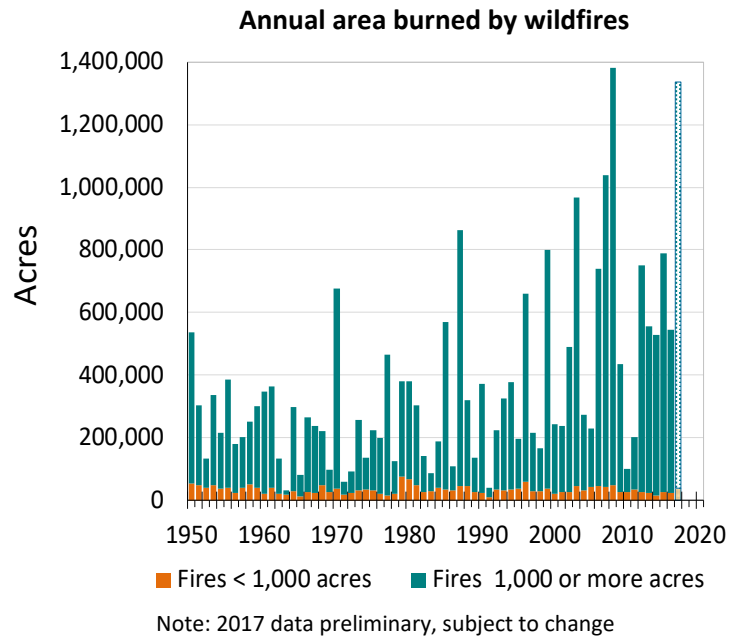
- Warming temperatures and changes in precipitation can affect **vector-borne** pathogen transmission and disease patterns in California. West Nile Virus currently poses the greatest mosquito-borne disease threat.
- **Heat-related deaths and illnesses**, which are severely underreported, vary from year to year. In 2006, they were much higher than any other year because of a prolonged heat wave.



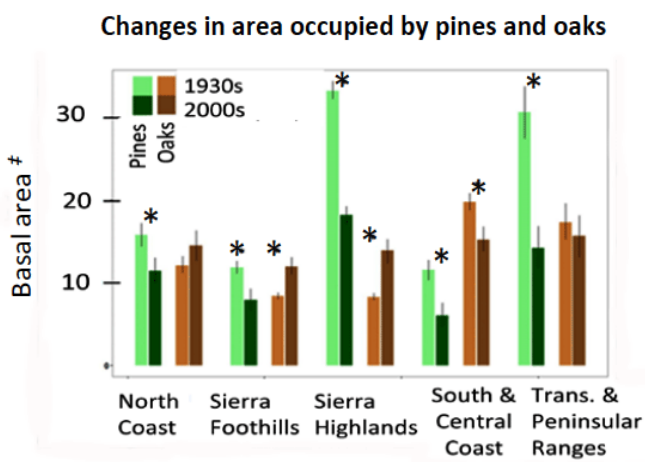
VEGETATION

Warming temperatures, declining snowpack, and earlier spring snowmelt runoff can create stresses on vegetation. A measure of plant stress, climatic water deficit, reflects the demand plants have for water relative to the availability of water in the soil. Increases in climatic water deficit are associated with a warming climate.

Since 1950, the area burned by **wildfires** each year has been increasing, as spring and summer temperatures have warmed and spring snowmelt has occurred earlier. During the recent “hotter” drought, unusually warm temperatures intensified the effects of very low precipitation and snowpack and created conditions for extreme, high severity wildfires that spread rapidly. Five of the largest fire years have occurred since 2006. The largest recorded wildfire in the state (Thomas Fire) occurred in December 2017.



Evidence of how the state’s **forests and woodlands** are responding to climate change has been found in studies that compared historical and current conditions. Historical data are from a 1930s survey of California’s vegetation.



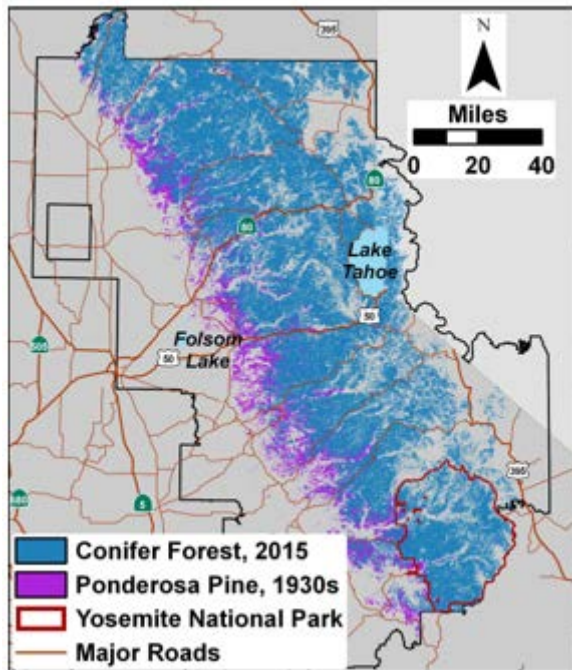
The structure and composition of the state’s forests and woodlands are changing. Compared to the 1930s, today’s forests have more small trees and fewer large trees. Pines occupy less area statewide and, in certain parts of the state, oaks cover larger areas. The decline in large trees and increased abundance of oaks are associated with statewide increases in climatic water deficit.

† Basal area refers to the area occupied by tree trunks
 *Statistically significant differences



On the western side of the northern Sierra Nevada Mountains, the lower edge of the Ponderosa pine forest has moved upslope. Since the 1930s, the forest has retreated from elevations that no longer experience freezing winter temperatures at night. The loss of conifers in this elevation was accompanied by an expansion of forests dominated by broadleaf trees.

Ponderosa Pine forest retreat in the Sierra Nevada Mountains since 1934



Other indicators of the impacts of climate change on vegetation show that:

- **Tree deaths** have increased dramatically since the 2012-2016 drought. Approximately 129 million trees died between 2012 and December 2017. Higher temperatures and decreased water availability made the trees more vulnerable to insects and pathogen attacks.
- **Vegetation distribution** has shifted across the north slope of Deep Canyon in the Santa Rosa Mountains in Southern California. Dominant plant species have moved upward by an average of about 65 meters (213 feet) in the past 30 years.
- Compared to the 1930s, today's **subalpine forests** (forests at elevations above 7,500 feet) in the Sierra Nevada are denser, as small tree densities increased by 62 percent while large tree densities decreased by 21 percent.
- In parts of the Central Valley, certain **fruits and nuts** (prunes and one walnut variety) are maturing more quickly with warming temperatures, leading to earlier harvests. Shorter maturation times generally lead to smaller fruits and nuts, potentially causing a significant loss of revenue for growers and suppliers.



WILDLIFE

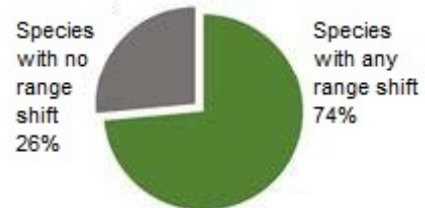
Changes in temperature, precipitation, food sources, competition for prey, and other physical or biological features of the habitat may force changes in the timing of key life cycle events for plants and animals and shift the ranges where these plants and animals live. These factors, along with the inherent sensitivity of the species, interact in ways that can affect species responses differently.

Certain birds and mammals are found at different elevations in three study regions of the Sierra Nevada Mountains today compared to a century ago.

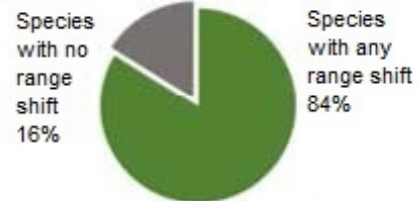
Range shifts have been observed in almost 75 percent of the small mammal species and over 80 percent of the bird species surveyed. High-elevation mammals tended to move upslope; birds and low-elevation mammals moved downslope as frequently as upslope. Across the three study regions, species did not show uniform shifts in elevation. The varied responses reflect the influence of intrinsic sensitivity to temperature, precipitation or other physical factors. They may also be due to changes in food sources, vegetation and interactions with competitors.

Sierra Nevada range shifts over the past century

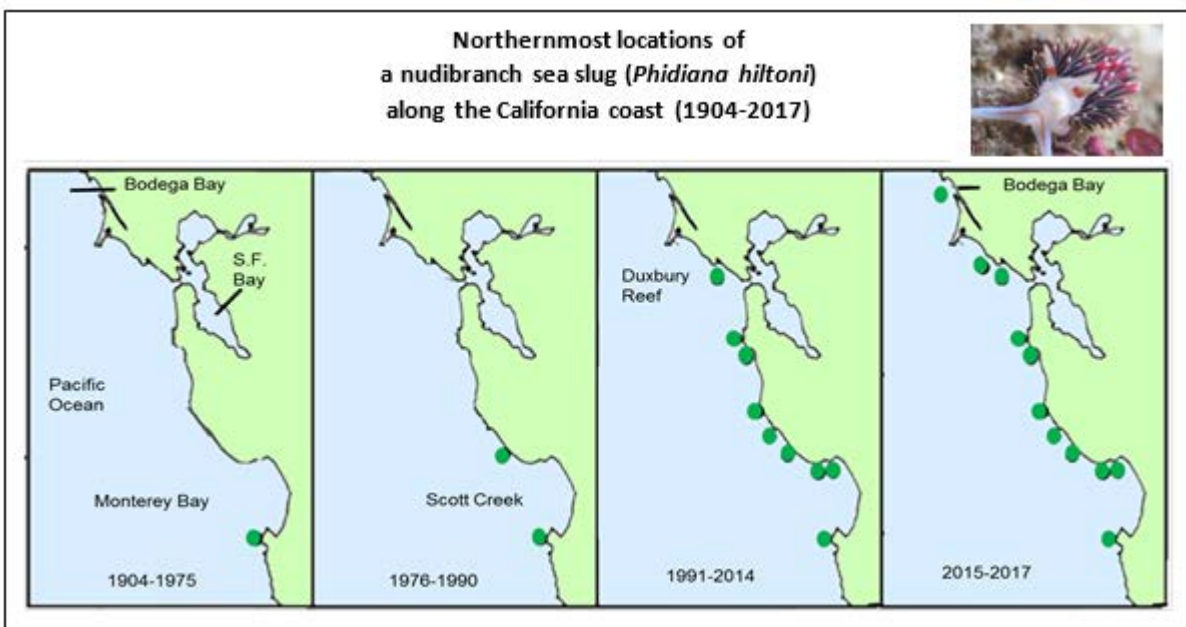
Small mammals



Birds



Marine species respond to changing ocean conditions, especially during periods of unusually warm sea surface temperatures. A **nudibranch** sea slug, *Phidiana hiltoni*, has expanded its range northward by 210 kilometers (130 miles) — from the Monterey Peninsula to Bodega Bay — since the mid-1970s in response to warming ocean conditions. This nudibranch was found for the first time in Bodega Bay in 2015. Unlike other nudibranch species, *P. hiltoni* has persisted at this northernmost location after warm water conditions ended.





Other indicators of the impacts of climate change on wildlife show that:

- Over the past 45 years, **Central Valley butterfly** species have been appearing earlier in the spring. Their earlier emergence is linked with hotter and drier regional winter conditions.
- Since 1980, the timing of spring and fall **migratory bird arrivals** at a coastal site in northern California have shown a diversity of changes.
- Across the state, **wintering bird species** have collectively shifted their range northward and closer to the coast over the past 48 years. In both cases, species' responses have not been uniform: some species have shifted to higher elevations or latitudes, and the shifts have occurred to varying degrees.
- The **effects of ocean acidification on marine organisms** involve a wide range of biological processes. The most widely observed effect is interference with shell-formation in mollusks. (Since there are no trend data tracking these effects, this is a "Type III" indicator.)
- Ocean conditions strongly influence marine organisms in the California Current, as seen with **copepod populations**. At the base of the food chain, the abundance and types of copepod species have been correlated with the abundance of many fish species.
- The number of adult **Chinook salmon** returning from the ocean to the Sacramento River has become more variable over the last two decades. This number is impacted by extreme mortality events among juvenile salmon. As residents of both marine and freshwater environments, salmon are at risk from the impacts of climate change on these habitats.
- Over a 45-year period, the **breeding success of Cassin's auklets** on Southeast Farallon Island near San Francisco has become increasingly variable. It is associated with the abundance of prey species that are influenced by ocean conditions such as warming.
- During years when sea surface temperatures are unusually warm in their breeding area, there have been fewer **California sea lion pup** births, higher pup mortality, and poor pup conditions at San Miguel Island off Santa Barbara. Sea lions are vulnerable to fluctuations in the abundance and distribution of their primary prey, which are directly influenced by ocean conditions.





EMERGING CLIMATE CHANGE ISSUES



Changes and impacts in California's environment that are plausibly influenced by climate change, though not yet established, are referred to in the report as emerging climate change issues. Scientifically defensible hypotheses, models, and/or limited data support the assertion that certain observed or anticipated changes are in part due to climate change.

Among the emerging issues described in this report are:

- Increased frequency, severity, and duration of harmful algal blooms in marine and freshwater environments, which are known to be influenced by water temperature and drought conditions.
- Reduced duration and extent of winter fog in the Central Valley and coastal fog, with warming winter temperatures and other climate changes.
- Increased survival and spread of forest disease-causing pathogens and insects, along with increased susceptibility of trees, which are affected by temperature, precipitation, and forest fires.
- More favorable conditions that allow invasive agricultural pest species like the Oriental fruit fly to thrive in places where they previously could not survive.

INDICATORS OF CLIMATE CHANGE IN CALIFORNIA



CLIMATE CHANGE DRIVERS

Greenhouse gas emissions

Atmospheric greenhouse gas concentrations

Atmospheric black carbon concentrations

Acidification of coastal waters



CHANGES IN CLIMATE

Annual air temperature

Extreme heat events

Winter chill

Cooling and heating degree days

Precipitation

Drought



IMPACTS OF CLIMATE CHANGE ON PHYSICAL SYSTEMS

Snowmelt runoff

Snow-water content

Glacier change

Lake water temperature

Coastal ocean temperature

Sea level rise

Dissolved oxygen in coastal waters



IMPACTS OF CLIMATE CHANGE ON BIOLOGICAL SYSTEMS

On humans

Vector-borne diseases

Heat-related mortality and morbidity

On vegetation

Forest tree mortality

Wildfires

Ponderosa pine forest retreat

Vegetation distribution shifts

Changes in forests and woodlands

Subalpine forest density

Fruit and nut maturation time

On wildlife

Spring flight of Central Valley butterflies

Migratory bird arrivals

Bird wintering ranges

Small mammal and avian range shifts

Effects of ocean acidification on marine organisms (*Type III**)

Nudibranch range shifts

Copepod populations

Sacramento fall-run Chinook salmon abundance

Cassin's auklet breeding success

California sea lion pup demography

Note: A "Type III" indicator is conceptual; no ongoing monitoring or data collection is in place.

TABLE OF CONTENTS

SUMMARY	S-1
INTRODUCTION	1
CLIMATE CHANGE DRIVERS	7
GREENHOUSE GAS EMISSIONS	9
ATMOSPHERIC GREENHOUSE GAS CONCENTRATIONS.....	24
ATMOSPHERIC BLACK CARBON CONCENTRATIONS.....	38
ACIDIFICATION OF COASTAL WATERS	45
CHANGES IN CLIMATE	53
ANNUAL AIR TEMPERATURE	55
EXTREME HEAT EVENTS	62
WINTER CHILL	71
COOLING AND HEATING DEGREE DAYS	82
PRECIPITATION.....	88
DROUGHT	98
IMPACTS ON PHYSICAL SYSTEMS	107
SNOWMELT RUNOFF.....	109
SNOW-WATER CONTENT	114
GLACIER CHANGE	124
LAKE WATER TEMPERATURE	131
COASTAL OCEAN TEMPERATURE	137
SEA LEVEL RISE.....	145
DISSOLVED OXYGEN IN COASTAL WATERS.....	154
IMPACTS ON BIOLOGICAL SYSTEMS	161
IMPACTS ON HUMANS	
VECTOR-BORNE DISEASES.....	164
HEAT-RELATED MORTALITY AND MORBIDITY	171

IMPACTS ON VEGETATION

FOREST TREE MORTALITY179
WILDFIRES185
PONDEROSA PINE FOREST RETREAT193
VEGETATION DISTRIBUTION SHIFTS (NO UPDATE)199
CHANGES IN FORESTS AND WOODLANDS205
SUBALPINE FOREST DENSITY211
FRUIT AND NUT MATURATION TIME219

IMPACTS ON WILDLIFE

SPRING FLIGHT OF CENTRAL VALLEY BUTTERFLIES.....226
MIGRATORY BIRD ARRIVALS232
BIRD WINTERING RANGES243
SMALL MAMMAL AND AVIAN RANGE SHIFTS255
EFFECTS OF OCEAN ACIDIFICATION ON MARINE ORGANISMS.....270
NUDIBRANCH RANGE SHIFTS276
COPEPOD POPULATIONS281
SACRAMENTO FALL- RUN CHINOOK SALMON ABUNDANCE290
CASSIN’S AUKLET BREEDING SUCCESS296
CALIFORNIA SEA LION PUP DEMOGRAPHY304

EMERGING CLIMATE CHANGE ISSUES 313

COASTAL FOG313
CENTRAL VALLEY FOG315
LIGHTNING316
FOREST DISEASE AND PEST INFESTATIONS.....317
INVASIVE AGRICULTURAL PESTS318
BLUETONGUE IN LIVESTOCK319
HARMFUL ALGAL BLOOMS320

INTRODUCTION

The world's climate is warming. Both globally and in California, this conclusion is supported by observations showing increasing air and ocean temperatures. Likewise, observed changes to freshwater systems, the oceans, and many plant and animal species have been attributed to climate change. The trends presented in this report, *Indicators of Climate Change in California*, serve as evidence that climate change is occurring in California and is having significant, measurable impacts on the state and its people. This third edition builds on the previous editions, and portrays an increasingly troubling story of accelerating rates of warming, record-breaking events, and species responses that have the potential to cause ecosystem disruptions.

This document presents 36 indicators that, both individually and collectively, show how climate change is affecting California. These scientifically-based measurements track trends in various aspects of climate change and are useful for communicating information about climate change issues confronting the state. This report is intended to promote scientific analysis to inform decision-making on mitigating and adapting to climate change, and to serve as a resource for decision makers, scientists, educators, and the public.

Science provides the foundation for the state's climate policy. By documenting historical trends, the *Indicators of Climate Change in California* report adds to the body of scientific information on the understanding of climate change and its impacts on the state. The indicators supplement, and serve as context for, projected climate change impacts presented in the CalAdapt web portal (<http://cal-adapt.org/>), and focused research conducted as part of *California's Fourth Climate Change Assessment* (CNRA, 2018a). The strategies to meet the state's greenhouse gas emission reduction goals in *California's 2017 Climate Change Scoping Plan* recognize the climate change impacts documented by the indicators in the 2013 edition of this report (CARB, 2017). Similarly, the *2018 Update to the Safeguarding California Plan* cites this indicator report as an example of the continuing reliance on scientific research in guiding state and local adaptation actions (CNRA, 2018b).

IDENTIFYING AND SELECTING INDICATORS TO TRACK CLIMATE CHANGE

The identification and selection of the climate change indicators presented in this report followed a commonly used conceptual framework and a process adopted by the Office of Environmental Health Hazard Assessment (OEHHA) for the Environmental Protection Indicators for California Project (OEHHA, 2002).

This conceptual framework, used by many environmental indicator programs, recognizes the relationships among pressures on the environment, ambient environmental conditions and societal responses. This “pressure-state-effects-response” framework can be applied to climate change. “Pressures” are the human-influenced changes in the environment (also known as “drivers”) that are linked to warming. These changes alter the “state” of the climate, as reflected in climate variables such as temperature and precipitation. These changes in climate, in turn, result in “effects,” namely impacts on physical systems (specifically hydrological resources and the oceans) and biological systems (humans and ecosystems).

Indicators were selected based on their usefulness for measuring climate change and its impacts, and by the body of evidence in the scientific literature. Each indicator had to be derived from scientifically acceptable data that support inferences about the studied impact, be sufficiently sensitive to detect change, and be meaningful for decision-making (OEHHA, 2002). Corroborating evidence from global and national assessments is particularly relevant. OEHHA relied upon the expertise of the researchers and technical experts who contributed to this report in ascertaining the influence of climate change.

Selecting climate change indicators is challenging due to the complexity and inherent variability of the climate system. Climate change refers to a change in the state of the climate that persists for an extended period, typically decades or longer. The earth's variable climate reflects the complex interactions and dependencies among its oceanic, terrestrial, atmospheric and living components. The climate responds to external disruptions, both natural (such as volcanic activity) and human (such as greenhouse gas emissions). The climate also changes according to inherent cyclical patterns of variability. Substantial seasonal, year-to-year and even decade-to-decade variations are superimposed on the long-term trend. To minimize the influence of natural variability on shorter time scales and to allow better analysis of long-term trends, climate is typically defined based on 30-year averages. Further difficulty in examining the impacts of climate change stems from the influence of non-climate stressors (such as land use and emissions of pollutants), which act in concert with the stresses associated with climate change.

CHARACTERIZING CLIMATE CHANGE AND ITS IMPACTS ON CALIFORNIA

Monitoring and research conducted by state and federal agencies, academia and research institutions across the state generate observational data that describe changes already underway. These data can serve as the basis for indicators that track climate change-related trends over time. For example, many of the indicators in the first edition of this report (and updated here) relied on research projects funded by the California Energy Commission, and on long-term hydroclimate data collected by the California Department of Water Resources.

OEHHA continually monitors the scientific literature, publications of research organizations, governmental entities and academia, and other sources for information relating to climate change and its impacts on California. Since 2013, OEHHA has compiled annotated bibliographies of selected publications presenting observations and new or emerging scientific information on climate change, with an emphasis on California. The bibliography includes publications from peer-reviewed journals and reports of governmental agencies, research institutions, universities and other authoritative bodies. The compilation of these bibliographies has supported efforts to update existing indicators and identify new indicators of climate change.

Report structure

This report presents indicators under the following chapters:

- Climate change drivers: Emissions and environmental concentrations of climate pollutants

- Changes in climate: Metrics that track temperature and precipitation over time
- Impacts of climate change
 - On physical systems: Changes to snow and ice cover, lakes and other freshwater bodies, and oceans
 - On biological systems: Changes to the abundance and distribution of species and the timing of growth or life stages

For each indicator, the trend is illustrated using one or more graphs or maps, and the following are discussed:

- What does the indicator show?
- Why is the indicator important?
- What factors influence the indicator?
- Technical considerations (describing characteristics and strengths and limitations of the data)
- Contact person(s) (generally the researcher or technical expert who contributed to, or collaborated with OEHHA on, the preparation of the information presented)
- References cited

Indicators are classified into three categories based on the availability of data:

- Type I, adequate data are available, supported by ongoing, systematic monitoring or collection. (All except one indicator in this report are in this category.)
- Type II, full or partial data generated by ongoing, systematic monitoring and/or collection are available, but either a complete cycle of data has not been collected, or further data analysis or management is needed. (None of the indicators in this report are in this category. Four Type II indicators in the previous editions of the report are now presented as Type I indicators.)
- Type III, conceptual indicators for which no ongoing monitoring or data collection is in place. (One indicator is in this category.)

Emerging climate change issues

A separate chapter identifies changes in California's environment that are plausibly — but not yet established to be — influenced by climate change. The link to climate change is supported by scientifically defensible hypotheses, models and/or limited data. However, factors such as land use and environmental pollution, as well as the inherent variability of the climate system, make it difficult to attribute these changes as impacts due to climate change. Environmental changes and trends for which the influence of climate change remains uncertain are discussed in this section as ***emerging climate change issues***. Additional data or further analyses are needed to determine the extent by which climate change plays a role.

This compilation of indicators will be updated periodically. OEHHA welcomes input from the research community, governmental agencies, non-governmental organizations, and other interested stakeholders. It is our goal that the indicators, both individually and collectively, address the key aspects of climate change and promote informed dialogue about the state's efforts to monitor, mitigate, and prepare for climate change and its impacts.

A summary of this report is available as a stand-alone document posted at <https://oehha.ca.gov/climate-change/document/indicators-climate-change-california>.

References:

CARB (2017). *California's 2017 Climate Change Scoping Plan*. California Air Resources Board. November 2017. Available at https://www.arb.ca.gov/cc/scopingplan/scoping_plan_2017.pdf

CNRA (2018a). California Natural Resources Agency. Resources and Tool Development. Available at <http://resources.ca.gov/climate/safeguarding/research/>

CNRA (2018b). California Natural Resources Agency. *Safeguarding California Plan: 2018 Update, California's Climate Adaptation Strategy*. January 2018. Available at <http://resources.ca.gov/docs/climate/safeguarding/update2018/safeguarding-california-plan-2018-update.pdf>

IPCC (2014). *Climate Change 2014: Synthesis Report. Contribution of Working Groups I, II and III to the Fifth Assessment Report of the Intergovernmental Panel on Climate Change*. [Core Writing Team, R.K. Pachauri and L.A. Meyer (eds.)]. Intergovernmental Panel on Climate Change. Geneva, Switzerland. Available at: <http://www.ipcc.ch/ipccreports/assessments-reports.htm>

Melillo, Jerry M, Terese (T.C.) Richmond, and Gary W. Yohe, Eds., 2014: *Highlights of Climate Change Impacts in the United States: The Third National Climate Assessment*. U.S. Global Change Research Program, 148 pp.

NRC (2010). *Advancing the Science of Climate Change*. National Academies of Science - National Research Council. America's Climate Choices: Panel on Advancing the Science of Climate Change. http://www.nap.edu/catalog.php?record_id=12782

OEHHA (2002). *Environmental Protection Indicators for California*. Office of Environmental Health Hazard Assessment, California Environmental Protection Agency. April, 2002. <http://www.oehha.ca.gov/multimedia/epic/2002epicreport.html>

OEHHA (2009). *Indicators of Climate Change in California*. Office of Environmental Health Hazard Assessment, California Environmental Protection Agency. April, 2009. <http://www.oehha.ca.gov/multimedia/epic/climateindicators.html>

Richardson AJ and Poloczanska ES (2008). Under-resourced, under threat. *Science* **320**(5881): 1294-1295. <http://www.sciencemag.org/content/320/5881/1294.short>

INDICATORS OF CLIMATE CHANGE IN CALIFORNIA



CLIMATE CHANGE DRIVERS

Greenhouse gas emissions
Atmospheric greenhouse gas concentrations

Atmospheric black carbon concentrations
Acidification of coastal waters



CHANGES IN CLIMATE

Annual air temperature
Extreme heat events
Winter chill

Cooling and heating degree days
Precipitation
Drought



IMPACTS OF CLIMATE CHANGE ON PHYSICAL SYSTEMS

Snowmelt runoff
Snow-water content
Glacier change
Lake water temperature

Coastal ocean temperature
Sea level rise
Dissolved oxygen in coastal waters



IMPACTS OF CLIMATE CHANGE ON BIOLOGICAL SYSTEMS

On humans

Vector-borne diseases
Heat-related mortality and morbidity

On vegetation

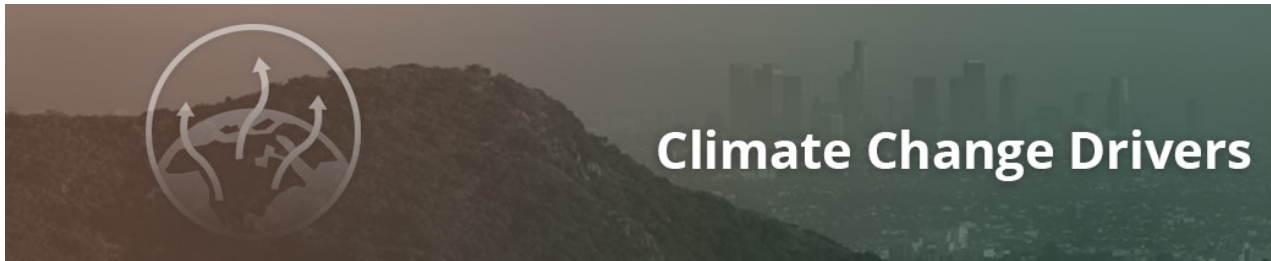
Forest tree mortality
Wildfires
Ponderosa pine forest retreat
Vegetation distribution shifts
Changes in forests and woodlands
Subalpine forest density
Fruit and nut maturation time

On wildlife

Spring flight of Central Valley butterflies
Migratory bird arrivals
Bird wintering ranges
Small mammal and avian range shifts
Effects of ocean acidification on marine organisms (*Type III**)
Nudibranch range shifts
Copepod populations
Sacramento fall-run Chinook salmon abundance
Cassin's auklet breeding success
California sea lion pup demography

Note: A "Type III" indicator is conceptual; no ongoing monitoring or data collection is in place.

Page intentionally blank



The Earth's climate is a complex, interactive system consisting of the atmosphere, land surfaces, snow and ice, oceans and other bodies of water, and living things. This system is influenced by its own internal dynamics and by changes in external factors, both natural and human-induced. External factors that affect climate are called "forcings." Solar radiation and volcanic eruptions are natural forcings. Changes in atmospheric composition resulting from greenhouse gases or aerosols from fossil fuel combustion are human-induced forcings (IPCC, 2014).

Earth has experienced natural cycles of climatic changes throughout its history. The current warming trend is unusual in that it is happening at an unprecedented rate, and is mostly due to human activity (IPCC, 2014).

Heat-trapping greenhouse gases are the major human-influenced drivers of climate change, with carbon dioxide (CO₂) being the largest contributor. Primarily emitted from the use of fossil fuels, annual average global concentrations of CO₂ exceeded a symbolic threshold of 400 parts per million (ppm) in 2015 for the first time since records began, a stark reminder that atmospheric greenhouse gases continue to increase (IPCC, 2014). Given that CO₂ can remain in the atmosphere for thousands of years, levels will likely stay above the 400 ppm benchmark for generations to come (see *Atmospheric greenhouse gas concentrations* indicator). Global atmospheric levels of other greenhouse gases, including methane (CH₄), nitrous oxide (N₂O), and certain fluorinated gases (F-gases), have also risen (IPCC, 2014).

International climate agreements aim to stabilize atmospheric greenhouse gas concentrations at a level that would prevent "dangerous anthropogenic interference with the climate system." The 2015 Paris Agreement calls for keeping the rise in the global average temperature to well below 2 degrees Celsius (°C) above pre-industrial levels. The Agreement also commits to pursue efforts to further limit the increase to 1.5°C. These efforts would significantly reduce the risks and impacts of climate change (UNFCCC, 2016).

Tracking emissions of greenhouse gases provides critical information to policymakers. Recent attention has focused on "short-lived climate pollutants," such as CH₄, certain F-gases and black carbon. Unlike CO₂, these pollutants do not persist for long periods of time in the atmosphere; thus, reducing their emissions can have more immediate effects in slowing the rate of warming.



As atmospheric concentrations of CO₂ increase, so do levels in the ocean. The ocean absorbs approximately 30 percent of the CO₂ released into the atmosphere by human activities every year, changing the chemistry of sea water — a process known as ocean acidification. This process has significantly slowed the CO₂ buildup in the atmosphere and reduced some of its impacts on global warming.

INDICATORS: CLIMATE CHANGE DRIVERS

Greenhouse gas emissions (*updated*)
Atmospheric greenhouse gas concentrations (*updated*)
Atmospheric black carbon concentrations (*updated*)
Acidification of coastal waters (*updated*)

References:

IPCC (2014). *Climate Change 2014 Synthesis Report. Contribution of Working Groups I, II and III to the Fifth Assessment Report of the Intergovernmental Panel on Climate Change* [Core Writing Team, Pachauri RK, and Meyer L (Eds.)]. Intergovernmental Panel on Climate Change. Geneva, Switzerland. Available at: http://www.ipcc.ch/pdf/assessment-report/ar5/syr/SYR_AR5_FINAL_full_wcover.pdf

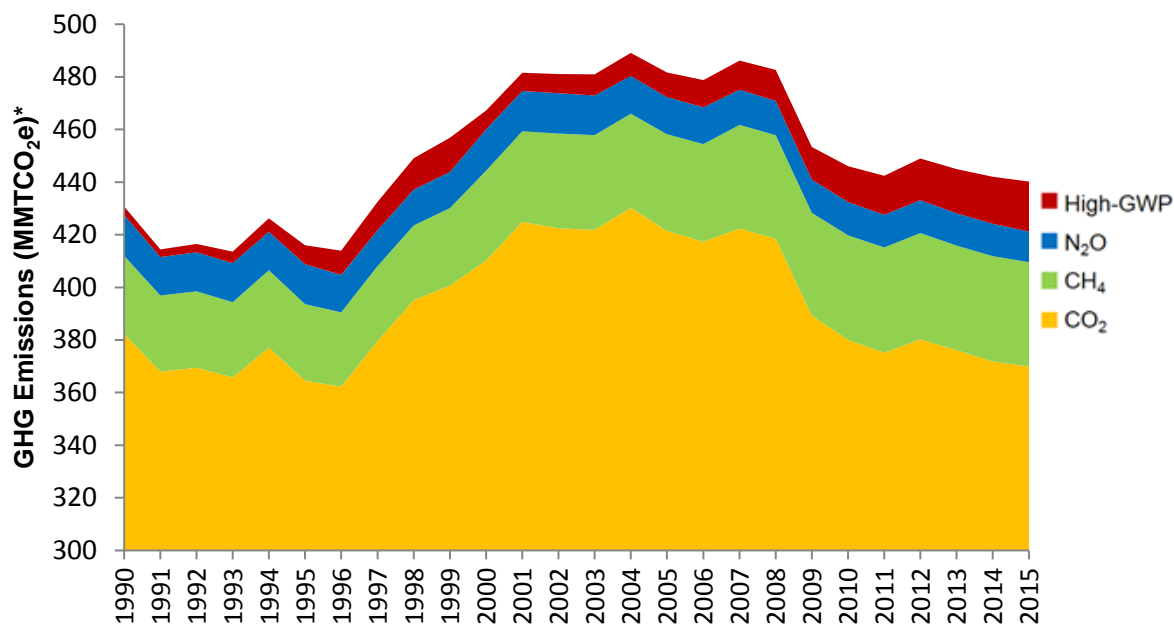
UNFCCC (2016). United Nations Framework Convention on Climate Change. Report of the Conference of the Parties on its twenty-first session, held in Paris from 30 November to 13 December 2015. Decision 1/CP.21: Adoption of the Paris Agreement. Paris, France. Available at <https://unfccc.int/resource/docs/2015/cop21/eng/10a01.pdf>



GREENHOUSE GAS EMISSIONS

Statewide emissions have increased since 1990, but have decreased by 10 percent since levels peaked in 2004. On a per capita and gross state product basis, emissions have steadily decreased.

Figure 1. Greenhouse gas emissions in California by pollutant: 1990-2015
(Based on IPCC Fourth Assessment Report 100-year global warming potentials)



*MMT_{CO₂e} = million metric tons of carbon dioxide equivalents

Source: CARB, 2007; CARB, 2017a

What does the indicator show?

California's combined emissions of the greenhouse gases (GHG) carbon dioxide (CO₂), methane (CH₄), nitrous oxide (N₂O), and high global warming potential (high-GWP) gases have increased since 1990, reaching peak levels in 2004, but have decreased by 10 percent since then (CARB, 2017a). GHG emissions are expressed in million metric tons (MMT) of carbon dioxide equivalents (CO₂e) based on 100-year Global Warming Potential values as specified in the Intergovernmental Panel on Climate Change (IPCC) Fourth Assessment Report (IPCC, 2006).

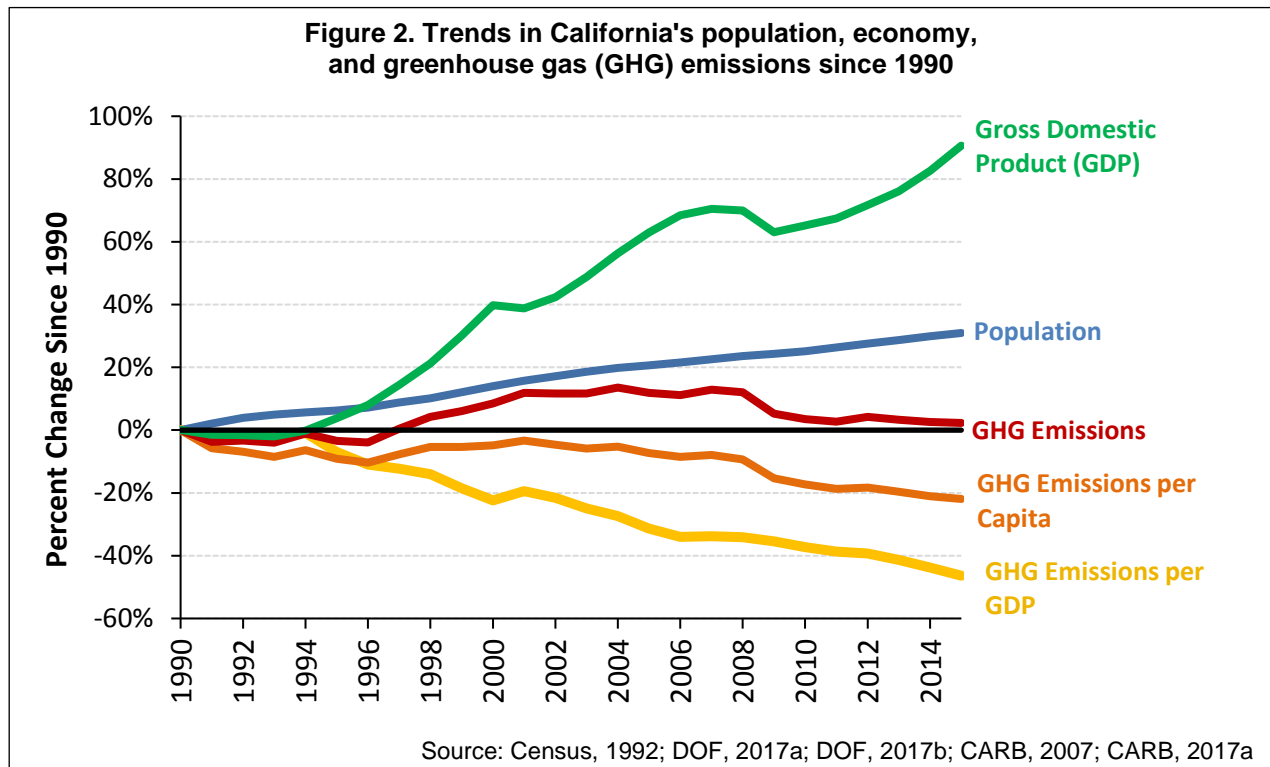
What are "CO₂ equivalents"?

Emissions of greenhouse gases other than carbon dioxide (CO₂) are converted to **carbon dioxide equivalents** or **CO₂e** based on their Global Warming Potential (GWP). GWP represents the warming influence of different greenhouse gases relative to CO₂ over a given time period and allows the calculation of a single consistent emission unit, CO₂e.

CO₂ accounts for the largest proportion of GHG emissions, making up 84 percent of total emissions in 2015. In comparison, CH₄ and N₂O account for 9 percent and 3 percent of total GHG emissions, respectively. The remaining GHG emissions consist of high-GWP gases including hydrofluorocarbons (HFC), perfluorocarbons (PFC),



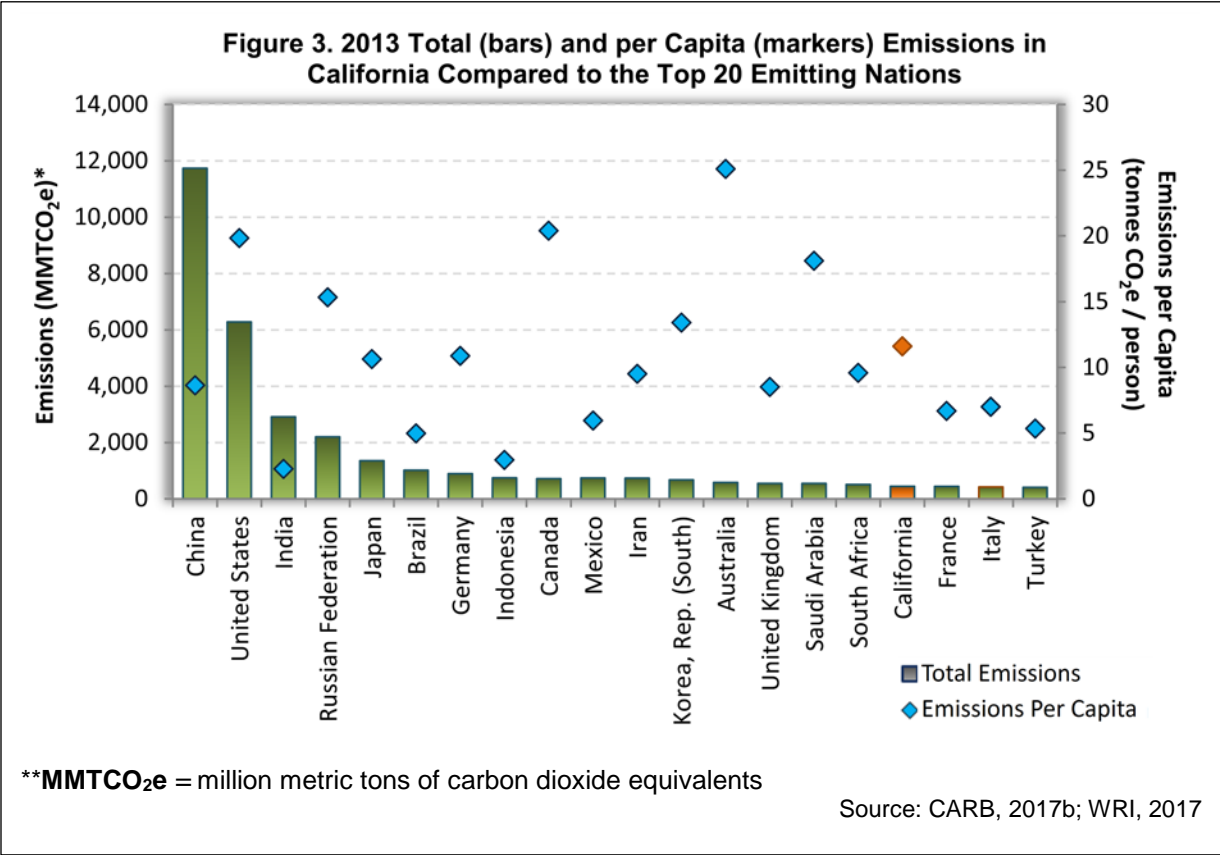
sulfur hexafluoride (SF₆), and nitrogen trifluoride (NF₃). Among these GHGs, methane and a subset of HFCs¹ are also considered short-lived climate pollutants (SLCPs), powerful climate forcers that remain in the atmosphere for a much shorter period of time than longer-lived climate pollutants such as CO₂. SLCPs are discussed further below (see *Why is this indicator important?*).



GHG emissions per person (per capita) and per dollar of gross domestic product (GDP, a measure of the state's economic output) show declining trends between 1990 and 2015 (Figure 2). During the same period, the state's population and GDP increased by 31 percent and 91 percent, respectively. California's 2015 GHG emissions are 2 percent higher than in 1990, but emissions per capita have declined by 22 percent and emissions per dollar of GDP (carbon intensity) have declined by 46 percent. Total GHG emissions have also decreased from the peak in 2004 by 10 percent. A combination of factors contributed to this decrease in carbon intensity of the California economy. These factors include incrementally higher energy efficiency standards, growths in renewable energy sources, carbon pricing in the cap-and-trade program, improved vehicle fuel efficiency, and other regulations.

¹ These include HFC-152a, HFC-32, HFC-245fa, HFC-365mfc, HFC-134a, HFC-43-10mee, HFC-125, HFC-227ea, and HFC-143a.

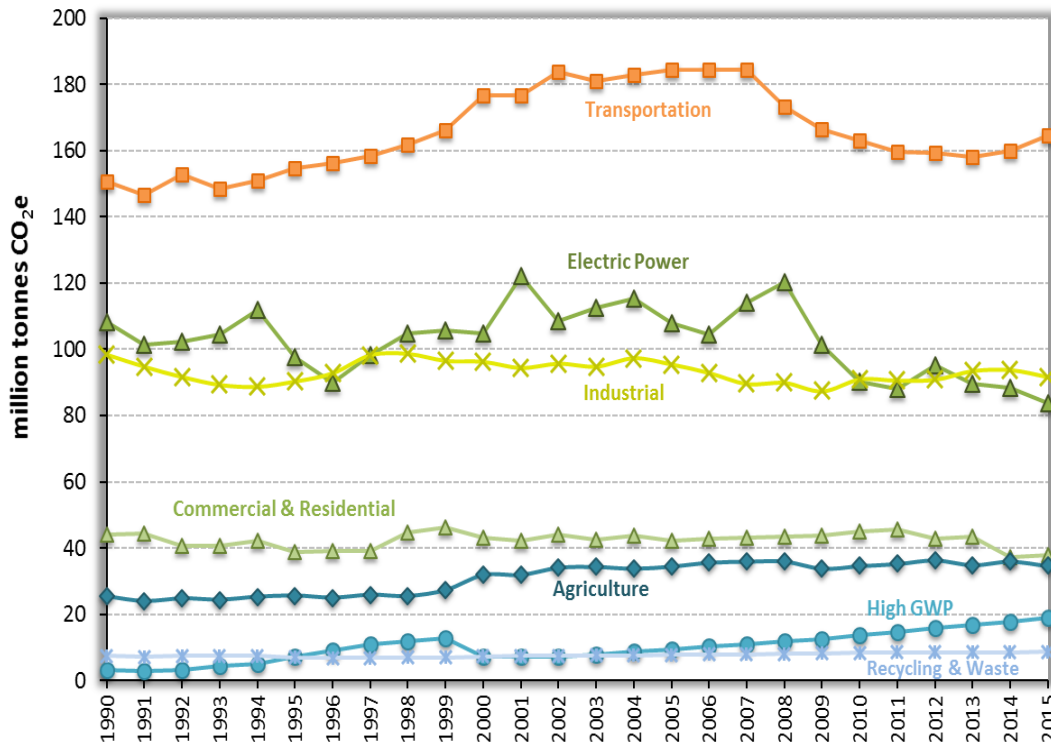




California has been an international leader in reducing GHG emissions. Figure 3 shows 2013 total emissions and emissions per capita for California compared to the top emitting nations. If California were a country, it would rank 17th in total emissions and 7th in per capita emissions among the top 20 emitting nations. The state’s 2013 per capita emissions are 42 percent lower than those of the United States (WRI, 2017).

Figure 4 shows emissions of GHGs from 1990 to 2015, organized by categories as defined in the California Air Resources Board’s *Initial Scoping Plan* (CARB, 2008). The transportation sector and the electric power sector are the primary drivers of year-to-year changes in statewide emissions. Transportation sector emissions increased between 1990 and 2007, followed by a period of steady decrease through 2013, and then a slight increase in 2014 and 2015. Emissions from the electric power sector are variable over time but have decreased by about 30 percent since 2008. High-GWP gases, while not representing a typical “economic sector,” are classified as such for purposes of organizing and tracking emissions, sources and emission reduction strategies. High-GWP gases make up a small portion of total emissions, but are steadily increasing as they replace ozone-depleting substances that are being phased out under international accord (UNEP, 2016). Emissions from the other sectors show some year-to-year variations, but their trends are relatively flat over time.

Figure 4. Greenhouse gas emissions in California by sector*: 1990-2015
(Based on IPCC Fourth Assessment Report 100-year global warming potentials)

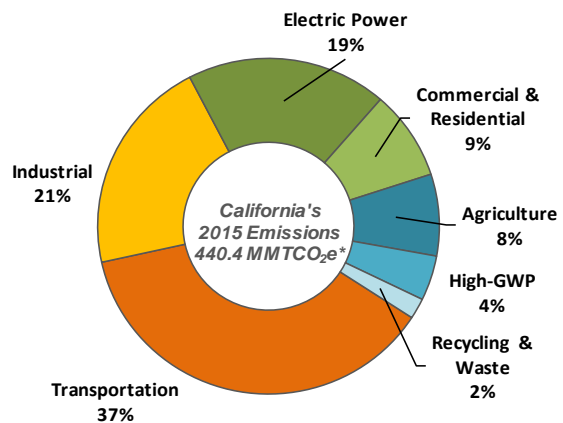


* This figure uses sector categories as defined in the Initial Scoping Plan (ARB 2008) Emissions on million metric tons of carbon dioxide equivalents

Source: CARB, 2017a

Transportation is the largest source of GHGs, accounting for over a third of the total emissions in 2015 (Figure 5). Cars, light duty trucks, and sport utility vehicles (SUVs) are the most important contributors to transportation emissions. Industrial activities account for 21 percent of emissions, and include fossil fuel combustion and fugitive emissions from a wide variety of activities such as manufacturing, oil and gas extraction, petroleum refining, and natural gas pipeline leaks. Electricity generated both in and out of the state accounts for 19 percent of emissions, followed by commercial and residential sources at 9 percent. The commercial sector includes schools, health care services, retail, and wholesale. The residential sector includes emissions from households such as heating with natural gas furnaces and the use of nitrogen fertilizer

Figure 5. Greenhouse gas emissions by sector



*MMTCO₂e = million metric tons of carbon dioxide equivalents

Source: CARB, 2017a



on residential lawns. Emissions from the agricultural sector come from livestock, crop production, and fuel combustion. High-GWP gases are primarily used in refrigeration and air conditioning, as well as foams and consumer products. Recycling and waste includes emissions from landfills, wastewater treatment, and compost.

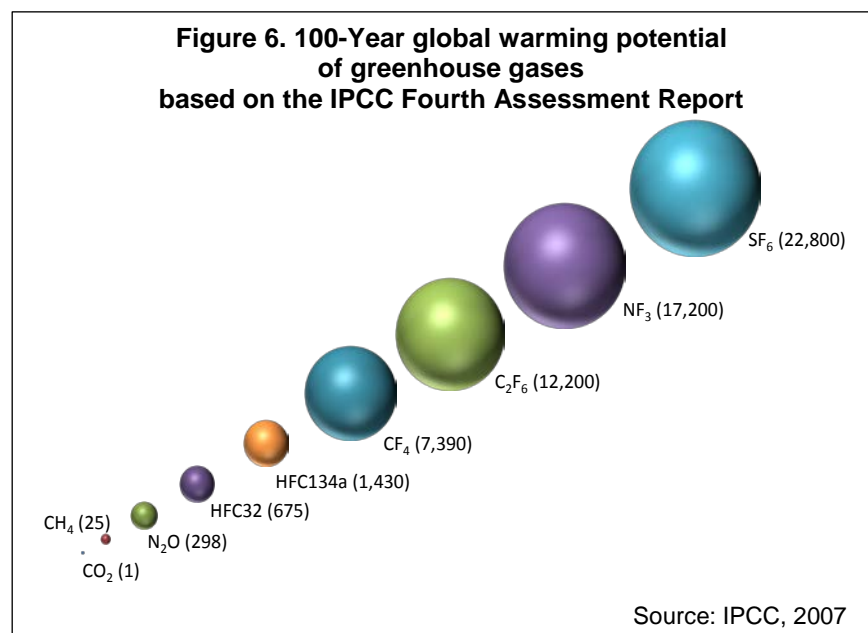
Why is this indicator important?

Atmospheric concentrations of GHGs have increased since the Industrial Revolution, enhancing the heat-trapping capacity of the earth's atmosphere. GHG emission reduction targets are intended to prevent atmospheric concentrations from reaching dangerous levels. Accurately tracking GHG emission trends in California provides critical information to policymakers as they assess climate change mitigation options and track the progress of GHG reduction programs. Businesses that track their GHG emissions can better understand processes that emit GHGs, establish an emissions baseline, determine the carbon intensity of their operations, and evaluate potential GHG emission reduction strategies.

The 2015 Paris Agreement aims to hold the increase in the global average temperature to well below 2°C above pre-industrial levels and to pursue efforts to limit the temperature increase even further to 1.5°C above pre-industrial levels (UNFCCC, 2016). These efforts would significantly reduce the risks and impacts of climate change (Xu and Ramanathan, 2017). Emissions scenarios leading to CO₂-equivalent concentrations of about 450 ppm or lower in 2100 are likely to maintain warming below 2°C over the 21st century relative to pre-industrial levels (IPCC, 2014).

Since each GHG pollutant absorbs energy and warms the atmosphere to a different degree, understanding the pollutants' relative effects on climate change is also important for setting priorities and meeting emission reduction goals. Current international and national GHG inventory practice, as defined by the IPCC Guidelines, uses 100 years as the standard timeframe for GHG inventories. (Other timeframes may be used for different purposes. For example, discussions related to SLCPs typically use the 20-year timeframe.)

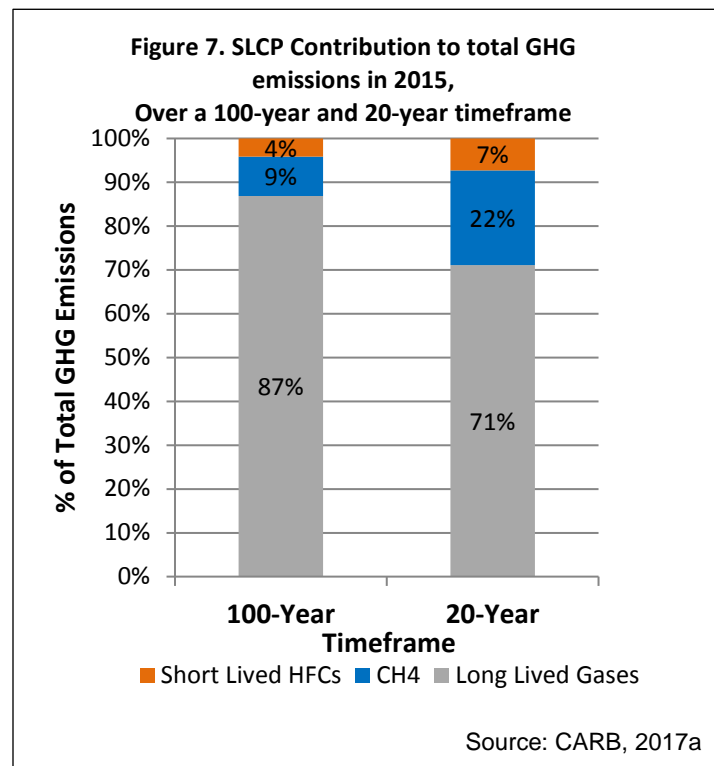
As illustrated in Figure 6, in a 100-year timeframe, CO₂ has the lowest GWP of all GHGs reported in the statewide inventory. Non-CO₂ emissions are converted to CO₂ equivalents (CO₂e) using GWP, which is a measure of the extent to which a particular GHG can alter the heat balance of the Earth relative to carbon dioxide over a specified



timeframe. For example, the GWP of SF₆ is 22,800, meaning that one gram of SF₆ has the same warming effect as 22,800 grams of CO₂.

Emissions of CO₂, the main contributor to climate change, stay in the atmosphere for hundreds of years. Reducing CO₂ emissions is critically important but will not result in near-term cooling. In contrast to CO₂, SLCPs remain in the atmosphere from days to decades; therefore, a reduction in these emissions can have more immediate effects. Moreover, their GWP values are tens to thousands of times greater than that of CO₂. Near-term reductions in SLCPs can help slow the rate of warming, providing additional time to reduce CO₂ emissions.

As noted earlier, GHG emissions are most commonly discussed using a 100-year timeframe. Because SLCPs do not persist in the atmosphere, however, it is useful to consider a 20-year timeframe when discussing their impacts on climate change and planning for mitigation measures. Figure 7 shows the contribution of SLCP emissions to total GHG emissions in 2015. This contribution is based on their effect on warming (GWP) and their atmospheric lifetime. Emissions of short-lived HFCs and methane in 2015 account for 13 percent of the total GHG emissions in a 100-year timeframe; however, when considering a 20-year timeframe, they account for 29 percent. In addition to methane and short-lived hydrofluorocarbons (HFCs), black carbon, a class of particulate matter, is also considered a SLCP (see *Atmospheric black carbon concentrations* indicator).



What factors influence this indicator?

Statewide GHG emissions reflect activities across all major economic sectors, which are influenced by a variety of factors including population growth, vehicle miles traveled, economic conditions, energy prices, consumer behavior, technological changes, drought, and regulations, among other things.

Because GHG emissions from each sector are simultaneously influenced by multiple factors, one-to-one attribution between these factors and their magnitude of influence can be difficult to quantify. For example, improved economic conditions can result in an increased number of motor vehicles per household, and can boost vehicle miles



traveled thus increasing GHG emissions, while using more fuel efficient vehicles, public transportation, or driving less can reduce emissions.

GHGs are emitted from a variety of sources, but most notably from the combustion of fossil fuels used in the industrial, commercial, residential, and transportation sectors. GHG emissions also occur from non-combustion activities at landfills, wastewater treatment facilities, and certain agricultural operations. A discussion of trends in the certain economic sectors, sources of SLCPs, and the influence of regulatory requirements is presented in the following sections. Further information is provided in CARB (2017b).

Transportation

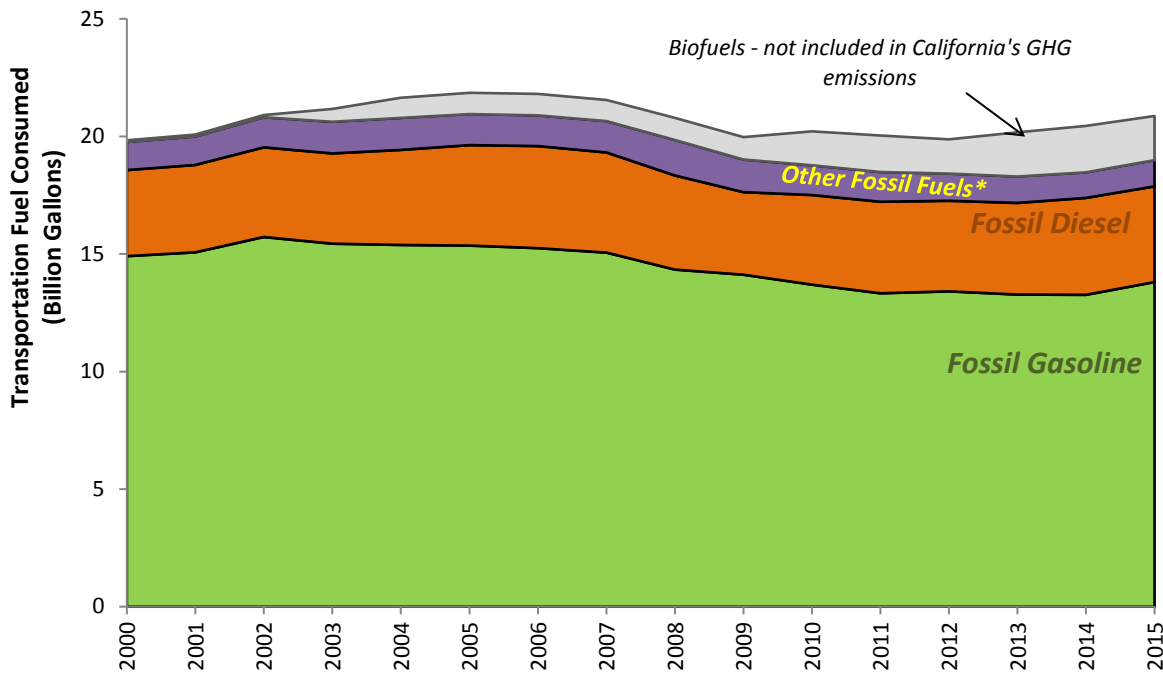
Although California's population has grown by 31 percent since 1990 (Figure 2), GHG emissions from the transportation sector have grown by only 12 percent (Figure 4). Furthermore, transportation emissions in 2015 were 11 percent lower than the peak level in 2007. This decline in transportation emissions is likely due to a combination of improved fuel efficiency of the vehicle fleet, higher market penetration of alternative fuel and zero emissions vehicles, increased use of biofuels, the economic recession, and fluctuations in fuel prices. California is a world leader in the adoption of advanced alternative vehicles, such as plug-in electric and hybrid vehicles. The state is the world's largest market for zero emission vehicles (ZEVs). The US comprises about one-third of the world's ZEV market, and 47 percent of ZEVs in the US are in California (GIWG, 2016). Building consumer awareness and demand, providing incentives and enabling the necessary infrastructure to support ZEVs are among the steps the state has undertaken to bring California towards the goal set by Executive Order B-16-2012 of 1.5 million ZEVs on the road by 2025 (Brown, 2012; GIWG, 2016). More recently, a new target of 5 million ZEVs by 2030 was established by Executive Order B-48-18 (Brown, 2018).

Transportation emissions are related to the amount of fuel burned. Combustion of fossil fuels, such as gasoline and diesel, produces GHGs that are counted towards California's inventory. On the other hand, emissions from the combustion of biofuels such as ethanol and biodiesel, which are derived from carbon that was recently absorbed from the atmosphere as a part of the global carbon cycle, are not counted pursuant to international GHG inventory practices (IPCC, 2006). Thus, displacing fossil fuels with biofuels can reduce the climate change impacts of the transportation sector.

The trends in use of fossil fuels (colored) and biofuels (grey) are shown in Figure 8. Gasoline use is declining and biofuel use is increasing — trends contributing to the reduction in GHG emissions from transportation. Declining gasoline consumption is related to higher ethanol use, as well as to improved fuel economy or increased use of alternative fuel vehicles such as electric or hydrogen fueled vehicles. Biofuel diesel alternatives (i.e., biodiesel and renewable diesel) have been in use since 2010, and volumes are increasing rapidly. Between 2012 and 2015, biofuel diesel alternatives increased from 1 percent to 6 percent of the total transportation diesel use.



Figure 8. Trends in transportation fuel combustion, 2000-2015



*Other fossil fuels include: aviation gasoline, jet fuel, LPG, residual fuel oil, and natural gas.

Source: CARB, 2017a

Residential and Commercial

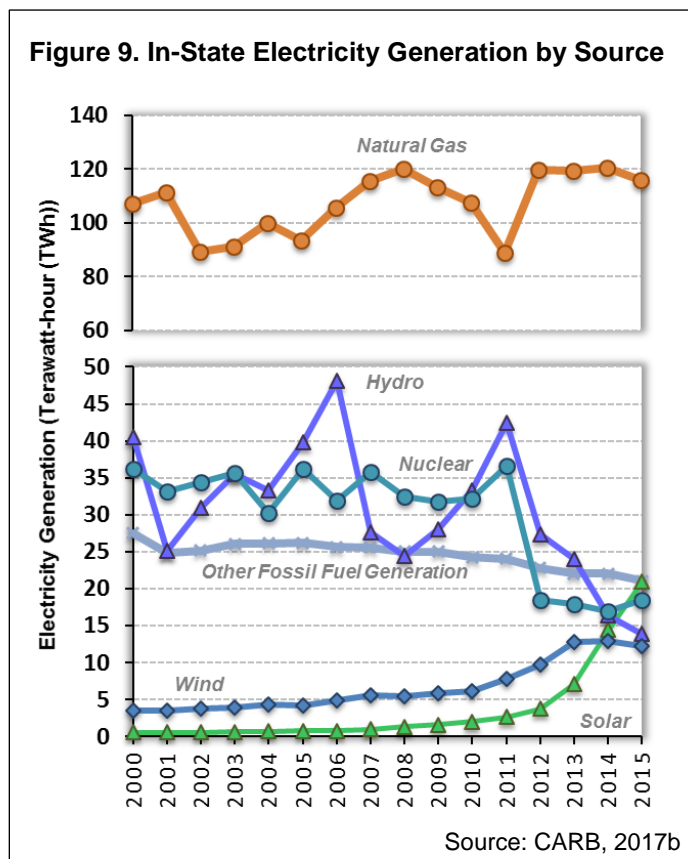
California's steady population growth from 1990 through 2015 has been accompanied by an increased demand for housing, among other things. More housing often means additional demand for residential energy and increased associated GHG emissions. Yet emissions from the residential and commercial sector have decreased in the same period. Residential and commercial building code standards are updated regularly to improve building efficiency (e.g., insulation thickness, window design, lighting systems, and heating/cooling equipment specification). These energy efficiency standards have saved Californians billions of dollars in reduced electricity bills (CEC, 2015), and have reduced the emissions of GHGs and other air pollutants. The per capita electricity consumption in California is near the lowest in the nation, primarily due to mild weather and energy efficiency programs (EIA, 2017).

Weather and precipitation can have notable influences on GHG emissions from the electricity sector. A warmer summer increases electricity demand for air conditioning, and consequently increases the emissions from power plants that must ramp up to meet the additional demand.



Electric Power

California's in-state electricity is derived from a variety of sources (see Figure 9). Natural gas, which is used to produce the majority of in-state electricity, accounted for 57 percent of the electricity production in 2015. Solar energy accounted for 10 percent, hydro accounted for 7 percent, and nuclear accounted for 9 percent. Nuclear power declined after the 2012 shutdown of the San Onofre Nuclear Generating Station. Hydro power reached historic lows in 2015 due to drought. An increase in solar and wind power has compensated for the decline in hydro power and nuclear generation in recent years. Wind, solar, hydro, and nuclear power are zero-emission sources. In 2015, California ranked first in the country in the production of solar energy, and second in net electricity generation from renewable resources (EIA, 2017).



Weather can also have notable influences on GHG emissions from the electricity sector. A warmer summer increases electricity demand for air conditioning, and consequently increases the emissions from power plants that must ramp up to meet the additional demand.

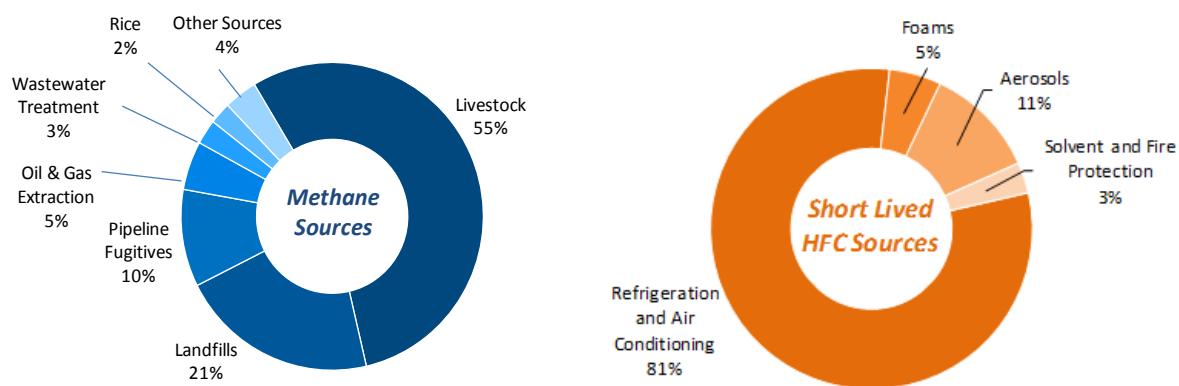
Short-Lived Climate Pollutants

Sources of methane and short-lived HFCs in California are shown in Figure 10. Livestock represents the largest source of methane. Methane is produced from livestock manure management and directly by ruminant animals such as cows, sheep, and goats. Organic waste streams deposited in landfills or managed in wastewater treatment plants also produce methane emissions. As the primary component of natural gas, methane is emitted by oil and gas extraction and during its storage, processing, and transport. Natural gas is used for many purposes including electricity production and heating.

Short-lived HFCs are used as replacements for ozone-depleting substances that are being phased out under the Montreal Protocol (UNEP, 2016). The majority of HFC emissions comes from refrigeration and air-conditioning systems used in the residential, commercial, industrial, and transportation sectors. Foams, aerosols, solvents, and fire protection are other sources of HFCs.



Figure 10. 2015 Sources of short-lived climate pollutants*



*Based on the 2017 edition of the GHG inventory and 100-year GWP

Source: CARB, 2017b

Policies and Regulations

California's pioneering efforts in the adoption and implementation of policies designed to curb GHG emissions have clearly impacted emission trends. The California Global Warming Solutions Act of 2006 (Nuñez, Chapter 488, Statutes of 2006), also known as AB 32, established the nation's first comprehensive program of regulatory and market mechanisms to achieve real, quantifiable, cost-effective GHG reductions. A complete list of initial AB 32 measures can be found on the California Air Resources Board's Scoping Plan webpage at: <https://www.arb.ca.gov/cc/scopingplan/scopingplan.htm>. AB 32 is among a collection of laws, executive orders and regulations that address emission reductions and energy efficiency in the state. These policies are discussed in the Appendix. For a complete list of climate change legislation enacted in California, see: <http://www.climatechange.ca.gov/state/legislation.html>.

Technical Considerations

Data Characteristics

A GHG inventory is an estimate of GHG emissions over a specified area and time period from known sources or categories of sources. Emission inventories generally use a combination of two basic approaches to estimate emissions. The top-down approach utilizes nationwide or statewide data from various federal and state government agencies to estimate emissions. The bottom-up approach utilizes activity data (such as fuel quantity, animal population, tons of waste deposited in the landfill, etc.) to compute unit level emissions that are then aggregated to the state level for a particular source category. In either approach, calculation assumptions are made to estimate statewide GHG emissions from different levels of activity data. These calculations typically reference the 2006 IPCC Guidelines for National Greenhouse Gas Inventories or the US EPA's national GHG inventory, but also incorporate California-specific methods and considerations to the extent possible.



Strengths and Limitations of the Data

The methods used to develop the California GHG inventory are consistent with international and national inventory guidelines to the greatest extent possible. Emission calculation methodologies are evaluated over time and refined by incorporating the latest scientific research and monitoring activities.

The California GHG inventory includes emissions from anthropogenic sources located within California's boundaries, as well as GHG emissions associated with imported electricity. Pursuant to AB 32, California has gone beyond the international inventory guidelines defined by the IPCC in including imported electricity in GHG emission tracking. The inventory, however, excludes emissions that occur outside California during the manufacture and transport of products and services consumed within the State. On the other hand, California is a net exporter of multiple products, especially agricultural commodities. California exported about a quarter of all agricultural products (CDFA, 2014), but the state's GHG inventory does not discount the carbon sequestered in California-produced agricultural products that are exported and consumed outside of the state. In addition, GHG mitigation action may cross geographic borders as part of international and sub-national collaboration, or as a natural result of implementation of a state policy, but the inventory also does not account for emission reductions outside of its geographic border that may have resulted from California's adopted programs.

For more information, contact:



Anny Huang, Ph.D.
California Air Resources Board
California Environmental Protection Agency
P.O. Box 2815
Sacramento, California 95812
(916) 323-8475
anny.huang@arb.ca.gov

References:

Brown EG (2012). Executive Order B-16-2012, March 23, 2012. Available at <https://www.gov.ca.gov/2012/03/23/news17472/>.

Brown EG (2018). Executive Order B-48-18, January 26, 2018. Available at <https://www.gov.ca.gov/2018/01/26/governor-brown-takes-action-to-increase-zero-emission-vehicles-fund-new-climate-investments/>.

CARB (2007). California Air Resources Board: 1990-2004 Inventory. Retrieved October 2017, from <https://www.arb.ca.gov/cc/inventory/1990level/1990data.htm>

CARB (2008). *Initial AB 32 Climate Change Scoping Plan Document*. California Air Resources Board. Available at https://www.arb.ca.gov/cc/scopingplan/document/adopted_scoping_plan.pdf

CARB (2016). California Air Resources Board: Low Carbon Fuel Standard. Retrieved October 2017, from <https://www.arb.ca.gov/fuels/lcfs/background/basics.htm>

CARB (2017a). California Air Resources Board: Greenhouse Gas Inventory 2017 Edition, Years 2000-2015. Retrieved October 2017, from <https://www.arb.ca.gov/cc/inventory/pubs/pubs.htm>



CARB (2017b). *California Greenhouse Gas Emissions from 2000 to 2015 – Trends of Emissions and Other Indicators* (2017 Edition). California Air Resources Board. Available at https://www.arb.ca.gov/cc/inventory/pubs/reports/2000_2015/ghg_inventory_trends_00-15.pdf

CEC (2015). California Energy Commission. California's Energy Efficiency Standards Have Saved Billions. Retrieved October 2017, from <http://www.energy.ca.gov/efficiency/savings.html>

Census (1992). *1990 Census of Population and Housing, Population and Housing Unit Counts, United States* (1990 CPH-2-1). U.S. Department of Commerce, Bureau of the Census. Washington DC: US Government Printing Office. Available at <https://www.census.gov/prod/cen1990/cph2/cph-2-1-1.pdf>

CDFA (2014). *California Agricultural Statistics Review: 2012 – 2013*. California Department of Food and Agriculture Sacramento, CA: Office of Public Affairs. Available at <https://www.cdfa.ca.gov/Statistics/PDFs/2013/FinalDraft2012-2013.pdf>

DOF (2017a). California Department of Finance. *E-6 Population Estimates and Components of Change by County July 1, 2010-2017*. Sacramento, CA. Available at <http://www.dof.ca.gov/Forecasting/Demographics/Estimates/E-6/>

DOF (2017b). California Department of Finance. *California Gross Domestic Product*. Retrieved October 2017, from http://www.dof.ca.gov/Forecasting/Economics/Indicators/Gross_State_Product/

EIA (2017). US Energy Information Administration. California Quick Facts. Retrieved October 2017, from <http://www.eia.gov/state/?sid=CA>

GIWG (2016). Governor's Interagency Working Group on Zero-emissions Vehicles, Governor Edmund G. Brown Jr. *2016 ZEV Action Plan – An Updated Roadmap Toward 1.5 Million Zero-Emission Vehicles in California Roadways by 2025*. Available at https://www.gov.ca.gov/wp-content/uploads/2017/09/2016_ZEV_Action_Plan.pdf

IPCC (2006). *2006 IPCC Guidelines for National Greenhouse Gas Inventories, Prepared by the National Greenhouse Gas Inventories Programme*. Eggleston HS, Buendia L, Miwa K, Ngara T, and Tanabe K (Eds.). Hayama, Kanagawa, Japan: Institute for Global Environmental Strategies. Available at <https://www.ipcc-nggip.iges.or.jp/public/2006gl/>

IPCC (2007). *Climate Change 2007: Synthesis Report. Contribution of Working Groups I, II, and III to the Fourth Assessment Report of the Intergovernmental Panel on Climate Change*. Core Writing Team, Pachauri RK and Reisinger A (Eds.). Geneva, Switzerland: International Panel on Climate Change. Available at https://www.ipcc.ch/publications_and_data/publications_ipcc_fourth_assessment_report_synthesis_report.htm

IPCC (2014). *Climate Change 2014 Synthesis Report. Contribution of Working Groups I, II and III to the Fifth Assessment Report of the Intergovernmental Panel on Climate Change* [Core Writing Team, Pachauri RK, and Meyer L (Eds.)]. Intergovernmental Panel on Climate Change. Geneva, Switzerland. Available at: http://www.ipcc.ch/pdf/assessment-report/ar5/syr/SYR_AR5_FINAL_full_wcover.pdf

UNEP (2016). United Nations Environment Programme: The Montreal Protocol on Substances that Deplete the Ozone Layer. Retrieved October 2017, from <http://ozone.unep.org/en/treaties-and-decisions/montreal-protocol-substances-deplete-ozone-layer>

UNFCCC (2016). United Nations Framework Convention on Climate Change. Report of the Conference of the Parties on its twenty-first session, held in Paris from 30 November to 13 December 2015. Decision 1/CP.21: Adoption of the Paris Agreement. Paris, France. Available at <https://unfccc.int/resource/docs/2015/cop21/eng/10a01.pdf>



WRI (2017). CAIT Climate Data Explorer. 2017. Washington, DC: World Resources Institute. Retrieved October 2017, from <http://cait.wri.org>

Xu Y and Ramanathan V (2017). Well- below 2° C: Mitigation strategies for avoiding dangerous to catastrophic climate changes. *Proceedings of the National Academy of Sciences* **114**(39): 10315-10323.



APPENDIX. California's Climate Change Policies

California's climate program has evolved through a series of statutory requirements and executive orders over almost 30 years (beginning with the enactment of Assembly Bill 4420 in 1988, which directed the California Energy Commission to maintain a greenhouse gas emissions inventory and to conduct research on the impacts of climate change). Most notably, California established the nation's first comprehensive program of regulatory and market mechanisms to achieve real, quantifiable, cost-effective GHG reductions with the enactment of the California Global Warming Solutions Act of 2006 (Nuñez, Chapter 488, Statutes of 2006). Also known as AB 32, this law caps California's greenhouse gas emissions at 1990 levels by 2020. In 2016, emission reduction targets were extended through 2030 with the passage of Senate Bill (SB) 32 (Pavley, Chapter 249, Statutes of 2016), which requires a reduction of statewide GHG emissions to 40 percent below the 1990 level by 2030. The same year, SB 1383 (Lara, Chapter 395, Statutes of 2016) was passed to reduce emissions of short-lived climate pollutants by 2030. SB 1383 specified emission reduction targets of 40 percent for methane, 40 percent for hydrofluorocarbon gases, and 50 percent for anthropogenic black carbon. The California Air Resources Board (CARB) is working in collaboration with other state agencies in adopting plans and regulations to achieve GHG and short-lived climate pollutant emission reductions.

AB 32 has led to the adoption of a suite of GHG emission reduction measures. Among these, the Cap-and-Trade Regulation and the Low Carbon Fuel Standard (LCFS) are expected to achieve approximately half of the total reductions needed for California to meet its 2020 emission goal. The Cap-and-Trade Regulation is a market-based program that sets a limit on GHG emissions from capped sectors and allows trading of carbon permits (allowances). CARB is working with other states and provinces on linked cap-and-trade programs to form a larger regional trading program. In 2017, the California Legislature passed AB 398 and authorized extension of the Cap-and-Trade program beyond 2020. The LCFS was adopted in 2009 with the goal of reducing the carbon intensity of transportation fuels by at least 10 percent by 2020 (CARB 2016). The LCFS is based on the principle that each fuel has "lifecycle" greenhouse gas emissions associated with the production, transportation, and use of the fuel. By using a performance-based approach and allowing the market to determine how the carbon intensity of transportation fuels will be reduced, the LCFS provides incentives to diversify the fuel pool, and to reduce the lifecycle carbon intensity, emissions of other air pollutants, and California's dependence on fossil fuels.

SB X1-2 (Simitian, Chapter 1, Statutes of 2011) codified into law a renewable portfolio standard (RPS) which sets a target of 33% use of renewable energy by 2020. In 2015, SB 350 (De Leon, Chapter 547, Statutes of 2015) took the state's RPS one step further to 50 percent by 2030. It also doubled the energy efficiency of electricity and natural gas end uses by 2030. These legislations put California on a path to reduce the GHG emissions from the electric power, residential, and commercial sectors, which together make up almost a third of the state's total GHG emissions.



California has a history of adopting technology-advancing vehicle emission standards to protect public health. Assembly Bill (AB) 1493 (Pavley, Chapter 200, Statutes of 2002) requires CARB to develop and adopt regulations that achieve the maximum feasible reduction of GHG emitted by passenger vehicles and light-duty trucks for model years through 2016. In 2012, CARB approved a new emissions-control program for model years 2017 through 2025. The program combines the control of smog, soot and global warming gases and requirements for greater numbers of zero-emission vehicles into a single package of standards called Advanced Clean Cars.

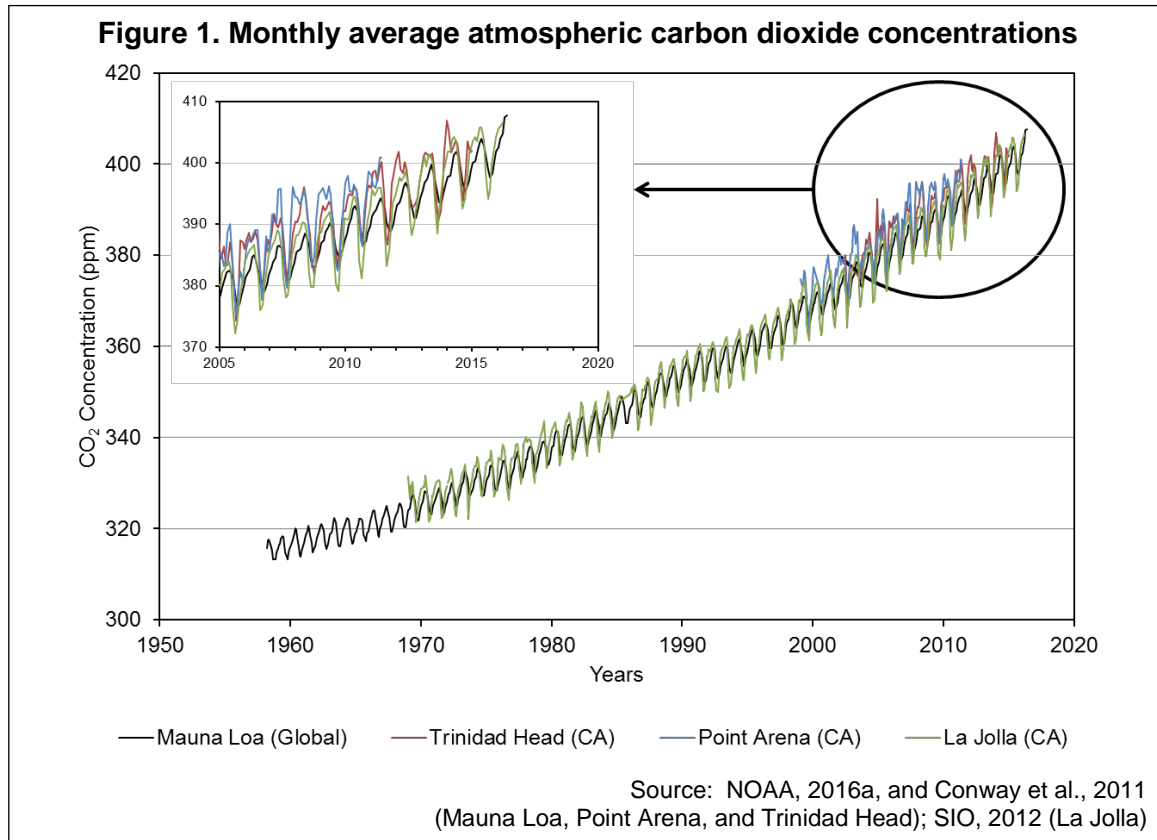
Senate Bill 375 (Steinberg, Chapter 728, Statutes of 2008) supports the state's climate action goals to reduce GHG emissions through coordinated transportation and land use planning with the goal of more sustainable communities. It requires CARB to develop regional GHG emission reduction targets from passenger vehicle use. CARB established targets for 2020 and 2035 for each region covered by one of the State's 18 metropolitan planning organizations and will periodically review and update the targets as needed (<https://www.arb.ca.gov/cc/sb375/sb375.htm>).

For a complete list of climate change legislations enacted in California, see: <http://www.climatechange.ca.gov/state/legislation.html>. A complete list of initial AB 32 measures can be found on CARB's Scoping Plan webpage at: <https://www.arb.ca.gov/cc/scopingplan/scopingplan.htm>



ATMOSPHERIC GREENHOUSE GAS CONCENTRATIONS

Atmospheric concentrations of greenhouse gases such as carbon dioxide, methane, nitrous oxide and certain fluorinated gases continue to increase globally and in California. In 2015, the annual average global concentrations of carbon dioxide exceeded 400 parts per million. Levels are expected to remain above this benchmark for many generations.



What does the indicator show?

Atmospheric concentrations of greenhouse gases are increasing, as illustrated in Figures 1-4. These graphs show the ambient concentrations of carbon dioxide (CO₂), methane (CH₄), nitrous oxide (N₂O), and a variety of fluorinated gases (F-gases) at a global background site at the peak of Mauna Loa on the island of Hawaii, and for CO₂ and CH₄, at three regional background sites in California. The measurements are presented in parts per million (ppm) or parts per billion (ppb). These are units of air pollution mixing ratios commonly used to describe ambient air pollution concentrations (1 ppm = 1,000 ppb).

Figure 1 shows the CO₂ measurements at Mauna Loa, and at three coastal sites in California (Trinidad Head, Point Arena, and La Jolla). Measurements at Mauna Loa first began in 1958. Since then, in under six decades, CO₂ concentrations have increased from 315 ppm to over 400 ppm, and continue to trend upward. In general, in the last five years, the annual average CO₂ concentrations have increased by 2 ppm or more per year (NOAA, 2017). The measurements in California have slightly higher values and



larger variabilities compared to those at Mauna Loa, primarily due to influences from anthropogenic CO₂ emission sources near the regional monitoring sites.

Figure 2 shows the atmospheric measurements of CH₄ at Mauna Loa since 1983. The figure also shows the CH₄ measurements at Point Arena and Trinidad Head since 1999 and 2002, respectively. Global CH₄ levels have increased since 1983, except for a brief period between 1999 and 2006 when they were relatively constant before increasing again in 2007. Pre-industrial (i.e., pre-1750) CH₄ concentrations were approximately 0.7 ppm. By contrast, today's atmospheric CH₄ concentrations exceed 1.8 ppm at Mauna Loa and the California sites – an increase of over 150 percent (WMO, 2016). However, the CH₄ concentrations at the California sites are higher than those observed at Mauna Loa. This is likely due to a strong latitudinal gradient that promotes elevated CH₄ concentrations in the northern latitudes, where there are more human activities that lead to greater emissions (Frankenberg et al., 2005).

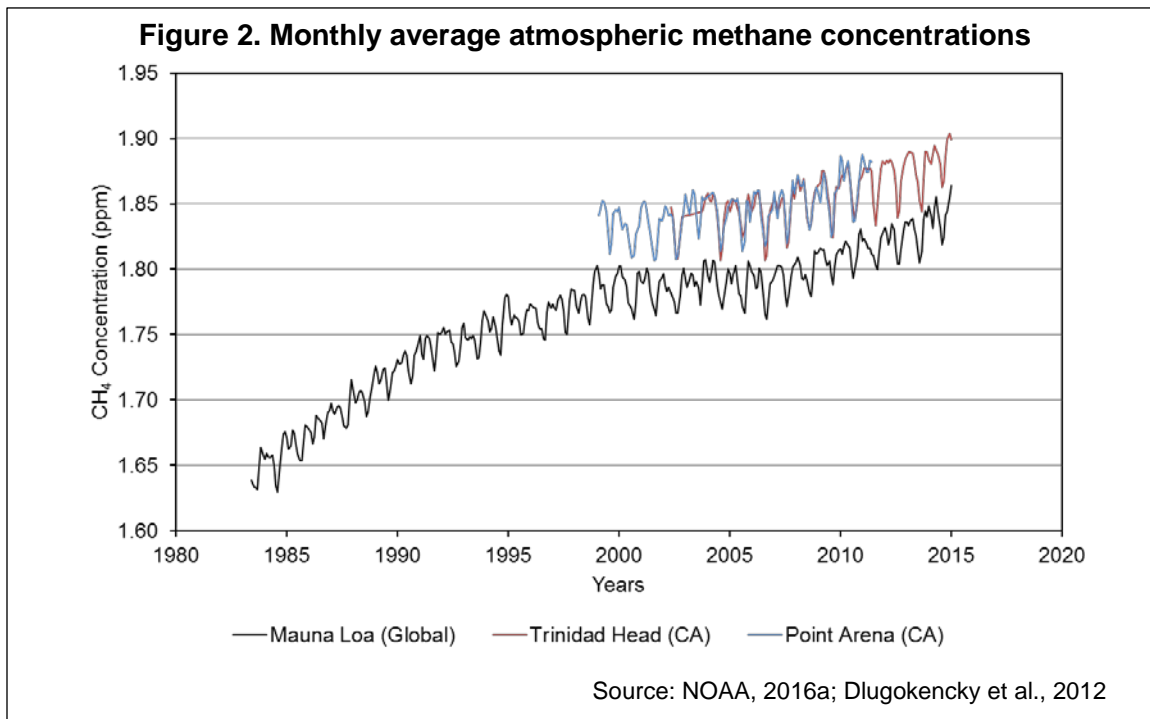


Figure 3 shows the atmospheric concentrations of N₂O at Mauna Loa since 1987. N₂O concentrations have been increasing globally at a rate of approximately 0.7 ppb per year over the past few decades (IPCC, 2014). Global N₂O levels in 2016 were approximately 22 percent greater than pre-industrial levels of 270 ppb (WMO, 2016).



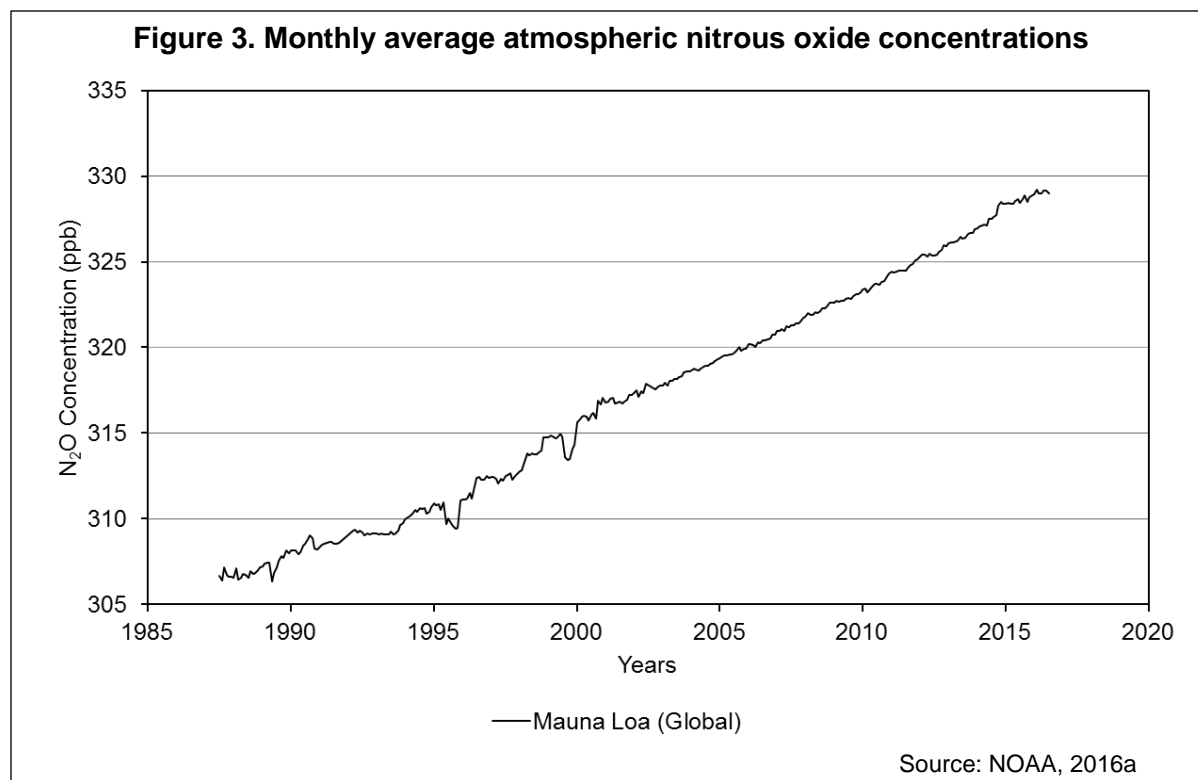
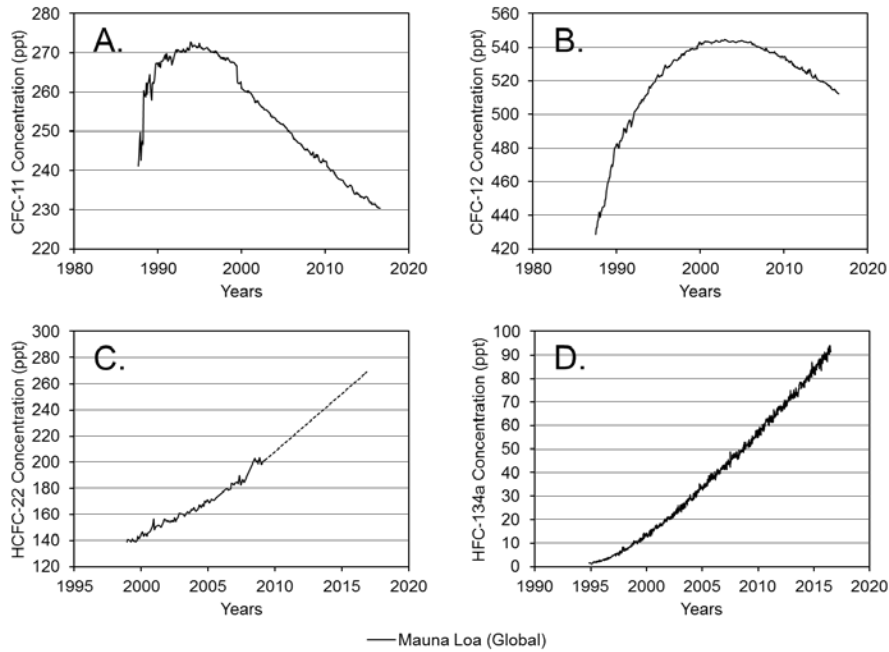


Figure 4 shows the atmospheric concentrations of select chlorofluorocarbons (CFCs) and hydrochlorofluorocarbons (HCFCs) which are the most prevalent F-gases in the atmosphere at Mauna Loa, specifically trichlorofluoromethane (CFC-11) (panel A), dichlorodifluoromethane (CFC-12) (panel B), chlorodifluoromethane (HCFC-22) (panel C), and 1,1,1,2-tetrafluoroethane (HFC-134a) (panel D). CFCs and HCFCs are synthetic compounds that began to appear in the atmosphere in the 20th century as a result of their increased usage as refrigerants. The pre-industrial CFC and HCFC concentrations are assumed to be zero. Hydrofluorocarbons (HFCs) are primarily used as substitutes for CFCs and HCFCs following the phase out and ban on these ozone-depleting substances pursuant to the Montreal Protocol of 1987.

Since they were first measured at Mauna Loa in 1987, concentrations of CFC-11 and CFC-12 have rapidly increased. Following their production ban in 1996, atmospheric CFC concentrations at Mauna Loa began to decrease steadily (UNEP, 2012). Atmospheric concentrations of HCFC-22 increased at Mauna Loa between the late 1990s, when they were first measured, and 2009; no data are available from 2009 to 2015. Atmospheric concentrations of HFC-134a have also been increasing globally over the past two decades at a steady rate of approximately 5 ppb per year since 2005. Its global background concentrations have increased by over 68 times since its first record at Mauna Loa in 1994, and now exceed 200 ppb.



Figure 4. Monthly average atmospheric F-gas concentrations

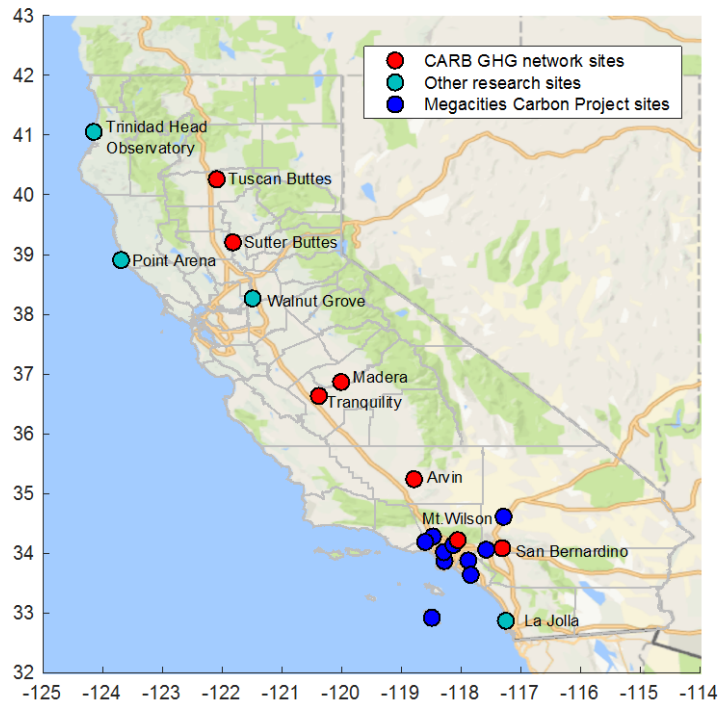


Note: HCFC-22 measurements were not available from 2009-2015, and have been marked with a dashed line on Panel C.

Source: NOAA, 2016a

California has undertaken additional efforts to track the changes in ambient GHG concentrations at several monitoring sites located throughout the state. As shown on the map in Figure 5, the California Air Resources Board (CARB) operates or funds eight GHG monitoring network sites in the state. The map inset also shows 13 additional monitoring sites that are operating under various research partnerships and collaborations (most notably the Megacities Carbon Project in Los Angeles (NASA-JPL, 2017)). These sites study the regional and local emission sources of important GHGs in California.

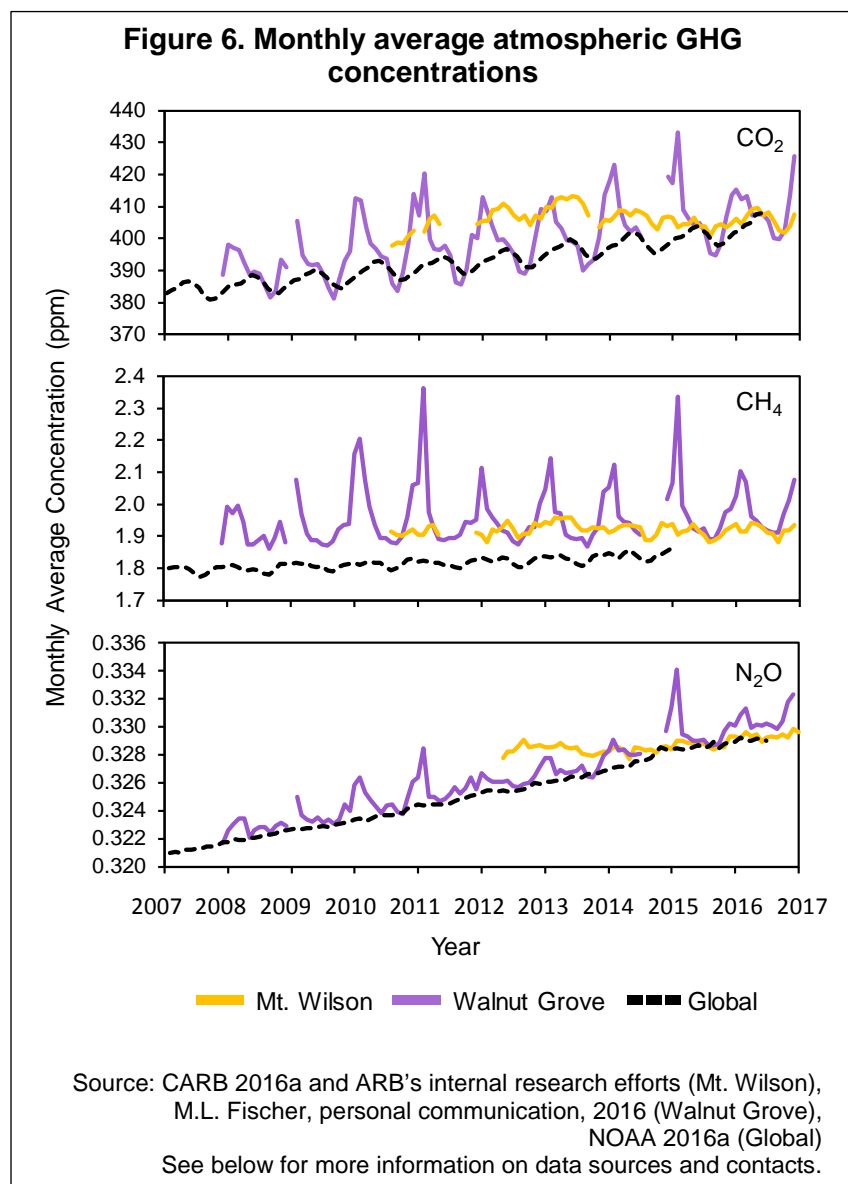
Figure 5. Greenhouse gas monitoring locations in California



Source: CARB, 2016



Aside from the three coastal background sites (NOAA, 2016a), California's GHG monitoring network also employs two stations that measure well-mixed regional air, which can be used to understand how GHG concentrations are changing in California relative to the global trends. The Mt. Wilson station, located on top of the San Gabriel Mountains in Los Angeles County, offers a good indication of air quality in Southern California, as it receives well-mixed air parcels from the Los Angeles air basin every day. The Walnut Grove station, an inland tower located near Sacramento, provides a signature of regional emissions from Northern and Central California.



CO₂ concentrations at inland locations in California track the global trends well, albeit with larger inter-annual variabilities and higher monthly average concentrations (Figure 6). The average CO₂ concentration at Mt. Wilson increased from roughly 400 ppm in 2010 to over 410 ppm by 2013, which translated to an enhancement of approximately 3 ppm per year. Since 2013, CO₂ concentrations at Mt. Wilson have not shown any significant annual variation. By comparison, the Walnut Grove tower experienced CO₂ enhancement of approximately 2 ppm per year. However, inter-annual variabilities were considerably larger with the monthly average concentrations at Walnut Grove reaching a maximum of over 420 ppm. The more

pronounced seasonal pattern at the Walnut Grove site can be attributed to influence from local sources as well as lower average mixing depths, which trap air pollution emissions closer to the ground during cooler months.



CH₄ concentrations in California also show higher values and larger variabilities relative to the global trend. At Mount Wilson, the monthly average CH₄ enhancement above the global background is typically within a fraction of a ppm. However, it continues to track the general trend of the global background measured at Mauna Loa. During summer months, CH₄ measurements at Walnut Grove are similar to measurements at Mt. Wilson. Higher concentrations during the winter months are likely due to influences from changing meteorological conditions and human activities. These measurements show that the general CH₄ concentration has remained relatively stable over the past decade.

Except for the years prior to 2015, N₂O concentrations at Mt. Wilson were similar to those at Mauna Loa. By contrast, the trend in N₂O concentrations at Walnut Grove closely mirrored the global trend, with summer time N₂O concentrations that were similar to global background concentrations. N₂O production rates change throughout the year based on parameters like soil moisture content, meteorology, and microbial activities, which may be contributing to the variability in N₂O concentrations observed at Walnut Grove. Furthermore, N₂O concentrations at Walnut Grove have been increasing by approximately 1 ppb per year, similar to the global trend.

Why is this indicator important?

Global temperatures are directly linked to GHG levels in the atmosphere (IPCC, 2013). The 2015 Paris Agreement aims to hold the increase in the global average temperature to well below 2°C above pre-industrial levels and to pursue efforts to limit the temperature increase even further to 1.5°C above pre-industrial levels (UNFCCC, 2016). Emissions scenarios leading to CO₂-equivalent concentrations of about 450 ppm or lower in 2100 are likely to maintain warming below 2°C over the 21st century relative to pre-industrial levels (IPCC, 2014). Some climate scientists argue that a reduction from the current level of CO₂ in the atmosphere to 350 ppm CO₂ by 2100 will be essential to avoid dangerous anthropogenic climate change (Hansen et al., 2013). Thus, ambient concentration trends are an important indicator for changes in GHG emissions and their accumulation in the atmosphere. In particular, CO₂, CH₄, N₂O, F-gases, and black carbon (discussed in the *Atmospheric black carbon concentrations* indicator) are considered to be the most important anthropogenic drivers of climate change.

CO₂ is a long-lived GHG responsible for roughly 65 percent of the total warming effect caused by GHGs globally. It contributes to over 84 percent of the current GHG emission inventory in California on a 100-year timescale (CARB, 2016a; WMO, 2016). Since CO₂ is typically well-mixed in the atmosphere, measurements at remote sites can provide integrated global background levels. The first and the longest continuous measurements of global atmospheric CO₂ levels were initiated by Charles D. Keeling in 1958 at Mauna Loa. For the first time, these measurements documented that atmospheric CO₂ levels were increasing globally. In the 1980s and the 1990s, it was recognized that greater coverage of CO₂ measurements was required to provide the basis for estimating the emission impacts of sources and sinks of atmospheric CO₂ over land as well as ocean regions. Since CO₂ remains in the atmosphere for many



centuries, its atmospheric levels can continue to increase even if its emissions are significantly reduced.

Atmospheric CH₄, N₂O, and F-gases contribute roughly 17 percent, 6 percent, and 12 percent respectively of the radiative forcing caused by globally well-mixed GHGs (IPCC, 2013; WMO, 2016). These pollutants could play an even more important role owing to their greater 100-year global warming potentials (100-year GWP) as compared to that of CO₂ (GWP = 1). Some of these GHGs have a much shorter life than that of CO₂. These can cause significant climate impact in the near term, and are considered short-lived climate pollutants (SLCPs). For instance, CH₄ has a 100-year GWP of 28, and remains in the atmosphere for about 12 years before removal, whereas F-gases such as HCFC-22 and HFC-134a have GWPs of over a thousand, and can remain in the atmosphere for one to two decades. On the other hand, N₂O has a GWP of 265 and remains in the atmosphere for roughly 120 years, which can result in long-term climate impacts (IPCC, 2014).

High-precision measurements, such as those presented in this indicator report, are essential to understanding GHG emissions from various sources – including human activities, atmospheric processes, plants, soils, and oceans. Tracking the life cycles of these GHGs provides information necessary for formulating mitigation strategies. Data on atmospheric GHG levels, in particular, are needed to project future climate change associated with various emission scenarios, and to establish and revise emission reduction targets (IPCC, 2013).

In California, regional GHG emission sources contribute to enhancements in the concentrations of CO₂, CH₄, and N₂O above global background levels. In addition to the monitoring and measurement efforts undertaken by various research teams, CARB has also funded several studies to utilize the atmospheric measurements from regional GHG monitoring sites to infer the most likely distribution and strength of regional CO₂, CH₄, and N₂O emission sources in California (Fischer and Jeong, 2016; Zhao et al., 2009).

What factors influence this indicator?

The concentrations of CO₂, CH₄, N₂O, and F-gases in the atmosphere reflect the difference between their rates of emission and their rates of removal. The majority of the changes observed in the global and regional GHG trends are directly related to human activities such as fossil fuel combustion, biomass burning, industrial processes, agricultural practices, and deforestation (IPCC, 2013). Additional discussion of factors affecting the emission of these GHGs in California is presented in the *Greenhouse gas emissions* indicator.

CO₂ is continuously exchanged between the land, the atmosphere, and the ocean through physical, chemical, and biological processes (IPCC, 2013). Prior to 1750, the global background CO₂ concentration was estimated to be less than 280 ppm (WMO, 2016). During this period, the amount of CO₂ released by natural processes (e.g., respiration and decomposition) was almost exactly in balance with the amount absorbed



by plants during photosynthesis and other removal processes (Tans and Keeling, 2012; WMO, 2016). The increase in the CO₂ concentration today derives primarily from emissions related to fossil fuel combustion and biomass burning. It is also directly related to changes in agricultural practices and deforestation (IPCC, 2013). While more than half of emitted CO₂ is removed through natural processes within a century, about 20 percent remains in the atmosphere for many millennia (Archer et al., 2009). Consequently, atmospheric CO₂ will continue to increase in the atmosphere even if annual CO₂ emissions are substantially reduced from present levels. It should be noted that, while increasing levels of atmospheric CO₂ are affecting climate, changes in climate are likewise affecting the processes that lead to CO₂ uptake from, and release into, the atmosphere (IPCC, 2013).

Atmospheric CO₂ concentrations reflect regional, as well as seasonal and inter-annual influences. Due to its higher fossil fuel emissions, the Northern Hemisphere has higher CO₂ concentrations than the Southern Hemisphere. Seasonal variations are attributed to seasonal patterns of plant growth and decay. Inter-annual variations have been attributed to El Niño and La Niña climate conditions; generally, higher-than-average increases in CO₂ correspond to El Niño conditions, and lower-than-average increases correspond to La Niña conditions (IPCC, 2013).

Atmospheric CH₄ originates from both natural and anthropogenic sources. CH₄ is emitted from wetlands, oceans, termites, and geological sources. Anthropogenic sources of methane include rice agriculture, livestock, landfills, waste treatment, biomass burning, and fossil fuel and natural gas exploitation (i.e., extraction, transmission, distribution, and use). The production of CH₄ by many of these sources is influenced by anaerobic fermentation processes and climate variables (notably temperature and moisture). Atmospheric removal of CH₄, on the other hand, is driven by oxidation processes, a process likewise affected by climate variables.

Atmospheric N₂O is naturally present in the atmosphere as part of the Earth's nitrogen cycle. Its primary driver is the breakdown of nitrogen by microorganisms that live in soil and water (Anderson et al., 2010). Human activities such as agriculture, fossil fuel combustion, wastewater management, and industrial processes account for 40 percent of total N₂O emissions globally (US EPA, 2016). In California, N₂O is emitted in large part from agricultural activities such as soil and manure management. In 2014, these contributed to roughly 65 percent of total statewide N₂O emissions (CARB, 2016a). Most of the remaining 35 percent were attributed to the transportation, industrial, commercial, and residential sectors. Commercial and residential application of synthetic fertilizers over soil and lawn, in particular, plays a significant role in the nitrogen cycle; the release of N₂O from such fertilizers has been shown to exhibit seasonal variability based on their rate of application and watering events.

N₂O from fossil fuel combustion can vary significantly based on the technology, maintenance, and operation of combustion equipment (Graham et al., 2009; Huai et al., 2004). N₂O is prevalent in the tail-pipe exhaust of motor vehicles when their engines and catalytic converters are operating at sub-optimal conditions. N₂O is also typically



generated as a by-product of synthetic fertilizer and other synthetic nitrogen production processes. On the other hand, N₂O is removed from the atmosphere through bacterial activities and through photochemical reactions (US EPA, 2016).

F-gases do not exist in the natural environment; they are only emitted from anthropogenic sources and are only removed through photochemical reactions in the upper atmosphere. F-gases have been used primarily as refrigerants in a variety of applications, including stationary refrigeration and air conditioning, industrial production and manufacturing processes, the transmission and distribution of electricity, and vehicle air conditioning systems. CFC-11, CFC-12, HCFC-22, and HFC-134a emissions derive largely from fugitive leaks, venting during the maintenance and servicing of equipment, leaks from improperly maintained or damaged equipment, and the improper disposal of equipment (Gallagher et al., 2014). International, national, and state regulations affect the use, emission, and eventual atmospheric concentrations of these substances. As noted above, pursuant to the Montreal Protocol of 1987, CFCs were phased out and banned in the United States in 1996; HCFCs will be phased out of new production and consumption by January 1, 2020. Driven by the phase-out of these ozone-depleting substances and by increased demand for refrigeration and air conditioning, HFCs became the fastest growing sources of GHG emissions in California and globally. They are now subject to a production and consumption phasedown under the Kigali Amendment (to the Montreal Protocol) starting in 2019 in ratified developed countries. The first group of developing countries ratified in the amendment will begin the phasedown in 2029. The second group of developing countries will have until 2032 to begin a phasedown. It is important to note that the Kigali Amendment has yet to be ratified by the United States. In addition, California's Senate Bill 1383 (Statutes of 2016) requires statewide reduction of HFC emissions to 40 percent below 2013 levels by 2030 (CARB, 2017). California is moving forward in adopting high global warming HFC prohibitions in certain stationary refrigeration and foam end uses that were originally subject to the US EPA Significant New Alternatives Policy program (SNAP) which was recently vacated by a court case. A legislative bill, Senate Bill 1013 (introduced in February 2018) proposes to adopt the federal SNAP program in its entirety and includes a provision for an incentive program to increase the adoption of low global warming refrigerant technologies. In addition to national and international measures, California has identified additional HFC reduction measures that will be needed to meet the SB 1383 target.

Technical Considerations

Data Characteristics

The CO₂ data presented above are a combination of data from the Scripps Institution of Oceanography (SIO), the National Oceanic and Atmospheric Administration's Earth System Research Laboratory (NOAA-ESRL), Lawrence Berkeley National Laboratory (LBNL), and CARB. In particular, NOAA-ESRL leads the Carbon Cycle Cooperative Global Air Sampling Network, an international effort which utilizes regular discrete samples from baseline observatories, cooperative fixed sites, and commercial ships (NOAA, 2016b). Air samples are collected weekly in glass flasks and CO₂ is measured by a non-dispersive infrared absorption technique (Keeling et al., 2001). The



measurements at Mauna Loa were initiated by C. David Keeling of SIO, and date back to March 1958 (Conway et al., 2007). Monitoring at Point Arena started in January 1999, and at Trinidad Head in April 2002. At the SIO La Jolla Pier, roughly one sample is collected each month during the period of record.

CARB initiated continuous GHG measurements at Mt. Wilson in 2010 (with pilot measurements in 2007) in efforts to improve spatial and temporal understanding of emission sources and regional GHG enhancements throughout California. Mt. Wilson is the longest running CARB site that employs real-time high-precision cavity ring-down spectroscopy (CRDS), and collects continuous CO₂ data every second. Mt. Wilson measures well-mixed urban emissions from the Los Angeles air basin at mid-day, when the atmospheric boundary layer height grows due to surface heating. The atmospheric boundary layer is the lowest part of the atmosphere that is most influenced by air pollution emissions from human activities. It also measures the well-mixed background concentration above the boundary layer during nighttime conditions.

Data collection at Walnut Grove tower began in 2007 through collaboration between researchers at LBNL and NOAA, with support from NOAA, the U.S. Department of Energy (DOE), California Energy Commission (CEC), and CARB. The site was equipped with an automated flask sampling system and real-time analyzers. These provide measurements of a suite of GHGs as well as other compounds including the radiocarbon of CO₂. The Walnut Grove site is the first tall tower site in the world with continuous CH₄ measurements (under NOAA-ESRL's Global monitoring Division).

CH₄ data presented in this report were obtained from the NOAA-ESRL, LBNL, and CARB networks. NOAA-ESRL collected ambient air samples in evacuated flasks to detect CH₄ using a flame ionization detector (FID) integrated with a gas chromatograph (GC) system. CARB conducts continuous air measurements of CH₄ using CRDS (as described previously) with the same collection frequency and quality control protocols. CH₄ monitoring at Mauna Loa began in 1983, Point Arena in 1999, Trinidad Head in 2002, and Mt. Wilson in 2010.

N₂O data presented in this report were obtained from the NOAA-ESRL, LBNL, and CARB. NOAA-ESRL collected ambient air samples in evacuated flasks and utilized *in situ* systems to measure N₂O. CARB and LBNL use off-axis integrated cavity output spectroscopy to continuously measure N₂O at Mt. Wilson and Walnut Grove, respectively. Quality control protocols similar to those applied for CH₄ and CO₂ measurements are instituted to obtain high-precision measurements.

F-gas data presented in this report were obtained from the NOAA-ESRL network. NOAA-ESRL utilizes evacuated flasks to collect ambient air at Mauna Loa and analyzes samples using GC systems integrated with an electron-capture detector (ECD) and a mass spectrometer (MS).



Strengths and Limitations of the Data

Measurement data from NOAA-ESRL undergoes critical evaluation for quality control (NOAA, 2016c). The long-term record at La Jolla, particularly when compared with the longer-term data at Mauna Loa, presents valuable time-series information for tracking CO₂ trends over the past half century (SIO, 2012). These data are useful for characterizing seasonal variations and provide information about the coastal air that travels into California. Although the La Jolla Pier at SIO extends considerably into the ocean, the site can receive some air currents polluted with urban CO₂ emissions from the Los Angeles area that mix with the oceanic and San Diego atmosphere. Likewise, the Point Arena monitors, although coastal, occasionally capture on-shore CO₂ emissions. The Trinidad Head monitor sits on a peninsula extending into the ocean with a tower, however, the air coming from the Pacific Ocean can back up on the nearby coastal range mountains and backflow to the site, thus impacting the measurements of CO₂ in the on-shore air.

CARB's Ambient GHG Monitoring Network was established in 2010 to study regional GHG emissions trends throughout California. The data collected from the GHG Monitoring Network is also critical in evaluating regional and statewide inventories in support of California's climate program (CARB, 2016b). These efforts rely heavily on highly accurate and precise measurements of ambient GHGs analyzed using state-of-the-science instruments. The network is comprised of eight monitoring stations located throughout California, and CARB has equipped these stations with highly accurate and precise analyzers used to measure crucial climate influencers such as CO₂, CH₄, N₂O, and black carbon (BC). Data from this network are used in several research studies. They also form the basis of a comprehensive statewide inverse receptor-oriented modeling effort (Fischer and Jeong, 2016), as well as various trend analysis studies used to verify and inform the statewide GHG emission inventory in California.

For more information, contact:



CO₂ data (except La Jolla): Pieter Tans and
Thomas J. Conway
CH₄ data: Edward J. Dlugokencky
Earth System Research Laboratory
National Oceanic and Atmospheric Administration
325 Broadway
Boulder, CO 80305-3328
Pieter.Tans@noaa.gov
Thomas.J.Conway@noaa.gov
Ed.Dlugokencky@noaa.gov



CO₂ data (La Jolla): Ralph Keeling and Stephen Piper
Scripps Institution of Oceanography
SIO CO₂ Program
University of California
La Jolla, CA 92093-0244
rkeeling@ucsd.edu, scpiper@popmail.ucsd.edu





Walnut Grove Data: Marc L. Fischer
Sustainable Energy Systems Group
Energy Technologies Area
E.O. Lawrence Berkeley National Laboratory
MS 90-2014
1 Cyclotron Road
Berkeley, CA 94720
(510) 486-5539
<http://energy.lbl.gov/env/mlf/mlfischer@lbl.gov>



Mt. Wilson Data: Toshihiro Kuwayama
Research Division, California Air Resources Board
1001 I Street
Sacramento, CA 95812
(916) 324-9287
toshihiro.kuwayama@arb.ca.gov

References:

Anderson B, Bartlett KB, Frohking S, Hayhoe K, Jenkins JC and Salas WA (2010). *Methane and Nitrous Oxide Emissions from Natural Sources*. US Environmental Protection Agency. Available at https://scholars.unh.edu/cgi/viewcontent.cgi?article=1483&context=earthsci_facpub

Archer D, Eby M, Brovkin V, Ridgwell A, Cao L, et al. (2009). Atmospheric lifetime of fossil fuel carbon dioxide. *Annual Review of Earth and Planetary Sciences* **37**(1): 117.

CARB (2017). California Air Resources Board. *Potential Impact of the Kigali Amendment on California HFC Emissions Estimates and Methodology used to Model Potential Greenhouse Gas Emissions Reductions in California from the Global Hydrofluorocarbon (HFC) Phase-down Agreement of October 15, 2016, in Kigali, Rwanda ("Kigali Amendment")*. Available at <https://www.arb.ca.gov/cc/shortlived/CARB-Potential-Impact-of-the-Kigali-Amendment-on-HFC-Emissions-Final-Dec-15-2017.pdf>

CARB (2016a). California Air Resources Board. California Greenhouse Gas Emission Inventory. Retrieved June 22, 2016, from <http://www.arb.ca.gov/cc/inventory/data/data.htm>

CARB (2016b). California Air Resources Board. Climate Change Programs. Retrieved January 2, 2016, from <https://www.arb.ca.gov/cc/cc.htm>

Conway T, Lang P and Masarie K (2007). Atmospheric Carbon Dioxide Dry Air Mole Fractions from the NOAA ESRL Carbon Cycle Cooperative Global Air Sampling Network, 1968–2006, version: 2007-09-19. 2007. Retrieved December 20, 2016.

Conway T, Lang P and Masarie K (2011). Atmospheric Carbon Dioxide Dry Air Mole Fractions from the NOAA/ESRL Carbon Cycle Global Cooperative Network, 1968–2010; version 2011-06-21. Retrieved from <ftp://ftp.cmdl.noaa.gov/ccg/co2/flask/event>

Dlugokencky EJ, Lang P, Crotwell A, Masarie K and Crotwell M (2012). Atmospheric Methane Dry Air Mole Fractions from the NOAA ESRL Carbon Cycle Cooperative Global Air Sampling Network, 1983–2011. Retrieved from <ftp://ftp.cmdl.noaa.gov/ccg/ch4/flask/event>

US EPA (2016). Overview of Greenhouse Gases: Nitrous Oxide Emissions. Retrieved August 24, 2016, from <https://www.epa.gov/ghgemissions/overview-greenhouse-gases>



Fischer ML and Jeong S (2016). Atmospheric Measurement and Inverse Modeling to Improve Greenhouse Gas Emission Estimates. Prepared for the California Air Resources Board and the California Environmental Protection Agency. Lawrence Berkeley National Laboratory. Available at <https://www.arb.ca.gov/research/apr/past/11-306.pdf>

Frankenberg C, Meirink JF, van Weele M, Platt U and Wagner T (2005). Assessing methane emissions from global space-borne observations. *Science* **308**(5724): 1010-1014.

Gallagher G, Zhan T, Hsu Y-K, Gupta P, Pederson J, et al. (2014). High-global warming potential F-gas emissions in California: Comparison of ambient-based versus inventory-based emission estimates, and implications of refined estimates. *Environmental Science & Technology* **48**(2): 1084-1093.

Graham LA, Belisle SL and Rieger P (2009). Nitrous oxide emissions from light duty vehicles. *Atmospheric Environment* **43**(12): 2031-2044.

Hansen J, Kharecha P, Sato M, Masson-Delmotte V, Ackerman F, et al. (2013) Assessing "Dangerous Climate Change": Required Reduction of Carbon Emissions to Protect Young People, Future Generations and Nature. *PLOS ONE* **8**(12): e81648.

Huai T, Durbin TD, Miller JW and Norbeck JM (2004). Estimates of the emission rates of nitrous oxide from light-duty vehicles using different chassis dynamometer test cycles. *Atmospheric Environment* **38**(38): 6621-6629.

IPCC (2013). *Climate Change 2013: The Physical Science Basis. Contribution of Working Groups I, II and III to the Fifth Assessment Report of the Intergovernmental Panel on Climate Change*. [Stocker TF, Qin D, Plattner G-K, Tignor M, Allen SK, et al. (Eds.)]. Intergovernmental Panel on Climate Change, Cambridge University Press, Cambridge, United Kingdom and New York, NY, USA, 1. Available at http://ipcc.ch/pdf/assessment-report/ar5/wg1/WG1AR5_Frontmatter_FINAL.pdf

IPCC (2014). *Climate Change 2014: Synthesis Report. Contribution of Working Groups I, II and III to the Fifth Assessment Report of the Intergovernmental Panel on Climate Change*. [Core Writing Team, R.K. Pachauri RK and Meyer LA (Eds.)]. Intergovernmental Panel on Climate Change, Geneva, Switzerland. Available at http://ar5-syr.ipcc.ch/ipcc/ipcc/resources/pdf/IPCC_SynthesisReport.pdf

Keeling CD, Piper SC, Bacastow RB, Wahlen M, Whorf TP, et al. (2001). Exchanges of atmospheric CO₂ and 13CO₂ with the terrestrial biosphere and oceans from 1978 to 2000. *I. Global Aspects*. SIO Reference No. 01-06 (Revised from SIO Reference No. 00-21), June 2001. Available at http://scrippsco2.ucsd.edu/assets/publications/keeling_sio_ref_series_exchanges_of_co2_ref_no_01-06_2001.pdf

NASA-JPL (2017). Megacities Project. Retrieved May 25, 2017, from <https://megacities.jpl.nasa.gov/portal/>

NOAA (2016a). National Oceanic and Atmospheric Administration, Earth System Research Laboratory, Global Monitoring Division. Retrieved December 12, 2016, from <http://www.esrl.noaa.gov/gmd/>

NOAA (2016b). CCGG Cooperative Air Sampling Network. National Oceanic and Atmospheric Administration, Earth System Research Laboratory. Retrieved December 12, 2016, from <http://www.esrl.noaa.gov/gmd/ccgg/flask.html>

NOAA (2016c). Carbon Cycle Trace Gas Measurement Details. National Oceanic and Atmospheric Administration, Earth System Research Laboratory. Retrieved December 12, 2016, from http://www.esrl.noaa.gov/gmd/dv/iadv/help/ccgg_details.html



NOAA (2017). Trends in Atmospheric Carbon Dioxide. Retrieved April 11, 2017, from <https://www.esrl.noaa.gov/gmd/ccgg/trends/gr.html>

SIO (2012). Monthly atmospheric CO₂ concentrations (ppm) derived from flask air samples. La Jolla Pier, California. Scripps Institution of Oceanography. Retrieved December 20, 2016, from <http://scrippsco2.ucsd.edu/data/ljo.html>

Tans P and Keeling R (2012). Trends in Atmospheric Carbon Dioxide - Global. <https://www.esrl.noaa.gov/gmd/ccgg/trends/>

UNEP (2012a). United Nations Environmental Programme. The Montreal Protocol: The Montreal Protocol on Substances that Deplete the Ozone Layer, Article 2A: CFCs. Retrieved August 24, 2016, from <http://ozone.unep.org/en/handbook-montreal-protocol-substances-deplete-ozone-layer/9>

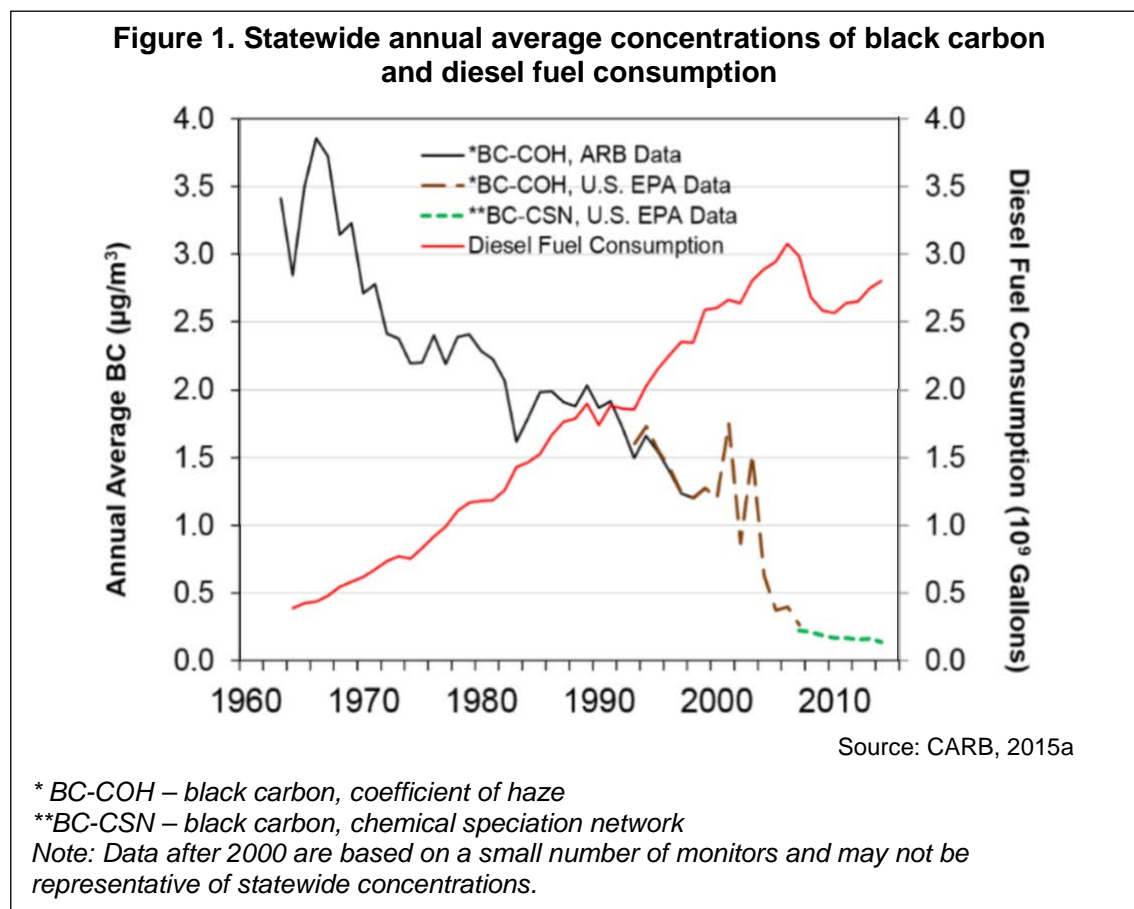
WMO (2016). *WMO Greenhouse Gas Bulletin: The State of Greenhouse Gases in the Atmosphere Using Global Observations through 2015*. Available at https://ane4bf-datap1.s3-eu-west-1.amazonaws.com/wmocms/s3fs-public/GHG_Bulletin_12_EN_web_JN161640.pdf?aZaKZhdpDfJdmHvtbSvLwbj6zb_PWwdz

Zhao C, Andrews AE, Bianco L, Eluszkiewicz J, Hirsch A, et al. (2009). Atmospheric inverse estimates of methane emissions from Central California. *Journal of Geophysical Research: Atmospheres* **114**(D16).



ATMOSPHERIC BLACK CARBON CONCENTRATIONS

Atmospheric levels of black carbon, a major short-lived climate pollutant, have decreased dramatically in California since the 1960s.



What does the indicator show?

Long-term data show that ambient black carbon (BC) concentrations in California have declined steadily (Figure 1). Annual average BC concentrations have dropped by more than 90 percent over the past 50 years, from an average of 3.4 micrograms per cubic meter ($\mu\text{g}/\text{m}^3$) in the 1960s to $0.14 \mu\text{g}/\text{m}^3$ since 2010. This dramatic decline in BC concentrations in the last five decades occurred despite a seven-fold increase in statewide diesel fuel consumption — the largest anthropogenic source of BC emissions in California. New emission standards and restrictions on diesel engines and biomass burning have significantly reduced atmospheric BC concentrations across the state (Kirchstetter et al., 2017).

Archived records of coefficient of haze (COH) were used to reconstruct historical BC concentrations. COH was one of the first measures of particulate matter (PM) pollution used by regulatory agencies and was determined to be a strong proxy for BC. (Please see *Technical Considerations* for a discussion of the data presented).



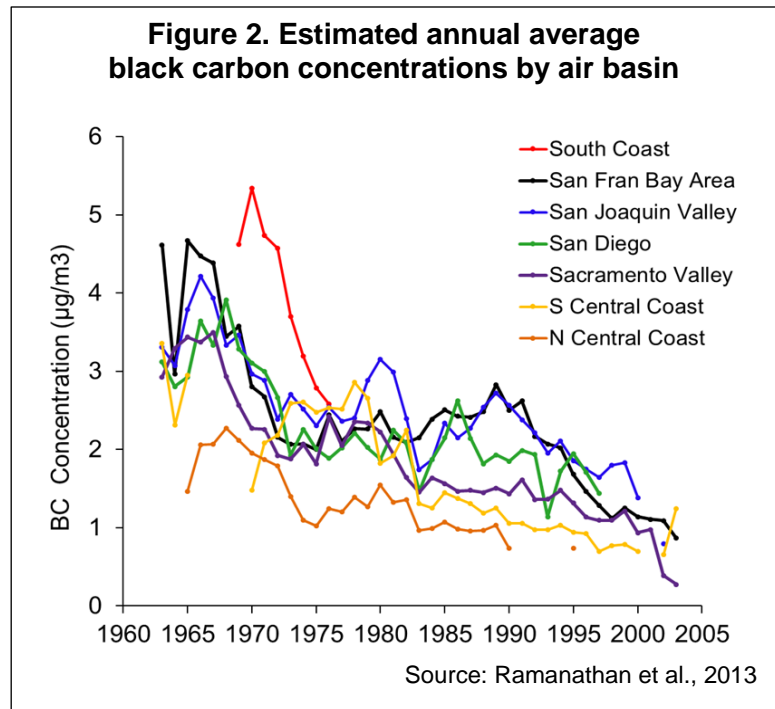
Although there is considerable variation, BC concentrations by air basin generally followed the decreasing statewide average trend. As shown in Figure 2, downward trends occur across all of the State's major air basins from the mid-1960s to the early 2000s. BC concentrations were considerably higher in the South Coast Air Basin than in the rest of California, at least until the mid-1970s; the lowest BC concentrations were in the North Central Coast Air Basin.

Why is this indicator important?

Black carbon is a light-absorbing particle in the air, commonly known as soot. Scientists recently determined that BC may be the second most important contributor to global warming after carbon dioxide (CO₂) (Bond et al., 2013). However, it behaves very differently than long-lived greenhouse gases such as CO₂ do. While greenhouse gases trap heat from the Earth's surface, BC contributes to climate warming by absorbing sunlight directly and releasing heat energy in the atmosphere. CO₂ remains in the atmosphere for hundreds of years, while BC particles are removed from the atmosphere by rain and by deposition after a few days or weeks. However, although BC has a shorter lifespan, it is a much more powerful warming agent than CO₂. For example, one ton of BC has a warming effect equal to 900 tons of CO₂ over a 100-year period. Over 20 years, one ton of BC has the warming impact of 3,200 tons of CO₂ (Bond et al., 2013). Hence, it is considered a critical short-lived climate pollutant.

Black carbon influences the climate in several complex ways. In addition to its direct warming effects, BC particles can deposit on snow, glaciers, and sea ice. This darkens these light, frozen surfaces and reduces their reflectivity. Darker surfaces absorb more solar energy, causing snow and ice to melt more quickly (Hadley et al., 2010; Hadley and Kirchstetter, 2012). This early melting could significantly affect California's summer water supplies, which rely heavily on snowmelt runoff from the Sierra Nevada. Less snowmelt runoff during the spring months, combined with warmer temperatures over already dry areas, increases wildfire risks — which can in turn release more BC particles.

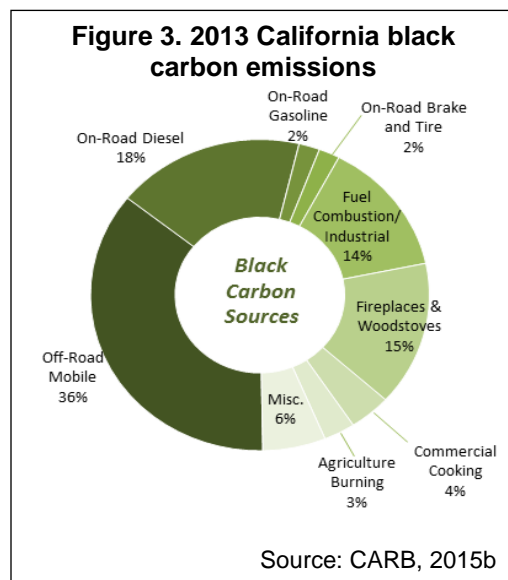
Black carbon can also change the reflectivity, stability, and duration of clouds. Its effects are different depending on how much of it is in the air and where it occurs in the atmosphere. Black carbon particles in a cloud layer can absorb solar radiation, heating the air in it, and leading to cloud evaporation and reduction. However, quantification of this indirect impact on the climate system is imprecise (Koch and Del Genio, 2010).



Reducing emissions of BC presents an opportunity to slow the rate of global warming in the near term. Black carbon is also a component of PM_{2.5} air pollution (fine particulate matter that is 2.5 microns or less in diameter). PM_{2.5} has been linked to respiratory and cardiovascular disease (US EPA, 2009). Hence, reduced BC emissions also provide public health benefits. Control measures are projected to lead to substantial reductions in BC emissions from mobile sources, preventing an estimated 5,000 premature deaths in the State each year (CARB, 2016). These reductions are especially beneficial to disadvantaged communities. For example, diesel particulate matter concentrations are highest along freight corridors and near ports and rail yards where disadvantaged communities are often located. Regardless of net climate forcing or other climatic effects, all BC mitigation options bring health benefits through reduced particulate matter exposure. A worldwide program along the lines of what is being done in California would avoid hundreds of thousands of premature deaths annually (Anenberg et al., 2011).

What factors influence this indicator?

In California, the major anthropogenic sources of BC in 2013 include a diesel-fueled mobile sources, fuel combustion and industrial processes, and residential fireplaces and woodstoves. Off-road mobile emissions account for over a third of statewide BC emissions. On-road mobile sources account for nearly a quarter of emissions, primarily from on-road diesel combustion, which contributes approximately 18 percent to California’s BC emissions. On-road gasoline, as well as brake wear and tire wear emissions of BC are relatively small. Residential fireplaces and woodstoves currently account for approximately 15 percent of BC emissions, with another 14 percent attributable to fuel combustion and industrial processes.



Other anthropogenic sources include dust, waste disposal, residential natural gas combustion, and unplanned structure and car fires. These sources and the ambient concentrations of BC vary geographically and temporally. Emissions standards and restrictions implemented on diesel engines and biomass burning activities have had a significant effect on decreasing ambient air BC concentrations across the State. In 2013, total anthropogenic BC emissions were about 38 million metric tons of carbon dioxide equivalent (MMTCO_{2e}), using the 20-year Global Warming Potential (GWP) value of 3,200 from the IPCC Fifth Assessment Report (IPCC, 2013).

Anthropogenic BC emissions do not include forest-related sources (i.e., wildfires and prescribed burning). Wildfire is the largest source of BC emissions in California, contributing an estimated 87 MMTCO_{2e} annually (calculated as a ten-year annual



average); prescribed fires, an important tool for forest managers, emit an estimated 4 MMTCO_{2e}. (To provide a more representative view of emissions without large year-to-year variability driven by natural forces, forestry emissions are calculated as a ten-year average) (CARB, 2017).

As shown in Figure 1, the largest decline in BC concentrations occurred in the years before 1975, coinciding with the adoption of state and federal air quality regulations. These include tailpipe emission limits established by California in the mid-1960s, federal emission standards for stationary sources and motor vehicles adopted in the mid-1960s, and diesel emission controls introduced nationally in 1970. Between 1975 and 1990, BC levels declined more gradually, likely due to the replacement of older, more polluting diesel vehicles as a result of on-road heavy-duty diesel particulate matter emission standards adopted in 1973 by California. BC concentrations decreased more rapidly after 1990, despite intermittent increases in the early 2000s (Kirchstetter et al., 2008). Retrofitting of urban transit buses with oxidation catalysts, limits on sulfur content in diesel fuel, changes in diesel engine technology, and restrictions on agricultural burning and residential wood combustion, among other measures, contributed to the reductions.

Existing regulatory programs, including ongoing efforts to reduce tailpipe emissions from trucks and buses, will continue to reduce BC emissions. For example, further reductions are expected from stricter diesel engine emission standards implemented by the state in 2007 and the complementary low-sulfur fuel introduced nationally in 2006. To comply with federal air quality standards, control measures that reduce PM_{2.5} pollution (including BC and other constituents) are projected to decrease BC emissions from mobile sources in California by 75 percent between 2000 and 2020 (CARB, 2016). Senate Bill 1383 (Chapter 395, Statutes of 2016) sets a target to reduce BC emissions by 50 percent below 2013 levels by 2030, with a focus on disadvantaged communities.

Technical Considerations

Data Characteristics

Because of their short residence time in the atmosphere and their strong dependence on local sources, particles exhibit high spatial and temporal variation, requiring frequent measurements at numerous sites to reliably track trends. However, few extensive records of particle concentrations are available. One of the first measures of PM pollution used by regulatory agencies, the coefficient of haze (COH), was determined to be a strong proxy for BC, based on co-located field measurements of BC and COH. Archived records of COH, a now-retired measure of light-absorbing PM, were used to reconstruct historical BC concentrations. BC concentrations were inferred from COH data based on a relationship determined from statistical analyses (see Chapter 2.0 of Ramanathan et al., 2013). Statewide average BC concentrations were computed separately using data from CARB (1963 to 2000), and US EPA (1993 to 2007).

Where the US EPA and CARB datasets overlap, agreement is very good. The location and number of COH monitors operating in California has varied over time. From the mid-1970s to 2000, 30 or more COH monitors were in operation for the majority of the year, but these dropped to 15 by mid-2000 (mainly in the US EPA dataset). Hence, the



data after 2000 are based on a smaller number of monitors, and may not be as representative of statewide concentrations.

Data from 2007 to 2017 are from the US EPA's Chemical Speciation Network (CSN). Since early 2000, about 17 CSN sites have been providing information on PM_{2.5} concentrations in California's ambient air. Samplers operate on a 24-hour schedule from midnight to midnight, generally sampling every third day or every sixth day. CSN must meet all federal and state requirements for monitoring methodology and quality assurance. CSN is designed to track the progress of PM_{2.5} emission reduction strategies through the characterization of trends of individual PM_{2.5} species, including BC. Although the CSN network has been collecting BC data since 2000, the collection and analysis methods were different during the first few years of the program (Chow et al., 2007). The differences were significant enough to affect the trends, therefore data from the CSN network prior to 2007 are not presented in Figure 1.

Strengths and Limitations of the Data

For the purposes of climate change study, BC is defined as the carbon component of PM that absorbs light. A significant advantage of monitoring BC by an optical method is that it delivers results in real time with a high time resolution (in minutes). However, BC as a component of PM is difficult to measure. Methods that measure light absorption in PM assume that BC is the only light-absorbing component present. However, some components of organic carbon can also be light-absorbing. The impact of BC on climate forcing is well established, but the magnitude and wavelength dependence of absorption by organic carbon (often called brown carbon, a by-product of the biomass burning) is poorly constrained. Existing methods, such as using an enhanced thermal/optical carbon analyzer with multi-wavelength capabilities, can add value to current PM monitoring programs by providing a complete identification and quantitation of the carbonaceous component of ambient aerosols in near-real time.

Emissions inventories for climate change studies have focused primarily on greenhouse gases. Most of the important sources of greenhouse gases are also important sources of health-related pollutants. Likewise, BC is emitted primarily from combustion sources which are also important sources of health-related pollutants. California's BC inventory relies on PM inventories coupled with speciation profiles that define the fraction of PM that is BC. However, it is a challenge to estimate statewide BC emissions, and to define speciation profiles for all sources. Hence, improved emissions inventory methodologies and tools developed for health-related pollutants can also provide opportunities for improving climate change emission inventories (and vice versa).



For more information, contact:



Ambient Concentrations: Nehzat Motallebi, Ph.D.
California Air Resources Board
P.O. Box 2815
Sacramento, California 95812
(916) 324-1744
nehzat.motallebi@arb.ca.gov



Emission Inventory: Anny Huang, Ph.D.
California Air Resources Board
P.O. Box 2815
Sacramento, California 95812
(916) 323-8475
anny.huang@arb.ca.gov

References:

Anenberg SC, Talgo K, Arunachalam S, Dolwick P, Jang C and West JJ (2011). Impacts of global, regional, and sectoral black carbon emission reductions on surface air quality and human mortality. *Atmospheric Chemistry and Physics* **11**: 7253-7267.

Bond TC, Doherty SJ, Fahey DW, Forster PM, Bernsten T, et al. (2013). Bounding the role of black carbon in the climate system: A scientific assessment. *Journal of Geophysical Research: Atmospheres* **118**(11): 5380-5552.

CARB (2015a). California Air Resources Board. *California Air Quality Data Products*. Retrieved November 2015, from <https://www.arb.ca.gov/html/ds.htm>

CARB (2015b). California Air Resources Board. *Short-Lived Climate Pollutant Inventory*. Retrieved November 2015, from <https://www.arb.ca.gov/cc/inventory/slcp/slcp.htm>

CARB (2016). California Air Resources Board. *Revised Proposed Short-Lived Climate Pollutant Reduction Strategy*. Available at <https://www.arb.ca.gov/cc/shortlived/meetings/11282016/revisedproposedslcp.pdf>

CARB (2017). California Air Resources Board. *Short-lived Climate Pollutant Reduction Strategy. Appendix C*. Available at <https://www.arb.ca.gov/cc/shortlived/meetings/11282016/appendixc.pdf>

Chow JC, Watson JG, Chen LWA, Chang MCO, Robinson NF, et al. (2007). The IMPROVE-A Temperature Protocol for Thermal/Optical Carbon Analysis: Maintaining Consistency with a Long-Term Database. *Journal of the Air and Waste Management Association* **57**: 1014–1023.

Hadley OL, Corrigan CE, Kirchstetter TW, Cliff SS and Ramanathan V (2010). Measured black carbon deposition on the Sierra Nevada snow pack and implication for snow pack retreat. *Atmospheric Chemistry and Physics* **10**: 7505-7513.

Hadley OL and Kirchstetter TW (2012). Black-carbon reduction of snow albedo. *Nature Climate Change* **2**: 437-440.



IPCC (2013). *Climate Change 2013: The Physical Science Basis. Contribution of Working Group I to the Fifth Assessment Report of the Intergovernmental Panel on Climate Change*. Cambridge, United Kingdom and New York, NY, USA: Cambridge University Press. Available at <http://www.ipcc.ch/report/ar5/wg1/>

Kirchstetter TW, Aguiar J, Tonse S, Novakov T and Fairley D (2008). Black carbon concentrations and diesel vehicle emission factors derived from coefficient of haze measurements in California: 1967-2003. *Atmospheric Environment* **42**: 480-491.

Kirchstetter TW, Preble CV, Hadley OL, Bond TC and Apte JS (2017). Large reductions in urban black carbon concentrations in the United States between 1965 and 2000. *Atmospheric Environment* **151**: 17-23.

Koch D, and Del Genio AD (2010). Black carbon absorption effects on cloud cover: Review and synthesis. *Atmospheric Chemistry and Physics* **10**: 7685-7696.

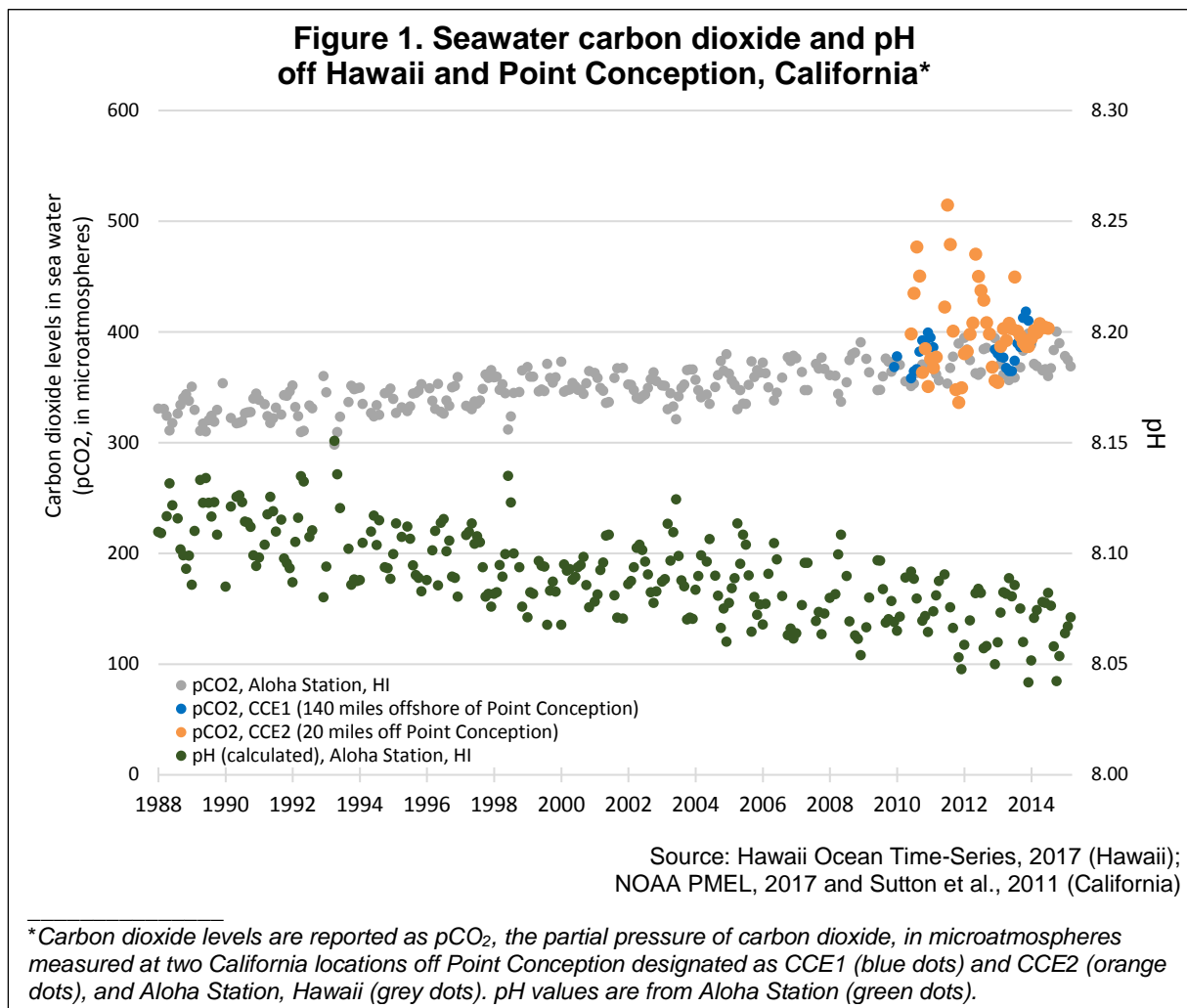
Ramanathan V, Bahadur R, Kirchstetter TW, Prather KA, et al. (2013). Black Carbon and the Regional Climate of California: Report to the Air Resources Board, Contract 08-323. Available at <http://www.arb.ca.gov/research/apr/past/08-323.pdf>

US EPA (2009). *Integrated Science Assessment (ISA) for Particulate Matter (Final Report, Dec 2009)* (EPA/600/R-08/139F, 2009). US Environmental Protection Agency. Washington, DC. Available at http://ofmpub.epa.gov/eims/eimscomm.getfile?p_download_id=494959



ACIDIFICATION OF COASTAL WATERS

As atmospheric concentrations of carbon dioxide increase, so do levels in the ocean, part of a process known as “ocean acidification.” While long-term data for California waters are limited, the values measured at the offshore location near Point Conception are similar to those from monitoring off Hawaii at the same time points. An increase in seawater carbon dioxide levels accompanied by declining pH (a measure of acidity) have been observed at the Hawaii station.



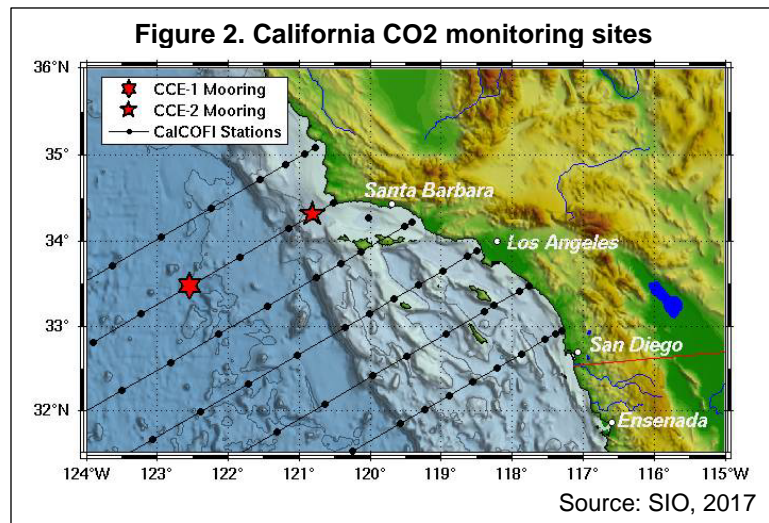
What is the indicator showing?

Figure 1 shows that levels of carbon dioxide (CO₂) in seawater measured relatively recently at an offshore location (CCE1) off Point Conception, California near Santa Barbara are similar to those measured at the same time points at Aloha Station off Hawaii; levels at CCE2, a station closer to the California coast, show greater variability. Measurements at CCE1, which began in September 2010, provide the longest-running publicly available data on CO₂ levels in seawater in California. Levels of CO₂ are expressed as the partial pressure of carbon dioxide, or pCO₂ (which refers to the pressure that CO₂ contributes to the total pressure of the mixture of gases present in seawater).



At Aloha Station pCO₂ levels have increased steadily at the rate of 1.92 microatmospheres per year (µatm/year), and the pH (a measure of acidity) has decreased at the rate of 0.002 unit per year from 1988 to 2015. At seven long-term monitoring sites around the globe, measurements of pCO₂ and pH show similar changes over the last three decades: pCO₂ has increased by 1.29 to 2.95 µatm/year, and pH has decreased by 0.0013 to 0.0025 unit/year (Bates et al., 2014). Monitoring at the Aloha Station off Hawaii provides the longest-running measurements of ocean acidity in the North Pacific Ocean.

In California, ongoing, continuous monitoring of CO₂ and pH is limited to a few sites (see *Technical Considerations*). Figure 1 presents pCO₂ data from two active monitoring sites off Point Conception (Figure 2): “CCE1,” about 140 miles offshore, and “CCE2,” positioned on the shelf break on the coast about 20 miles off Point Conception (blue and orange dots, respectively). The greater variability in the CO₂ levels in CCE2 (orange dots) is due to its location closer to shore, where levels are influenced by seasonal changes in upwelling (see discussion in *What factors influence this indicator?*). Given the duration of the period covered by the data set, and the gaps in the data, there are insufficient data at these locations with which to derive trends.



Why is this indicator important?

CO₂ is considered to be the largest and most important anthropogenic driver of climate change. It is continuously exchanged between land, the atmosphere, and the ocean through physical, chemical, and biological processes. The ocean absorbs approximately 30 percent of the CO₂ released into the atmosphere by human activities every year (Sabine et al., 2004); this process has significantly reduced the CO₂ concentrations in the atmosphere and minimized some of the impacts of global warming (Rhein et al., 2013). Consequently, as atmospheric CO₂ concentrations continue to increase, so do CO₂ values in the ocean, changing the carbonate chemistry of seawater — a process termed “ocean acidification” (Caldeira and Wickett, 2003; Doney et al., 2009). The mean pH of surface waters in the open ocean currently ranges between 7.8 and 8.4, which means that the ocean is mildly basic (pH > 7). The net result of adding CO₂ to seawater is an increase in hydrogen ions (H⁺) — which increases seawater acidity and lowers seawater pH — along with decreasing carbonate ion, a fundamental ‘building block’ for organisms forming shells of calcium carbonate.

Many economically and ecologically important West Coast species have been documented to show direct responses to acidification; bivalves, for example, are



economically valuable, while also serving an ecological role in providing ecosystem services such as water filtration and habitat for other species. While field observations of impacts on marine organisms are limited (see *Effects of ocean acidification on marine organisms* indicator), laboratory experiments on bivalves have documented mechanisms by which negative effects arise (Miller et al., 2009; Gaylord et al., 2011; Hettinger et al., 2012 and 2013; Barton et al., 2012; Waldbusser et al., 2013) as well as repercussions for species interactions (Sanford et al., 2014). Ocean acidification is also likely to exacerbate the impact of other stressors — including overfishing, input of chemical contaminants, exotic and invasive species, temperature change, and deoxygenation — on coastal ecosystems.

What factors influence the indicator?

The air-sea exchange of carbon dioxide is determined largely by the difference in the partial pressure of CO₂ between the atmosphere and the ocean; as more atmospheric CO₂ is produced, the ocean absorbs some of it to reach equilibrium. Long-term measurements of ocean carbon content at seven monitoring sites around the globe (including the Hawaii Ocean Time Series presented in Figure 1) collectively show consistent and coherent changes in the uptake of CO₂ by the ocean; at decadal time scales, the rate of ocean acidification in these open ocean surface waters generally approximates the rate of CO₂ increase in the atmosphere (Bates et al., 2014).

The air-sea CO₂ interchange is governed by both chemical and biologically-mediated reactions (photosynthesis, respiration, and precipitation and dissolution of calcium carbonate). Photosynthesis and respiration remove and add CO₂ to seawater, respectively. Precipitation of calcium carbonate by marine organism calcifiers also affects the carbonate chemistry of surrounding seawater. These biological processes play an especially key role in determining shorter-term variability in pH and CO₂ in seawater, whereas air-sea exchange processes dominate the longer-term interannual-to-decadal trends.

Along the West Coast, ocean acidification adds to the already naturally high values of carbon dioxide in “upwelled” waters. Upwelling is the wind-driven movement of deep, cool, carbon- and nutrient-rich ocean water to the surface, replacing the warmer, usually nutrient-depleted surface water (see *Coastal ocean temperature* indicator).

In addition to seasonal patterns in ocean chemistry tied to upwelling processes, changes associated with large-scale climate oscillations such as El Niño and the Pacific Decadal Oscillation can alter the oceanic CO₂ sink/source conditions. This can occur through seawater temperature changes as well as through ecosystem variations that occur via complex physical-biological interactions (Chavez et al., 2007). For example, during El Niño, upwelling of high CO₂ waters is dramatically reduced along central California so that flux out of the ocean is reduced; at the same time, ocean uptake of CO₂ is also reduced because of lower photosynthetic activity, as nutrients that would have been carried to the surface by upwelled waters are less available. Modeled estimates of pH and *aragonite saturation state* (another measure used to monitor ocean acidity) along the southern California coast from 1985 to 2014 suggest a persistent shift



in ocean acidification-related seawater conditions from the decade prior to the strong 1997–1998 El Niño event to the decade after it (McClatchie et al., 2016). Summertime warming has been shown to increase surface $p\text{CO}_2$ at certain locations, including Station Aloha, so that these waters seasonally transition to being net sources of CO_2 to the atmosphere (Bates et al., 2014). In the southern California Current System, subdecadal (2005–2011) estimates for pH and related parameters reveal a pronounced seasonal cycle and inter-annual variability in the upper water column (Alin et al., 2012).

The variability in the data of $p\text{CO}_2$ levels in Figure 1 (CCE2 location) compared to open ocean waters (CCE1 location) reflects the more complex acid-base chemistry dynamic of coastal waters (NAS, 2010). In addition to climate processes, coastal waters can be affected by localized freshwater and atmospheric inputs, organic matter and nutrients from land, and processes in the underlying sediments. The seasonal, monthly and daily variability that can occur from biological and oceanographic processes has been observed at other monitoring stations along the California coast (e.g., M1 mooring in Monterey, Hog Island Oyster Company store station, Carlsbad Aquafarm shore station) (CenCOOS (Monterey), 2018; IPACOA (shore stations), 2018; see references for URLs to access data from these stations). Knowledge of short-term variability of CO_2 in seawater is important to interpret any changes attributed to anthropogenic processes at a given location.

Technical Considerations

Data Characteristics

Monitoring along the California coast includes moorings with carbon dioxide and pH sensors, regular measurements of inorganic carbon species on oceanographic cruises, calculation of aragonite saturation state, and shore-based observations of carbon chemistry in nearshore waters. These monitoring efforts are included in large-scale monitoring programs, for example within the US Integrated Ocean Observing System (IOOS) and the National Oceanic and Atmospheric Administration (NOAA) ocean acidification observing network, all carried out in collaboration with a wide range of national, regional, and international partners. Many of these efforts can be viewed in real time through an online data portal (IPACOA, 2018).

The CCE1 mooring (205 km southwest of Point Conception) was deployed in November 2008 as part of a multi-investigator, multi-disciplinary project by NOAA's Pacific Marine Environmental Laboratory. The project expanded to include the CCE2 mooring, at the shelf break offshore Point Conception, in 2010. Sensors on these moorings measure aspects of biological, chemical, and physical oceanography as well as meteorology; data are collected every 3 hours. This project is closely coordinated with other projects off of Southern California such as the California Cooperative Oceanic Fisheries Investigations (<http://www.calcofi.org/>), the California Current Ecosystem Long Term Ecological Research (<http://cce.lternet.edu/>), and the Consortium on the Oceans Role in Climate (<http://mooring.ucsd.edu/index.html?projects/corc>).

Figure 1 features data from the Hawaii Ocean Time-series (HOT) program for comparison. This program has been making repeated observations of the chemistry,

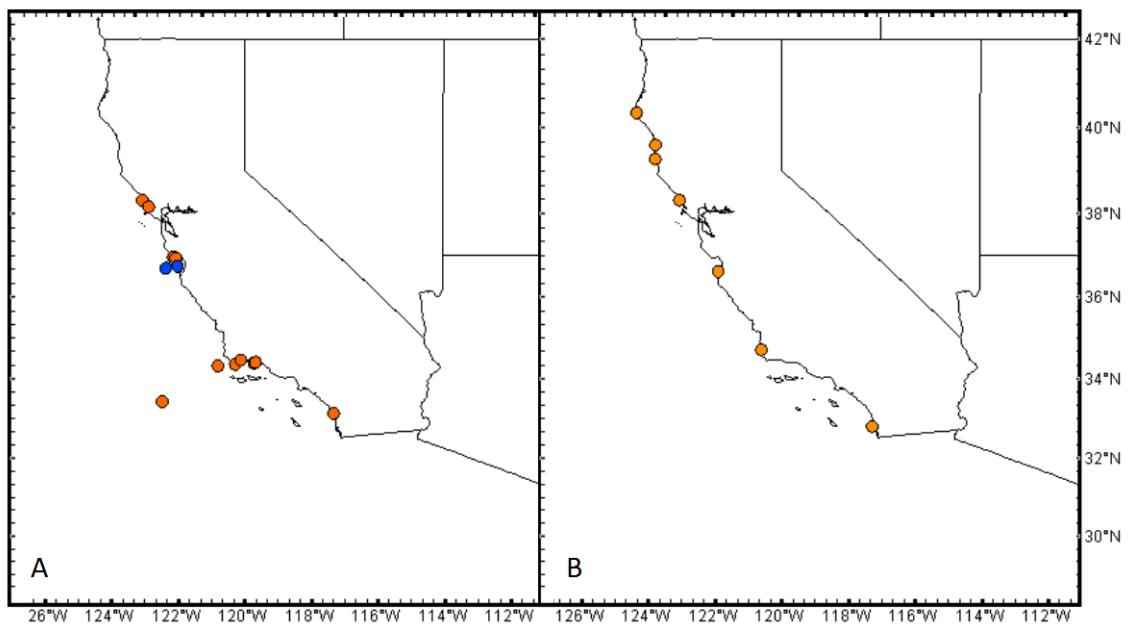


and biology of the water column at a station north of Oahu, Hawaii since October 1988. Cruises are made approximately once per month to the deep-water Station ALOHA located 100 kilometers north of Oahu, Hawaii. Calculated values of pH and pCO₂ are obtained from measured parameters; direct measurements of pH are also made at sea.

Despite the central importance of data for detecting long-term changes in the ocean's carbon system, coordinated observing networks in the US coastal and estuarine waters did not exist until recently. Historically, assessments of changes to the carbonate system relied on a handful of data records worldwide (none of which operated in California waters, and the longest of which began only in the early 1980's) (Bates et al., 2014).

To date, indicators of acidification (pH, pCO₂, and/or aragonite saturation state: a calculation of the stability of shell material) have been monitored at 36 sites (moorings, instrument deployments, or regular bottle sampling) along the California coast (Figure 3) — a small number compared to 300 sites for ocean temperature. In the figure, only publicly available datasets from stationary instruments are presented. The panel on the left shows the datasets that are ongoing (N=13); the panel on the right indicates the datasets that may have been terminated or may not be ongoing. There are no datasets longer than 50 years. There are an additional twelve datasets in California collected on oceanographic vessels that are not displayed here.

Figure 3. Stationary monitoring sites for CO₂-relevant parameters off California



Panel (A) shows carbonate chemistry datasets that are ongoing. Panel (B) shows carbonate chemistry datasets that have been terminated or may not be ongoing.

The colors of the dots refer to dataset length: Blue: 10+years; Orange: 0-9 years

Source: UC Davis Bodega Marine Laboratory, 2016



Strengths and Limitations of the Data

Given that pH and/or pCO₂ of seawater are variable in many of California's marine ecosystems, datasets of these carbonate chemistry parameters will need to be at least a decade or more in length before trends can be detected beyond natural variability (Henson et al., 2016). Hence, a limitation of the ability to detect long-term trends in carbonate chemistry off California's coast is that many of the monitoring sites have not been continuously operated, due to funding limitations, and many focused on ocean acidification were more recently initiated. A surface seawater pH sensor was only recently (September 2012) added to the CCE1 mooring. Measurements of pH in addition to pCO₂, will allow a more accurate and precise evaluation of the changes associated with ocean acidification. Future expansion and extension of the current monitoring network for ocean acidification was a major recommendation of the West Coast Ocean Acidification and Hypoxia Panel (Chan et al., 2016). Ideally this will take shape via a robust, integrated monitoring system for ocean acidification and hypoxia that is integrated with biological monitoring.

For more information, contact:



Tessa M. Hill, Ph.D.
University of California, Davis
Bodega Marine Laboratory
P. O. Box 247
Bodega Bay, CA 94923
(707) 875-1910
tmhill@ucdavis.edu

Emily Rivest, Ph.D.
Virginia Institute of Marine Science
Department of Biological Sciences
College of William & Mary
PO Box 1346
Gloucester Point, VA 23062
804-684-7942
ebrivest@vims.edu

2013 Report contributed by S. Alin and F. Chavez

This report update provided by UC Davis team: Rivest, Hill, Gaylord, Sanford, Myhre, Largier

References:

Alin SR, Feely RA, Dickson AG, Hernández-Ayón JM, Juranek LW, et al. (2012). Robust empirical relationships for estimating the carbonate system in the southern California Current System and application to CalCOFI hydrographical cruise data (2005–2011). *Journal of Geophysical Research* **117**: C05033.

Barton A, Hales B, Waldbusser GG, Langdon C and Feely RA (2012). The Pacific oyster, *Crassostrea gigas*, shows negative correlation to naturally elevated carbon dioxide levels: Implications for near term ocean acidification effects. *Limnology & Oceanography* **57**(3): 698-710.



Bates NR, Best MHP, Neely K, Garley R, Dickson AG, and Johnson RJ (2012). Detecting anthropogenic carbon dioxide uptake and ocean acidification in the North Atlantic Ocean. *Biogeosciences* **9**: 2509-2522.

Bates N, Astor Y, Church M, Currie K, Dore J, et al. (2014). A time-series view of changing ocean chemistry due to ocean uptake of anthropogenic CO₂ and ocean acidification. *Oceanography* **27**: 126-141.

Caldeira K and Wickett ME (2003). Oceanography: anthropogenic carbon and ocean pH. *Nature* **425**: 365.

CenCOOS (2018). Data for Monterey M1 mooring provided by Monterey Bay Aquarium Research Institute. Available at <http://www.cencoos.org/data/buoys/mbari/m1ph>

Chan F, Boehm AB, Barth JA, Chornesky EA, Dickson AG, et al. (2016) *The West Coast Ocean Acidification and Hypoxia Science Panel: Major Findings, Recommendations, and Actions*. California Ocean Science Trust. Oakland, CA. Available at <http://westcoastoah.org/wp-content/uploads/2016/04/OAH-Panel-Key-Findings-Recommendations-and-Actions-4.4.16-FINAL.pdf>

Chavez FP, Takahashi T, Cai WJ, Friederich G, Hales B, et al. (2007). *Chapter 15: Coastal Oceans*. In: The First State of the Carbon Cycle Report (SOCCR): The North American Carbon Budget and Implications for the Global Carbon Cycle. Synthesis and Assessment Product 2.2, Report by the U.S. Climate Change Science Program and the Subcommittee on Global Change Climate Change. King AK (lead editor) and Dilling L (co-lead). Available at <http://cdiac.ess-dive.lbl.gov/SOCCR/pdf/sap2-2-final-all.pdf>

Doney SC, Fabry VJ, Feely RA and Kleypas JA (2009). Ocean acidification: The other CO₂ problem. *Annual Review of Marine Science* **1**: 169-192.

Dore JE, Lukas R, Sadler DW, Church MJ and Karl DM (2009). Physical and biogeochemical modulation of ocean acidification in the central North Pacific. *Proceedings of the National Academy of Sciences* **106**: 12235-12240.

Fabry VJ, Seibel BA, Feely RA and Orr JC (2008). Impacts of ocean acidification on marine fauna and ecosystem processes. *ICES Journal of Marine Science* **65**: 414-432.

Feely RA, Alin SR, Newton J, Sabine CL, Warner M, et al. (2010). The combined effects of ocean acidification, mixing, and respiration on pH and carbonate saturation in an urbanized estuary. *Estuarine, Coastal and Shelf Science* **88**: 442-449.

Gaylord B, Hill TM, Sanford E, Lenz EA, Jacobs LA, Sato KN, et al. (2011). Functional impacts of ocean acidification in an ecologically critical foundation species. *Journal of Experimental Biology* **214**: 2586-2594.

Gaylord B, Kroeker KJ, Sunday JM, Anderson KM, Barry JP, et al. (2015). Ocean acidification through the lens of ecological theory. *Ecology* **96**: 3-15.

Hawaii Ocean Time-Series (2017). *Hawaii Ocean Time-series surface CO₂ system data product*. [As adapted from: Dore JE, Lukas R, Sadler DW, M.J. Church MJ, and D.M. Karl DM (. 2009). Physical and biogeochemical modulation of ocean acidification in the central North Pacific. *Proceedings of the National Academy of Sciences USA* **106**:12235-12240] Retrieved December 22, 2017, from http://hahana.soest.hawaii.edu/hot/products/HOT_surface_CO2.txt

Hettinger A, Sanford E, Hill TM, Russell AD, Sato KNS, et al. (2012). Persistent carry-over effects of planktonic exposure to ocean acidification in the Olympia oyster. *Ecology* **93**: 2758-2768.



Hettinger A, Sanford E, Hill TM, Lenz EA, Russell AD and Gaylord B (2013). Larval carry-over effects from ocean acidification persist in the natural environment. *Global Change Biology* **19**: 3317-3326.

IPACOA (2018). IOOS Pacific Region Ocean Acidification Data Portal. Available at <http://www.ipacoa.org>. See “Data Explorer” for an interactive map to access data for Hog Island Oyster Company store station and Carlsbad Aquafarm shore station.

Kroeker KJ, Kordas RL, Crim R, Hendriks IE, Ramajo L, et al. (2013). Impacts of ocean acidification on marine organisms: quantifying sensitivities and interaction with warming. *Global Change Biology* **19**:1884-1896.

McClatchie S, Thompson AR, Alin SR, Siedlecki S, Watson W and Bograd SJ (2016). The influence of Pacific Equatorial Water on fish diversity in the southern California Current System. *Journal of Geophysical Research Oceans* **121**: 6121–6136

Miller AW, Reynolds AC, Sobrino C and Riedel GF (2009). Shellfish face uncertain future in high CO₂ world: Influence of acidification on oyster larvae calcification and growth in estuaries. *PLoS One* **4**(5): e5661

NAS (2010). *Ocean Acidification: A National Strategy to Meet the Challenges of a Changing Ocean. Committee on the Development of an Integrated Science Strategy for Ocean Acidification Monitoring, Research, and Impacts Assessment; National Research Council*. Washington DC: National Academies Press.

NOAA PMEL (2017). CO₂ Moorings and Time Series Project, California Current Ecosystem 1 (CCE1) Mooring at 33.5°N, 112.5°W. Retrieved December 22, 2017 from https://www.nodc.noaa.gov/ocads/oceans/Coastal/CCE1_122W_33N.html

Rhein M, Rintoul SR, Aoki S, Campos E, Chambers D, et al. (2013): Observations: Ocean. In: *Climate Change 2013: The Physical Science Basis. Contribution of Working Group I to the Fifth Assessment Report of the Intergovernmental Panel on Climate Change*. Stocker TF, Qin D, Plattner GK, Tignor M, Allen SK, et al. (Eds.)]. Cambridge, United Kingdom and New York, NY, USA: Cambridge University Press.

Sabine CL, Feely RA, Gruber N, Key RM, Lee K and Bullister JL (2004). The oceanic sink for anthropogenic CO₂. *Science* **305**: 367-371.

Sanford E, Gaylord B, Hettinger A, Lenz EA, Meyer K and Hill TM (2014). Ocean acidification increases the vulnerability of native oysters to predation by invasive snails. *Proceedings of the Royal Society B*. **281**: 20132681.

SIO (2017) Scripps Institution of Oceanography: California Current Ecosystem Moorings map. Retrieved February 2, 2018 from http://mooring.ucsd.edu/index.html?/projects/cce/cce_data.html

Sutton A, Sabine C, Send U, Ohman M, Dietrich C, et al. (2011). High-resolution ocean and atmosphere pCO₂ time-series measurements from mooring CCE1_122W_33N. http://cdiac.esd.ornl.gov/ftp/oceans/Moorings/CCE1_122W_33N/. Carbon Dioxide Information Analysis Center, Oak Ridge National Laboratory, US Department of Energy, Oak Ridge, Tennessee.

UC Davis Bodega Marine Laboratory (2016). Map showing location of stationary monitoring sites for CO₂-relevant parameters off California.

Waldbusser GG, Brunner EL, Haley BA, Hales B, Langdon CJ and Prah F, et al. (2013). A developmental and energetic basis linking larval oyster shell formation to acidification sensitivity. *Geophysical Research Letters* **40**(10): 2171-2176.





Climate, which is generally defined as “average weather”, is usually described in terms of the mean and variability of temperature, precipitation and wind over a period of time.

Warming of the climate system is unequivocal, and since the 1950s, many of the observed changes are unprecedented over decades to millennia (IPCC, 2013). Globally, each of the last three decades has been successively warmer than any preceding decade. The period from 1983 to 2012 was likely the warmest 30-year period of the last 1400 years in the Northern Hemisphere.

In the US, annual average temperatures have increased by 1.3°F to 1.9°F since record-keeping began in 1895. Most of this increase has occurred since about 1970, with the most recent decade being the warmest on record. Over the last 50 years, much of the United States has seen an increase in prolonged periods of excessively high temperatures (Melillo et al., 2014).

Consistent with global and US observations, California temperatures have risen since records began in 1895. The last four years showed unprecedented temperatures: 2014 is the warmest on record, followed by 2015, 2017 and 2016. In a warming climate, nighttime temperatures increase faster than daytime temperatures. Warmer nights can impact public health, especially for certain sensitive groups, and can affect fruit and nut tree production in our agricultural regions. Extreme heat events have become more frequent since 1950, especially in the last 30 years. These warming trends have been accompanied by an increase in “cooling degree days”, indicating a greater need for energy for cooling homes and buildings.

From 2012 to 2016, during the years of record warmth, and a year (2015) of record low snowpack, California experienced the most extreme drought since instrumental records began in 1895. A growing body of evidence suggests that anthropogenic warming has increased the likelihood of extreme droughts.



INDICATORS: CHANGES IN CLIMATE

Annual air temperature (*updated*)
Extreme heat events (*updated*)
Winter chill (*updated*)
Cooling and heating degree days (*new*)
Precipitation (*updated*)
Drought (*new*)

References:

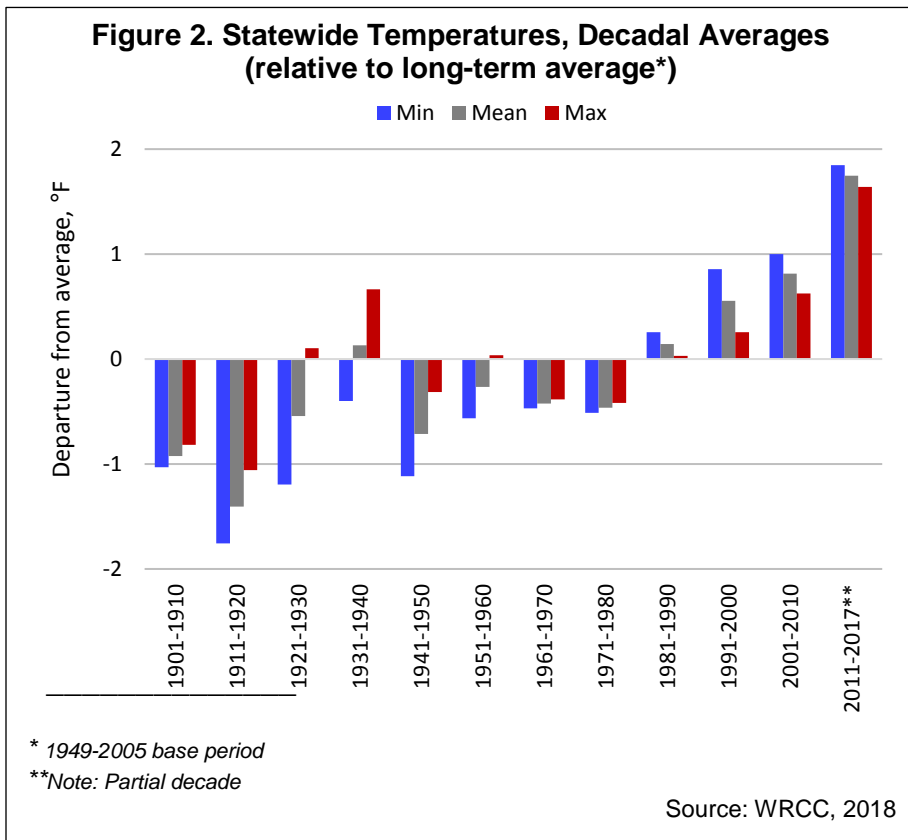
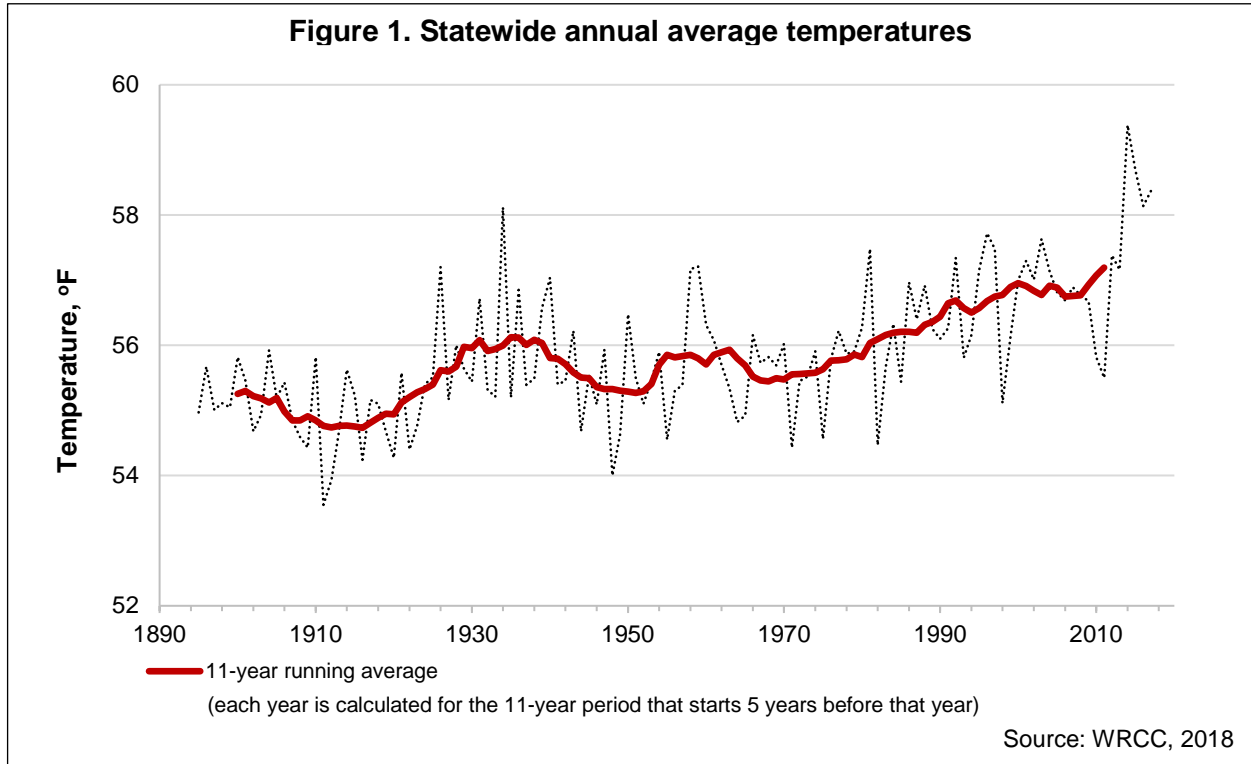
IPCC (2013). Summary for Policymakers. In: *Climate Change 2013: The Physical Science Basis. Contribution of Working Group I to the Fifth Assessment Report of the Intergovernmental Panel on Climate Change*. Stocker TF, Qin D, Plattner G-K, Tignor M, Allen SK, et al. (Eds.). Cambridge, United Kingdom and New York, NY, USA: Cambridge University Press. Available at http://www.ipcc.ch/pdf/assessment-report/ar5/wg1/WGIAR5_SPM_brochure_en.pdf

Melillo, Jerry M., Terese (T.C.) Richmond, and Gary W. Yohe, Eds., 2014: Highlights of Climate Change Impacts in the United States: The Third National Climate Assessment. U.S. Global Change Research Program, 148 pp.



ANNUAL AIR TEMPERATURE

Air temperatures have increased over the past century.



Temperature Departures: Definition of terms used

Average is the long-term average temperature based on data from 1949 to 2005.

Departure is the difference between the long-term average and the value for the period of interest. Positive values are above the long-term average (which is set at zero) and negative values are below the long-term average.

Maximum and minimum temperature is an average of the maximum or minimum temperature values for a given length of time.

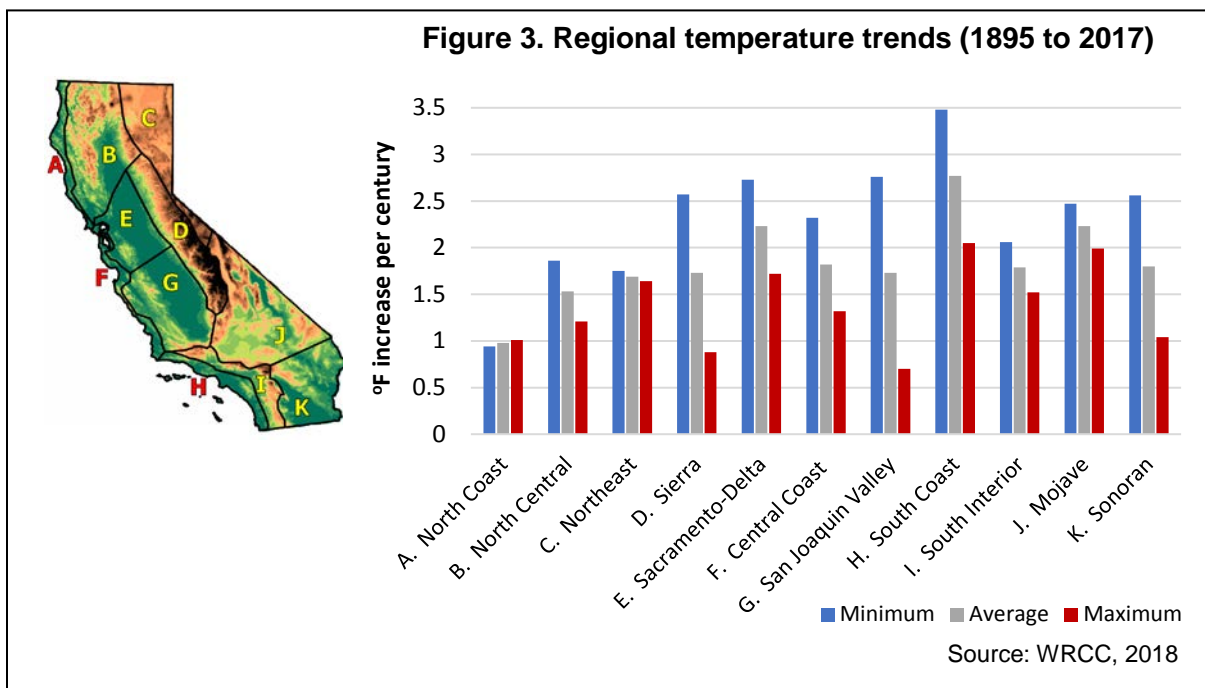
Mean temperature is the average of the maximum and minimum temperatures, or the sum of maximum + minimum, divided by 2.



What does the indicator show?

Statewide air temperatures have been recorded since 1895 and have shown a warming trend consistent to that found globally (IPCC, 2013). Figure 1 shows annual mean temperatures averaged over the state. Since 1895, annual mean temperatures have increased by about 2.2 degrees Fahrenheit (°F) (or about 1.8 °F per century, which is a common way of measuring long-term temperature changes). The last four years were notably warm, with 2014 being the warmest on record, followed by 2015, 2017 and 2016. These warm years coincided with some of the driest years in the instrumental record leading to exacerbated drought conditions due to increased land surface temperatures, evapotranspiration, and evaporative demand.

Figure 2 shows “departures” by decade from a long-term average (base period of 1949 to 2005) for minimum, average (mean) and maximum temperatures — i.e., the difference between each decade’s value and the long-term average. Minimum, average and maximum temperatures have been increasing overall, particularly since the 1980s. Minimum temperatures (that reflect overnight low temperatures) have increased the fastest. Minimum temperatures rose by 2.8 °F since 1895 (at a rate of 2.3 °F per century). Maximum temperatures rose by 1.6 °F since 1895 (at 1.3 °F per century). The increasing trend in mean California temperature is driven more by nighttime processes than by daytime processes.



All of California’s 11 climate regions show warming trends over the last century, although at varying rates (see Figure 3). The greatest increase is observed in the South Coast region. Minimum temperatures showed the greatest rate of increase in all the regions, except the North Coast. Minimum temperatures rose up to four times faster than maximum temperatures in the San Joaquin Valley, and three times faster in the Sierra Region. Graphs showing annual minimum, average and maximum temperatures



from 1895 to 2017 for the North Coast, Sierra, San Joaquin Valley, and South Coast regions are presented under “What factors influence this indicator?” (see “Regional Annual (Jan-Dec) Temperature Departures”).

Why is this indicator important?

Temperature is a basic physical factor that affects many natural processes and human activities. Warmer air temperatures alter precipitation and runoff patterns, affecting the availability of freshwater supplies. Increased temperature leads to a wide range of impacts on ecosystems — including changes in species’ geographic distribution, in the timing of life cycle events, and in their abundance — as well as human health and well-being. In addition, warming temperatures affect energy needed for cooling and heating, which in turn influences the types of energy generation, infrastructure, and management policies needed to meet these demands. Temperature changes can also increase the risk of severe weather events such as heat waves and intense storms. Understanding observed temperature trends is important for refining future climate projections for climate sensitive sectors and natural resources within the state (Cordero et al., 2011).

What factors influence this indicator?

Globally, the increase in the concentration of carbon dioxide and other greenhouse gases in the Earth’s atmosphere since the Industrial Revolution in the mid-1700s has been a principal factor causing warming (IPCC, 2013). Emissions of these greenhouse gases are intensifying the natural greenhouse effect, causing surface temperatures to rise. Greenhouse gases absorb heat radiated from the Earth’s surface and lower atmosphere, and radiate much of the energy back toward the surface.

Temperatures are influenced by local topography, proximity to the ocean, and global and regional atmospheric and oceanic circulations. Climate patterns can vary widely from year to year and from decade to decade, in accordance with large-scale circulation changes around the Earth. The Pacific Ocean has a major effect on California temperatures all year along the coast, especially summer, and farther inland in winter. In addition to topography, local influences on temperature include changes in land surface and land use. For example, urbanization of rural areas is generally known to have a warming effect, due in large part to the heat absorbing concrete and asphalt in building materials and roadways. Expansion of irrigation has been shown to have a cooling effect on summertime temperatures (Bonfils and Lobell, 2007).

There are unequal warming trends in each season, and spring is of particular interest due to its apparent larger warming trend. Abatzoglou and Redmond (2007) found that the difference between spring and autumn temperature trends observed in western North America is most likely due to global atmospheric circulation changes over the last several decades that exacerbate regional warming in the spring, and counteract warming in autumn (hence producing cooling).

Statewide seasonal temperature trends are listed in Table 1. The values are linear trends reported by the California Climate Tracker (WRCC, 2018). The greatest increases in maximum and mean temperatures occurred in the spring, while increases



in minimum temperatures were greatest in the summer and in the fall. Trends since 1975 are greater than trends since 1895, except for maximum temperatures in the winter.

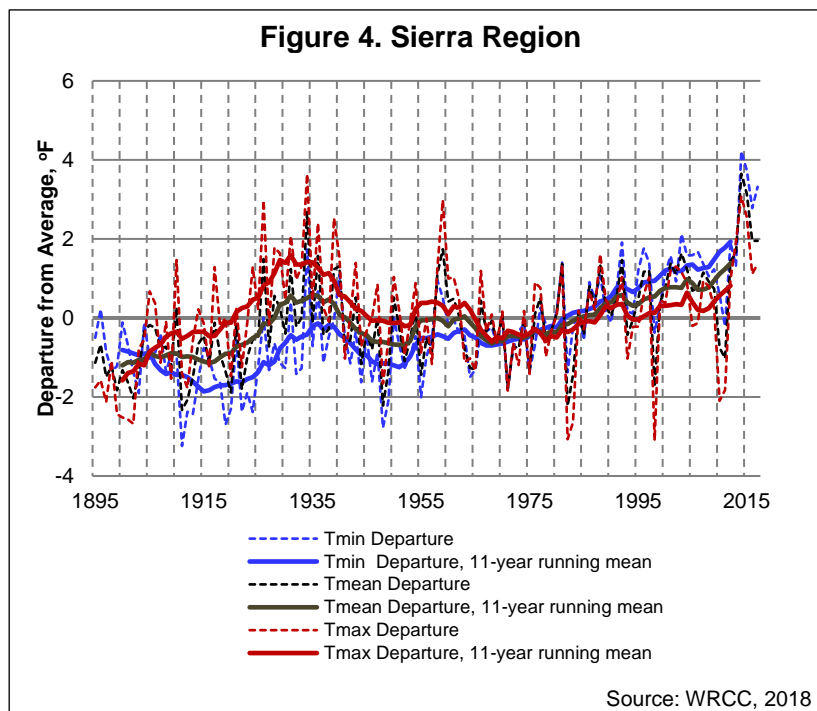
Table 1. Statewide trends by season

Season	Trend, °F/100 years					
	1895 to Present			1975 to Present		
	Minimum	Average	Maximum	Minimum	Average	Maximum
Fall (Sep-Nov)	2.74	1.94	1.15	6.96	5.78	4.61
Winter (Dec-Feb)	1.57	1.44	1.31	1.93	1.27	0.61
Spring (Mar-May)	2.08	2.00	1.92	4.86	5.82	6.77
Summer (Jun-Aug)	2.76	1.82	0.88	5.93	5.46	5.00
Annual (Jan-Dec)	2.30	1.82	1.34	5.23	4.84	4.45

Source: WRCC, 2018

Regional Annual (Jan-Dec) Temperature Departures (based on 1949-2005 averages)

To illustrate the varied nature of temperature trends in different regions of the state, data are presented for four of the 11 California climate regions. The South Coast showed the greatest warming of all regions, the San Joaquin Valley and the Sierra regions showed the largest and second largest difference between the increase in minimum temperatures compared to maximum temperatures, and the North Coast showed fairly equal trends in minimum, average, and maximum temperatures (see Figure 3). In the graphs that follow, the red line is the maximum temperature; the blue line is the minimum temperature; and the black line is mean temperature. Thin lines are values for annual departures from the long term (1949 to 2005) average. Bold lines are the 11-year running mean, where the value shown for each year is calculated for the 11-year period that starts five years before that year.

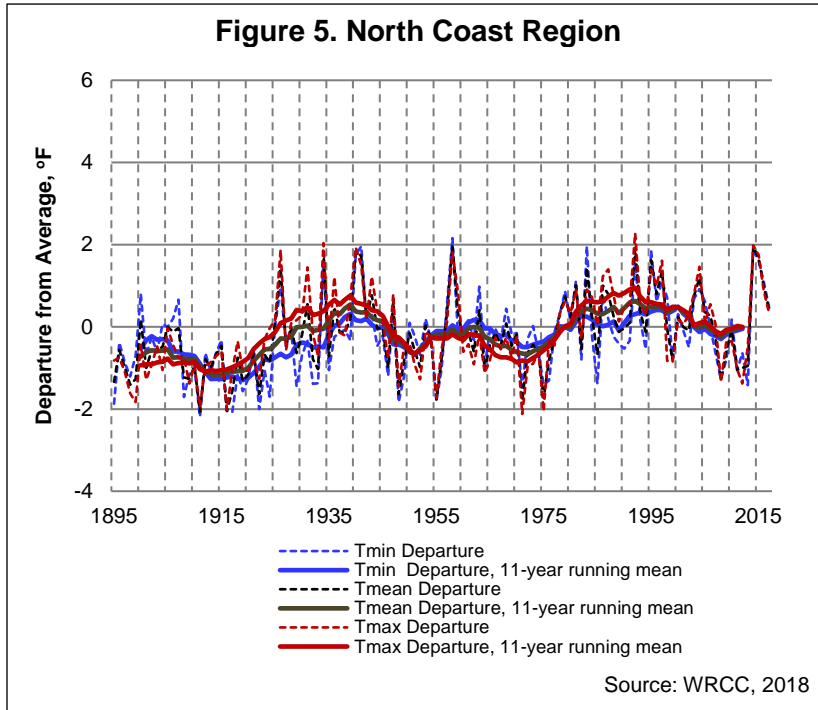


The Sierra Region contains the natural winter snowpack storage for the state's water supply. It stretches from the Feather River in the north to the Kern River in the south, ranging from about 2,000 feet to above 14,000 feet in elevation. Minimum temperatures in this region have increased about three times faster than maximum temperatures. The rise in spring season minimum temperatures and decrease in the number of days with

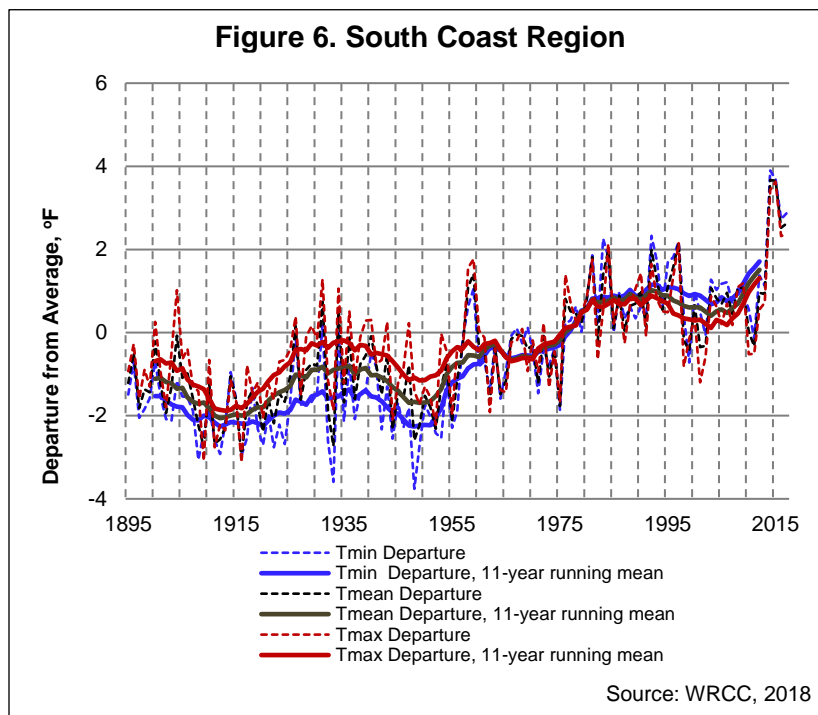
Source: WRCC, 2018



temperatures below freezing have impacted snowpack and snowmelt. Snow cover is a factor affecting temperature in this region: the disappearance of snow cover exposes surfaces that absorb solar energy, resulting in further warming (a phenomenon known as “snow albedo feedback”) (Walton et al., 2017).



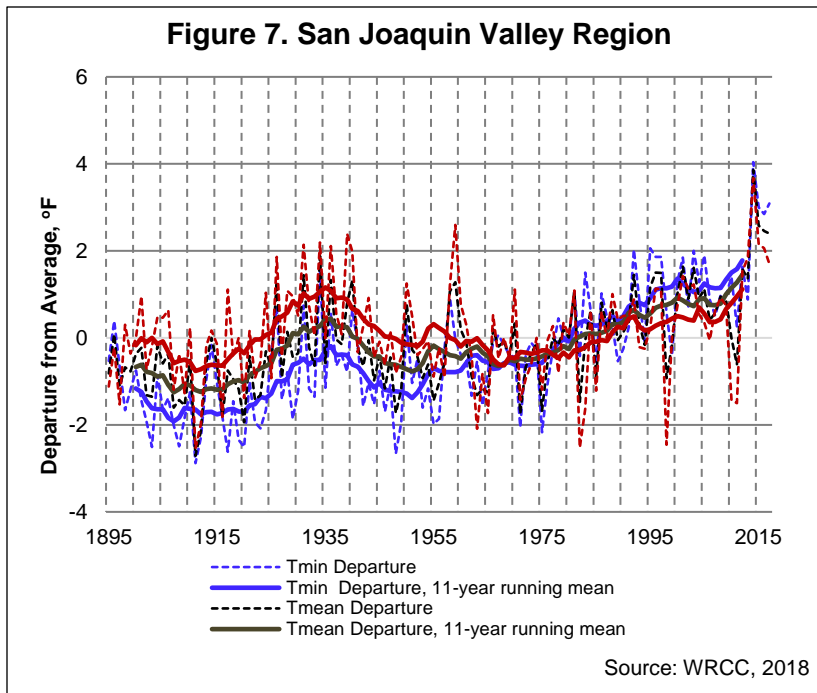
The North Coast region is a narrow coastal strip from the Oregon border to just south of Point Reyes. The region shows less of an increase in minimum and average temperatures than the rest of the state. Further, the overall trends for minimum, mean and maximum temperatures are similar. These trends may reflect the moderating influence of maritime air on temperatures (Abatzoglou et al., 2009).



The South Coast region encompasses a narrow band along the coast from Point Conception to the Mexican border, including the Los Angeles Basin and San Diego. It has experienced the greatest warming among the regions since 1895. Although the region experiences the moderating influence of maritime air, rapid urbanization may have contributed to its relatively steep overall warming trend (LaDochy et al., 2007). More recently,

increased sea breeze activity due to the gradient created by inland warming is thought to have created a cooling effect in the summer (Lebassi et al., 2009).





Minimum temperatures in the San Joaquin Valley region have been rising about four times faster than maximum temperatures. Studies in this region suggest that urbanization has primarily increased minimum temperatures (LaDochy et al., 2007), while irrigation has both decreased maximum temperatures and increased minimum temperatures (e.g., Bonfils and Lobell, 2007; Kueppers et al., 2007).

Technical Considerations

Data Characteristics

Two data sources are used to create a single value for each temperature variable each month: (1) data for nearly 200 climate stations in the NOAA Cooperative Network within California (from the Western Regional Climate Center database archive of quality controlled data from the National Climatic Data Center); and (2) gridded climate data from the Parameter-elevation Regressions on Independent Slopes Model (PRISM) (Daly et al., 1997) acquired from the PRISM group at Oregon State University. PRISM provides complete spatial coverage of the state. Because climate stations are not evenly spaced, the PRISM data are used to provide even and complete coverage across the state. This operational product, the California Climate Tracker, is updated monthly online at the Western Regional Climate Center at <http://www.wrcc.dri.edu/monitor/cal-mon/index.html>. Software and analyses were produced by Dr. John Abatzoglou (Abatzoglou et al., 2009).

Strengths and Limitations of the Data

The datasets used are subjected to their own separate quality control procedures, to account for potentially incorrect data reported by the observer, missing data, and to remove inconsistencies such as station relocation or instrument change.

The PRISM dataset offers complete coverage across the state for every month of the record. Limitations include the bias of station data toward populated areas, and limited ability of quality control processes in remote or high terrain areas. The results cited here offer a hybrid using both gridded (full coverage) and station data, which is suggested to be more robust than either dataset used independently (Abatzoglou et al., 2009).



For more information, contact:



Dan McEvoy and Nina Oakley
Western Regional Climate Center
Division of Atmospheric Science
Desert Research Institute
2215 Raggio Parkway
Reno, NV 89512-1095
(775) 674-7010
Daniel.McEvoy@dri.edu
Nina.Oakley@dri.edu

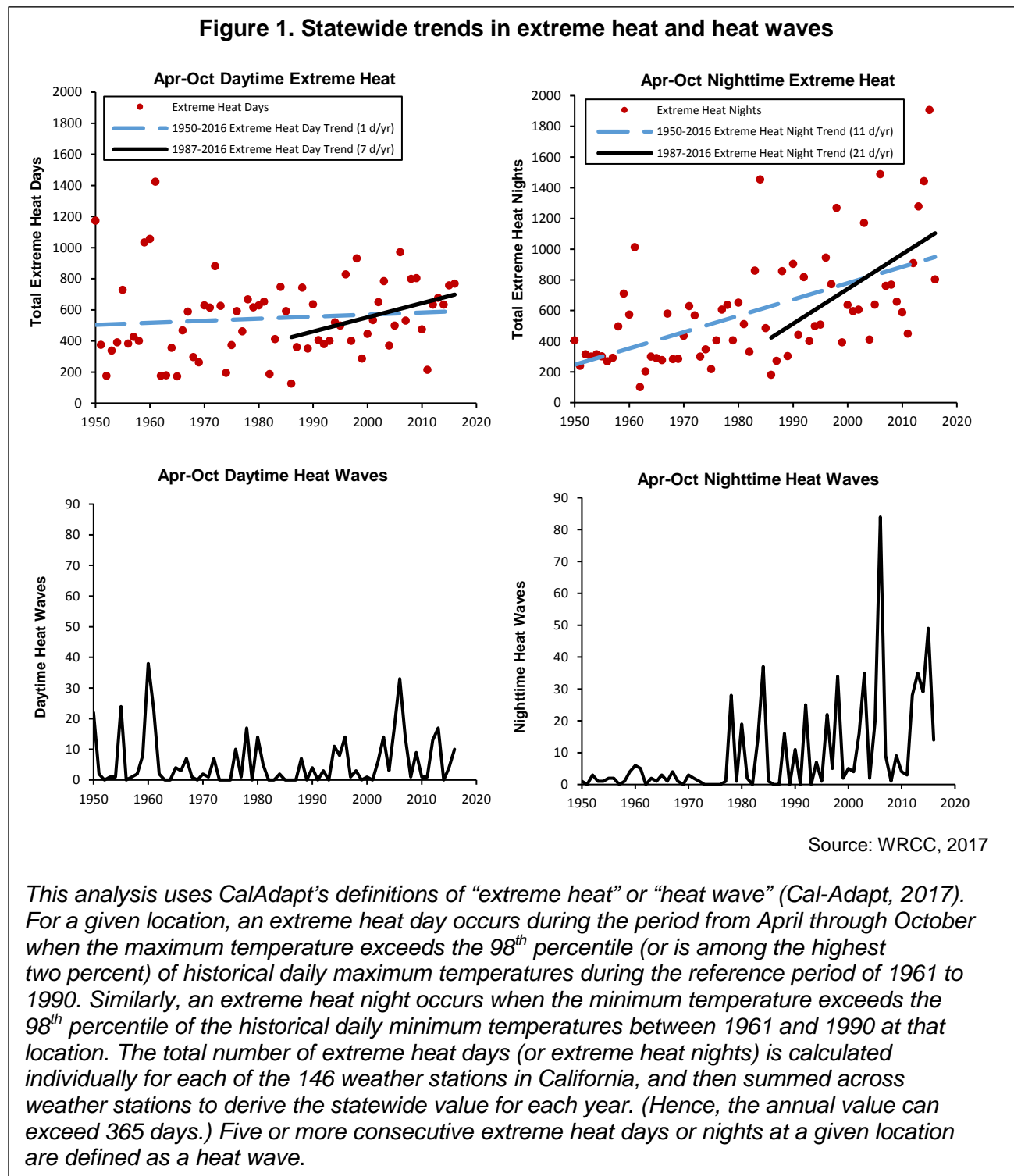
References:

- Abatzoglou JT and Redmond KT (2007). Asymmetry between trends in spring and autumn temperature and circulation regimes over western North America. *Geophysical Research Letters* **34**(18): L18808.
- Abatzoglou JT, Redmond KT and Edwards LM (2009). Classification of regional climate variability in the state of California. *Journal of Applied Meteorology and Climatology* **48**(8): 1527-1541.
- Bonfils C and Lobell D (2007). Empirical evidence for a recent slowdown in irrigation-induced cooling. *Proceedings of the National Academy of Sciences* **104**(34): 13582-13587.
- Cordero E, Kessomkiat W, Abatzoglou JT and Mauget S (2011). The identification of distinct patterns in California temperature trends. *Climatic Change* **108**(1-2): 357-382.
- Daly C, Taylor G and Gibson W (1997). *The PRISM approach to mapping precipitation and temperature. 10th Conference on Applied Climatology*. American Meteorological Society. Available at <http://citeseerx.ist.psu.edu/viewdoc/summary?doi=10.1.1.730.5725>
- IPCC (2013). *Climate Change 2013: The Physical Science Basis. Contribution of Working Group I to the Fifth Assessment Report of the Intergovernmental Panel on Climate Change*. Stocker TF, Qin D, Plattner GK, Tignor M, Allen SK, et al. (Eds.). Available at <http://www.ipcc.ch/report/ar5/wg1/>
- Knowles N, Dettinger MD and Cayan DR (2006). Trends in snowfall versus rainfall in the western United States. *Journal of Climate* **19**(18): 4545-4559.
- Kueppers LM, Snyder MA and Sloan LC (2007). Irrigation cooling effect: Regional climate forcing by land-use change. *Geophysical Research Letters* **34**(3): L03703.
- LaDochy S, Medina R and Patzert W (2007). Recent California climate variability: spatial and temporal patterns in temperature trends. *Climate Research* **33**(2): 159-169.
- Lebassi B, Gonzáles J, Fabris D, Maurer E, Miller N, et al. (2009). Observed 1970-2005 cooling of summer daytime temperatures in coastal California. *Journal of Climate* **22**(13): 3558-3573.
- Walton DB, Hall A, Berg N, Schwartz M and Sun F (2017). Incorporating snow albedo feedback into downscaled temperature and snow cover projections for California's Sierra Nevada. *Journal of Climate* **30**: 1417-1438.
- WRCC (2018). Western Regional Climate Center: California Climate Tracker. Retrieved January 10, 2018, from <http://www.wrcc.dri.edu/monitor/cal-mon/index.html>



EXTREME HEAT EVENTS

Extreme heat days and nights have become more frequent since 1950. Heat waves have been variable each year, but nighttime heat waves have shown a marked increase since the mid-1970s.



What does the indicator show?

The two top graphs in Figure 1 show statewide trends in the number of extreme heat days and nights from April through October. The dashed blue lines show the linear trend for the period from 1950 to 2016. The solid line shows the trend for the last 30 years (1987-2016). Since 1950, the number of extreme heat days has increased slightly statewide, at a rate of about one day per year. In contrast, the rate of increase in the occurrence of extreme heat nights for the same period is over 10 times higher, at 11 days per year. For both extreme heat days and nights, the rate of change has been greater over the most recent 30 years. From 1987 to 2016, extreme heat days and nights increased by 7 and 21 days per year, respectively.

Statewide heat waves are shown in the two bottom graphs in Figure 1. The number of daytime heat waves shows considerable year-to-year variability, without a clear trend. Nighttime heat waves, which occurred infrequently until the mid-1970s, have increased in frequency over the past 40 years.

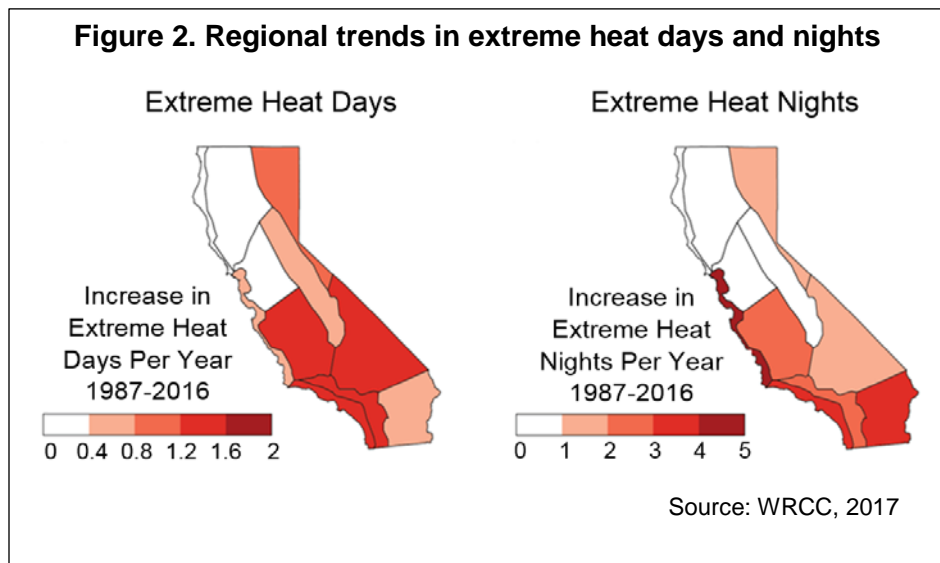
Regional trends in the number of extreme heat days and nights over the 30-year period from 1987 to 2016 are illustrated in the maps in Figure 2. For most regions, the rate of increase in the number of extreme heat nights was twice that of the rate of increase in extreme heat days. The greatest

increase in the total number of daytime and nighttime extreme heat events occurred in Southern California. Nighttime heat increased the most in the Central Coast region.

Why is this indicator important?

Periods of extremely high temperatures have significant public health, ecological, and economic impacts. Among these are heat-related illnesses and deaths, livestock deaths, increased water demand, increased air pollution, and strains on the power supply. Heat causes the most weather-related deaths in the United States (NOAA, 2017).

Heat events are projected to become more frequent and last longer (USGCRP, 2016). Taking action to mitigate the impacts of extreme heat is critical, particularly given the largely preventable adverse effects on public health. Anticipating the effects of



unusually high temperatures on wildfires, agriculture, and energy demand will also help inform planning and resource allocation.

A recent study found a changing pattern of heat waves in California. Since the 1980s, heat waves have become more humid, in part due to ocean warming (Gershunov et al., 2009). Humidity prevents surfaces from cooling down at night, leading to higher nighttime temperatures. Warmer nighttime temperatures have a significant biological impact. People, animals, and plants that are adapted to California's traditionally dry daytime heat and nighttime cooling are unable to recover from extreme heat, especially when humidity is high at night. The increase in nighttime heat waves presents an additional risk factor for vulnerable populations.

What factors influence the indicators?

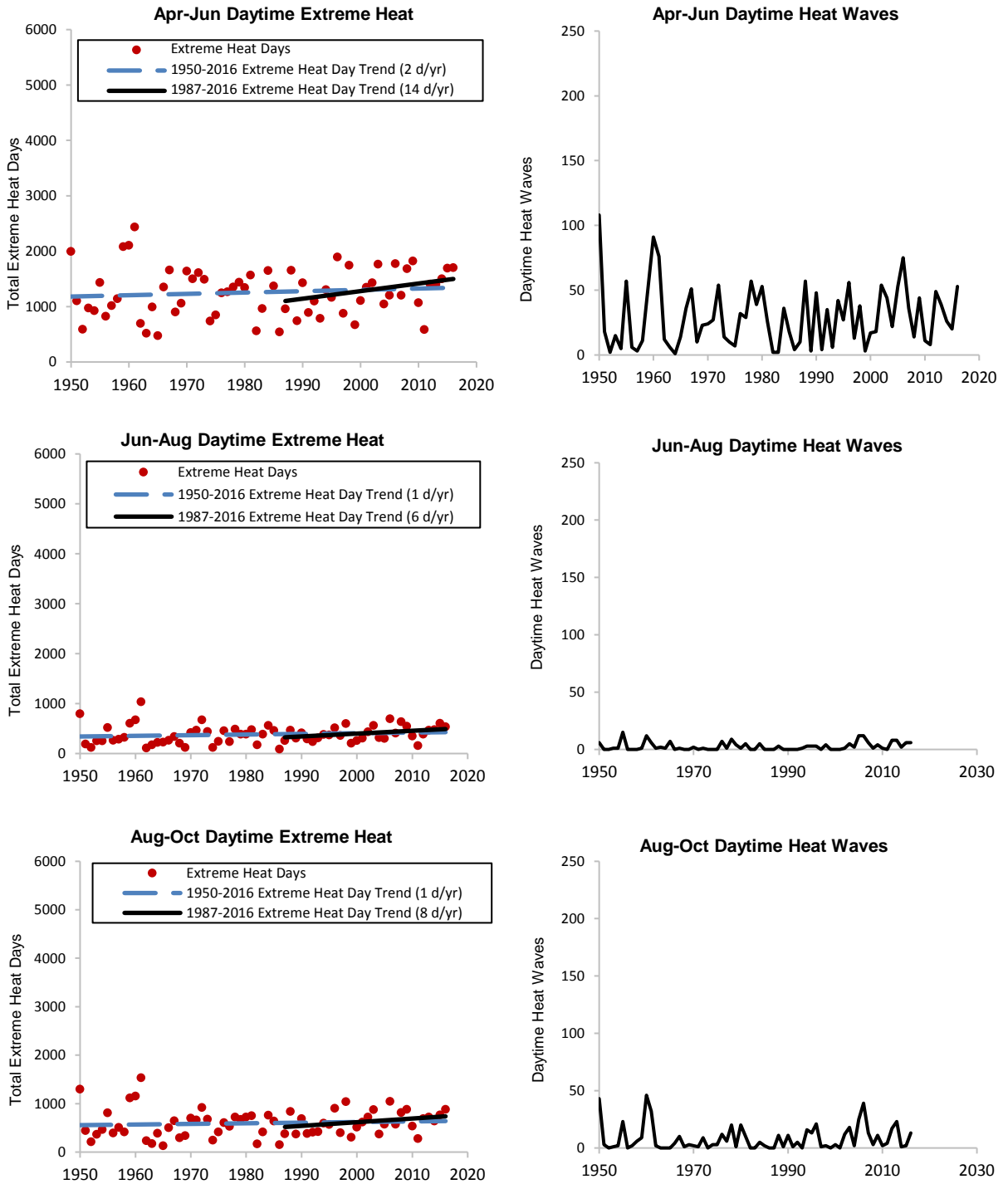
Air temperature varies according to the time of day, the season of the year, and geographic location. Temperatures in urban areas can also be affected by the urban heat island effect due to land surface modification and other human activities. However, rural locations see comparable increases in extreme heat days and nights and all regions of California are affected by regional climate change. This suggests that urbanization and land use does not explain the changes observed in California. The asymmetric increase in nighttime California heat wave activity and extreme heat nights compared to daytime heat extremes is consistent with impacts expected under global climate change.

As noted above, heat waves are becoming more humid. Although concern over greenhouse gas emissions tends to focus on carbon dioxide, water vapor is the most abundant greenhouse gas in the atmosphere, and the largest contributor to warming (Myhre et al, 2013). Human activities have little direct influence on the amount of atmospheric water vapor (Forster et al., 2007). As air temperatures rise due to anthropogenic emissions of other greenhouse gases, the water vapor content of the atmosphere increases. Water vapor absorbs outgoing longwave terrestrial radiation and re-radiates energy back to the surface, thus impeding radiative cooling. Therefore, there is less nighttime respite from heat when specific humidity is high. Moreover, humid heat waves tend to last longer due to the stronger coupling of maximum and minimum temperatures during humid heat waves (Gershunov et al., 2009).

The influence of the time of year (or season) is evident in the extreme heat trends presented in the graphs (Figures 3 and 4) and Table 1. The period from April to June showed the greatest increase in the number of extreme heat days and nights (see Figure 3, 4 and 5). This suggests that these months are warming at a faster rate than other months of the year. Further, the increase in extreme heat occurred at a faster rate during the past 30 years (1987-2016) than the past 67 years (1950-2016), suggesting that warming has increased during the recent decades.



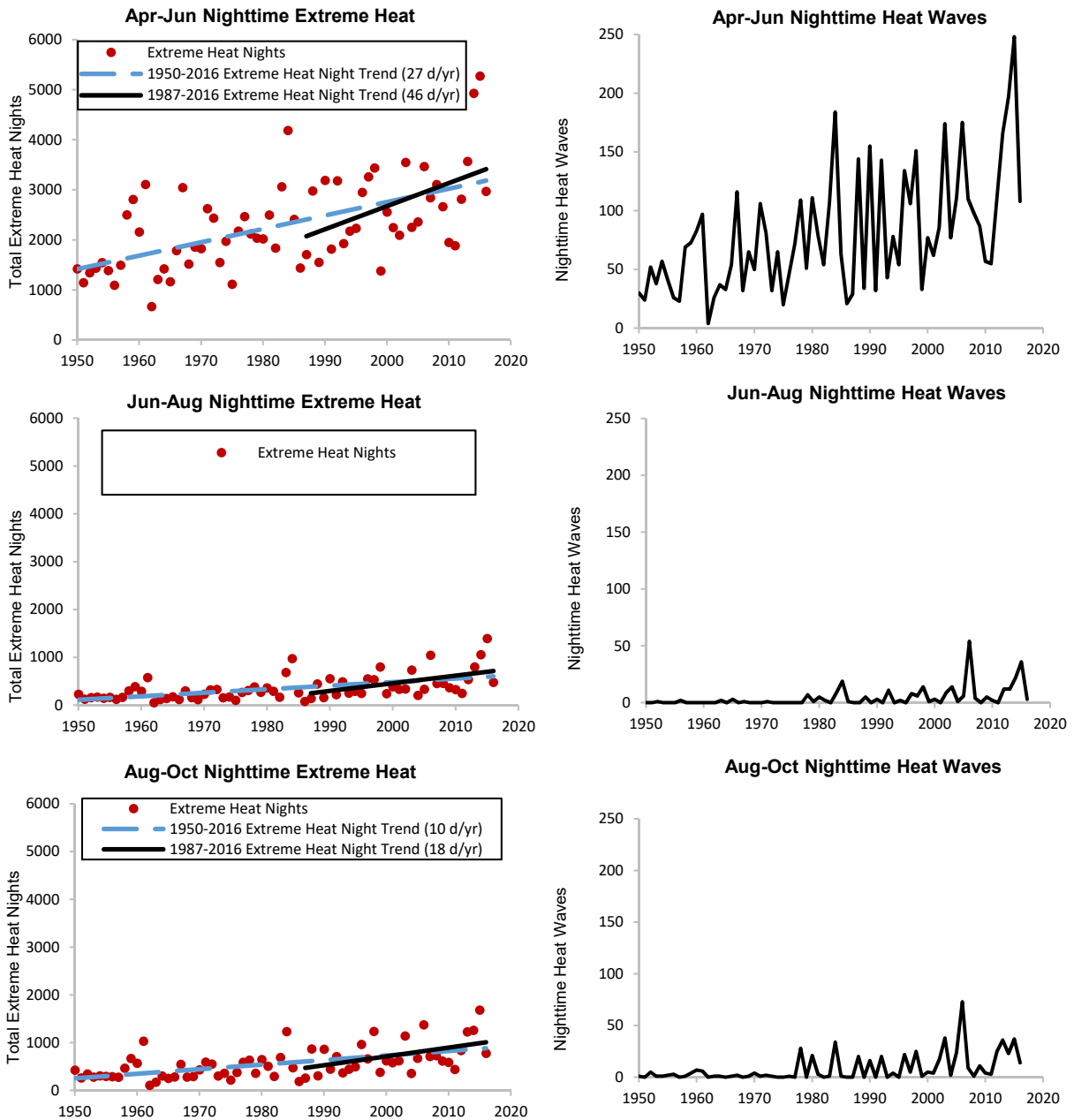
Figure 3. Statewide trends in daytime heat waves and extreme heat days



Source: WRCC, 2017



Figure 4. Statewide trends in nighttime heat waves and extreme heat nights

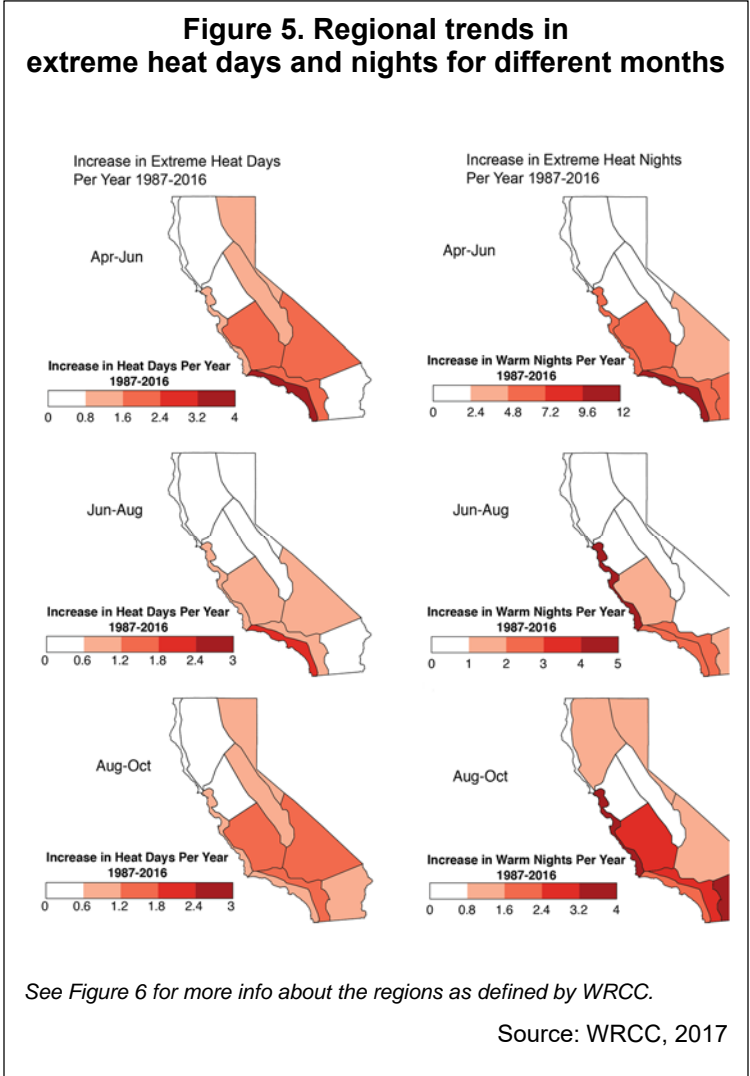


Source: WRCC, 2017



Table 1. Summary of extreme heat trends				
Rate of increase in the number of extreme heat days or nights per year for different periods during the warm months at 146 CA weather stations				
Period	Daytime extreme heat trend (days/year)		Nighttime extreme heat trend (days/year)	
	1950-2016	1987-2016	1950-2016	1987-2016
April-October	1	7	11	21
April-June	2	14	27	46
June-August	1	6	7	16
August-October	1	8	10	18

Nighttime trends are at least two times greater than daytime trends in extreme heat. The greatest increases are found in Southern California. The South Coast has experienced the greatest increases in both daytime and nighttime heat extremes during late spring (April-June). Note that the spring season nighttime extreme heat increases are on the order of two to four times greater than other seasons. Summer (June-August) increases in nighttime heat extremes are most pronounced along the Central Coast followed by the South Coast and South Interior regions. Early fall (August-October) increases in nighttime extreme heat is more widespread throughout southern California with the Central Coast and Mojave Desert regions experiencing the greatest increases, followed by the South Interior and San Joaquin Valley regions.

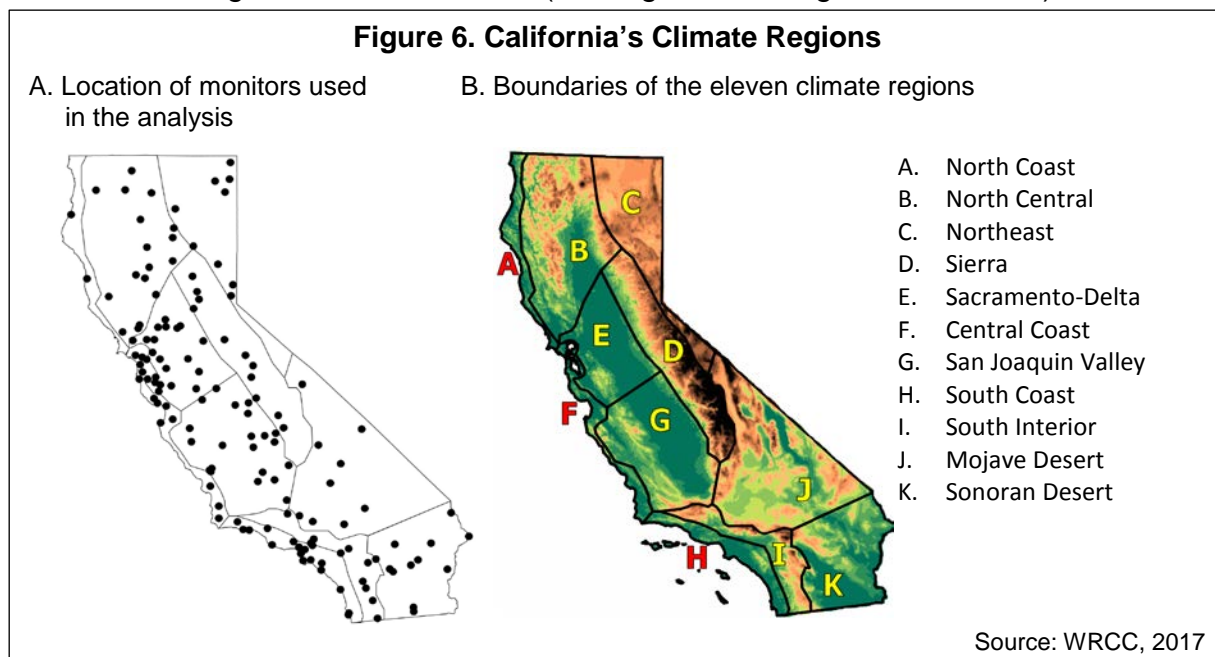


Technical Considerations

Data Characteristics

This indicator uses station data from the National Weather Service (NWS) cooperative observation network acquired from the Applied Climate Information System (via <https://wrcc.dri.edu/csc/scenic/>). The vast majority of the observers are trained volunteers, and the network also includes the NWS principal climatological stations. The observing equipment used at all of the stations, whether at volunteer sites or federal installations, are calibrated and maintained by NWS field representatives, Cooperative Program Managers, and Hydro-Meteorological Technicians. Only stations with at least 90 percent complete records were used in the analysis for a total of 146 stations. These stations are shown in Figure 6.

Regional trends are presented according to California's climate regions, as defined by the Western Regional Climate Center (see Figure 6 for region boundaries).



Strengths and Limitations of the Data

The station data have received a high measure of quality control through computer and manual edits, and are subjected to internal consistency checks, compared against climatological limits, checked serially, and evaluated against surrounding stations. Station coverage is not uniformly distributed geographically and coverage can be quite sparse in mountainous areas such as the Sierra Nevada and Klamath Mountain regions, therefore there is a bias towards populated areas and lower elevations. Recorded temperatures in urban areas can also be affected by the urban heat island effect due to land surface modification and other human activities. The majority of California's population resides in urban areas, implying that the heat impacts from urban-induced warming on health are non-negligible. The statewide and climate region-based estimates should be interpreted as maximum estimates of changes in heat extremes due to the contribution of urban warming. Quantification of the specific



magnitudes of station-based urban heat contributions and its influence on regional and statewide trends in heat extremes are beyond the scope of the present study but are the subject of ongoing research. The stations used in this analysis have undergone a homogenization technique applied by the National Center for Environmental Information to reduce urban heat-related biases (Hausfather et al., 2013).

For more information, contact:



Western Regional
Climate Center

Benjamin Hatchett, Ph.D.
Desert Research Institute
Western Regional Climate Center
2215 Raggio Parkway
Reno, Nevada, 89512
Benjamin.Hatchett@dri.edu
(775) 674-7111

References:

CCSP (2008). *Analyses of the Effects of Global Change on Human Health and Welfare and Human Systems. Final Report, Synthesis and Assessment Product 4.6. A Report by the U.S. Climate Change Science Program and the Subcommittee on Global Change Research.* U.S. Climate Change Science Program. Available at <http://www.climate-science.gov/Library/sap/sap4-6/final-report>

Gershunov A, Cayan DR and Iacobellis SF (2009). The Great 2006 Heat Wave over California and Nevada: Signal of an Increasing Trend. *Journal of Climate* **22**(23): 6181–6203.

Guirguis KJ and Avissar R (2008). A precipitation climatology and dataset intercomparison for the western United States. *Journal of Hydrometeorology* **9**(5): 825-841.

Hausfather, Z, Menne MJ, Williams CN, Masters T, Broberg R and Jones D (2013). Quantifying the effect of urbanization on U.S. Historical Climatology Network temperature records. *Journal of Geophysical Research: Atmospheres* **118**: 481-494.

Forster P, Ramaswamy V, Artaxo P, Bernsten T, Betts R, et al. (2007). Changes in Atmospheric Constituents and in Radiative Forcing. In: *Climate Change 2007: The Physical Science Basis. Contribution of Working Group I to the Fourth Assessment Report of the Intergovernmental Panel on Climate Change.* Solomon S, Qin D, Manning M, Chen Z, Marquis M, et al. [Eds.]. Cambridge University Press, Cambridge, United Kingdom and New York, NY, USA. Available at http://www.ipcc.ch/publications_and_data/ar4/wg1/en/ch2.html

Maurer EP, Wood AW, Adam JC, Lettenmaier DP and Nijssen B (2002). A long-term hydrologically based dataset of land surface fluxes and states for the conterminous United States. *Journal of Climate* **15**(22): 3237-3251. data updated to 2010 at: http://www.engr.scu.edu/~emaurer/gridded_obs/index_gridded_obs.html

Myhre G, Shindell D, Bréon F-M, Collins W, Fuglestedt J, et al. (2013). Anthropogenic and Natural Radiative Forcing. In: *Climate Change 2013: The Physical Science Basis. Contribution of Working Group I to the Fifth Assessment Report of the Intergovernmental Panel on Climate Change.* Stocker TF, Qin D, Plattner GK, Tignor M, Allen SK, et al. [Eds.]. Cambridge University Press, Cambridge, United Kingdom and New York, NY, USA. Available at https://www.ipcc.ch/pdf/assessment-report/ar5/wg1/WG1AR5_Chapter08_FINAL.pdf

NOAA (2017). National Weather Service: 77-Year List of Severe Weather-Related Fatalities (1940-2016). Retrieved July 10, 2017, from <http://www.nws.noaa.gov/om/hazstats.shtml>.



Richman MB and Lamb PJ (1985). Climatic Pattern Analysis of Three- and Seven-Day Summer Rainfall in the Central United States: Some Methodological Considerations and a Regionalization. *Journal of Climate and Applied Meteorology* **24**(12): 1325-1343.

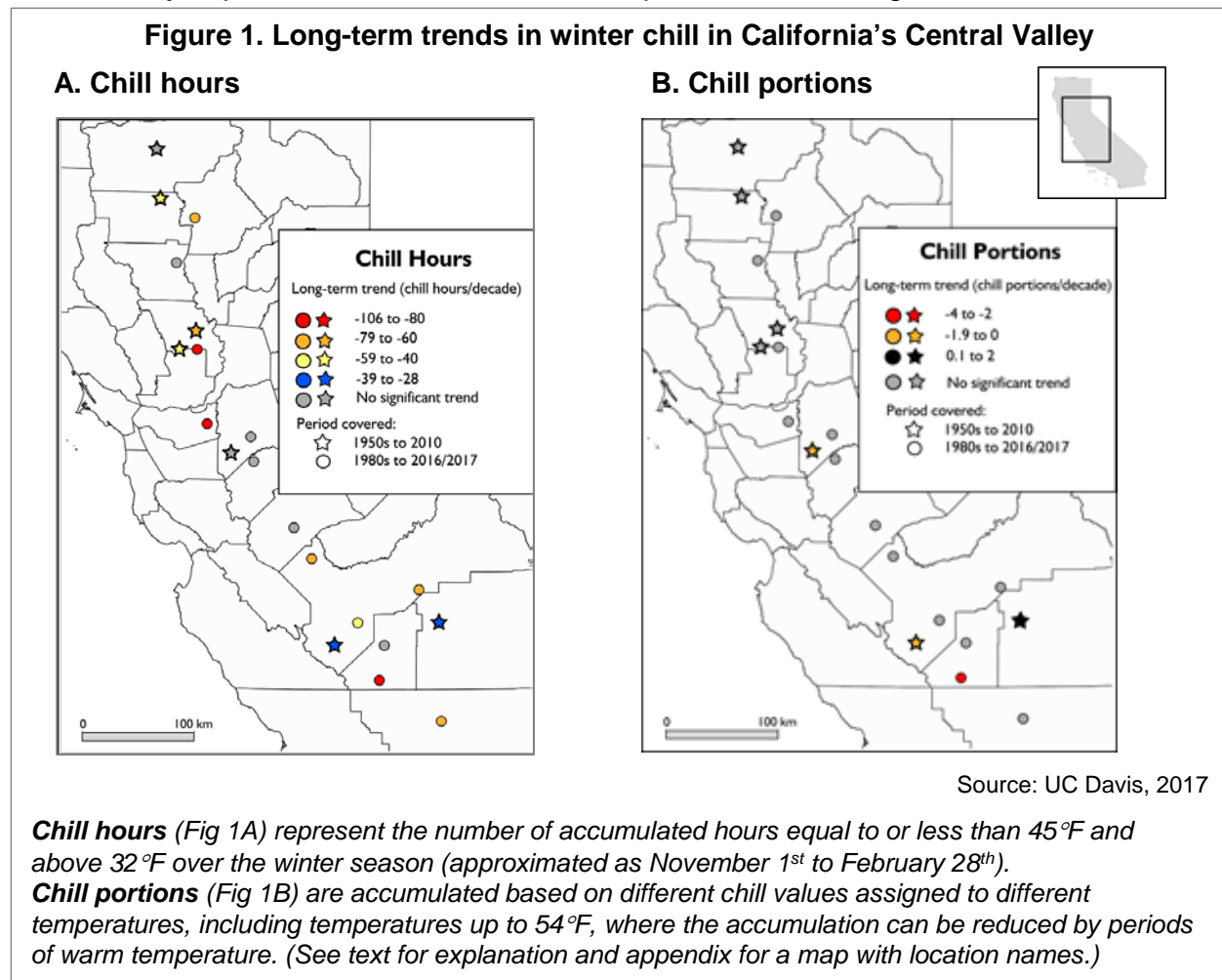
USGCRP (2016). *Chapter 2: Temperature-Related Death and Illness. The Impacts of Climate Change on Human Health in the United States: A Scientific Assessment*. US Global Change Research Program. Available at <https://health2016.globalchange.gov/temperature-related-death-and-illness>

WRCC (2017). Western Regional Climate Center. National Weather Service Cooperative Observation Network, accessed 10 March 2017 via the Applied Climate Information System. Data analyzed by Ben Hatchett, Desert Research Institute.



WINTER CHILL

Winter “chill hours,” a very sensitive and rudimentary metric that has been used since the 1940s, have been declining in more than half of the sites studied in the state. However, “chill portions,” a biologically based metric that more closely approximates how California’s agricultural trees experience winter chill, have shown declines at far fewer sites. While warming winter temperatures in California’s Central Valley are reflected in the “chill hours” metric, temperatures have not warmed enough to substantially impact the accumulation of “chill portions” in the region.



What does the indicator show?

Winter chill is a period of cold temperatures above freezing required for deciduous fruit and nut trees to produce flowers and fruit. The amount of chill that is required is dependent on the type of tree, for example, whether they are almonds, apricots, cherries, grapes, peaches, pistachios or walnuts. As shown in Figure 1, winter chill in California’s fruit- and nut-growing Central Valley has shown different trends over the past three to six decades, depending on how chill is calculated. Figure 1A presents chill hours, which have been declining in more than half of the sites studied (13 out of 20, $p < 0.05$). However, chill portions, presented in Figure 1B, show significant negative trends at only a few sites.



Different models have been developed to approximate how trees respond to the passage of this cold period. Chill hours have been used to measure winter chill since the 1940s; however, recent research favors the use of a more biologically based metric, chill portions (Luedeling et al., 2009). Chill portion is a better suited measurement of winter chill than chill hours for California's Mediterranean climate and mild winters. The *Technical Considerations (Data Characteristics)* section below provides a description of the differences in how chill hours and chill portions are calculated.

The increase in winter temperatures in the Central Valley is reflected in the decrease in chill hours at most of the sites. Given their lower temperature threshold (45°F), chill hours are more sensitive to warming temperatures. Unlike chill hours, chill portions show declining trends at just three sites – Coalinga, Kettleman, and Tracy-Carbona – and an increasing trend at one site (Visalia). At two additional sites – Orland and Winters, chill portions also appear to be declining ($0.1 \geq p \geq 0.05$; see Appendix for graphs). The fact that the increase in winter temperatures is not reflected in the chill portions metric indicates that temperatures have not warmed enough to affect the accumulation of biologically based chill portions, which are based on a higher temperature threshold (54°F).

Why is this indicator important?

An extended period of cold temperatures above freezing and below a threshold temperature is required for fruit and nut trees to become and remain dormant, and subsequently bear fruit. This chill requirement can vary widely from one fruit or nut to another, and even by variety of the same fruit (or nut). Fruit and nut trees need between 200 and 1,500 hours between 32 and 45°F during the winter (Baldocchi and Wong, 2006), or between 13 and 75 chill portions to produce flowers and fruit (Pope et al., 2014).

The importance of winter chill was demonstrated during the warm winter of 2013-2014. During this period, average chill portions dropped by 25 percent in the Central Valley. Orchards for many crops showed delayed and extended bloom, poor pollinizer overlap, and weak leaf-out. Low chill was likely responsible for much of the unusual tree behavior and low yields. Delayed bloom can extend later into spring, when conditions may be too warm for successful pollination. Extended bloom can result in changes in fruit or nut maturation timing, which could mean a more prolonged, costly harvest and increased risk of pests eating crops. Poor pollinizer overlap—when the pollen-producing flowers and the fruit-producing flowers are not opening at the same time—can result in decreased yield (Pope, 2014).

Current climate conditions provide the needed dormancy requirements partly as a result of prolonged periods of fog during the winter in the California Central Valley. In an analysis of weather data and satellite imagery for the Central Valley during the years 1981-2014, scientists found the number of winter fog events decreased 46 percent, on average, with much year-to-year variability (Baldocchi and Waller, 2014). If prolonged periods of winter fog disappear in the future, the Central Valley may experience larger diurnal swings in winter temperature and reduced hours below the critical temperature.



Future trend projections show that continued warming will reduce the accumulated winter chill for the Central Valley. By the middle to the end of the 21st century, it is projected that climatic conditions will no longer support current varieties of some of the main tree crops currently grown in California; chill hours are projected to show greater declines than chill portions. Current varieties of major tree crops may tolerate a 20 percent decline in winter chill. The tree crop industry will likely need to develop agricultural adaptation measures (e.g., the use of chill-compensating products, or by growing low-chill varieties) to cope with these projected changes. For some crops, production might no longer be possible (Luedeling et al., 2009). This would jeopardize the region's ability to sustain its production of high value nuts and fruits like almonds, cherries and apricots, resulting in serious economic, dietary and social consequences.

What factors influence this indicator?

The indicator is derived from temperature data, and as such, is influenced by the same factors that influence temperature. An additional consideration relates to the location where temperature measurements are taken, and whether they are close enough to the areas where fruits and nuts are grown to be representative of those air temperatures.

As discussed above, the choice of metric makes a difference in quantifying the magnitude of winter chill accumulation. The difference presented here between chill hours and chill portions is consistent with research that has modeled the potential impact of continued climate change. One study using weather data and several greenhouse gas emissions scenarios throughout California's Central Valley projected chill portions to decrease by 14 to 21 percent and chill hours to decrease by 29 to 39 percent between 1950 and 2050 (Luedeling et al., 2009). Projected impacts appear far more dramatic when seen through the lens of chill hours, although the chill hours model appears to be more sensitive to change than the trees themselves.

The influence of temperature on the biological processes underlying the breaking of dormancy — and the processes themselves — are poorly understood. It is known, however, that not all “chill” is effective. Temperatures above 45°F — which is common during the winter months in California — can cancel the effect of previous chill accumulation. Chill hours, which simply count the number of winter hours when temperatures are between the freezing point and 45°F, do not account for this cancelling effect. Chill portions, on the other hand, reflect a more biologically based theoretical framework, incorporating temperature fluctuations (see Luedeling et al., 2009 for details).



Technical Considerations

Data Characteristics

The indicator presents a metric for chill hours and the more mathematically complex metric for chill portions. The primary differences in the calculations for these two metrics are:

- Chill hours equally count any hour when temperatures are between 32-45°F. Chill portions give different chill values for temperatures, with those between 43-47°F having the most value. Chill values on either side of the range are lower.
- Chill hours only count up to 45°F. Chill portions count up to 54°F, which better approximates effective chilling for trees grown in fairly mild climates.
- Chill hours are a sum of hours between the temperatures described above, without accounting for warm hours. With chill portions, the running total of chill accumulation is reduced when warm hours closely follow cold periods.

Chill hours and chill portions were calculated using “chillR,” a statistical model for phenology analysis (Leudeling, 2017). The model is an extension to a commonly used statistics software, R. It includes a library that provides a number of utilities for phenology analysis in fruit trees, including automated retrieval of climate data from weather station databases including the University of California Statewide Integrated Pest Management Program (UCIPM) archive for California, modeling of hourly temperatures from daily minimum and maximum temperatures, and computation of three different horticultural chill metrics (Chilling Hours, Chill Units, and Chill Portions) and one heat metric. Climate data for Central Valley locations listed in Baldocchi and Wong (2008) were retrieved through the chillR downloading interface. Climate stations for which data were not retrievable from the UCIPM archive were omitted from the analysis.

The UCIPM archive includes data from the California Irrigation Management Information System (CIMIS) and the National Weather Service Cooperative Network (NWS COOP). Hourly temperature records, which are needed to calculate chill accumulation, are available from CIMIS. However, these stations only have data back to 1982; some stations were established even more recently. NWS COOP has records that date back decades earlier (the earliest records used in this indicator start in 1951), but only for daily maximum and minimum temperature; hourly temperatures were estimated using an algorithm based on diurnal temperature trends and reported maximum and minimum temperature (chillR, Leudeling, 2017).

NWS COOP station winter records were analyzed for trends from 1953 to 2010. CIMIS station winter records were analyzed from the beginning of the record, which was in the early-to-mid 1980s, depending on the station, until 2017.

Strengths and Limitations of the Data

Summary statistics that are commonly used to track temperature (such as average, minimum and maximum) generally do not provide the resolution necessary to examine temperature trends relevant to agriculture. Deriving winter chill accumulation from temperature data for the winter months yields a more meaningful measure for tracking a



change in climate that would be more predictive of fruit production. Winter chill accumulation provides an indication of whether specific fruit and nut trees are experiencing sufficient periods of dormancy.

The hourly data from CIMIS provide direct inputs into the calculation of winter chill degree hours, unlike daily minimum and maximum temperature data from NWS, which require the use of an algorithm. CIMIS weather stations are designed to monitor agricultural climate conditions. Thus, they are almost exclusively in agricultural areas, with the monitoring equipment located in a well-irrigated pasture. NWS COOP weather stations are designed with a broader use in mind. As such, they are generally located in developed, paved areas – in towns and cities, or at airports. As a result, temperatures at the NWS COOP stations in the winter are likely higher than they would be in an open field a few miles away. While this means that the chill accumulation at each NWS COOP weather station may not be precisely representative of what an orchard in that area would experience, any trends of increased or decreased chill accumulation of years and decades would likely be similar.

Historic temperature records are rarely complete. Many different approaches are used to fill in gaps in temperature records to analyze long term trends. In this study, hourly or daily temperatures were interpolated following Luedeling (2017). If more than 50 percent of the winter record required interpolation, that winter was not included in the analysis.

The chill portions model has become increasingly popular for climates with Mediterranean or otherwise mild winters. Multiple studies have found the chill portions model to count winter chill accumulation does as well as or better than the chill hours model.

For more information, contact:

University of California
Agriculture and Natural Resources

Katherine Jarvis-Shean
Sacramento-Solano-Yolo Orchard Systems Advisor
University of California Cooperative Extension
70 Cottonwood Street
Woodland, CA 95695
(530) 377-9528

Modeling and data analysis provided by Allan Hollander, UC Davis Information Center for the Environment.



References:

Baldocchi D and Waller E (2014). Winter fog is decreasing in the fruit growing region of the Central Valley of California. *Geophysical Research Letters*. **41**(9).

Baldocchi D and Wong S (2006). *An Assessment of the Impacts of Future CO₂ and Climate on Californian Agriculture*. #CEC-500-2005-187-SF California Climate Change Center. Available at <http://www.energy.ca.gov/2005publications/CEC-500-2005-187/CEC-500-2005-187-SF.PDF>

Baldocchi D and Wong S (2008). Accumulated winter chill is decreasing in the fruit growing regions of California. *Climatic Change* **87**(1): 153-166.

Luedeling E, Zhang M, Luedeling V, and Girvetz EH (2009). Sensitivity of winter chill models for fruit and nut trees to climatic changes expected in California's Central Valley. *Agriculture, Ecosystems & Environment* **133**(1–2): 23-31.

Luedeling E (2017). chillR: Statistical Methods for Phenology Analysis in Temperate Fruit Trees. R package version 0.66. Available at <https://cran.r-project.org/web/packages/chillR/index.html>

Pope KS (2014). Is Last Year's Warm Winter the New Normal? Retrieved December 12, 2017, from http://thealmonddoctor.com/2014/11/08/warm_winter_new_normal/

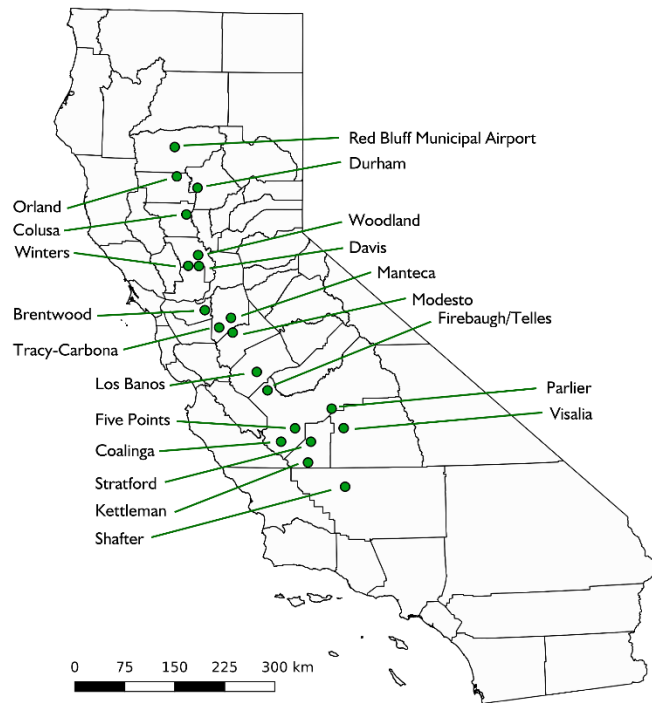
Pope KS, Brown PH, DeJong TM, and Da Silva D (2014). A biologically based approach to modeling spring phenology in temperate deciduous trees. *Agricultural and Forest Meteorology* **198**:15-23.

UC Davis (2017). Chill hours and chill portions at selected Central Valley sites, estimated using chillR (Luedeling 2017), using data from UC IPM (Weather, Models, and Degree Days. University of California Statewide Integrated Pest Management System). November, 2017.



APPENDIX

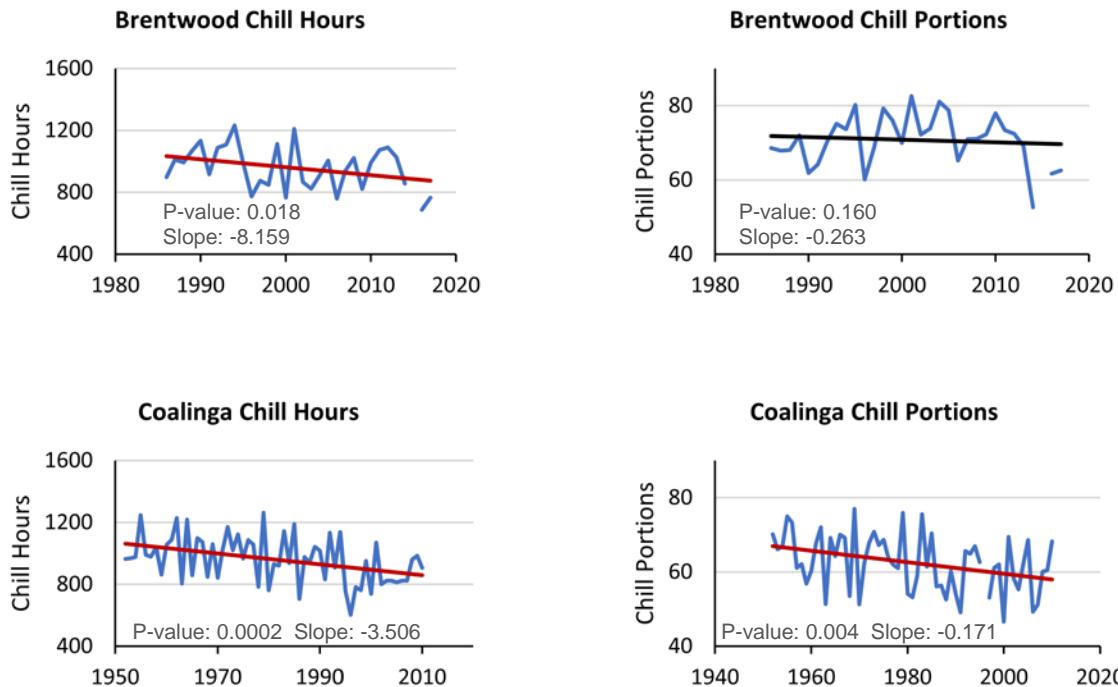
Figure A1. Map of winter chill sites in California

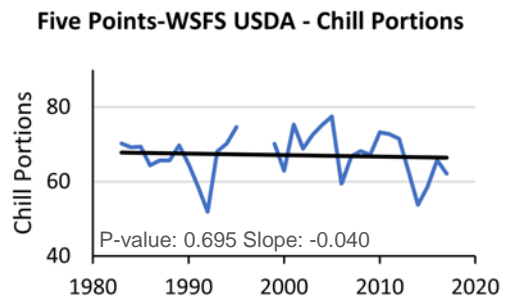
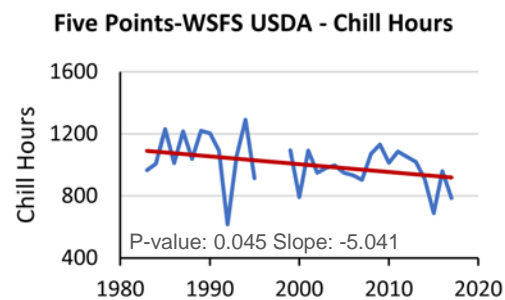
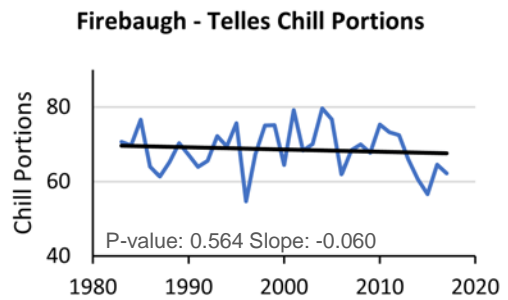
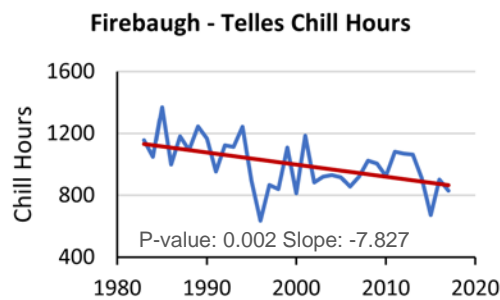
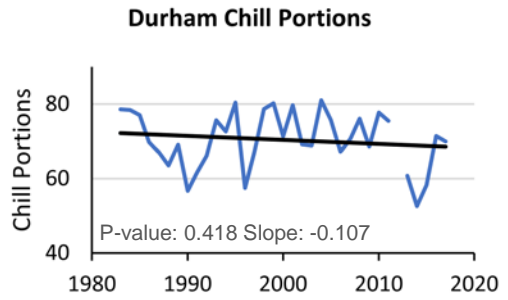
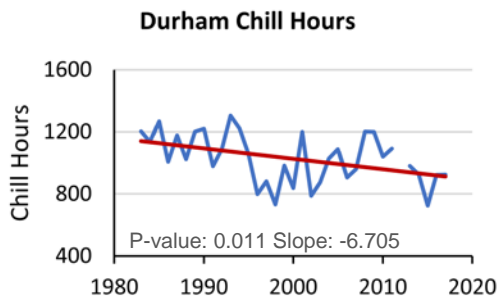
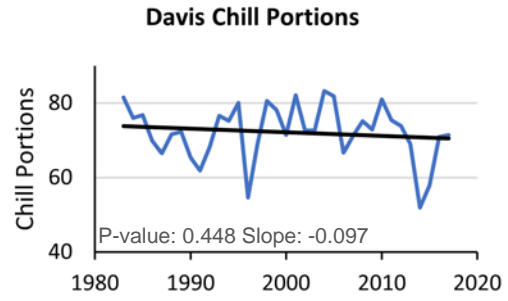
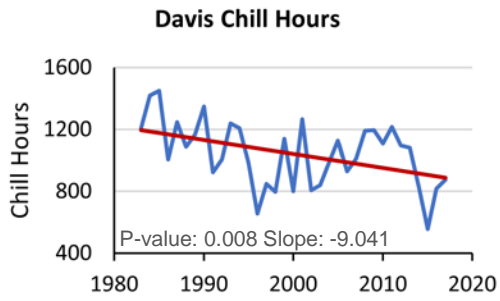
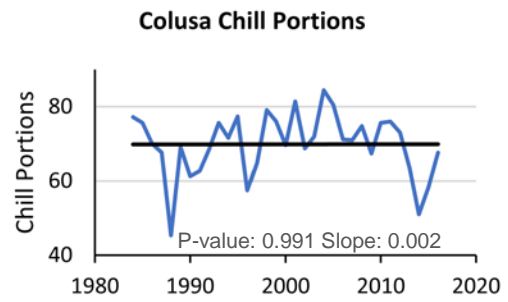
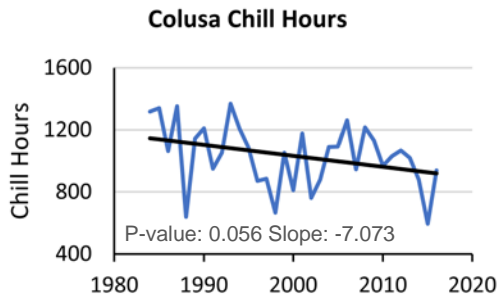


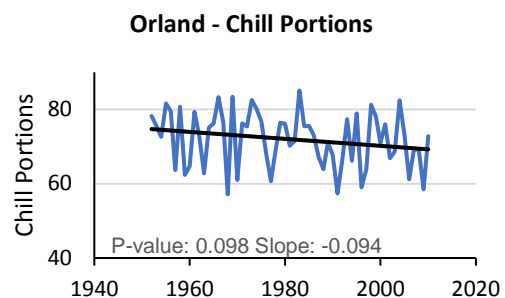
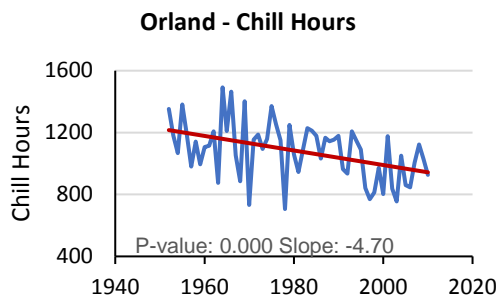
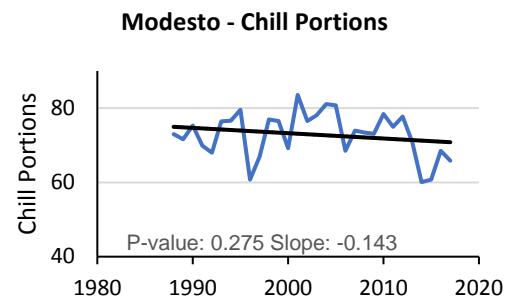
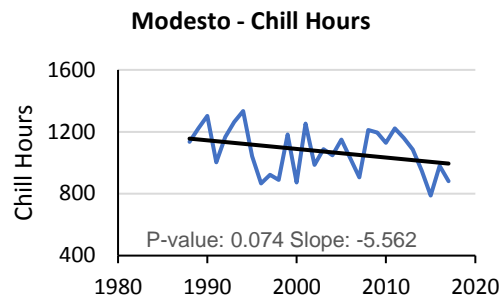
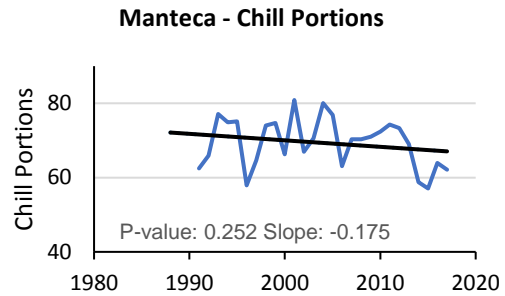
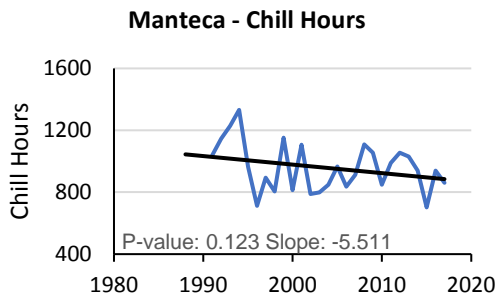
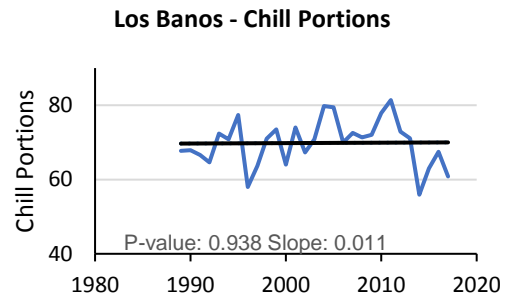
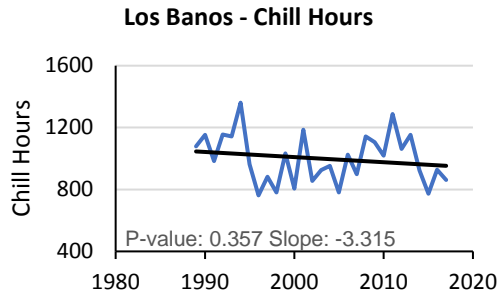
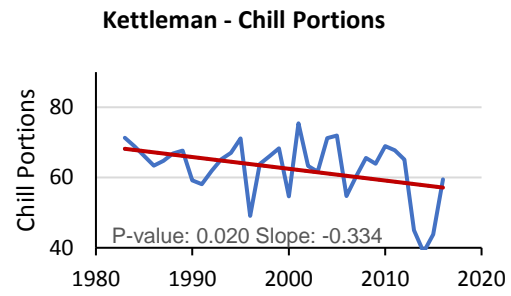
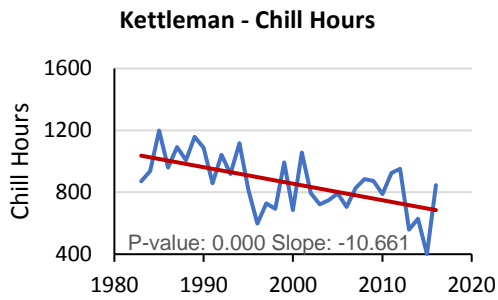
Source: UC Davis, 2017

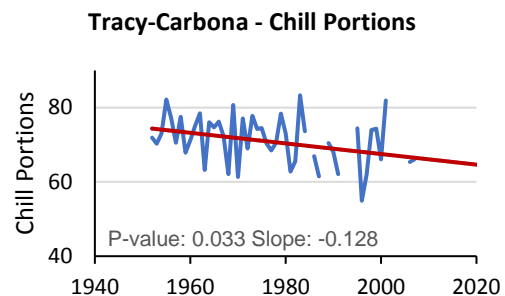
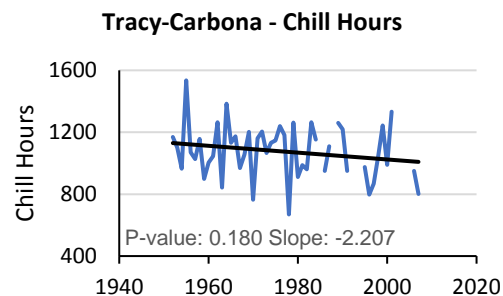
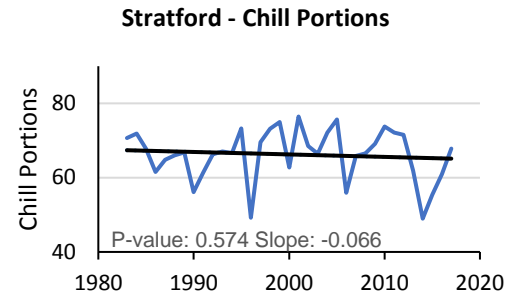
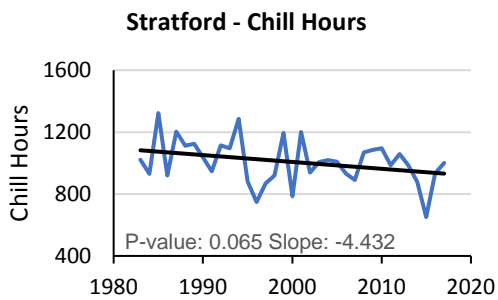
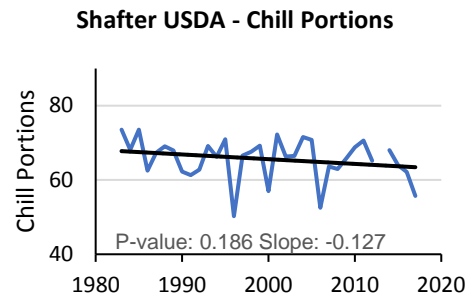
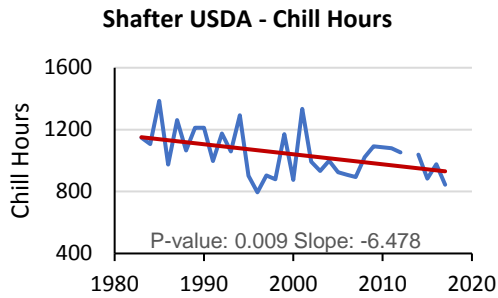
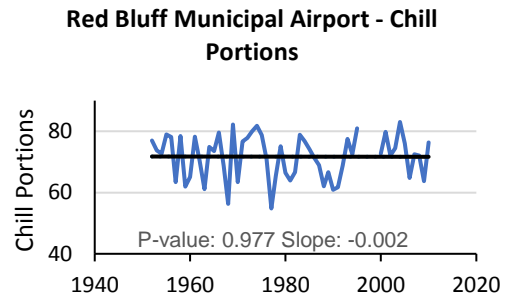
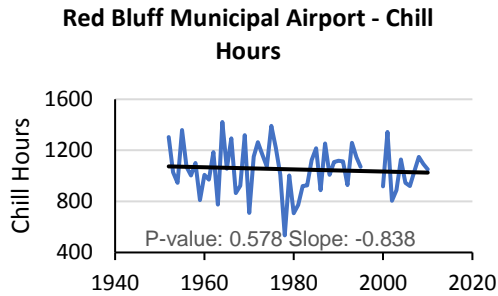
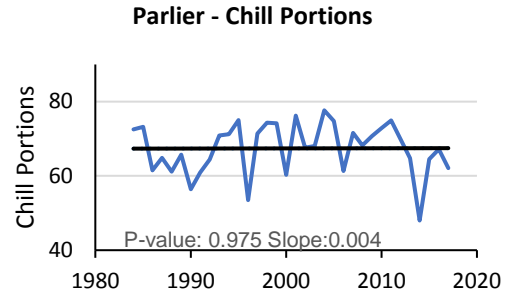
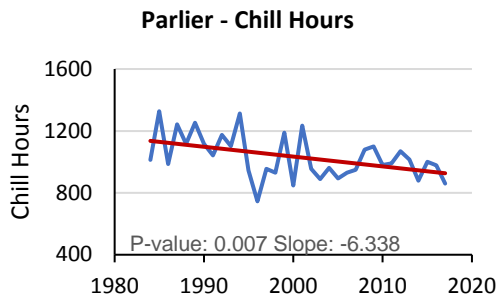
Figure A2. Long-term trends in chill hours and chill portions, by location

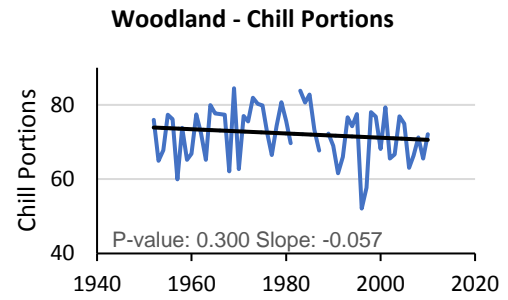
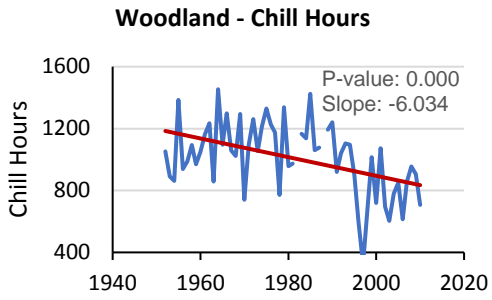
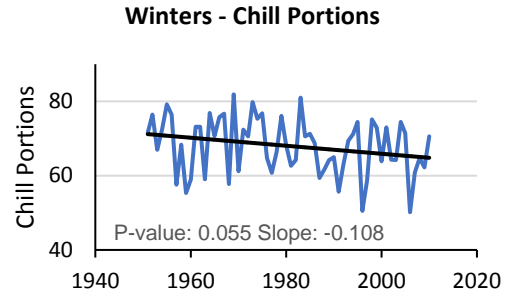
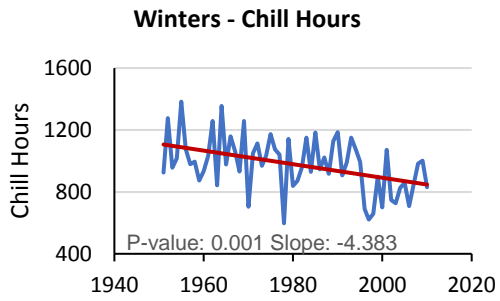
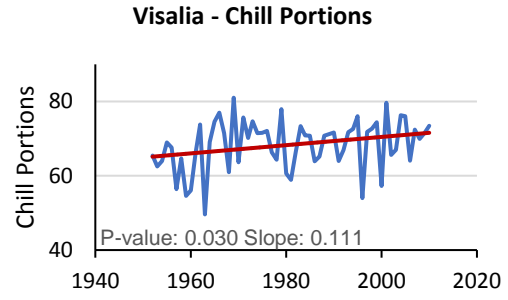
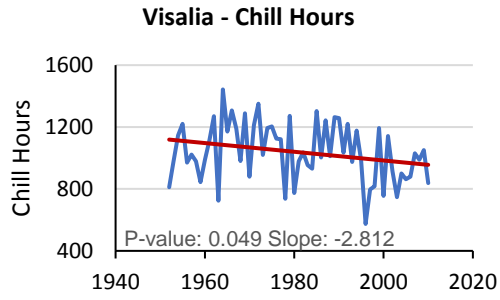
Statistically significant trends ($p < 0.05$) are shown as red lines; non-significant trends, as gray lines.









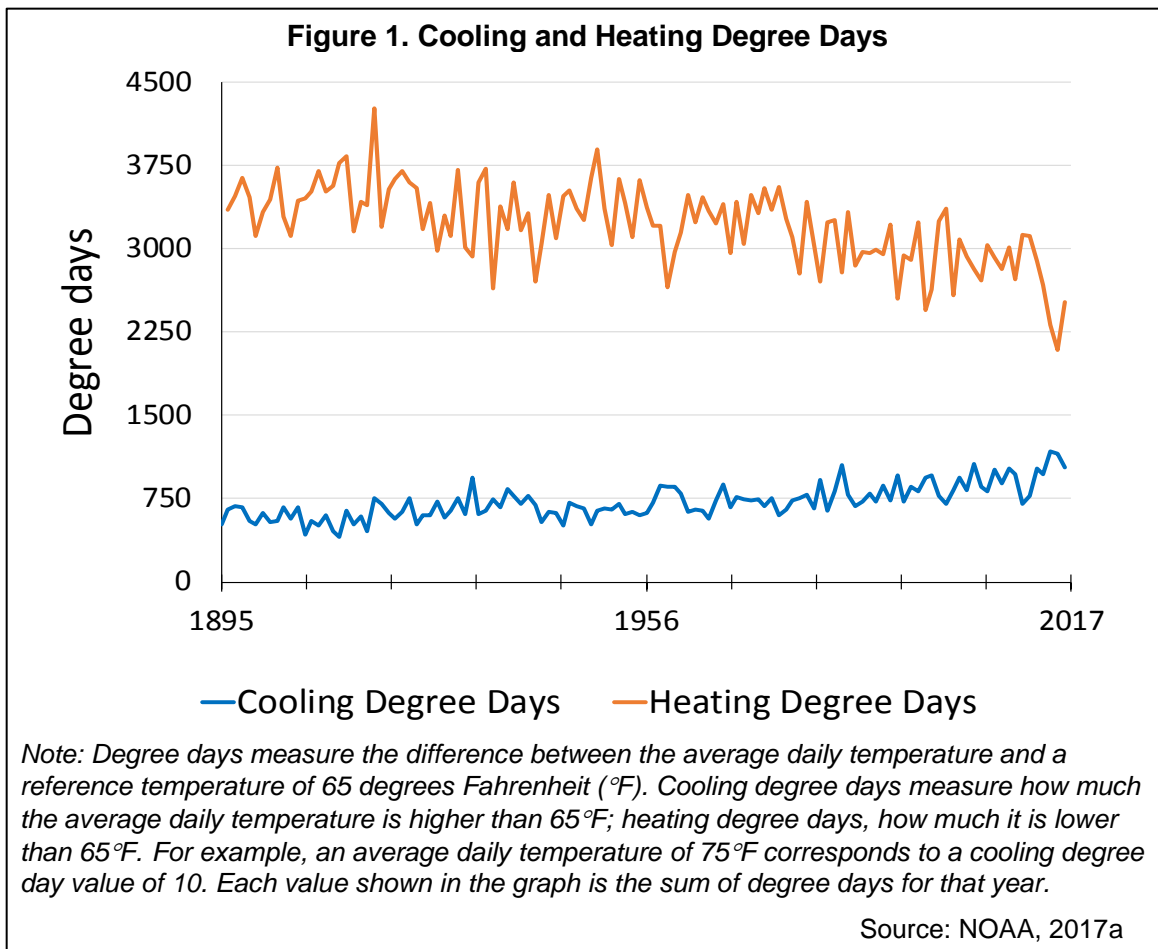


UC Davis, 2017



COOLING AND HEATING DEGREE DAYS

Average temperatures have increased in California over the past century. As a result, the energy needed to cool buildings during warm weather — measured by “cooling degree days” — has increased. The energy needed to heat buildings during cold weather — measured by “heating degree days” — has decreased.

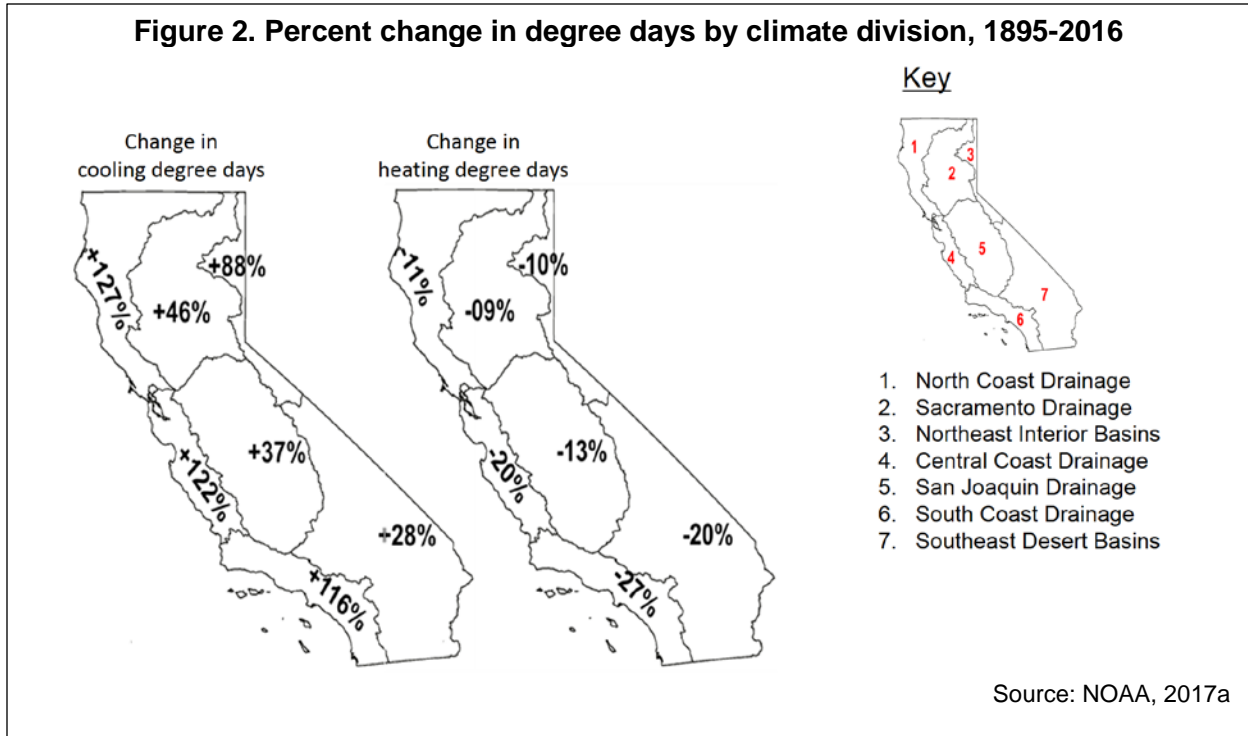


What does the indicator show?

Annual cooling degree days (CDD) in California increased between 1895 and 2016, while heating degree days (HDD) decreased over the same time period (Figure 1). Both trends are consistent with national trends (US EPA, 2016). The past few years have seen anomalously high ambient temperatures, as reflected in the unusually high CDDs and unusually low HDDs observed statewide and regionally. Trends in CDD and HDD for the seven California climate divisions as defined by the National Oceanic and Atmospheric Administration (NOAA)² are shown in Figures 2-5.

² Note: NOAA’s climate divisions span the contiguous United States, subdividing each state into ten or fewer climate divisions; other indicators in this report are based on data from the Western Regional Climate Center, which divides California into eleven climate regions.





All seven divisions show an increase in CDD and a decrease in HDD over the last century, but to varying extents (see Figure 2). Interestingly, coastal California shows greater increases in CDD over the last century compared to inland areas of the state. Larger declines in HDD are found in the Central Coast and South Coast, with the latter showing the greatest decrease. Graphs of degree days for each division are provided below in Figure 3 and 4.

California’s 100 million acres encompass diverse terrains and geographies with various climates. Not surprisingly, long-term trends in degree days show regional variations. Table 1 presents these trends in terms of the average annual change in heating and cooling days for the seven climate divisions.

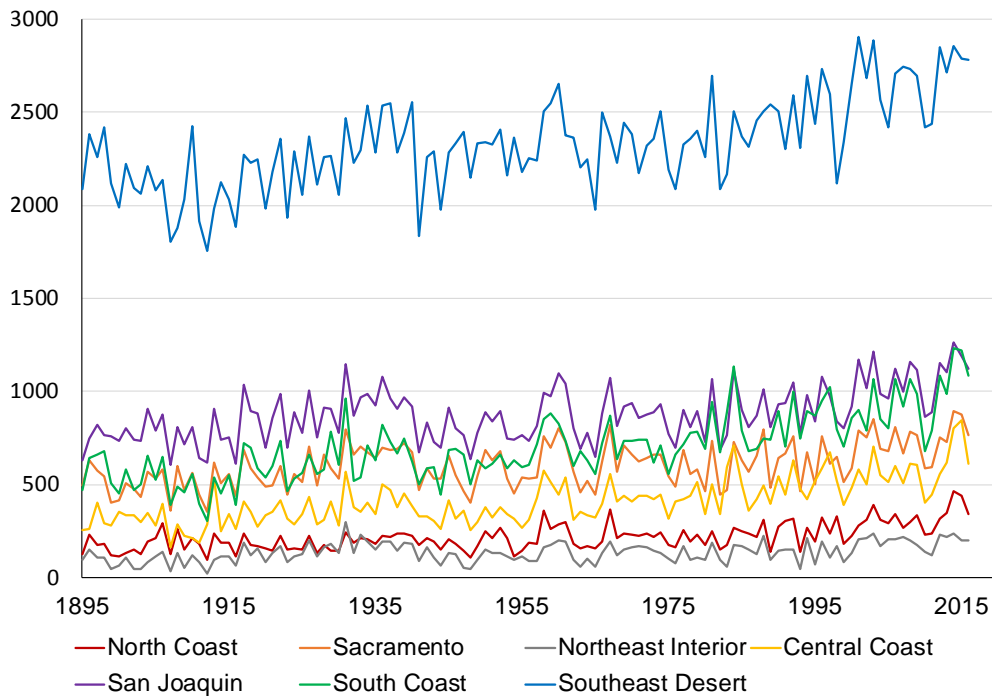
Table 1. Divisional Trends in Cooling and Heating Degree Days

Trends are presented for each of California’s climate divisions. Values presented are the slope of linear trends, representing the rate of change in cooling or heating degree days per year.

Climate Division	Trends, 1895-2016 (Degree Days per Year)	
	Cooling	Heating
Southeast Desert Basins	+4.7	-4.4
North Coast Drainage	+1.2	-5.1
Central Coast Drainage	+2.5	-6.0
South Coast Drainage	+3.8	-7.4
San Joaquin Drainage	+2.1	-4.3
Sacramento Drainage	+1.6	-3.6
Northeast Interior Basins	+0.6	-6.4

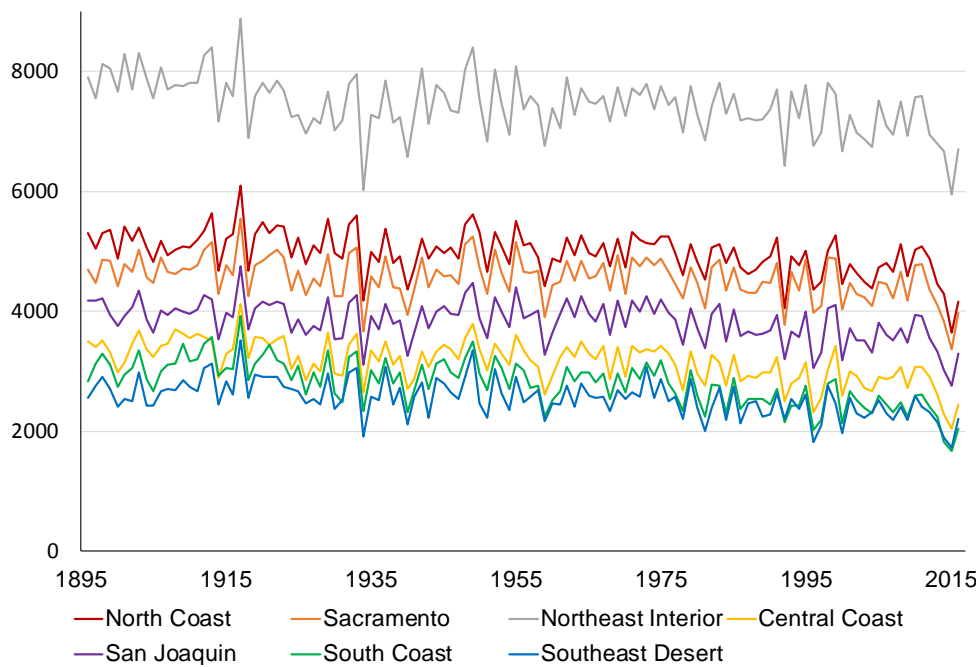


Figure 3. Cooling degree days by Division, 1895-2016



Source: NOAA, 2017a

Figure 4. Heating degree days by Division, 1895-2016



Source: NOAA, 2017a



Why is this indicator important?

The need to cool or heat indoor living spaces depends on the outdoor temperature. Warmer summers increase the need for air conditioning, and warmer winters decrease the need for heating. Measurements of degree days offer a way to track the demand for energy to cool homes and buildings (NOAA, 2005). They inform utility planning and construction decisions (USGCRP, 2014), along with other factors that influence energy demand including energy-efficient heating systems, cooling technologies, home insulation, behavior change, and population shifts (US EPA, 2016).

As the climate continues to warm, energy consumption will shift from cooler months to warmer months (CEC, 2015). Demand for air conditioning electricity will grow and demand for heating sources will shrink (US EPA, 2016). Space heating represents about 18 percent of average total household energy expenditures in California, while air conditioning represents 13 percent (US EIA, 2013).

Meeting a growing demand for air conditioning may require investments in new energy generation and distribution infrastructure and new ways to manage peak demand and system reliability (US EPA, 2016). At the same time, studies suggest climate change may hamper the ability to meet the increased demand in electricity for cooling. Warming temperatures, sea level rise, and wildfires can impact the operation or the efficiency of power plants, transmission networks, and natural gas facilities (US EPA, 2016; CEC, 2009, 2012; Patrick and Fardo, 2009). Climate change can also affect renewable energy, given its dependence on natural resources like water, wind, biomass and available incoming solar radiation which are all influenced by climate variations (CEC, 2009).

The increasing demand for cooling can impact communities in California. Although the state, on average, consumes less electricity per household than most of the nation, the higher electricity prices in California raise household electricity costs closer to the national average (US EIA, 2009). In addition, certain populations in California may face disproportionately greater impacts than other groups. Lower-income households are less likely to own air conditioners, making them more vulnerable to health effects of summer heat extremes. For households that do own air conditioners, the cost of energy associated with cooling represents a greater proportion of household income in lower income groups (CalEPA, 2010).

What factors influence this indicator?

Since heating and cooling degree days reflect trends in temperature, factors that influence temperature affect this indicator. These factors are discussed in the *Annual air temperature* indicator.

Technical Considerations

Data Characteristics

Degree day values were downloaded from an online NOAA database, Climate at a Glance, at <https://www.ncdc.noaa.gov/cag/> (NOAA, 2017b).



The values for degree days are derived by NOAA using daily temperature observations at major weather stations in the United States. A mean daily temperature (average of daily maximum and minimum temperatures) of 65°F serves as the reference temperature for degree day calculations. Cooling degree days are calculated by summing the positive differences between the mean daily temperature and the 65°F reference temperature. Heating degree days are calculated by summing the negative differences between the mean daily temperature and 65°F. Heating degree days during July 1 through June 30 and cooling degree days during January 1 through December 31 are added together to calculate total heating degree days per “heating year” and total cooling degree days per “cooling year,” respectively.

Long-term trends of degree days over time (1895 to 2016) for each climate division were analyzed with trendlines. Slopes of trendlines provided the rates of change in degree days per year for Table 1.

Strengths and Limitations of the Data

The nCLIMDIV dataset is an improved version of an older climate dataset from NOAA. It goes through quality assurance reviews and temperature bias adjustments and provides more robust values than its predecessor (NOAA, 2017b).

For more information, contact:



Guido Franco
California Energy Commission
1516 9th Street, MS-50
Sacramento, CA 95814
(916) 654-3940
Guido.Franco@energy.ca.gov

References:

CalEPA (2010). *Indicators of Climate Change in California: Environmental Justice Impacts*. Available at <http://oehha.ca.gov/media/downloads/risk-assessment/document/climatechangeej123110.pdf>

CEC (2009). *Potential Impacts of Climate Change on California's Energy Infrastructure and Identification of Adaptation Measures* (CEC-150-2009-001). California Energy Commission. Available at <http://www.energy.ca.gov/2009publications/CEC-150-2009-001/CEC-150-2009-001.PDF>

CEC (2012). *Our Changing Climate 2012: Vulnerability & Adaptation to the Increasing Risks from Climate Change in California* (CEC-500-2012-007). California Energy Commission. Available at <http://www.energy.ca.gov/2012publications/CEC-500-2012-007/CEC-500-2012-007.pdf>

CEC (2015). *2015 Integrated Energy Policy Report* (CEC-100-2015-001-CMF). California Energy Commission. Available at http://www.energy.ca.gov/2015_energy/policy/

NOAA (2005). NOAA National Weather Service Climate Prediction Center Degree Day Monitoring and Data: Explanation. Retrieved October 2016, from http://www.cpc.ncep.noaa.gov/products/analysis_monitoring/cdus/degree_days/ddayexp.shtml

NOAA (2017a). NOAA Climate at a Glance: U.S. Time Series. Retrieved March 2017, from <http://www.ncdc.noaa.gov/cag/time-series/us>



NOAA (2017b). NOAA Monitoring References: U.S. Climate Divisions. Retrieved November 2017, from <https://www.ncdc.noaa.gov/monitoring-references/maps/us-climate-divisions.php>

Patrick DR and Fardo SW (2009). Ch 7: Power Distribution Equipment. *In: Electrical Distribution Systems* (2nd ed). Lilburn, Georgia: The Fairmont Press, Inc.

US EIA (2009). *Household Energy Use in California*. U.S. Energy Information Administration. Available at https://www.eia.gov/consumption/residential/reports/2009/state_briefs/pdf/ca.pdf

US EIA (2013). *Residential Energy Consumption Survey*. U.S. Energy Information Administration. Available at <https://www.eia.gov/consumption/residential/data/2009/>

US EPA (2016). US Environmental Protection Agency: Climate Change Indicators in the United States. Retrieved December 15, 2017, from <https://www.epa.gov/climate-indicators>

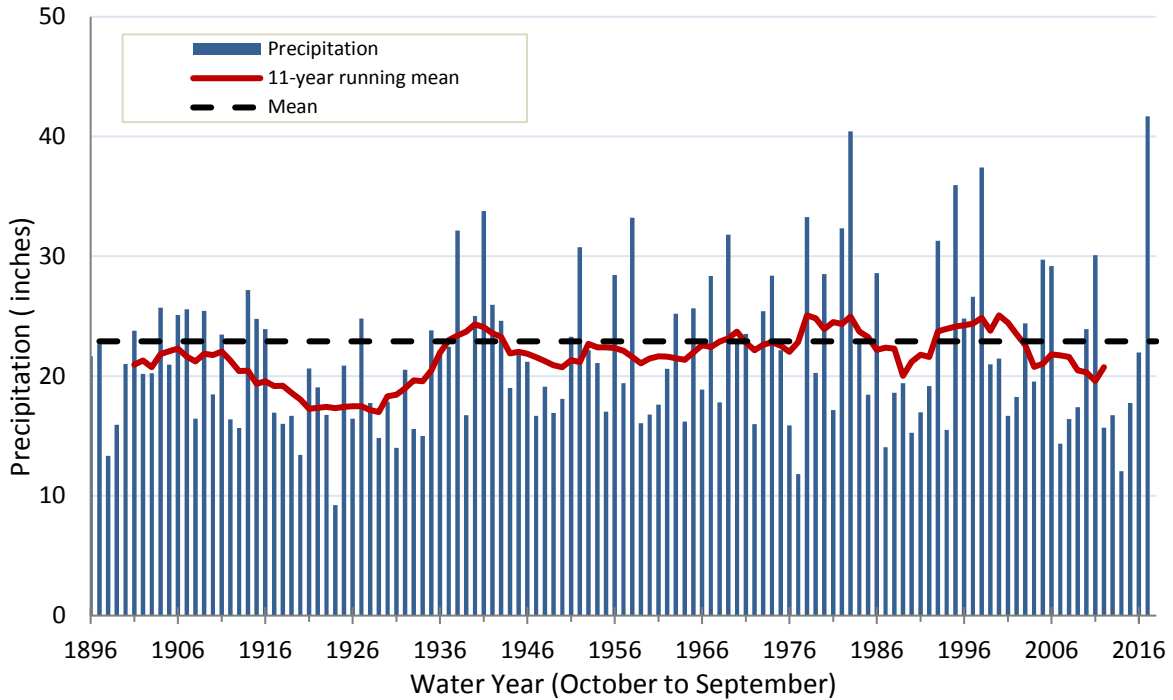
USGCRP (2014). U.S. Global Change Research Program National Climate Assessment. Retrieved December 15, 2017, from <http://nca2014.globalchange.gov/report>



PRECIPITATION

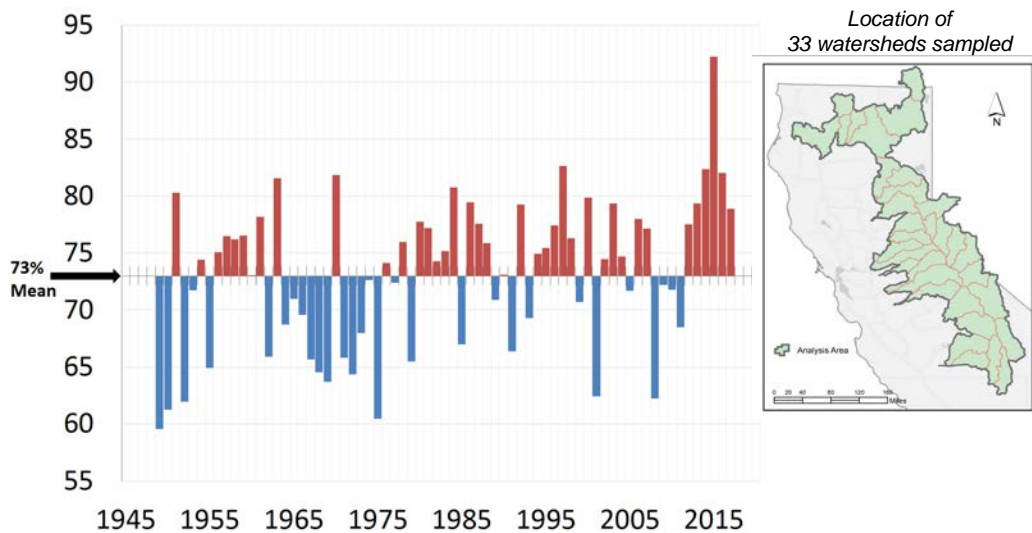
The total amount of precipitation varies greatly from year to year and statewide shows no apparent trend, however year to year variability has increased since 1980. In recent years, the fraction of precipitation that falls as rain over the watersheds that provide most of California's water supply has been increasing.

Figure 1. Statewide annual precipitation



Source: WRCC, 2017

Figure 2. Rain as percentage of total precipitation (1949-2017)



Red bars show years with a higher percentage of rain than the mean; blue bars have a lower percentage of rain than the mean.

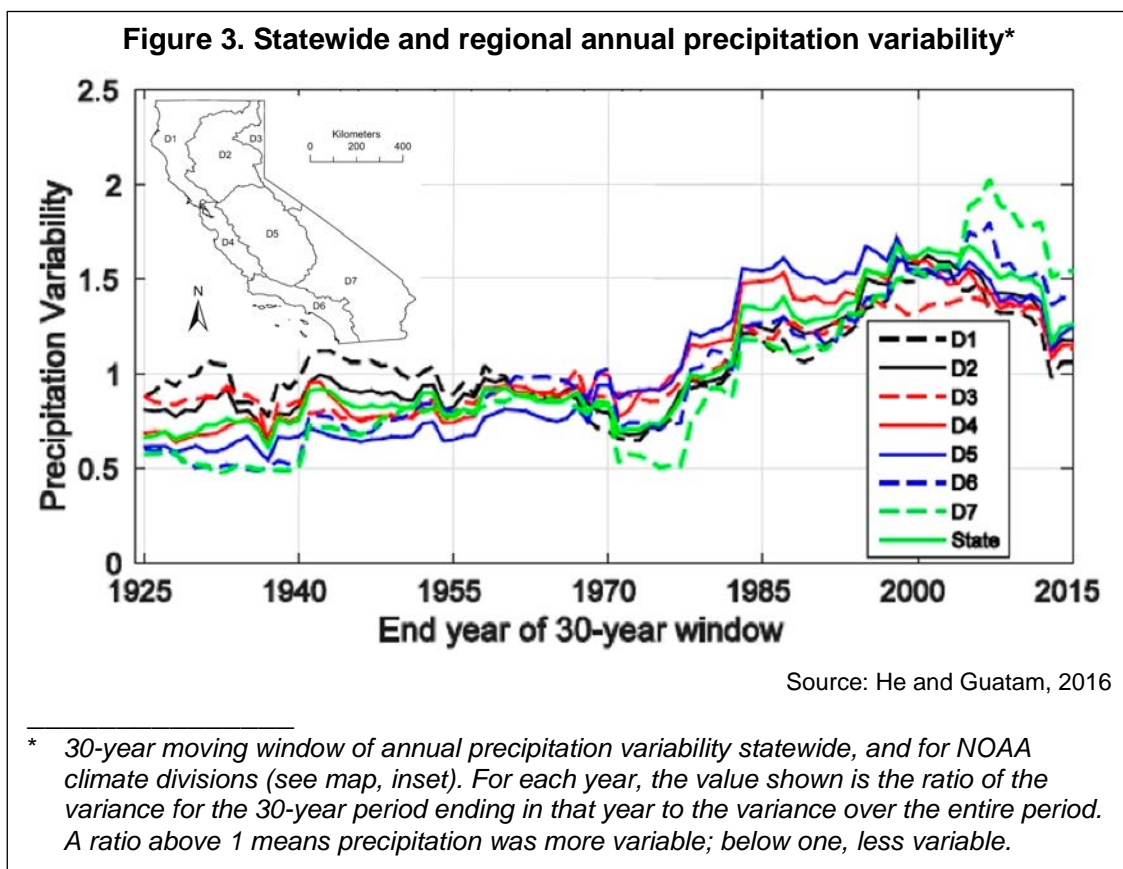
Source: DWR, 2017



What does the indicator show?

No clear trend is evident in the amount of annual precipitation. Statewide precipitation has been variable from year to year, with a consecutive dry then wet year occurring many times since 1895. Statewide precipitation is the area-weighted average of regional precipitation values. (In other words, the regional precipitation values — computed as an area-weighted average of precipitation at the climate stations in the region — are weighted by the area covered by each region, and an average calculated as the statewide value).

Variability in annual precipitation statewide and across the regions of the state has increased since the early 1980s, peaking in the late 1990s for most climate divisions (Figure 3) (He & Guatam, 2016). This shows that dry and wet precipitation extremes have become more frequent.



Since records began in 1895, statewide annual precipitation has ranged from a low of 9.4 inches in 1924 to a high of 41.66 inches in 2017. Precipitation in seven of the last ten years has been below the statewide average of 22.9 inches (the dashed line in Figure 1). The water years of 2012 to 2015 set a record for the driest consecutive four-year period of statewide precipitation.

With regard to physical state, precipitation lands on the surface as rain or snow depending on the temperature of the air and the ground, the local geography, and the



characteristics of the storm itself. Figure 2 shows the percentage of yearly precipitation falling as rain over the 33 watersheds that provide most of the state's water supply (see inset map). Each value shown represents the difference between that year's percentage of rain compared to the average for the entire period (1949 to 2016), which is 73 percent. Red bars show years with more rain than average (and thus less snow), and blue bars show years with less rain than average. While there is high year-to-year variability, recent years clearly show a trend toward more precipitation falling as rain. The 2015 water year, which had the lowest snowpack on record, also had the highest percentage of rain, at about 92 percent.

Why is this indicator important?

Precipitation, in the form of rain and snow, is the primary source of California's water supply. On average, 75 percent of the state's annual precipitation occurs from November through March, with 50 percent occurring from December through February. Precipitation totals are tracked by "water year," from the beginning of the rainy season in October through the following September, the end of the dry season.

Under climate change, more intense dry periods under warmer conditions are anticipated, leading to extended, more frequent drought in California. A higher proportion of precipitation falling as rain instead of snow and an increase in the duration, frequency, and intensity of warm, wet "atmospheric river" storms are also projected (see *What factors influence this indicator?*). In recent years, greater attention on atmospheric rivers has revealed their role in ending persistent droughts (Dettinger, 2013) and in producing large floods (Dettinger, 2011).

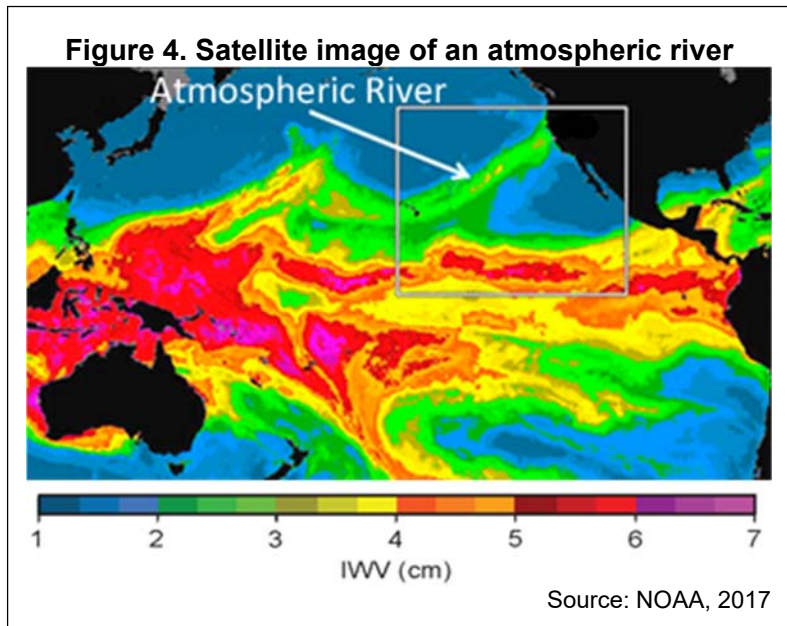
Tracking trends in the amount and physical state of precipitation, and in the patterns of storm events, is critical to water management in California. During warmer months, the state relies on snowpack melting from the Sierras to meet its water demand. The fraction of precipitation falling as rain significantly affects how much water is stored in snowpack. Information on trends plays an important role in balancing the multiple water management objectives of reservoir operations, including storage and flood protection. Historical trends help inform short-term water management planning, and provide the basis for future projections.

What factors influence this indicator?

Global scale weather patterns bring moisture to California, primarily from the Pacific Ocean. Most of the water vapor that provides the state's precipitation comes from the Pacific Ocean. The variability in the state's precipitation is related to El Niño and La Niña in the tropical Pacific, and to conditions in the northern Pacific and near Indonesia. Ocean conditions change slowly, over periods of months to years to decades, with similarly prolonged effects on adjacent land.



Atmospheric rivers, mentioned above, represent an important feature of California's precipitation. These storms provide 30 to 50 percent of California's annual precipitation, and 40 percent of the Sierra Nevada snowpack. Atmospheric rivers are long, narrow bands of water vapor, greater than 1,000 miles long and typically about 250 to 370 miles wide, that originate over the Pacific Ocean (see Figure 4; colors represent the amount of water vapor, or IWV). A natural part of the global water cycle, these constantly moving atmospheric rivers are responsible for most of the horizontal transport of water vapor outside of the tropics (NOAA, 2017).



In California's Mediterranean climate, summers are typically dry. In the southeastern desert regions, including the Sonora and Mojave deserts, some monsoonal activity in the summertime may bring thunderstorm precipitation. Summers are characterized by a blocking high pressure zone that diverts atmospheric moisture away from the state. Precipitation deficits during the recent drought have been associated with a prominent region of high pressure nicknamed the "ridiculously resilient ridge" that diverted storm tracks northward during California's rainy season in 2012 to 2015 (Swain, 2015).

Local terrain influences precipitation. For example, as the atmosphere is pushed up the slope of a mountain range, the water vapor cools and condenses if the air is moist enough. This often forms clouds on the upslope and over the mountain crest, and can cause precipitation to fall. This phenomenon is called orographic forcing.

Average annual precipitation varies greatly among California's eleven climate regions, as defined by the Western Regional Climate Center: from 4.4 inches in the Sonora Desert to 64.4 inches in the North Coast. As with statewide precipitation, annual variability has increased across most regions, peaking in the late 1990s, except in Southern California (which includes the South Coast, South Interior, Mojave Desert and Sonoran Desert regions) where it peaked in 2007 (He and Guatam, 2016). Regional graphs are shown in the appendix.

In the Sierra Nevada, the last 35 years have brought some of the wettest and driest winters, including several multi-year wet and dry periods. Dry years since and including 1976-77 have approached the driest single year ever recorded in 1924; two of the past ten years, 2014 and 2015 were among the ten driest years (third and eighth,



respectively). Snowpack in the Sierra Nevada provides natural water storage for California, therefore precipitation in this area has major statewide impacts and draws intense interest.

Technical Considerations

Data Characteristics

Data are from the California Climate Tracker, an operational database tracker for weather and climate monitoring information. This indicator tracks precipitation amount in a “water year” defined as October 1 to September 30. This is more useful than a calendar year in California due to the typically dry summer and wet winter (“Mediterranean”) climate. This operational product, the California Climate Tracker, is updated monthly online at the Western Regional Climate Center <http://www.wrcc.dri.edu/monitor/cal-mon/index.html>. Software and analyses were produced by Dr. John Abatzoglou (Abatzoglou et al., 2009).

Precipitation data for nearly 200 climate stations in the NOAA Cooperative Network (COOP) within California were obtained from the Western Regional Climate Center database archive of quality controlled data from National Climatic Data Center. For this study, COOP data from 1948-2007 were utilized. Gridded climate data from Parameter-elevation Regressions on Independent Slopes Model (Daly et al., 1997) was acquired from the PRISM group at Oregon State University for the period 1895-2007. PRISM provides complete spatial coverage of the state, where the station data serve to fill in recent data, until PRISM is processed each month. Because climate stations are not evenly spaced, the PRISM data are used to provide even and complete coverage across the state. These are combined to create a time series of annual statewide precipitation dating back to 1895.

Strengths and Limitations of the Data

The datasets used in this work were subjected to their own separate quality control procedures, to account for potentially incorrect data reported by the observer, missing data, and to remove inconsistencies such as station relocation or instrument change. The PRISM data offers complete coverage across the state for every month of the record. Limitations include the bias of station data toward populated areas, and limited ability of quality control processes in remote or high terrain areas. The results cited here offer a hybrid using both gridded and station data, which is suggested to be more robust than either data set used independently (Abatzoglou et al., 2009).

For more information, contact:



Michael Anderson, Ph.D., P.E.
State Climatologist
California Department of Water Resources
Division of Flood Management
3310 El Camino Ave Rm 200
Sacramento, CA 95821
(916) 574-2830
Michael.L.Anderson@water.ca.gov



References:

Abatzoglou JT, Redmond KT and Edwards LM (2009). Classification of regional climate variability in the state of California. *Journal of Applied Meteorology and Climatology* **48**(8): 1527-1541.

Daly C, Taylor G and Gibson W (1997). *The PRISM approach to mapping precipitation and temperature. 10th Conference on Applied Climatology*. American Meteorological Society. Available at <http://citeseerx.ist.psu.edu/viewdoc/summary?doi=10.1.1.730.5725>

Dettinger MD (2013). Atmospheric rivers as drought busters on the U.S. west coast. *Journal of Hydrometeorology* **14**: 1721-1732.

Dettinger MD (2011). Climate change, atmospheric rivers, and floods in California-A multimodel analysis of storm frequency and magnitude changes. *Journal of the American Water Resources Association* **47**: 514-523.

DWR (2015). *California's Most Significant Droughts: Comparing Historical and Recent Contributions*, California Department of Water Resources. February 2015. Available at http://www.water.ca.gov/waterconditions/docs/California_Significant_Droughts_2015_small.pdf

DWR (2017). *Water Year 2017*, California Department of Water Resources. September 2017. Available at <http://water.ca.gov/waterconditions/docs/2017/Water%20Year%202017.pdf>

He M and Guatam M (2016). Variability and trends in precipitation, temperature and drought indices in the state of California. *Hydrology* **3**(2): 14.

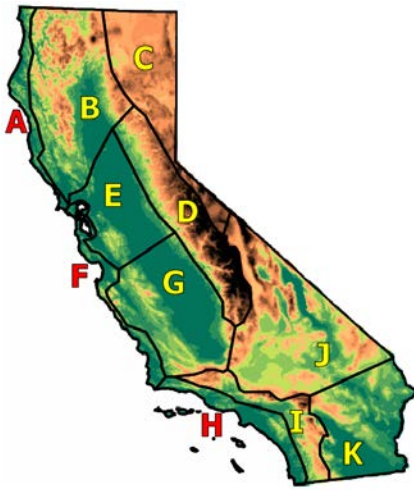
NOAA (2017). Atmospheric River Q&A. National Oceanic and Atmospheric Administration. Retrieved August 7, 2017 from <https://www.esrl.noaa.gov/psd/atmrivers/questions/>

Swain DL (2015). A tale of two California droughts: Lessons amidst record warmth and dryness in a region of complex physical and human geography, *Geophysical Research Letters* **42**: 9999-10,003.

WRCC (2017). "California Climate Tracker," Western Regional Climate Center. Retrieved November 14, 2017 from <http://www.wrcc.dri.edu/>



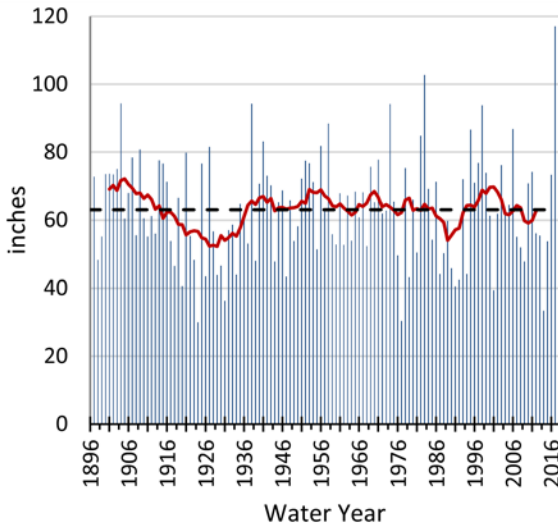
APPENDIX. Regional precipitation trends in California's climate regions (as defined by the Western Regional Climate Center)



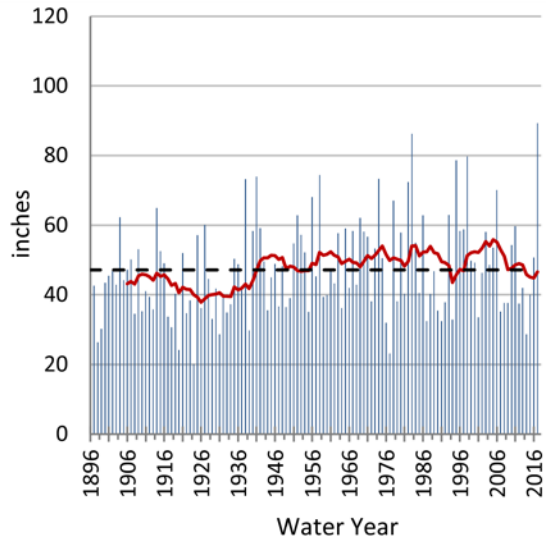
Region	Average precipitation (inches)
A. North Coast	64.4
B. North Central	51.0
C. Northeast	23.8
D. Sierra	39.2
E. Sacramento-Delta	19.7
F. Central Coast	25.2
G. San Joaquin Valley	12.5
H. South Coast	17.4
I. South Interior	17.8
J. Mojave Desert	7.3
K. Sonoran Desert	4.4
Statewide	22.9

Source: WRCC, 2017

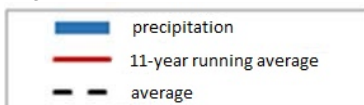
North Coast Region



North Central Region



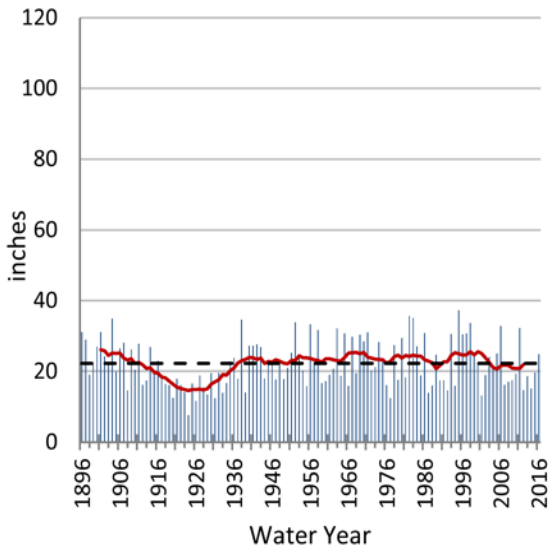
Legend



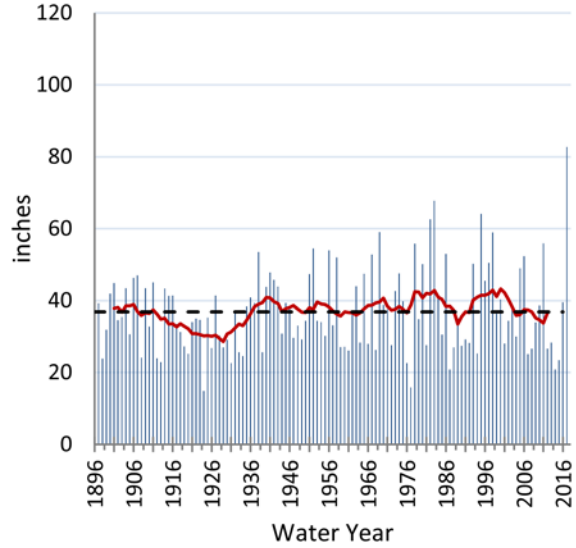
Source: WRCC, 2018



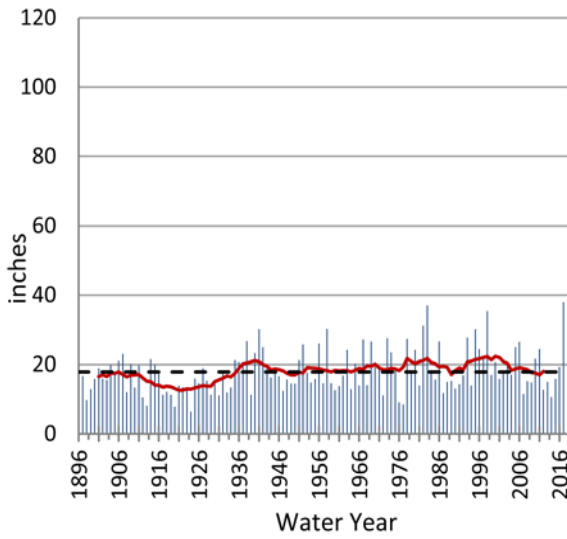
Northeast Region



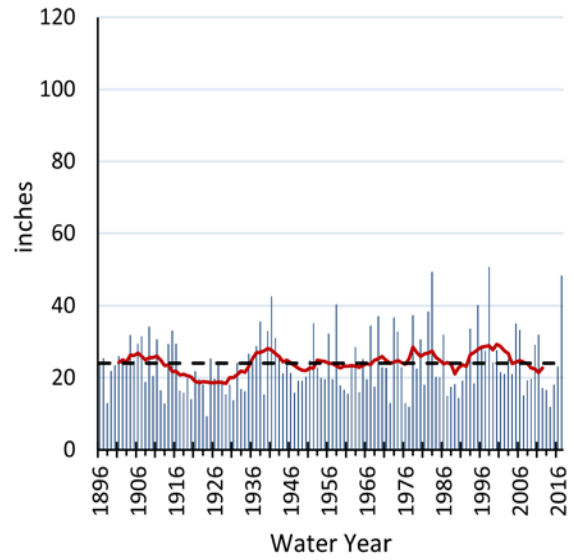
Sierra Region



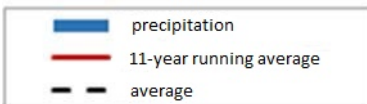
Sacramento Delta Region



Central Coast Region



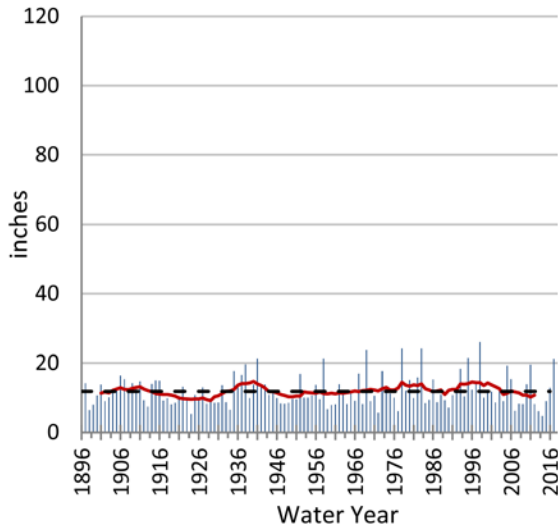
Legend



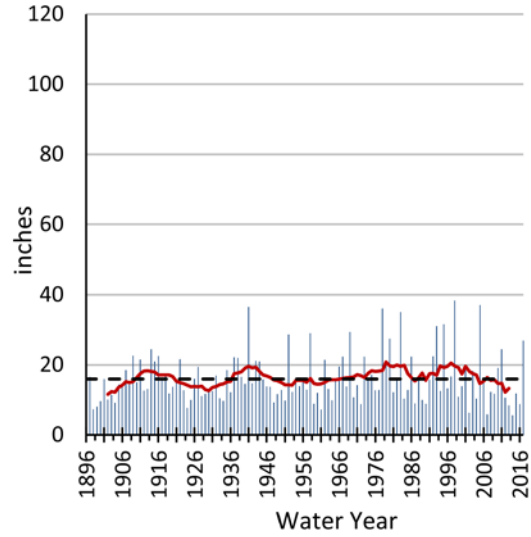
Source: WRCC, 2018



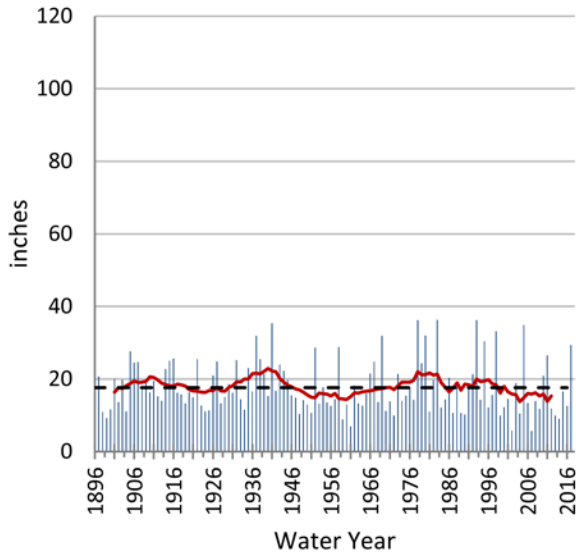
San Joaquin Region



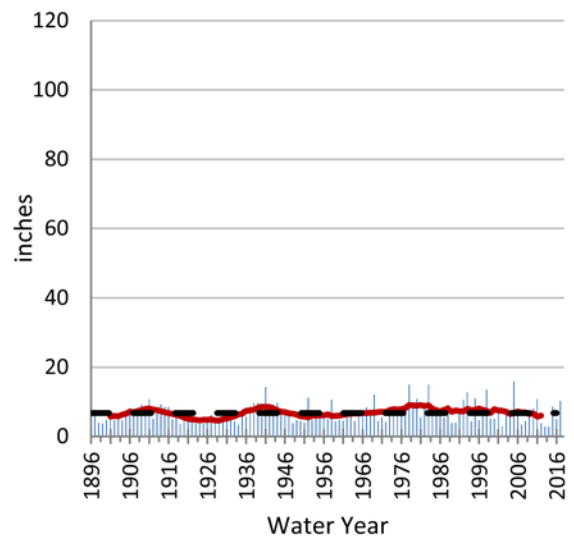
South Coast Region



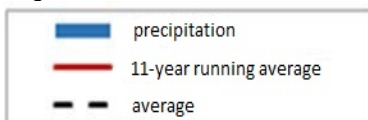
South Interior Region



Mojave Region



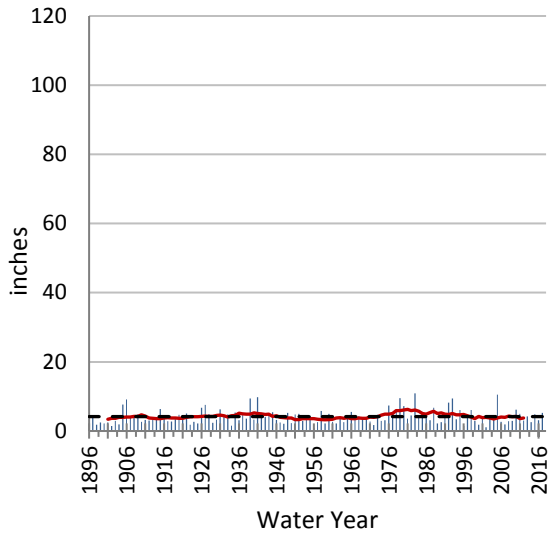
Legend



Source: WRCC, 2018

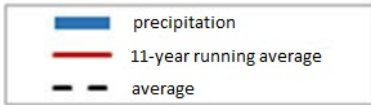


Sonoran Desert Region



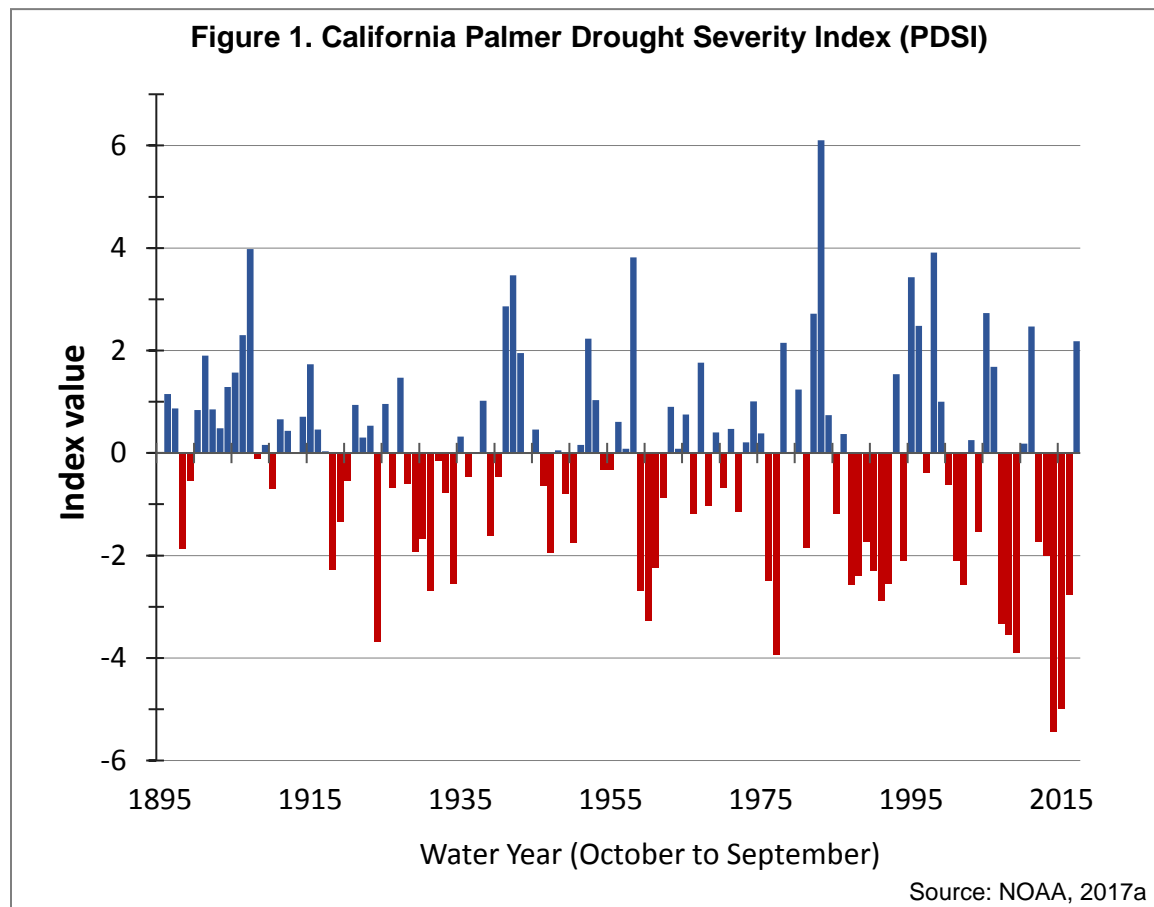
Source: WRCC, 2018

Legend



DROUGHT

Over the past 120 years, California has become increasingly dry. The most recent drought from 2012 to 2016 was the most extreme since instrumental records began. Extraordinarily high precipitation in 2017 ended the drought.



What does the indicator show?

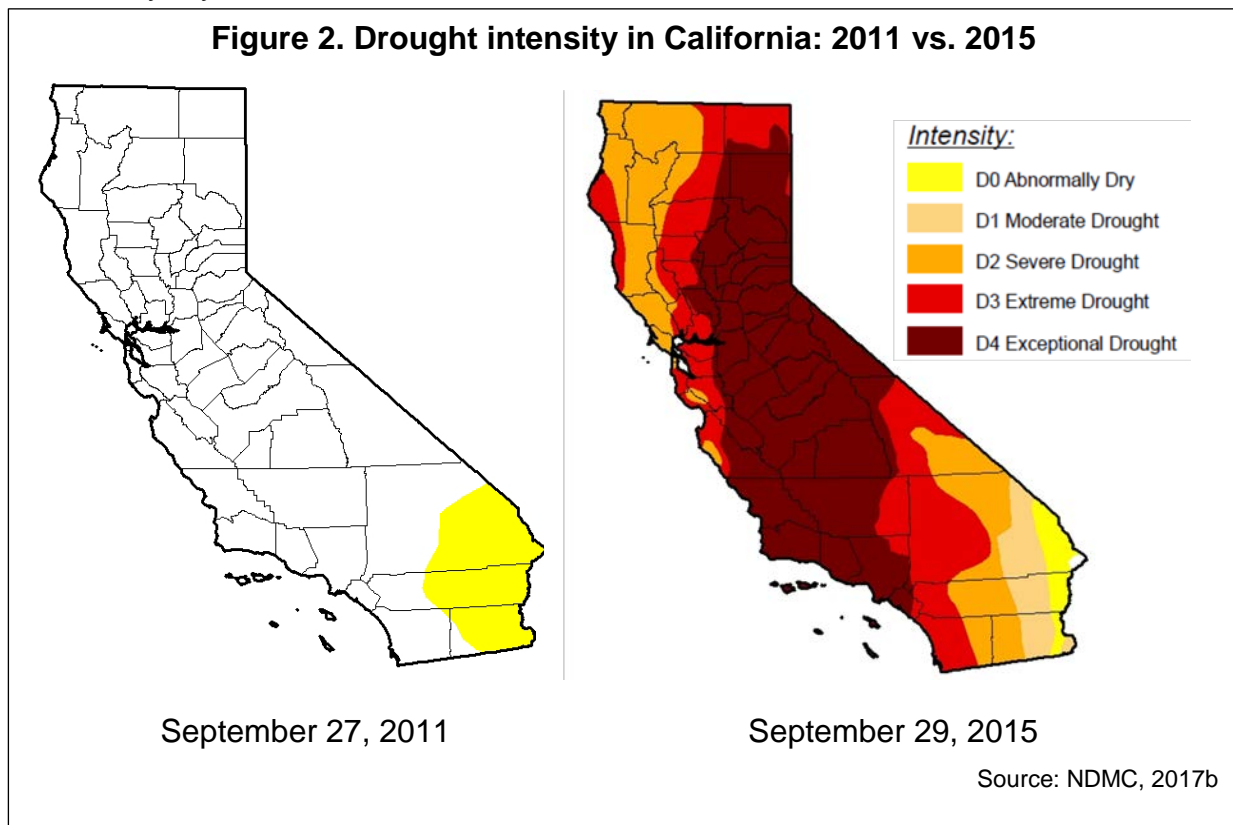
Droughts are generally thought of as periods of unusually dry weather that last long enough to cause a shortage of water (IPCC, 2014). Figure 1 shows values for the Palmer Drought Severity Index (PDSI) over the past 120 years: positive values (blue bars) indicate “wet” years; negative values (red bars) are “dry” years. Although drought can be defined in multiple ways and tracked using different metrics, the PDSI is a universally used indicator of drought; it measures relative dryness of a region using readily available temperature and precipitation data and local available water content of the soil (NDMC, 2017a). Values below -3 represent severe to extreme drought. Five of the eight years when PDSI values fell below -3 were between 2007 and 2016, with unprecedented dry years in 2014 and 2015.

As noted above, from 2012 to 2016, California experienced the most extreme drought since instrumental records began in 1895 (AghaKouchak et al., 2014; Diffenbaugh et al., 2015; Griffin and Anchukaitis, 2014; Robeson, 2015; Swain et al., 2014; Williams et al., 2015). It was possibly the most extreme for a millennium or more (Griffin and



Anchukaitis, 2014; Robeson, 2015). This drought occurred at a time of record warmth — 2014 is the warmest year on record, followed by 2015 — accompanied by record low snowpack, less than 5 percent of average in 2015. In response to the drought, a State of Emergency was declared in 2014 (<https://www.gov.ca.gov/news.php?id=18368>). Other periods of major droughts in California include 1929-1934, 1976-1977, and 1987-1992 (DWR, 2015). The drought ended with unusually high precipitation in 2017; however, because precipitation is only one component of PDSI (temperature and soil moisture are two others), an unusually high precipitation value does not necessarily result in an equally high PDSI value, particularly given the unusually hot temperatures in 2016 and 2017.

The maps in Figure 2 compare the intensity of the drought in 2015 to conditions in 2011 (NDMC, 2017b). Drought conditions fall under one of five drought categories, from least intense (“D0, abnormally dry”) to most intense (“D4, exceptional drought”). These categories are based on five key indicators, including PDSI and measures of soil moisture, streamflow and precipitation; they also incorporate numerous supplementary indicators including drought impacts (such as on crops, pastures and water supply) and local reports from expert observers. In 2015, the entire state was under one of the five drought categories, with almost half of the state’s area (46 percent) in the “exceptional drought” category. By comparison, in 2011 only 11 percent of the state was considered “abnormally dry.”



Why is this indicator important?

Droughts have major environmental, social, and economic repercussions, affecting the availability of water both for human use — such as urban uses (including drinking), agriculture, hydroelectricity generation — and for ecosystems. People most reliant on annual rainfall are generally the first to feel the impacts of drought. A single dry year can impair activities like dryland farming or livestock grazing that depend on unmanaged water supplies (DWR, 2015).

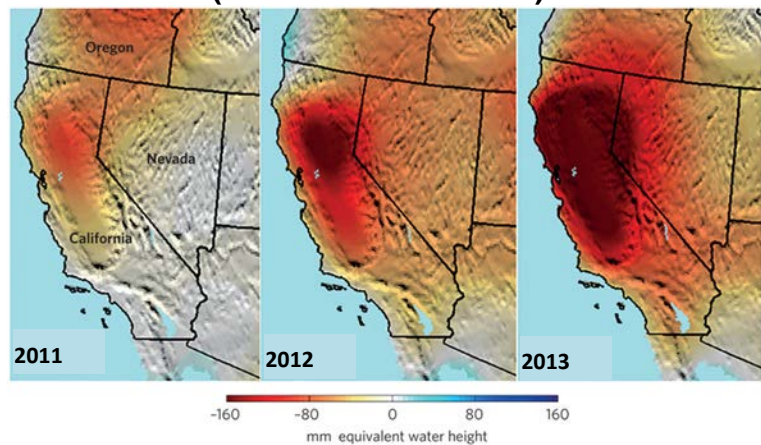
Drinking water shortages primarily occur among small drinking water systems. By late 2015, more than 100 small water systems lacked enough water and more than 2,000 domestic wells went dry, particularly in the Central Valley and Sierra Nevada foothills (PPIC, 2016). Drinking water shortages place a disproportionate burden on lower income households, as financial costs of water services tend to rise during droughts (Famiglietti, 2014; Feinstein et al., 2017).

Drought also impacts the generation of hydroelectricity, a major source of power in California. Hydroelectricity, which is dependent on snowmelt runoff and rainfall, costs less than most other forms of electricity, produces no greenhouse gases, and helps satisfy peak energy demands (Gleick, 2016). In 2014, the state's driest year, hydroelectric power generation provided 6 percent of the in-state electricity generation, down from 12 percent in 2013 (CEC, 2017). The total reductions in hydroelectricity generation during the recent drought may have increased state electricity costs by about \$2.0 billion (Gleick, 2016).

Negative economic impacts on California's agricultural sector as a whole from the recent drought were significant (Howitt et al., 2014 and 2015). Impacts included abandoned orchards and vineyards, fallowed land (more than 500,000 acres, or 6 percent of irrigated acreage, were fallowed in 2015), and lost jobs (DWR, 2015; PPIC, 2016). The livelihoods of many farmworkers disappeared (Swain, 2015).

Approximately 30 to 46 percent of the state's total water supply comes from groundwater (DWR, 2017a). Reliance on groundwater increases during droughts. Between 2011 and 2016, groundwater levels decreased by at least 10 feet in over 40 percent of monitored wells in the state (DWR, 2017b). Figure 3 illustrates how groundwater levels in California significantly dropped between 2011 and 2013 (Famiglietti, 2014).

Figure 3. Groundwater storage anomalies (relative to 2005-2010)



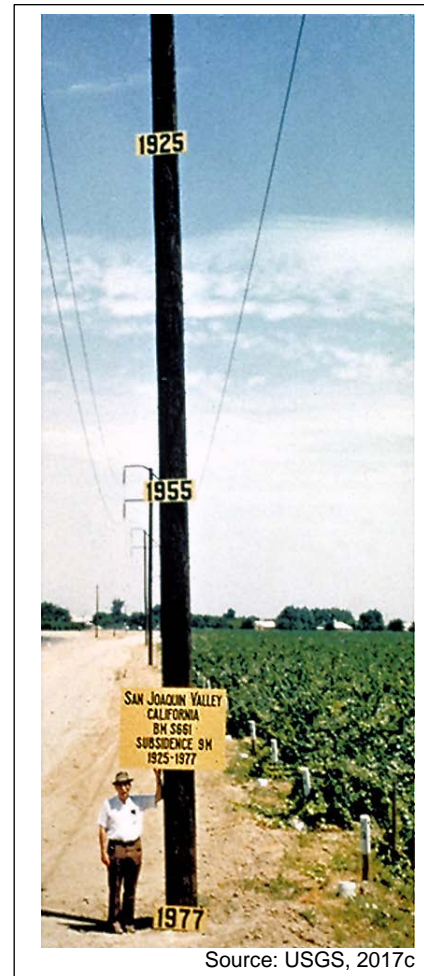
Maps of dry season (September-November) total water storage anomalies (mm equivalent water height, anomalies with respect to 2005-2010), constructed using data from NASA's Gravity Recovery and Climate Experiment satellite mission.

Source: Famiglietti, 2014



Over pumping of groundwater results in aquifer compaction, reducing its water-holding capacity, and land subsidence (i.e., the land surface sinks). Land subsidence can impact infrastructure — including water conveyance systems, roads, railways, bridges — aquifer storage capacity, and land topography (USGS, 2017a and 2017b).

The San Joaquin Valley, one of the most productive agricultural regions in the nation, has been impacted by the over pumping of groundwater. Starting in the early 1900s, farmers relied on groundwater for water supply. By 1970, about half of San Joaquin Valley experienced land subsidence. Some areas had dropped by as much as 28 feet. Reduced surface water availability during 1976-77, 1986-92, 2007-09, and 2012-2015 caused even more groundwater pumping. The photograph on the right from the San Joaquin Valley shows the approximate height of the land surface in 1925 compared to much lower levels in 1955 and 1977 as a result of excessive groundwater pumping.



Droughts can harm aquatic ecosystems. During the latest drought, rivers in California experienced record-low flows and poor water quality. Various coastal and mountain streams that are home to native fish like salmon and steelhead dried up. Rivers below Central Valley dams deteriorated. As many as 18 native fish species may face extinction with continued drought, which could put other species at risk of extinction. In addition, water shortages in wildlife refuges in the Central Valley and Klamath Basin during the recent drought forced birds to gather in smaller areas, making them more vulnerable to disease outbreaks and predation (PPIC, 2016).

Droughts produce drier-than-normal conditions that can increase the intensity and severity of wildfires (USGS, 2017a). Droughts and wildfires, in combination with altered land cover, disease, and human activity, can contribute to expanding or contracting vegetation ranges. Forests may convert to shrubland and grassland. Die-offs in whitebark pine in the Sierra Nevada and conifers in southern California have been related to drought. A rapid redistribution of coniferous and broadleaf species occurred in the mountains of southern California during droughts in the early 2000s (Clark et al., 2016). Droughts can contribute to bark beetle outbreaks, which cause tree mortality. Between 2010 and late 2015, aerial surveys conducted by the US Forest Service found that around 40 million trees had died in California. Nearly three quarters of this total died from drought and insect infestation from September 2014 to October 2015 alone (Tree



Mortality Task Force, 2017). Droughts also affect most ecosystem services provided by forests, including carbon storage (Clark et al., 2016).

Finally, drought may affect human health by altering patterns of certain diseases like West Nile (see *Vector-borne diseases* indicator), and by increasing air pollution from wildfires and dust storms, (DWR, 2015; see *Wildfires* indicator). These drought-related changes potentially can impact respiratory health (CDC, 2016). Interestingly, however, a study by Berman et al. (2017) found a lowered incidence of hospital admissions for respiratory illness among older people in the western US during drought periods compared to non-drought periods. The reduced incidence of respiratory admissions may be due to less exposure to pollen and allergenic spores during dry spells. In the same study, California had an overall decreased risk of mortality among the elderly during drought. Counties in the western US that have less frequent droughts showed significantly greater risks for cardiovascular admissions and mortality when droughts occurred. Another study found that the stress caused by drought may induce anxiety, depression, or other adverse mental health outcomes for some people (Vins et al., 2015).

What factors influence this indicator?

Droughts in California are influenced by the El Niño-Southern Oscillation, regional atmospheric pressure anomalies, and “drought-busting” atmospheric rivers (Griffin and Achukaitis, 2014; Dettinger, 2013). Historically dry winters in California have been associated with a ridge of high atmospheric pressure off the west coast, and wet winters have been associated with a trough off the west coast and an El Niño event. A study using climate change models and observational data found the precipitation deficit during the most recent drought to be dominated by natural variability, although sea surface temperatures were found to also play a role (Seager et al., 2015).

While precipitation is a main driver of drought variability, a growing body of evidence suggests that anthropogenic warming has increased the likelihood of extreme droughts in the state (AghaKouchak et al., 2014; Williams et al., 2015; Diffenbaugh et al., 2015; Shukla et al., 2015; Swain et al., 2014). Climate change has increased the chances of co-occurring temperature and precipitation conditions that have historically led to drought in California (Diffenbaugh et al., 2015). In fact, a combination of record high temperatures and low (but not unprecedented) precipitation contributed to the severity of the recent drought (Griffin and Achukaitis, 2014). Anthropogenic warming has been linked to the unusually intense atmospheric pattern that initiated the dry 2013-2014 winter in California (Wang et al., 2014). Mao et al. (2015) determined that the effect of anthropogenic warming in the winter of 2013-2014, although modest, likely exacerbated drought conditions. In the future, climate change is expected to continue to make dry and warm years happen more often (Diffenbaugh et al., 2015). More heat from climate change will likely increase the rate of drying, which will further exacerbate drought (Trenberth et al., 2014).

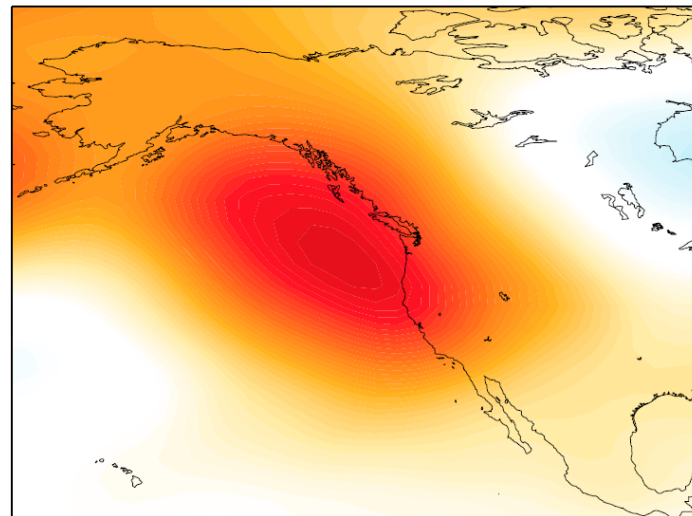
Atmospheric circulation patterns like those observed during California’s most extreme dry and hot years have increased during recent decades (Swain et al., 2016). In



particular, patterns characterized by a persistent ridge near the West Coast of North America — similar to those during the latter half of the most recent drought — have occurred more frequently; these patterns lead to both extremely low precipitation and extremely warm temperatures.

In 2012-2015, a region of atmospheric high pressure, nicknamed the “ridiculously resilient ridge” (see Figure 5) resulted in a northward shift in the Pacific storm track during the rainy season, preventing storms from reaching California. Studies (such as Swain et al., 2014 and Wang et al., 2014) suggest that climate change may be increasing the likelihood of the type of rare atmospheric event associated with the recent and unusually severe drought California.

Figure 5. The “ridiculously resilient ridge”



Oct-May 500mb geopotential height anomaly, meters

-45 -40 -35 -30 -25 -20 -15 -10 -5 0 5 10 15 20 25 35 40 45

Colors represent the mean cool season 500mbar geopotential height anomaly (meters) over four consecutive years (i.e., October–May 2012, 2013, 2014, and 2015).

Source: Swain, 2015

Technical Considerations

Data Characteristics

PDSI identifies droughts by incorporating data on temperature, precipitation, and the water-holding capacity of soil. The index takes into consideration moisture received as precipitation and moisture stored in the soil, accounting for potential loss of water due to temperature. It originally functioned to identify drought affecting agriculture but has since been used to identify drought associated with other types of impacts (WMO and GWP, 2016). PDSI is used to assess long-term drought patterns (NOAA, 2017b).

Strengths and Limitations of the Data

Considered a robust index of drought, PDSI is universally used and has been employed since the 1960s. However, PDSI assumes all precipitation comes as rain (Williams et al., 2015) and does not account for frozen precipitation or frozen soils very well (WMO and GWP, 2016). PDSI also does not provide information on human water demand, streamflow and reservoir storage, or groundwater accessibility (Williams et al., 2015).

Another metric for drought, the Palmer Hydrological Drought Index (PHDI), accounts for longer-lasting dryness that can perturb water storage, streamflow, and groundwater (WMO and GWP, 2016). It measures hydrological impacts, including reservoir levels and groundwater data, and responds more slowly to changing conditions than the PDSI (NOAA, 2017b). It does not account for human influences like irrigation or management practices (WMO and GWP, 2016).



For more information, contact:



Michael L. Anderson, Ph.D., P.E.
State Climatologist
California Department of Water Resources
Division of Flood Management
3310 El Camino Ave Rm 200
Sacramento, CA 95821
(916) 574-2830
Michael.L.Anderson@water.ca.gov

References:

- AghaKouchak A, Cheng L, Mazdidasni O and Farahmand A (2014). Global warming and changes in risk of concurrent climate extremes: Insights from the 2014 California drought. *Geophysical Research Letters* **41**: 8847–8852.
- Berman JD, Ebisu K, Peng RD, Dominici F and Bell ML (2017). Drought and the risk of hospital admissions and mortality in older adults in western USA from 2000 to 2013: A retrospective study. *The Lancet Planetary Health* **1**(1): e17-e25.
- CDC (2016). Centers for Disease Control and Prevention: Drought and Your Health. Retrieved November 11, 2017, from <https://www.cdc.gov/features/drought/>
- CEC (2017). California Energy Commission: Hydroelectric power in California. Retrieved December 14, 2017, from <http://www.energy.ca.gov/hydroelectric/>
- Clark JS, Iverson L, Woodall CW, Allen CD, Bell DM, et al. (2016). The impacts of increasing drought on forest dynamics, structure, and biodiversity in the United States. *Global Change Biology* **22**(7): 2329-2352.
- Dettinger MD (2013). Atmospheric rivers as drought busters on the U.S. west coast. *Journal of Hydrometeorology* **14**: 1721-1732.
- Diffenbaugh NS, Swain DL and Touma D (2015). Anthropogenic warming has increased drought risk in California. *Proceedings of the National Academy of Sciences* **112**(13): 3931-3936.
- DWR (2015). *California's Most Significant Droughts: Comparing Historical and Recent Conditions*. California Department of Water Resources. Sacramento, CA. Available at https://www.water.ca.gov/LegacyFiles/waterconditions/docs/California_Significant_Droughts_2015_small.pdf
- DWR (2017a). California Department of Water Resources: Groundwater Information Center. Retrieved November 15, 2017, from <http://www.water.ca.gov/groundwater/gwinfo/>
- DWR (2017b). California Department of Water Resources: Groundwater Level Change – Fall 2011 to Fall 2016. Retrieved November 15, 2017, from http://www.water.ca.gov/groundwater/maps_and_reports/MAPS_CHANGE/DOTMAP_F2016-F2011.pdf
- Famiglietti JS (2014). The global groundwater crisis. *Nature Climate Change* **4**: 945-948.
- Feinstein L, Phurisamban R, Ford A, Tyler C and Crawford A (2017). *Drought and Equity in California*. Pacific Institute. Oakland, CA. Available at http://pacinst.org/wp-content/uploads/2017/01/PI_DroughtAndEquityInCA_Jan_2017.pdf



Gleick PH (2016). *Impacts of California's Ongoing Drought: Hydroelectricity Generation – 2015 Update*. Pacific Institute. Oakland, CA. Available at <http://pacinst.org/wp-content/uploads/2016/02/Impacts-Californias-Ongoing-Drought-Hydroelectricity-Generation-2015-Update.pdf>

Griffin D and Anchukaitis KJ (2014). How unusual is the 2012–2014 California drought? *Geophysical Research Letters* **41**: 9017–9023.

Howitt R, Medellín-Azuara J, MacEwan D, Lund J, and Sumner D (2014). *Economic Analysis of the 2014 Drought for California Agriculture*. UC Davis Center for Watershed Science. Davis, CA. Available at https://watershed.ucdavis.edu/files/biblio/DroughtReport_23July2014_0.pdf

Howitt R, MacEwan D, Medellín-Azuara J, Lund J and Sumner D (2015). *Economic Analysis of the 2015 Drought for California Agriculture*. UC Davis Center for Watershed Science. Davis, CA. Available at https://watershed.ucdavis.edu/files/biblio/Final_Drought%20Report_08182015_Full_Report_WithAppendices.pdf

IPCC (2014): Annex II: Glossary. Mach KJ, Planton S and von Stechow C (Eds.). In: *Climate Change 2014: Synthesis Report. Contribution of Working Groups I, II and III to the Fifth Assessment Report of the Intergovernmental Panel on Climate Change*. [Core Writing Team, Pachauri RK and Meyer LA (Eds.)]. Intergovernmental Panel on Climate Change. Geneva, Switzerland. Available at https://www.ipcc.ch/pdf/assessment-report/ar5/syr/AR5_SYR_FINAL_Glossary.pdf

Mao Y, Nijssen B and Lettenmaier DP (2015). Is climate change implicated in the 2013-2014 drought? A hydrologic perspective. *Geophysical Research Letters* **42**(8): 2805-2813.

NDMC (2017a). National Drought Mitigation Center: How Do I Measure Drought? Retrieved November 15, 2017, from <http://drought.unl.edu/ranchplan/DroughtBasics/WeatherDrought/MeasuringDrought.aspx>

NDMC (2017b). National Drought Mitigation Center U.S. Drought Monitor. Map Archive. Retrieved May 2, 2017, from <http://droughtmonitor.unl.edu/Maps/MapArchive.aspx>

NOAA (2017a). NOAA National Centers for Environmental information: Climate at a Glance, Time Series. Palmer Drought Severity Index, 12-month starting October. Retrieved December 26, 2017, from <http://www.ncdc.noaa.gov/cag/>

NOAA (2017b). NOAA Historical Palmer Drought Indices. Retrieved December 26, 2017, from <https://www.ncdc.noaa.gov/temp-and-precip/drought/historical-palmers/overview>

PPIC (2016). *Managing Droughts*. Public Policy Institute of California, Water Policy Center. Sacramento, CA. Available at http://www.ppic.org/content/pubs/report/R_1016JM2R.pdf

Robeson SM (2015). Revisiting the recent California drought as an extreme value. *Geophysical Research Letters* **42**(16): 6771-6779.

Seager R, Hoerling M, Schubert S, Wang H, Lyon B, et al. (2015). Causes of the 2011-14 California drought. *Journal of Climate* **28**(18): 6997–7024.

Shukla S, Safeeq M, AghaKouchak A, Guan K and Funk C (2015). Temperature impacts on the water year 2014 drought in California. *Geophysical Research Letters* **42**(11): 4384-4393.

Swain DL, Tsiang M, Haugen M, Singh D, Charland A, et al. (2014). The extraordinary California drought of 2013/2014: Character, context, and the role of climate change. *Bulletin of American Meteorological Society* **95**(9): S3-S7.



Swain DL (2015). A tale of two California droughts: Lessons amidst record warmth and dryness in a region of complex physical and human geography. *Geophysical Research Letters* **42**(22): 9999-10003.
Swain DL, Horton DE, Singh D and Diffenbaugh NS (2016). Trends in atmospheric patterns conducive to seasonal precipitation and temperature extremes in California. *Science Advances* **2**(4): e1501344.

Tree Mortality Task Force (2017). *Tree Mortality: Facts and Figures*. Available at http://www.fire.ca.gov/treetaskforce/downloads/TMTFMaterials/Facts_and_Figures_April_2017.pdf

Trenberth KE, Dai A, van der Schrier G, Jones PD, Barichivich J, et al. (2014). Global warming and changes in drought. *Nature Climate Change* **4**: 17-22.

USGS (2017a). USGS California Water Science Center: Drought Impacts. Retrieved November 22, 2017, from <https://ca.water.usgs.gov/data/drought/drought-impact.html>

USGS (2017b). USGS California Water Science Center: Land Subsidence: Cause & Effect. Retrieved December 14, 2017, from https://ca.water.usgs.gov/land_subsidence/california-subsidence-cause-effect.html

USGS (2017c). USGS Groundwater Information: Groundwater Resources for the Future. Retrieved December 14, 2017, from <https://water.usgs.gov/ogw/pubs/fs00165/>

Vins H, Bell J, Saha S, and Hess JJ (2015). The mental health outcomes of drought: A systematic review and causal process diagram. *International Journal of Environmental Research and Public Health* **12**(10): 13251-13275.

Wang S-Y, Hipps L, Gilles RR and Yoon JH (2014). Probable causes of the abnormal ridge accompanying the 2013-2014 California drought: ENSO precursor and anthropogenic warming footprint. *Geophysical Research Letters* **41**(9): 3220-3226.

Williams AP, Seager R, Abatzoglou JT, Cook BI, Smerdon JE, et al. (2015). Contribution of anthropogenic warming to California drought during 2012-2014. *Geophysical Research Letters* **42**(16): 6819-6828.

WMO and GWP (2016). *Handbook of Drought Indicators and Indices*. Integrated Drought Management Programme, World Meteorological Organization and Global Water Partnership. Geneva, Switzerland. Available at http://www.droughtmanagement.info/literature/GWP_Handbook_of_Drought_Indicators_and_Indices_2016.pdf





Warming temperatures and changing precipitation patterns have altered hydrological systems on a global scale, affecting water resources (IPCC, 2014). Among the most visible indicators of climate change, glaciers continue to shrink almost worldwide due to a warming climate. Glacier shrinkage has affected some of the largest Sierra Nevada glaciers, which have lost an average of about 70 percent of their area since the early 1900s.

Winter snowpack and spring snowmelt runoff provide approximately one-third of the state's annual water supplies. Warmer winter temperatures mean less precipitation falling as snow and reduced snowpack. The earlier arrival of warmer temperatures in the spring causes snow to melt earlier in the year. These changes have tremendous implications for California's water resources, impacting rural and urban communities, agriculture, and vegetation and wildlife.

As increasing atmospheric concentrations of greenhouse gases trap heat energy, the excess heat is absorbed and stored by the oceans and atmosphere. The oceans absorbed over 90 percent of the excess energy accumulated between 1971 and 2010 (Field et al., 2014). On a global scale, the ocean warming is largest near the surface. Thermal expansion of ocean waters and melting glaciers have contributed to the rise in global mean sea level by 0.19 meter (7 inches). Warmer temperatures also alter water chemistry, impacting the marine ecosystem.

In California, coastal sea surface temperatures are increasing, levels of dissolved oxygen are decreasing and sea levels are rising. Fresh waterbodies are also affected by a warming climate. Increased temperatures in Lake Tahoe waters have hindered seasonal deep mixing, which brings nutrients to the surface and distributes oxygen throughout the lake — a process essential to the health of its ecosystem.

INDICATORS: IMPACTS ON PHYSICAL SYSTEMS

Snowmelt runoff (*updated*)
Snow-water content (*updated*)
Glacier change (*updated*)
Lake water temperature
Coastal ocean temperature (*updated*)
Sea level rise (*updated*)
Dissolved oxygen in coastal waters (*updated*)



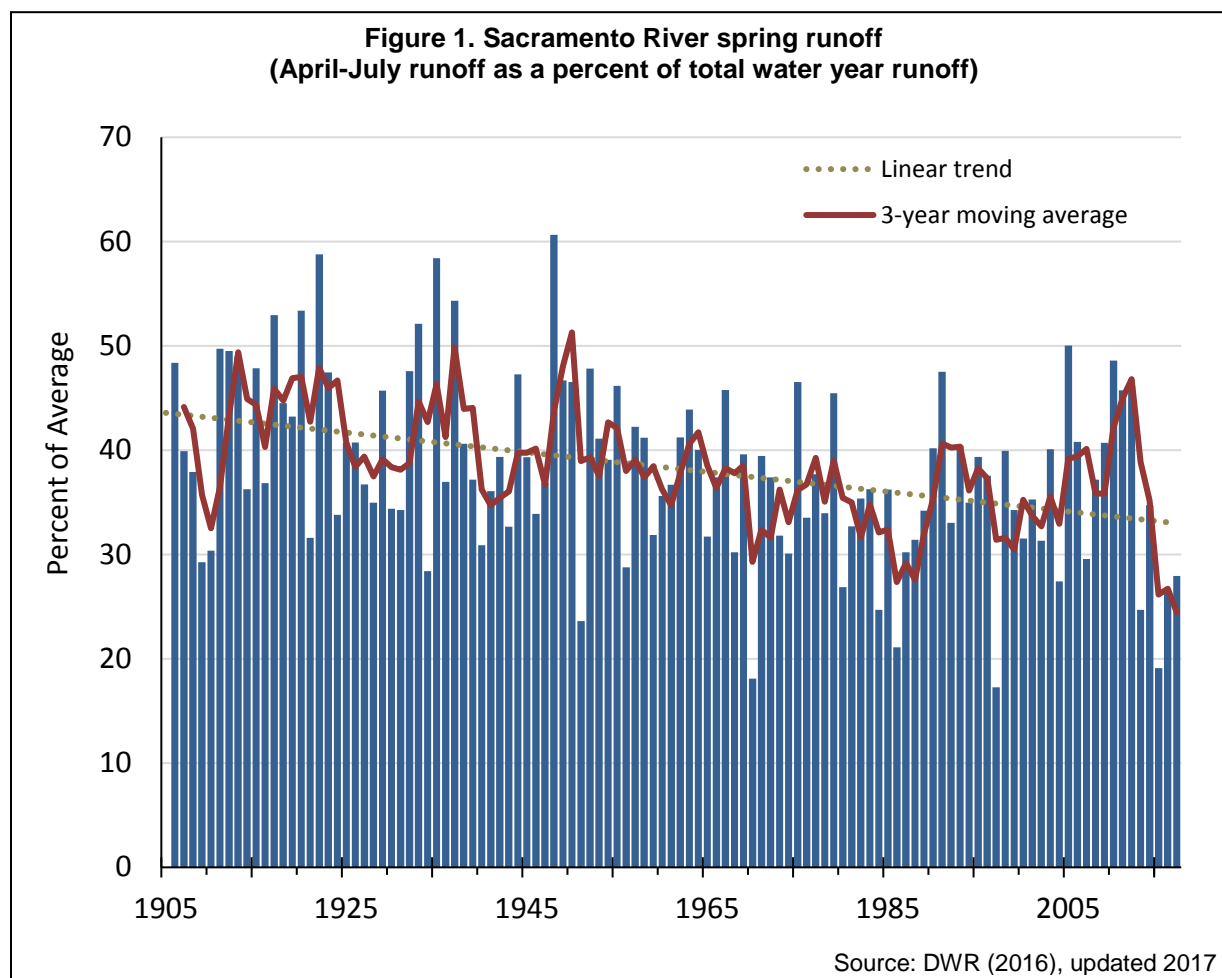
Reference:

Field CB, Barros VR, Mach KJ, Mastrandrea MD, van Aalst M, et al. (2014). *Technical summary*. In: *Climate Change 2014: Impacts, Adaptation, and Vulnerability. Part A: Global and Sectoral Aspects. Contribution of Working Group II to the Fifth Assessment Report of the Intergovernmental Panel on Climate Change* [Field CB, Barros VR, Dokken DJ, Mach KJ, Mastrandrea MD et al. (Eds.)]. Cambridge University Press, Cambridge, United Kingdom and New York, NY, USA, pp. 35-94.
http://www.ipcc.ch/pdf/assessment-report/ar5/wg2/WGIIAR5-TS_FINAL.pdf



SNOWMELT RUNOFF

The fraction of snowmelt runoff into the Sacramento River between April and July relative to total year-round water runoff has declined over the past century.



What does the indicator show?

Since 1906, the fraction of annual unimpaired snowmelt runoff that flows into the Sacramento River between April and July (“spring”) has decreased by about nine percent. Figure 1 shows this spring fraction as the percentage of total runoff for the entire water year, the period from October through the following September. The 2015 water year had the third lowest percentage of spring runoff on record (the lowest snowpack on record also occurred in 2015). This decreased runoff was especially evident after 1950. There is no significant trend in total water year runoff into the Sacramento River (not shown), just a change in the timing of runoff.

Why is this indicator important?

In the Sierra Nevada and southern Cascade Mountains, snow accumulates from October to March. The snowpack preserves much of California’s water supply in cold storage. Less snowpack accumulates when winter temperatures are warmer because more precipitation falls as rain instead of snow. As temperatures warm in the spring,



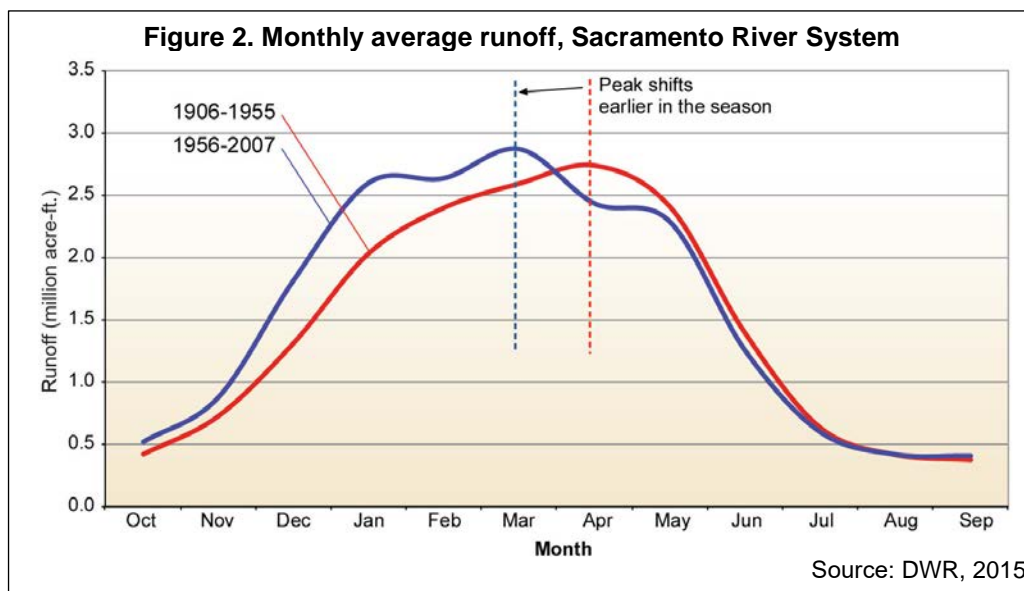
water stored in snowpack is released as snowmelt runoff, typically from April through July.

Spring runoff averages around 15 million acre feet (18 billion cubic meters) water, which is about 35 percent of the usable annual supply for agriculture and urban needs (Roos and Anderson, 2006). Spring runoff data, along with related snow pack information, are used for water supply and flood forecasting. Much of the state's flood protection and water



Source: NPS, 2017

supply infrastructure was designed to capture the slow spring runoff and deliver it during the drier summer and fall months. This infrastructure was designed and optimized for historical conditions. As shown in Figure 2, the timing of peak monthly runoff had shifted earlier by nearly a month in 1956-2007 (blue line), compared to 1906-1955 (red line), indicating an earlier onset of springtime temperatures. This shift in timing strains the current water management system. As the climate continues to change, water storage, and flood strategies may also have to change.



With less spring runoff, less water is available during the summer to meet the state's water needs, including domestic and agricultural uses, hydroelectric power production, and recreation. Reduced runoff impacts ecosystems, leading to impaired cold water habitat for salmonid fishes (Roos, 2000), tree deaths (see *Forest tree mortality* indicator), and increased wildfires (see *Wildfires* indicator). Precipitation in the form of rain instead of snow may increase flood risk and impact snow-related recreation.



What factors influence this indicator?

Lower water volumes of spring snowmelt runoff compared to the rest of the water year may indicate warmer winter temperatures or unusually early warm springtime temperatures. With warmer winter temperatures, a greater proportion of precipitation occurs as rain, and snow falls and accumulates at higher elevations than in the past. Higher elevations of the snow line mean reduced snow pack and flows from watersheds in the spring.

Spring runoff from mountain snowmelt has declined throughout California:

River Runoff	% Decline in the 20th Century
Sacramento River system*	9
San Joaquin River system	6
Kings	6
Kern	8
Mokelumne	7
Trinity	8
Truckee	13
Carson and Walker	5

** includes the Sacramento River and its major tributaries, the Feather, Yuba, and American Rivers.*

Other possible factors, such as the Pacific Decadal Oscillation (PDO) and air pollution, probably contribute to the patterns observed. The PDO is a pattern of Pacific climate variability that shifts phases on at least an interdecadal time scale, usually 20 to 30 years. It is detected as warm or cool surface waters in the Pacific Ocean, which in turn impact coastal and inland climate in Washington, Oregon and Northern California (Mantua and Hare, 2002). There appears to be a PDO effect concurrent with decreasing spring snowmelt percentages due to warming temperatures.

Technical Considerations

Data Characteristics

Runoff for the Sacramento River system is the sum of the estimated unimpaired runoff of the Sacramento River and its major tributaries, the Feather, Yuba, and American Rivers. “Unimpaired” runoff refers to the amounts of water produced in a stream unaltered by upstream diversions, storage, or by export or import of water to or from other basins. The California Cooperative Snow Surveys Program of the California Department of Water Resources (DWR) collects the data. Runoff forecasts are made systematically, based on historical relationships between the volume of April through July runoff and the measured snow water content, precipitation, and runoff in the preceding months (Roos, 1992). The snow surveys program began in 1929.

Related snow pack information is used to predict how much spring runoff to expect for water supply purposes. Each spring, about 50 agencies, including the United States



Departments of Agriculture and Interior, pool their efforts in collecting snow data at about 270 snow courses throughout California. A snow course is a transect along which snow depth and water equivalent observations are made, usually at ten points. The snow courses are located throughout the state from the Kern River in the south to Surprise Valley in the north. Courses range in elevation from 4,350 feet in the Mokelumne River Basin to 11,450 feet in the San Joaquin River Basin.

Since the relationships of runoff to precipitation, snow, and other hydrologic variables are natural, it is preferable to work with unimpaired runoff. To get unimpaired runoff, measured flow amounts have to be adjusted to remove the effect of man-made works, such as reservoirs, diversions, or imports (Roos, 1992). The water supply forecasting procedures are based on multiple linear regression equations, which relate snow, precipitation, and previous runoff terms to April-July unimpaired runoff.

Major rivers in the forecasting program include the Sacramento, Feather, Yuba, American, San Joaquin, Merced, Tuolumne, Stanislaus, and Kings on the western slopes of the Sierra; the Truckee, Walker, Carson and Owens on the eastern slopes; the Kern at the south end of the Sierra; and the Trinity in the North Coast.

Strengths and Limitations of the Data

River runoff data have been collected for almost a century for many monitoring sites. Stream flow data exist for most of the major Sierra Nevada watersheds because of California's dependence on their spring runoff for water resources and the need for flood forecasting. The April to July unimpaired flow information represents spring rainfall, snowmelt, as adjusted for upstream reservoir storage calculated depletions, and diversions into or out from the river basin. Raw data are collected through water flow monitoring procedures and used along with the other variables in a model to calculate the unimpaired runoff of each watershed.

Over the years, instrumentation has changed and generally improved; some monitoring sites have been moved short distances to different locations. The physical shape of the streambed can affect accuracy of flow measurements at monitoring sites, but most foothill sites are quite stable.

For more information, contact:



Maurice Roos
Department of Water Resources
Division of Flood Management
3310 El Camino Avenue
P. O. Box 219000
Sacramento, CA 95821-9000
(916) 574-2625
mroos@water.ca.gov



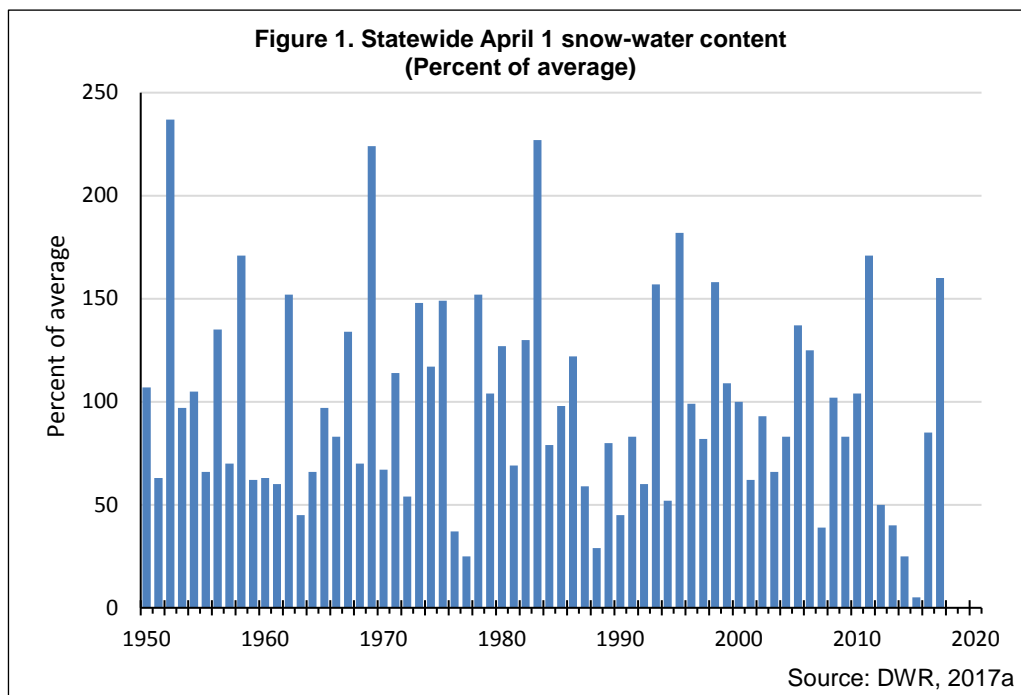
References:

- DWR (2015). *California Climate Science and Data for Water Resources Management*. Sacramento, CA: California Department of Water Resources. Available at https://www.water.ca.gov/LegacyFiles/climatechange/docs/CA_Climate_Science_and_Data_Final_Release_June_2015.pdf
- DWR (2016). California Department of Water Resources: Chronological Reconstructed Sacramento and San Joaquin Valley Water Year Hydrologic Classification Indices. Retrieved August 16, 2017, from <http://cdec.water.ca.gov/cgi-progs/iodir/WSIHIST>. (2017 data provided by California Department of Water Resources)
- Mantua NJ and Hare SR (2002). The pacific decadal oscillation. *Journal of Oceanography* **58**(1): 35-44.
- NPS (2017). National Park Service: Hydrology, Yosemite National Park. Retrieved August 2017, from <http://www.nps.gov/yose/naturescience/hydrology.htm>
- Roos M (1992). Water Supply Forecasting Technical Workshop. California Department of Water Resources.
- Roos M (2000). *Possible Effects of Global Warming on California Water or More Worries for the Water Engineer*. W. E. F. Water Law and Policy Briefing. San Diego, CA: Department of Water Resources.
- Roos M and Anderson M (2006). Monitoring monthly hydrologic data to detect climate change in California. *Third Annual Climate Change Research Conference*. Sacramento, CA.



SNOW-WATER CONTENT

The amount of water stored in the state's snowpack has been highly variable from year to year, ranging from a high of about 240 percent of average in 1952 to a record low of 5 percent in 2015.



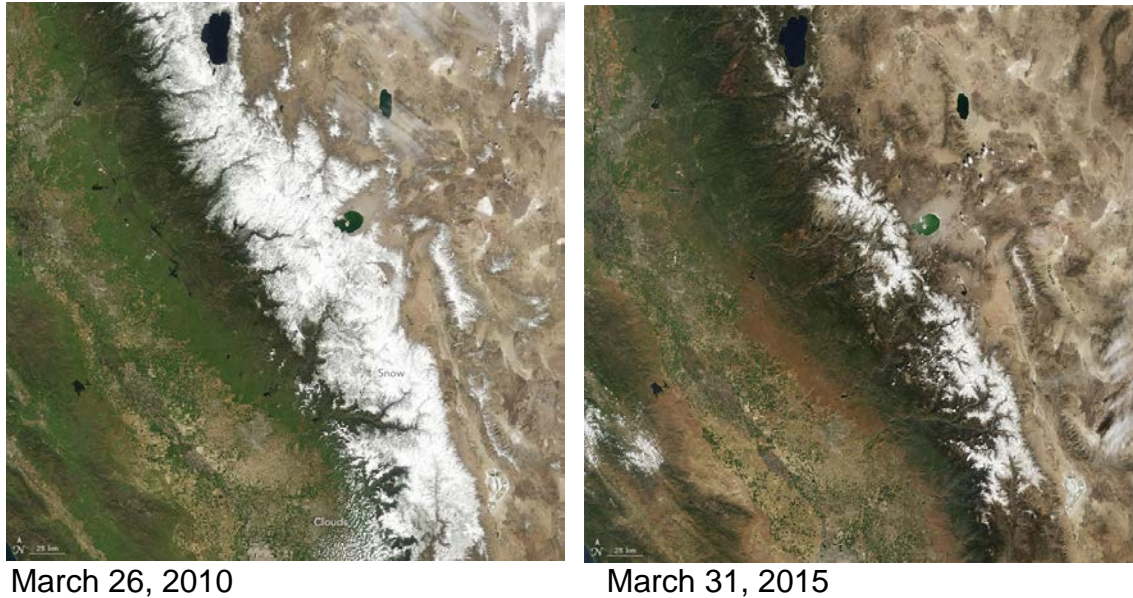
What does the indicator show?

The amount of water contained in California's snowpack — expressed as “snow water content” — is highly variable from year to year. Snow-water content is the depth of water, usually expressed in inches, that would cover the ground if the snow cover was in a liquid state (NWS, 2018). It is traditionally measured by weighing the mass of a core of snow — from snow surface to soil — collected by an observer (snow gauger) in the field; more recently, sensing devices take measurements of the mass of snow laying on top of a large scale, called a snow pillow. In either case, the weight of snow is a measure of how much liquid water would be obtained by melting the snow over a given area. Manual measurements are taken near the first of the month starting about January 1 and ending in May. The most important one is taken around April 1, when the snowpack has historically been deepest; these measurements are used by water managers for water supply forecasting and operations. The historical average snow-water content on April 1 is about 28 inches.

As shown in Figure 1, since 1950, statewide snow-water content has ranged from more than 200 percent of average in 1952, 1969 and 1983, to the lowest value on record, 5 percent, during the drought in 2015 (see satellite images comparing the 2015 snowpack with average conditions, Figure 2). In 2017, snowpack was at 160 percent of average. These statewide values reflect measurements taken at about 250 stations from the Trinity Alps and Mount Shasta in northern California, and throughout the Sierra Nevada down to the Kern River basin in the south.



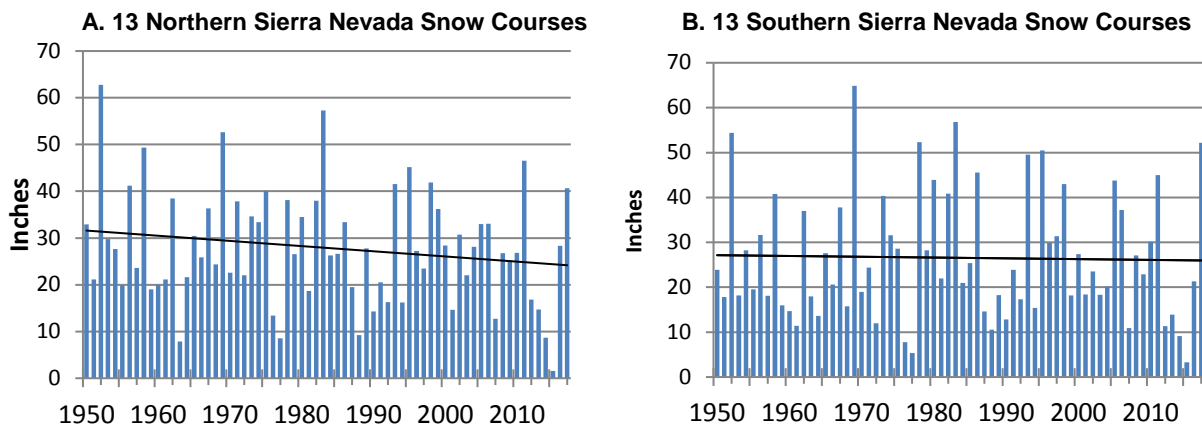
Figure 2. Satellite images showing average conditions of the Sierra Nevada snowpack in 2010 (left) and the record-low snowpack in 2015



Source: NASA, 2017

Over the time period from 1950 to present, snow-water content in both the northern and southern Sierra Nevada long-term snow courses have been declining (Figure 3A and B), part of a broader pattern of declining snowpack across the West. Snow courses are permanent locations that represent snowpack conditions at a given elevation in a given area; further details are provided in *Technical Considerations*.

Figure 3. April 1 Snow-Water Content*



Source: DWR, 2017a

* Snow-water content is measured in inches, equivalent to amount of water that would be obtained by melting snow over a given area.

When snowpack trends were examined in 2009 and 2012, the northern Sierra Nevada showed a decline, but courses in the southern Sierra Nevada showed a small increase. Factors which may account for this difference in trends are discussed in *What factors*



influence this indicator? A more recent reevaluation of snowpack trends showed that the southern Sierra group is now declining although the slope is flatter than in the northern Sierra group of snow courses (DWR, 2017a; Roos and Fabbiani-Leon, 2017). In 2017, the snowpack trend for the southern Sierra group showed an overall decline of about 1.2 inches since 1950, compared to 7.4 inches for the northern Sierra group of snow courses (DWR, 2017a).

Why is this indicator important?

Snow-water content is a measure of how much water is locked up in the snowpack at a given location. Although some of this water will be lost to direct evaporation, most will be available to run off into streams and rivers or percolate into soils once the snow melts in spring and summer.

The Sierra Nevada snowpacks are an integral part of the state's water-supply. They serve as natural water storage, adding about 35 percent to the reservoir capacity available in the state. Information on the amount of water stored in the snowpack is used by water managers to forecast the availability of water to meet the state's water needs for domestic and agricultural uses, hydroelectric power production, and recreation. The water stored in the snowpack also plays a role in the ecosystem, providing cold water habitat for salmonid fishes (Roos, 2000), and water for forests.

Traditionally, California's snowpacks are thickest and contain the most water by about April 1 of each year — at which time they have historically stored about 15 million acre-feet of water. While the date of maximum snow-water content may vary from year to year and place to place, measurements taken on April 1 have been used to estimate how much water stored in the state's snowpacks will be released as snowmelt later in the year. Although the timing of maximum snowpack is predicted to come earlier in the year as the climate warms, continued monitoring of the April 1 snowpack should provide the data needed to determine changes in total warm-season water supplies from snowmelt.

California receives its largest and most dangerous storms during the wintertime. Likewise, its most devastating floods have occurred during the same season. In order to balance flood-risk management and water-supply considerations, California's water managers have developed a strategy of maintaining empty space in the major reservoirs during winter, so that flood flows can be captured or at least reduced when necessary. By about April 1, when most of the winter storms stop reaching California, flood risks generally decline considerably. At this time, reservoir managers change strategies and instead capture as much streamflow as possible to fill flood-control spaces to store water in the reservoirs for the summer when water demands are highest. This strategy works primarily because, during winter, the state's snowpacks are holding copious amounts of the winter's precipitation in the mountain watersheds, only releasing most of it to reservoirs after about April 1. In a big snowpack year like 2017, some of the early portion of the snowmelt will be released in March and April prior to the normal peak snowmelt. The gradual release of snowmelt during the spring precludes



the need for overly high-volume reservoir releases later in the runoff season. The forecasted volume becomes a tool to guide reservoir operations.

To the extent that climate change depletes the state's snowpacks in the future (Knowles and Cayan, 2004), this historical flood- and water-management strategy will be severely challenged. Thus, it is important to monitor whether the state's snowpacks are declining, increasing, or staying the same.

What factors influence this indicator?

April 1 snow-water content is determined by winter and spring precipitation totals and by air temperatures, which affect whether precipitation falls as rain or as snow. Elevation matters. Cooler air temperatures at higher elevations generally mean higher snow accumulations compared to lower elevations. The average elevation of the northern Sierra group of 13 courses is 6,900 feet, whereas the average is 8,900 feet for the southern group.

The record low snowpack in 2015 was accompanied by the warmest winter temperatures since 1950. The average minimum winter temperature in 2015 was 37.1°F, about 5 °F higher than the long-term average (WRCC, 2017). In addition to enhancing the likelihood of rain instead of snow, warm temperatures increase the frequency of melt events, leading to a reduction of snow-water content. A study of trends in the Sierra Nevada snowpack found warm daily maximum temperatures in March and April to be associated with a shift toward earlier timing of peak snow mass by 0.6 day per decade since 1930; this earlier trend is associated with snow melting earlier, which also results in trends toward lower snow-water equivalent (Kapnick and Hall, 2010). Over the past decade, the average snow level (altitude where precipitation changes from snowfall to rain) along the western slope of the northern Sierra Nevada has risen over 1,200 feet — a change hypothesized to be related to atmospheric rivers that are predominantly associated with low snow-fraction storms and anomalously warm coastal sea surface temperatures (Hatchett et al., 2017). A decade of available data is not sufficient to connect this change to longer term snow-rain trends in recent decades (Knowles et al., 2006). However, the change is large enough and important enough so that following the altitudes of snowlines offers a metric to assess hydrologic impacts of climate change in the mountains.

The declines in snow-water content are part of a much broader pattern of declining snowpacks across the western United States — a pattern that has been associated with springtime warming trends and earlier snowmelt seasons in recent years by several different scientific studies (e.g., Mote, 2003; Barnett et al., 2008). Prior to the 2012-2016 drought, increases in the southern Sierra Nevada were part of a more localized pattern associated with El Niño climate conditions since about the mid-1970s (e.g., McCabe and Dettinger, 2002). During El Niño winters, the southwestern United States, including the southern Sierra Nevada, is typically wetter (Cayan and Webb, 1992), so that snowpacks are consequently thicker and store more water by April. The southern Sierra Nevada snowpack may also be influenced by weather modification programs that generate snow through cloud seeding programs.



Under climate change, warming is likely to lead to less snowpack if precipitation does not increase too markedly (Knowles and Cayan, 2004). If precipitation increases, snow-water content could increase in those areas above the retreating snowlines that are still cold enough to receive snowfall; if precipitation decreases, snow-water content may be expected to decline even faster than due to warming alone.

To a lesser extent, snow-water content may be influenced by the amount of solar radiation that falls on the snowpack in each season, which, in turn, depends on cloudiness and timing of the beginning of the snowmelt season (Lundquist and Flint, 2006). Cloudiness decreases solar radiation on the snowfields, and would tend to result in less wintertime snowmelt and thus more snow-water content left by April 1 (the opposite would occur if cloudiness declines in the future).

A potential confounding factor in the variation and trends in snowpack is the effect of dust and air pollutants (including black carbon, a component of soot) on both the initial formation of mountain snowpacks and on snowmelt timing. Recent field measurements and modeling have provided potentially important indications that the presence or absence of dust in the atmosphere, including dust carried to California by high-altitude winds from Asia, may help to determine amounts of snowfall over the Sierra Nevada, which in turn could contribute to variations and trends in April 1 snowpack (Ault et al., 2011). Recent studies in the Colorado River Basin have helped to quantify important influences on snowmelt timing and, ultimately, amounts that are due to springtime snow albedo (reflectivity) changes associated with dust (mostly from within the region) falling onto snow surfaces across the Western US (e.g., Painter et al., 2010). Black carbon has been measured in the Sierra Nevada snowpack at concentrations sufficient to affect snowmelt and surface temperatures (Hadley et al., 2010). These factors likely play roles in past and future variations of April 1 snowpack amounts, but the long-term past and future trends in these additional factors in California remain largely unknown at present.

In its *Climate Change Indicators Report*, the US Environmental Protection Agency presents an indicator showing declining trends in April snowpack for the Western United States from 1955 to 2016 (US EPA, 2016); an interactive map can be accessed from the US EPA's website. Of the 233 sites in California, all except for 24 showed declining trends.

Technical Considerations

Data Characteristics

Snow-water content has traditionally been measured by weighing cores of snow pulled from the whole depth of the snowpack at a given location. Since the 1930s, within a few days of the beginning of each winter and spring month, measurements have been taken along permanent snow courses — locations that represent snowpack conditions at a given elevation in a given area. Measurements are taken by skiing or flying to remote locations and extracting 10 or more cores of snow along ¼ mile-long pre-marked “snow course” lines on the ground. The depth of snow and the weight of snow in the cores are measured, the weights are converted to a depth of liquid water that would be released by melting that weight of snow; the results from all the measurements at the snow



course are averaged to arrive at estimates of the snow-water content at that site (Osterhuber, 2014). More than 50 state, federal and private entities pool their efforts in collecting snow data from over 300 snow courses in California.

To examine trends for the Northern and Southern Sierra Nevada, snow courses that have fairly complete records from 1950 (that is, sites with the fewest missing years of data), and that provide a good representation of the region were selected (by DWR, see Roos and Sahota, 2012). The thirteen snow courses selected for each region are as follows:

<u>Northern Sierra Nevada</u>	River Basin	Elevation, in feet
North Fork Sacramento	Upper Sacramento	6900
Cedar Pass	Upper Sacramento	7100
Adin Mountain	Upper Sacramento	6800
Mount Dyer	Feather	7100
Harkness Flat	Feather	6600
Feather River Meadow	Feather	5400
Webber Peak	Yuba	7800
Meadow Lake	Yuba	7200
Cisco	Yuba	5900
Lake Spaulding	Yuba	5200
Upper Carson Pass	American	8500
Silver Lake	American	7100
Blue Lakes	Mokelumne	8000
<u>Southern Sierra Nevada</u>	River Basin	Elevation, in feet
Piute Pass	San Joaquin	11300
Agnew Pass	San Joaquin	10300
Kaiser Pass	San Joaquin	9100
Florence Lake	San Joaquin	7200
Blackcap Basin	Kings	10300
Beard Meadow	Kings	9800
Upper Burnt Corral	Kings	9700
Long Meadow	Kings	8500
Helms Meadow	Kings	8250
Panther Meadow	Kaweah	8600
Giant Forest	Kaweah	6400
Ramshaw Meadows	Kern	8700
Little Whitney Meadows	Kern	8500

Data from monthly snow surveys are supplemented by daily information from an automatic snow sensor network (often called snow pillows), developed and deployed over the last 30 years. The snow sensors measure the accumulation and melting cycles

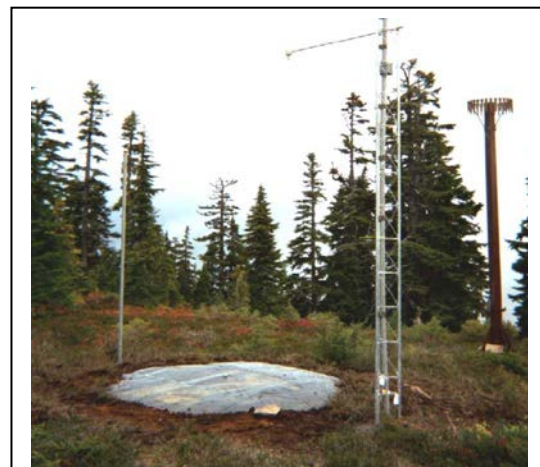


in the snowpack, providing data on the effect of individual storms or hot spells. In addition to tracking changes during the snow accumulation season, snow sensor data help greatly in forecasting water volumes involved in the late-season filling of reservoirs. There are now approximately 130 snow sensor sites from the Trinity Alps to the Kern River, with 36 sites included from the Trinity area south to the Feather and Truckee basins, 57 sites from the Yuba and Tahoe basins to the Merced and Walker basins, and 36 sites from the San Joaquin and Mono basins south to the Kern basin. Snow-water content data for snow courses and snow sensors can be downloaded from the Department of Water Resources' California Data Exchange Center website (DWR, 2017b).

Strengths and Limitations of the Data

The measurements are relatively simple, and the methods have not changed since monitoring started. Averaging of the 10 or more measurements at each course yields relatively accurate and representative results. During the past three decades, continuous snow-measurement instrumentation has been established at many of the snow courses. These sensors provide snow-water content information at more frequent time intervals, and serve as a valuable check on the representativeness and accuracy of the snow-course measurements.

The sensors measure the weight of snow on the ground (along with several meteorological variables) with a snow pillow (see photograph, right). Snow pillows are large (10 foot (') diameter), flat, flexible tanks or a group of four interconnected 4' x 5' sheet metal tanks filled with denatured alcohol or other liquids that do not freeze at winter temperatures, buried just below the ground surface. As snow piles up on the pillows, it squeezes the tanks and liquids they contain, raising the pressure in the tanks, and that pressure change is used to determine the weight of snow on the tank and ground. The sensor network provides important data for assessing changes in snowpack and the effect of storms, supplementing data from monthly snow course measurements.



A typical snowpack telemetry site includes a snow pillow, an antenna with solar panels and a temperature sensor, and a precipitation gauge (brown structure in background, right)

Source: NRCS, 2018



For more information, contact:



Michael Dettinger
California Applications Program/California Climate Change Center
Scripps Institution of Oceanography, UCSD, Dept. 0224
9500 Gilman Drive
La Jolla, CA 92093-0224
(858) 822-1507
mdettinger@ucsd.edu



Frank Gehrke, Chief
Department of Water Resources
California Cooperative Snow Surveys
P.O. Box 219000
Sacramento, CA 95821-9000
(916) 574-2635
gridley@water.ca.gov



Maurice Roos
Department of Water Resources
Division of Flood Management
P.O. Box 219000
Sacramento, CA 95821-9000
(916) 574-2625
mroos@water.ca.gov

References:

Ault AP, Williams CR, White AB, Neiman PJ, Creamean JM, et al. (2011). Detection of Asian dust in California orographic precipitation, *Journal Geophysical Research* **116**(D16).

Barnett TP, Pierce DW, Hidalgo HG, Bonfils C, Santer BD, et al. (2008). Human-Induced Changes in the Hydrology of the Western United States. *Science* **319**(5866): 1080-1083.

Cayan DR and Webb R (1992). El Niño/Southern Oscillation and streamflow in the western United States. In: *El Niño: Historical and Paleoclimatic Aspects of the Southern Oscillation*. Diaz HF and Markgraf V (Eds.). New York: Cambridge University Press, 29-68.

DWR (2017a). California Department of Water Resources: Snow Course Data, California Data Exchange Center. Retrieved July 2017, from <http://cdec.water.ca.gov/cgi-progs/snowQuery> and <http://cdec.water.ca.gov/cgi-progs/selectSnow>

DWR (2017b). California Department of Water Resources: California Data Exchange Center—Snow. Retrieved January 2018, from <http://cdec.water.ca.gov/snow/current/snow/index.html>

Hadley OL, Corrigan CE, Kirchstetter TW, Cliff SS, and Ramanathan V (2010). Measured black carbon deposition on the Sierra Nevada snow pack and implication for snow pack retreat. *Atmospheric Chemistry and Physics* **10**:7505-7513.

Hatchett BJ, Daudert B, Garner CB, Oakley NS, Putnam AE, and White AB (2017). Winter Snow Level Rise in the Northern Sierra Nevada from 2008 to 2017. *Water* **9**(11): 899.



- Kapnick S and Hall A (2010). Observed Climate–Snowpack Relationships in California and their Implications for the Future. *Journal of Climate* **23**: 3446–3456.
- Knowles N, Dettinger MD, and Cayan DR (2006). Trends in Snowfall versus Rainfall in the Western United States. *Journal of Climate* **19**:4545–4559.
- Knowles N and Cayan DR (2004). Elevational dependence of projected hydrologic changes in the San Francisco estuary and watershed. *Climatic Change* **62**(1-3): 319-336.
- Lundquist JD and Flint AL (2006). Onset of snowmelt and streamflow in 2004 in the western United States: How shading may affect spring streamflow timing in a warmer world. *Journal of Hydrometeorology* **7**(6): 1199-1217.
- McCabe GJ and Dettinger MD (2002). Primary modes and predictability of year-to-year snowpack variations in the western United States from teleconnections with Pacific Ocean climate. *Journal of Hydrometeorology* **3**(1): 13-25.
- Mote, PW, Hamlet AF, Clark MP, and Lettenmaier DP (2005). Declining mountain snowpack in western North America. *American Meteorological Society* **86**(1):39–49.
- Mote PW (2003). Trends in snow water equivalent in the Pacific Northwest and their climatic causes. *Geophysical Research Letters* **30**(12): 1601.
- NASA (2017). National Aeronautics and Space Administration: *Snowpack in the Sierra Nevada*. Retrieved March 27, 2017, from https://earthobservatory.nasa.gov/Features/WorldOfChange/sierra_nevada.php?all=y
- NRCS (2018). Natural Resources Conservation Service: Snow Surveys and Water Supply Forecasting. Retrieved February 21, 2018, from https://www.wcc.nrcs.usda.gov/factpub/sect_4b.html
- NWS (2018). National Weather Service: Snow water equivalent and depth information. Retrieved February 21, 2018, from <http://www.weather.gov/marfc/snow>
- Osterhuber R (2014). *Snow Survey Procedure Manual*. Prepared for the California Department of Water Resources, California Cooperative Snow Surveys. Available at <https://cdec.water.ca.gov/cgi-progs/products/SnowSurveyProcedureManualv20141027.pdf>
- Painter TH, Deems JS, Belnap J, Hamlet AF, Landry CC and Udall B (2010). Response of Colorado River runoff to dust radiative forcing in snow. *Proceedings of the National Academy of Sciences* **107**(40):17125-17130.
- Roos M (2000). Possible Effects of Global Warming on California Water or More Worries for the Water Engineer. *W.E.F. Water Law and Policy Briefing*. San Diego, CA, Department of Water Resources.
- Roos M and Sahota S (2012). *Contrasting Snowpack Trends in the Sierra Nevada of California*. Presented at the 2012 Western Snow Conference. Available at <http://www.westernsnowconference.org/sites/westernsnowconference.org/PDFs/2012Roos.pdf>
- Roos M and Fabbiani-Leon A (2017). *Recent Changes in the Sierra Snowpack in California*. Presented at the 2017 Western Snow Conference. Available at <https://westernsnowconference.org/node/1828>
- US EPA (2016). US Environmental Protection Agency: Climate Change Indicators: Snowpack. Retrieved December 1, 2017, from <https://www.epa.gov/climate-indicators/climate-change-indicators-snowpack>

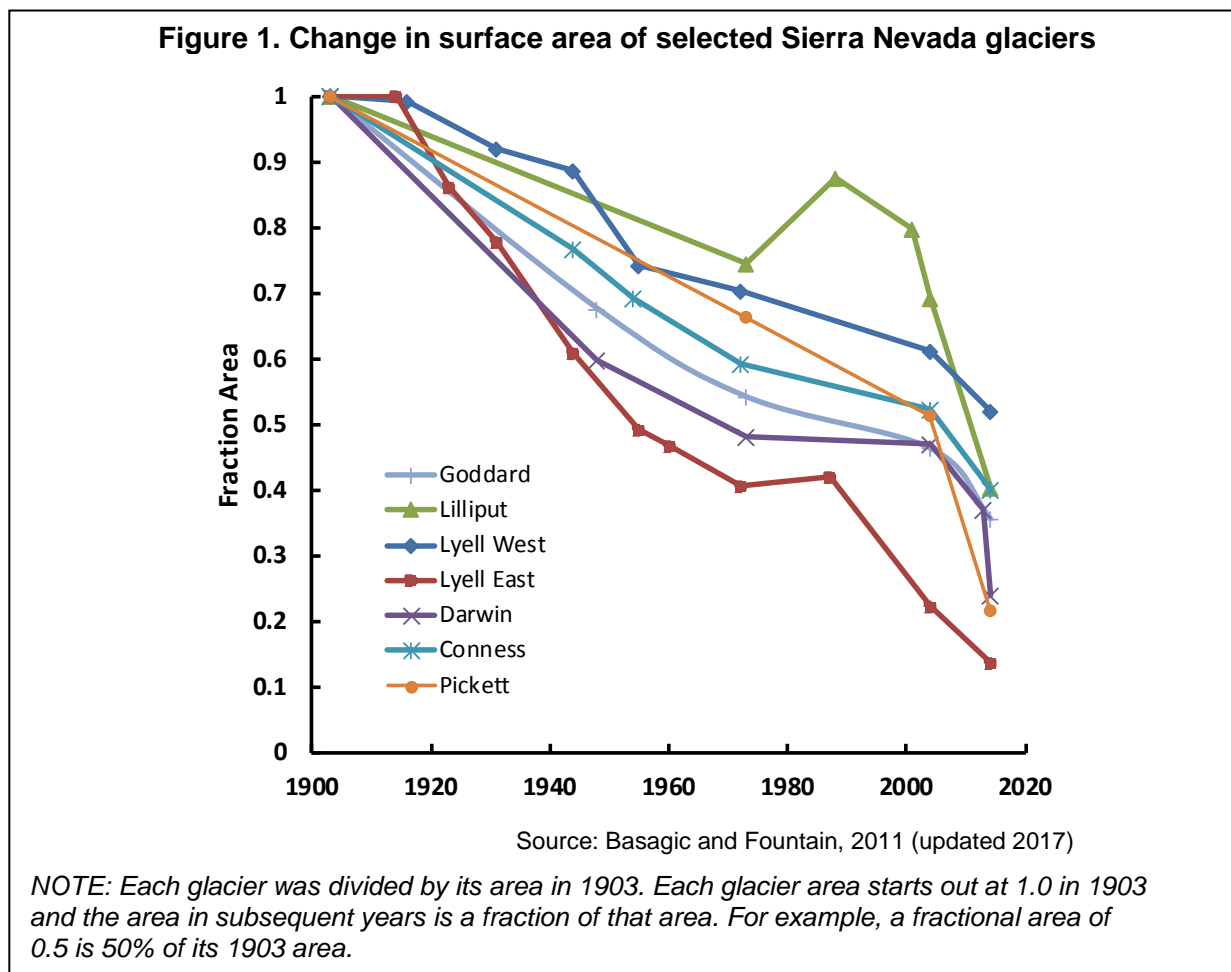


WRCC (2017). Western Regional Climate Center: *California Climate Tracker*: Time series, minimum temperature, winter (December to February). Retrieved November 27, 2017, from https://wrcc.dri.edu/monitor/cal-mon/frames_version.html



GLACIER CHANGE

Glaciers in the Sierra Nevada have retreated dramatically. From the beginning of the twentieth century to 2014, some of the largest glaciers have lost an average of about 70 percent of their area, with losses ranging from about 50 to 85 percent.



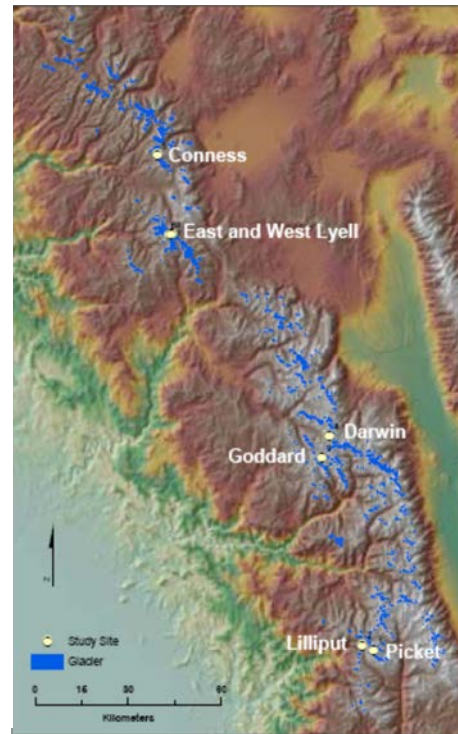
What does the indicator show?

Figure 1 shows that the surface area of seven Sierra Nevada glaciers (Figure 2) has decreased dramatically during the past century (Basagic and Fountain, 2008, updated to 2014). Changes in area are relative to 1903. By 2014, these seven glaciers lost between 48 to 86 percent of their 1903 area. About half the area was lost since the 1970s.

These findings are consistent with those from a separate study of 769 glaciers and perennial snowfields that were identified within the Sierra Nevada in the 1970s and 1980s based on the US Geological Survey's 1:24,000-scale, topographic maps (Fountain et al., 2017). The largest 39 glaciers, free of rock debris mantling the surface, covered an area of 2.74 ± 0.12 square kilometers (km^2) in the 1970s and 1980s. By 2014, overall, they lost about 50 percent of their area.



Figure 2. Location of the Sierra Nevada glaciers (left), and the seven glaciers studied (right)



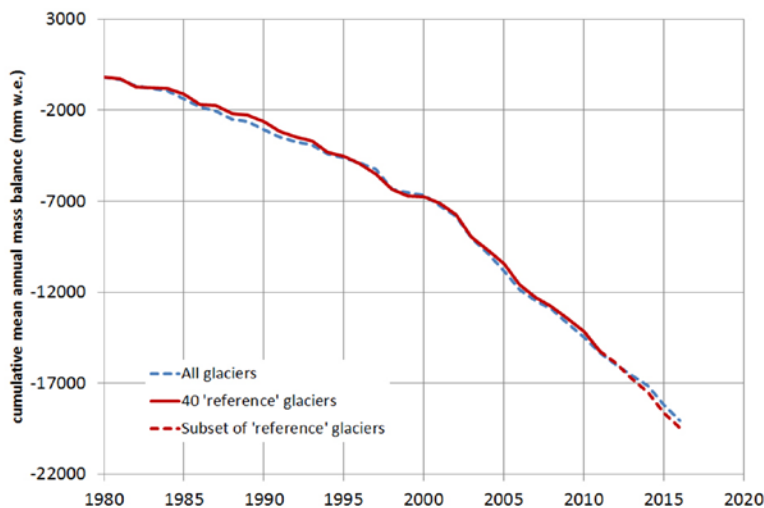
Glacier locations:

- Conness: Inyo National Forest, east of Yosemite National Park
- Lyell: Headwaters of Tuolumne River, in eastern Yosemite
- Darwin and Goddard: Northern Kings Canyon National Park
- Lilliput and Pickett: Sequoia National Park

Source: Basaglin and Fountain, 2008

The results from the Sierra Nevada are consistent with global averaged glacier mass, which has been decreasing for the past 100 years (global measurements date back to 1917 or earlier). The trend since 1980 is shown in Figure 3. The graph is based on standardized observations on glaciers around the globe collected by the World Glacier Monitoring Service (WGMS, 2017). Glacier mass change is reported as “cumulative mean annual mass balance in millimeters of water equivalent (mm w.e.),” the equivalent depth of water (spread out over the entire glacier area) that would be produced from the amount of snow or ice on the glacier. The global average smooths out the variations of individual glaciers like those shown for the Sierra.

Figure 3. Global average glacier mass changes



“Cumulative mean annual mass balance” is reported in millimeters of water equivalent (mm w.e.)

All glaciers — more than 130 glaciers worldwide;

40 reference glaciers — glaciers in ten mountain ranges with more than 30 years of continuous data;

Subset of “reference” glaciers — a subset of reference glaciers for which data have been reported

Source: WGMS, 2017



The late summer photographs in Figure 4 show the area change in the Dana and Conness glaciers over the past century. Losses in both glacier area and volume over time are evident from the photographs. Additional photographs can be viewed at the “Glaciers of the American West” web site (PSU, 2017).

Figure 4. Historical and contemporary photographs of two Sierra Nevada glaciers

Dana Glacier



Credit: U.S. Geological Service, photo station ric046 (left); H. Basagic (right)

Conness Glacier



Credit: National Park Service, photo station Conness 5555 (left); H. Basagic (right)

Why is this indicator important?

Glaciers are important indicators of climate change. Over the 20th century, with few exceptions, alpine glaciers were receding throughout the world in response to a warming climate. Historical glacier responses preserved in photographic records, and prehistoric responses preserved as landscape modifications are important records of past climates in high alpine areas where few other climate records exist.

Glaciers are also important to alpine hydrology. They begin to melt most rapidly in late summer after the bright, reflective seasonal snow disappears, revealing the darker ice



beneath. This causes peak runoff to occur in late summer when less water is available and demand is high. Glacier shrinkage reduces this effect, resulting in earlier peak runoff and drier summer conditions. These changes are likely to have ecological consequences for flora and fauna in the area that depend on available water resources. Finally, glacier shrinkage worldwide is an important contribution to global sea level rise.

What factors influence this indicator?

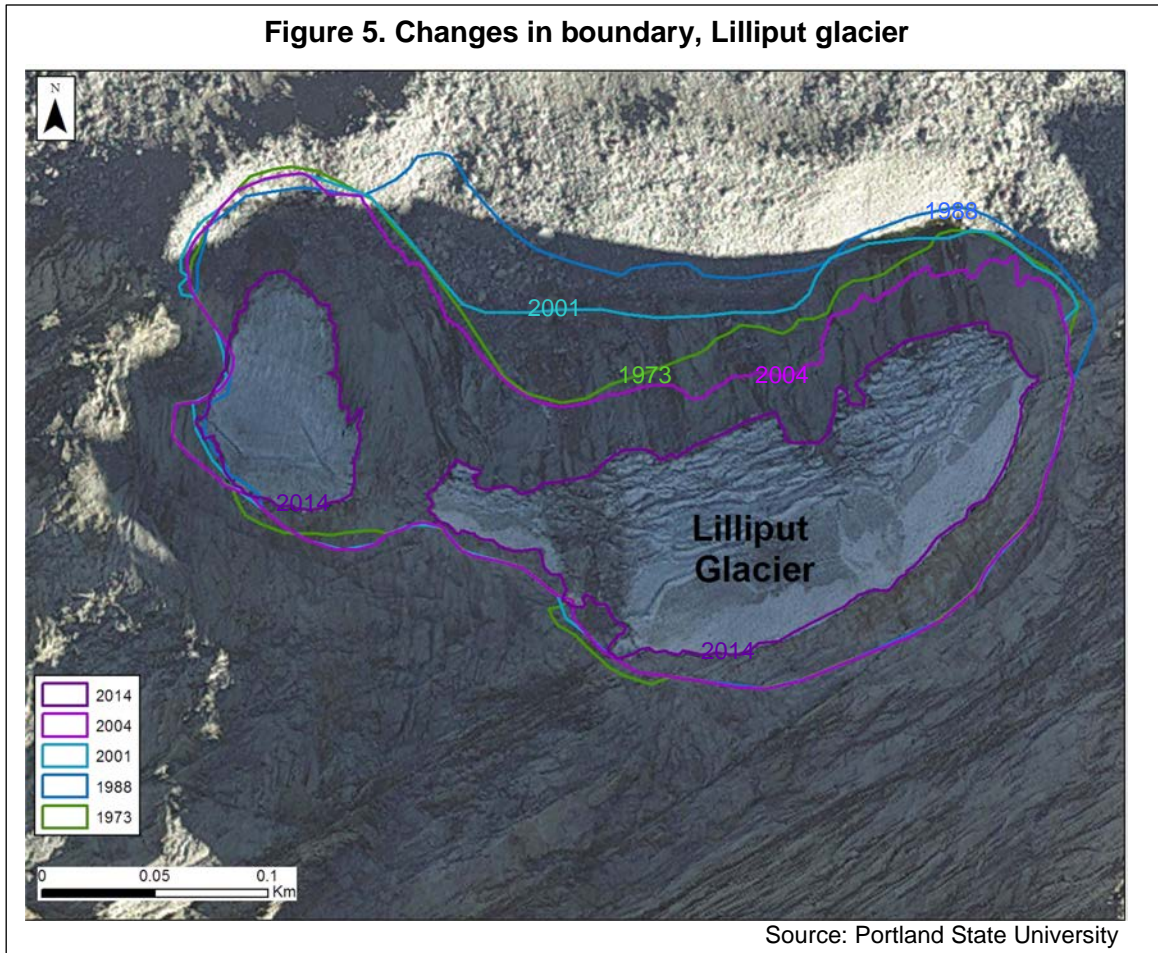
A “glacier,” by definition, is a mass of perennial snow or ice that moves (Cogely et al., 2011). As such, glaciers are a product of regional climate, responding to the combination of winter snow and spring/summer temperatures. Winter snowfall nourishes the glaciers, and spring/summer temperatures melt ice and snow. Summer air temperature affects the rate of snow and ice melt. Winter temperature determines whether precipitation falls as rain or snow and therefore affects snow accumulation and glacier mass gain. The greater the winter snowfall, the healthier the glacier. Based on their assessment of studies of glaciers in various parts of the world, the Intergovernmental Panel on Climate Change concluded that human-induced warming likely contributed substantially to widespread glacier retreat during the 20th century (IPCC, 2014).

Analysis for the Sierra Nevada (Basagic and Fountain, 2008) shows a 0.6 degree centigrade (°C) increase in mean annual air temperature over the past century. Seasonal spring, summer and winter mean temperatures likewise increased, with spring mean temperatures showing the greatest change (+1.8°C). The glacier retreat (i.e., decrease in size) in the Sierra Nevada occurred during extended periods of above average spring and summer temperatures. Winter snowfall appears to be a less important factor. Following a cool and wet period in the early part of the century during which glacier area was constant, the Sierra Nevada glaciers began to retreat rapidly with warmer and drier conditions in the 1920s. The glaciers ceased retreating, while some glaciers increased in size (or “advanced”) during the wet and cool period between the 1960s and early 1980s with below average temperatures. By the late 1980s, with increasing spring and summer temperatures, glacier retreat resumed, accelerating by 2001. Hence, the timing of the changes in glacier size appears to coincide with changes in air temperatures. In fact, glacier area changes at East Lyell and West Lyell glaciers were found to be significantly correlated with spring and summer air temperatures.

Figure 5 illustrates how the area of Lilliput Glacier changed over time and split into two glaciers. The changing glacier boundary is derived from five aerial photographs from 1973 to 2014, by Portland State University.



Figure 5. Changes in boundary, Lilliput glacier



As can be seen from Figure 1, the seven glaciers studied have all decreased in area. However, the magnitude and rates of change are variable, suggesting that factors other than regional climate influenced these changes. One of these factors is glacier geometry. A thin glacier on a flat slope will lose more area compared to a thick glacier in a bowl-shaped depression, even if the rate of melting is the same. In addition, local topographic features, such as headwall cliffs, influence glacier response through shading solar radiation, and enhancing snow accumulation on the glacier through avalanching from the cliffs.

A glacier gains or loses mass through climatic processes, then responds by either advancing or retreating. The area changes observed in the photographs of the study glaciers were instigated by climatic changes, but modified by the dynamics of ice flow. Hence, glacier change is a somewhat modified indicator of climate change, with local variations in topography and climate either enhancing or reducing the magnitude of change so that each glacier's response is unique.

Technical Considerations

Data Characteristics

To quantify the change in glacier extent, seven glaciers in the Sierra Nevada were selected based on the availability of past data and location: Conness, East Lyell,



West Lyell, Darwin, Goddard, Lilliput, and Picket glaciers. Glacier extents were reconstructed using historical photographs and field measurements. Aerial photographs were scanned and imported into a geographic information system (GIS). Only late summer photographs, largely snow free, were used in the interpretation of the ice boundary. The historic glacier extents were interpreted from aerial photographs by tracing the ice boundary. Early 1900 extents are based on ground-based images and evidence from moraines. To obtain recent glacier areas, the extent of each glacier was recorded using a global positioning system (GPS) in 2004. The GPS data were processed (2-3 m accuracy), and imported into the GIS database. Glacier area was calculated within the GIS database.

The Fountain et al. (2017) study cited above as having consistent findings provided estimates of area change considered to be preliminary. The area estimates of glaciers and perennial snowfields in that study are based on a comparison of recent aerial photographs to older US Geological Survey topographic maps. The recent photography is quite good, with little seasonal snow obscuring the glacier boundaries. The older maps were also based on aerial photographs taken when the landscape was snowy, thus masking some glacier boundaries. This could have caused a small overestimate of the glacier area; consequently, the difference in area between then and now is likely to be larger than in reality in the Fountain et al. (2017) study. However, the similarity in the findings from two entirely different sources using different methods provides confidence in the results.

Strengths and Limitations of the Data

The observation of tangible changes over time demonstrates the effects of climate change in an intuitive manner. This indicator relies on data on glacier change based on photographic records, which are limited by the availability and quality of historical photographs. Increasing the number of studied glaciers and the number of intervals between observations would provide a more robust data set for analyzing statistical relationships between glacier change and climatological and topographic parameters. Additionally, volume measurements would provide valuable information and quantify changes that area measurements alone may fail to reveal.

For more information, contact:



Andrew G. Fountain and Hassan J. Basagic
Department of Geology
Portland State University
P. O. Box 751
Portland, OR 97207-0751
andrew@pdx.edu
(503) 725-3386
www.glaciers.us

This work was supported by the Western Mountain Initiative of the US Geological Survey and by the US Forest Service. Bryce Glenn helped in the preparation of this report.



References:

Basagic HJ and Fountain AG (2011, updated by Basagic H, 2017). Quantifying 20th century glacier change in the Sierra Nevada, California. *Arctic, Antarctic, and Alpine Research* **43**(3): 317-330.

Cogley JG, Hock R, Rasmussen LA, Arendt AA, Bauder A, et al. (2011). *Glossary of Glacier Mass Balance and Related Terms, IHP-VII Technical Documents in Hydrology No. 86, IACS Contribution No. 2, UNESCO-IHP*. Available at <http://unesdoc.unesco.org/images/0019/001925/192525e.pdf>

Fountain AG, Glenn B and Basagic HJ (2017). The geography of glaciers and perennial snowfields in the American West. *Arctic, Antarctic, and Alpine Research* **49**(3): 391-410.

IPCC (2014). *Climate Change 2014: Synthesis Report. Contribution of Working Groups I, II and III to the Fifth Assessment Report of the Intergovernmental Panel on Climate Change*. [Core Writing Team, Pachauri RK and Meyer LA (Eds.)]. Intergovernmental Panel on Climate Change. Geneva, Switzerland. Available at <https://www.ipcc.ch/report/ar5/syr/>

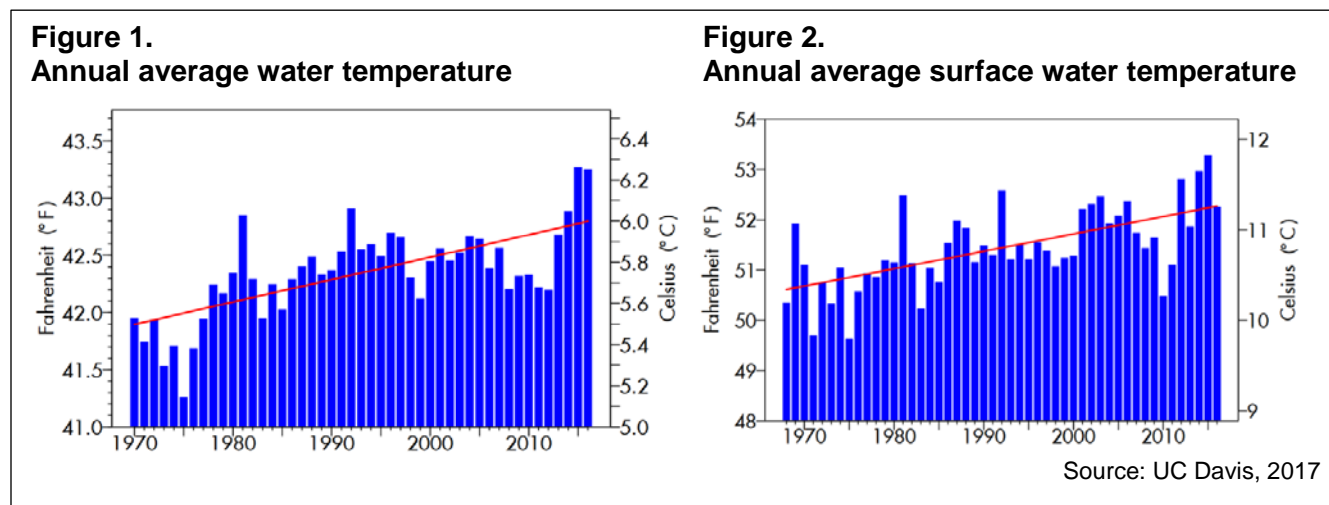
PSU (2017). Portland State University: Glaciers of the American West. Retrieved January 2, 2018, from <http://www.glaciers.us>

WGMS (2017). World Glacier Monitoring Service: Latest Glacier Mass Balance Data. Retrieved April 27, 2017 from <http://wgms.ch/latest-glacier-mass-balance-data>



LAKE WATER TEMPERATURE

Lake Tahoe waters are warming in response to warming air temperatures in the Sierra Nevada.



What does the indicator show?

Average lake water temperatures at Lake Tahoe have increased by nearly a full degree Fahrenheit (°F) since 1970 at an average rate of 0.02°F per year (Figure 1). The lake warmed from 1970 until the 1990s, began to cool between 1997 and 2011 due to deep mixing (see below), and has since warmed again. Warming accelerated in the last four years by about 10 times faster than the long-term rate.

Surface water temperatures have also increased (Figure 2). The overall warming of the lake surface is on average almost 0.04°F per year. Temperatures fell in 2016 due to cool summertime air temperatures and a large increase in winds. In 2015, the average surface water temperature was the warmest on record.

Why is this indicator important?

Climate change is among the greatest threats to lakes (O'Reilly et al., 2015). Lakes are sensitive to climate, respond rapidly to change and integrate changes in the land areas that drain into them (catchment). Thus, they also serve as good sentinels for climate change. Aquatic habitats most vulnerable to climate effects, especially rising temperatures, are alpine lakes like Lake Tahoe that sit at high altitude and latitude.

In a warming climate, tracking changes that are detrimental to lake water quality is critically important. Even seemingly small changes in lake temperature can significantly affect key physical and biological processes (O'Reilly et al., 2015). Rising water temperatures reduce water quality by increasing thermal stability and altering mixing patterns (discussed in next section). These changes can result in the creation of niches for species that previously could not survive in the lake but could now survive if introduced, potentially disadvantaging native species that have evolved under clear,



cold water conditions. Elevated water temperatures can also increase metabolic rates of organisms, from plankton to fish (UC Davis, 2017).

During the summer, Lake Tahoe waters are stratified, with warm, lighter waters at the surface, and cold, denser waters at depth. Between these layers is the “thermocline,” a region in which the temperature declines rapidly with depth. Thermal stratification occurs in the warm season because of the large differences in density between the warm and cold waters. In the late fall and winter, Lake Tahoe’s waters undergo “deep mixing,” as surface waters cool and sink to the bottom, and upwelling brings nutrients to the surface. This mixing plays a critical role in providing nutrients to the food web and distributing oxygen throughout the lake. Without this circulation, oxygen-rich surface water does not make it to the lake bottom, depriving fish and other aquatic life of oxygen.

Since 1968, the lake’s waters have undergone deep mixing every three to four years, on average. However, Lake Tahoe has not mixed to its full depth in the past five years.

Resistance to lake mixing across the thermocline increases markedly even at a temperature gradient of only a few degrees between stratified layers (Sahoo et al., 2015). Record-high water temperature in 2016 hindered the lake’s deep mixing. The lake mixed to a depth of only 540 feet, one-third of its maximum depth. Scientists are predicting that in a warming climate mixing in Lake Tahoe will become less frequent — a change that will disrupt fundamental processes that support a healthy ecosystem (UC Davis, 2017).



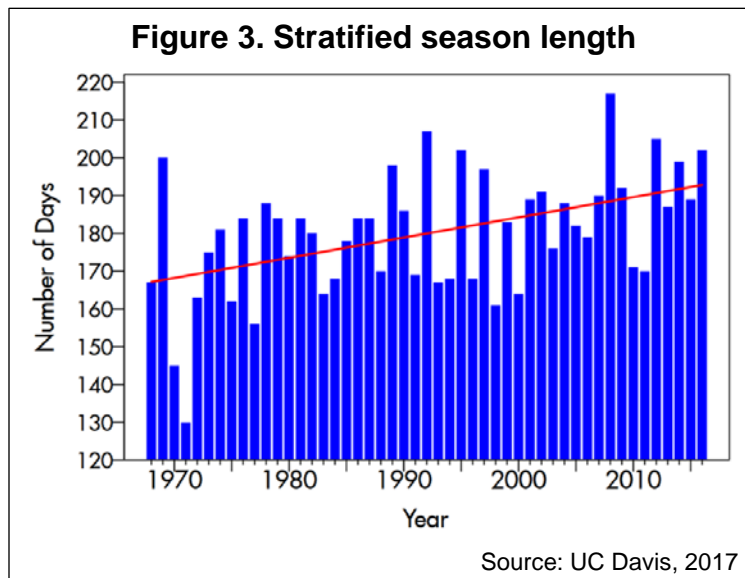
Credit: California Tahoe Conservancy

Lake Tahoe is a crystal-clear high altitude alpine lake, considered one of the jewels of the Sierra. World-renowned for its striking blue color and amazing clarity, majestic beauty, close proximity to urban areas, and opportunities for hiking, skiing, camping, boating and a host of other recreational activities, the lake draws millions of visitors to the area every year (CTC, 2017).

Lake Tahoe is 22 miles long, has a surface area of 190 square miles, and a total volume of 130 million acre feet. Its maximum depth of 1,644 feet makes it the third deepest lake in North America, and the eleventh deepest lake in the world.



Thermal stability determines “stratified season length,” the number of days when the lake is resistant to mixing (based on the amount of energy required to mix the lake). The stratification season has been starting earlier with the early arrival of spring temperatures, and ending later as the fall season for the lake has been ending later. Figure 3 shows increasing stratified season length in Lake Tahoe over the years 1968-2016. Although there is considerable year-to-year variation, overall the stratification season has lengthened by almost 26 days. A prolonged season length can potentially impact species composition, organism abundance, and lake productivity.



The lack of seasonal lake mixing can cause shifts in Lake Tahoe’s algal species and their distribution (UC Davis, 2017). Most algae are free-floating in the lake’s turbulent environment, which prevents algae from sinking out of the sunlight. Turbulence suppression, due to stratification, causes the larger algae to sink and leaves the smallest algae at the surface with no competition for nutrients. One of the most common is *Cyclotella gordonensis*, a tiny diatom. When *Cyclotella gordonensis* is suspended in the water for extended lengths of time it scatters light and decreases the lake’s clarity. As clarity decreases, greater warming of the surface water takes place, increasing stratification and the likelihood of more small algal species. This vicious cycle presents an additional climate-induced challenge. Reduced mixing may also prolong periods of reduced lake clarity that occur following years of heavy stream runoff, by causing fine particles to be retained in the upper layer of the lake (Coats et al., 2006).

Water clarity measurements have been taken continuously at Lake Tahoe since 1968 using an instrument called a Secchi disk (UC Davis, 2017). This monitoring has allowed a better understanding of how various factors, including temperature, precipitation, and nutrient and sediment inputs into the lake associated with land use and human activities are changing physical, chemical, and biological processes that affect the lake’s clarity. Although lake clarity over this period has been declining overall, the rate of decline has slowed somewhat over the last decade, with notable differences between winter and summer clarity. Since 1968, winter clarity (December–March) has shown a general improvement. However, summer clarity (June–September) shows an overall decrease over time. In 2016, decreased clarity was caused by large increases in the concentration of *Cyclotella gordonensis* due to an early onset of spring and strongly stratified lake conditions.



In addition to Lake Tahoe, warming has been reported in other lakes in the western United States. Temperature data derived from satellite observations show increasing summertime surface water temperatures in a study of four lakes in Northern California (including Lake Tahoe) and two in Nevada (Schneider et al., 2009). From 1992 to 2008, these six lakes showed a significant warming trend for summer (July through September) nighttime surface temperatures, ranging from 0.05 degrees Celsius (°C) per year at Clear Lake to 0.15°C per year at Lake Almanor and Mono Lake. The lakes exhibited a fairly similar rate of change, with the mean warming rate of 0.11°C per year ($\pm 0.03^\circ\text{C}$ per year).

The scenic beauty of Lake Tahoe offers recreational and cultural opportunities. The annual tourist population of 4.5 million makes it a region of national economic significance, with estimated annual revenues of 4.7 billion dollars (Mooney and Zavaleta, 2016). A decline in the famous water clarity and ecosystem health of the lake could jeopardize future tourism.

What factors influence this indicator?

Key drivers controlling lake surface water temperature are air temperature, solar radiation, humidity, ice cover, and wind. Lake temperatures are also mediated by local factors such as lake surface area, volume, and depth. A study of lakes around the world found summer air temperature to be the single most important and consistent predictor of lake summer surface water temperature (LSSWT) (O'Reilly et al., 2015). The study reported that LSSWT is warming significantly, with a mean trend of 0.34°C per decade across 235 globally distributed lakes between 1985 and 2009. This warming water surface rate is consistent with the annual average increase in air temperatures and ocean surface temperatures over a similar time period (1979–2012).

Lake Tahoe warming trends reflect overall air temperature trends in the region (UC Davis, 2017). Lake Tahoe's accelerated warming over the last four years is of special concern, since its enormous volume should make it less vulnerable to change. Over the last 105 years, the average daily maximum air temperature at Tahoe City has risen by 1.1°C (2°F) and the nighttime minimum temperature by 2.4°C (4.3°F). A warming climate is affecting other physical changes at Lake Tahoe — including a shift from snow to rain and a shift in snowmelt timing to earlier dates — that may have significant impacts on lake ecology and water quality. For more information about meteorological trends in the Lake Tahoe area, refer to: *Tahoe: State of the Lake 2017* (UC Davis, 2017).

Technical Considerations

Data Characteristics

The University of California, Davis and its research collaborators collect the measurements used for monitoring Lake Tahoe. They have recorded water temperature measurements at two locations in Lake Tahoe since 1969:

- (1) at the Index Station (about 0.3 kilometers off the California side west shore) at depth increments of 2 to 15 meters starting at the surface to a depth of about



- 100 meters, on an approximately weekly basis (and since 1996 at 1-meter increments to a depth of 125 meters biweekly);
- (2) at the Midlake Station, the exact location of which has varied slightly over time, at nominal depths of 0, 50, 100, 200, 300 and 400 meters, on an at least monthly basis (Coats, 2006).

Strengths and Limitations of the Data

A variety of thermometers and digital thermographs have been used at the Index Station over the years. Although the sensitivity, accuracy, and calibrations of these instruments have varied over time, these data are adequate for characterizing the thermal structure of the epilimnion and thermocline. Temperatures at the Midlake Station were originally measured at 13 depths with mercury-reversing thermometers, as follows: a protected thermometer, unaffected by pressure, records the temperature at reversal depth; readings from this thermometer are corrected for glass expansion and, along with a second, unprotected thermometer affected by pressure in deep water, provide measure of the actual depth of the temperature reading (Coats et al., 2006). These instruments were accurate to 0.01°C. More recently temperature is measured using a high precision thermistor that is part of a suite of instruments on a Seabird SBE-25 profiler. Accuracy of the thermistor is 0.001°C. The Seabird measures at a rate of 8 times per second as it falls through the water at a velocity of 60 centimeters/sec.

Lake temperature data derived from thermal infrared satellite imagery (ATSR and MODIS), when validated against corresponding *in situ* data for Lake Tahoe, were found to agree very well over the entire range of temperatures. This, along with an additional assessment of inter-sensor bias between all ATSR sensors, indicates that accurate and stable time series of lake surface temperature can be retrieved from ATSR and MODIS satellite data.

For more information, contact:

S. Geoffrey Schladow
Professor of Water Resources and Environmental Engineering
Director, Tahoe Environmental Research Center
University of California Davis
Department of Civil & Environmental Engineering
(530) 752-3942
<http://edl.engr.ucdavis.edu>

References:

Coats R, Perez-Losada J, Schladow G, Richards R and Goldman C (2006). The warming of Lake Tahoe. *Climatic Change* **76**(1): 121-148.

CTC (2017). California Tahoe Conservancy: Public Access and Recreation Program. California Tahoe Conservancy. Retrieved January 2017, from <http://tahoe.ca.gov/recreation-public-access/>

Mooney H and Zavaleta E (Eds.) (2016). *Ecosystems of California*. Oakland, California: University of California Press. Available at <https://www.ucpress.edu/book.php?isbn=9780520278806>



O'Reilly CM, Sharma S, Gray DK, Hampton SE, Read JS, et al. (2015). Rapid and highly variable warming of lake surface waters around the globe. *Geophysical Research Letters* **42**(24): 10,773-10,781.

Sahoo GB, Forrest AL, Schladow SG, Reuter JE, Coats R and Dettinger M (2015). Climate change impacts on lake thermodynamics and ecosystem vulnerabilities. *Limnology and Oceanography* **61**(2): 496-507.

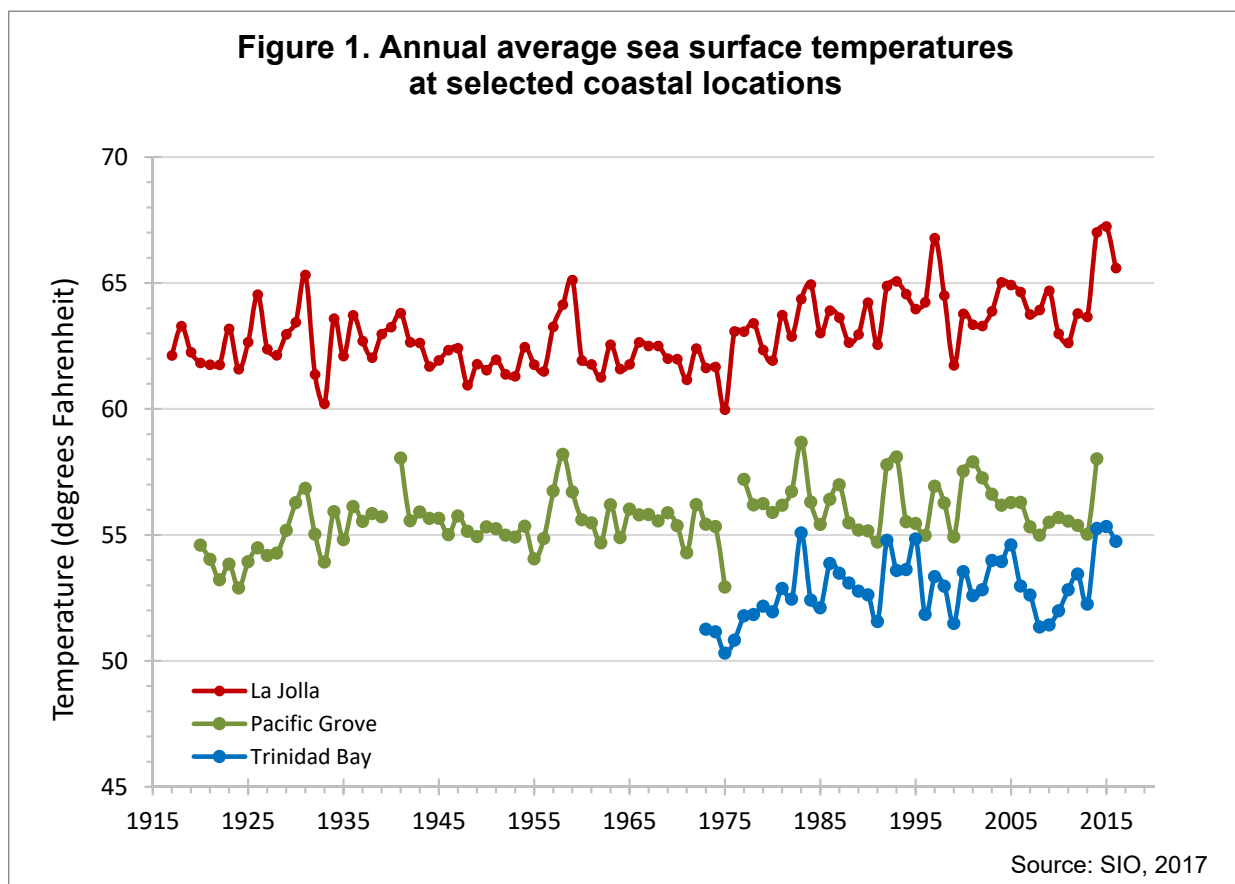
Schneider P, Hook SJ, Radocinski RG, Corlett GK, Hulley GC, et al. (2009). Satellite observations indicate rapid warming trend for lakes in California and Nevada. *Geophysical Research Letters* **36**(22): L22402.

UC Davis (2017). *Tahoe: State of the Lake Report 2017*. University of California, Davis. Davis, CA: Tahoe Environmental Research Center. Available at <http://terc.ucdavis.edu/stateofthelake/>



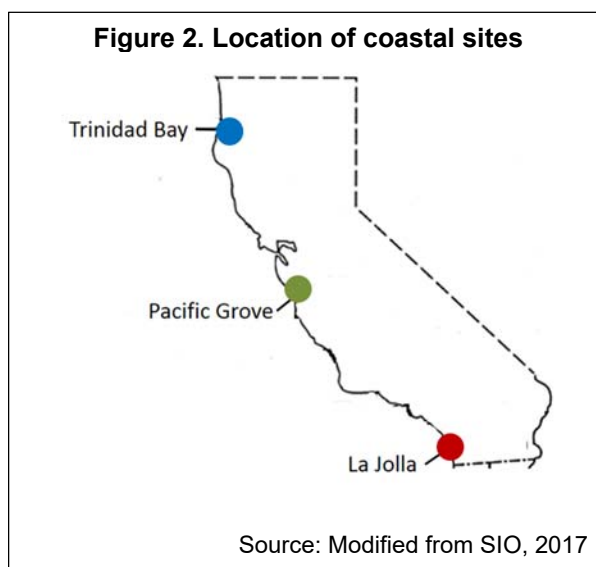
COASTAL OCEAN TEMPERATURE

Like global ocean temperatures, California coastal temperatures have warmed over the past century.



What does the indicator show?

California coastal ocean temperatures have warmed over the past century. Although sea surface temperature (SST) fluctuates naturally each year, trends of sea surface warming are clearly detected. Specifically, as shown in Figure 1, SST has increased at the rate of 0.2 Fahrenheit (°F) per decade at Pacific Grove between 1920 and 2014. SSTs at La Jolla increased at about the same rate between 1917-2016, but at a faster rate of 0.6°F per decade since 1973. At Trinidad Bay, SSTs increased at the rate of 0.4°F per decade over the same shorter time period (1973-2016). (See Figure 2 for coastal measurement locations.)



These observations are consistent with those observed globally. Global scale changes in sea and land surface temperature are unequivocal (IPCC, 2013). From 1950 to 2016, globally averaged sea surface temperatures warmed at a rate of about 1.8°F per century, while the rate of warming for 2000 to 2016 is 2.9°F per century, reflecting sharper increases in sea surface temperatures over the recent 16-year period (NOAA, 2017).

Why is this indicator important?

Temperature is one of the best-measured signals of climate change. The ocean's large mass and high heat capacity allow it to store large amounts of heat. As atmospheric concentrations of greenhouse gases increase, excess heat is absorbed and stored by the oceans and atmosphere. It is estimated that over 90 percent of the observed heat energy increase on the Earth over the past 50 years has occurred in the ocean (Rhein et al., 2013; NOAA, 2015).

Changes in temperature can affect the physical and chemical properties of the ocean. Since warmer water is less dense than colder water, changes in SST can alter currents and transport patterns. Warming SSTs can cause more stable layers of seawater to form near the surface, thus increasing "stratification"; when this happens, vertical mixing that transports nutrients, oxygen, carbon, plankton and other material across ocean layers is reduced (Roemmich and McGowan, 1995). Temperature also impact affects air-sea gas exchange. Surface water temperature affects weather, specifically the occurrence of coastal fog and the strength of winds, as well as the thickness of the marine atmospheric boundary layer. The latter is a primary factor controlling the inland intrusion of cool coastal air and therefore inland weather patterns. Warmer waters play a role in extreme weather events by increasing the energy and moisture of the atmosphere. Warmer ocean temperatures also contribute to global sea level rise because warming water not only expands but also accelerates the melting of land-based ice sheets.

Changes in SST along the coast of California can alter the distribution and abundance of many marine organisms, including commercially important species. Fluctuations in the distribution and abundance of many California coastal marine populations have been related to temperature variability (e.g., Sagarin et al., 1999; Goericke et al., 2007). The direct effects of temperature on the physiological performance of marine organisms and the timing of their key developmental stages (such as from egg to larva) are the likely mechanisms underlying these patterns. Water temperature can also influence species indirectly, by altering interactions between species and their competitors, predators, parasites, facilitators, and prey.

The period of unusually high SSTs in 2014-2015 (discussed further in the next section) was accompanied by northward shifts in the geographic distributions of a variety of marine animals including fish, sea turtles, pelagic red crabs, southern copepods and many other marine invertebrates (Leising et al., 2015; Cavole et al., 2016). The 2014-2015 warm-water anomaly was also associated with mass strandings of some marine mammals and sea birds (Cavole et al., 2016). High temperatures initiated toxic algal



blooms that affected the commercial and recreational crab fishing season (Gentemann et al., 2017). Temporary shifts in species distributions have also occurred during past warm-water anomalies, including major El Niño-Southern Oscillation (ENSO) events (Pearcy and Schoener, 1987). While these impacts of coastal temperature change are beginning to be documented, offshore temperature variability is complex and may influence a suite of other biological processes, including migration patterns.

What factors influence this indicator?

As noted above, global SSTs have increased due to a net heat flux from the atmosphere stemming from the greenhouse effect. Deeper regions of the oceans have also warmed, to depths of 3000 meters during the past several decades (Levitus et al., 2001).

Regionally, near-surface ocean water temperatures along the California coast are influenced by seasonal upwelling. Upwelling is a wind-driven process in the spring and summer months that brings deep, colder, nutrient-rich waters to the surface. Trends in coastal temperatures are complex owing to the simultaneous interaction of surface warming and the cooling effect of upwelling. In general, it is expected that surface temperatures will increase offshore and in sheltered coastal waters, where upwelling does not occur. In contrast, cooler SSTs are observed during the upwelling season in open shelf waters, especially off central and northern California (Largier et al., 2010; Garcia-Reyes and Largier, 2010; Sydeman et al., 2014). In certain upwelling regions, including the California Current, studies suggest that upwelling favorable winds may intensify with climate change (Bakun, 1990; Garcia-Reyes and Largier, 2010; Sydeman et al., 2014). In parts of coastal California, summer SSTs decreased between the 1980s and 2000s, at rates of 0.2-0.4°C per decade with stronger upwelling favorable winds (Garcia-Reyes and Largier, 2010).

Natural fluctuations in temperature, wind, and circulation patterns that occur in coastal waters can introduce variability observed in long-term trends. Although the long-term increase in SST in California waters is clearly evident, significant interannual and interdecadal fluctuations are also observed. A recent notable event occurred when anomalously warm waters were observed across the northeast Pacific in 2014 and 2015 (Figure 3). A large area of exceptionally high SSTs first appeared in the Gulf of Alaska in November 2013. Known as the “warm blob” or a “marine heat wave”, this phenomenon resulted in unprecedented sea surface temperatures off central/northern California (Di Lorenzo and Mantua, 2016). While marine heat waves have occurred in the past, the magnitude and duration of the warming during this event was unprecedented for the west coast of North America. Further, it was followed by El Niño-Southern Oscillation (ENSO) conditions during the 2015-2016 winter. ENSO is responsible for anomalously warm (or cool) ocean temperatures during El Niño (or La Niña) events, with major El Niño events occurring every 5-10 years (UCAR, 1994). Additionally, the West Coast is affected by multi-decadal variability in temperature, characterized by patterns such as the Pacific Decadal Oscillation, or PDO



(Mantua et al., 1997), and the North Pacific Gyre Oscillation, or NPGO (Di Lorenzo et al., 2008). While these natural fluctuations make it more difficult to isolate the magnitude of anthropogenic climate change, they also provide an indication of the ecosystem's sensitivity to extremes in temperature and other factors. Recent work projects that future SSTs (by year 2070) will always be warmer than the warmest year in the historical record, despite all of the natural variability inherent to this system (Alexander et al., 2018).

Technical Considerations

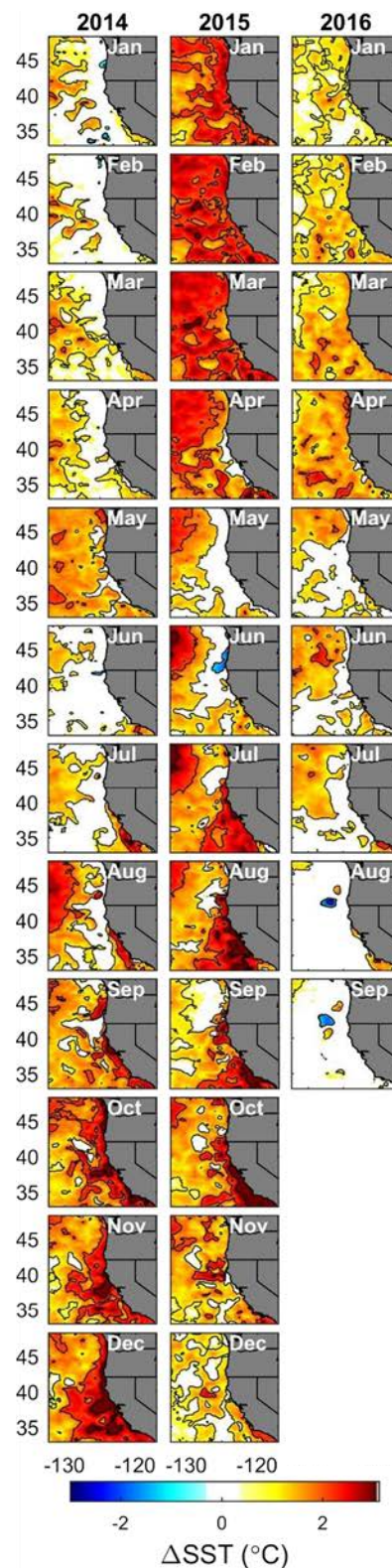
Data Characteristics

Coastal California is home to the longest continuous record of SST on the US West Coast and the Pacific Rim. In total, there are over 300 sites with SST time series along the shore and in the nearshore region of California (see Figure 4).

Long-term time series from three sites — Trinidad Bay in Humboldt County, Pacific Grove in Monterey County, and La Jolla in San Diego — are presented in this report; these sites were chosen based upon their long operational duration (~40 to 100 years), public data availability, and regional/geographic coverage. Data for the three sites have been collected by the Shore Stations Program (SIO, 2017), which provides access to current and historical data records of SST from 9 coastal California sites. The time series at Scripps Pier, La Jolla Shores, which extends back to 1916, is the longest running SST data set in the state.

Trinidad Bay temperature measurements are taken daily by staff from the [Humboldt State University Marine Laboratory](#), located on the rocky headland between the ocean and Trinidad Bay. Bay temperature is measured from the fishing pier on the southeast side of the headland. Pacific Grove measurements are taken daily by staff from [Stanford University's Hopkins Marine Station](#) from a beach on the north side of Point Cabrillo. This location is representative of coastal conditions on

Figure 3. Monthly SST anomalies* during the marine heatwave



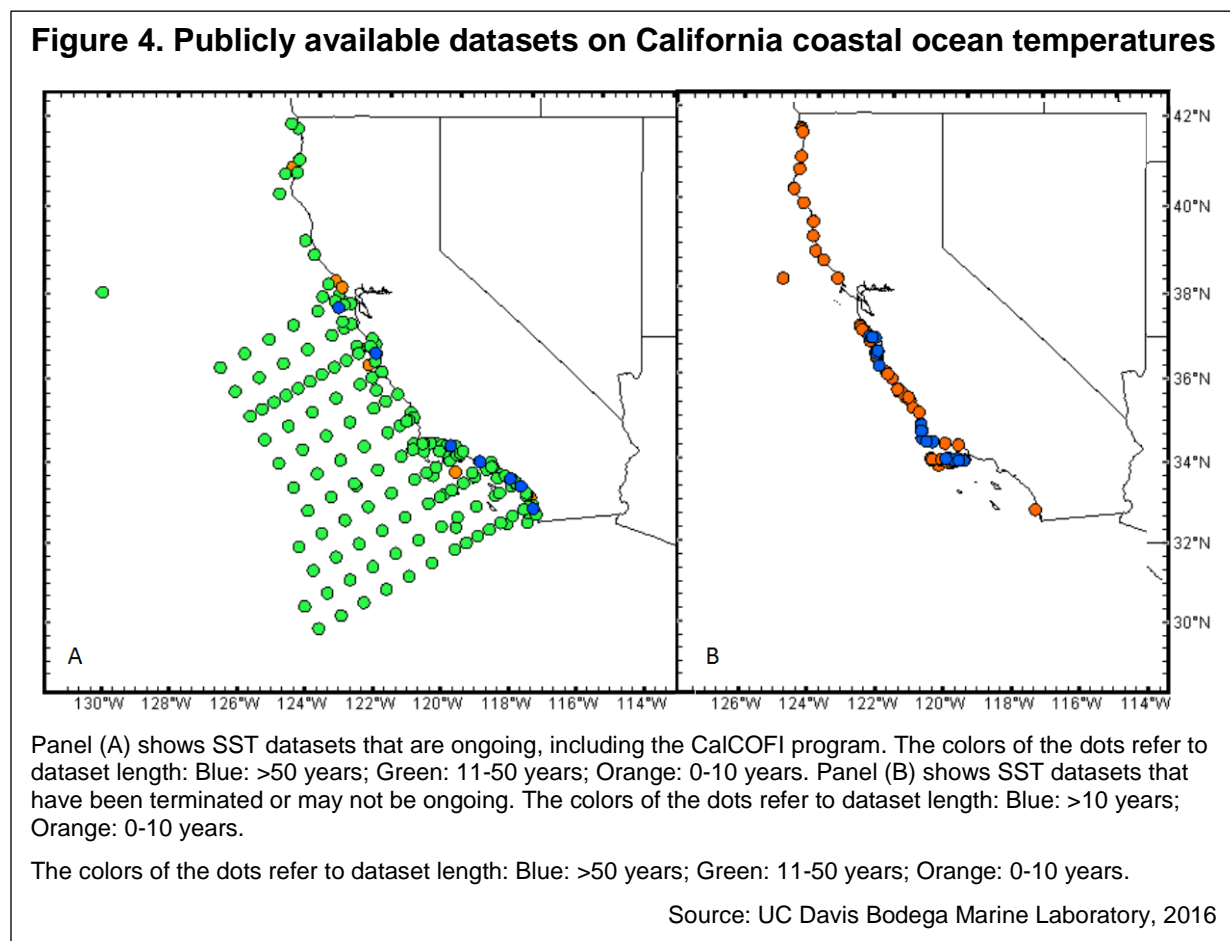
*relative to 2002-2012

Source: Gentemann et al., 2017



the south side of Monterey Bay. La Jolla temperature measurements are taken daily at Scripps Pier by representatives from Scripps Birch Aquarium. The proximity of the pier to the deep waters at the head of La Jolla submarine canyon results in data representative of oceanic conditions.

Publicly available datasets on coastal ocean temperatures in California are presented in Figure 4. While SST is being measured throughout the entire state (N=300 datasets), more data are being collected south of San Francisco Bay; 71 percent of datasets (N=214) are 10 years or longer (green and blue dots); however, only 65 percent of datasets (N=194) are both ongoing and 10 or more years long (green and blue dots, Panel A). Long-term, ongoing datasets present the greatest opportunity to detect a signature of climate change in SST along the California coast. It is also important to sustain more recently established datasets to better understand SST trends.



A growing network of ocean monitoring along California is an important resource for separating natural and anthropogenic influences on increasing temperatures. The California Cooperative Oceanic Fisheries Investigations (CalCOFI) and National Oceanic and Atmospheric Administration (NOAA) National Data Buoy programs represent the largest coordinated efforts to collect SST data across broad spatial scales. In addition, the Central and Northern California Ocean Observing System and



the Southern California Coastal Observing System provide coordinated long-term monitoring of environmental conditions to support ocean management decisions as part of an eleven-region US Integrated Ocean Observing System (IOOS, 2018).

Many SST datasets for California are short and/or terminated time series (41 percent), providing limited utility in separating anthropogenic and natural processes. Climate-related trends are challenging to distinguish from natural variability for SST datasets covering less than 10 years (Henson et al., 2016). Longer data sets are ideal in light of the natural fluctuations that recur at subdecadal and multi-decadal intervals. Thus, it is critical that data collection continues and is extended to increase the coverage of datasets from which to evaluate climate change-induced SST in California waters.

One collective limitation of the datasets currently available is that there is less information to describe the effects of climate change in Northern California, because fewer time series have been collected in that region. While SST is being measured throughout the entire state, data collections to date have been concentrated south of the San Francisco Bay, in Central and Southern California.

For more information, contact:



Eric Sanford, Ph.D.
University of California, Davis
Bodega Marine Laboratory
P. O. Box 247
Bodega Bay, CA 94923
(707) 875-1910
edsanford@ucdavis.edu

John Largier, Ph.D.
University of California, Davis
Bodega Marine Laboratory
P. O. Box 247
Bodega Bay, CA 94923
(707) 875-1930
jlargier@ucdavis.edu

2009 indicator contributed by Frank Schwing, NOAA.

2017 updates provided by UC Davis team: Hill, Largier, Sanford, Rivest, Myhre, Gaylord

References:

Alexander AA, Scott JD, Friedland KD, Mills KE, Nye JA, et al. (2018). Projected sea surface temperatures over the 21st century: Changes in the mean, variability and extremes for large marine ecosystem regions of Northern Oceans. *Science of the Anthropocene* 6(9).

Bakun A (1990). Global climate change and intensification of coastal ocean upwelling. *Science* 247: 198-201.

Barry JP, Baxter CH, Sagarin RD and Gilman SE (1995). Climate-related, long-term faunal changes in a California rocky intertidal community. *Science* 267(5198): 672- 675.



Cavole LM., Demko AM, Diner RE, Giddings A, Koester I, et al. (2016). Biological impacts of the 2013–2015 warm-water anomaly in the Northeast Pacific: Winners, losers, and the future. *Oceanography* **29**: 273–285.

Di Lorenzo E and Mantua N (2016) Multi-year persistence of the 2014/15 North Pacific marine heatwave. *Nature Climate Change* **6**(11): 1042–1048.

García-Reyes M and Largier J (2010). Observations of increased wind-driven coastal upwelling off Central California. *Journal of Geophysical Research* **115**(C4).

Gentemann C, Fewings M and Garcia-Reyes M (2017). Satellite sea surface temperature along the West Coast of the United States during the 2014-2016 Northeast Pacific marine heat wave. *Geophysical Research Letters* **44**: 312-310.

Goerck R, Venrick EL, Koslow TL, Sydeman WJ, Schwing FB, et al. (2007). The State of the California Current, 2006-2007: Regional and local processes dominate. *CalCOFI Report* **48**: 33-66.
http://www.calcofi.org/newhome/publications/CalCOFI_Reports/v48/033-066_State_Of_Current.pdf

Henson SH, Beaulieu C and Lampitt R (2016). Observing climate change trends in ocean biogeochemistry: When and where. *Global Change Biology* **22**:1561-1571.

IPCC (2013). Summary for Policymakers. In: *Climate Change 2013: The Physical Science Basis. Contribution of Working Group I to the Fifth Assessment Report of the Intergovernmental Panel on Climate Change*. Stocker TF, Qin D, Plattner G-K, Tignor M, Allen SK, et al. (Eds.). Cambridge, United Kingdom and New York, NY, USA: Cambridge University Press. Available at
http://www.ipcc.ch/pdf/assessment-report/ar5/wg1/WGIAR5_SPM_brochure_en.pdf

Largier, JL, Cheng BS and Higgason KD (2010). *Climate Change Impacts: Gulf of the Farallones and Cordell Bank National Marine Sanctuaries. Report of a Joint Working Group of the Gulf of the Farallones and Cordell Bank National Marine Sanctuaries Advisory Councils* (Marine Sanctuaries Conservation Series ONMS-11-04). National Oceanic and Atmospheric Administration. Available at
https://nmssanctuaries.blob.core.windows.net/sanctuaries-prod/media/archive/science/conservation/pdfs/climate_cbnms.pdf

Leising AW, Schroeder ID, Bograd SJ, Abell J, Durazo R, et al. (2015). State of the California Current 2014-15: Impacts of the warm water “blob”. *CalCOFI Report* **56**:31-68.

Levitus S, Antonov JI, Wang J, Delworth TL Dixon KW and Broccoli AJ (2001). Anthropogenic warming of Earth's climate system. *Science* **292**(5515): 267-270.

Mantua N, Hare S, Zhang Y, Wallace J and Francis R (1997). A Pacific interdecadal climate oscillation with impacts on salmon production. *Bulletin of the American Meteorological Society* **78**: 1069-1079.

McGowan JA, Cayan DR and Dorman LM (1998). Climate-ocean variability and ecosystem response in the Northeast Pacific. *Science* **281**(5374): 210-217.

Mendelssohn R and Schwing F (2002). Common and uncommon trends in SST and wind stress in the California and Peru-Chile Current Systems. *Progress in Oceanography* **53**: 141-162.

Mendelssohn R, Schwing F and Bograd S (2003). Spatial structure of subsurface temperature variability in the California Current, 1950-1993. *Journal of Geophysical Research -Oceans* **108** (C3): 3093.

NOAA (2012). Global Surface Temperature Anomalies. The Global Anomalies and Index Data: The Annual Global Land Temperature Anomalies (degrees C); The Annual Global Ocean Temperature Anomalies (degrees C); The Annual Global (land and ocean combined) Anomalies (degrees C). Retrieved April 3, 2012, from <http://www.ncdc.noaa.gov/cmbfaq/anomalies.php>



NOAA (2015). Climate change: Ocean Heat Content. Retrieved August, 2017 from <https://www.climate.gov/news-features/understanding-climate/climate-change-ocean-heat-content>

NOAA (2017). *State of the Climate in 2016. Report Highlights* (Bulletin of the American Meteorological Vol. 98 No. 8). Available at: <https://www.ncdc.noaa.gov/bams>

Palacios D, Bograd S, Mendelssohn R and Schwing F (2004). Long-term and seasonal trends in stratification in the California Current, 1950-1993. *Journal of Geophysical Research - Oceans* **109** (C10).

Pearcy WG and Schoener A (1987). Changes in marine biota coincident with the 1982-83 El Niño in the northeastern subarctic Pacific Ocean. *Journal of Geophysical Research* **92**: 14417–14428.

Rhein M, Rintoul SR, Aoki S, Campos E, Chambers D, et al. (2013). Observations: Ocean. In: *Climate Change 2013: The Physical Science Basis. Contribution of Working Group I to the Fifth Assessment Report of the Intergovernmental Panel on Climate Change*. Stocker TF, Qin D, Plattner G-K, Tignor M, Allen SK, et al. (Eds.). Cambridge, United Kingdom and New York, NY, USA: Cambridge University Press. Available at <http://www.ipcc.ch/report/ar5/wg1/>

Roemmich D (1992). Ocean warming and sea level rise along the Southwest U.S. coast. *Science* **257**(5068): 373-375.

Roemmich D and McGowan J (1995). Climatic warming and the decline of zooplankton in the California Current. *Science* **267**(5202): 1324-1326.

Sagarin RD, Barry JP, Gilman SE and Baxter CH (1999). Climate-related change in an intertidal community over short and long time scales. *Ecological Monographs* **69**(4): 465-490.

SIO (2017). Shore Stations Program. Trinidad temperature measurements and salinity samples collected by staff at Humboldt State University Marine Laboratory; Pacific Grove measurements collected by the Stanford University Hopkins Marine Station; Scripps Pier measurements collected by the Birch Aquarium at Scripps staff and volunteers. Data provided by the Shore Stations Program, sponsored at Scripps Institution of Oceanography by California State Parks and Recreation, Division of Boating and Waterways, Award C1670003. Retrieved December 7, 2017, from <http://shorestations.ucsd.edu/>

Smith T and Reynolds R (2005). A global merged land air and sea surface temperature reconstruction based on historical observations (1880-1997). *Journal of Climate* **18**: 2021-2036.

Snyder M, Sloan L, Diffenbaugh N and Bell J (2003). Future climate change and upwelling in the California Current. *Geophysical Research Letters* **30**: 1823.

Sydeman WJ, Garcia-Reyes M, Schoeman DS, Rykaczewski RR, Thompson SA, et al. (2014). Climate change and wind intensification in coastal upwelling ecosystems. *Science* **345**: 77-80.

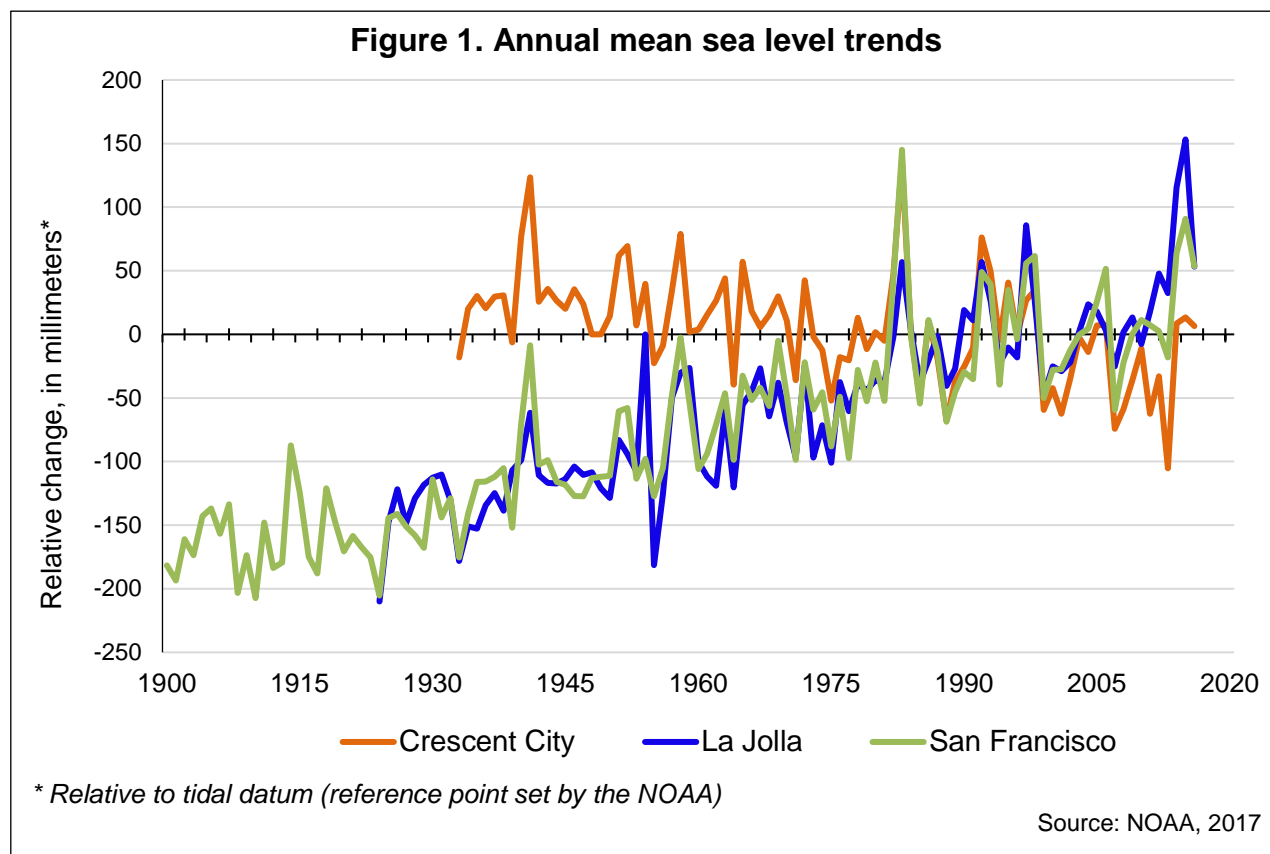
UCAR (1994). *El Niño and Climate Prediction, Reports to the Nation on our Changing Planet. University Corporation for Atmospheric Research, pursuant to National Oceanic and Atmospheric Administration (NOAA) Award No. NA27GP0232-01*. Available at <http://www.pmel.noaa.gov/tao/elnino/report/el-nino-report.html>.

UC Davis Bodega Marine Laboratory (2016). Map showing location of stationary monitoring sites for dissolved oxygen off California. Unpublished data.



SEA LEVEL RISE

Sea levels along the California coast have generally risen over the past century, except along the far north coast where uplift of the land surface has occurred due to the movement of the Earth's plates.



What does the indicator show?

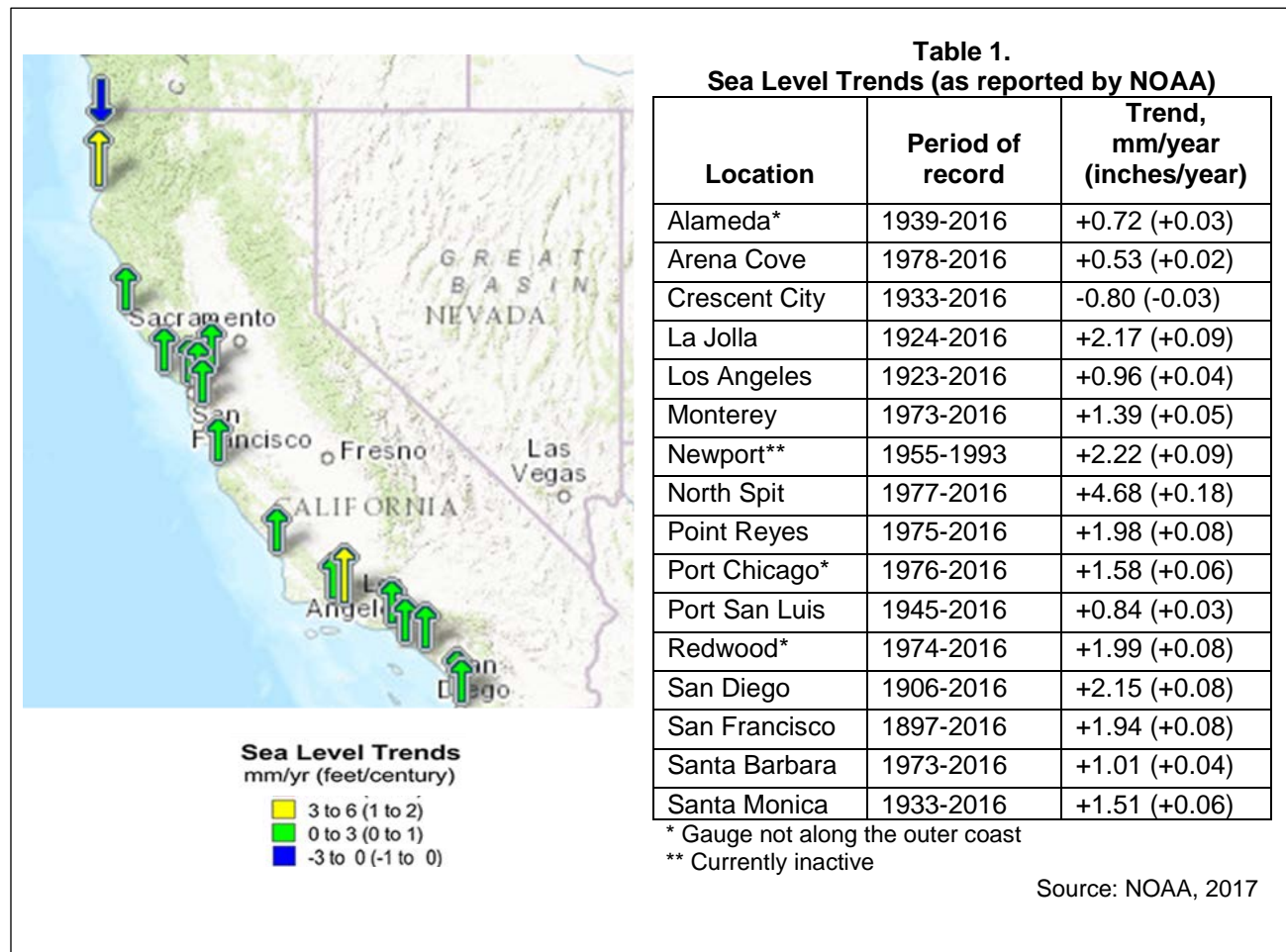
Mean sea levels along the California coast show year-to-year variability, peaking during El Niño years (when the waters of the eastern Pacific Ocean are warmer). Over the long term, mean sea levels — the average height of the ocean relative to land — have been rising. Figure 1 shows annual changes relative to a standard elevation established by the National Oceanic and Atmospheric Administration (NOAA) as a reference point (see *Technical Considerations* for details).

Mean sea level has increased by 180 millimeters (mm) (7 inches (")) since 1900 in San Francisco, and by about 150 mm (6") since 1924 in La Jolla. In contrast, sea level at Crescent City has declined by about 70 mm (3") since 1933 due to plate tectonics. Levels at all three locations rose in 2014 and 2015, possibly due to unusually warm sea surface temperatures in the Pacific Ocean during that period.

Trends at 16 tide stations operated by NOAA in California are presented in Table 1, with graphs for individual locations in the Appendix (NOAA, 2017). (One NOAA tide station has been excluded from the table: Rincon Island, an artificial offshore island in



Ventura County built for oil and gas production, reported a linear trend of +3.22 mm/year based on measurements from 1962 to 1990.)



The general trend towards higher sea levels in California is consistent with global observations (IPCC, 2014). Global sea-level rise is the most obvious manifestation of climate change in the ocean (Griggs et al., 2017). Since the mid-19th century, global mean sea levels have been rising at a higher rate than during the previous two millennia. More recently, the rate of increase has been at 3.2 mm/year (about 0.1 inch/year) between 1993 and 2010, faster than the rate of 1.7 mm/year (0.07 inch/year) between 1901 and 2010, during which sea levels rose by 0.19 meters (7.5 inches) (IPCC, 2014). Similarly high rates occurred between 1920 and 1950.

Why is this indicator important?

More than 70 percent of California residents live and work in coastal counties, and almost 86 percent of the state's total gross domestic product comes from these counties (Caldwell et al., 2013). California's hundreds of miles of scenic coastline contain ecologically fragile estuaries, expansive urban centers, and fisheries that could be impacted by future changes in sea level elevation. Critical infrastructure lies less than 4 feet above the high tide, including two international airports--Oakland and



San Francisco — and about 172,000 homes (DWR, 2016). Rising sea levels place the airports, already vulnerable to storms and flooding, at greater risk. Loss of service at either airport would result in major economic consequences regionally, nationally, and internationally (San Francisco Bay Conservation and Development Commission, 2012). Other critical infrastructure, such as natural gas lines, power plants, and wastewater treatment plants, will also become more vulnerable to storms and flooding (CEC, 2017; Caldwell et al., 2013).

The risks of flooding, coastal erosion, and shoreline retreat increase with rising sea levels. Short-term processes that result in significant short-term increases in water levels such as “King tides” (extremely high tides that typically occur during a new or full moon), seasonal cycles, winter storms and patterns of climate variability (e.g., the Pacific Decadal Oscillation or the El Niño Southern Oscillation (ENSO)) will likely continue to cause the greatest impacts on infrastructure and coastal development due to the significantly higher water levels they produce compared to sea level rise alone (Griggs et al., 2017).

Rising sea levels can disrupt ecosystems along the coast, including wetlands, estuaries, and fisheries. These coastal ecosystems provide flood protection, water treatment, carbon sequestration, biodiversity, wildlife habitat, and recreation (CEC, 2009). The coast also supports economically valuable commercial and recreational fishing activities (Caldwell et al., 2013).

Rising seas present serious threats to the Sacramento-San Joaquin Delta. During storms and high water flood events, higher sea levels increase the likelihood of Delta island levee failures. Sea level rise would tend to increase the Delta’s salinity, particularly during periods of reduced fresh water outflows from snowmelt. This puts the water supply for over half of California’s population and much of the Central Valley’s agriculture at risk. Saltwater intrusion into groundwater may also increase with sea level rise, putting further pressure on limited drinking water supplies (DWR, 2013).

Coastal communities may lose revenue under extreme flood events (Caldwell et al., 2013). Hazards in vulnerable areas can disproportionately affect communities that are least able to adapt. Compared to higher-income communities and property owners, people with lower incomes and residents of rental units are more likely to be displaced by flooding or related impacts because they are not as able to rebuild, have less control over their safety, and have less access to insurance. Importantly, tribal communities are often tied to specific regions and cannot easily relocate. In addition, loss of local public beaches and recreational areas would disproportionately affect low-income communities that have few options for low-cost recreation (CCC, 2015).

To assist with local adaptation strategies, online coastal flooding hazard maps using data produced by the scientific and research community in California may be accessed at: <http://beta.cal-adapt.org/>. These maps show predicted inundation for the San Francisco Bay, Sacramento-San Joaquin River Delta and California coast resulting from storm events at different sea level rise scenarios.



What factors influence this indicator?

The ocean has absorbed more than 90 percent of the excess energy associated with anthropogenic greenhouse gas emissions, leading to ocean warming. As the ocean warms, water expands and sea levels rise (IPCC, 2014). Heat-driven expansion accounts for about half of the sea level rise that occurred in the past one hundred years (Griggs, et al., 2017).

The other major contributor to sea level rise is water from melting mountain glaciers, ice caps, and polar ice sheets. Within days of ice water entering the ocean, regions around the globe experience a rise in sea level (IPCC, 2014). The ice sheets in Greenland and Antarctica, while not expected to melt completely even on millennial time scales, contain enough ice to raise global mean sea level by 24 feet and 187 feet, respectively. In addition to the large volume of water they contain, the accelerating rate of ice loss from these ice sheets is of particular concern (Griggs et al., 2017).

Other sources of land-based water that contribute to sea level include anthropogenic activities. Groundwater that is pumped for farming and drinking tends to end up in the ocean more than returning into the ground, thereby raising the sea level (Griggs, et al., 2017; Cazenave and Cozannet, 2014). Dam building along rivers and associated reservoir impoundment can lower the sea level; however, estimates for the past few decades suggest that the effect of groundwater depletion and dam/reservoir contribution to sea level rise may cancel each other (Cazenave and Cozannet, 2014).

Global sea levels vary by region. Wind and water density gradients push sea levels higher in some places and lower in others. Climatic variability in different regions also affects local sea levels. ENSO in the eastern Pacific Ocean, for instance, produces alternating warm and cool phases that can bring sharp swings in sea level that are transient and do not last multiple decades. Additionally, ice masses around Earth's poles exert a gravitational pull. When the ice melts, water that had once been pulled toward the ice mass due to gravitational attraction migrates away (NASA, 2017).

In the short term, local sea level is modulated by processes which produce higher-than-normal rises of coastal waters, such as storm surges or exceptionally high tides known as King tides. Over the long term, subsidence and plate tectonics play a role in local sea levels. When the land itself sinks, as in the California Bay Delta, relative sea levels rise. Many of the islands in the California Bay Delta have dropped below sea level due to microbial oxidation and soil compaction caused by more than a century of farming (NASA, 2017). Conversely, plate tectonics can cause land uplift along the coast to outpace sea level rise, as is happening in Crescent City in northern California where NOAA's records show a drop in sea level over time. The far north coast is the only area along California where sea level is dropping relative to land surface (Russell and Griggs, 2012).



Technical Considerations

Data Characteristics

Sea level measurements came from federally-operated tide gages located along the California coast which are managed by the National Water Level Observation Network, part of what is now NOAA. Data are available online at <https://tidesandcurrents.noaa.gov/>.

Tide stations measure sea level relative to specific locations on land. Short-term changes in sea level (e.g., monthly mean sea level or yearly mean sea level) are determined relative to a location's Mean Sea Level, the arithmetic mean of hourly heights observed over a specific 19-year period called the "National Tidal Datum Epoch" (NTDE) established by NOAA's National Ocean Service. The NTDE accounts for the effect of the 18.6-year lunar nodal cycle on variations in tidal range. The current NTDE is 1983-2001 (previous NTDEs were for the periods 1924-1942, 1941-1959, and 1960-1978); NTDEs are updated roughly every 20 years (NOAA, 2000; Szabados, 2008).

The United States federal government first started collecting measurements of sea levels in the mid-19th century to assist with accurate navigation and marine boundary determinations. Data from these early observation efforts and continued monitoring are used to assess long-term changes in sea level in multiple locations in California. Monitoring efforts have expanded over the years to include more locations with tidal stations, allowing for analysis of sea level trends at more regions, although for shorter time scales (NOAA, 2006).

Strengths and Limitations of the Data

Due to astronomical forces, such as the lunar cycle, it is difficult to isolate possible changes due to global warming by looking at short time periods in the sea level tidal record. Monthly mean sea levels tend to be highest in the fall and lowest in the spring, with differences of about 6 inches. Local warming or cooling resulting from offshore shifts in water masses and changes in wind-driven coastal circulation patterns also seasonally alter the average sea level by 8.4 inches (Flick, 1998). For day-to-day activities, the tidal range and elevations of the high and low tides are often far more important than the elevation of mean sea level. Shoreline damage due to wave energy is a factor of wave height at high tide and has a higher impact on the coast than mean sea level rise.

As noted above, geological forces such as subsidence, in which the land falls relative to sea level, and the influence of shifting tectonic plates complicate regional estimates of sea level rise. Much of the California coast is experiencing elevation changes due to tectonic forces. Mean sea level is measured at tide gauges with respect to a tide gauge benchmark on land, which traditionally was assumed to be stable. This only allows local changes to be observed relative to that benchmark. There are studies in progress that will study the feasibility of monitoring absolute changes in sea level on a global scale through the use of global positioning systems (GPS) satellite altimetry. The GPS may be useful to record vertical land movement at the tide gauge benchmark sites to correct for seismic activity and the earth's crustal movements.



For more information, contact:



Maurice Roos
Department of Water Resources
Division of Flood Management
3310 El Camino Avenue, Suite 200
P.O. Box 219000
Sacramento, CA 95821-9000
(916) 574-2625
mroos@water.ca.gov

References:

Caldwell MR, Hartge EH, Ewing LC, Griggs G, Kelly RP, et al. (2013). Coastal Issues. *In: Assessment of Climate Change in the Southwest United States: A Report Prepared for the National Climate Assessment*. Garfin G, Jardine A, Merideth R, Black M, and LeRoy S (Eds.). Southwest Climate Alliance. Washington, DC: Island Press. pp. 168–196.

Cazenave A and Cozannet GL (2014). Sea level rise and its coastal impacts. *Earth's Future* 2(2): 15-34.

CEC (2009). *The Impacts of Sea-Level Rise on the California Coast* (CEC-500-2009-024-D). California Energy Commission. Available at <http://www.energy.ca.gov/2009publications/CEC-500-2009-024/CEC-500-2009-024-D.PDF>

CEC (2017). *Assessment of California's Natural Gas Pipeline Vulnerability to Climate Change* (CEC-500-2017-008). California Energy Commission. Berkeley, CA: University of California, Berkeley. Available at <http://www.energy.ca.gov/2017publications/CEC-500-2017-008/CEC-500-2017-008.pdf>

CCC (2015). *California Coastal Commission Sea Level Rise Policy Guidance: Interpretive Guidelines for Addressing Sea Level Rise in Local Coastal Programs and Coastal Development Permits*. California Coastal Commission. San Francisco, CA. Available at https://documents.coastal.ca.gov/assets/slr/guidance/August2015/0_Full_Adopted_Sea_Level_Rise_Policy_Guidance.pdf

DWR (2013). *California Water Plan Update 2013: Sacramento-San Joaquin Delta* (Regional Reports, Vol. 2). California Department of Water Resources. Sacramento, CA. Available at https://www.water.ca.gov/LegacyFiles/waterplan/docs/cwpu2013/Final/Vol2_DeltaRR.pdf

DWR (2016). *Quick Guide Coastal Appendix: Planning for Sea-Level Rise*. California Department of Water Resources. Sacramento, CA: The National Flood Insurance Program in California. Available at https://www.water.ca.gov/LegacyFiles/floodmgmt/lrafmo/fmb/docs/QGCoastalAppendix_FINALDRAFT_2016dec02.pdf

Flick RE (1998). Comparison of California tides, storm surges, and mean sea level during the El Niño winters of 1982-1983 and 1997-1998. *Shore and Beach* 66(3): 7-11.

Griggs G, Arvai J, Cayan D, DeConto R, Fox R, et al. (2017). *Rising Seas in California: An Update on Sea-Level Rise Science*. California Ocean Science Trust. Available at <http://www.opc.ca.gov/webmaster/ftp/pdf/docs/rising-seas-in-california-an-update-on-sea-level-rise-science.pdf>

IPCC (2014). *Climate Change 2014: Synthesis Report. Contribution of Working Groups I, II and III to the Fifth Assessment Report of the Intergovernmental Panel on Climate Change*. Core Writing Team, Pachauri RK, and Meyer LA (Eds.). Geneva, Switzerland: Intergovernmental Panel on Climate Change. Available at <http://www.ipcc.ch/report/ar5/syr/>



NASA (2017). National Aeronautics and Space Administration Sea Level Change: Observations from Space. Retrieved July 2017, from <https://sealevel.nasa.gov/>

NOAA (2000). *Tidal Datums and their Applications* (NOAA Special Publication NOS CO-OPS 1). National Oceanic and Atmospheric Administration. Silver Spring, MD: Center for Operational Oceanographic Products and Services. Available at https://tidesandcurrents.noaa.gov/publications/tidal_datums_and_their_applications.pdf

NOAA (2006). *Sea Level Variations of the United States 1854-2006* (NOS CO-OPS 053). National Oceanic and Atmospheric Administration. Silver Spring, MD: Center for Operational Oceanographic Products and Services. Available at https://tidesandcurrents.noaa.gov/publications/Tech_rpt_53.pdf

NOAA (2017). National Oceanic and Atmospheric Administration, Center for Operational Oceanographic Products and Services: Tides and Currents. Retrieved July 2017, from www.co-ops.nos.noaa.gov

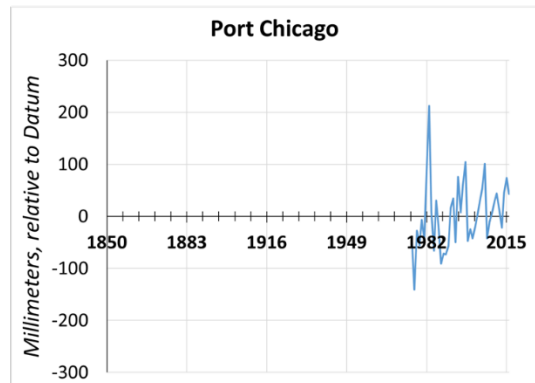
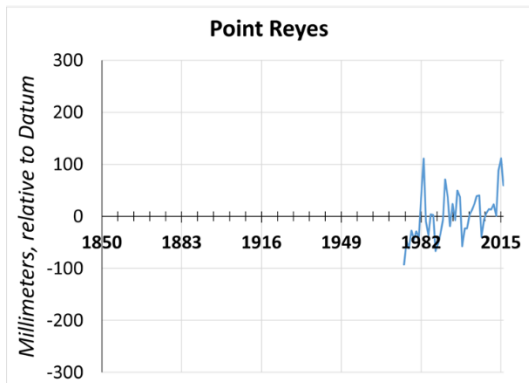
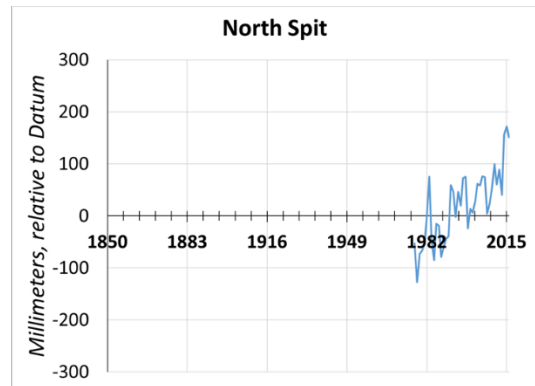
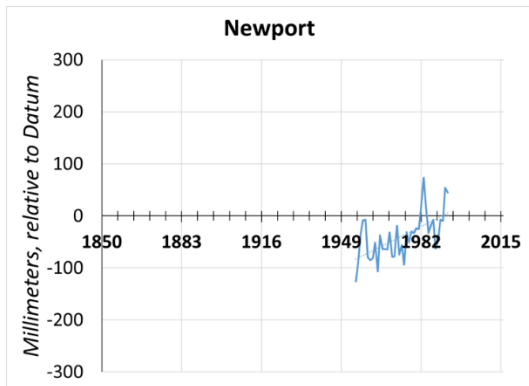
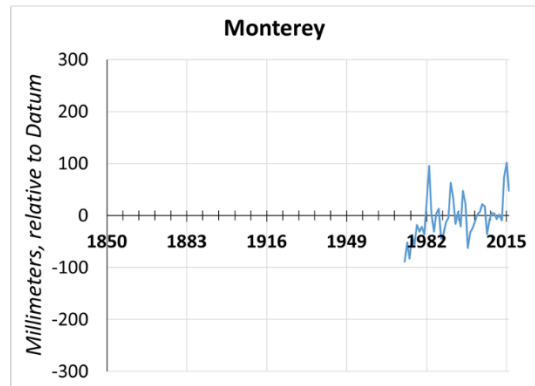
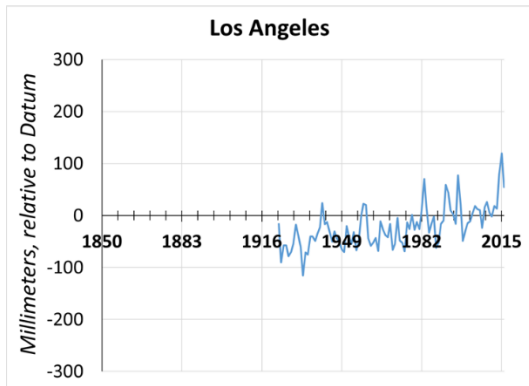
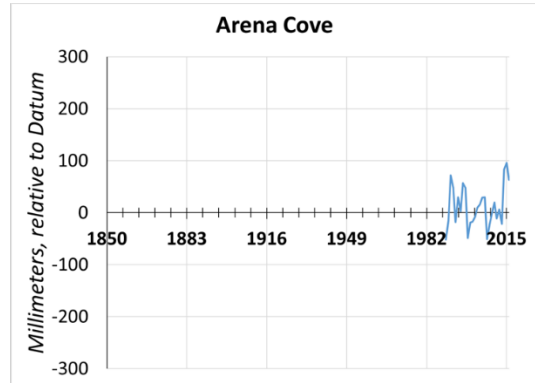
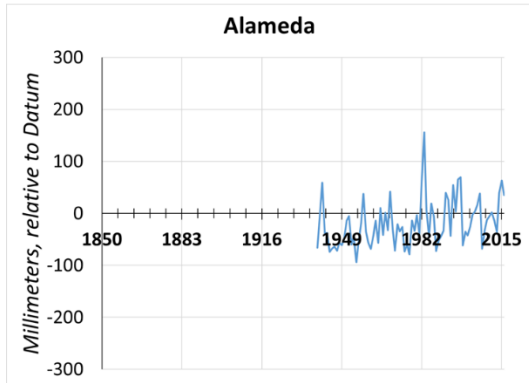
Russell N and Griggs G (2012). *Adapting to Sea Level Rise: A Guide for California's Coastal Communities*. California Energy Commission Public Interest Environmental Research Program. Available at <http://climate.calcommons.org/bib/adapting-sea-level-rise-guide-california%E2%80%99s-coastal-communities>

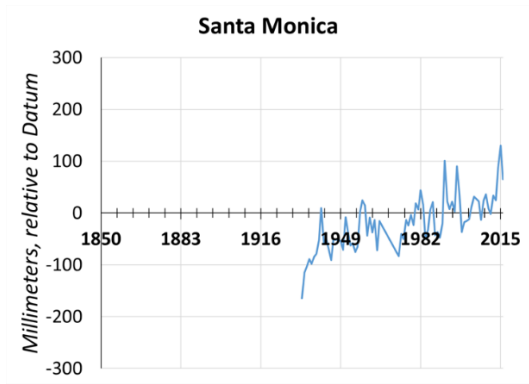
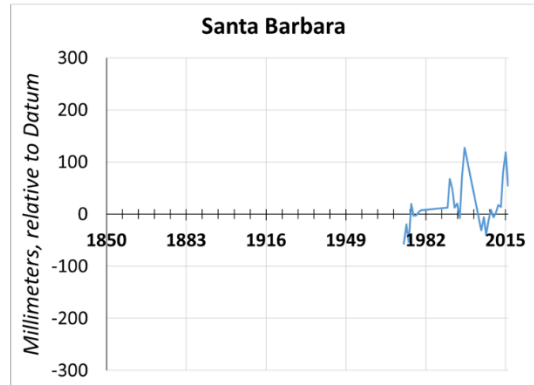
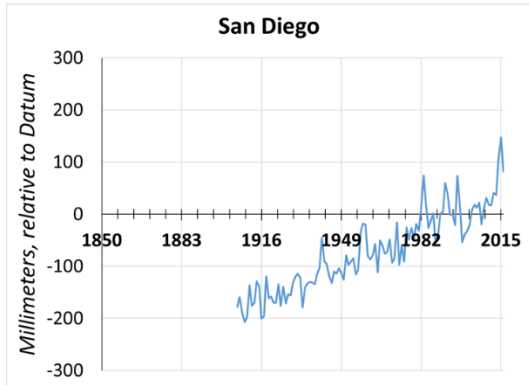
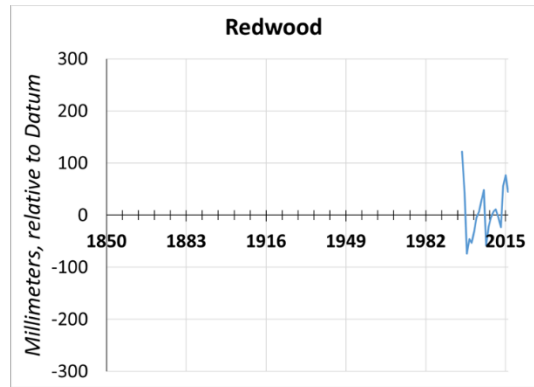
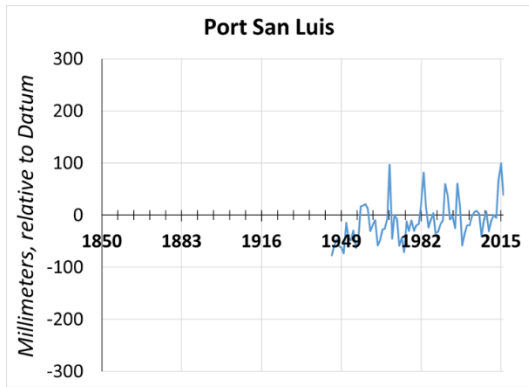
San Francisco Bay Conservation and Development Commission (2012). Adapting to Rising Tides; Airports. Retrieved June, 2017 from <http://www.adaptingtorisingtides.org/portfolio/airport/>

Szabados M (2008). *Understanding Sea Level Change*. Reprint from ACSM Bulletin, 236: 10-14. Available at <https://tidesandcurrents.noaa.gov/pub.html>



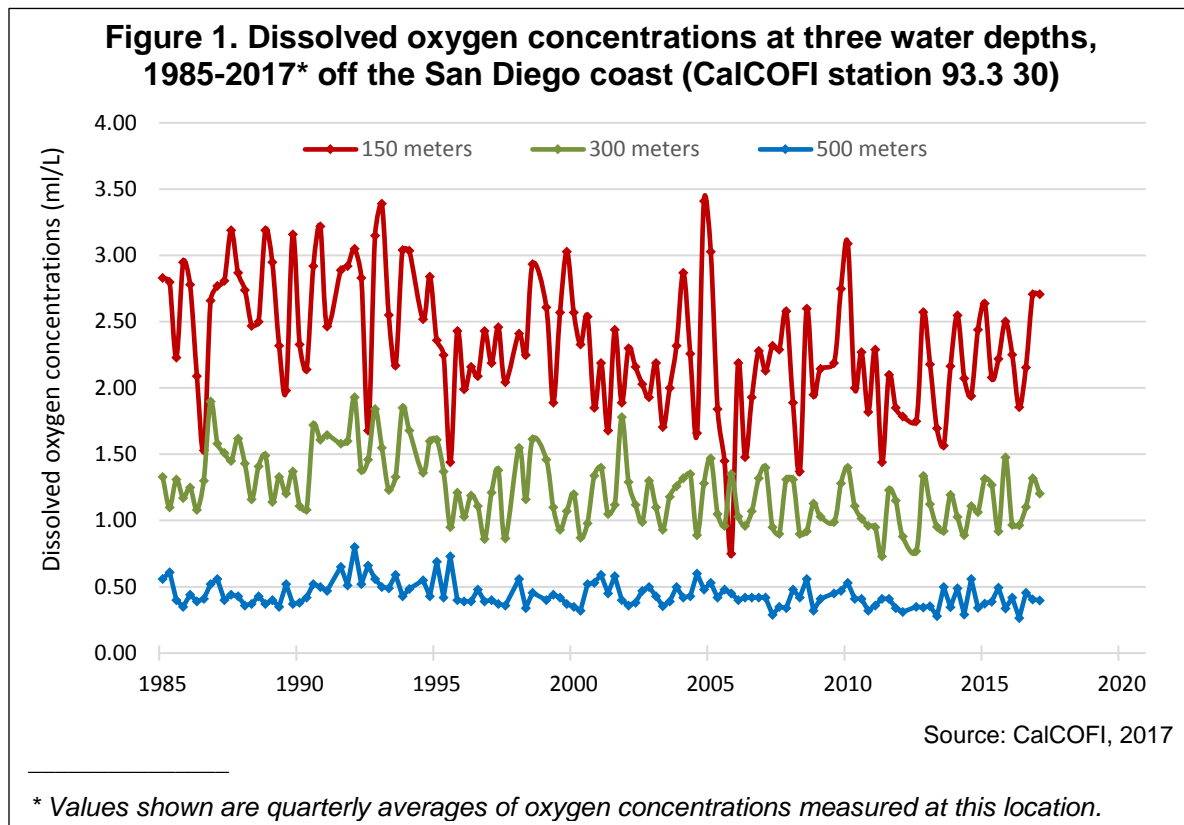
**APPENDIX. Mean sea level trends for 16 California tide stations
(data from NOAA, 2017)**





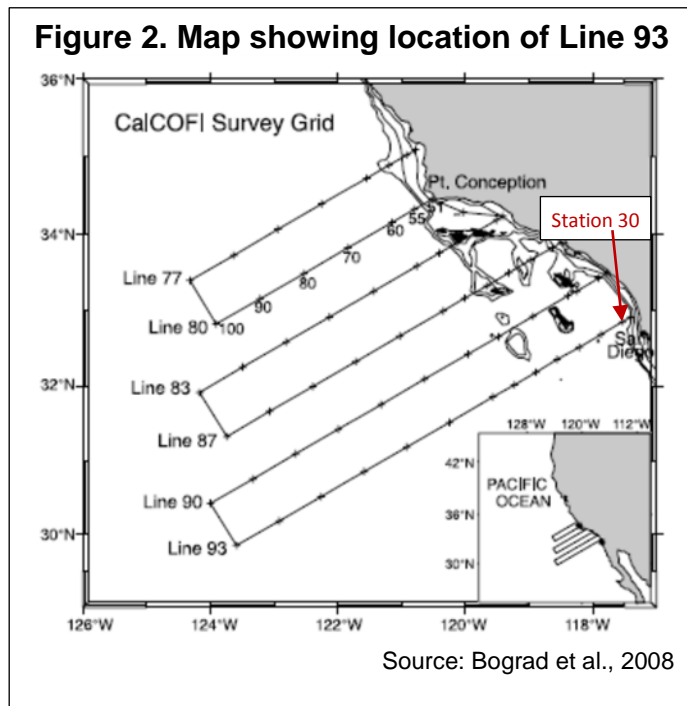
DISSOLVED OXYGEN IN COASTAL WATERS

Dissolved oxygen concentrations are declining in ocean waters off southern California.



What does this indicator show?

Instrumental measurements of dissolved oxygen (DO) concentrations point to decreasing oxygenation of coastal waters within the California Current. As shown in Figure 1, DO concentrations at three water depths offshore of San Diego indicate overall mean decreases as well as significant low-oxygen events since the mid-1990's. The measurements were taken by the California Cooperative Oceanic Fisheries Investigations (CalCOFI) as the location "Line 93.3, station 30" shown in Figure 2. This location is where the influence of the California Undercurrent is typically observed. This current is a



major supplier of source waters to the region and has a large influence on oxygen content for much of the survey area. Declines in DO over time have been observed throughout the CalCOFI survey region (to at least 500 m depth) (Bograd et al., 2008).

Why is this indicator important?

Declining DO concentrations in ocean waters, and the associated changes in the depth and extent of low oxygen zones, can lead to significant and complex ecological changes in marine ecosystems, including wide-ranging impacts on diversity, abundance, and trophic structure of communities (e.g., Levin et al., 2009; Stramma et al., 2010; Somero et al., 2015). Changing ocean chemistry, in concert with changes in temperature, may lead to even greater and more diverse impacts on coastal marine ecosystems (e.g., Somero et al., 2015).

Globally since 1950, more than 500 coastal sites have been reported to have experienced hypoxic conditions (waters with low or depleted oxygen concentrations, <1.4 mL/L, or 2 mg/L). Fewer than 10 percent of these were known to have hypoxia before then (Breitburg et al., 2018). Separate from these episodic hypoxic events, coastal California is characterized by the presence of a zone of depleted oxygen concentrations (Oxygen Minimum Zone, or OMZ) at depths from 600 to 1100 meters. The OMZ near California is expanding both vertically (moving upward towards the ocean surface (e.g., Bograd et al., 2008) and horizontally (Somero et al., 2015). The declines in oxygenation observed off California are consistent with an observed expansion of the low oxygen zones elsewhere around the world (Stramma et al., 2008; Breitburg et al., 2018).

The expansion of oxygen-deficient zones can lead to a compression of favorable habitat for certain marine species and an expansion of favorable habitat for other species. For example, during the last decade, the Humboldt squid (*Dosidicus gigas*) — which thrives in low-oxygen environments — has expanded its range northward from Baja California to southeast Alaska, a shift that may have been affected by changes in the extent of oxygen-deficient zones (Gilly and Markaida, 2007). Recent studies have indicated that low-oxygen waters can reach nearshore coastal habitats via upwelling; impacts on coastal habitats have not yet been observed (e.g., Booth et al., 2012; Frieder et al., 2012).

Oxygen plays a role in the cycling of nutrients such as nitrogen, phosphorus and iron. As a result, changes in oxygen levels can influence nutrient budgets, biological productivity and carbon fixation. In oxygen-depleted waters, anaerobic microbial processes can produce chemicals such as hydrogen sulfide, which is toxic to other organisms, and methane, a potent greenhouse gas (Breitburg et al., 2018).

What factors influence this indicator?

DO levels reflect a complex interplay between physical and biological drivers. Warmer waters hold less oxygen, as the gas becomes less soluble, and surface warming produces stratification that reduces the overturning circulation essential in ocean ventilation processes. Warming also accelerates the rate of oxygen consumption by



marine organisms (e.g., Somero et al., 2015; Breitburg et al., 2018). In addition to these processes, DO is influenced by high surface productivity, regional circulation of the North Pacific Ocean, and anthropogenic nutrient inputs to the coastal ocean, as discussed below.

Upwelling is a wind-driven physical process wherein deep, nutrient rich waters move upward into the shallow surface ocean. There is evidence that upwelling has increased in some locations along the California coast due to anthropogenic impacts (García-Reyes and Largier, 2010; Wang et al., 2015; see also discussion in *Coastal ocean temperature* indicator). Upwelling brings nutrient rich waters to the surface, where it drives surface ocean productivity (photosynthesis). The amount of surface water productivity affects DO concentrations because as biological material sinks downward from the surface ocean and decays, oxygen is utilized in the decay and decomposition process. Thus, DO concentrations decrease in the subsurface below regions of high biological productivity.

DO concentrations are also controlled by regional and global oceanographic processes. For example, the Southern California Bight is impacted seasonally by the northward flowing California Undercurrent. The Southern California Bight is the 400 miles of coastline from Point Conception in Santa Barbara County to Cabo Colnett, south of Ensenada, Mexico. Much of the Bight is included in the CalCOFI survey region. Declining oxygen concentrations in this region imply a change in the properties of these equatorial source waters, although the precise mechanisms of the decline are unknown (Bograd et al., 2015).

Local nutrient inputs from human practices (e.g., agriculture, wastewater discharge) can also decrease oxygen concentrations in coastal waters. Fertilizers and nutrient enrichment from wastewater promote algal growth. As this material sinks and decays, it can create localized areas of low oxygen. Management of coastal pollution is an important aspect of minimizing changes in oxygen concentrations on a local scale.

Scientists estimate that about 15 percent of global oxygen decline between 1970 and 1990 can be explained by ocean warming and the remainder by increased stratification. In coastal areas, especially nutrient-enriched waters, warming is predicted to exacerbate oxygen depletion (Breitburg et al., 2018). Climate change models predict a decline in concentrations of DO under future scenarios, based primarily on decreased oxygen solubility in seawater with warming ocean temperatures.

Technical considerations:

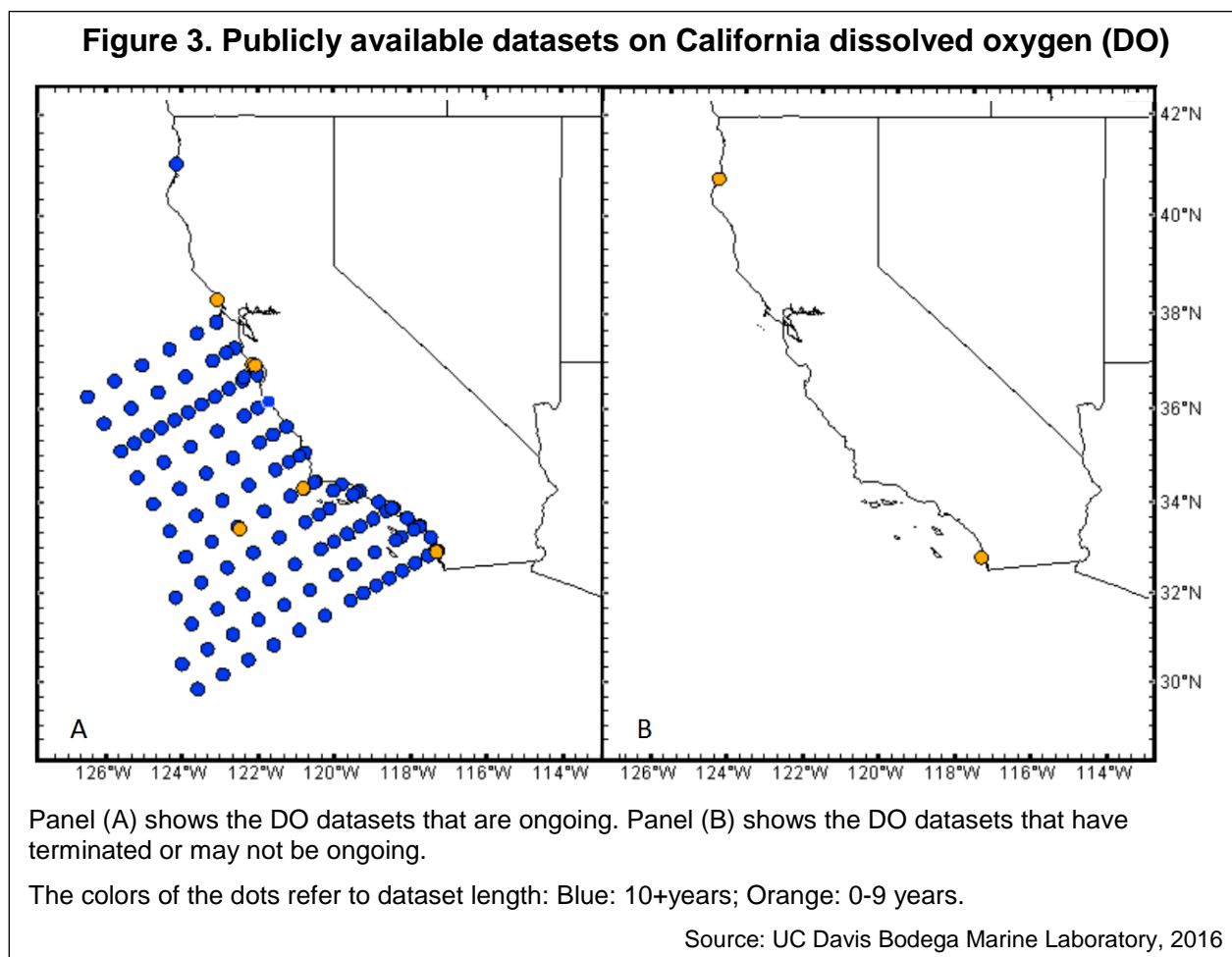
Data Characteristics

This indicator is based on data from the CalCOFI program. As noted above and illustrated in Figures 1 and 2, DO measurements were taken between the surface and depths of up to 500 meters at CALCOFI Line 93.3 Station 30.0, offshore of San Diego from 1951 to 2016. Data were downloaded from the CalCOFI website at <http://calcofi.org/data.html>. Quarterly averages were derived from oxygen concentrations reported for that calendar quarter. While sampling did occur between



1950 and 1980, there are data gaps during this period (notably between 1952-1955, and 1966-1976).

The locations and lengths of collection periods of publicly available DO datasets for California are shown in Figure 3. DO is currently measured and monitored within California at 124 sites. Most data are collected south of San Francisco Bay, with only two collection sites north of Bodega Bay. The vast majority of the central and south coast data (>90%) are from offshore stations monitored by the CalCOFI Program. The majority of the datasets that are 10 years or longer (97 percent) are from the CalCOFI Program. There are no datasets longer than 50 years. The CalCOFI data collection presents a significant opportunity to detect the signature of climate change in DO concentrations along the California coast.



Strengths and Limitations of the Data

Very few datasets describe DO conditions north of San Francisco and/or in coastal regions. One analysis suggests that 20-30 years of data are needed to robustly detect long-term declines in DO above natural variability (Henson et al., 2016). All of the CalCOFI datasets meet this criterion, thus CalCOFI currently represents our best resource for distinguishing long-term trends in DO from natural variability. CalCOFI has



limited sampling availability in nearshore/coastal habitats, so establishing additional coastal monitoring sites may be critical for characterizing DO conditions in these areas.

These observations are limited by sites where oxygen concentration measurements are currently monitored along the coast and do not reflect oxygen declines that may be occurring across the entire California Current System. As described above, the observed DO concentrations could be influenced by both local thermodynamic or biological processes, as well as remote, large-scale changes. The oxygen concentrations can vary with the depth, temperature and time of year DO levels are measured.

For more information, contact:



Tessa M. Hill, Ph.D.
University of California, Davis
Bodega Marine Laboratory
P. O. Box 247
Bodega Bay, CA 94923
(707) 875-1910
tmhill@ucdavis.edu

John Largier, Ph.D.
University of California, Davis
Bodega Marine Laboratory
P. O. Box 247
Bodega Bay, CA 94923
(707) 875-1930
jlargier@ucdavis.edu

2013 report provided by S. Bograd, NOAA.

2018 updates provided by UC Davis team: Myhre, Hill, Rivest, Gaylord, Sanford, Largier

References:

Bograd SJ, Castro CG, Di Lorenzo E, Palacios DM, Bailey H, Gilly W, et al. (2008). Oxygen declines and the shoaling of the hypoxic boundary in the California current. *Geophysical Research Letters* **35**(12): L12607.

Bograd SJ, Buil MP, Di Lorenzo E, Castro CG, Schroeder ID, et al. (2015). Changes in source waters to the Southern California Bight. *Deep-Sea Research Part II: Topical Studies in Oceanography* **112**:42-52.

Booth JAT, McPhee-Shaw EE, Chua P, Kingsley E, Denny M, Philips R, Bograd SJ, Zeidberg LD and Gilly WF (2012). Natural intrusions of hypoxic, low pH water into nearshore marine environments on the Californian coast. *Continental Shelf Research* **45**:108-115.

Breitburg D, Levin LA, Oschlies A, Gregoire M, Chavez FP, et al. (2018). Declining oxygen in the global ocean and coastal waters. *Science* **359** (6371).

CalCOFI (2017): California Cooperative Oceanic Fisheries Investigations: Hydrographic Data – 1949 to Latest Update. Retrieved December 29, 2017 from <http://calcofi.org/data.html>



Frieder CA, Nam SH, Martz TR and Levin LA (2012). High temporal and spatial variability of dissolved oxygen and pH in a nearshore California kelp forest. *Biogeosciences* **9**: 3917-3930.

García-Reyes M and Largier J (2010). Observations of increased wind-driven coastal upwelling off Central California. *Journal of Geophysical Research* **115**(C4).

Gilly W and Markaida U (2007). Perspectives on *Dosidicus gigas* in a changing world. Olson R and Young J (Eds.). The role of squid in open ocean ecosystems. Report of a GLOBEC-CLIOTOP/PFRP workshop, 16-17 November 2006, Honolulu, Hawaii, USA. GLOBEC. Report 24: vi, 81-90.

Henson SH, Beaulieu C, Lampitt R (2016). Observing climate change trends in ocean biogeochemistry: when and where. *Global Change Biology* **22**:1561-1571.

Levin LA, Ekau W, Gooday AJ, Jorissen F, Middelburg JJ, Naqvi SWA, et al. (2009). Effects of natural and human-induced hypoxia on coastal benthos. *Biogeosciences* **6**(10): 2063-2098.

Rhein M, Rintoul SR, Aoki S, Campos E, Chambers D, et al. (2013): Observations: Ocean. In: *Climate Change 2013: The Physical Science Basis. Contribution of Working Group I to the Fifth Assessment Report of the Intergovernmental Panel on Climate Change*. Stocker TF, Qin D, Plattner G-K, Tignor M, Allen SK, et al. (Eds.]. Cambridge, United Kingdom and New York, NY, USA: Cambridge University Press.

Somero GN, Beers JM, Chan F, Hill TM, Klinger T and Litvin SY (2015). What changes in the carbonate system, oxygen, and temperature portend for the northeastern Pacific Ocean: A physiological perspective. *BioScience* **66**(1): 14-26.

Stramma L, Johnson GC, Sprintall J and Mohrholz V (2008). Expanding oxygen minimum zones in the tropical oceans. *Science* **320**(5876): 655-658.

Stramma L, Schmidtko S, Levin L and Johnson GC (2010). Ocean oxygen minima expansions and their biological impacts. *Deep Sea Research Part I: Oceanographic Research Papers* **57**(4):587–595.

UC Davis Bodega Marine Laboratory (2016). Map showing location of stationary monitoring sites for dissolved oxygen off California.

Wang D, Gouhier TC, Menge BA and Ganguly AR. (2015). Intensification and spatial homogenization of coastal upwelling under climate change. *Nature* **518**: 390-394.



Page intentionally blank



Climate change impacts on terrestrial, marine and freshwater ecosystems have been observed globally. Studies have demonstrated species responses consistent with warming trends, including poleward and elevational shifts in range; changes in the timing of growth stages (known as “phenology”); and changes in the abundance of species and in community composition. With continued climate change, many species will be unable to adapt or to migrate to suitable climates. This could result in decreased abundance or extinction in part or all of their ranges (Field et al., 2014). In addition, climate change interacts with other factors (such as land use, habitat alteration, and emissions of pollutants) in ways that can either moderate or intensify their impacts (Melillo et al., 2014).

Climate change can impair the ability of ecosystems to provide goods and services, many of which represent cultural, social and economic benefits. For example, forests provide wildlife habitat, timber and recreational opportunities. They also play an important role in regulating levels of atmospheric carbon by removing carbon dioxide from the atmosphere.

Globally, the human health burden associated with climate change is relatively small compared to the effects of other stressors and is not well quantified (IPCC, 2014). Nevertheless, climate change is increasing the risk of heat-related illness and deaths, and the spread of certain infectious diseases. Children, the elderly, the sick, the poor and some communities of color are especially vulnerable (Melillo et al., 2014).

This chapter presents climate change impacts on biological systems using three categories: *human health, vegetation, and wildlife*.

Human Health

Climate change poses a threat to public health. Heat causes more reported deaths per year on average in the United States than any other weather hazard (NOAA, 2017). In addition to the long-recognized health impacts of extreme heat, hospital admissions and emergency room visits, deaths and other adverse health outcomes have been associated with the warm season in California.

In 2006, dramatic increases in many heat-related illnesses and deaths were reported in California following a record-breaking heat wave. During the summer months, large urbanized areas can experience higher temperatures compared to nonurban outlying regions. “Urban heat islands” create health risks both because of the increased temperatures and because of the enhanced formation of air pollutants. Warming



temperatures can amplify the transmission of mosquito-borne diseases (such as West Nile Virus) and make conditions more hospitable for invasive species that may transmit diseases.

While difficult to track using indicators, climate change can impact human well-being in many ways, including injuries and fatalities from extreme events, and respiratory stress from poor air quality (Mellilo et al., 2014).

Vegetation

Changing precipitation patterns and increased temperatures reduce the amount of water available to plants. The resulting stress on vegetation has been associated with changes to California's forested lands and woodlands. Since the 1930s, forests have more small trees, fewer large trees, less areas occupied by pine, and more areas occupied by oaks. Conifer-dominated forests of the Sierra Nevada have been retreating upslope, and plant species in Southern California have shifted their distribution upslope. Tree deaths in forested lands increased dramatically during the 2012-2016 drought, the most severe in recorded history. Warm and dry conditions have led to larger and more severe wildfires and longer fire seasons, posing significant threats to public health, infrastructure and natural resources.

Warming temperatures have been associated with faster maturation of certain fruit and nut varieties in the Central Valley, leading to earlier harvests. In general, shorter maturation times lead to smaller fruits and nuts, a change that can lead to a significant loss of revenue for growers and suppliers.

Wildlife

The impacts on wildlife observed globally have also been documented in California. Small mammals and birds in the Sierra Nevada have shifted their elevation in response to changing climatic conditions. Common butterfly species have started to appear in the Central Valley earlier in the spring due to hotter and drier conditions in the region in recent decades. Over the past five decades, wintering bird species have collectively shifted their range northward and closer to the California coast. Changes in the timing of migratory bird arrivals have also been observed.

Marine species respond to changing ocean conditions, especially during periods of unusually warm sea surface temperatures. The abundance and species composition of planktonic populations, important food sources for many marine species, change with ocean conditions. Chinook salmon abundance in California's rivers has become more variable for many reasons, including warming temperatures in both freshwater and ocean habitats. Increasing ocean temperatures can negatively alter the food web on which salmon depend, changing the range of predators and prey species. The reproductive success of colonies of Cassin's auklet, a seabird on the Southeast Farallon Island near San Francisco, has also been found to be associated with ocean conditions that affect the availability of krill, their food source. Finally, unusually warm sea surface temperatures have been associated with declines in California sea lion pup births, increased pup mortality and poor pup condition.



INDICATORS: IMPACTS ON BIOLOGICAL SYSTEMS

HUMANS

Vector-borne diseases (*updated*)
Heat-related mortality and morbidity (*updated*)

VEGETATION

Forest tree mortality (*updated*)
Wildfires (*updated*)
Ponderosa pine forest retraction (*updated*)
Vegetation distribution shifts (*no update*)
Changes in forests and woodlands (*new*)
Subalpine forest density (*updated*)
Fruit and nut maturation (*new*)

WILDLIFE

Spring flight of Central Valley butterflies (*updated*)
Migratory bird arrivals (*updated*)
Bird wintering ranges (*new*)
Small mammal and avian range shifts (*updated*)
Effects of ocean acidification on marine organisms (*updated*)
Nudibranch range shifts (*new*)
Copepod populations (*updated*)
Sacramento fall-run Chinook salmon abundance (*updated*)
Cassin's auklet breeding success (*updated*)
California sea lion pup demography (*updated*)

References:

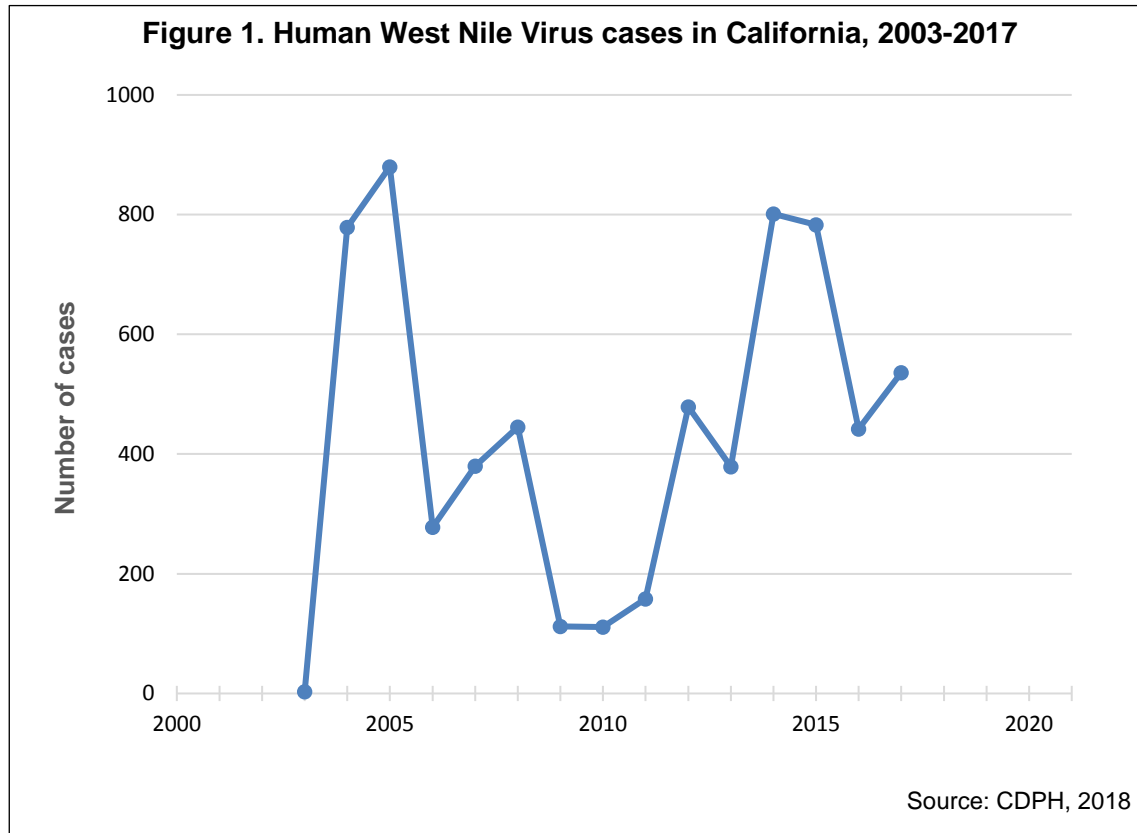
Field CB, Barros VR, Mach KJ, Mastrandrea MD, van Aalst M, et al. (2014). *Technical summary*. In: *Climate Change 2014: Impacts, Adaptation, and Vulnerability. Part A: Global and Sectoral Aspects. Contribution of Working Group II to the Fifth Assessment Report of the Intergovernmental Panel on Climate Change* [Field CB, Barros VR, Dokken DJ, Mach KJ, Mastrandrea MD et al. (Eds.)]. Cambridge University Press, Cambridge, United Kingdom and New York, NY, USA, pp. 35-94.
http://www.ipcc.ch/pdf/assessment-report/ar5/wg2/WGIIAR5-TS_FINAL.pdf

Melillo, Jerry M., Terese (T.C.) Richmond, and Gary W. Yohe, Eds., 2014: Highlights of Climate Change Impacts in the United States: The Third National Climate Assessment. U.S. Global Change Research Program, 148 pp.



VECTOR-BORNE DISEASES

Warming temperatures and changes in precipitation can affect vector-borne pathogen transmission and disease patterns in California. West Nile Virus currently poses the greatest mosquito-borne disease threat.



What does the indicator show?

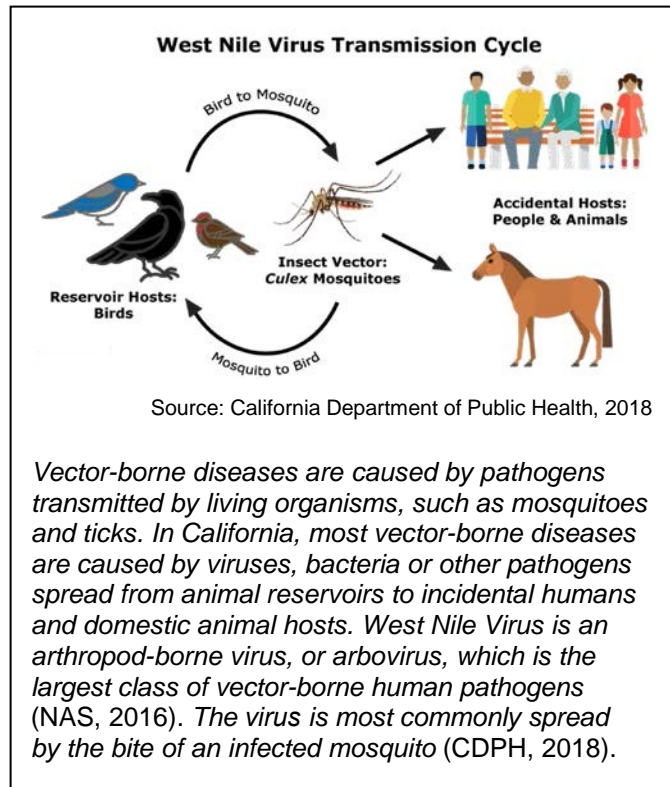
Figure 1 shows human cases of West Nile Virus (WNV) reported in California. Of the 15 mosquito-borne viruses known to occur in California, WNV in particular continues to seriously impact the health of humans, horses and wild birds throughout the state (CDPH, 2016). First detected in the state in 2003 (when three cases were reported), WNV cases show no clear trend, varying from year to year over the 16-year period shown. The number of cases peaked in 2004-2005, and in 2014-2015.

Why is this indicator important?

Tracking vector-borne disease is critical for understanding the associations between disease prevalence and climate trends. Climate change will likely affect vector-borne disease transmission patterns. Changes in temperature and precipitation can influence seasonality, distribution, and prevalence of vector-borne diseases (USGRCP, 2016). In fact, due to their widespread occurrence and sensitivity to climatic factors, vector-borne diseases are some of the illnesses that have been most closely associated with climate change (Smith et al., 2014).



For most Californians, WNV poses the greatest mosquito-borne disease threat. The majority of infections are undetected and therefore not reported since symptoms can be very mild or absent. Symptomatic infections involve generalized health effects that may include fever, headache, body aches, nausea, vomiting, swollen lymph glands or a skin rash, and in some cases fatigue or weakness that lasts for weeks or months. “Neuroinvasive cases” (generally less than one percent of WNV infections) can result in encephalitis or meningitis, with symptoms that may include high fever, neck stiffness, disorientation, tremors, numbness and paralysis and coma, and in the most severe cases, death; the fatality rate is reported at 10 percent (CDC, 2015). Over the past decade, cases of WNV neuroinvasive disease have increased at a greater rate than non-neuroinvasive cases, although this is likely due to underreporting; the latter are milder cases which generally do not require medical attention. The number of human cases reported in California in 2015 (783) was the third highest since 2003 and the number of fatal cases (53) was the highest ever reported. As discussed below, drought appears to increase the prevalence of WNV. The record hot temperatures statewide and extended drought may have contributed to the elevated activity (CDPH, 2016).



In addition to WNV, other mosquito-borne viruses that can cause significant illness are the western equine encephalomyelitis virus (WEEV) and St. Louis encephalitis virus (SLEV) (Reisen and Coffey, 2014). While WEEV has been detected only rarely in recent years (Bergren et al., 2014), SLEV has re-emerged in California starting in 2015 after over a decade without detection, causing three reported cases of human disease in 2016 (White et al., 2016). WEEV activity has been shown to decrease with increasing temperatures (Reeves et al., 1994), whereas SLEV activity and outbreaks have long been associated with elevated temperatures (Monath, 1980).

Two invasive mosquito species recently found in several California counties can potentially spread to other areas of the state: *Aedes aegypti* (the yellow fever mosquito) and *Aedes albopictus* (the Asian tiger mosquito) (see map posted at: <https://arcg.is/00j1P8>). Both mosquitoes have the potential to transmit several viruses, including Zika, dengue fever, chikungunya, and yellow fever viruses. Although all cases of these viruses detected in California through April 2017 have been associated with travel, the presence of its vectors adds to the potential risk of local mosquito-borne



transmission of these viruses, especially if these species become more widely established in the state. The emergence of new infectious diseases associated with invasive species can be influenced by a number of factors, including land use changes (e.g., urbanization), the introduction of new hosts and climate change (NAS, 2016).

In addition to mosquito vectors, climate change will invariably impact the prevalence of tick-borne pathogens in California. Lyme disease, the most commonly reported tick-borne disease, is transmitted by the western blacklegged tick (*Ixodes pacificus*). The abundance of the western blacklegged tick is limited by abiotic conditions during the summer dry season (Swei et al., 2011). Prolonged hot dry periods may reduce tick abundance and therefore decrease Lyme disease risk in some locations, although if relative humidity is maintained, an increase in temperature may increase the number of infected ticks (Eisen et al., 2003). In contrast, the distribution of one vector of Rocky Mountain spotted fever (RMSF), the brown dog tick (*Rhipicephalus sanguineus*), may expand with increased frequencies of El Niño Southern Oscillation (ENSO) events. This could cause an increase in RMSF cases (Fisman et al., 2016). The on-going outbreak of RMSF in northern Mexico, which occasionally results in human cases in the United States through imported dogs or ticks, is a multifactorial problem involving climate and socioeconomic factors (Álvarez-Hernández et al., 2017).

Extreme precipitation events often associated with ENSO events are thought to impact hantavirus activity by expanding rodent habitat, particularly in normally arid habitats adjacent to humans (Carver et al., 2015). Hantavirus prevalence in rodents continues to be monitored in California in locations where rodents and humans may come in contact. Although the 2012 hantavirus outbreak in Yosemite National Park was associated with rodent habitat enrichment provided by cabin construction rather than with weather abnormalities, it was an example of how human hantavirus infection risk can increase when rodent densities are given the opportunity to increase.

What factors influence this indicator?

In California, changes in temperature and precipitation have been associated with WNV activity (Paull et al., 2017; Hartley et al., 2012). Such change may also alter the transmission risk of hantavirus and tick-borne diseases such as Lyme disease, by affecting the distribution and abundance of deer mice (host animal) and ticks (vector), respectively (Carver et al., 2015; Ogden and Lindsay, 2016). Finally, as discussed above, a changing climate may create conditions favorable for the establishment of invasive mosquito vectors in California (Ogden et al., 2014).

Above-normal temperatures are among the most consistent factors associated with WNV outbreaks (Hahn et al., 2015). Mild winters have been associated with increased WNV transmission possibly due, in part, to less mosquito and resident bird mortality. Warmer winter and spring seasons may also allow for transmission to start earlier. Such conditions also allow more time for virus amplification in bird-mosquito cycles, possibly increasing the potential for mosquitoes to transmit WNV to people. The effects of increased temperature are primarily through acceleration of physiological processes within mosquitoes, which results in faster larval development and shorter generation



times, faster blood meal digestion and therefore more frequent mosquito biting, and shortening of the incubation period time required for infected mosquitoes to transmit WNV (Hoover and Barker, 2016).

A useful measure of the efficiency of transmission of a vector-borne pathogen is the number of bites or blood meals required by the vector before the pathogen can be transmitted. Investigators have studied the efficiency of transmission of mosquito-borne pathogens when mosquitoes were incubated at different temperatures (Reisen et al., 2006). They report that with increasing temperatures, fewer blood meals are required for transmission and there is a higher probability that the virus can be transmitted within a mosquito's lifetime. Similar data have been used to delineate the effective global distribution of different malaria parasites and how climate change may have altered this pattern (Chaves and Koenraadt, 2010; Parham and Michael, 2010).

Precipitation and associated hydrological impacts also influence the likelihood of WNV transmission. Expected shifts of winter precipitation from snow to rain at high elevations (see *Precipitation* indicator) will limit water storage and cause spring runoff to occur earlier and faster, which would result in increased mosquito habitat during wet years (DWR, 2017). Periods of elevated rainfall (for example during El Niño events) can increase immature habitats for mosquitoes and increase population survival due to higher humidity (Linthicum et al., 2016).

During periods of drought, especially in urban areas, mosquitoes tend to thrive more due to changes in stormwater management practices. Under drought conditions, mosquitoes in urban areas can reach higher abundance due to stagnation of underground water in stormwater systems that would otherwise be flushed by rainfall. Runoff from landscape irrigation systems mixed with organic matter can also create ideal mosquito habitat (Hoover and Barker, 2016). Drought conditions may also force birds to increase their utilization of suburban areas where water is more available, thereby bringing these WNV hosts into contact with urban vectors (Reisen, 2013). Drought was found to be an important predictor of reported annual WNV neuroinvasive disease cases in California and nationwide (Paull et al., 2017).

Although a changing climate will likely alter the distribution of disease vectors in both time and space, it is important to recognize the role of social and environmental drivers (USGCRP, 2016). Vector-borne disease transmission can be influenced by such factors as how pathogens adapt and change, the availability of susceptible hosts, human behavior (for example time spent indoors), and mosquito and vector control programs. These factors were found to be major drivers of changes in mosquito populations over the last eight decades in areas on both coasts of North America (Rochlin et al., 2016).



Technical Considerations

Data Characteristics

California has a comprehensive mosquito-borne disease surveillance program that has monitored mosquito abundance and mosquito-borne virus activity since 1969 (CDPH, 2017). Statewide, diagnosis of human infection with WNV and other arboviruses is performed at the California Department of Public Health (CDPH) Health Viral and Rickettsial Disease Laboratory, nine local county public health laboratories, and multiple commercial laboratories. Human WNV cases in California have been reported to the Centers for Disease Control and Prevention (CDC) since the virus was first detected in 2003. Surveillance also includes monitoring virus activity in mosquitoes and vertebrate hosts that enzootically amplify the virus for purposes of providing warning of human disease risk. In addition to mosquito-borne diseases, CDPH works with local, state, and federal agencies, universities, the medical community and others in its efforts to monitor, prevent, and control rodent-, flea-, and tick-borne diseases.

Strengths and Limitations of the Data

For human disease surveillance, local mosquito control agencies rely on the detection and reporting of confirmed cases to plan emergency control and prevention activities. However, human cases of mosquito-borne viruses are an insensitive surveillance measure because less severe fever cases are rarely diagnosed and most infected persons do not develop disease (CDPH, 2017). With WNV, most people infected do not develop symptoms and these infections are not detected, except by blood bank screening.

For more information, contact:



Vicki Kramer or Anne Kjemtrup
California Department of Public Health
Vector-borne Disease Section
1616 Capitol Ave. MS 7307
P.O. Box 997377
Sacramento, CA 95899-7377
(916) 552-9730



Christopher Barker or William Reisen
Center for Vectorborne Diseases
4206 Vet Med 3A
One Shields Avenue
Davis, CA 95616
(530) 752-0124
cmbarker@ucdavis.edu, wkreisen@ucdavis.edu

References:

Álvarez-Hernández G, Roldán JF, Milan NS, Lash RR, Behravesh CB and Paddock CD (2017). Rocky Mountain spotted fever in Mexico: past, present, and future. *Lancet Infectious Disease* 17(6): 189-196.



Bergren NA, Auguste AJ, Forrester NL, Negi SS, Braun WA and Weaver SC (2014). Western equine encephalitis virus: Evolutionary analysis of a declining alphavirus based on complete genome sequences. *Journal of Virology* **88**(16): 9260-9267.

CDC (2015). Centers for Disease Control and Prevention: General Questions about West Nile Virus. Retrieved February 2, 2018, from <https://www.cdc.gov/westnile/faq/genquestions.html>

CDPH (2016). *Vector-Borne Disease Section Annual Report*. Kjemtrup AM and Kramer V (Eds.). California Department of Public Health. Sacramento, CA. Available at: <https://www.cdph.ca.gov/Programs/CID/DCDC/CDPH%20Document%20Library/VBDSAnnualReport16.pdf>

CDPH (2017). *California Mosquito-Borne Virus Surveillance and Response Plan*. California Department of Public Health. Sacramento, CA: California Department of Public Health, Mosquito and Vector Control Association of California, and University of California. Available at: <https://www.cdph.ca.gov/Programs/CID/DCDC/CDPH%20Document%20Library/2017CAMBVirusSurveillanceResponsePlan.pdf>

CDPH (2018). California Department of Public Health California, Human West Nile Virus Activity, California, 2003-2017 (Reported as of February 2, 2018). Retrieved February 2, 2018, from <http://westnile.ca.gov/>

Carver S, Mills JN, Parmenter CA, Parmenter RR, Richardson KS, et al. (2015). Toward a mechanistic understanding of environmentally forced zoonotic disease emergence: Sin nombre hantavirus. *Bioscience* **65**(7): 651-666.

Chaves LF and Koenraadt CJ (2010). Climate change and highland malaria: Fresh air for a hot debate. *The Quarterly Review of Biology* **85**(1): 27-55.

DWR (2017). *Hydroclimate Report Water Year 2016*. California Department of Water Resources. Sacramento, CA. Available at https://www.water.ca.gov/LegacyFiles/climatechange/docs/2017/DWR_Hydroclimate_Report_2016.pdf

Eisen RJ, Eisen L, Castro MB and Lane RS (2003). Environmentally related variability in risk of exposure to lyme disease spirochetes in Northern California: Effect of climatic conditions and habitat type. *Environmental Entomology* **32**(5): 1010-1018.

Fisman DN, Tuite AR and Brown KA (2016). Impact of El Niño Southern Oscillation on infectious disease hospitalization risk in the United States. *Proceedings of the National Academy of Sciences USA* **113**(51): 14589-14594.

Hahn MB, Monaghan AJ, Hayden MH, Eisen RJ, Delorey MJ, et al. (2015). Meteorological conditions associated with increased incidence of West Nile Virus disease in the United States, 2004–2012. *American Journal of Tropical Medicine and Hygiene* **92**(5): 1013–1022.

Hartley DM, Barker CM, Menach AL, Niu T, Gaff HD and Reisen WK (2012). Effects of temperature on emergence and seasonality of West Nile virus in California. *American Journal of Tropical Medicine and Hygiene* **86**(5): 884-894.

Hoover KC and Barker CM (2016). West Nile virus, climate change, and circumpolar vulnerability. *WIREs Climate Change* **7**(2): 283-300.

Linthicum KJ, Anyamba A, Britch SC, Small JL and Tucker CJ (2016). Appendix A7: Climate teleconnections, weather extremes, and vector-borne disease outbreaks. In: *Global Health Impacts of Vector-Borne Diseases Workshop Summary*. National Academies of Sciences, Engineering, and Medicine. Washington, DC: The National Academies Press.



Monath TP (1980). Epidemiology. In: *St Louis Encephalitis*. Monath TP (Ed.) St. Louis Washington, DC: American Public Health Association. pp. 239-312.

NAS (2016). *Global Health Impacts of Vector-Borne Diseases: Workshop Summary*. National Academies of Sciences, Engineering, and Medicine. Washington, DC: The National Academies Press. Available at: <https://www.ncbi.nlm.nih.gov/books/NBK355538/>

Ogden NH and Lindsay LR (2016). Effects of climate and climate change on vectors and vector-borne diseases: ticks are different. *Trends in Parasitology* **32**(8): 646-56.

Ogden NH, Milka R, Caminade C and Gachon P (2014). Recent and projected future climatic suitability of North America for the Asian tiger mosquito. *Aedes albopictus*. *Parasites and Vectors* **7**: 532.

Parham PE and Michael E (2010). Modelling climate change and malaria transmission. *Advances in Experimental and Medical Biology* **673**: 184-199.

Paull SH, Horton DE, Ashfaq M, Rastogi D, Kramer LD, et al. (2017). Drought and immunity determine the intensity of West Nile virus epidemics and climate change impacts. *Proceedings of the Royal Society B* **284**(1848): 2016-2078.

Reeves WC, Hardy JL, Reisen WK and Milby MM (1994). Potential effect of global warming on mosquito-borne arboviruses. *Journal of Medical Entomology* **31**(3): 323-332.

Reisen WK, Fang Y and Martinez VM (2006). Effects of temperature on the transmission of West Nile virus by *Culex tarsalis* (Diptera: Culicidae). *Journal of Medical Entomology* **43**(2): 309-317.

Reisen WK (2013). Ecology of west nile virus in North America. *Viruses* **5**(9): 2079-2105.

Reisen WK and Coffey LL (2014). Arbovirus threats to California. *Proceedings of Mosquito and Vector Control Association of California* **82**: 64-68.

Rochlin I, Faraji A, Ninivaggi DV, Barker CM and Kilpatrick AM (2016). Anthropogenic impacts on mosquito populations in North America over the past century. *Nature Communications* **7**: 13604.

Smith KR, Woodward A, Campbell-Lendrum D, Chadee DD, Honda Y, et al. (2014). Human health: Impacts, Adaptation, and Co-benefits. In: *Climate Change 2014: Impacts, Adaptation, and Vulnerability. Part A: Global and Sectoral Aspects. Contribution of Working Group II to the Fifth Assessment Report of the Intergovernmental Panel on Climate Change*. Field CB, Barros VR, Dokken DJ, Mach KJ, Mastrandrea MD et al. (Eds.). Cambridge and New York: Cambridge University Press. pp. 709-754.

Swei A, Meentemeyer R and Briggs CJ (2011). Influence of abiotic and environmental factors on the density and infection prevalence of *Ixodes pacificus* (Acari:Ixodidae) with *Borrelia burgdorferi*. *Journal of Medical Entomology* **48**: 20-28.

USGCRP (2016). *The Impacts of Climate Change on Human Health in the United States: A Scientific Assessment*. United States Global Change Research Group. Washington, DC. Available at <https://health2016.globalchange.gov/downloads#climate-change-and-human-health>

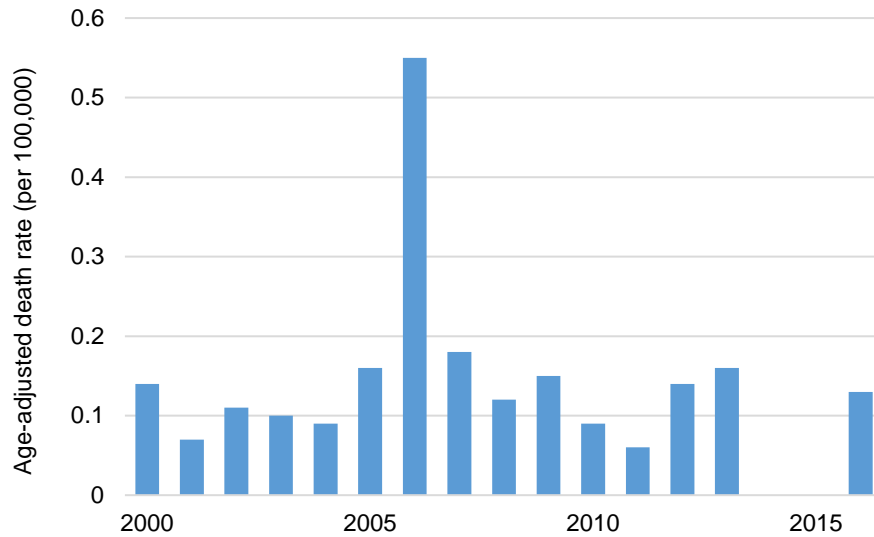
White GS, Symmes K, Sun P, Fang Y, Garcia S, et al. (2016). Reemergence of St. Louis Encephalitis Virus, California, 2015. *Emerging Infectious Diseases* **22**(12): 2185-2188.



HEAT-RELATED MORTALITY AND MORBIDITY

Deaths and illnesses from heat exposure are severely underreported, and vary from year to year. In 2006, numbers of deaths and illnesses were much higher than any other year because of a prolonged heat wave.

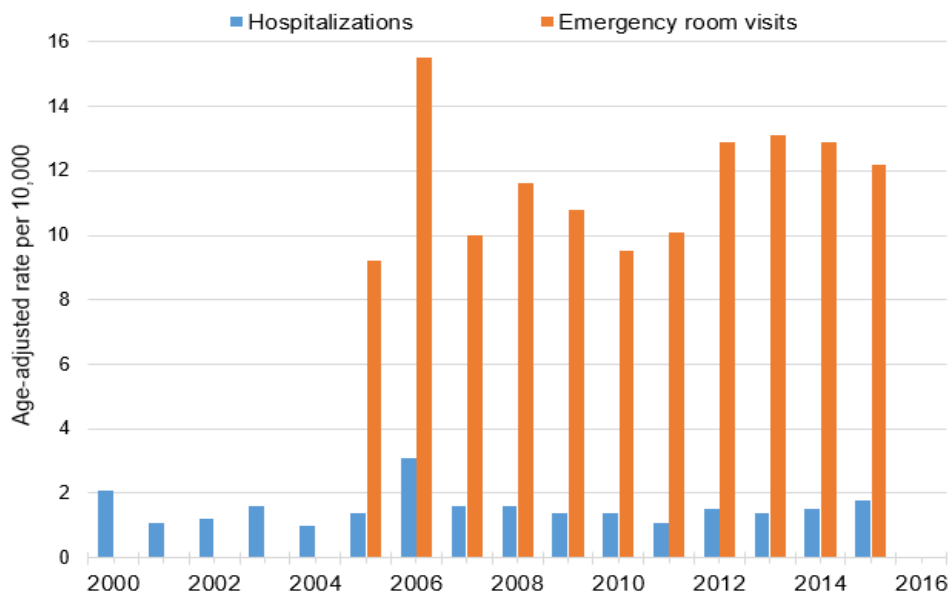
Figure 1. Heat-related deaths



*Mortality data with all causes of death were not available for 2014 and 2015 at the time of analysis.

Source: Data set compiled by Tracking California, using data from the Center for Health Statistics (PHI, 2018)

Figure 2. Heat-related illnesses*



*Data for emergency room visits were not available until 2005.

Source: Data set compiled by Tracking California, using data from the Office of Statewide Health Planning and Development. (PHI, 2017a)



What does the indicator show?

Exposure to high temperatures can lead to illness (morbidity) and deaths (mortality). Heat-related illnesses are a broad spectrum of diseases, ranging from mild heat cramps to severe, life-threatening heat stroke, to death. Figure 1 presents annual heat-related death rates for 1999 to 2013 and for 2016. (At this time, mortality data for all causes of death are not available for the years 2014 and 2015.) Figure 2 shows both heat-related hospitalizations (2000 to 2015) and heat-related emergency room (ER) visits (2005 to 2015). No trend is evident in either heat-related illnesses or deaths in California, both of which vary from year to year. In 2006, dramatic increases in many heat-related illnesses and deaths were reported following a record-breaking heat wave. Over 16,000 excess emergency room visits, over 1,100 excess hospitalizations (Knowlton et al., 2009), and at least 140 deaths (Margolis et al., 2008) occurred between July 15 and August 1, 2006.

Heat-related illnesses and deaths are often misclassified as another underlying cause or unrecognized. Hence, the available data on heat-related illnesses and deaths likely underestimate the full health impact of exposure to periods of high temperatures, including heat waves.

Why is this indicator important?

Heat causes more reported deaths per year on average in the United States than any other weather hazard, yet heat-related illnesses and deaths are generally preventable (NOAA, 2017; Luber et al., 2014). Certain groups such as infants, children, pregnant women, the elderly, those with pre-existing health conditions, and those who are socioeconomically disadvantaged are especially vulnerable to overexposure to heat (Luber et al., 2014).

Tracking heat-related illnesses and deaths provides critical information for developing adaptation plans and evaluating their successes, especially in relation to heat waves. State and local policies, plans, and programs focusing on heat are already in place in some locations. These may include heat wave early warning and surveillance (observation) systems, accessible cooling centers, public education campaigns on preventing heat-related illnesses, and worker heat-safety regulations. The use of air conditioning has been associated with significant reductions in heat-related hospital visits in California (Ostro et al., 2010). However, during periods of high heat, there is likely to be a greater risk of brownouts or blackouts from overuse of gas and electricity.

Periods of warmer temperatures and heat waves are expected to rise in frequency, duration, and intensity over the next century (IPCC, 2014; Luber et al., 2014). Projections for California estimate about a 10- to 20-fold increase in the number of extremely hot days by the mid-21st century, and about a 20- to 30-fold increase by the end of the century (CCAT, 2013). These projection numbers suggest an increasing public health burden from heat-related deaths and illnesses.



What factors influence this indicator?

Heat-related health outcomes are affected by the magnitude and duration of exposures to heat, as well as by factors relating to the exposed individuals, such as age, health status, and access to air conditioning.

As shown in figures 1 and 2, heat-related illnesses and deaths in 2006 peaked during the prolonged heat wave that occurred from July 16 to 26 (Knowlton et al., 2009; Margolis et al., 2008). Average apparent temperatures ranged from 81°F to 100°F, which is 4°F greater than the average statewide temperatures in July. The Central Valley region had the highest number of uninterrupted hot days ever recorded, with each day reaching 100°F and greater. Multiple locations in California broke records for the highest number of uninterrupted days over 100°F ever recorded: 11 in Sacramento; 12 in Modesto; and 21 in Woodland Hills near Los Angeles (Kozlowski and Edwards, 2007).

As noted above, certain groups are more vulnerable to heat exposure. These include the elderly, young children, people with pre-existing health conditions (such as heart or lung disease), African Americans, socially isolated people, the poor, and those who have difficulty getting medical care (CCAT, 2013; Basu and Ostro, 2008). Those engaged in vigorous physical activity are also at risk, such as workers in construction, firefighting, and agriculture. The rate of occupational heat-related deaths in California slightly exceeds the national average (Gubernot et al., 2016).

Urban residents may be more vulnerable to heat waves than people who live in surrounding suburban and rural areas. Buildings, dark paved surfaces, lack of vegetation and trees and heat emitted from vehicles and air conditioners cause cities to generate and retain heat, a phenomenon known as the “urban heat island effect.” On the other hand, people living in historically cooler areas may be less acclimated to heat than people living in historically warm areas and are less likely to have air conditioners installed in their homes (CDPH, 2007).

Communities with measures to prevent adverse heat-related health effects will likely fare better during times of extreme heat as California continues to warm. Such measures include early warning and surveillance systems, access to air conditioning, and public outreach and education.

Other findings studies on the effect of various factors on heat-related deaths and illnesses are discussed below.

Heat-related deaths

Investigators worldwide have documented relationships between elevated ambient temperature and mortality (Basu, 2009; Anderson and Bell, 2011). Deaths related to the July 2006 heat wave were largely attributed to elevated nighttime temperatures (Gershunov et al., 2009). Minimum temperatures, which reflect nighttime temperatures, have been increasing at a higher rate than daytime temperatures in California (see *Annual air temperature* indicator). In addition, heat waves have become increasingly



more humid since the 1980's. People who are adapted to California's traditionally dry daytime heat and nighttime cooling are less able to recover from extreme heat, especially when humidity levels are high.

Studies conducted in California have also documented increased mortality risk not only with extreme heat events, but also with increasing apparent temperature (Basu and Ostro, 2008; Basu et al., 2008; Basu and Malig, 2011). One California study found deaths from non-accidental causes increased by approximately 2.6 percent for every 10° F increase in mean daily apparent temperature. The effects were acute, with same-day effects being most significant, supporting the notion that public health actions to prevent heat-related mortality should be immediate. The investigators found that these effects not only impacted frail, elderly individuals but a broader population, and therefore, have the potential for greater public health risk.

Heat-related illnesses

Dramatic increases across a wide range of illnesses were observed during the summer of 2006 for emergency department visits, including heat stroke, electrolyte imbalance, acute kidney failure, diabetes, and cardiovascular diseases (Knowlton et al., 2009).

A 2014 study investigated the public health impacts of 19 heat waves throughout six regions of California from 1999 to 2009 (Guirguis et al., 2014). On average, hospital admissions were found to increase by seven percent on the peak heat-wave day, with a significant impact for cardiovascular diseases, respiratory diseases, dehydration, acute renal failure, heat illnesses, and mental health. Statewide, there were 11,000 excess hospitalizations that were due to extreme heat over the study period. The strongest health impacts occurred in the Central Valley and in the north and south coasts, with the north coast disproportionately affected. In the face of more frequent and severe heat waves, public health officials will be tasked with implementing plans to protect the high population areas along the coast, where heat acclimation is poor and air conditioners are less common.

In one study, apparent temperature, a combination of temperature and relative humidity, and hospital admissions were evaluated in nine counties across California from 1999 to 2005 (Green et al., 2010). Significantly increased risk of hospitalizations for multiple diseases, including ischemic heart disease, respiratory diseases, pneumonia, dehydration, heat stroke and diabetes were associated with a 10°F increase in mean daily apparent temperature. Increased mean daily apparent temperature was found to have same-day associations with emergency room admissions for several health outcomes, particularly for certain age and race/ethnic groups, which varied by disease (Basu et al., 2012).

Warming temperatures can increase emergency room visits for mental health-related outcomes, including violence and self-harm (Basu et al., 2017b). Apparent temperature has also been found to be associated with preterm delivery, with younger mothers and Black and Asian mothers at greatest risk (Basu et al., 2010). The week before preterm delivery was found to be associated with the most profound effects. Mothers with pre-



existing and/or gestational diabetes, hypertension, pre-eclampsia, or depression, as well as those who were underweight, Medicaid users, alcohol consumers or smokers were at greater risk for heat-associated preterm delivery (Basu et al., 2017a). Another study has also shown an association between apparent temperature and increase in stillbirths during the warm season two to six days before the fetal loss (Basu et al., 2016). These studies add to the growing body of literature identifying pregnant women and their fetuses as subgroups vulnerable to heat exposure.

Notably, even without extremes in temperatures, investigators observe associations between temperature, deaths, hospital or emergency room admissions, and adverse birth outcomes during the warm season in California (Basu and Ostro, 2008; Basu et al., 2008; Basu et al., 2010; Green et al., 2010; Basu et al., 2012; Basu et al., 2017b).

Technical considerations

Data Characteristics

Heat-related hospitalizations and emergency room visits were identified for the months of May -September by the California Environmental Health Tracking Program (CEHTP, recently renamed “Tracking California”). CEHTP is a program of the Public Health Institute, in partnership with the California Department of Public Health. Heat-related diseases were identified using Incident Classification of Disease (ICD)-9 codes for: heat stroke and sunstroke; heat syncope; heat cramps; heat exhaustion; heat fatigue; heat edema; other specified heat effects; unspecified effects of heat and light; health effect caused by excessive heat due to weather; and effect from unknown cause of excessive heat. Causes that were due to a man-made source of heat were excluded.

Hospitalization data were available for the years 2000 to 2015, and data on emergency room visits for the years 2005 to 2015.

CEHTP also identified heat-related deaths for the months of May-September, from 2000 to 2013, and for 2016, using ICD-10 codes for the following causes of death: heat stroke and sun stroke; heat syncope; heat cramps; heat exhaustion; heat fatigue; heat edema; exposure to excessive natural heat; other specified heat effects; and unspecified effects of heat and light. CEHTP did not have access to all causes mortality data for the years 2014 and 2015 at the time of analysis; hence, heat-related deaths for those years could not be identified. As with the morbidity dataset, deaths due to a man-made source of heat were excluded. More information about data and methods, including rate calculations, can be found at the CEHTP website (PHI, 2017b).

Strengths and limitations of the data

As noted earlier, the available data on heat-related illnesses and death likely underestimates the full health impact of exposure to heat. Heat-related health effects can manifest in a number of clinical outcomes, and people with chronic health problems are more susceptible to the effects of heat than healthy individuals. Heat-related illnesses and deaths are often misclassified or unrecognized.

During a heat wave, the number of heat-related deaths from coroners' reports rely on deaths coded as “heat-related” without any universal classification of these diseases.



Few deaths are recorded on death certificates as being heat-related (English et al., 2009). Heat illness is rarely listed as a main cause of deaths that occur in hospitals or emergency rooms, even when exposure to heat is a contributing factor. It is likely that there were three to four times as many deaths in the July 2006 heat wave than were actually reported (Ostro et al., 2009; Joe et al., 2016).

Despite these known limitations, heat-related health effects are tracked nationally. This data can be used to identify trends in heat-related morbidity and mortality and can be compared across states (US EPA, 2016).

For more information, contact:



Rupa Basu, PhD, MPH
California Environmental Protection Agency
Office of Environmental Health Hazard Assessment
1515 Clay Street, 16th floor
Oakland, CA 94612
(510) 622-3156
Rupa.Basu@oehha.ca.gov

Data: Heat-related deaths and Heat-related illnesses
Paul B. English, PhD, MPH
Senior Branch Science Advisor
Environmental Health Investigations Branch
California Department of Public Health
850 Marina Bay Parkway, P-3
Richmond, CA 94804
(510) 620-3038
Paul.English@cdph.ca.gov

References:

Anderson GB and Bell ML (2011). Heat waves in the United States: Mortality risk during heat waves and effect modification by heat wave characteristics in 43 U.S. communities. *Environmental Health Perspectives* **119**: 210-218.

Basu R and Ostro BD (2008). A multicounty analysis identifying the populations vulnerable to mortality associated with high ambient temperature in California. *American Journal of Epidemiology* **168**(6): 632-637.

Basu R, Feng W and Ostro B (2008). Characterizing temperature and mortality in nine California counties, 1999-2003. *Epidemiology* **19**(1): 138-145.

Basu R (2009). High ambient temperature and mortality: A review of epidemiologic studies from 2001 to 2008. *Environmental Health Perspectives* **8**: 40.

Basu R, Malig B and Ostro B (2010). High ambient temperature and the risk of preterm delivery. *American Journal of Epidemiology* **172**(10): 1108-1117.

Basu R and Malig B (2011). High ambient temperature and mortality in California: Exploring the roles of age, disease, and mortality displacement. *Environmental Research* **111**(8): 1286-1292.



Basu R, Pearson D, Malig B, Broadwin R and Green S (2012). The effect of high ambient temperature on emergency room visits in California. *Epidemiology* **23**(6): 813-20.

Basu R, Sarovar V and Malig B (2016). Association between high ambient temperature and risk of stillbirth in California. *American Journal of Epidemiology* **183**(10): 894-901.

Basu R, Chen H, Li D-K and Avalos LA (2017a). The impact of maternal factors on the association between temperature and preterm delivery. *Environmental Research* **4**: 109-114.

Basu R, Gavin L, Pearson D, Ebisu K and Malig B (2017b). Examining the association between temperature and emergency room visits for mental health-related outcomes in California. *American Journal of Epidemiology* (accepted).

CCAT (2013). *Preparing California for Extreme Heat: Guidance and Recommendations*. California Climate Action Team. Available at http://www.climatechange.ca.gov/climate_action_team/reports/Preparing_California_for_Extreme_Heat.pdf

CDPH (2007). *Public Health Impacts of Climate Change in California: Community Vulnerability Assessments and Adaptation Strategies. Report No. 1: Heat-Related Illness and Mortality. Information for the Public Health Network in California*. California Department of Public Health. Available at <http://www.energy.ca.gov/2008publications/DPH-1000-2008-014/DPH-1000-2008-014.PDF>

English PB, Sinclair AH, Ross Z, Anderson H, Boothe V, et al. (2009). Environmental health indicators of climate change for the United States: Findings from the State Environmental Health Indicator Collaborative. *Environmental Health Perspectives* **117**(11):1673-1681.

Gershunov A, Cayan DR and Lacobellis SF (2009). The great 2006 heat wave over California and Nevada: Signal of an increasing trend. *Journal of Climate Change* **22**: 6181-6203.

Green R, Basu R, Malig B, Broadwin R, Kim J, et al. (2010). The effect of temperature on hospital admissions in nine California counties. *International Journal of Public Health* **55**(2): 113-121.

Gubernot DM, Anderson CG and Hunting KL (2016). Characterizing occupational heat-related mortality in the United States, 2000-2010: An analysis using the census of fatal occupational injuries database. *American Journal of Industrial Medicine* **58**(2): 203-211.

Guirguis K, Gershunov A, Tardy A and Basu R (2014). The impact of recent heat waves on human health in California. *Journal of Applied Meteorology and Climatology* **53**(1): 3-19.

IPCC (2014). *Climate Change 2014: Impacts, Adaptation and Vulnerability. Contribution of Working Group II to the Fifth Assessment Report of the Intergovernmental Panel on Climate Change*. [Field CB, Barros VR, Dokken DJ, Mach KJ, Mastrandrea MD (Eds.)]. Intergovernmental Panel on Climate Change. Geneva, Switzerland. Available at <http://www.ipcc.ch/ipccreports/ar4-wg1.htm>

Joe L, Hoshiko S, Dobraca D, Jackson R, Smorodinsky S, et al. (2016). Mortality during a Large-Scale Heat Wave by Place, Demographic Group, Internal and External Causes of Death, and Building Climate Zone. *International Journal of Environmental Research and Public Health* **13**(3): 299.

Knowlton K, Rotkin-Ellman M, King G, Margolis HG, Smith D, et al. (2009). The 2006 California heat wave: Impacts on hospitalizations and emergency department visits. *Environmental Health Perspectives* **117**(1): 61-67.

Kozlowski DR and Edwards LM (2007). An Analysis and Summary of the July 2006 Record-Breaking Heat Wave Across the State of California. (Western Region Technical Attachment 07-05). Available at https://www.cnrfc.noaa.gov/publications/heatwave_ta.pdf



Luber G, Knowlton K, Balbus J, Frumkin H, Hayden M, et al. (2014). Chapter 9: Human Health. In: *Climate Change Impacts in the United States: The Third National Climate Assessment*. Melillo JM, Richmond TC, and Yohe GW (Eds.). U.S. Global Change Research Program. pp. 220-256.

Margolis HG, Gershunov A, Kim T, English P and Trent R (2008). 2006 California heat wave high death toll: Insights gained from coroner's reports and meteorological characteristics of event. *Epidemiology* **19**(6): S363-S364.

NOAA (2017). National Oceanic and Atmospheric Administration National Weather Service: 77-Year List of Severe Weather-Related Facilities (1940-2016). Retrieved July 10, 2017, from <http://www.nws.noaa.gov/om/hazstats.shtml>

Ostro BD, Roth LA, Green RS and Basu R (2009). Estimating the mortality effect of the July 2006 California heat wave. *Environmental Research* **109**(5): 614-619.

Ostro BD, Rauch S, Green R, Malig B and Basu R (2010). The effects of temperature and use of air conditioning on hospitalizations. *American Journal of Epidemiology* **172**(9): 1053-1061.

PHI (2017a). Public Health Institute. Tracking California. Climate Change Data: Heat-Related Illness Data Query, using data from the Office of Statewide Health Planning and Development. Retrieved August 11, 2017, from http://www.cehtp.org/page/hri/query#_faq_0_0

PHI (2017b). Public Health Institute. Tracking California. Climate Change Data: Heat-Related Illness and Death Data: Methods and Limitations. Retrieved August 11, 2017, from http://www.cehtp.org/faq/climate_change/heatrelated_illness_and_death_data_methods_and_limitations

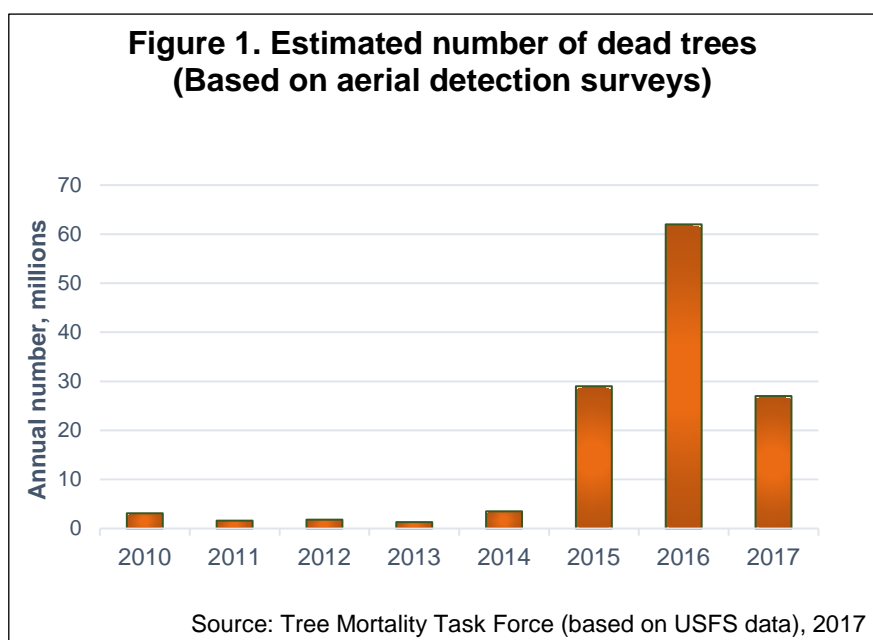
PHI (2018). Public Health Institute. Tracking California. Climate Change Data: Heat-Related Deaths Summary Tables, using data from the Center for Health Statistics, 2000-2011. Retrieved August 11, 2017, from http://www.cehtp.org/faq/climate_change/climate_change_data_heat_related_deaths_summary_tables#_faq_0_0. Data for 2012 through 2016 provided by Tracking California.

US EPA (2016). *Climate Change Indicators in the United States, 2016. US Environmental Protection Agency Technical Documentation: Heat-Related Deaths*. United States Environmental Protection Agency. Available at https://www.epa.gov/sites/production/files/2017-01/documents/heat-deaths_documentation.pdf



FOREST TREE MORTALITY

Since the 2012-2016 drought — the most severe since instrumental records began — tree deaths in forest lands in California increased dramatically. Annual tree mortality was elevated beginning in 2014 and a cumulative total of 129 million trees in forest lands died between 2012 and December 2017. Most of these trees were stressed from higher temperatures and decreasing water availability, making them more vulnerable to insects and pathogens.



What does the indicator show?

Annual tree mortality in California forests increased in 2014, two years into the 2012-2016 drought, followed by steep increases in 2015 and 2016. Tree deaths in 2017 were also considerably above levels at the beginning of the decade. Figure 1 shows the estimated annual number of dead trees in California forests killed by a variety of agents (not limited to drought or drought-related insect activity), as measured by US Forest Service aerial detection surveys. The largest number of tree deaths in any one year (62 million) was recorded in 2016. The cumulative number of dead trees in forested areas between 2012 and 2017 was an estimated 129 million (USFS, 2017a).

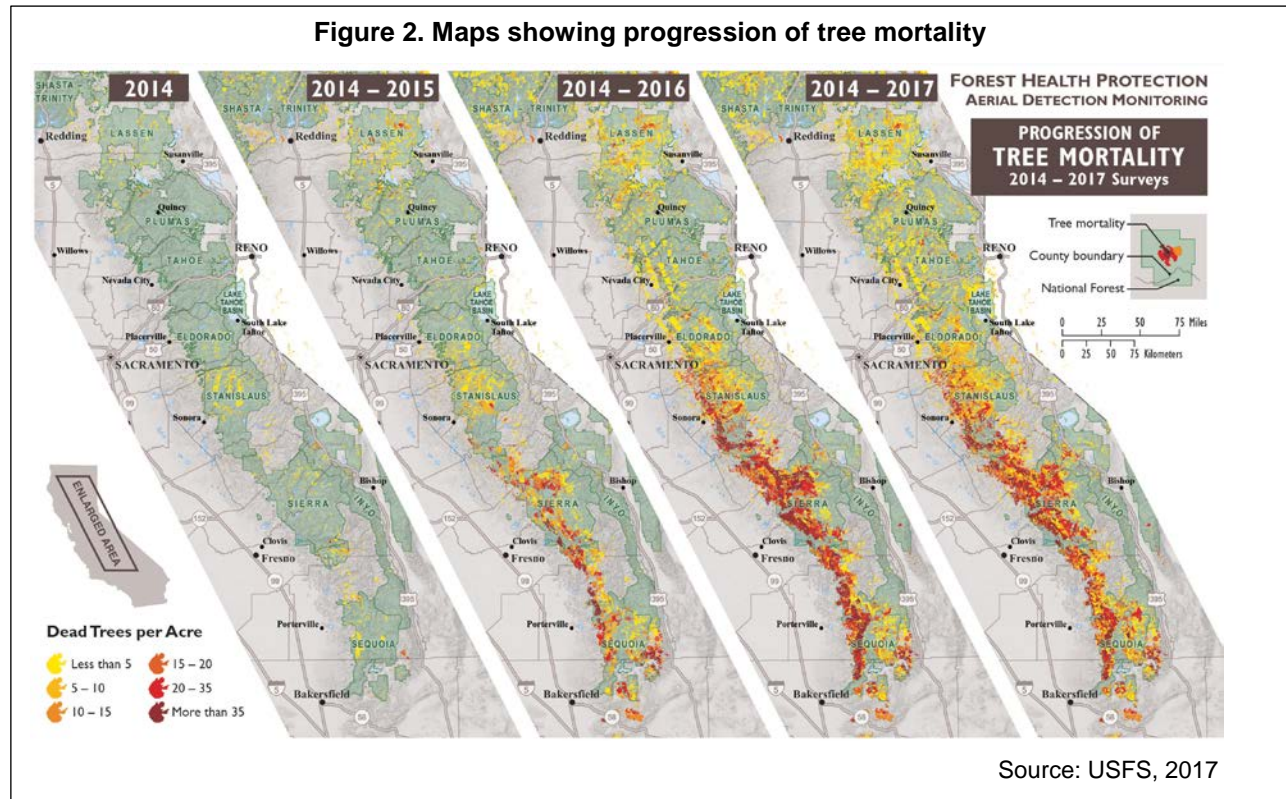
Based on the aerial detection surveys, the maps in Figure 2 show the progression of tree mortality in California's Sierra Nevada Mountains in recent years. The spatial extent and severity of tree mortality have increased since 2014, as the drought in California progressed (USFS, 2017a).

Why is this indicator important?

Forests occupy almost one-third of California and are a vital resource for the state, providing important ecosystem services including water provision, air purification, carbon sequestration, and recreational opportunities (CNRA, 2016). Accelerating tree mortality and the increasing frequency of large-scale high mortality events (known as



forest dieback) could have profound effects on these processes. Additionally, there is a potential that increased tree mortality will amplify other climate change-related phenomena such as forest type conversion (a change in tree species or group of species present, for example, from conifers to hardwood; see *Changes in forests and woodlands* indicator) and increased fire risk (see *Wildfires* indicator).



The majority of the trees that have died in California forests are conifers; the majority of deaths involved trees weakened by the drought succumbing to beetle outbreaks (rather than direct physiological stress from the drought) (Moore et al., 2016). Using tree ring data, researchers estimated 2014 to be the worst single drought year in at least the last 1,200 years in the state, as seen in the tree rings of blue oak (*Quercus douglasii*) — the result of unusually low (yet not unprecedented) precipitation and record high temperatures (Griffin and Anchukaitis, 2014). California's pattern of tree mortality corresponds with global trends: increasing tree mortality has been documented on all vegetated continents and in most bioregions over the past two decades and is linked to increasingly dry and hot climatic conditions (Allen et al., 2010).

If forest tree mortality continues at the current elevated rates, it could lead to changes in the species comprising the state's forest ecosystems, conversion of forests to vegetation types with less trees, or even the outright loss of forests (Kobe, 1996; Lenihan et al., 2003; Thorne et al., 2008; Millar et al., 2015).

Recognizing the unprecedented extent of the recent tree mortality, Governor Brown proclaimed a state of emergency in October 2015 to address its impacts to communities



in the affected regions (Brown, 2015). Among other things, the proclamation directs state agencies to take action to minimize the risks to public safety associated with the large number of dead trees, and to address the increased threat of wildfires and erosion in the affected areas.

What factors influence this indicator?

Tree mortality is a complex process that often involves a chain of events and a wide range of factors, often making it difficult to assign a single ultimate cause of death. In fact, many of the disturbances contributing to tree mortality are overlapping and integrative events that may play a role in observed large stand-level forest dieback and changes in the composition of forest trees and their structure, and shifts in tree species ranges in the western United States (Clark et al., 2016).

Regional warming and the consequent drought stress were found to be the most likely drivers of increased background tree mortality in old growth western forests; the observed regional warming from the 1970s to 2000s contributed to hydrologic changes — less precipitation falling as snow, declining snowpack water content, earlier spring snowmelt and runoff, and a lengthening of the summer drought (van Mantgem et al., 2009). The 2012-2016 drought occurred at a time of record warmth — 2014 is the warmest year on record, followed by 2015 — accompanied by record low snowpack (DWR, 2017) (also see *Drought* indicator).

Climatic water deficit (CWD) is used as a measure of water stress experienced by plants (Stephenson, 1998). CWD can be thought of as the amount of additional water that would have evaporated or been transpired by plants had it been present in the soils; it integrates plant water demand relative to soil moisture availability. Increases in CWD are associated with a warming climate, as warmer air temperatures increase plant water demand for evapotranspiration (Flint et al., 2013; Thorne et al., 2015); reduced precipitation and earlier snowmelt also contribute to a higher CWD by decreasing available water. Under increased CWD conditions, trees could lose their ability to convey water from root to leaf via a tree's xylem — a mechanism that has been shown to lead to drought-induced tree mortality (Adams et al., 2010). The tree mortality during the drought correlated with increases in CWD (Young et al., 2017).

The frequency, severity, and extent of large forest dieback events, such as the one discussed here, are of concern. The most recent drought in California may foreshadow an increasingly common condition in which warm temperatures coincide with periodically occurring dry years — “hotter drought” — contributing to increasing physiological stress in trees (Young et al., 2017; Diffenbaugh et al., 2015). In fact, rising global temperatures have contributed to droughts of a severity that is unprecedented in the last century or more (Millar et al., 2015).

Competition for resources is also a factor. Most of California's coniferous forests have more trees now than 100 years ago, a consequence of fire suppression (Stephens et al., 2018). Tree mortality increased disproportionately in areas that were both dry and dense (Young et al., 2017).



Another effect of warming temperatures is the enhanced growth and reproduction of insects and pathogens that attack trees (van Mantgem et al., 2009). In recent decades, the outbreaks of insects and pathogens have resulted in extensive forest defoliation, canopy dieback, declines in growth, and forest mortality in western North America. Some widespread dieback events have occurred concomitant with infestation outbreaks where the insect populations increased due to warmer winter temperatures (Bentz et al., 2010); in California, however, the effect of warmer winter temperatures on insect populations has not been demonstrated. In many regions, drought and unusually warm temperatures have weakened trees and accelerated the bark beetle population growth (Adams et al., 2010). Temperature-driven insect population increases in combination with water deficit can have disproportionate consequences on tree mortality than would have occurred due to drought or insects alone (Anderegg, 2015).

Technical Considerations

Data Characteristics

The aerial tree mortality surveys are based on annual small plane reconnaissance over California's forested lands. Forested areas are mapped on a one-acre basis, and the following recorded: (a) damage type, (b) number of trees affected, and (c) affected tree species. Generally, areas with <1 tree per acre of mortality are considered to have "background" or "normal" levels of mortality and are not usually mapped during the flight. If low levels of mortality are indicative of a localized pest-related event, the areas are supposed to be mapped; however, it is usually not possible to systematically discern the cause of such low-level mortality using visual aerial surveys.

Lands dominated by hardwood and conifer tree species are considered forest lands in California. Affected tree species are recorded to species level if possible (Sugar Pine and White Fir), or to genus level (pine, fir). In areas where two or more tree species are affected, the surveyor will designate the proportion of damage affecting each species (e.g., 25 percent Sugar Pine, 75 percent White Fir), or preferably, an estimate of trees per acre for each species affected is recorded. Lands characterized as urban, orchards, and windbreaks are not mapped. Tree injuries that are recorded are typically defoliation, discoloration, dieback or more commonly death. Survey results provide a reasonable estimate of dead trees that aid in the understanding of the mortality event (USFS, 2017b). It is possible there is some level of error in the density estimates. However, over large areas covered, the results will show the correct trends.

Strengths and Limitations of the Data

Aerial surveys cannot detect mortality until the trees have been dead some months and the foliage has dried out and faded from green to a red or yellow color. Thus, currently infested, but dead, trees still look healthy from a distance but may not be counted in the aerial survey.



For more information, contact:



James Thorne
Department of Environmental Science and Policy
University of California Davis
2132 Wickson Hall, 1 Shields Avenue
Davis, CA 95616
(530) 752-4389
jthorne@ucdavis.edu



Mark Rosenberg or Tadashi Moody
Department of Forestry and Fire Protection
Fire and Resource Assessment Program
P.O. Box 944246
Sacramento, CA 94244-2460
(916) 327-3939
Tadashi.Moody@fire.ca.gov or Mark.Rosenberg@fire.ca.gov

References:

- Adams HD, Macalady AK, Breshears DD, Allen CD, Stephenson NL, et al. (2010). Climate-Induced Tree Mortality: Earth System Consequences. *EOS Transactions, American Geophysical Union* **91**(17): 153–154.
- Allen CD, Macalady AK, Chenchouni H, Bachelet D, McDowell N, et al. (2010). A global overview of drought and heat-induced tree mortality reveals emerging climate change risks for forests. *Forest Ecology and Management* **259**(4): 660-684.
- Anderegg WRL, Hicke JA, Fisher RA, Allen CD, Aukema J, et al. (2015). Tree mortality from drought, insects, and their interactions in a changing climate. *New Phytologist* **208**: 674-683.
- Bentz B, Regniere J, Fettig C, Hansen E, Hayes JL, et al. (2010). Climate Change and Bark Beetles of the Western United States and Canada: Direct and Indirect Effects. *BioScience* **60**(8): 602-613.
- Brown EG (2015). *Proclamation of a State of Emergency, October 30, 2015*. Executive Department, State of California. Available at https://www.gov.ca.gov/docs/10.30.15_Tree_Mortality_State_of_Emergency.pdf
- CNRA (2016). *Safeguarding California: Implementation Action Plan. Forestry Sector Plan*. California Natural Resources Agency. Available at <http://resources.ca.gov/docs/climate/safeguarding/Safeguarding%20California-Implementation%20Action%20Plans.pdf>
- Clark JS, Iverson L, Woodall CW, Allen CD, Bell DM, et al. (2016). The impacts of increasing drought on forest dynamics, structure, and biodiversity in the United States. *Global Change Biology* **22**(7): 2329–2352.
- Diffenbaugh NS, Swain DL, and Touma D (2015). Anthropogenic warming has increased drought risk in California. *Proceedings of the National Academy of Sciences* **112**(13): 3931-3936.
- DWR (2017). *Hydroclimate Report: Water Year 2016*. California Department of Water Resources. Office of the State Climatologist. Available at https://www.water.ca.gov/-/media/DWR-Website/Web-Pages/Programs/All-Programs/Climate-Change-Program/Files/a3037_Hydroclimate_report_v11.pdf



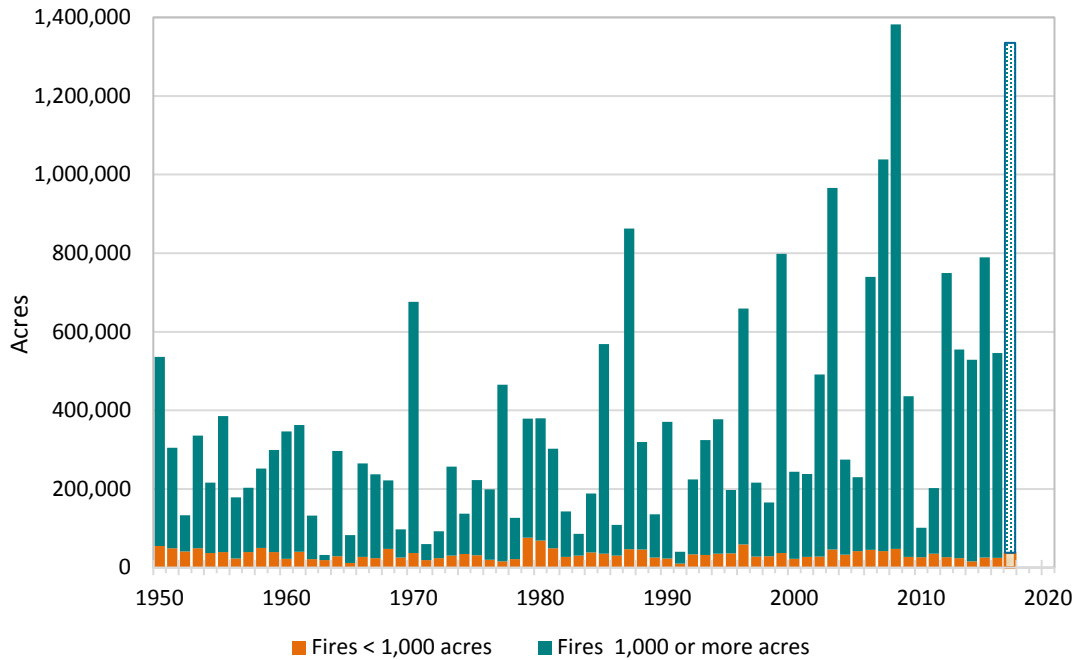
- Flint LE, Flint AL, Thorne JH and Boynton RM (2013). Fine-scale hydrological modeling for regional landscape applications: Model development and performance. *Ecological Processes* **2**(25).
- Griffin D and Anchukaitis KJ (2014). How unusual is the 2012–2014 California drought?. *Geophysical Research Letters* **41**(24): 9017–9023.
- Kobe RK (1996). Intraspecific variation in sapling mortality and growth predicts geographic variation in forest composition. *Ecological Monographs* **66**(2): 181-201.
- Lenihan JM, Drapek R, Bachelet D and Neilson RP (2003). Climate change effects on vegetation distribution, carbon, and fire in California. *Ecological Applications* **13**(6): 1667-1687.
- Millar CI and Stephenson NL (2015). Temperate forest health in an era of emerging megadisturbance. *Science* **349**(6250): 823-826.
- Moore J, Jirka A, McAfee L, Heath Z, Matthews K, et al. (2016). *2015 Aerial Highlights for California*. Board of Forestry and Fire Protection. Available at http://bofdata.fire.ca.gov/board_business/binder_materials/2016/jan_2016/full/full_14.2_pest_council_poster.pdf
- Stephens SL, Collins BM, Fettig CJ, Finney MA, Hoffman CM, et al. (2018). Drought, Tree Mortality, and Wildfire in Forests Adapted to Frequent Fire. *Bioscience* **68**(2): 77-88.
- Stephenson N (1998). Actual evapotranspiration and deficit: biologically meaningful correlates of vegetation distribution across spatial scales. *Journal of Biogeography* **25**(5): 855–870.
- Tree Mortality Task Force (2017). *2017 Tree Mortality Aerial Detection Survey Results*. U.S. Department of Agriculture, Forest Service, Pacific Southwest Region. Available at https://www.fs.usda.gov/Internet/FSE_DOCUMENTS/fseprd566199.pdf
- Thorne JH, Morgan BJ and Kennedy JA (2008). Vegetation Change over 60 Years in the Central Sierra Nevada. *Madroño* **55**(3): 223-237.
- Thorne JH, Boynton RM, Flint LE and Flint AL (2015). Comparing historic and future climate and hydrology for California’s watersheds using the Basin Characterization Model. *Ecosphere* **6**(2).
- USFS (2017a). *Progression of Tree Mortality, 2014-2017 Surveys*. U.S. Department of Agriculture, Forest Service. Available at https://www.fs.usda.gov/Internet/FSE_DOCUMENTS/fseprd565841.pdf
- USFS (2017b). *Aerial Detection Survey: Methodology*. U.S. Department of Agriculture, Forest Service. Available at <https://www.fs.usda.gov/detail/r5/forest-grasslandhealth/?cid=stelprdb5429568>
- van Mantgem PJ, Stephenson NL, Byrne JC, Daniels LD, Franklin JF, et al. (2009). Widespread Increase of Tree Mortality Rates in the Western United States. *Science* **323**(5913): 52 –4.
- Young DJN, Stevens JT, Earles JM, Moore J, Ellis A, et al. (2017). Long-term climate and competition explain forest mortality patterns under extreme drought. *Ecological Letters* **20**(1): 78–86.



WILDFIRES

The area burned by wildfires across the state is increasing in tandem with rising temperatures.

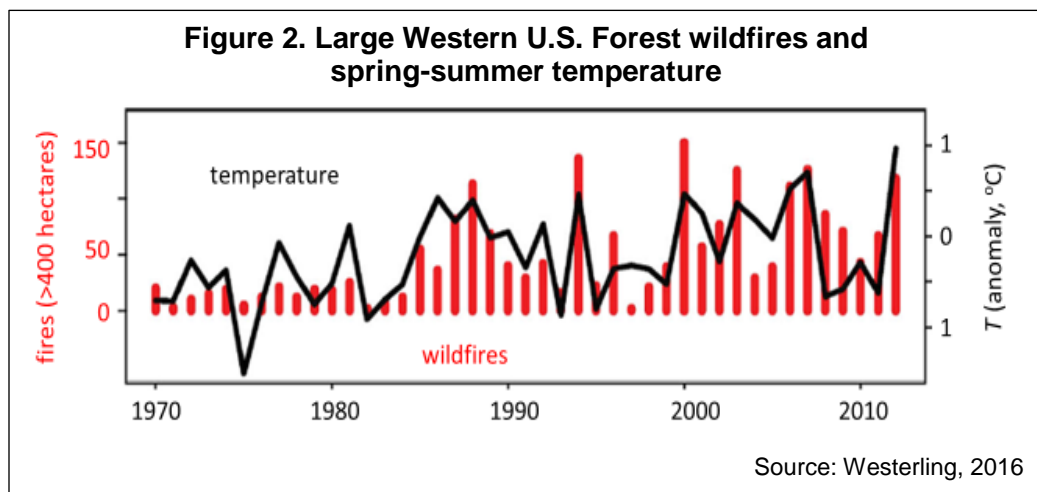
Figure 1. Statewide annual acres burned, 1950-2017*



*2017 data preliminary and subject to change

Source: CalFire, 2018

Figure 2. Large Western U.S. Forest wildfires and spring-summer temperature



Source: Westerling, 2016

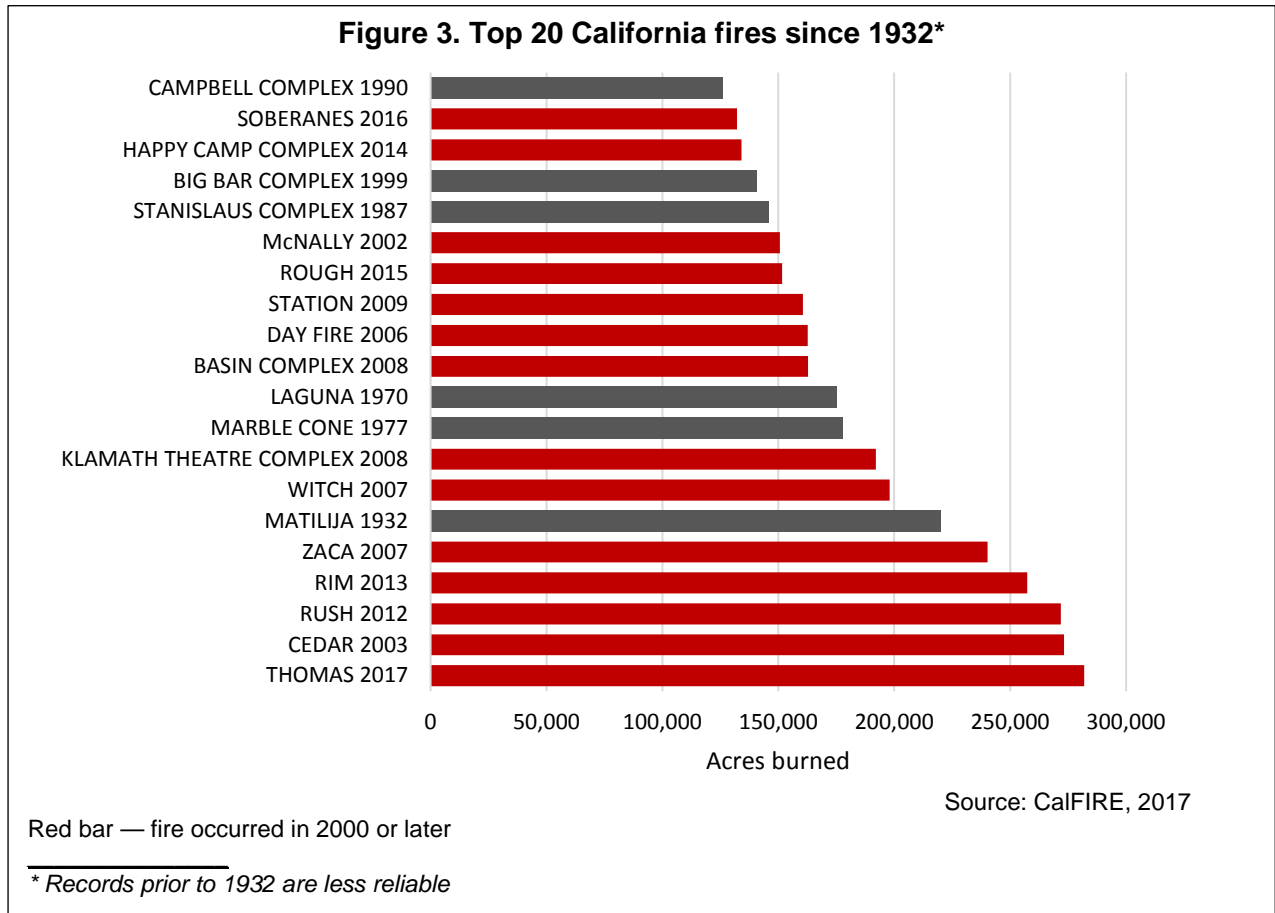
What does the indicator show?

The data presented in Figure 1 show a trend toward increasing acres burned by wildfires statewide. The total area burned annually since 1950 ranged from a low of 32,000 acres in 1963 to a high of 1.4 million acres in 2008.



Although they are fewer in number than fires affecting smaller areas, fires affecting 1,000 acres or more account for most of the area burned each year. The vast majority of wildfires are less than 1,000 acres, yet they account for only about 10 percent of the total area burned each year.

The recent increase in areas burned by wildfires in California is reflected in the fact that, five of the largest fire years since 1950 occurred in about the past decade, in the years 2006, 2007, 2008, 2012, and 2015. Moreover, 14 of the 20 largest wildfires have occurred since 2000 (Figure 3).



Throughout the western United States, large wildfires (affecting more than 400 hectares, or approximately 1000 acres) have increased in number and acreage burned over recent decades (Westerling, 2016; Dennison et al., 2014). The number of large forest wildfires in the western US (consisting of the Rockies, the Sierra Nevada, Cascades, the Coast Ranges, and the mountain ranges of Arizona and New Mexico) has been found to be strongly correlated with mean temperatures from March through August (see Figure 2; Westerling, 2016). As with large forest fires, wildfire activity in grass and shrubland in the western US have also increased significantly over the same time period in terms of frequency and area burned (Westerling, 2016).



Why is this indicator important?

Wildfires are a natural element of California's landscape, playing a critical role in the structure and function of ecosystems. The state's native vegetation is adapted to the periodic recurrence of fire. This pattern has been significantly altered since Euro-American settlement by fire exclusion, land use practices, and development. These human influences have modified the types and distribution of vegetation. This, in turn, affects the likelihood and severity of wildfires (CalFire, 2010).

Wildfires can have a wide ranges of impacts on ecosystems. Recovery of plant communities following a fire determines biodiversity, ecosystem services, future fire activity and other ecosystem conditions. Animals exhibit a wide range of strategies in dealing with fires; recovery of animal communities is affected by the nature of the fire, along with factors such as the type of vegetation burned, the availability of refugia, and habitat fragmentation outside the burned area. Fires can affect soil, water, and carbon storage (Keeley and Safford, 2016). More frequent, expansive and exceptionally severe fires can result in habitat loss, disrupt watershed integrity, adversely impact small mammal populations, and degrade scenery.

Forests play an important part in regulating levels of atmospheric carbon (Settele et al, 2014; Gonzalez et al., 2015). Trees remove carbon dioxide, a greenhouse gas, from the atmosphere and store it through natural processes. Wildfires release carbon dioxide and black carbon into the atmosphere and in doing so contribute to increasing carbon dioxide levels and climate change. With the increasing size and intensity of wildfires, scientists are concerned that some forest lands are releasing carbon faster than they are able to store it (Schimmel and Braswell, 2005).

Wildfires threaten public health and safety, property and infrastructure. The October 2017 wildfires in Sonoma and Napa counties devastated the affected communities: 44 deaths, more than 100,000 residents evacuated, and over \$9 billion in residential and commercial insurance claims, making it the deadliest and most destructive fire in the state's history (CDI, 2017). The Thomas Fire that swept through Ventura and Santa Barbara counties in December 2017 is the largest recorded wildfire in the state's history, even though it occurred outside of what has traditionally been considered the state's fire season. As demonstrated by these two disasters, California's environment is increasingly at risk from wildfire. Scientists predict that the largest changes in property damage will occur in wildland/urban interfaces proximate to major metropolitan areas in coastal southern California, in the San Francisco Bay Area, and in the Sierra foothills northeast of Sacramento (Westerling and Bryant, 2008). By the end of the century, substantial increases in residential wildfire risk are projected to result from rapid, sprawling growth in areas on the periphery of the Sierra Nevada (Bryant and Westerling, 2014).

Wildfires severely impact air quality both locally and in areas downwind of the fire (Luber et al., 2014). Exposures to wildfire smoke, which contains particulate matter (PM), carbon monoxide, nitrogen oxides, and various volatile organic compounds, have been associated with general respiratory illnesses and exacerbations of asthma and



COPD (Reid et al., 2016; Liu et al., 2017). Medical costs in 2007 associated with wildfires in Southern California were estimated to have exceeded \$3.4 million (Kochi et al., 2016). Globally, hundreds of thousands of deaths annually have been attributed to exposures to landscape fire smoke.

Larger and more extreme wildfires could be especially challenging for rural, low-income households residing in fire-prone areas. Property loss is more likely to occur in smaller, more isolated housing clusters that are difficult for firefighters to reach and suppress (Syphard, 2012). Rural residents may have a lower capacity to protect themselves and recover from fire impacts than people living in more affluent communities (Collins and Bolin, 2009). Wildfires on or near native lands threaten the health, safety, and economy of those tribes, culturally important species, medicinal plants, traditional foods, and cultural sites (Bennett et al., 2014).

The increased number and severity of fires and losses of property, lives, and natural resources has made fire suppression in California an increasingly higher priority for federal, state, and local land management agencies. As large wildfires increase in size and number and the fire season has grown longer, firefighting consumes more of the annual resource management budgets for federal and state lands that otherwise could be spent on sustainable programs for fuel management and forest health. Threats posed by wildfires are expected to rise in the face of changing climate conditions and shifts in land use, especially population growth and housing development (USDA, 2015).

What factors influence this indicator?

California's Mediterranean climate predisposes its landscape to fires. Winter rains lead to abundant vegetation that, following the warm, dry summer months, become potential fuel for fires. Prior to Euro-American settlement, the state's diverse vegetation experienced the periodic recurrence of low-severity fires: more than 40 percent of the state supported high fire frequencies (that is, "fire return intervals" of less than 35 years), and another 15 to 20 percent supported moderate fire frequencies (fire return intervals of 35 to 100 years) (Keeley and Safford, 2016).

Increased spring and summer temperatures and earlier spring snowmelt have been associated with increased large wildfire activity (higher large-wildfire frequency, longer wildfire durations, and longer wildfire seasons) in western US forests beginning in the mid-1980s (Westerling et al., 2006; Westerling, 2016). The earliest third of spring snowmelt years accounted for over 70 percent of the area burned in large forest wildfires and more than 40 percent of the area burned in non-forest wildfires. Another study found that increasing trends in the number of large wildfires and area burned annually in the western US across ecoregions representing a wide range of vegetation types, latitudes, and precipitation regimes (Dennison et al., 2014). In ecoregions with the largest increases in fire activity, temperatures trended hotter and precipitation trended drier — coinciding with trends toward increased drought severity — compared to ecoregions without significant changes in fire activity. This study's findings implicate climate as a dominant driver of changing fire activity in the western US.



In western US forests, increases in temperature and vapor pressure deficit linked to anthropogenic climate change significantly enhanced fuel aridity over the past several decades, allowing for a more favorable fire environment (Abatzoglou and Williams, 2016). California has recently experienced extreme drought intensified by unusually warm temperatures, known as a hotter drought. With a hotter drought comes very low precipitation and snowpack, decreased streamflow, dry soils, and large-scale tree deaths. These conditions create increased risk for extreme wildfires that spread rapidly, burn with a severity that damages the ecosystem, and are costly to suppress (Crockett and Westerling, 2017).

Higher altitude forests are buffered against climate change warming effects to some extent by available moisture from colder conditions (more snowpack and abundant spring runoff). The runoff provides moisture to soil and vegetation, reducing the flammability of these forests. Interestingly, researchers have reported an increasing frequency of wildfire at higher elevations in the Sierra Nevada using a 105-year dataset (Schwartz et al., 2015). Several factors are likely contributing to this trend, including warming temperatures (especially nighttime) and earlier snowpack melt; increased fuel loads from increasing tree densities; changes in fire management such as reduced fire suppression at high elevations; and increasing ignition frequencies (both lightning and human-caused). These factors are not mutually exclusive and may have synergistic effects. An analysis of forests in the western US found that the number of large wildfires increased exponentially with a measure of moisture deficit (a forest-area weighted moisture deficit index) that incorporates both temperature and precipitation (Westerling, 2016). Forests at elevations with snow-free seasons averaging two to four months and relatively high cumulative warm-season actual evapotranspiration have been most affected.

The large differences in wildfire acres burned from year to year in California are primarily due to variable weather conditions and situations in which lightning-ignited fires occur in remote locations that are difficult to access (CalFire, 2010). For example, the size of a fire is influenced by the presence of strong winds, the dryness of vegetation due to lack of rainfall, and the ease of accessibility to firefighters. In Southern California, the influence of Santa Ana (SA) winds on wildfires is evident; a study found that non-Santa Ana fires, which occur mostly in June through August affected higher elevation forests, while SA fires, which occur mostly in September through December, spread three times faster and occurred closer to urban areas (Jin et al., 2015).

Changes in population and land use can have immediate and dramatic effects on the number and sources of ignitions and on the availability and flammability of fuels. For example, the escalation of fire losses at the wildland-urban interface is often attributed to new housing development within or adjacent to wildland vegetation (Syphard et al., 2012). This results in increasing shrubland acreage burned. Over the long term, fire management and land uses that suppress surface fires can lead to changes in the density and structure of the vegetation biomass that fuels wildfires, increasing the likelihood of a large or severe fire occurring.



Technical Considerations

Data Characteristics

Data on statewide annual acres burned (Figure 1) were downloaded from a fire perimeter database made publicly available online through CalFire. CalFire works with the USDA Forest Service (USFS) Region 5 Remote Sensing Lab, the Bureau of Land Management (BLM), and the National Park Service (NPS) to track fires on public and private lands throughout California. The data for the period 1950 to 2001 includes USFS wildland fires 10 acres and greater, and CalFire fires 300 acres and greater. In 2002, BLM and NPS fires 10 acres and greater were added, as were CalFire timber fires 10 acres and greater, brush fires 50 acres and greater, grass fires 300 acres and greater, wildland fires destroying three or more structures, and wildland fires causing \$300,000 or more in damage. Further details are available at: http://frap.fire.ca.gov/projects/fire_data/fire_perimeters_methods

Fire data for the western U.S. (Figure 2) are from the U. S. Department of Interior and the U.S. Forest Service, as described in Westerling (2016).

Strengths and Limitations of the Data

The CalFire database contains the most complete digital record of fires in California. However, some fires may be missing for a variety of reasons (e. g., lost historical records, inadequate documentation). In addition, although every attempt is made to remove duplicate fires, some duplicates may still exist. Overgeneralization may also be an issue, in which unburned regions within old, large fires may appear as burned.

Fire records used for Figure 2 were reviewed and obvious duplications and errors corrected, as described in Westerling (2016).

For more information, contact:



David Sapsis
Department of Forestry and Fire Protection
Fire and Resource Assessment Program
P.O. Box 944246
Sacramento, CA 94244-2460
(916) 445-5369
dave.sapsis@fire.ca.gov



Anthony L. Westerling
Sierra Nevada Research Institute
University of California, Merced
P.O. Box 2039
Merced, CA 95344
(209) 756-8793
awesterling@ucmerced.edu



References:

- Abatzoglou JT and Williams AP (2016). Impact of anthropogenic climate change on wildfire across western US forests. *Proceedings of the National Academy of Sciences* **113**(42): 11770-11775.
- Bennett TMB, Maynard NG, Cochran R, Gough K, Lynn J, et al. (2014). Ch. 12: Indigenous Peoples, Lands, and Resources. In: *Climate Change Impacts in the United States: The Third National Climate Assessment*. Melillo JM, Richmond TC, and Yohe GW (Eds.). U.S Global Research Program. pp. 297-317.
- Bryant BP and Westerling AL (2014). Scenarios for future wildfire risk in California: Links between changing demography, land use, climate, and wildfire. *Environmetrics* **25**: 454-471.
- CalFire (2010). *California's Forests and Rangelands: 2010 Assessment*. California Department of Forestry and Fire Protection. Available at http://frap.fire.ca.gov/data/assessment2010/pdfs/california_forest_assessment_nov22.pdf
- CalFire (2017). Top 20 Largest California Wildfires. California Department of Forestry and Fire Protection. Retrieved December 26, 2017, from http://www.fire.ca.gov/communications/downloads/fact_sheets/Top20_Acres.pdf
- CalFire (2018). FRAP Mapping, Fire Perimeters Version 16_1. Statewide data set "fires_100.xls" California Department of Forestry and Fire Protection. Retrieved February, 2018, from http://frap.fire.ca.gov/data/frapgisdata-sw-fireperimeters_download. 2017 update provided by CalFire.
- CDI (2017). California Department of Insurance, Press Release dated December 6, 2017: October wildfire claims top \$9. 4 billion statewide. Retrieved December, 2017, from <https://www.insurance.ca.gov/0400-news/0100-press-releases/2017/release135-17.cfm>.
- Collins T and Bolin B (2009). Situating hazard vulnerability: people's negotiations with wildfire environments in the US Southwest. *Environmental Management* **44**(3):441-455.
- Crockett JL and Westerling AL (2017). Greater temperature and precipitation extremes intensify western U. S. droughts, wildfire severity, and Sierra Nevada tree mortality. *Journal of Climate* **31**(1): 341-354.
- Dennison PE, Brewer SC, Arnold JD, and Moritz MA (2014). Large wildfire trends in the western United States, 1984–2011. *Geophysical Research Letters* **41**(8): 2928–2933.
- Gonzalez P, Battles J, Collins B, Robards T, and Saah D (2015). Above ground live carbon stock changes of California wildland ecosystems, 2001-2010. *Forest Ecology and Management* **348**: 68-77.
- Jin Y, Goulden M, Faivre N, Veraverbeke S, Sun F, et al. (2015). Identification of two distinct fire regimes in Southern California: Implications for economic impact and future change. *Environmental Research Letters* **10**: 094005.
- Keeley JE and Safford HD (2016). Chapter 3: Fire as an Ecosystem Process. In: *Ecosystems of California*. Mooney H and Zavaleta E (Eds). University of California Press.
- Kochi I, Champ P, Loomis J, and Donovan G (2016). Valuing morbidity effects of wildfire smoke exposure from the 2007 Southern California wildfires. *Journal of Forest Economics* **25**: 29-54.
- Liu J, Wilson A, Mickley L, Dominici F, Ebisu K, et al. (2017). Wildfire-specific fine particulate matter and risk of hospital admissions in urban and rural counties. *Epidemiology* **28**(1): 77-85.
- Luber G, Knowlton K, Balbus J, Frumkin H, Hayden M, et al. (2014). Ch. 9: Human Health. In: *Climate Change Impacts in the United States: The Third National Climate Assessment*, Melillo JM, Richmond TC, and Yohe GW (Eds.). U. S. Global Change Research Program. pp. 220-256.

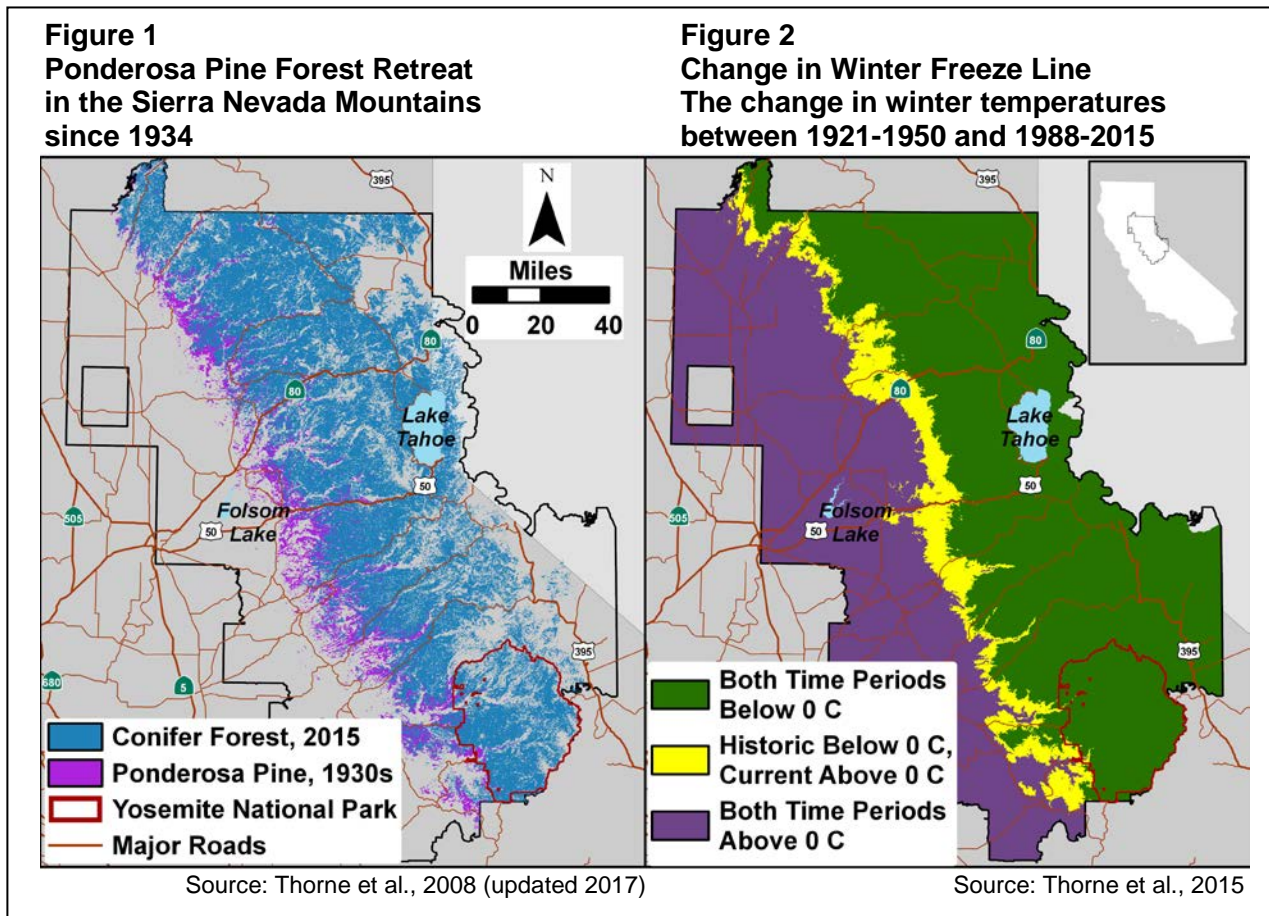


- Reid C, Brauer M, Johnston F, Jerrett M, Balmes J, and Elliot C (2016). Critical Review of health impacts of wildfire smoke exposure. *Environmental Health Perspectives* **124**: 1334-1343.
- Schimmel D and Braswell B (2005). Global Change and Mountain Regions: An Overview of Current Knowledge. In: *Advances in Global Change Research*. (Vol. 23). Huber W, Bugmann H and Reasoner. M (Eds.), Dordrecht, Netherlands: Springer. pp 449-456.
- Schwartz M, Butt N, Dolanc C, Holguin A, Moritz M, et al. (2015). Increasing elevation of fire in the Sierra Nevada and implications for forest change. *Ecosphere* **6**(7): 1-10.
- Settele J, Scholes R, Betts R, Bunn S, Leadley P, et al. (2014). Terrestrial and inlandwater systems. In: *Climate Change 2014: Impacts, Adaptation, and Vulnerability. Part A: Global and Sectoral Aspects. Contribution of Working Group II to the Fifth Assessment Report of the Intergovernmental Panel on Climate Change*. Field CB, Barros VR, Dokken DJ, Mach KJ, Mastrandrea MD, et al. (Eds.). Cambridge University Press, Cambridge, United Kingdom and New York, NY, USA. pp. 271-359.
- Syphard A, Keeley J, Massada A, Brennan T, and Radeloff V (2012). Housing arrangement and location determine the likelihood of housing loss due to wildfire. *PLoS ONE* **7**(3): e33954.
- USDA (2015). *The Rising Costs of Wildfire Operations: Effects on the Forest Service Non-Fire Work*. U.S. Department of Agriculture, U.S. Forest Service. Available at <https://www.fs.fed.us/sites/default/files/2015-Fire-Budget-Report.pdf>
- Westerling A (2016). Increasing western US forest wildfire activity: sensitivity to changes in the timing of spring. *Philosophical Transactions of the Royal Society B: Biological Sciences* **371**: 20150178.
- Westerling AL and Bryant BP (2008). Climate change and wildfire in California. *Climatic Change* **87** (Suppl 1): S231-S249.
- Westerling A, Hidalgo H, Cayan D, and Swetnam T (2006). Warming and earlier spring increase in western U.S. Forest wildfire activity. *Science* **313**(5789): 940-943.



PONDEROSA PINE FOREST RETREAT

Ponderosa pine forests in the Sierra Nevada have retreated uphill over the past 80 years.



What does the indicator show?

The lower edge of the conifer-dominated forests of the Sierra Nevada has been retreating upslope over the past 80 years. The dark blue areas in Figure 1 are the regions that still are dominated by the Sierran conifer forests, including the well-known forests leading up to the Lake Tahoe Basin. The area in purple was historically occupied by ponderosa pine (*Pinus ponderosa*), the pine that extends the lowest of the group of conifers making up the mixed conifer forests of the Sierra Nevada Mountains (Thorne et al., 2008). This lower edge is contracting along a 186-mile long front, which is consistent with predicted forest response to future climate change (Lenihan et al., 2003) – that is, an expansion of broadleaf-dominated forests in this elevation zone, with the accompanying loss of conifer-dominated forests.

Figure 2 shows the change in winter nighttime freezing temperatures (that is, minimum temperatures during December, January and February) (adapted from Thorne et al., 2015) over the past several decades. Winter nighttime temperatures were historically below freezing in the 4015-square kilometer (km²) area in yellow, but are currently above 0°C on average. The purple region to the west represents the area where winter



average minimum temperatures have always exceeded 0°C, while the green region to the east is the area that had, and on average still has, freezing winter nighttime temperatures.

The area that no longer has freezing nighttime winter temperatures (the yellow area in Figure 2) occupies elevations from 476 to 1861 meters (m). These elevations fall within those from which ponderosa pine has retreated — between 92 and 2310 m (shown in purple in Figure 1).

Why is this indicator important?

Since plant species are adapted to environmental conditions, changes in the distribution of dominant plants can be both an indicator of, and a response to, climate change. As conditions warm, species are generally expected to move towards the poles and to higher elevations. At the lower edge of the Sierra Nevada Mountains' conifer forests, there has been a transition to oak-dominated and chaparral vegetation concurrent with the uphill retreat of ponderosa pines.

The shift in vegetation from needle-leafed to broad-leafed trees and chaparral is a significant change, with consequences for the species of this region. Birds, mammals and other species that rely on acorns and oaks for food and habitat will find more of this type of habitat available, while species that depend on pine nuts and pine trees will find fewer resources. Increasing temperatures and the change to oak-dominated ecosystems means these areas will dry out more quickly due to both increased plant evaporative demand (Goulden and Bales, 2014) and earlier onset to the summer seasonal drought (see *Snow-water content and Snowmelt runoff* indicators). The vegetation transformation may also lead to more frequent wildfires (see *Wildfires* indicator). Moreover, the temperature of microenvironments will also be different, due to the differing amount of shade and the physical structure of the trees and shrubs making up the majority of the area.

The upslope retreat of conifers is a clear biological signal that conditions are changing. Since the snowpack of the Sierra Nevada is a vitally important resource for people, plants and animals, and the lower edge of the snowpack is also associated with the conifer belt, the upslope retreat of conifers may be a visible measure for monitoring what regions of the Sierra can still support a snowpack.

What factors influence this indicator?

The Sierra Nevada foothills have a Mediterranean climate that includes a summer seasonal drought, and the mixed conifer forests found higher upslope do not often occur in this zone. As temperatures warm, these drought-dominated conditions are moving upslope, as evidenced by the upslope movement of the freezeline. This change in the freezeline means that, should a rare winter storm drop snow in the yellow zone, it will likely melt within a few days, and not accumulate in a snowpack. In turn, this means that the countdown to summer drought conditions starts from the last precipitation event of the year, since there is no stored water in a snowpack to be released through melting. Therefore, summer drought conditions begin earlier, as also evidenced by the



advancing spring snow melt, which has been documented throughout the western United States (Stewart et al., 2005) and in the Sierra Nevada (see *Snowmelt runoff* indicator). The uphill retreat of the ponderosa pines in the Sierra Nevada roughly corresponds to the upward migration of the freezeline shown in Figure 2.

Vegetation changes occurring along elevation gradients are linked to changes in climate as well as many other factors such as species competition, topographic conditions, and land use (Macias-Fauria and Johnson, 2013). The discovery of tree seedlings recently established in alpine areas above the tree line suggests that those trees had found some suitable condition and moved upslope into the area. This phenomenon is a leading edge dynamic — that is, successful establishment of seedlings at the advancing edge of a species' range. An increase or decrease in the area of a vegetation type within its elevational limits is reflective of the population changes among the dominant plant species of that type. At the retreating, lower end of a species' range, as shown here, change is likely driven by mortality of adults, along with the inability of seedlings to survive under unfavorable conditions.

This rise in temperature and associated drying in the Sierra Nevada is not likely to kill adult ponderosa pine trees directly. This tree species is resistant to heat and drought, and a gradual warming may not kill the adult trees. However, if the seedling establishment conditions have changed enough, the sequence of events is likely to proceed as follows: 1) A disturbance occurs on a site; this can be a fire that kills the adult trees (fires are increasing throughout the western US (Westerling, 2016) and in California [see *Wildfires* indicator]), a logging clear cut or other land use change, or disturbances such as a bark beetle outbreak or a disease that affects the adult trees; 2) Subsequent to the adults being killed off, the seeds and seedlings are not able to survive long enough to allow a new stand of trees to establish. Seedlings may be susceptible to a number of causes of mortality: desiccation due to increased aridity; root competition for water by other species, particularly chaparral shrubs and non-native grasses; or increased fire frequency, which kills all the seedlings. Long-term vegetation plot studies corroborate the trend that this map analysis illustrates, by documenting an increase in seedling mortality in Sierra Nevada conifers (van Mantgem and Stephenson, 2007). The upslope retreat of ponderosa pine overlaps but is also slightly lower than the upslope movement of the freezeline, suggesting a lag time during which forest tree species are adjusting to the new climate conditions.

Technical Considerations

Data Characteristics

This indicator is based on a study that compared vegetation maps made in two time periods spanning 80 years: the Wieslander Vegetation Type Survey of the 1930s, and the California Department of Forestry and Fire Protection's 2015 landcover map (FRAP, 2015). The climate trend information depends on reconstructions of historical climate from weather stations in the study area. The climate data comparison uses 30-year averages of winter nighttime low temperature (1921-1950 for the historical period and 1986-2015 to represent the current time period). These temperature values are derived from the monthly Parameter-elevation Regressions on Independent Slopes Model



(PRISM) (Daly et al., 1997) 800-meter (m) data, downscaled to 270 m (Flint et al., 2013). The mean minimum monthly temperatures for December, January and February were combined to represent the winter quarter and the average of the 30 years used to track changes in winter freezing conditions.

The Wieslander Vegetation Type Mapping (VTM) project was a US Forest Service survey program that began in the late 1920s and ended in the early 1940s, and was meant to inventory the forests of California (Wieslander, 1935a; Wieslander, 1935b). Directed by Albert Wieslander, project surveyors would ascend to ridge lines and draw the patterns of the vegetation they observed on topographic maps, coding the polygons they drew with symbols representing the dominant species in each mapped unit. Maps were drawn for about half of the state, including most of the Sierra Nevada Mountains, the Coast Ranges from the San Francisco Bay Area to the Mexican border, and scattered quadrangles in the far northwest of the state. They also surveyed over 16,000 vegetation plots, took over 3,000 landscape photographs, and left notes associated with each quadrangle surveyed. University groups have digitized the survey (Kelly et al., 2005; Kelly et al., 2016): UC Berkeley digitized the photographs (<http://www.lib.berkeley.edu/BIOS/vtm/>) and the vegetation plots (<http://vtm.berkeley.edu/>); UC Davis digitized the vegetation maps (Thorne et al., 2006; Thorne and Le, 2016). The Sierra Nevada VTM maps used here were surveyed from 1934-1937, meaning that this dataset provides a potential for assessing change in vegetation over the past 80 years. The analysis presented here compares parts of the central and northern Sierra Nevada which were mapped in both time periods and comprise 25 30' quadrangles and 47,955 km² (11,849,939 acres; Figure 1).

The Wieslander maps were compared to a 2015 digital vegetation map. Because the level of spatial detail in each map was different, a 200-m grid was created for the study area. Vegetation types occupying the most area were identified within each grid cell (about 1,198,887 cells for this study), and assigned to that cell. Once the dominant vegetation from each time period was identified for each cell, those cells that had been listed as ponderosa pine forest but had become a non-conifer vegetation type, were identified, and the pattern of loss at the lower edge was revealed.

The VTM survey data are used in two other indicators in this report. In the *Subalpine forest density* indicator, vegetation plots were revisited to see how tree size and the composition of species of trees at a particular location have changed since the original VTM survey; and in the *Changes in forest and woodlands* indicator, plots from independent surveys were summarized to describe changes in forest structure and composition since the VTM survey.

Strengths and Limitations of the Data

Historical reconstructions, whether of climate or vegetation, are dependent on the quality of the data. In the case of the Wieslander maps, the historic maps upon which the vegetation was surveyed have spatial inaccuracies of up to ~300 m. Registration methods allow the historical base maps and digitized vegetation maps to be registered to contemporary topography with an average RMSE of 98 m. This permitted the



comparison between times at 200 m grid resolution. The Wieslander Vegetation Type Map survey was one of the most complete and thorough efforts to document the forests of California. The use of these data is a unique opportunity. The general trend is consistent across the entire western flank of the Sierra Nevada, which also lends credence to the findings.

Generally, the high elevation zones of the Sierra Nevada are the least well represented by weather stations that were used in generating the monthly climate maps. This study reports phenomenon more than two-thirds of the way down from the peaks of the Sierra, an area where there are more weather stations. Hence, while the historical climate maps of California as a whole may have some areas of high uncertainty, the region reported here was fairly well documented.

For more information, contact:



James Thorne
Department of Environmental Science and Policy
University of California Davis
2132 Wickson Hall, 1 Shields Avenue
Davis, CA 95616
(530) 752-4389
jhthorne@ucdavis.edu

References:

Daly C, Taylor G and Gibson W (1997). The PRISM approach to mapping precipitation and temperature. 10th Conference on Applied Climatology, American Meteorological Society. Reno, NV.

Flint LE, Flint AL, Thorne JH and Boynton R (2013). Fine-scale hydrologic modeling for regional landscape applications: the California Basin Characterization Model development and performance. *Ecological Processes* 2: 1–21.

FRAP (2015). California Department of Forestry and Fire Protection: Fire Resource and Assessment Program, "A raster representation of statewide vegetation". Retrieved February 2016, from http://frap.fire.ca.gov/data/frapgisdata-sw-fveg_download

Goulden ML and Bales RC (2014). Mountain runoff vulnerability to increased evapotranspiration with vegetation expansion. *Proceedings of the National Academy of Sciences*, 111(39): 14071-14075.

Kelly M, Allen-Diaz B and Kobzina N (2005). Digitization of a historic dataset: the Wieslander California Vegetation Type Mapping Project. *Madroño* 52(3): 191-201.

Kelly MK, Easterday G, Rapacciuolo MS, Koo P, McIntyre J, et al. (2016). Rescuing and sharing historic vegetation data for ecological analysis: the California Vegetation Type Mapping project. *Biodiversity Informatics* 11: 40-62.

Lenihan JM, Drapek R, Bachelet D and Neilson RP (2003). Climate change effects on vegetation distribution, carbon, and fire in California. *Ecological Applications* 13(6): 1667-1687.

Macias-Fauria M and Johnson EA (2013). Warming-induced upslope advance of subalpine forest is severely limited by geomorphic processes. *Proceedings of the National Academy of Sciences* 110: 8117-8122.



Stewart IT, Cayan DR and Dettinger MD (2005). Changes toward earlier streamflow timing across western North America. *Journal of Climate* **18**(8): 1136-1155.

Thorne JH, Boynton RM, Flint LE and Flint AL (2015). Comparing historic and future climate and hydrology for California's watersheds using the Basin Characterization Model. *Ecosphere* **6**(2).

Thorne J, Kelsey TR, Honig J and Morgan B (2006). *The development of 70-year old Wieslander Vegetation Type Maps and an assessment of landscape change in the central Sierra Nevada* (CEC-500-2006-107). California Energy Commission. Available at <http://www.energy.ca.gov/2006publications/CEC-500-2006-107/CEC-500-2006-107.PDF>

Thorne JH, Morgan BJ, and Kennedy JA (2008, updated 2017). Vegetation change over 60 years in the central Sierra Nevada. *Madroño* **55**:223-237.

Thorne JH and Le TN (2016). California's historic legacy for landscape change, the Wieslander Vegetation Type Maps. *Madroño* **63**: 293-328.

van Mantgem PJ and Stephenson N (2007). Apparent climatically induced increase of tree mortality rates in a temperate forest. *Ecology Letters* **10**(10): 909-916.

Westerling AL (2016). Increasing western US forest wildfire activity: sensitivity to changes in the timing of spring. *Philosophical Transactions of the Royal Society B*, **371**: 20150178.

Westerling AL, Hidalgo HG, Cayan DR and Swetnam TW (2006). Warming and earlier spring increase western U.S. Forest wildfire activity. *Science* **313**(5789): 940-943.

Wieslander AE (1935a). First Steps of the Forest Survey in California. *Journal of Forestry* **33**(10): 877-884.

Wieslander AE (1935b). A vegetation type map for California. *Madroño* **3**: 140-144.



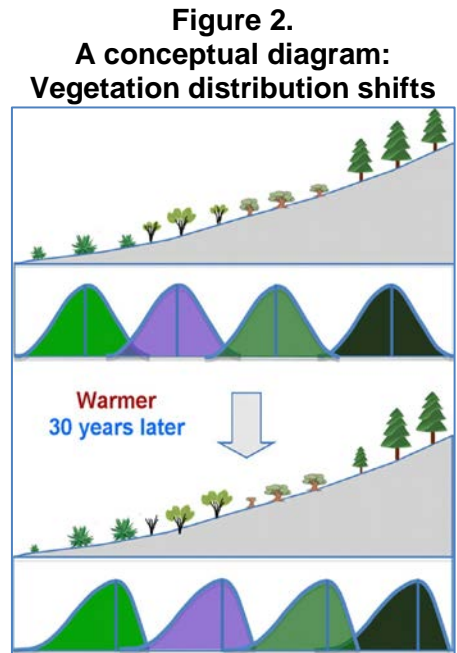
VEGETATION DISTRIBUTION SHIFTS (NO UPDATE)

The distribution of vegetation across the north slope of Deep Canyon in the Santa Rosa Mountains has moved upward 213 feet in the past 30 years.

Figure 1. Change in mean elevation* of plant species in the Deep Canyon Transect

Common Name	Mean elevation, m		Change
	1977	2006-2007	
White Fir	2,421	2,518	96
Jeffrey Pine	2,240	2,267	28
Canyon Live Oak	1,987	2,033	47
Sugar Bush	1,457	1,518	61
Desert Ceanothus	1,602	1,671	70
Muller's Scrub Oak	1,485	1,522	37
Creosote Bush	317	459	142
Burrobush	630	748	118
Brittlebush	574	674	100
Desert Agave	693	643	-50
Mean change in elevation		65 m (213 ft)	
95% confidence interval		34 m (112 ft)	

* Change in cover-weighted mean elevation of ten most widely distributed species in the Deep Canyon Transect



Source: Breshears et al., 2008

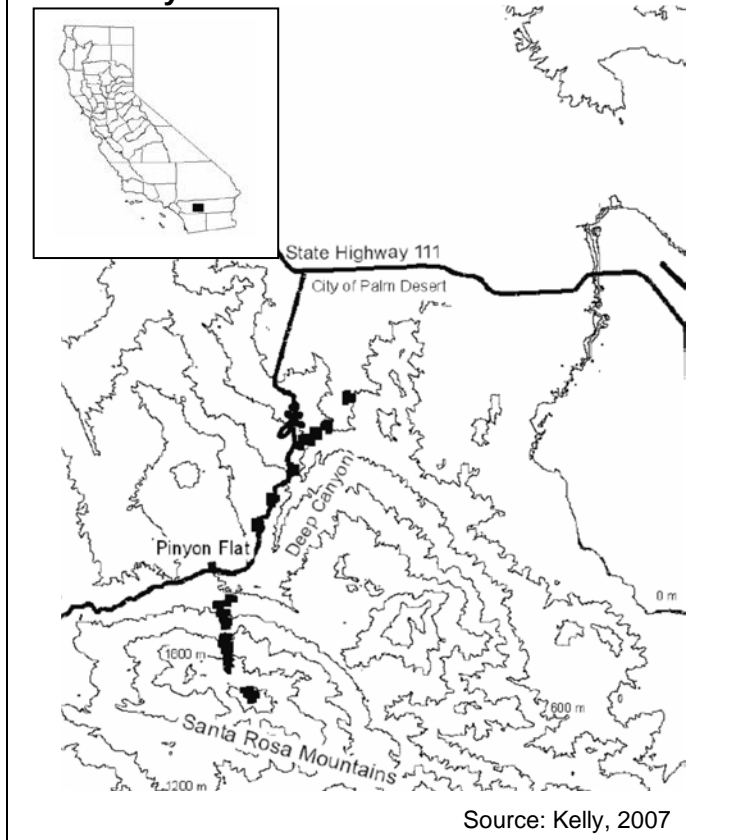
What does the indicator show?

The mean elevation of nine of the ten dominant plant species in the Deep Canyon Transect of Southern California's Santa Rosa Mountains (see map, Figure 3) have moved upslope in the past 30 years (Kelly and Goulden, 2008). A comparison of two vegetation surveys of plant cover — one in 1977 and the other in 2006-2007 — along an 8,400-foot elevation gradient found that the average elevation of the dominant species rose by 65 meters (213 feet) between the surveys. All vegetation types moved upward, including small desert shrubs, chaparral, Canyon oak, and large conifers.

Although the species distribution moved upslope, the upper and lower range limits of these species have not changed. At the lower half of the species' ranges, individual plants have pruned limbs or completely died, reducing their dominance. An increase in cover was observed at the upper half of the species' ranges, where mature plants have reproduced and grown in size, increasing their dominance.



Figure 3. The sites of the Deep Canyon surveys and their location in California



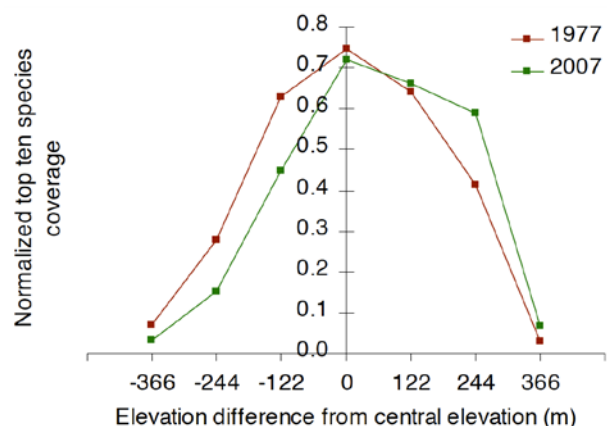
The conceptual diagram above illustrates these changes. Vegetation species along the mountain slope were distributed in a bell curve along the slope in 1977, with the highest abundances at the middle of each species' range. After 30 years of warming and drought, vegetation experienced die-off at the lower edges of each species' range, while plants at the cooler, wetter, upper elevations increased in dominance.

Vegetation distribution changes at Deep Canyon can be compared to the conceptual diagram using the graph in Figure 4. A detailed discussion of the derivation of the metrics presented is beyond the scope of this narrative (see Kelly and Goulden, 2008 for details).

In simple terms, Figure 4 shows plant coverage (which represents the percent of ground surface covered by vegetation) plotted against elevation, with "0" representing the "center elevation" (the midpoint of the lowest and highest elevations where each species was found.) (The y-axis of the graph shows "normalized" coverage, derived by dividing each species' coverage at each elevation in 2007 by its maximum coverage at any elevation in 1977 and averaging across the ten dominant species.)

Figure 4 shows that the ten dominant species in the survey area had a symmetric normalized distribution in 1977. This changed to an upwardly skewed distribution in 2007. From 1977 to 2007, cover declined in the lower parts of the species' original ranges (by a median of 46 percent) and increased in the upper parts of the original ranges (by 12 percent).

Figure 4. Vegetation distribution, ten dominant species at Deep Canyon



Source: Kelly and Goulden, 2008



Why is this indicator important?

Plant ranges are limited by environmental conditions. On a mountain slope, the climate of the lower extent of a species' range experiences warmer and drier conditions, while the upper extent of a species' range is cooler and wetter. Climate warming or drought is expected to increase stress on plants at lower elevations, pushing them upward into the cooler, wetter climates higher on the slope. Recent climate warming and drying has been found to be pushing conifers upslope across the Southwestern United States by killing the trees at the lower, warmer, drier edges of their ranges (Allen and Breshears, 1998; McDowell et al., 2010).

The climate and vegetation gradient of Deep Canyon's slopes is analogous to the south-to-north gradient of California. Deep Canyon's climate ranges from hot desert at the mountain base, stretching upward through warm chaparral, and finally into mild conifer forests at the mountain peak. This vegetation and climate gradient is similar to the transition along the state of California, from the southern deserts, northward through chaparral-covered foothills and mountains, and into the mild evergreen forests of northern California. Understanding the effects of local climate change on Deep Canyon's vegetation gradient will help to predict how California's vegetation will respond to a warmer or drier climate.

This indicator is consistent with biological range shifts seen around the globe (Chen et al., 2011). Plant, bird, mammal, and insect ranges are retreating away from the equator and up mountain slopes, generally tracking the temperature changes observed within each species' range. There is major uncertainty surrounding any individual species' ability to migrate in response to climate change. In Deep Canyon, no species were found outside their historic range. If species are not able to establish in new locations, this study might be revealing the beginning of a local extinction of each species and local ecosystem collapse.

What factors influence this indicator?

The climate of Deep Canyon has become warmer and drier in the past 30 years. Temperatures have increased 1.1 °F from 1977 to 2007, and droughts have intensified. The combination of warming and drying has effectively moved the climate zones of Deep Canyon upslope about 200 feet, similar to the amount the vegetation has shifted upslope.

The change in plant distribution observed in Deep Canyon may be attributed in part to a severe drought from 1999 to 2002. This drought caused marked vegetation mortality throughout Southern California, directly through drought stress and indirectly through insect attack, and many recently dead plants were observed during the survey. However, recent mortality alone cannot explain the elevation shifts. Many plants that had died before the 1999–2002 drought were also noted, as well as an increase in cover in the upper half of the species' ranges. These trends indicate that warming and/or drying of climate has been stressing the lower elevation plants and providing more favorable conditions for plants at higher elevations over the 30-year period. These



changes are consistent with predictions of the effects of climate warming and drought on mountain ecosystems.

Four considerations provide evidence that the observed vegetation redistribution is attributable to climate:

- Vegetation shifts were uniform across elevation, implying that the ultimate causal factor was uniformly distributed. Recent climatic trends in Southern California do not appear to vary strongly with elevation.
- The vegetation shifts are consistent with the expected bioclimatic effects of most of the observed climatic shifts. Increased temperature, longer frost-free period, increased elevation of the snow line, and occurrence of severe drought should increase plant stress in some years. This increased stress would be expected to decrease a species' ability to survive in the drier, warmer, lower parts of its range and increase its ability to survive in the wetter, cooler, upper parts of its range.
- The change from a symmetrical vegetation distribution to an upwardly skewed distribution (see Figure 4), when averaged across species and elevation, can be interpreted as a sign of the impact of climate change on vegetation distribution.
- The vegetation shifts resulted in part from mortality during the 1987–1990 and 1999–2002 droughts. The connection between mortality and drought is consistent with a fingerprint of climate change.

Two alternative explanations for the vegetation redistribution, changes in fire frequency or air pollution, merit consideration. The wildfire regime in Southern California has changed over the last century, resulting in plant demographic shifts, especially in montane forest. However, the fire regime in Deep Canyon is similar to its historical norm, and fire effects would not produce uniform changes across the elevation gradient. Schwilk and Keeley (2012) claim that the upslope redistribution of one species in Deep Canyon, *Ceanothus greggii*, was due to elevational differences in historic fires and not by climate warming. However, observations of postfire recovery of *C. greggii* outlined in Zammit and Zedler (1993) support the conclusion that an influence stronger than fire history is redistributing Deep Canyon's dominant species upwards. Air pollution as an explanation is similarly problematic: ozone-related mortality is concentrated only at higher elevations, and would not produce the uniform changes that were observed across the elevation gradient.

The upward movement of the dominant species at Deep Canyon in just 30 years can also be attributed to recent changes in the local climate. The establishment of species at locations well above their previous ranges appears to have been minimal, and the observed upslope movement is a result of shifting dominance within existing communities, rather than the expansion of ranges to new elevations. The climate factor most influential on species redistribution could not be determined. In fact, the various observed climatic changes may interact and reinforce each other; climate warming



coupled with increasing climate variability intensifies the effects of extreme yet unexceptional droughts.

The local changes could be caused by regional urban heat island effects or long-term climate fluctuations, such as the Pacific Decadal Oscillation. Nonetheless, the climate changes observed are similar to climate changes that have been predicted with or attributed to greenhouse gas-forced global climate change. The study results imply that surprisingly rapid shifts in the distribution of plants can be expected with climate change, at least in areas where seed dispersal is not a major constraint, and that global climate change may already be influencing the distribution of vegetation.

Additionally, the exact mechanisms of the plant mortality are unknown. How a tree dies in response to drought is a surprisingly difficult question that the scientific community continues to discuss (Waring, 1987; Breshears et al., 2009; van Mantgem et al., 2009). Drought and warming have caused forest mortality worldwide and no other plausible explanation for the vegetation shifts were observed.

Technical Considerations

Data Characteristics

This indicator is based on a re-survey of an initial vegetation study conducted in 1977 (Zabriskie, 1979). Zabriskie's survey consisted of 22 belt-transect surveys 400 yards long, at 400' elevation intervals, from 0' to 8400' elevation along the north face of the Santa Rosa Mountains. These surveys counted live perennial vegetation crossing the 400-yard transect and noted species and coverage amount.

The exact location of Zabriskie's original surveys is lost. The study investigators were able to relocate the surveys within 10-20 yards of the original location using the original selection criteria: north-facing slopes, with transects centered on north-facing ridgelines and following the 400' interval isocontour. Jan Zabriskie also toured the sites with the investigators to explain his original sampling strategy and point out original locations.

Strengths and Limitations of the Data

A common problem in revisiting historic studies is finding the exact location of the original sites. Discussion with Zabriskie, original maps, careful and consistent site location criteria, and a relatively small geographic area, provide confidence in the investigators' accuracy in relocating the original survey sites. Location inaccuracy is the largest source of uncertainty in the data. The vegetation coverage methodology was identical to Zabriskie's and could result in biases of less than a few percent per transect. Year-to-year fluctuations could be a problem in extrapolating one survey to a 30-year trend. A major strength of this survey is that the species evaluated in this survey are generally long-lived, thus the vegetation changes observed are the result of long-term trends and not short-term variability. Species in the survey such as yucca, white fir, creosote, and California lilac have lifespans of decades to centuries, and thus high mortality rates within 30 years are considered significant changes. Finally, weather station data do not come from within the survey site; the climate data come from nearby stations around the Southern California desert mountains.



For more information, contact:



Anne E. Kelly
Department of Earth System Science
Croul Hall
University of California
Irvine, CA 92697
(949) 824-9273
a.kelly@uci.edu

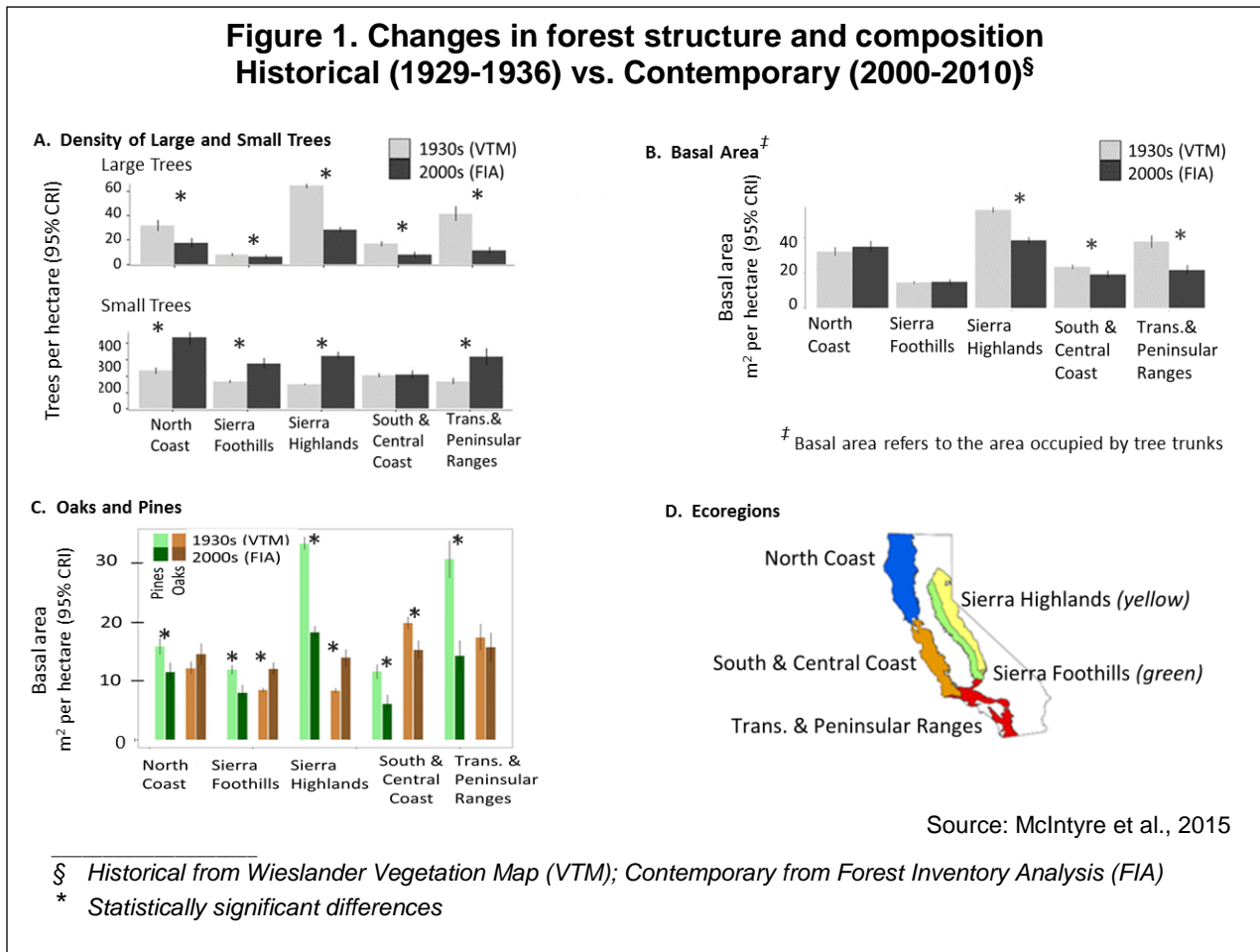
References:

- Breshears DD (1998). Drought-induced shift of a forest–woodland ecotone: Rapid landscape response to climate variation. *Proceedings of the National Academy of Sciences* **95**(25): 14839-14842.
- Breshears DD, Huxman TE, Adams HD, Zou CB, and Davison JE (2008). Vegetation synchronously leans upslope as climate warms. *Proceedings of the National Academy of Sciences* **105**(33): 11591-11592.
- Breshears DD, Myers OB, Meyer CW, Barnes FJ, Zou CB, et al. (2009). Tree die-off in response to global-change-type drought: Mortality insights from a decade of plant water potential measurements. *Ecology and the Environment* **7**(4): 185-189.
- Chen I-C, Hill JK, Ohlemüller R, Roy DB and Thomas CD (2011). Rapid range shifts of species associated with high levels of climate warming. *Science* **333**(6045): 1024-1026.
- Kelly AE (2007). “Shifts in the deep canyon ecotone. 1977-2007”. California State University, Los Angeles. Master of Science.
- Kelly AE and Goulden ML (2008). Rapid shifts in plant distribution with recent climate change. *Proceedings of the National Academy of Sciences* **105**(33): 11823-11826.
- McDowell NG, Allen CD and Marshall L (2010). Growth, carbon-isotope discrimination, and drought-associated mortality across a *Pinus ponderosa* elevational transect. *Global Change Biology* **16**(1): 399-415.
- Schwilk, D.W. and J.E. Keeley (2012) A plant distribution shift: temperature, drought, or past disturbance? *PLoS ONE* **7**(2):e31173.
- van Mantgem PJ, Stephenson NL, Byrne JC, Daniels LD, Franklin JF, Fulé PZ, et al. (2009). Widespread increase of tree mortality rates in the western United States. *Science* **323**(5913): 521-524.
- Waring RH (1987). Characteristics of trees predisposed to die. *Bioscience* **37**(8): 569-574.
- Zabriskie JG (1979). *Plants of Deep Canyon and the Central Coachella Valley, California*. (1st ed.). Riverside, CA: Philip L. Boyd Deep Canyon Desert Research Center, University of California.
- Zammit CA and Zedler PH (1993). Size structure and seed production in even-aged populations of *Ceanothus greggii* in mixed chaparral. *Journal of Ecology* **81**(3): 499-511.



CHANGES IN FORESTS AND WOODLANDS

Compared to 80 years ago, California's forests today have more small trees, fewer large trees, and less biomass. The areas occupied by pines have decreased in all regions studied, while the areas occupied by oaks have increased in the Sierra Nevada but have decreased in the South and Central Coast. These changes are associated with decreased water availability driven by warmer temperatures.



What does this indicator show?

The structure and composition of California's forests have changed, and this is associated with climate change related water availability. This indicator consists of three metrics tracking changes in the structure and composition of forests across five regions in California. These metrics are based on a comparison of data from a 1930s survey of the state's vegetation (documented in the Wieslander Vegetation Type Map, or VTM) with data from surveys conducted between 2000 to 2010 (as part of the US Forest Service's Forest Inventory Analysis, or FIA) (McIntyre et al., 2015). Forest structure refers to the distribution of small, medium, and large-sized trees, while species composition refers to the diversity of tree species present.

Figure 1A displays the first metric, which shows changes in the density of large and small trees. Large trees are defined as greater than (>) 61 centimeters (cm), or



>24 inches (in), in diameter at a height of 4.5 feet (“diameter at breast height,” or dbh), and small trees are defined as 10-30 cm, or 4-12 in, dbh. Decreases in large tree density were observed in all regions studied (top row). The greatest decrease occurred in the Transverse and Peninsular ranges of Southern California, where large tree density in the contemporary period was less than 30 percent of the density in the historical dataset (40.8 vs. 10.6 trees per hectare (trees/ha)). Declines of about 50 percent in large tree densities were observed in the Sierra Nevada highlands (64.3 vs. 28.03 trees/ha), the Coast Ranges of southern and central California (16.6 vs. 7.5 trees/ha), and northern California (30.6 vs. 16.7 trees/ha). Declines in large trees were lowest in the Sierra Nevada foothills (7.6 vs. 5.7 trees/ha), the region where large tree densities are lowest.

From the historical to the contemporary period, densities of small trees increased over two-fold within the Sierra Nevada highlands (149 vs. 315 trees/ha), and over 50 percent in the Sierra Nevada foothills (165 vs. 268 trees/ha), the North Coast region (229 vs. 412 trees/ha) and the Transverse and Peninsular ranges (165 vs. 301 trees/ha) (Figure 1, bottom row). The density of small trees was unchanged in the South and Central Coast Region (200 vs. 197 trees/ha). Patterns of change for intermediate-sized trees (31–60 cm or 12-24 in dbh) were variable across the two time periods (not shown).

Figure 1B illustrates the second metric, which shows changes in basal area — the amount of area occupied by tree trunks within a given area (here expressed in units square meters per hectare (m²/ha)). Basal area, which reflects biomass, decreased in three of the five regions: up to 40 percent in the Transverse and Peninsular Ranges Region (37.8 vs. 21.6 m²/ha, 30 percent in the Sierra Nevada Highlands Region (55.9 vs. 38.5 m²/ha), and 18 percent in the South and Central Coast Region (23.3 vs. 19.0 m²/ha). In the North Coast and Sierra Nevada Foothills Regions, the reductions in basal area due to large tree declines were balanced by increases in smaller size classes, hence no decline in overall basal area was observed.

The third metric is displayed in Figure 1C, which compares historical and contemporary basal area occupied by pines and oaks. Changes in the relative abundance of these tree species represent changes in forest composition. Pines have declined in all regions, whereas oaks increased in two Sierra Nevada regions but decreased in the South and Central Coastal ranges.

Why is this indicator important?

The pine and oak-dominated forests and woodlands of California provide ecosystem benefits such as erosion control, water provision and carbon sequestration, as well as wildlife habitat, timber, and opportunities for recreation. Changes in forest structure and tree species composition can impact these functions.

This indicator describes how forest conditions have changed relative to historical climate change by comparing the 80-year old VTM survey with modern-day observations. It shows that the state’s forests are transitioning from one set of species



to another. Since these changes may be a natural ecosystem response to warming and drying conditions, monitoring them provides valuable insight into future forest responses to climate change. There is evidence that wildfires at elevations up to about 5,000 feet where pines and oaks grow together can initiate this shift in species dominance by removing the dominant conifers (including pines but also other needle-leafed trees), allowing resident oaks and chaparral to establish and become the dominant vegetation. Another VTM-based study estimates that 13.5 million acres in California are at risk of this conversion (Goforth and Minnich, 2008). Decreases in large coniferous trees, including pines and firs in California montane (mountainous) forests have also been documented in other studies (van Mantgem and Stephenson, 2007; Dolanc et al., 2013; Lutz et al., 2009); furthermore, dieback of trees has been reported on all continents (Allen et al., 2015) and across the western USA (van Mantgem et al., 2009).

Despite a nearly 40 percent overall increase in tree density, the decline in large trees has resulted in about a 20 percent decline in basal area and associated biomass (not shown).

What factors influence this indicator?

Statewide, the decline in large trees and increases in the relative abundance of oaks compared to pines are associated with climatic water deficit (CWD), while changes in small tree densities are not (McIntyre et al, 2015). CWD is the cumulative annual excess of potential versus actual evapotranspiration of water from plants. It can be thought of as the amount of additional water that would have evaporated or been transpired by plants (beyond what was actually evaporated or transpired) if the water had been present in the soils for the plants to take up. CWD is a useful metric because it integrates plant water demand relative to soil moisture availability, and provides a measure of potential plant drought stress. Increases in CWD, which reflect decreases in soil moisture, are associated with a warming climate because increased air temperatures increase plant water demand (Thorne et al., 2015). CWD can be further increased if there is less precipitation under future conditions, and if snowpack melts sooner, leading to drier soils during summer months. CWD has been associated with patterns of forest mortality and vegetation distributions in a number of studies. Following four years of severe drought (2012-2015) in California, areas with high CWD experienced substantially more tree mortality than areas with low CWD (Young et al., 2017). Much of the mortality was caused by beetle attacks on trees weakened by the drought (see *Forest tree mortality* indicator).

The ratio of oak to pine basal area was correlated with estimates of CWD in the time periods of both forest surveys (McIntyre et al., 2015). In addition, the contemporary survey shows an increased relative dominance by oaks that was associated with increases in CWD. The paleological record is consistent with this: in the past 150,000 years, oaks dominated in warmer, drier interglacial periods, and pines in colder, more mesic (characterized by moderate or well-balanced supply of moisture) glacial periods (Heusser, 1992).



The changes in forest species composition and basal area described here are occurring in California forest and woodland areas at elevations that are subject to seasonal drought; these areas represent water-limited ecosystems throughout the low to mid-elevations of the state, from the southern coastal and transverse mountains to near the northern end of the foothills of the Sierra Nevada Mountains. Although there are several potential causes for these dynamics at lower elevations, hotter drought conditions are the lead environmental cause.

That conifer trees are potentially at higher climatic risk than broadleaf trees is supported by the findings of Lutz et al. (2010). The authors mapped the climate occupied by 17 Sierra Nevada tree species in Yosemite National Park relative to the entire range of climate conditions each species encounters in its geographic range. They found seven species, all except one of which is a conifer, occupy the arid end of their North American climate distributions: *Pseudotsuga menziesii*, *Pinus ponderosa*, *Calocedrus decurrens*, *Pinus lambertiana*, *Abies concolor*, *Abies magnifica*, and *Quercus kelloggii*.

Other factors potentially contributing to shifts in the oak: pine ratio include fire suppression, wildfires, and logging practices. Widespread fire suppression in the western USA has led to the buildup of forest litter and increased density of small trees, including the establishment of the highly flammable white fir (*Abies concolor*) — changes which have potentially contributed to the more frequent and larger wildfires today. Further, a warming climate is contributing to the increasing frequency and intensity of wildfires in the western US (Westerling et al., 2006) (see *Wildfires* indicator).

As noted above, wildfires can initiate the conversion of coniferous to broadleaf forests and woodlands or chaparral by removing dominant conifers. A large stand-replacing fire at Cuyamaca Rancho State Park near San Diego (the Cedar fire, October 24-28, 2003) happened after eight decades of fire suppression. A seedling census four years after the fire found that while various oak species had re-established, few to no conifer seedlings had done so, resulting in the conversion of a mixed conifer-oak forest to one dominated principally by oaks (Goforth and Minnich, 2008). The authors did not examine changes in climatic conditions. The authors predict this transition is to be expected for the ~13.6 million acres of this forest type in California, including large swaths of the Sierra Nevada foothills and most of the forests and woodlands near coastal urban areas. This prediction is also in line with change documented on the western slope of the Sierra Nevada Mountains where lower elevations of coniferous forests are retracting upslope (Thorne et al., 2008; see *Ponderosa pine forest retreat* indicator). This is corroborated by a recent study that examined post-fire seedling regeneration after 14 large wildfires in Northern California. Welch et al. (2016) found that in 10 of the 14 fires, conifer regeneration was not high enough to meet US Forest Service stocking standards, indicative of a return of the site to a conifer forest.

Technical Considerations

Data characteristics

The indicator is based on a study comparing forested plots from the Wieslander Vegetation Type Map (VTM) survey (between 1929 and 1936) with US Forest Service



Forest Inventory Analysis (FIA) plots (between 2000 and 2010). Across California, 9,388 VTM plots and 5,198 FIA plots were identified as forested (having at least one tree >10.2 cm dbh, the cutoff for a tree in the VTM data). Only plots occurring within 5 km of a plot from the other time period were selected, resulting in 6,572 VTM and 1,909 FIA focal plots. The plots were similar in slope, aspect, and elevation, as well as location across latitudinal and longitudinal gradients.

A modified version of the Jepson Manual eco-regions of California was used in identifying plots by region, as follows: South and Central Coast; Transverse and Peninsular Ranges; North Coast; Foothills of the Sierra Nevada and southern Cascades; Highlands of the Sierra Nevada and southern Cascades. (The Central Valley and desert regions are not included because they did not have a sufficient number of forested plots). Changes in tree density were compared with changes in CWD between 1910–1940 and 1981–2010 using 30-year averages from each time period. CWD is the seasonally integrated excess in potential evapotranspiration (PET) versus actual evapotranspiration. Details on the methodology are described in McIntyre et al. (2015).

Strengths and limitations of the data

Historical reconstructions, whether of climate or vegetation, are dependent on the quality of the data. In the case of the 1930s historical vegetation survey, the plot areas surveyed were not permanently marked, and this comparison used contemporary US Forest Service plots to compare densities of trees in similar locations as paired plots that had similar slope, aspect and elevation. The VTM survey only classed trees to size classes, so the modern survey, which has actual diameter at breast height values for every tree was re-classed to the same size classes. This reduced some of the precision with regards to tree size. However, the historical VTM was one of the most complete and thorough efforts to document the forests of California, and the use of these data was a unique opportunity to examine shifts statewide.

For more information, contact:



Patrick J. McIntyre
NatureServe
1680 38th St., Suite 120
Boulder, CO 80301
(703) 797-4812
Patrick_McIntyre@natureserve.org



James Thorne
Department of Environmental Science and Policy
University of California Davis
2132 Wickson Hall, 1 Shields Avenue
Davis, CA 95616
(530) 752-4389
jhthorne@ucdavis.edu



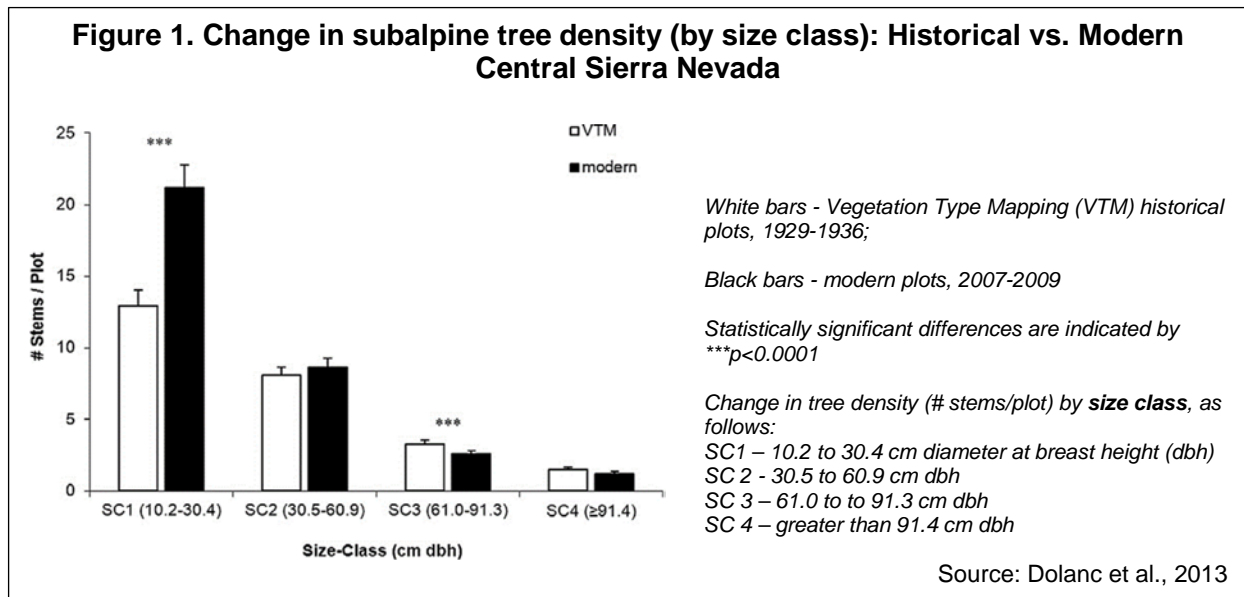
References:

- Allen CD, Breshears DD, and McDowell NG (2015). On underestimation of global vulnerability to tree mortality and forest die-off from hotter drought in the Anthropocene. *Ecosphere* **6**(8): 129.
- Dolanc CR, Thorne JH, and Safford HD (2013). Widespread shifts in the demographic structure of subalpine conifer forests over last 80 years in the central Sierra Nevada. *Global Ecology and Biogeography* **22**: 264–276.
- Goforth BR and Minnich RA (2008). Densification, stand-replacement wildfire, and extirpation of mixed conifer forest in Cuyamaca Rancho State Park, southern California. *Forest Ecology and Management* **256**: 36-45.
- Heusser LE (1992). Pollen stratigraphy and paleoecologic interpretation of the 160-ky record from Santa Barbara Basin, Hole 893A1. Proceedings of the Ocean Drilling Program, *Scientific Results* **146**(2): 265-279.
- Lutz JA, Van Wagtendonk JW, and Franklin JF (2009). Twentieth-century decline of large-diameter trees in Yosemite National Park, California USA. *Forest Ecology and Management* **257**:2296–2307.
- Lutz JA, van Wagtendonk JW, and Franklin JF (2010). Climatic water deficit, tree species ranges, and climate change in Yosemite National Park. *Journal of Biogeography* **37**: 936-950.
- McIntyre P, Thorne JH, Dolanc CR, Flint A, Flint L, et al. (2015). Twentieth century shifts in forest structure in California: denser forests, smaller trees, and increased dominance of oaks. *Proceedings of the National Academy of Sciences* **112**: 1458–1463.
- Thorne JH, Morgan BJ, and Kennedy JA (2008). Vegetation change over 60 years in the central Sierra Nevada. *Madroño* **55**: 223-237.
- Thorne JH. and Le TN (2016). California's Historic Legacy for Landscape Change, the Wieslander Vegetation Type Maps. *Madroño* **63**(4): 293-328. VTM website available at <http://vtm.berkeley.edu/#/about/>
- Thorne JH, Boynton RM, Flint LE, and Flint AL (2015). Comparing historic and future climate and hydrology for California's watersheds using the Basin Characterization Model. *Ecosphere* **6**(2).
- van Mantgem PJ and Stephenson N (2007). Apparent climatically induced increase of tree mortality rates in a temperate forest. *Ecology Letters* **10**(10): 909-916.
- van Mantgem PJ, Stephenson NL, Byrne JC, Daniels LD, Franklin JF, et al. (2009). Widespread increase of tree mortality rates in the western United States. *Science* **323**: 521-524.
- Wright DH, Nguyen CV, and Anderson S (2016). Upward shifts in recruitment of high-elevation tree species in the northern Sierra Nevada, California. *California Fish and Game* **102**: 17-31.
- Welch KR, Safford HD, and Young TP (2016). Predicting conifer establishment post wildfire in mixed conifer forests of the North American Mediterranean-climate zone. *Ecosphere* **7**(12): e01609.
- Westerling AL, Hidalgo HG, Cayan DR, and Swetnam TW (2006). Warming and earlier spring increase western U.S. Forest wildfire activity. *Science* **313**(5789): 940-943.
- Young DJN, Stevens JT, Mason Earles J, Moore J, Ellis A, et al. (2017) Long-term climate and competition explain forest mortality patterns under extreme drought. *Ecology Letters* **20**: 78-86.



SUBALPINE FOREST DENSITY

Subalpine forests in the Sierra Nevada have more small trees and fewer large trees than they did in the early decades of the 20th century.



What does the indicator show?

Figure 1 shows an increase in the density of small trees (measured as the number of stems in each plot) in higher-elevation (subalpine) forests in the central Sierra Nevada since the 1930s. The figure compares the densities of trees by size class in historical plots (based on Vegetation Type Mapping (VMT) data collected between 1929 and 1936), with modern-day plots (based on resampling data between 2007 and 2009).

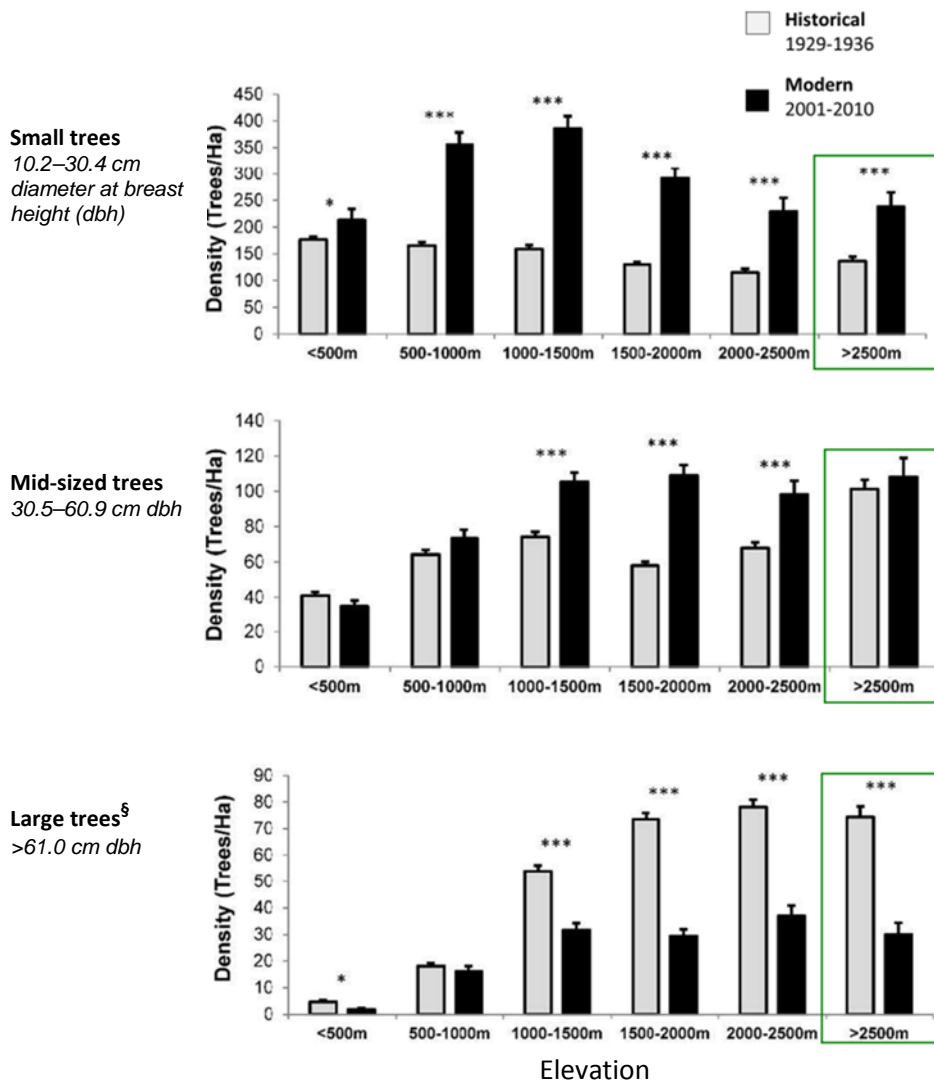
There are now many more small trees (categorized as SC1, with diameters measuring 10.2 to 30.4 centimeters (cm) (4 to 12 inches) at a height of 1.4 meters (4.5 feet) – a measurement referred to as “diameter at breast height,” or dbh. Also, there are fewer large trees (those categorized as SC3 and SC4, exceeding 61 cm (24”) dbh). Thus, in the subalpine zone, the density of small trees increased by 62 percent while large tree densities decreased by 21 percent — a net increase of 30 percent more trees present today than in the 1930s. These shifts are ubiquitous throughout the subalpine zone (2300 to 3400 meters (m) or approximately 7,500 to 11,000 feet elevation) of the central Sierra Nevada (see map, Figure 3); further, the shifts occurred to a surprisingly consistent degree for the eight most common tree species native to this zone.

Figure 2 shows that declines in the density of large trees and increases in the density of small trees also occurred at lower elevations. These findings are from a more recent study by Dolanc et al. (2014a), which compared contemporary Forest Inventory Analysis (FIA) forest survey plots to the historical VMT data across a larger area that spans a broader range of elevations in the north and central Sierra Nevada. At subalpine elevations (>2500 m), the increases in small trees and the decrease in large trees recorded in this study are similar to those found in the first study (Figure 1; Dolanc



et al., 2013). The similarity between the two studies provides further evidence of widespread and prevalent changes in the Sierra Nevada forest structure.

Figure 2. Change in tree density by elevation* and size class: Historical vs. Modern, North and Central Sierra Nevada



Gray bars - Vegetation Type Mapping (VTM) historical plots, 1929-1936
Black bars - Forest Inventory and Analysis (FIA) modern plots, 2001-2010
 The last set of bars (outlined in green) show changes at the subalpine elevation (>2500m)
 Statistically significant differences are indicated by * $p < 0.05$, ** $p < 0.001$, and *** $p < 0.0001$

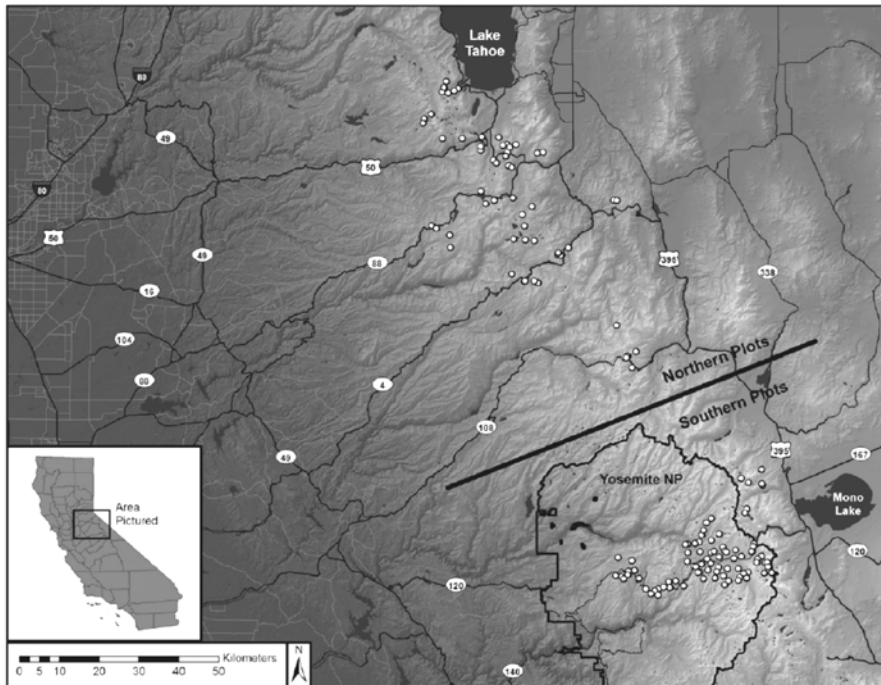
[§]“Large trees” in this figure are classified as “SC3” and “SC4” in Figure 1.

Source: Dolanc et al., 2014a

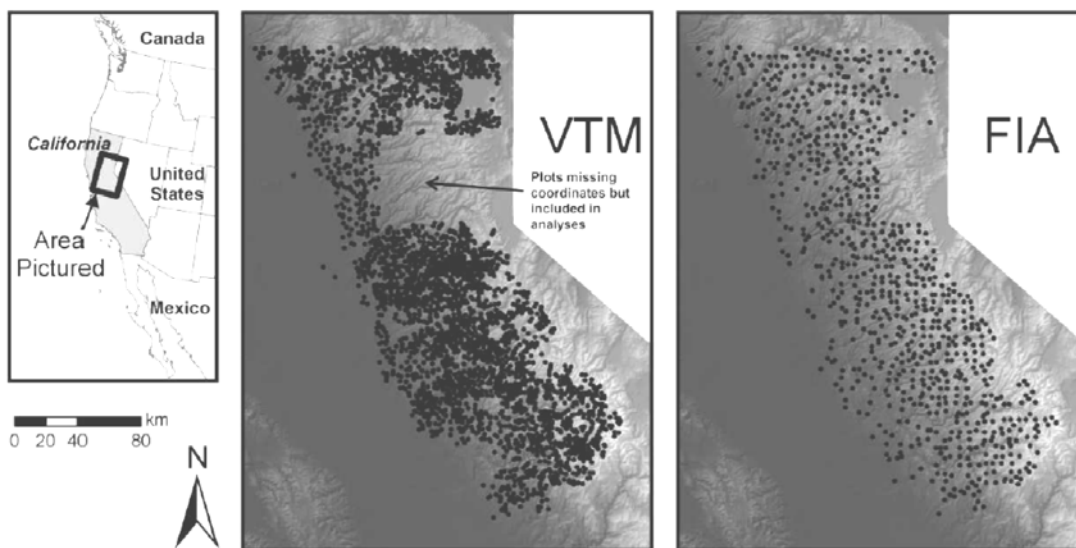


Figure 3. Maps showing Sierra Nevada study areas

A. Central Sierra Nevada study area for Figure 1 (circles show survey plots)



B. Northern and Central Sierra Nevada study area for Figure 2 (dots show study plots; arrow points to VTM plots with missing coordinates but for which elevation and tree data are available; these are included in analyses)



Sources: (A) Dolanc et al, 2013;
(B) Dolanc et al., 2014a

Why is this indicator important?

Shifts in forest structure could have detrimental effects on the ecology of the Sierra Nevada. Compared to small trees, large trees store considerable amounts of carbon, provide soil nutrients, provide nests and shelters, and play critical roles in hydrological



regimes. Younger and smaller trees cannot provide these functions to the same extent as large trees, if at all (Lindenmayer et al., 2012).

In addition, increased tree density from small trees provides more fuel for larger and more frequent fires. Though much of California's vegetation is adapted to frequent fire, fire in the subalpine zone has historically been infrequent and isolated (van Wagtenonk and Fites-Kaufman, 2006). Recently, however, wildfires have been documented to be increasing in elevation in the Sierra Nevada (Schwartz et al., 2015). Subalpine forests have historically been sparse, with insufficient accumulation of dead, woody residue on the forest floor to act as fuel to carry a fire very far. However, an increasing number of smaller trees will naturally lead to increased fuel and could ultimately lead to larger and more frequent fires. Since most species native to subalpine regions are not adapted to fire, this has the potential to shift dominance at these elevations toward lower-elevation, fire-adapted species, effectively accelerating an upward shift of ecological zones.

Densification of forests and warming temperatures could also make conditions more favorable for insect outbreaks and disease. Beetle infestations have caused widespread mortality in high-elevation forests in the Pacific Northwest and Rocky Mountain regions, including two species present in Sierran subalpine, lodgepole and whitebark pine. These infestations were linked to changing climate and forest conditions that are conducive to the beetle's life cycle (Kurz et al., 2008). Increased density of Sierran subalpine forests and warming temperatures are expected to lead to increased tree mortality and conditions ripe for outbreaks in the Sierra Nevada. Such outbreaks have occurred during the recent drought (Meyer et al., 2016; Sierra Nevada Conservancy, 2017). A similar situation exists for white-pine blister rust, which affects 5-needle pines throughout the western mountains, including western white pine and whitebark pine, two species found in Sierran subalpine (Tomback and Achuff, 2010). Continued large-scale beetle outbreaks and/or disease could lead to a compositional shift in favor of species more resistant to these pathogens. In addition to these potential negative effects, major shifts in composition and structure to an ecosystem are likely to lead to numerous other, unforeseen biological changes in the ecosystem.

Tracking trends and patterns in how the high elevation forests in this region are changing helps advance the understanding of the factors driving these changes, and improves the ability to anticipate future changes.

What factors influence this indicator?

In the subalpine zone of the Sierra Nevada, deep spring snowpack and low summer moisture limit the germination and establishment of seedlings (known as "recruitment"), and the growth and survival of young trees. The Sierra Nevada is experiencing warmer temperatures, a greater proportion of rain to snow, and earlier snowmelt dates (Dettinger and Cayan, 1995; Coats, 2010; Millar et al., 2012; Knowles et al., 2006), as well as overall decreases in snowpack during the recent drought (Berg and Hall, 2017). These climate-related changes could be making growing seasons longer, creating favorable conditions for tree recruitment and enhancing the survival of small trees (Dolanc et al., 2014a). At the same time large trees, which have a higher water demand,



may be dying off due to insufficient moisture (McIntyre et al., 2015). Thus, the changes in tree densities are likely influenced by regional climatic changes since the 1930s. Interestingly, no apparent change in the relative abundance of tree species were observed (Dolanc et al., 2013).

Certain factors that help explain the increased tree densities at low to mid-elevations may not explain the changes observed at subalpine elevations. Fire suppression appears to be a primary factor for increased tree density at low to mid-elevations. However, fire suppression activities have been minimal at sub-alpine elevations due to the low occurrence of wildfire, implicating changing climatic conditions as the factor associated with increased small tree densities at these elevations. (Dolanc et al., 2014a; Dolanc et al., 2014b). Timber harvest and logging may explain some of the declines in large trees over time at lower elevations as well. However, logging has been minimal in Yosemite National Park, which has also experienced significant declines in large trees (Dolanc et al., 2014a; Lutz et al., 2010).

Increasing concentration of nitrogen may also contribute to densification of small trees. Increased deposition of nitrogen from pollution sources upwind has been documented in the Lake Tahoe Basin. However, because nitrogen deposition is highly contingent upon the location of pollution sources, its effects are highly variable across the landscape (Fenn et al., 2003) and therefore not likely to account for the rather consistent and widespread shift in subalpine structure. It has also been suggested that higher concentrations of carbon dioxide could cause major structural shifts, but research has shown that this is unlikely to happen in high-elevation forests (Grace et al., 2002). Similarly, although ozone pollution from upwind areas may increase mortality of ponderosa and Jeffrey pine in the Sierra Nevada, its effects on densification are likely minimal. The greatest tree mortality impacts from ozone have been observed south of the study area shown in Figure 3. In addition, declines in ponderosa and Jeffrey pine large tree densities were roughly in line with that of other species not affected by ozone (Dolanc et al., 2014a).

Technical Considerations

Data Characteristics

Data for Figure 1: Plots of approximately 809 m² (8712 ft²) were originally sampled from 1929-1934 as part of the Wieslander Vegetation Type Mapping (VTM) project that represented the US Forest Service's original forest inventory in California (Wieslander et al., 1933; Thorne and Le, 2016). From 2007-2009, 139 historic vegetation plots were resampled throughout wilderness areas at 2300-3400 m elevation in the central Sierra Nevada. Care was taken to sample modern stand conditions with a protocol compatible with the original surveys, matching plot size, shape and orientation as closely as possible. Nearly half of the 139 plots were concentrated in the Tioga Pass area of Yosemite National Park, with the other half coming from passes located as far north as the Desolation Wilderness. The study area encompasses approximately 5500 km².

Analysis was centered on differences between numbers of stems in historic VTM versus modern stands, using the four size-class dbh (diameter at breast height) categories set



by the VTM team (SC1, SC2, SC3, and SC4). Comparisons were made for all species combined as well as each of the eight most-common tree species.

To determine change in climate over the same time period, data from two weather stations at either end of the study area, Tahoe City in the north and Huntington Lake in the south, were accessed. Thirty-year means were calculated for 1916-1945 and 1976-2005, representing the historic and modern periods influencing each of the sample periods in the vegetation data. Differences in climate between the two time periods were calculated for annual minimum temperature, annual maximum temperature and annual precipitation. Differences in these variables during the July through September growing season were also calculated.

Data for Figure 2:

The US Department of Agriculture Forest Service (USFS) runs the Forest Inventory and Analysis (FIA) program, which collects, compiles and archives data on forest status across the United States. The FIA protocol divides plots into four 7.3-m radius circular subplots, with one central subplot and three outer subplots arranged at 120° angles from each other at distances of 36.5 m from plot center to plot center. Each subplot has a 2.1-m radius circular microplot nested within its boundaries. For all subplots, every tree >12.7 cm (5 in) is measured (DBH, height, etc.) and identified to species. Within microplots, every tree >2.5 cm is measured. The total area of all four subplots combined is 672.45 m².

This study used 4321 historical VTM plots and compared stand composition and structure to 1000 FIA plots occupying the central Sierra Nevada from Lake Tahoe to the southern end of Yosemite National Park. Tree sizes in the FIA plots were re-classed into three size classes used in the VTM study and tree densities were converted to per-area measures. Separate generalized linear model statistical tests were conducted for each elevation band and latitude category using a negative binomial distribution (Dolanc et al., 2014a).

Strengths and Limitations of the Data

The structural shifts observed from subalpine of the Sierra Nevada are the first empirical-based observations of changes in high elevation forests in the Sierra Nevada mountains.

Using VTM data as historic references has been criticized because VTM field crews did not permanently mark their plots, meaning precise relocation of plots is not possible. However, it is possible to navigate to the same slope face and likely the same forest stand using their data on canopy composition, elevation, slope, aspect and several other environmental variables. As long as many locations are resampled, this approach should be sufficient and preferable to studies that use entirely different sets of modern data for comparison with VTM conditions. With resampling, differences between each pair of historic vs. modern plots have been minimized. Because of these considerations, the analysis for this study is focused on overall change (all 139 plots combined). The modern resampling effort covered a large region, with a large sample size. Numerous



recent papers have used the VTM data set as a historic reference and it appears as though this trend will continue. A critique that the VTM plots may have been systematically biased to sampling larger trees has been suggested but never substantiated. Evidence from high elevation plots in the form of downed large trees suggests that the historical densities of large trees recorded are accurate (Dolanc et al., 2013) while the field manual for the VTM surveys instructs the surveyors to sample vegetation representative of the mapped vegetation (Thorne and Le, 2016).

VTM and FIA data differ in sampling protocol and plot selection. However, trends in comparisons of VTM and FIA data are similar in direction and magnitude to those reported in regional studies using a variety of methods, supporting the use of comparing these two data sets. In addition, scatterplot analyses suggest that the VTM crew sampled as wide a variety of stands as the current FIA program (Dolanc et al., 2014b).

For more information, contact:



Christopher R. Dolanc
Mercyhurst University
501 East 38th Street
Erie, PA 16546
Phone: 814-824-2540
cdolanc@mercyhurst.edu



James H. Thorne
Department of Environmental Science and Policy
University of California Davis
2132 Wickson Hall, 1 Shields Avenue
Davis, CA 95616
(530) 752-4389
jhthorne@ucdavis.edu

References:

Berg N and Hall A (2017). Anthropogenic warming impacts on California snowpack during drought. *Geophysical Research Letters* **44**(5): 2511.

Coats R (2010). Climate change in the Tahoe basin: regional trends, impacts and drivers. *Climatic Change* **102**: 435–466.

Dettinger MD and Cayan DR (1995). Large-scale atmospheric forcing of recent trends toward early snowmelt runoff in California. *Journal of Climate* **8**: 606-623.

Dolanc CR, Thorne JH and Safford HD (2013). Widespread shifts in the demographic structure of subalpine forests in the Sierra Nevada, California. *Global Ecology and Biogeography* **22**: 264–276.

Dolanc CR, Safford HD, Thorne JH and Dobrowski SZ (2014a). Changing forest structure across the landscape of the Sierra Nevada, CA, USA, since the 1930s. *Ecosphere* **5**(8):101.

Dolanc CR, Safford HD, Dobrowski SZ and Thorne JH (2014b). Twentieth century shifts in abundance and composition of vegetation types of the Sierra Nevada, CA, US. *Applied Vegetation Science* **17**: 442-455.

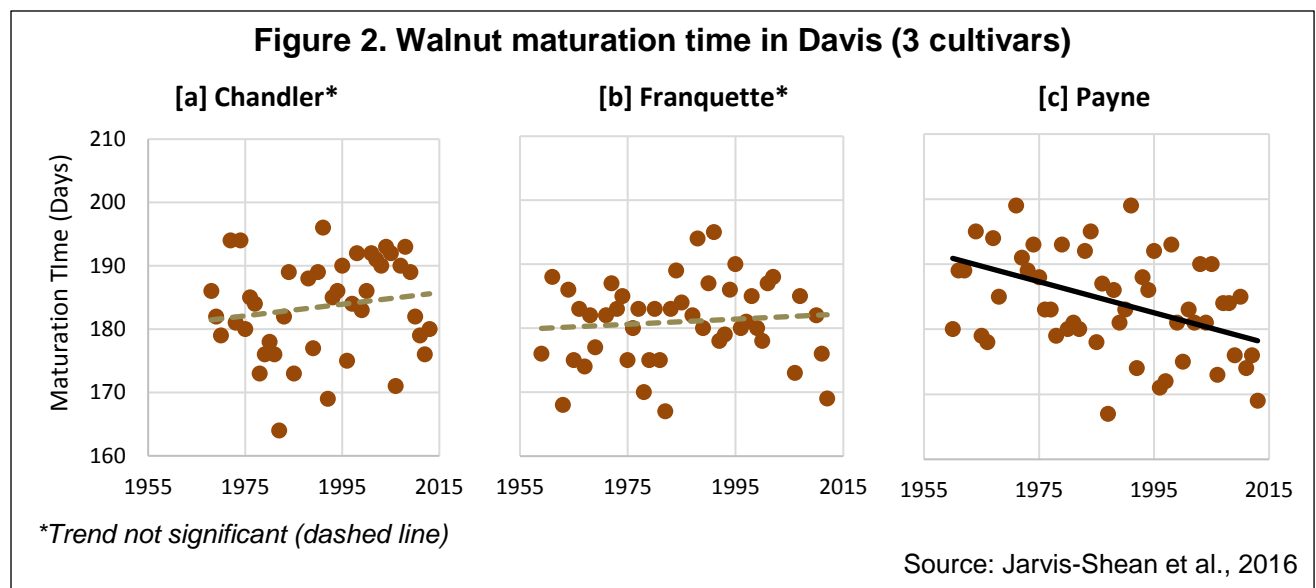
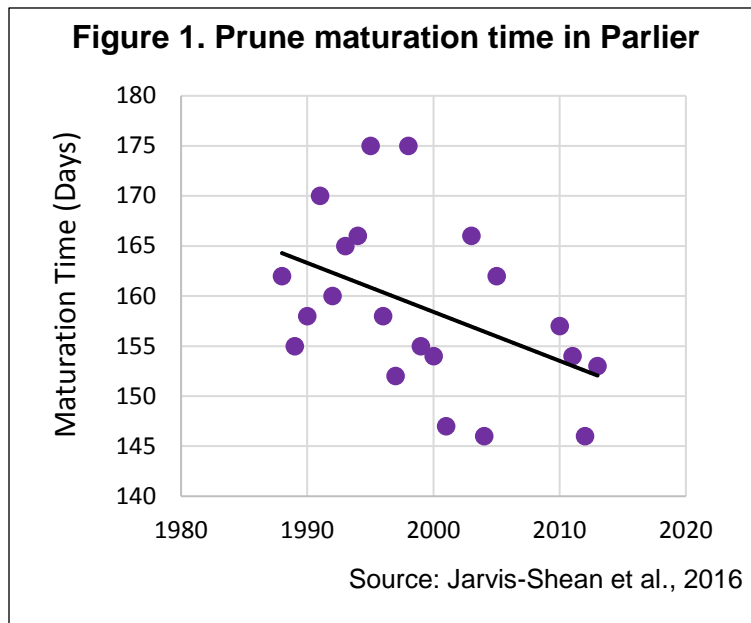


- Fenn ME, Haeuber R, Tonnesen GS, Baron JS, Grossman-Clarke S, et al. (2003). Nitrogen emissions, deposition, and monitoring in the western United States. *Bioscience* **53**(4): 391-403.
- Grace J, Berninger F and Nagy L (2002). Impacts of climate change on the tree line. *Annals of Botany* **90**(4): 537-544.
- Knowles N, Dettinger MD and Cayan DR (2006). Trends in snowfall versus rainfall in the western United States. *Journal of Climate* **19**(18): 4545-4559.
- Kurz WA, Dymond CC, Stinson G, Rampley GJ, Neilson ET, et al. (2008). Mountain pine beetle and forest carbon feedback to climate change. *Nature* **452**(7190): 987-990.
- Lindenmayer DB, Laurance WF and Franklin JF (2012). Global decline in large trees. *Science* **338**(6112): 1305-1306.
- Lutz JA, van Wagtendonk JW and Franklin JF (2010). Climatic water deficit, tree species ranges, and climate change in Yosemite National Park. *Journal of Biogeography* **37**: 936-950.
- McIntyre PJ, Thorne JH, Dolanc CR, Flint AL, Flint LE, et al. (2015). Twentieth-century shifts in forest structure in California: Denser forests, smaller trees, and increased dominance of oaks. *Proceedings of the National Academy of Sciences* **112**(5):1458-1463.
- Millar CI, Westfall RD, Delany DL, Bokach MJ, Flint AL, et al. (2012). Forest mortality in high-elevation whitebark pine (*Pinus albicaulis*) forests of eastern California, USA; influence of environmental context, bark beetles, climatic water deficit, and warming. *Canadian Journal of Forest Research* **42**:749–765.
- Meyer MD, Bulaon B, MacKenzie M and Safford HG (2016). Mortality, structure, and regeneration in whitebark pine stands impacted by mountain pine beetle in the southern Sierra Nevada. *Canadian Journal of Forest Research* **46**: 572-581.
- Sierra Nevada Conservancy (2017). State of California Sierra Nevada Region: Tree Mortality in the Sierra Nevada. Retrieved December 28, 2017, from <http://www.sierranevadaconservancy.ca.gov/our-region/tree-mortality>
- Schwartz MW, Butt N, Dolanc CR, Holguin AJ, Moritz MA, et al. (2015). Increasing elevation of fire in the Sierra Nevada and implications forest change. *Ecosphere* **6**(7): 121.
- Thorne JH and Le TN (2016). California's historic legacy for Landscape Change, the Wieslander Vegetation Type Maps. *Madroño* **63**: 293-328.
- Tomback DF and Achuff P (2010). Blister rust and western forest biodiversity: ecology, values and outlook for white pines. *Forest Pathology* **40**(3-4): 186-225.
- van Wagtendonk JW and Fites-Kaufman JA (2006). Sierra Nevada Bioregion. In: *Fire in California's Ecosystems*. Sugihara NG, Van Wagtendonk JW, Shaffer KE, Fites-Kaufman JA and Thode AE (Eds.). Berkeley, Los Angeles, London: University of California Press. pp594.
- Wieslander AE, Yates HS, Jensen AE and Johannsen PL (1933). *Manual of Field Instructions for Vegetation Type Map of California*. USDA Forest Service.



FRUIT AND NUT MATURATION TIME

With warming air temperatures, one walnut variety and prunes in the Central Valley are maturing more quickly, leading to earlier harvests.



What does the indicator show?

The graphs above show maturation times for California prunes (Figure 1) and three cultivated walnut varieties (“cultivars”) (Figure 2) grown respectively in two Central Valley locations: Parlier (Fresno County) and Davis (Yolo County). “Maturation time” refers to the period between bloom and harvest — specifically, flowering and fruit maturity for the prune, and leaf-out and first harvest for the walnut.



From 1988 to 2013, prune maturation (Figure 1) time decreased on average by about 12 days. The maturation time for one of the walnut cultivars, the Payne walnut (Figure 2[c]), similarly decreased by approximately 11 days since 1960. Maturation times for two other walnut cultivars, the Chandler and the Franquette (Figure 2[a] and [b]), have remained relatively constant since 1968 and 1959, respectively.

Why is this indicator important?

California accounts for an estimated 96 percent of the prunes grown in the US, with about half consumed domestically and half exported. The state currently supplies about 40 percent of the world's prunes (Lazicki et al., 2016). The prune industry in California is dependent on a single cultivar, the "Improved French Prune."

California growers produce 99 percent of the commercial US supply of walnuts with about a third of the crop exported (Geisseler and Horwath, 2016). The industry generates \$1.4 billion in farm gate revenue annually (net value after subtracting marketing costs) and supports some 60,000 jobs directly and indirectly (California Walnut Board, 2017).

Climatic conditions following flowering and leaf-out for fruits and nuts are critical to the development of a robust crop. In general, shorter maturation times lead to smaller fruits and nuts. Because larger fruits command a premium price, this change can lead to a significant loss of revenue for growers and suppliers. For prunes, this can be somewhat offset by fruit thinning earlier in the year, which can promote larger fruits. This is not practical for walnuts, due to the size of the trees.

Shorter maturation times mean that crops are ripening more quickly. This results in a shorter timeframe for harvest and processing. During harvest season, farmers draw on a limited supply of workers and equipment. If the harvest timeframe shortens, hiring workers and renting equipment can present challenges. Thus, a compressed harvest schedule puts farmers at risk for significant loss of crop quality.

The trend toward earlier maturation for some cultivars of walnuts has some positive impact. Walnuts are often harvested in October — the beginning of the rainy season in the Central Valley. Rain immediately before or during the harvest can be catastrophic, making it difficult to properly dry the nuts, leaving them vulnerable to mold growth. The earlier in the season that walnuts mature, the less likely they are to encounter rain at harvest time.

Warming is expected on an annual, seasonal, and even daily basis in California, with impacts differing by region. The significant, overall outcome of warming is the likely reduction in yield of some of California's most valuable specialty crops, particularly perennial crops.



What factors influence this indicator?

Temperature influences how fast the fruits on a plant develop and mature. Following a period of dormancy in the winter (see *Winter chill* indicator), fruit and nut trees begin to bloom by opening flower or leaf buds. Prune trees have flower buds that produce flowers and vegetative buds that produce leaves. Flowering occurs before vegetative bud break. Walnuts have male buds that produce pollen and mixed buds that produce leaves and female flowers. Leaf emergence precedes the opening of the female flowers (Ramos, 1997).

During the first 30 to 90 days after bloom, the amount and duration of warm weather experienced by the plant — referred to as heat accumulation — is the most significant factor that determines harvest timing. This period occurs during the months of April, May, June and July, depending on the variety of walnut. With warmer temperatures, the fruit or nut develops and matures more quickly, leading to an earlier harvest. However, temperatures that are too high (such as during hot days in the Central Valley) can slow development as trees divert energy from fruit development towards self-cooling and preventing or repairing heat damage (Jarvis-Shean et al., 2016)

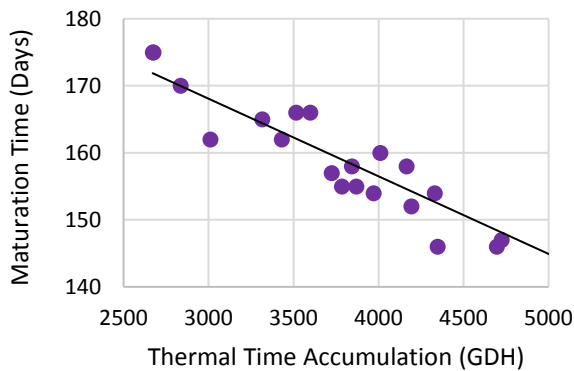
Different crops have different heat requirements for fruit development; these requirements are typically expressed as **thermal time accumulation**. In its simplest form, thermal time measures the difference between a given temperature and a certain threshold or base temperature, and the length of time this difference occurs in a day or other unit of time. Thermal time accumulation is calculated by summing hourly thermal time. A fruit or nut reaches maturity when it has accumulated sufficient thermal time. “Growing degree hours” (GDH) is a commonly used unit of thermal time accumulation.

Fruit or nut maturity represents the first possible harvest date. The timing of maturity is partially determined by the timing of flowering. Generally, a tree that blooms earlier will also be ready to harvest earlier. Consequently, changes in harvest readiness date can be due to changes in flowering dates as well as changes in temperature after flowering. Time to Maturity tracks the time between flowering and maturity, and thus the influence of temperature on changes occurring after flowering.

As shown in Figure 3, prune maturation time responded very strongly to thermal time accumulation: the greater the thermal time accumulation in a given season, the shorter the maturation time. In fact, thermal time accumulation for French prunes in Parlier has been increasing since 1988 (Figure 4) — a trend consistent with the decreasing season length. There is, however, too much variation in the data to make any strong conclusions at this time. If thermal time accumulation in Parlier continues to increase as the trend suggests, prune maturation times will most likely continue to shorten with increasing temperatures projected with climate change. Since 1931, minimum temperatures have been increasing for most months of the year in Parlier, while maximum temperatures have been decreasing.

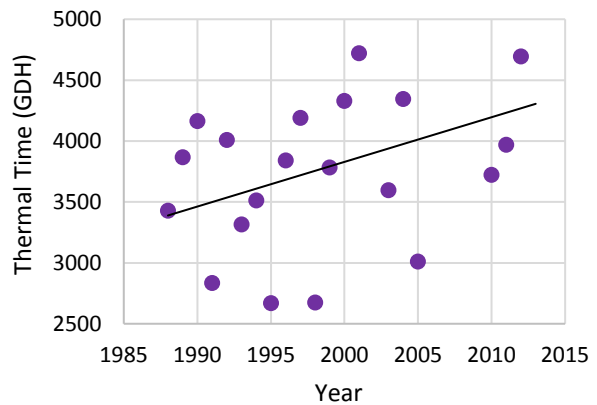


Figure 3. Prune maturation time in response to thermal time accumulation in Parlier



Source: Jarvis-Shean et al., 2016

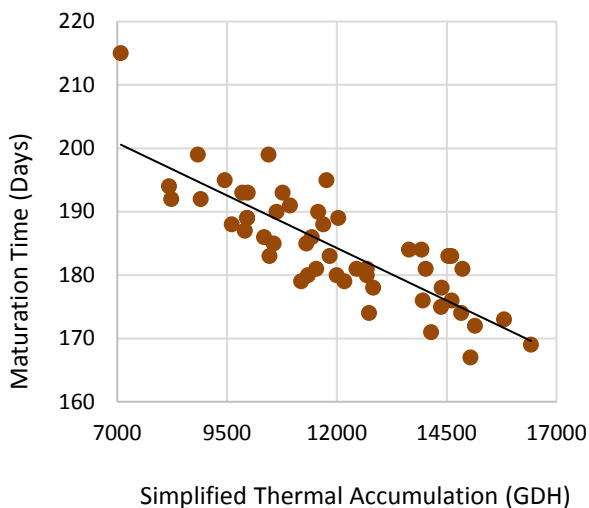
Figure 4. Thermal time accumulation for prunes in Parlier



Source: Jarvis-Shean et al., 2016

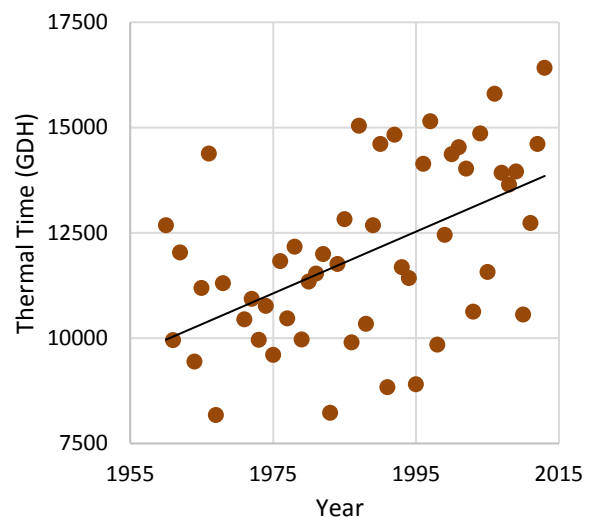
Of the three walnut varieties, only Payne showed a significant decreasing trend in maturation time length over the past 60 years. As with the prune, Payne maturation time responded strongly to thermal time accumulation, showing decreasing maturation times with increasing thermal time accumulation (Figure 5). Payne thermal time accumulation has been increasing since 1960 (Figure 6), indicating that maturation time for these walnuts will shorten with warming conditions associated with climate change. Although maturation times for both the Chandler and Franquette walnuts did not change appreciably over the past 46 and 54 years, respectively, thermal time accumulation for both cultivars increased over time, and showed a strong relationship with maturation time (not shown). Researchers anticipate that maturation times for these cultivars will likely shorten in the future with increasing thermal time accumulation.

Figure 5. Payne walnut maturation time in response to thermal time accumulation in Davis



Source: Jarvis-Shean et al., 2016

Figure 6. Thermal time accumulation for Payne walnut in Davis



Source: Jarvis-Shean et al., 2016



No definitive conclusions can be drawn regarding trends in the maturation times of three almond cultivars, given the short period for which observations are available (nine years).

Technical Considerations

Data Characteristics

Climate data:

Temperature data were obtained from the National Climatic Data Center of the National Oceanic and Atmospheric Administration (Menne et al., 2015) and from the California Irrigation Management Information System (CIMIS). CIMIS, developed by the California Department of Water Resources and the University of California at Davis, is a repository of climatological data collected at more than 100 computerized weather stations throughout California.

Temperature data were retrieved from stations closest to the fruit and nut orchard locations. When data was missing from a primary station, temperature data from a nearby station were used to supplement the dataset. In Davis, for days when climatological data was absent from the primary station, temperatures from other surrounding locations were used in a model to estimate Davis temperatures.

Temperature time series going back to 1988 (prune) and 1960 (walnut) were analyzed to match up with the duration of maturation time.

Spring thermal time accumulation was calculated using the Growing Degree Hours (GDH) model of Anderson et al. (1986). This model counts the highest GDH accumulation at an optimal temperature of 25 degrees centigrade (°C); at temperatures above a minimum (4°C) and below a maximum (36°C), heat accumulates at fractions of the highest possible amount.

Prune bloom/leaf-out data and walnut maturity/harvest data:

Flowering onset and maturity data for prunes were provided by the University of California Dried Plum/Prune Cultivar Development Program. Full bloom is defined as when 50 percent of the flower buds on the tree have opened. The maturity date is defined as when the fruit can withstand 3 to 4 pounds of pressure (a penetrometer measures the pressure necessary to force a plunger of specified size into the pulp of a fruit).

The leaf-out and harvest data for walnuts were obtained from the University of California at Davis Walnut Breeding Program. Leaf-out is defined as the time at which 50 percent of the vegetative buds have started to open. The harvest date is the time at which the hull, the outer fleshy part, separates from the shell of the nut.

Strengths and Limitations of the Data

The prune and walnut orchards from which data were collected were at the same or nearby locations over the entire study periods. The walnut dataset is long by phenology data standards, with an average of 44 years of observation, a minimum of 35 years, and



a maximum of 59 years, depending on cultivar. The prune dataset, although 25 years in length, provides sufficient information for evaluating phenology trends. In both cases, it would be advantageous to have records of walnut and prune phenology at multiple locations. Not only do crops responses change at different latitudes, but the climate effects may vary throughout California. Evaluating data at multiple sites would allow for a better understanding of how climate change may be affecting different agricultural regions within the state.

To measure prune maturity, the amount of pressure a fruit can withstand when punctured, is a very precise and consistent method. For walnuts, the measure of harvest readiness (hullsplit) is affected by humidity. Higher humidity accelerates nut maturity and can introduce uncertainty in timing of harvest readiness date.

For both the prune and the walnut data sets, a small number of researchers were collecting prune bloom/leaf-out data and walnut maturity/harvest data measurements. Researchers trained their successors to ensure consistency in data collection over time.

For more information, contact:



Katherine Jarvis-Shean
Sacramento-Solano-Yolo Orchard Systems Advisor
University of California Cooperative Extension
70 Cottonwood Street
Woodland, CA 95695
(530) 377-9528
kjarvisshean@ucanr.edu

Elise Hellwig
Ecology Graduate Group
University of California, Davis
echellwig@ucdavis.edu

Robert J. Hijmans
Department of Environmental Science and Policy
University of California, Davis
One Shields Avenue, Davis, 95616
rhijmans@ucdavis.edu

References:

Anderson JL, Richardson EA and CD Kesner (1986). Validation of Chill Unit and Flower Bud Phenology Models for 'Montmorency' Sour Cherry. *Acta Horticulturae* **184**: 71-78.

California Walnut Board (2017). Walnut Industry. Retrieved February 14, 2018, from <https://walnuts.org/walnut-industry/>

Geisseler D and Horwath WR (2016). *Walnut Production in California*. Document prepared in collaboration between the University of California at Davis and the California Department of Food and Agriculture Fertilizer Research and Education Program.



Jarvis-Shean K, Hellwig E and Hijmans R (2016). *Effects of Climate Change on Tree Crop Phenology in California*. University of California, Davis. Report submitted to the Office of Environmental Health Hazard Assessment.

Lazicki P, Geisseler D and Horwath W (2016). *Prune and Plum Production in California*. University of California at Davis, funded by the California Department of Food and Agriculture Fertilizer Research and Education Program. Available at https://apps1.cdfa.ca.gov/FertilizerResearch/docs/Prune_Plum_Production_CA.pdf

Menne MJ, Durrel, Korzeniewski B, McNeal S, Thomas K, et al. (2015). *NOAA National Climatic Data Center: Global Historical Climatology Network - Daily (GHCN-Daily), Version 3.22*. Available at <http://doi.org/10.7289/V5D21VHZ>

Ramos DE (1997). *Walnut Production Manual* (Vol. 3373). UCANR Publications.

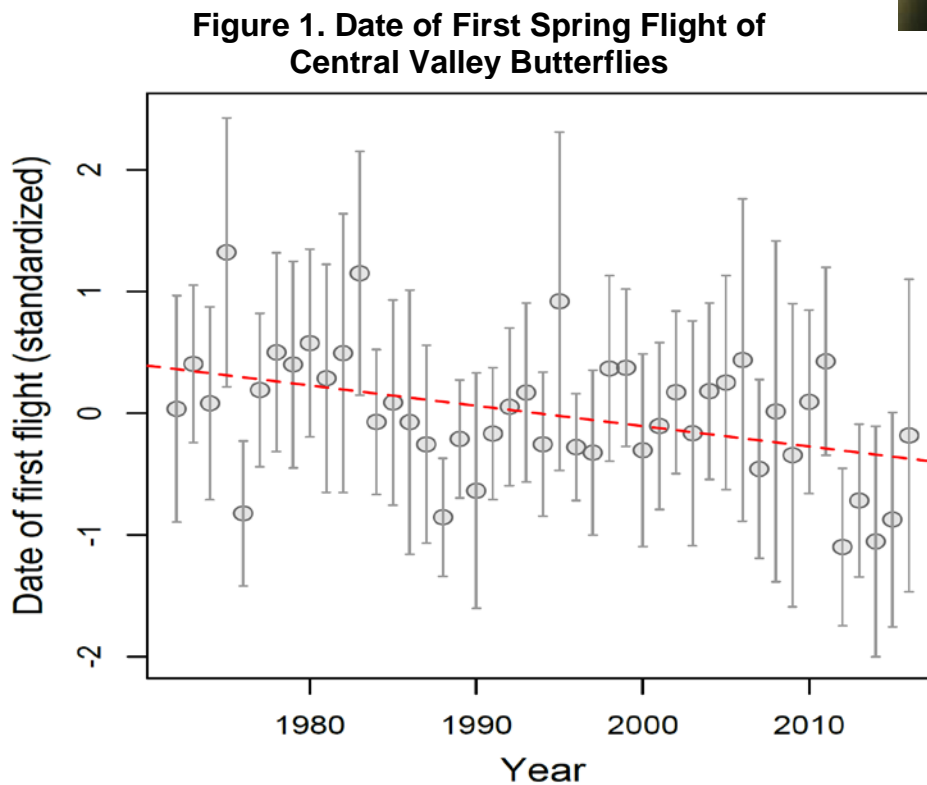


SPRING FLIGHT OF CENTRAL VALLEY BUTTERFLIES

Over the past 45 years, common butterfly species have been appearing in the Central Valley earlier in the spring.



Painted lady
(*Vanessa cardui*)
Photo: Jim Ellis



Source: Forster and Shapiro (2003), updated 2017

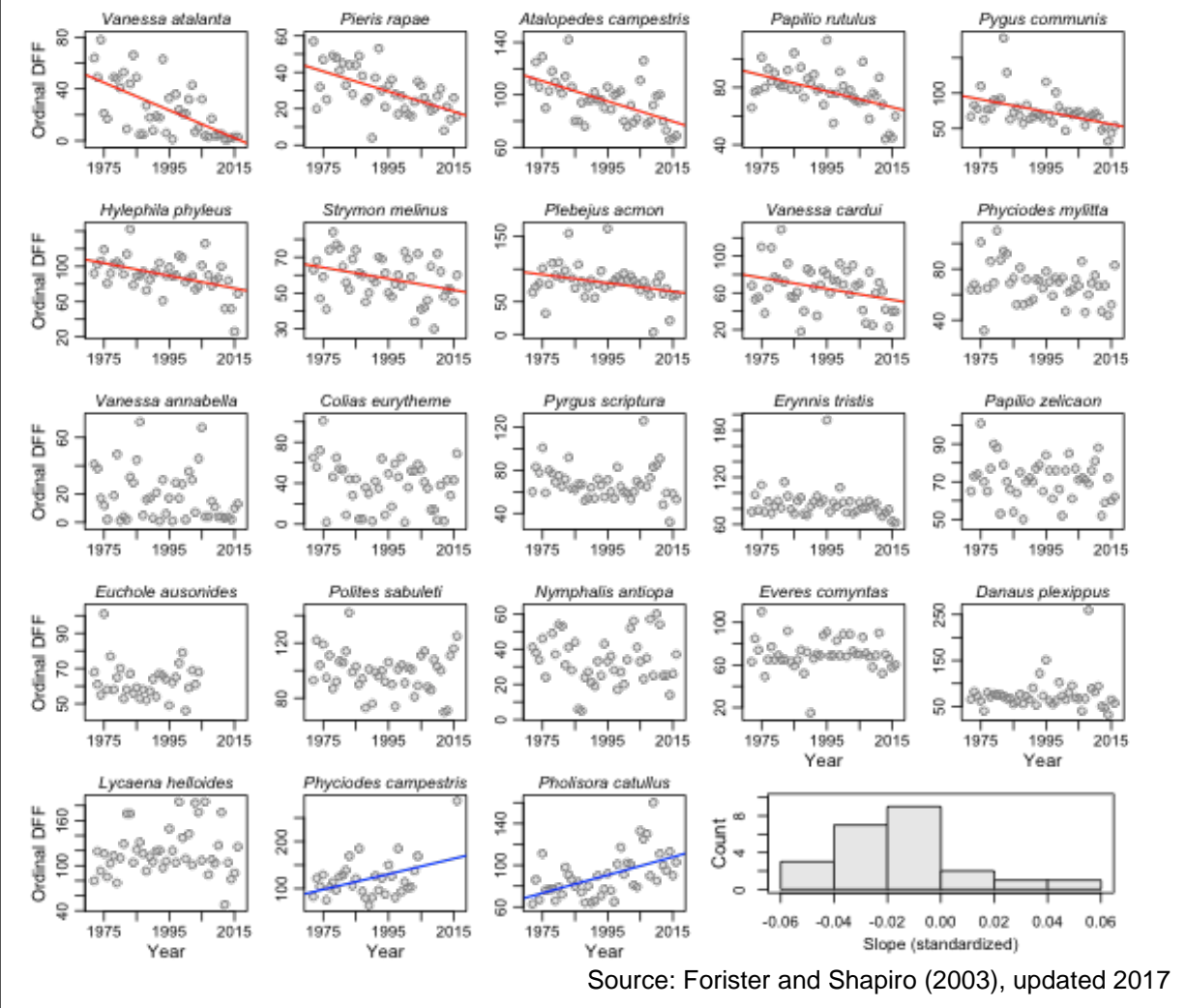
What does the indicator show?

Over the past 45 years, the average date of first flight (DFF) of a suite of 23 butterfly species in the Central Valley of California has been shifting towards an earlier date in the spring. The DFF refers to the date that the first adult of a species is observed in the field in a given calendar year. In Figure 1, the value shown for each year is the aggregate of DFFs across the 23 species, calculated as described in the *Technical Considerations* section below. The higher the value on the graph, the later the DFF.

Figure 2 presents graphs showing DFF (untransformed) by year for each butterfly species, starting with the species showing stronger trends towards earlier emergence, and ending with the species showing trends towards later emergence. Values plotted are days since the start of the calendar year (also known as "ordinal" dates). Lines on plots indicate that the trend is significant (at $P < 0.05$): red lines are used for species emerging earlier, and blue lines for those emerging later. The histogram in the lower right shows the distribution of slopes of DFF values against years for the different species, calculated using z-scores (see *Technical Considerations*).



Figure 2. Date of first spring flight for 23 butterfly species



Source: Forster and Shapiro (2003), updated 2017

Nine species each independently show significant trends towards earlier emergence, while only two species show significant trends for later emergence. Across the nine species with significantly earlier emergence, the average slope is -0.67 day per year. This means that on average these species have emerged earlier in the spring by roughly one month over the 45 years of observations. The slopes of the two later-emerging species are 1.64 and 0.87 days per year, respectively. As shown in the histogram in Figure 2, slopes of DFF values against years have shifted toward negative values, indicating overall earlier emergence across species, consistent with the pattern shown in Figure 1.

Why is this indicator important?

This indicator tracks the response of common butterfly species as a way of studying biological shifts consistent with the impacts of a changing climate. Plants and animals reproduce, grow, and survive within specific ranges of climatic and environmental conditions. Changes in these conditions beyond a species' tolerances can elicit a

change in phenology — that is, a change in the timing of seasonal life-cycle events, such as leaf unfolding, flowering, bird migration, egg-laying and the appearance of butterflies. Studies that have investigated the relationship between phenology and changes in climate conditions have largely been conducted in higher, temperate latitudes, where minor climatic changes can have large impacts on species that are often at the limits of their geographic ranges. By contrast, species from lower latitudes, where the climate is highly variable (including areas of California that have a Mediterranean climate), and where there are large fluctuations in temperature and precipitation, might be expected to be less sensitive to such variability.

The shifting phenology of these 23 butterfly species is correlated with the hotter and drier conditions in the region in recent decades (Forister and Shapiro, 2003) (see *Annual air temperature* and *Precipitation* indicators). The data supporting this indicator suggest that Central Valley butterflies not only are responding to changing climate conditions, but also that their responses have been similar to those of butterflies from higher-latitude climates. These findings complement similar studies from Europe and demonstrate the apparently ubiquitous phenological response of spring butterflies to warming and drying conditions (e.g., Roy and Sparks, 2000; Peñuelas et al., 2002). It is also worth noting that the Central Valley has undergone intense land conversion, both to urban development and to agriculture (Forister et al., 2016). Thus, the data indicate that the phenological impacts of climate change are not restricted to northern latitudes or to areas with pristine ecological conditions.

What factors influence this indicator?

Climatic conditions have a significant impact on the phenology of butterflies. Butterflies in the temperate latitudes enter a dormant state during the winter months; in the spring, temperature cues cause them to hatch, resume feeding, or emerge from pupae as adults (Dennis, 1993; Shapiro, 2007). As climatic conditions during key times of the year have changed, the timing of butterfly life-history events has undergone a corresponding change. The butterfly species monitored overwinter (i.e., spend the winter) in different life-history stages as: eggs (1 species); larvae (8 species); pupae (9 species); and adults (3 species). Two of the species emigrate in the spring from distant overwintering sites.

Statistical analyses were conducted to determine the association between DFF and different weather variables: total precipitation, average daily maximum temperature and average daily minimum temperature in the winter and spring of the year in question, and in the summer and fall of the previous year. Winter conditions — specifically winter precipitation, average winter daily maximum temperature, and average winter daily minimum temperature — were found to have the strongest associations with the date of first flight (Forister and Shapiro, 2003).

Other factors may impact the phenological observations described here, such as nectar and host plant availability. Plant resources may in turn be affected by habitat conversion, though it is not clear how these factors could lead to the earlier emergence of a fauna in a specific area. Finally, the impacts that a shifting insect phenology may



have on other species at higher and lower trophic levels, including larval hosts and predators, are also unknown.

Technical Considerations

Data Characteristics

The data described here consist of the date of first spring adult flight (DFF) for 23 butterfly species. These were first reported by Forister and Shapiro (2003). Fourteen years of data have been added to that original data set. The primary result remains unchanged by the updated data: an overall shift towards earlier emergence, with more dramatic shifts in a subset of species.

The values for Figure 1 were derived as follows:

- Calendar dates were first converted into days since the start of the year, also known as "ordinal" dates.
- The ordinal dates of first flight (DFF values) were transformed into z-scores separately for each species. To do this, the mean and standard deviation of DFF values across years were calculated. The difference between each DFF value and the mean was then found, and that result divided by the standard deviation to produce a z-score corresponding to the number of standard deviations a value is from the long-term average DFFs for that species. For example, a z-score of -1 indicates a DFF that is one standard deviation earlier than the average for that species, and a value of 1 indicates a DFF that is one standard deviation later than average.
- The mean of the z-scores across the 23 species for each year is shown in Figure 1, along with the standard deviation of the z-score values.
- The red line in Figure 1 is fit to the mean z-score values across years. It shows that the mean values have decreased over time, and corresponds to an overall trend towards earlier emergence that is significant ($F_{1,43} = 8.92$, $P = 0.0046$).

The study area is located in the Central Valley portions (below 65 meters elevation) of three Northern California counties: Yolo, Sacramento, and Solano. Three permanent field sites in these counties are visited by an investigator at two-week intervals during "good butterfly weather." Most of the observations (> 90%) of DFF come from these permanent sites; however, in a given year, if a butterfly is first observed to be flying at a location within the three counties, but outside the permanent sites, that observation is included as well.

Weather data were obtained from the University of California/National Oceanic and Atmospheric Administration climate station in Davis, California, a World Meteorological Organization station centrally located among the study sites. Weather variables are not



independent, and some were excluded as redundant before use in multiple regressions or other analyses.

Strengths and Limitations of the Data

Since the data are collected and compiled entirely by one observer (Arthur Shapiro of University of California at Davis), any biases in data collection should be consistent across years. This would not be true in studies which involve multiple workers — with variable levels of training — across years.

The primary limitation of the data stems from the fact that DFF is only one aspect of a potentially multi-faceted suite of population-level dynamics. For example, if the spring phenology of a species shifts, does this affect the total flight window? Does it affect peak or total abundance throughout the season? The picture becomes even more complex when one considers the general declines in low-elevation butterfly populations in the region that have been reported by Forister et al. (2010). If populations are in overall decline, with lower densities of individuals throughout the year, this could lower detection probabilities. This is true particularly early in the season for multivoltine species (i.e., species that produce more than one generation in a season, where the first generation tends to be smaller). Lower detection probabilities could appear as later phenological emergence (i.e., a “backwards” shift in time as is shown for *P. catullus* in the bottom right of the second figure). These issues are addressed in more detail in Forister et al. (2011). For further discussion of relevant biological complexities, see Shapiro et al. (2003) and Thorne et al. (2006).

For more information, contact:



Matthew L. Forister
Department of Biology
University of Nevada Reno
Mail Stop 314
Reno, NV 89557
(775) 784-4053
mforister@unr.edu



Arthur Shapiro
Department of Evolution and Biology
University of California Davis
6347 Storer Hall
Davis, CA 95616
(916) 752-2176
amshapiro@ucdavis.edu

References:

Dennis RLH (1993). *Butterflies and Climate Change*. Manchester, NY: Manchester University Press.

Forister ML, Cousens B, Harrison JG, Anderson K, Thorne JH, et al. (2016). Increasing neonicotinoid use and the declining butterfly fauna of lowland California. *Biology Letters* **12**(8): 20160475.



Forister ML, Jahner JP, Casner KL, Wilson JS and Shapiro AM (2011). The race is not to the swift: long-term data reveals pervasive declines in California's low-elevation butterfly fauna. *Ecology* **92**(12): 2222-2235.

Forister ML, McCall AC, Sanders NJ, Fordyce JA, Thorne JH, et al. (2010). Compounded effects of climate change and habitat alteration shift patterns of butterfly diversity. *Proceedings of the National Academy of Sciences* **107**(5): 2088-2092.

Forister ML and Shapiro AM (2003). Climatic trends and advancing spring flight of butterflies in lowland California. *Global Change Biology* **9**(7): 1130-1135.

Peñuelas J, Filella I, and Comas P (2002). Changed plant and animal life cycles from 1952 to 2000 in the Mediterranean region. *Global Change Biology* **8**(6): 531-544.

Roy DB and Sparks TH (2000). Phenology of British butterflies and climate change. *Global Change Biology* **6**(4): 407-416.

Shapiro A (2007). *Field Guide to Butterflies of the San Francisco Bay and Sacramento Valley Regions*. Berkeley, CA: University of California Press.

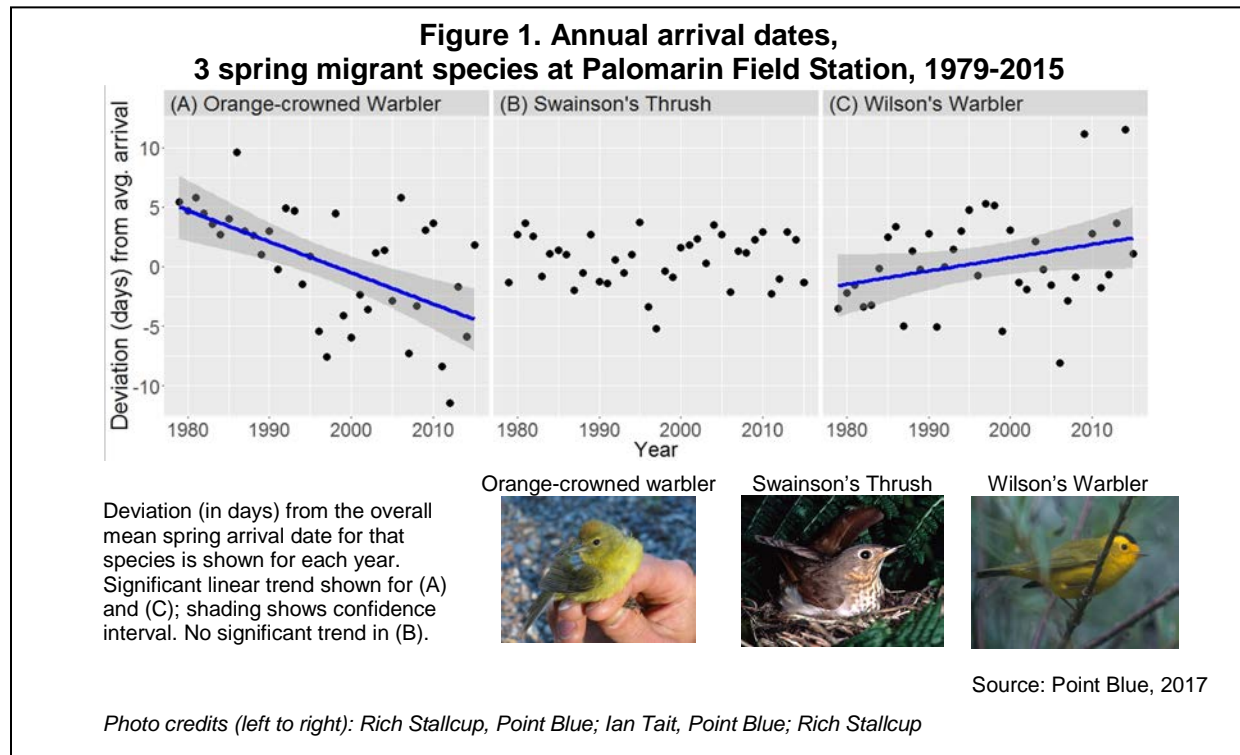
Shapiro A, Van Buskirk R, Kareofelas G and Patterson W (2003). Phenofaunistics: Seasonality as a Property of Butterfly Faunas. In: *Butterflies: Ecology and Evolution Taking Flight*. Boggs CL, Watt WB and Ehrlich PR (Eds.). Chicago: University of Chicago Press. pp. 111-147.

Thorne J, O'Brien J, Forister M and Shapiro A (2006). Building phenological models from presence/absence data for a butterfly fauna. *Ecological Applications* **16**(5): 1842-1853.



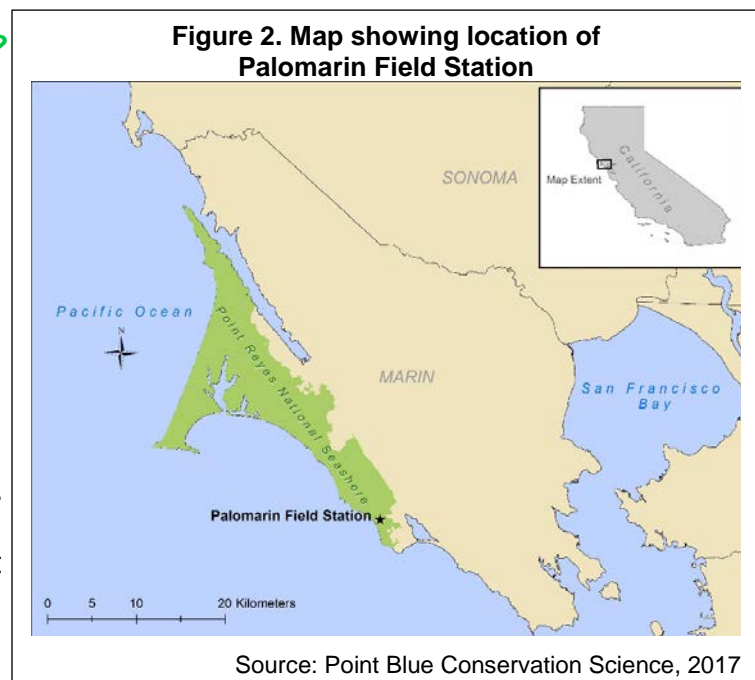
MIGRATORY BIRD ARRIVALS

Migratory songbird species are showing a diversity of changes in arrival dates. Of the three species studied that arrive at a coastal California site in the spring, two are showing opposite trends in timing (one shows no significant change). Of the four species that arrive in the fall, two have been arriving earlier over the past 35 years, while one has been showing a trend toward earlier arrival since 1995. The fourth species shows no significant change.



What does the indicator show?

Trends in spring and fall arrival dates of birds migrating to their breeding grounds in the spring (Figure 1) and their wintering grounds in the fall (Figure 3) differ among seven species of songbirds that spend part of the year at the Point Blue Conservation Science's Palomarin Field Station in Point Reyes National Seashore, Marin County, California (see Figure 2). Arrival dates are based on a 36-year record of observations at this location, where the habitat is



a mix of coastal scrub and mixed-evergreen hardwood forest with encroaching Douglas-fir forest.

As shown in Figure 1, of the spring species migrating to their breeding grounds, the Wilson's Warbler (*Wilsonia pusilla*) has been arriving later (1.1 days later per decade), while the Orange-crowned Warbler (*Oreothlypis celata*) has been trending towards earlier arrivals (2.6 days earlier per decade) over the past 36 years. No significant trend was observed for the Swainson's Thrush (*Catharus ustulatus*).

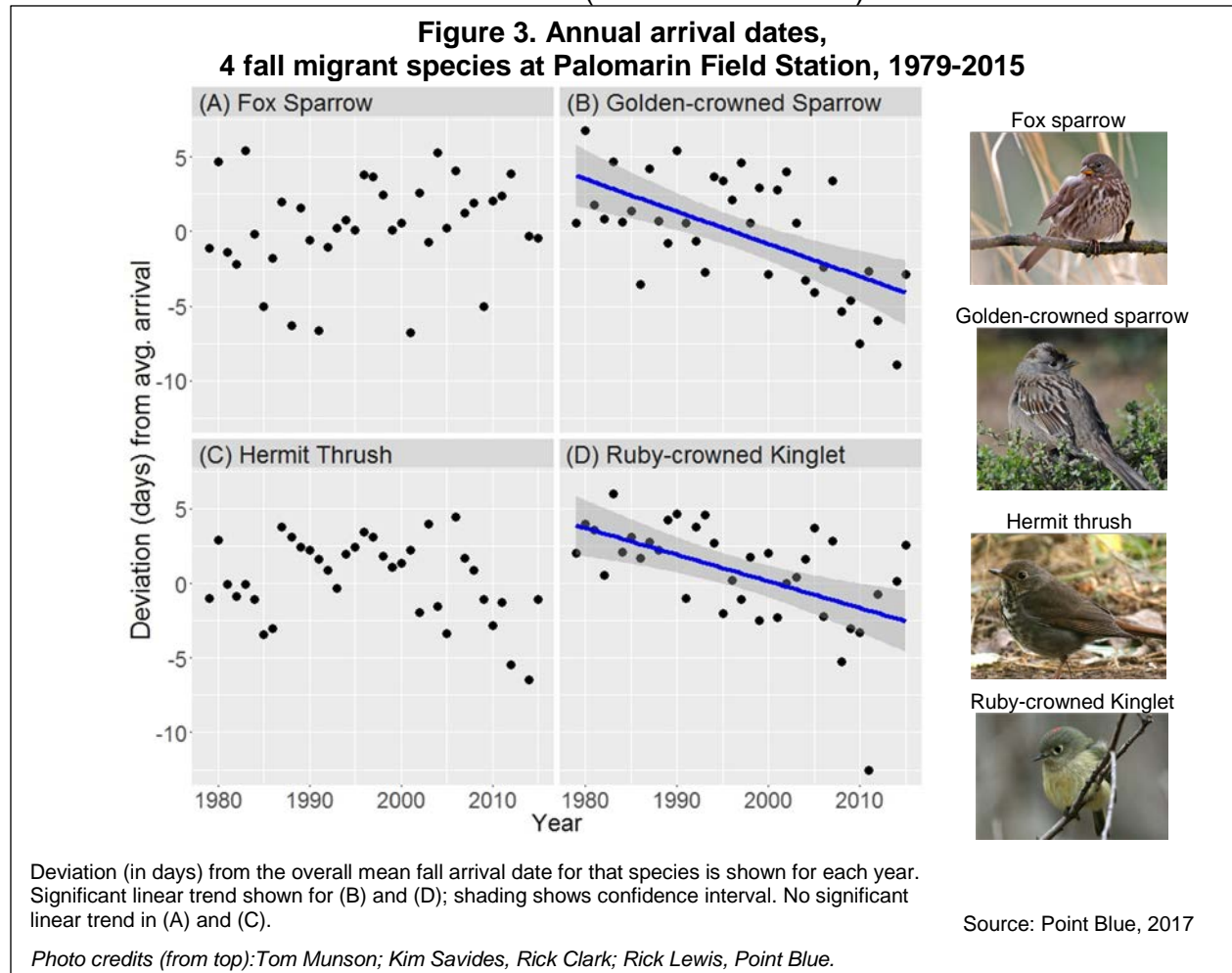


Figure 3 shows that, among species migrating to their wintering grounds in the fall, the Ruby-crowned Kinglet (*Regulus calendula*) and the Golden-crowned Sparrow (*Zonotrichia atricapilla*) have been arriving earlier (1.8 and 2.1 days per decade, respectively) since 1980. The overall linear trend over the 36-year period is not significant for the Hermit Thrush (*Catharus guttatus*); however, the data show a trend toward earlier arrival beginning in 1995. This response is similar to that of the Golden-crowned Sparrow, which has been arriving at increasingly earlier dates (the data show a significant acceleration in the past two decades). The Fox Sparrow (*Passerella iliaca*) shows no significant linear trend.



Globally, a general trend of earlier arrival of birds migrating in the spring has been reported, associated with warming temperatures and the earlier onset of spring and with it, the emergence of the plant and insect resources the birds rely on (Usui et al., 2017; Herbert and Liang, 2012; Parmesan, 2006). However, there is considerable variation, with different species (or even populations of the same species) exhibiting both earlier and later timing of spring migration. While there are less data on fall migration, some studies have indicated shifts to later arrivals (Jarjour et al., 2017).

Why is this indicator important?

Tracking changes in migratory bird arrivals adds to the body of evidence of how terrestrial species have responded to regional changes in climate. A growing number of studies have examined changes in the timing of migration in recent decades across the Northern Hemisphere. Changes in the timing of spring migration (Marra et al., 2005; MacMynowski et al., 2007; van Buskirk et al., 2009; Ward et al., 2015) and, to a lesser extent fall migration, have been documented (Cotton, 2003; Jenni and Kéry, 2003; Mills, 2005).

The timing of bird arrivals on breeding territories and wintering grounds is a key determinant of reproductive success and survival (Cotton, 2003). To the extent that migrating birds species are adapted to arrive at the optimum stage in the growth season — thus maximizing the availability of resources — shifts in migration timing can be expected to be disadvantageous (Travers et al., 2015). An analysis of changes in spring arrival dates among 48 bird species and the emergence of vegetation (spring “green-up” dates) across North America from 2001-2012 found that both have changed over time, usually in the same direction; however arrival of eastern species increasingly lagged behind greenup, while in the west, where green-up typically shifted later, birds arrived increasingly earlier (Mayor et al., 2017). These findings highlight mismatches in timing that may potentially lead to adverse consequences on bird populations.

Knowledge of how migratory birds are responding to changing climatic conditions is critical in assessing and projecting the impacts of those changes on bird populations. Of particular concern are species or populations that are unable to modify their arrival times; reduced genetic variability due to a decline in their population size could limit their ability to adapt to climate change, potentially hastening further population declines (Hurlbert and Liang, 2012) . A study of changes in spring migration timing among 100 European bird species found that population declines occurred in species that did not advance their spring migration in the period 1990-2000; those with stable or increasing populations advanced their migration considerably (Møller et al., 2008).

This indicator illustrates the value of long-term data, gathered in a systematic way, in revealing trends in spring and fall arrival dates of migratory songbirds. It adds California and western North American observations to the growing body of data describing temporal patterns in bird migration patterns (Seavy et al., in press). Such regional information helps improve the scientific understanding of factors that may be influencing the timing of migration and how these factors may be reflected in global trends. The data presented can serve as a baseline with which to compare future observations and



to develop long-term projections under future climate change scenarios. While there is no definitive explanation for why the responses of the seven species differ, this information can also help inform studies that seek to elucidate the mechanisms and consequences of these phenological changes — particularly studies that examine whether shifts in timing are synchronous with changes in the timing of optimal conditions in breeding or wintering grounds.

What factors influence this indicator?

Bird migrations are seasonal movements between wintering and breeding grounds that allow individuals to take advantage of abundant resources, or to avoid predators or exposure to harsh conditions. As environmental conditions change over time, birds can potentially adjust the timing of migration — a response that reflects the interactions among several intrinsic and extrinsic factors. Migratory birds exhibit seasonal physiological changes in preparation for migration, triggered by environmental cues such as photoperiod (the length of day or night) and temperature (Hurlbert and Liang, 2012).

Researchers have investigated the association between changes in migration timing and a number of factors. Species that migrate more slowly and over short distances, and that occupied broader climatic niches (that is, habitats with a wider range of physical and biological resources) were found to have advanced arrival dates the earliest in a study of 18 common bird species in eastern North America (Hurlbert and Liang, 2012). An analysis of over 70 published studies on the timing of spring migration of 413 species across five continents found that, correlated with warmer spring conditions on arrival grounds, short distance migrants advanced their arrival dates by more than long distance migrants; no relationship was found between species' habitat or diet and arrival time (Usui et al., 2017). In contrast, a study of 19 songbird species in Quebec, Canada from 2005 to 2015 found a significant association between changes in migration timing and feeding habits: 10 of 14 insectivores, and only one of five granivores showed evidence of a shift in migration (Jarjour et al., 2017); overall spring arrival dates shifted earlier, while fall departure dates varied considerably.

As fall temperatures increase, insects and plants may be available as food for longer, delaying fall departure as individuals improve their condition to increase survival during migration (Jarjour et al., 2017) Similarly, some species may be shifting their spring arrival timing in response to climatic conditions at their wintering grounds, which has been shown to affect the physiological condition of migrants and thus their departure dates (Marra et al., 2015).

Environmental conditions in the wintering or breeding grounds, stopover locations along the migration route, or in the final settling location — all of which affect arrival times — may, in turn be affected by factors operating on multiple spatial scales. The variety of factors and the multiplicity of temporal and spatial scales at which birds operate during migration undoubtedly contribute to the considerable inter-annual variation in arrival dates.



The earlier arrival of the Orange-crowned Warbler at Palomarin is not surprising. Earlier onset of spring conditions has been documented over much of the Northern Hemisphere (Root et al., 2005; Parmesan, 2006). This can influence the timing of migration and breeding (Gordo, 2007; Møller et al., 2010; Seavy et al., in press). However, Both and Visser (2001) found that changes in conditions on the breeding grounds influenced laying date but did not lead to changes in spring arrival dates for a long-distance migrant. The contrasting arrival patterns of the two warbler species — both small, insectivorous songbirds in the same taxonomic family — presents a paradox, however, and indicates the need for further research.

In contrast, less research has investigated fall arrival patterns of birds to their wintering grounds (Gallinat et al., 2015). Trends in fall arrival dates likely relate, in part, to spring breeding ground conditions elsewhere: If breeding conditions persist later in the season, fall arrivals could be delayed; if breeding conditions support earlier breeding or if drier conditions result in earlier cessation of breeding, fall arrivals could advance.

The species described here migrate to the Point Reyes area from different wintering or breeding locations. Among the spring arrivals to the Point Reyes area, Swainson's Thrushes (which show no trend in arrival dates) winter predominantly in western Mexico (Cormier et al., 2013); Wilson's Warblers, which have been arriving later, winter in a larger area covering Baja California as well as western Mexico (Ruegg et al., 2014). Baja California and western Mexico are characterized by different wintering habitats that may influence departure timing from the wintering grounds. The migratory pathways of Orange-crowned Warblers have not been documented; while their wintering range includes areas farther north than the other species (Gilbert et al., 2010), the wintering location of the population migrating to Palomarin is unknown.

The four species that arrive in the fall migrate from temperate regions. The Golden-crowned Sparrow (arriving earlier) and Fox Sparrow (no change in arrivals) both breed predominantly in the Gulf of Alaska (Seavy et al., 2012, Cormier et al., 2016; Point Blue unpublished data). The difference in these species' arrival patterns suggests that either conditions on the breeding grounds are not having a direct effect on timing of arrival or that the species are responding differently. Hermit Thrush, whose pattern is similar to Golden-crowned Sparrows (tendency to earlier arrival), breed in the Pacific Northwest, in particular, coastal British Columbia and the Olympic Peninsula of Washington (Nelson et al., 2016). It is not known where the population of Ruby-crowned Kinglets breed, although subspecies-related plumage patterns at Palomarin (Point Blue unpublished data) suggest that the majority are likely from either or both of the above two regions (Pacific Northwest and Gulf of Alaska), with some originating from interior Alaska or Canada (Swanson et al., 2008). Thus it is possible that either finer-scale differences in conditions at breeding grounds or along migratory stopover sites, or differential responses to shared conditions, may be influencing their arrival timing on their wintering grounds.



Technical Considerations

Data Characteristics

The data for this analysis consist of banding records of individual birds captured and marked as part of a constant-effort mist-netting program at the Palomarin Field Station (Ralph et al., 1993; Point Blue, 2016). Although mist-netting was initiated in 1966, the period of analyses was restricted to 1979, when constant-effort mist netting became fully standardized, through fall 2015. Fall 2013 was excluded due to a 15-day October hiatus in banding operations resulting from the federal government shutdown. This provides a 37-year dataset for spring arrivals and 36 years for fall arrivals.

The dataset was restricted to the first capture of each individual in each season. In spring, newly fledged birds were excluded from the analysis, thus all individuals analyzed were approximately 1 year or older; in the fall, all age classes were included, including immature birds that fledged earlier in the year (during the breeding season immediately preceding fall arrival).

The species selected for this analysis were chosen for their migratory status and high capture rates. These species differed somewhat from the previous iteration of this report (OEHHA, 2009), by including analyses of three species not previously reported, namely Hermit Thrush, Golden-crowned Sparrow and Orange-crowned Warbler, and the removal of three species due to modest sample sizes: Black-headed Grosbeak, Warbling Vireo, and Yellow Warbler.

The distribution of first capture dates for each species was assessed to determine species-specific “arrival windows.” The beginning of the arrival window was determined by the first captures; the end of the arrival period was determined by the date at which first captures had declined to relatively low “baseline” levels (see Nur et al., 2017 for details). Any further captures after the arrival window’s end-date were determined to be individuals that likely had been present in the study area but had avoided capture until then. Thus, the arrival window encompassed the first wave of captures during the season in its entirety.

Arrival window dates are as follows:

- Swainson’s Thrush: 6 April – 8 June
- Wilson’s Warbler: 12 March – 29 May
- Orange-crowned Warbler: 20 February – 19 May
- Ruby-crowned Kinglet: 8 September – 15 November
- Hermit Thrush: 13 September – 15 December
- Fox Sparrow: 29 August – 5 November
- Golden-crowned Sparrow: 6 September – 30 November

Of these species, two occur in the region in small numbers year-round. In addition to the overwintering population in this study, a small number of Hermit Thrushes also breed in the region and migrate south in the fall (Phillips, 1991); however, the small number of post-breeding individuals from this population that were captured in early fall did not overlap in time with the window for arrivals from the north. Similarly, in addition to the



breeding population of Orange-crowned Warblers studied here, a relatively small number of individuals winter in the region; again, the capture window allowed those few breeding individuals to be excluded from this study.

None of the species in this study are passage migrants at the Palomarin Field Station; rather, Palomarin is the final stopping location (either for breeding or wintering) for all 7 species. In addition, the arrival window was set to exclude individuals that may have been present at the location for some period of time in order to better identify the timing of the wave of migrants as they first arrive on their wintering or breeding grounds.

The 25th percentile of capture dates during the arrival window was used to track the initial wave of arrival of migrants. Linear models were then fit to the capture dates for each species to analyzing a linear-only trend (reported in Figures 1 and 3). To better analyze changes in trend, quadratic models were also fit to the same data (depicted as blue lines in Figures 1 and 3). Details on data processing and analysis are provided in the companion Technical Report (Nur et al., 2017).

One concern was that a change in population size could result in fewer captures which could affect measures of arrival date. Reduced sample size will bias the metric of the very earliest arrival date (Miller-Rushing et al., 2008). In order to provide a more robust metric, not biased by sample size, the 25th percentile value was used, though other quantiles could have been used, e.g., the median.

Strengths and Limitations of the Data

These data provide a long-term record of bird migration phenology. There were sufficient data to analyze these seven migrant songbirds, including both fall and spring migrants; species included came from four taxonomic families, thus providing taxonomic breadth. The time series is extensive for biological monitoring: 37 years as of 2015.

Monitoring efforts have been strictly standardized since 1979. In general, sampling efforts and net hours per season (where each “net hour” equals a single net open for one hour) have remained relatively stable during the period included in these analyses. Frequency of mist netting was generally three days per week (April through Thanksgiving) or 6 days per week (May through Thanksgiving), weather permitting; one significant change in effort was a switch from banding 6 days/week to 3 days/week in the month of April starting in 1989. This change, as well as the generally small variation in effort in other months due to weather and other variables, was addressed by standardizing the analysis with regard to bird captures per 1000 net hours (a full banding day at Palomarin results in 120 net hours) and pooling captures into 5-day periods.

The 2013 *Indicators of Climate Change in California* Report provided results for four of the seven species analyzed here, using the long-term mist-netting data from the Palomarin Field Station. For one of the species, Swainson’s Thrush, previous results are very similar to what is presented here. However, for the other three species (Wilson’s Warbler, Ruby-crowned Kinglet, and Fox Sparrow) there were noticeable



differences in trend. The principal reason for the differences was that the earlier analysis used 1971-1978 (which, as noted earlier, were excluded here because mist-netting was not fully standardized until 1979), while the current analysis included the years 2006-2015. These more recent years made a substantial difference in characterizing the trend. The bottom line is that most species analyzed demonstrate both year-to-year variability and a trend over time that is not constant over the entire time series and, therefore, two different time intervals can produce two different trend values.

For more information, contact:



Point Blue
Conservation
Science

Nadav Nur, Ph.D.
Point Blue Conservation Science
3820 Cypress Dr. #11
Petaluma, CA 94954
(707) 781-2555 ext. 301
nnur@pointblue.org

Diana Humple
Point Blue Conservation Science
Palomarin Field Station
PO Box 1157 / 999 Mesa Road
Bolinas, CA 94924
(415) 868-0655 ext. 386
dhumple@pointblue.org

Leo Salas, Ph.D.
Point Blue Conservation Science
3820 Cypress Dr. #11
Petaluma, CA 94954
(707) 781-2555 ext. 334
lsalas@pointblue.org

References:

Bitterlin LR, and Van Buskirk J (2014). Ecological and life history correlates of changes in avian migration timing in response to climate change. *Climate Research* **61**(2): 109-121.

Both C and Visser ME (2001). Adjustment to climate change is constrained by arrival date in a long-distance migrant bird. *Nature* **411**: 296–298.

Charmantier A and Gienapp P (2014). Climate change and timing of avian breeding and migration: evolutionary versus plastic changes. *Evolutionary Applications*, **7**(1): 15-28.

Cormier RL, Humple DL, Gardali T and Seavy NE (2013). Light-level geolocators reveal strong migratory connectivity and within winter movements for a coastal California Swainson's Thrush population. *The Auk* **130**(2): 283-290.

Cormier RL, Humple DL, Gardali T and Seavy NE (2016). Migratory connectivity of Golden-crowned Sparrows from two wintering regions in California. *Animal Migration* **3**: 48-56.



Cotton PA (2003). Avian migration phenology and global climate change. *Proceedings of the National Academy of Sciences USA* **100**(21):12219–12222.

Gallinat AS, Primack RB and Wagner DL (2015). Autumn, the neglected season in climate change research. *Trends in Ecology & Evolution* **30**(3):169–176.

Gilbert WM, Sogge MK and Van Riper III C (2010). Orange-crowned Warbler (*Oreothlypis celata*). In: *The Birds of North America*. Rodewald PG (Ed.). Ithaca, NY: Cornell Lab of Ornithology.

Gordo O (2007). Why are bird migration dates shifting? A review of weather and climate effects on avian migratory phenology. *Climate Research* **35**(1-2): 37-58.

Hurlbert AH and Liang Z (2012). Spatiotemporal variation in avian migration phenology: citizen science reveals effects of climate change. *PLoS One* **7**(2):e31662.

Jarjour C, Frei B, Elliott KH (2017). Associations between sex, age and species-specific climate sensitivity in migration. *Animal Migration* **4**: 23-36.

Jenni L and Kéry M (2003). Timing of autumn bird migration under climate change: advances in long-distance migrants, delays in short-distance migrants. *Proceedings of the Royal Society B* **270**(1523): 1467–1471.

Kellermann JL, Enquist CAF, Humple DL, Seavy NE, Rosemartin A, *et al.* (2015). A bird's-eye view of the USA National Phenology Network: an off-the-shelf monitoring program. In: *Phenological synchrony and bird migration: changing climate and seasonal resources in North America*. Wood EM and Kellermann JL (Eds.). Studies in Avian Biology, Number 47. Boca Raton, FL: CRC Press, pp.47-60.

MacMynowski DP, Root TL, Ballard G and Geupel GR (2007). Changes in spring arrival of Nearctic-Neotropical migrants attributed to multiscalar climate. *Global Change Biology* **13**(11): 2239-2251.

Marra PP, Francis CM, Mulvihill RS and Moore FR (2005). The influence of climate on the timing and rate of spring bird migration. *Oecologia* **142**(2): 307–315.

Marra, PP, Studds CE, Wilson S, Sillett TS, Sherry TW and Holmes RT (2015). Non-breeding season habitat quality mediates the strength of density-dependence for a migratory bird. *Proceedings of the Royal Society B* **282**: 20150624.

Mayor SJ, Guralnick RP, Tingley, MW, Otegui J, Withey JC, *et al.* (2017). Increasing phenological asynchrony between spring green-up and arrival of migratory birds. *Scientific Reports* **7**(1).

Miller-Rushing AJ, Lloyd-Evans TL, Primack RB and Satzing P (2008). Bird migration times, climate change, and changing population sizes. *Global Change Biology* **14**(9): 1959-1972.

Mills AM (2005). Changes in the timing of spring and autumn migration in North American migrant passerines during a period of global warming. *Ibis* **147**:259–269.

Møller, AP., Rubolini D, and Lehikoinen E (2008). Populations of migratory bird species that did not show a phenological response to climate change are declining. *Proceedings of the National Academy of Sciences USA*, **105**: 16195–16200.



Møller AP, Fiedler W and Berthold P (2010). *Effects of Climate Change on Birds*. Oxford: Oxford University Press.

Morton ML (2002). *The Mountain White-Crowned Sparrow: Migration and Reproduction at High Altitude*. Studies in Avian Biology, Number 24. Camarillo, CA: Cooper Ornithological Society.

Nelson AR, Cormier RL, Humple DL, Scullen JC, Sehgal R and Seavy NE (2016). Migration patterns of San Francisco Bay Area Hermit Thrushes differ across a fine spatial scale. *Animal Migration* **3**: 1-13.

Nur N, Humple D and Salas L (2017). Migratory Bird Arrivals Indicator Technical Report. Unpublished Report. Available from Point Blue Conservation Science, Petaluma, CA 94954.

Office of Environmental Health Hazard Assessment (2009). *Indicators of Climate Change in California*. Sacramento, CA: California Environmental Protection Agency.

Parmesan C (2006). Ecological and evolutionary responses to recent climate change. *Annual Review of Ecology, Evolution, and Systematics* **37**(1): 637-669.

Phillips AR (1991). *The Known Birds of North and Middle America, Part 2*. Denver, CO.

Point Blue Conservation Science (2016). *The Palomarin Handbook: Point Blue's Landbird Procedures Manual* (16.2 ed).

Porzig EL, Dybala KE, Gardali T, Ballard G, Geupel GR and Wiens JA (2011). Forty-five years and counting: reflections from the Palomarin field station on the contribution of long-term monitoring and recommendations for the future. *The Condor* **113**(4): 713-723.

Ralston J, DeLuca WV, Feldman RE and King DI (2016). Population trends influence species ability to track climate change. *Global Change Biology* **23**(4): 1390-1399.

Ralph C, John G, Geupel GR, Pyle P, Martin T and DeSante D (1993). *Handbook of Field Methods for Monitoring Landbirds* (General Technical Report). Albany, CA: US Department of Agriculture Forest Service Pacific Southwest Research Station.

Root TL, Price JT, Hall KR, Schneider SH, Rosenzweig C and Pounds JA (2003). Fingerprints of global warming on wild animals and plants. *Nature* **421**(6918): 57-60.

Seavy NE, Humple DL, Cormier RL and Gardali T (2012). Establishing the breeding provenance of a temperate-wintering North American passerine, the Golden-crowned Sparrow, using light-level geolocation. *PLoS One* **7**(4): e34886.

Seavy NE, Porzig EL, Cormier RL, Humple DL and Gardali T (*In press*). Evidence of climate change impacts on landbirds in western North America: A review and recommendations for future research. *Studies of Western Birds*.

Swanson DL, Ingold JL and Wallace GE (2008). Ruby-crowned Kinglet (*Regulus calendula*). In: *The Birds of North America*. Rodewald PG (Ed.). Ithaca, NY: Cornell Lab of Ornithology.

Travers SE, Marquardt M, Zerr NJ, Finch JB, Boche MJ, et al. (2015). Climate change and shifting arrival date of migratory birds over a century in the northern Great Plains. *The Wilson Journal of Ornithology* **127**(1):43-51.



Usui T, Butchart SHM and Phillimore AB (2017). Temporal shifts and temperature sensitivity of avian spring migratory phenology: a phylogenetic meta-analysis. *Journal of Animal Ecology* **86**(2): 250-261.

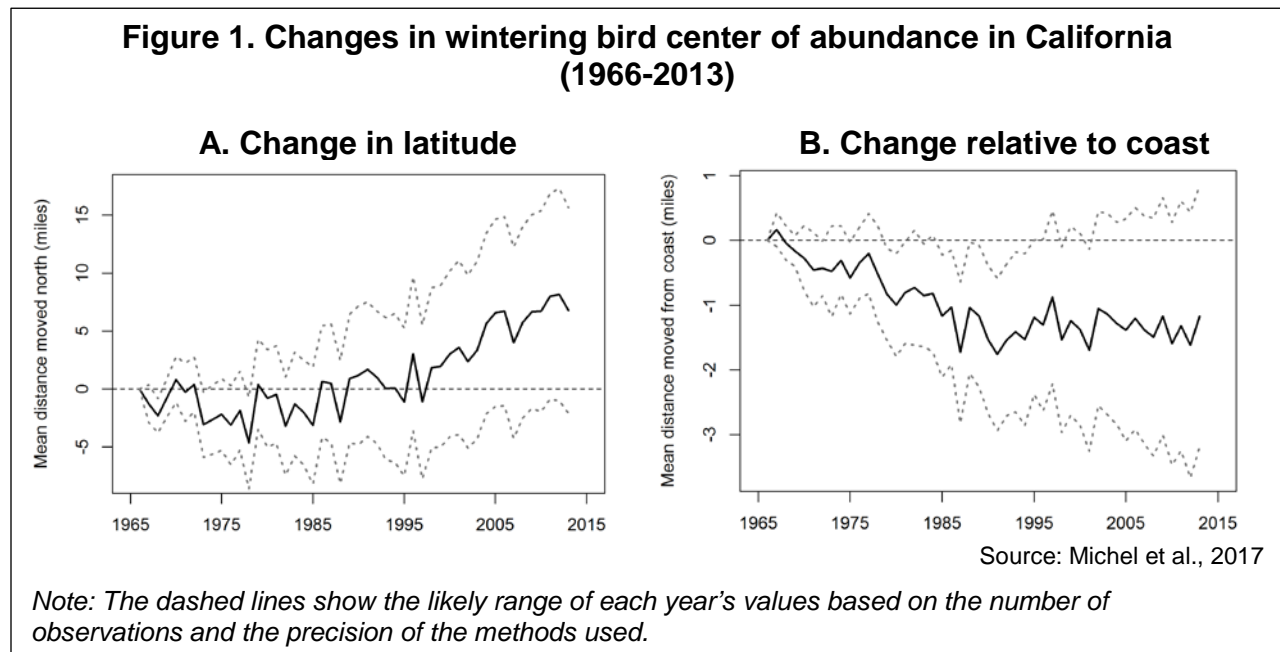
Van Buskirk J, Mulvihill RS and Leberman RC (2009). Variable shifts in spring and autumn migration phenology in North American songbirds associated with climate change. *Global Change Biology* **15**(3): 760–771.

Ward DH, Helmericks J, Hupp JW, McManus L, Budde M, et al. (2015). Multi-decadal trends in spring arrival of avian migrants to the central Arctic coast of Alaska: effects of environmental and ecological factors. *Journal of Avian Biology* **46**(2):197–207.



BIRD WINTERING RANGES

Over the past 48 years, wintering bird species have collectively shifted their range northward and closer to the coast in California.



What does the indicator show?

This indicator examines changes in the ranges of 234 migratory and resident wintering California bird species between 1966 and 2013 and shows, in aggregate, a shift northward. Data for this indicator are the California subset of observations from the Christmas Bird Count (CBC), managed by the National Audubon Society. The CBC consists of observations recorded from December 14 to January 5 each year by over 50,000 volunteers across the Western Hemisphere, following a specified methodology. It is the longest-running census of birds that relies on public participation and collaboration (often referred to as “citizen science”).

The graphs show the position of the center of abundance (the center of the population distribution) for each year relative to the winter of 1965-1966, averaged across the species for latitude (Figure 1A) and for distance from the coast (Figure 1B). An overall northward movement of about seven miles was observed between 1966 and 2013, as birds moved a farther distance north than south (Figure 1A). Over the same time period, a shift of approximately 1 mile toward the coast occurred (Figure 1B).

The center of abundance is a common way to characterize the general location of a population. In terms of latitude, half of the individuals in the population live north of the center of abundance and the other half live to the south. Similarly, in terms of distance to coast, half of the individuals live closer to the coast than the center of abundance, and the other half live further from the coast.



Why is this indicator important?

Monitoring changes in the geographic distribution of birds provides scientists with a way to track which birds may be responding to a changing climate — one of many factors that are threatening bird populations. A better understanding of these responses will help inform conservation strategies. As the climate continues to change, its pace may exceed many bird species' capacities to migrate to more favorable habitats (La Sorte and Jetz, 2012). The predicted increase in extreme weather events, such as severe storms, might also impact the ability of birds to make these range shifts. Birds that cannot adapt to changing conditions could experience a population decline as a result.

Birds are a particularly good indicator of environmental change for several reasons:

- Each species of bird has adapted or evolved to favor certain habitat types, food sources, and temperature ranges. In addition, the timing of certain events in their life cycles — such as migration and reproduction — is driven by cues from the environment. For example, many North American breeding birds follow a regular seasonal migration pattern; moving north to feed and breed in the summer, then moving south to spend the winter in warmer areas. Changing conditions can influence the distribution of both migratory and non-migratory birds as well as the timing of important life cycle events (La Sorte and Thompson, 2007).
- Birds are relatively easy to identify and count, and thus there is a wealth of scientific knowledge about their distribution and abundance. People have kept detailed records of bird observations for more than a century.
- There are many different species of birds living in a variety of habitats, including water birds, coastal birds, and land birds. If a change in behavior or range occurs across a range of bird types, it suggests that a common external factor might be the cause.

When bird wintering ranges shift, human and ecological communities lose not just the birds themselves, but also the valuable functions and services they provide. For example, western bluebirds eat insects that damage crops, nectar-eating birds like hummingbirds pollinate flowers, and birds like woodpeckers build roosting cavities in trees that other bird and mammal species use (Kearns et al., 1998; Sekercioglu, 2006; Jedlicka et al., 2011). The movement of a species to places where it was not previously present, or where it was present in lower numbers, may also disrupt complex ecosystem interactions. For example, a newcomer species may compete for food or other resources with species that already inhabit the area (Kearns and Inouye, 1997).

What factors influence this indicator?

In the Northern Hemisphere, a changing climate has been associated with shifts in the habitat ranges of certain animals toward more northern latitudes and higher elevations (Field et al., 2014; Ralston et al., 2016; Moritz et al., 2008). Warming temperatures may cause species to expand their wintering ranges further north into regions that were, until recently, too cold to support populations, and away from regions that are now too hot.



A continental-scale analysis of 305 bird species found that their wintering ranges moved approximately 40 miles north between 1966 and 2013, and that this change was related to warming winter temperatures (National Audubon Society, 2009; USEPA, 2013). In California, the seven-mile northward shift in bird wintering ranges was found to be closely associated with warmer minimum December temperatures.

The movement of species toward the coast in California is the opposite of both what was expected and what was observed in the continental-scale study. The latter analysis found that bird wintering ranges moved about 13 miles away from the coast — a shift associated with a warming climate and a decrease of extreme cold inland. In California, in contrast, birds moved closer to the coast as temperatures increased. The California trend may be the result of the combined influence of climate and topography. Inland areas of the state, already drier compared to the coast, are further drying due to warming temperatures, causing birds to move towards the coast to seek wetter conditions.

Both the continental and the California analysis found no significant longitudinal movement. This is not surprising given that there are no clear longitudinal gradients in temperature or precipitation, which instead vary in response to topographical features (e.g., elevation or location relative to mountain ranges).

Latitudinal range movement varied among the California species: 87 species (37 percent) moved northward, 74 species (32 percent) moved southward, and 73 (31 percent) showed no significant change. Some bird species moved farther than others. Snow goose showed the greatest northward shift of 326 miles, while Ross' goose showed the greatest southward shift of 242 miles. Similarly, distance shifted relative to the coast ranged from 84 miles towards the coast by Canada goose to 60 miles inland by Barrow's goldeneye. Eighty-six species (37 percent) moved towards the coast, while 86 other species moved inland and 62 (26 percent) showed no significant change. While equal numbers of species moved inland and towards the coast, the range shifts towards the coast involved greater distances than inland, resulting in an overall shift toward the coast. These differences in range shifts are not surprising. Species have been found to respond to environmental change in a highly variable and idiosyncratic fashion, reflecting the complex interplay between land cover, climate, species interactions, and other factors.

Many factors can influence bird ranges, including food availability, habitat alteration, and interactions with other species, and these factors may also be influenced by climate change. Some of the birds covered in this indicator might have moved northward or inland for reasons other than changing temperatures. Responses to climate change may also vary among different types of birds. However, within California, there were no differences in average movements north or towards the coast between birds differing in habitat use, diet, body size, life expectancy, clutch size, age at sexual maturity, or urban affiliation. Though moderate- and short-distance migrants moved slightly further north than year-round residents, migratory status did not influence movement towards the coast.



Technical Considerations

Data Characteristics

This indicator is based on data collected by the annual Christmas Bird Count (CBC), managed by the National Audubon Society. Data are collected in a citizen science activity by volunteer birdwatchers who systematically survey certain areas and identify and count all bird species they encounter within a specified area. Bird surveys take place each year in approximately 2,000 different locations throughout the contiguous 48 states and the southern portions of Alaska and Canada. This indicator used only data from CBC circles within the state of California. All local counts take place between December 14 and January 5 of each winter. Each local count takes place over a 24-hour period in a defined “count circle” that is 15 miles in diameter. A variable number of volunteer observers separate into field parties which survey different areas of the count circle and tally the total number of individuals of each species observed (National Audubon Society, 2009).

CBC data starting in 1966 are used, as data prior to 1966 lack sufficient quality and quantity for a North American-scaled analysis. At the end of the 24-hour observation period, each count circle tallies the total number of individuals of each species seen in the count circle. Audubon scientists then run the data through several levels of analysis and quality control to determine final count numbers from each circle and each region. Data processing steps include corrections for different levels of sampling effort — for example, if some count circles had more observers and more person-hours of effort than others. Population trends over the 48-year period of this indicator and annual indices of abundance were estimated for the entire survey area with hierarchical models in a Bayesian analysis using Markov chain Monte Carlo techniques (Soykan et al., 2016).

This indicator covers 234 bird species, listed in Table 1 (Appendix). These species were included because they are widespread, occur within California, and meet specific criteria for data availability. Information on study methods is available on the National Audubon Society website at: <http://web4.audubon.org/bird/bacc/techreport.html> and in Soykan et al. (2016). Methods are largely based on those used for an earlier analysis, which is documented in the National Audubon Society (2009) report: *Northward Shifts in the Abundance of North American Birds in Early Winter: A Response to Warmer Winter Temperatures?*. For additional information on CBC survey design and methods, see Soykan et al. (2016) and the reports classified as “Methods” in the list at: <http://www.audubon.org/conservation/christmas-bird-count-bibliography>.

Strengths and Limitations of the Data

Although the indicator relies on human observation rather than precise measuring instruments, the people who collect the data are skilled observers who follow strict protocols that are consistent across time and space. These data have supported many peer-reviewed studies, a list of which can be found on the National Audubon Society’s website at <http://www.audubon.org/christmas-bird-count-bibliography>.



Data Characteristics

This indicator is based on data collected by the annual Christmas Bird Count (CBC), managed by the National Audubon Society. Data are collected in a citizen science activity by volunteer birdwatchers who systematically survey certain areas and identify and count all bird species they encounter within a specified area. Bird surveys take place each year in approximately 2,000 different locations throughout the contiguous 48 states and the southern portions of Alaska and Canada. This indicator used only data from CBC circles within the state of California. All local counts take place between December 14 and January 5 of each winter. Each local count takes place over a 24-hour period in a defined “count circle” that is 15 miles in diameter. A variable number of volunteer observers separate into field parties which survey different areas of the count circle and tally the total number of individuals of each species observed (National Audubon Society, 2009).

CBC data starting in 1966 are used, as data prior to 1966 lack sufficient quality and quantity for a North American-scaled analysis. At the end of the 24-hour observation period, each count circle tallies the total number of individuals of each species seen in the count circle. Audubon scientists then run the data through several levels of analysis and quality control to determine final count numbers from each circle and each region. Data processing steps include corrections for different levels of sampling effort — for example, if some count circles had more observers and more person-hours of effort than others. Population trends over the 48-year period of this indicator and annual indices of abundance were estimated for the entire survey area with hierarchical models in a Bayesian analysis using Markov chain Monte Carlo techniques (Soykan et al., 2016).

This indicator covers 234 bird species, listed in Table 1 (Appendix). These species were included because they are widespread, occur within California, and meet specific criteria for data availability. Information on study methods is available on the National Audubon Society website at: <http://web4.audubon.org/bird/bacc/techreport.html> and in Soykan et al. (2016). Methods are largely based on those used for an earlier analysis, which is documented in the National Audubon Society (2009) report: *Northward Shifts in the Abundance of North American Birds in Early Winter: A Response to Warmer Winter Temperatures?*. For additional information on CBC survey design and methods, see Soykan et al. (2016) and the reports classified as “Methods” in the list at: <http://www.audubon.org/conservation/christmas-bird-count-bibliography>.

Strengths and Limitations of the Data

Although the indicator relies on human observation rather than precise measuring instruments, the people who collect the data are skilled observers who follow strict protocols that are consistent across time and space. These data have supported many peer-reviewed studies, a list of which can be found on the National Audubon Society's website at <http://www.audubon.org/christmas-bird-count-bibliography>.

Uneven effort between count circles, such as inconsistent level of effort by volunteer observers, could lead to data variations. However, these differences are carefully



corrected in Audubon's statistical analysis (Soykan et al., 2016). Rare or difficult-to-observe bird species could lead to increased variability. Gregarious species (i.e., species that tend to gather in large groups) can also be difficult to count, and they could be either overcounted or undercounted, depending on group size and the visibility of their roosts. These species tend to congregate in known and expected locations along CBC routes, however, so observers virtually always know to check these spots. Locations with large roosts are often assigned to observers with specific experience in estimating large numbers of birds. For this analysis, the National Audubon Society included only 234 widespread bird species that met criteria for abundance and the availability of data to enable the detection of meaningful trends.

The tendency for saltwater-dependent species to stay near coastlines could impact the change in distance to coast calculation for species living near the Pacific Ocean. By integrating these species into the distance to coast calculation, Figure 2 may understate the total extent of coastward or inland movement of species.

This indicator is based solely on shifts in the center of abundance of birds observed within the state of California. As a result, it represents only a small portion of the wintering range of many species, and may either overestimate or underestimate distances moved across the species' entire wintering ranges.

Figures 1 and 2 show average distances moved north and towards the coast, based on an unweighted average of all species. Thus, no adjustments are made for population differences across species. No attempt was made to estimate trends prior to 1966 (i.e., prior to the availability of complete spatial coverage and standardized methods), and no attempt was made to project trends into the future. The entire study description, including analyses performed, can be found in National Audubon Society (2009), Soykan et al. (2016), and references therein. Information on this study is also available on the National Audubon Society website at: <http://web4.audubon.org/bird/bacc/techreport.html>.

For more information, contact:



Nicole Michel, Ph.D.
Senior Quantitative Ecologist
National Audubon Society
220 Montgomery St, Suite 1000
San Francisco, CA 94104
415.644.4611
nmichel@audubon.org



References:

- Field CB, Barros VR, Mach KJ, Mastrandrea MD, van Aalst M, et al. (2014). *Technical summary*. In: *Climate Change 2014: Impacts, Adaptation, and Vulnerability. Part A: Global and Sectoral Aspects. Contribution of Working Group II to the Fifth Assessment Report of the Intergovernmental Panel on Climate Change* [Field CB, Barros VR, Dokken DJ, Mach KJ, Mastrandrea MD et al. (Eds.)]. Cambridge University Press, Cambridge, United Kingdom and New York, NY, USA, pp. 35-94.
http://www.ipcc.ch/pdf/assessment-report/ar5/wg2/WGIIAR5-TS_FINAL.pdf
- Jedlicka HA, Greenberg R, and Letourneau DK (2011). Avian Conservation Practices Strengthen Ecosystem Services in California Vineyards. *PLoS ONE* **6**(11):e27347.
- Kearns CA and Inouye DW (1997). Pollinators, flowering plants, and conservation biology. *Bioscience* **47**(5): 297-307.
- Kearns CA, Inouye DW and Waser NM (1998). Endangered mutualisms: the conservation of plant-pollinator interactions. *Annual Review of Ecology and Systematics* **29**: 83-112.
- La Sorte FA and Thompson FR (2007). Poleward shifts in winter ranges of North American birds. *Ecology* **88**: 1803–1812.
- La Sorte FA and Jetz W (2012). Tracking of climatic niche boundaries under recent climate change. *Journal of Animal Ecology* **81**(4): 914–925.
- Michel NL, Soykan CU, Niven D, Sauer J, Schuetz JG, et al. (2017). Winter range shifts by California birds over 48 years. Unpublished analysis of data from: Soykan CU, Sauer J, Schuetz JG, LeBaron GS, Dale K, and Langham GM (2016). Population trends for North American winter birds based on hierarchical models. *Ecosphere* **7**(5): e01351.
- Moritz C, Patton JL, Conroy CJ, Parra JL, White GC and Beissinger SR (2008). Impact of a century of climate change on small-mammal communities in Yosemite National Park, USA. *Science* **322**(5899): 261-264.
- National Audubon Society (2009). Northward shifts in the abundance of North American birds in early winter: A response to warmer winter temperatures? Retrieved October 11, 2017 from <http://web4.audubon.org/bird/bacc/techreport.html>.
- Ralston J, Deluca W, Feldman RE and King D (2016). Population trends influence species ability to track climate change. *Global Change Biology* **23**(4): 1390-1399.
- Sekercioglu C (2006). Increasing awareness of avian ecological function. *Trends in Ecology and Evolution* **21**: 464-471.
- Soykan CU, Sauer J, Schuetz JG, LeBaron GS, Dale K and Langham GM (2016). Population trends for North American winter birds based on hierarchical models. *Ecosphere* **7**(5): e01351.
- US EPA (2016). US Environmental Protection Agency: Climate Change Indicators—Bird Wintering Ranges. Retrieved August, 2017 from <https://www.epa.gov/climate-indicators/climate-change-indicators-bird-wintering-ranges>



APPENDIX

Table 1. Bird species included in the California wintering bird range shift climate change indicator analysis.

Common name	Scientific name
Acorn Woodpecker	<i>Melanerpes formicivorus</i>
American Avocet	<i>Recurvirostra americana</i>
American Bittern	<i>Botaurus lentiginosus</i>
American Coot	<i>Fulica americana</i>
American Crow	<i>Corvus brachyrhynchos</i>
American Dipper	<i>Cinclus mexicanus</i>
American Goldfinch	<i>Spinus tristis</i>
American Kestrel	<i>Falco sparverius</i>
American Pipit	<i>Anthus rubescens</i>
American Robin	<i>Turdus migratorius</i>
American Wigeon	<i>Anas americana</i>
Anna's Hummingbird	<i>Calypte anna</i>
Arctic and Pacific Loon ^{fl}	<i>Gavia arctica and G. pacifica</i>
American Tree Sparrow	<i>Spizelloides arborea</i>
American White Pelican	<i>Pelecanus erythrorhynchos</i>
Bald Eagle	<i>Haliaeetus leucocephalus</i>
Baltimore Oriole	<i>Icterus galbula</i>
Band-tailed Pigeon	<i>Patagioenas fasciata</i>
Barrow's Goldeneye	<i>Bucephala islandica</i>
Barn Owl	<i>Tyto alba</i>
Bell's and Sagebrush Sparrow ^{††}	<i>Amphispiza belli and A. nevadensis</i>
Belted Kingfisher	<i>Megaceryle alcyon</i>
Bewick's Wren	<i>Thryomanes bewickii</i>
Black-and-white Warbler	<i>Mniotilta varia</i>
Black-bellied Plover	<i>Pluvialis squatarola</i>
Black-billed Magpie	<i>Pica hudsonia</i>
Black-capped Chickadee	<i>Poecile atricapillus</i>
Black-crowned Night-Heron	<i>Nycticorax</i>
Blue-gray Gnatcatcher	<i>Polioptila caerulea</i>
Blue-headed, Cassin's, and Plumbeous Vireo ^{†††}	<i>Vireo solitarius, V. cassini, and V. plumbeus</i>
Blue-winged Teal	<i>Anas discors</i>
Brown-headed Cowbird	<i>Molothrus ater</i>
Black Brant	<i>Branta b. nigricans</i>
Black Phoebe	<i>Sayornis nigricans</i>
Black Rail	<i>Laterallus jamaicensis</i>
Black Scoter	<i>Melanitta americana</i>
Black Turnstone	<i>Arenaria melanocephala</i>
Black-necked Stilt	<i>Himantopus mexicanus</i>
Bonaparte's Gull	<i>Chroicocephalus philadelphia</i>
Brewer's Blackbird	<i>Euphagus cyanocephalus</i>



Common name	Scientific name
Brown Creeper	<i>Certhia americana</i>
Bufflehead	<i>Bucephala albeola</i>
Burrowing Owl	<i>Athene cunicularia</i>
Bushtit	<i>Psaltriparus minimus</i>
Cackling and Canada Goose [†]	<i>Branta hutchinsii</i> and <i>B. canadensis</i>
Cactus Wren	<i>Campylorhynchus brunneicapillus</i>
California and Canyon/Brown Towhee [#]	<i>Melospiza crissalis</i> and <i>M. fuscus</i>
California Gull	<i>Larus californicus</i>
California Quail	<i>Callipepla californica</i>
Canvasback	<i>Aythya valisineria</i>
Canyon Wren	<i>Catherpes mexicanus</i>
Caspian Tern	<i>Hydroprogne caspia</i>
Cassin's Finch	<i>Haemorhous cassinii</i>
Cattle Egret	<i>Bubulcus ibis</i>
Cedar Waxwing	<i>Bombycilla cedrorum</i>
Chestnut-backed Chickadee	<i>Poecile rufescens</i>
Chipping Sparrow	<i>Spizella passerina</i>
Chukar	<i>Alectoris chukar</i>
Cinnamon Teal	<i>Anas cyanoptera</i>
Clapper Rail	<i>Rallus crepitans</i>
Clark's Nutcracker	<i>Nucifraga columbiana</i>
Clark's and Western Grebe ^{§§§}	<i>Aechmophorus clarkii</i> and <i>A. occidentalis</i>
Common Goldeneye	<i>Bucephala clangula</i>
Common Ground-Dove	<i>Columbina passerina</i>
Common Loon	<i>Gavia immer</i>
Common Merganser	<i>Mergus merganser</i>
Common Moorhen	<i>Gallinula galeata</i>
Common Murre	<i>Uria aalge</i>
Common Raven	<i>Corvus corax</i>
Common Yellowthroat	<i>Geothlypis trichas</i>
Cooper's Hawk	<i>Accipiter cooperii</i>
Dark-eyed Junco	<i>Junco h. hyemalis</i>
Double-crested Cormorant	<i>Phalacrocorax auritus</i>
Downy Woodpecker	<i>Picoides pubescens</i>
Dunlin	<i>Calidris alpina</i>
Eared Grebe	<i>Podiceps nigricollis</i>
Eastern and Spotted Towhee ^{‡‡}	<i>Pipilo erythrophthalmus</i> and <i>P. maculatus</i>
Eastern and Western Screech-Owl ^{¶¶¶¶}	<i>Megascops asio</i> and <i>M. kennicottii</i>
European Starling	<i>Sturnus vulgaris</i>
Evening Grosbeak	<i>Coccothraustes vespertinus</i>
Ferruginous Hawk	<i>Buteo regalis</i>
Forster's Tern	<i>Sterna forsteri</i>
Fox Sparrow	<i>Passerella iliaca</i>
Gadwall	<i>Anas strepera</i>
Gambel's Quail	<i>Callipepla gambelii</i>



Common name	Scientific name
Glaucous Gull	<i>Larus hyperboreus</i>
Glaucous-winged Gull	<i>Larus glaucescens</i>
Golden Eagle	<i>Aquila chrysaetos</i>
Golden-crowned Kinglet	<i>Regulus satrapa</i>
Golden-crowned Sparrow	<i>Zonotrichia atricapilla</i>
Gray Jay	<i>Perisoreus canadensis</i>
Great Blue Heron	<i>Ardea herodias</i>
Great Egret	<i>Ardea alba</i>
Great Horned Owl	<i>Bubo virginianus</i>
Greater Roadrunner	<i>Geococcyx californianus</i>
Greater Scaup	<i>Aythya marila</i>
Greater White-fronted Goose	<i>Anser albifrons</i>
Greater Yellowlegs	<i>Tringa melanoleuca</i>
Green Heron	<i>Butorides virescens</i>
Green-tailed Towhee	<i>Pipilo chlorurus</i>
Green-winged Teal	<i>Anas crecca</i>
Hairy Woodpecker	<i>Picoides villosus</i>
Harlequin Duck	<i>Histrionicus histrionicus</i>
Harris's Sparrow	<i>Zonotrichia querula</i>
Hermit Thrush	<i>Catharus guttatus</i>
Herring Gull	<i>Larus argentatus</i>
Hooded Merganser	<i>Lophodytes cucullatus</i>
Horned Grebe	<i>Podiceps auritus</i>
Horned Lark	<i>Eremophila alpestris</i>
House Finch	<i>Haemorhous mexicanus</i>
House Sparrow	<i>Passer domesticus</i>
House Wren	<i>Troglodytes aedon</i>
Hutton's Vireo	<i>Vireo huttoni</i>
Iceland and Thayer's Gull §	<i>Larus glaucoides and L. thayeri</i>
Inca Dove	<i>Columbina inca</i>
Juniper and Oak Titmouse##	<i>Baeolophus ridgwayi and B. inornatus</i>
Killdeer	<i>Charadrius vociferus</i>
Ladder-backed Woodpecker	<i>Picoides scalaris</i>
Lapland Longspur	<i>Calcarius lapponicus</i>
Lark Sparrow	<i>Chondestes grammacus</i>
Least Bittern	<i>Ixobrychus exilis</i>
Least Sandpiper	<i>Calidris minutilla</i>
Lesser Goldfinch	<i>Spinus psaltria</i>
Lesser Scaup	<i>Aythya affinis</i>
Lesser Yellowlegs	<i>Tringa flavipes</i>
Lewis's Woodpecker	<i>Melanerpes lewis</i>
Lincoln's Sparrow	<i>Melospiza lincolni</i>
Little Blue Heron	<i>Egretta caerulea</i>
Loggerhead Shrike	<i>Lanius ludovicianus</i>
Long-billed Dowitcher	<i>Limnodromus scolopaceus</i>



Common name	Scientific name
Long-eared Owl	<i>Asio otus</i>
Long-tailed Duck	<i>Clangula hyemalis</i>
Marbled Godwit	<i>Limosa fedoa</i>
Marbled Murrelet	<i>Brachyramphus marmoratus</i>
Marsh Wren	<i>Cistothorus palustris</i>
Merlin	<i>Falco columbarius</i>
Mew Gull	<i>Larus canus</i>
Mountain Bluebird	<i>Sialia currucoides</i>
Mountain Chickadee	<i>Poecile gambeli</i>
Mourning Dove	<i>Zenaida macroura</i>
Nashville Warbler	<i>Oreothlypis ruficapilla</i>
Northern Cardinal	<i>Cardinalis cardinalis</i>
Northern Goshawk	<i>Accipiter gentilis</i>
Northern Harrier	<i>Circus cyaneus</i>
Northern Flicker	<i>Colaptes a. cafer</i>
Northern Mockingbird	<i>Mimus polyglottos</i>
Northern Pintail	<i>Anas acuta</i>
Northern Pygmy-Owl	<i>Glaucidium gnoma</i>
Northern Saw-whet Owl	<i>Aegolius acadicus</i>
Northern Shoveler	<i>Anas clypeata</i>
Northern Shrike	<i>Lanius excubitor</i>
Orange-crowned Warbler	<i>Oreothlypis celata</i>
Osprey	<i>Pandion haliaetus</i>
Palm Warbler	<i>Setophaga palmarum</i>
Pelagic Cormorant	<i>Phalacrocorax pelagicus</i>
Peregrine Falcon	<i>Falco peregrinus</i>
Pied-billed Grebe	<i>Podilymbus podiceps</i>
Pileated Woodpecker	<i>Dryocopus pileatus</i>
Pine Siskin	<i>Spinus pinus</i>
Pinyon Jay	<i>Gymnorhinus cyanocephalus</i>
Prairie Falcon	<i>Falco mexicanus</i>
Purple Finch	<i>Haemorhous purpureus</i>
Pygmy Nuthatch	<i>Sitta pygmaea</i>
Red Crossbill	<i>Loxia curvirostra</i>
Redhead	<i>Aythya americana</i>
Red Knot	<i>Calidris canutus</i>
Red-breasted Merganser	<i>Mergus serrator</i>
Red-breasted Nuthatch	<i>Sitta canadensis</i>
Red-necked Grebe	<i>Podiceps grisegena</i>
Red-shouldered Hawk	<i>Buteo lineatus</i>
Red-winged Blackbird	<i>Agelaius phoeniceus</i>
Ring-billed Gull	<i>Larus delawarensis</i>
Ring-necked Duck	<i>Aythya collaris</i>
Ring-necked Pheasant	<i>Phasianus colchicus</i>
Rock Sandpiper	<i>Calidris ptilocnemis</i>



Common name	Scientific name
Rock Wren	<i>Salpinctes obsoletus</i>
Ross's Goose	<i>Chen rossii</i>
Rough-legged Hawk	<i>Buteo lagopus</i>
Royal Tern	<i>Thalasseus maximus</i>
Ruby-crowned Kinglet	<i>Regulus calendula</i>
Ruddy Turnstone	<i>Arenaria interpres</i>
Rufous-crowned Sparrow	<i>Aimophila ruficeps</i>
Sanderling	<i>Calidris alba</i>
Sandhill Crane	<i>Antigone canadensis</i>
Savannah Sparrow	<i>Passerculus sandwichensis</i>
Say's Phoebe	<i>Sayornis saya</i>
Semipalmated Plover	<i>Charadrius semipalmatus</i>
Sharp-shinned Hawk	<i>Accipiter striatus</i>
Short-billed Dowitcher	<i>Limnodromus griseus</i>
Short-eared Owl	<i>Asio flammeus</i>
Snow Goose	<i>Chen caerulescens</i>
Snowy Egret	<i>Egretta thula</i>
Snowy Plover	<i>Charadrius nivosus</i>
Song Sparrow	<i>Melospiza melodia</i>
Sora	<i>Porzana carolina</i>
Spotted Sandpiper	<i>Actitis macularius</i>
Steller's Jay	<i>Cyanocitta stelleri</i>
Surfbird	<i>Calidris virgata</i>
Surf Scoter	<i>Melanitta perspicillata</i>
Swamp Sparrow	<i>Melospiza georgiana</i>
Townsend's Solitaire	<i>Myadestes townsendi</i>
Townsend's Warbler	<i>Setophaga townsendi</i>
Tree Swallow	<i>Tachycineta bicolor</i>
Tricolored Heron	<i>Egretta tricolor</i>
Tundra Swan	<i>Cygnus columbianus</i>
Turkey Vulture	<i>Cathartes aura</i>
Varied Thrush	<i>Ixoreus naevius</i>
Verdin	<i>Auriparus flaviceps</i>
Vermilion Flycatcher	<i>Pyrocephalus rubinus</i>
Vesper Sparrow	<i>Pooecetes gramineus</i>
Virginia Rail	<i>Rallus limicola</i>
Western Bluebird	<i>Sialia mexicana</i>
Western Meadowlark	<i>Sturnella neglecta</i>
Western Scrub-Jay	<i>Aphelocoma californica</i>
Whimbrel	<i>Numenius phaeopus</i>
White-breasted Nuthatch	<i>Sitta carolinensis</i>
White-crowned Sparrow	<i>Zonotrichia leucophrys</i>
White-tailed Kite	<i>Elanus leucurus</i>
White-throated Sparrow	<i>Zonotrichia albicollis</i>
White-winged Dove	<i>Zenaida asiatica</i>



Common name	Scientific name
White-winged Scoter	<i>Melanitta fusca</i>
Wild Turkey	<i>Meleagris gallopavo</i>
Willet	<i>Tringa semipalmata</i>
Williamson's Sapsucker	<i>Sphyrapicus thyroideus</i>
Wilson's Snipe	<i>Gallinago delicata</i>
Wilson's Warbler	<i>Cardellina pusilla</i>
Winter Wren	<i>Troglodytes hiemalis</i>
Wood Duck	<i>Aix sponsa</i>
Yellow-bellied Sapsucker	<i>Sphyrapicus varius</i>
Yellow-headed Blackbird	<i>Xanthocephalus xanthocephalus</i>
Yellow-rumped Warbler	<i>Setophaga coronata</i>

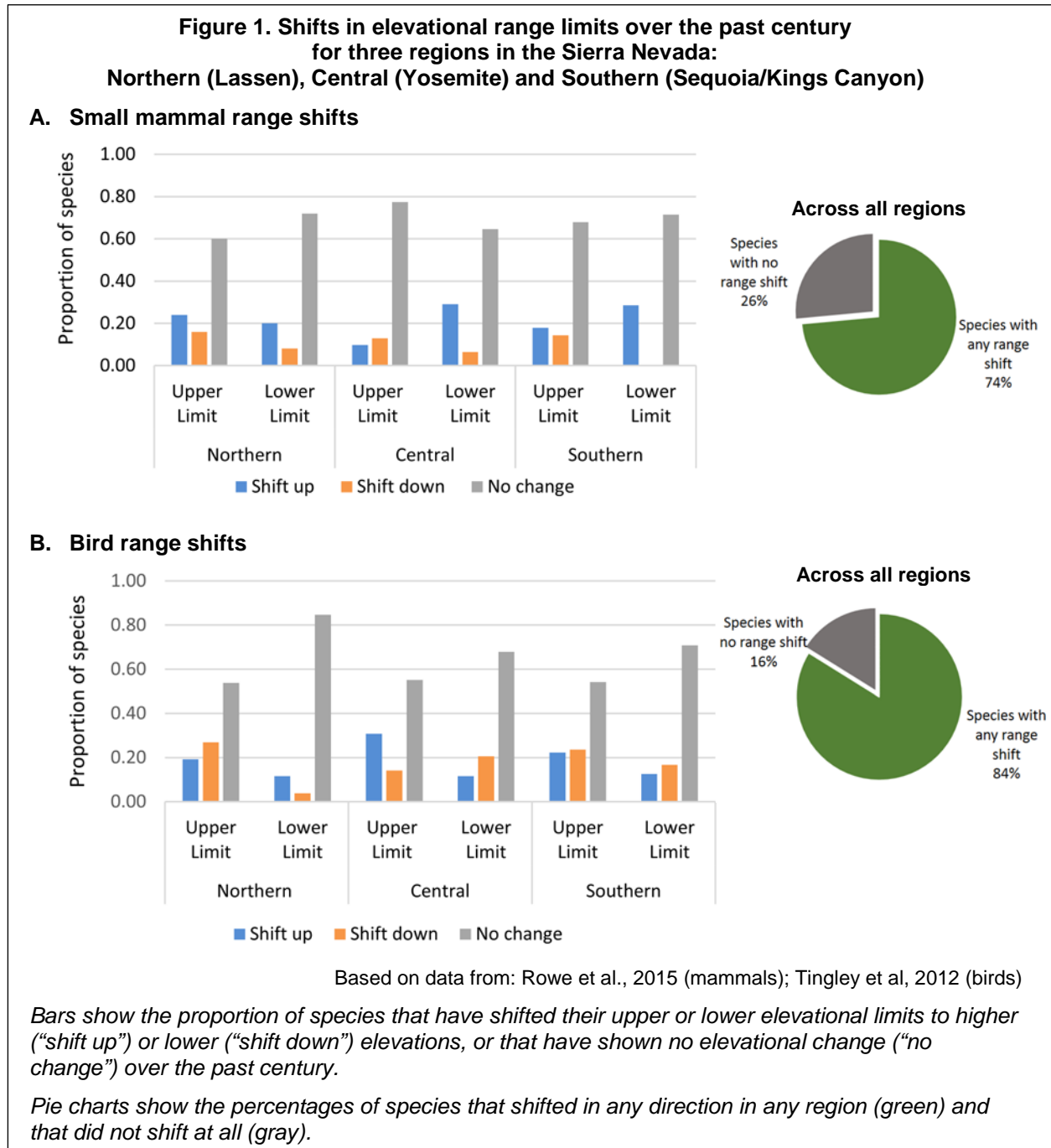
Notes:

- † Since the Cackling and Canada Goose (*Branta hutchinsii* and *B. canadensis*) were not distinguished in CBC counts until after 1966, the two species were lumped for trend analyses.
- § Since the Iceland and Thayer's Gull (*Larus glaucooides* and *L. thayeri*) were not distinguished in CBC counts until after 1966, the two species were lumped for trend analyses.
- ¶ Since the Arctic and Pacific Loon (*Gavia arctica* and *G. pacifica*) were not distinguished in CBC counts until after 1966, the two species were lumped for trend analyses.
- # Since the California and Canyon/Brown Towhee (*Melospiza crissalis* and *M. fuscus*) were not distinguished in CBC counts until after 1966, the two species were lumped for trend analyses.
- ‡ Since the Eastern and Spotted Towhee (*Pipilo erythrophthalmus* and *P. maculatus*) were not distinguished in CBC counts until after 1966, the two species were lumped for trend analyses.
- †† Since the Bell's and Sagebrush Sparrow (*Amphispiza belli* and *A. nevadensis*) were not distinguished in CBC counts until after 1966, the two species were lumped for trend analyses.
- ## Since the Juniper and Oak Titmouse (*Baeolophus ridgwayi* and *B. inornatus*) were not distinguished in CBC counts until after 1966, the two species were lumped for trend analyses.
- ‡‡ Since the Blue-headed, Cassin's, and Plumbeous Vireo (*Vireo solitarius*, *V. cassinii*, and *V. plumbeus*) were not distinguished in CBC counts until after 1966, the three species were lumped for trend analyses.
- §§§ Since the Clark's and Western Grebe (*Aechmophorus clarkii* and *A. occidentalis*) were not distinguished in CBC counts until after 1966, the two species were lumped for trend analyses.
- ¶¶¶ Since the Eastern and Western Screech-Owl (*Megascops asio* and *M. kennicottii*) were not distinguished in CBC counts until after 1966, the two species were lumped for trend analyses.



SMALL MAMMAL AND AVIAN RANGE SHIFTS

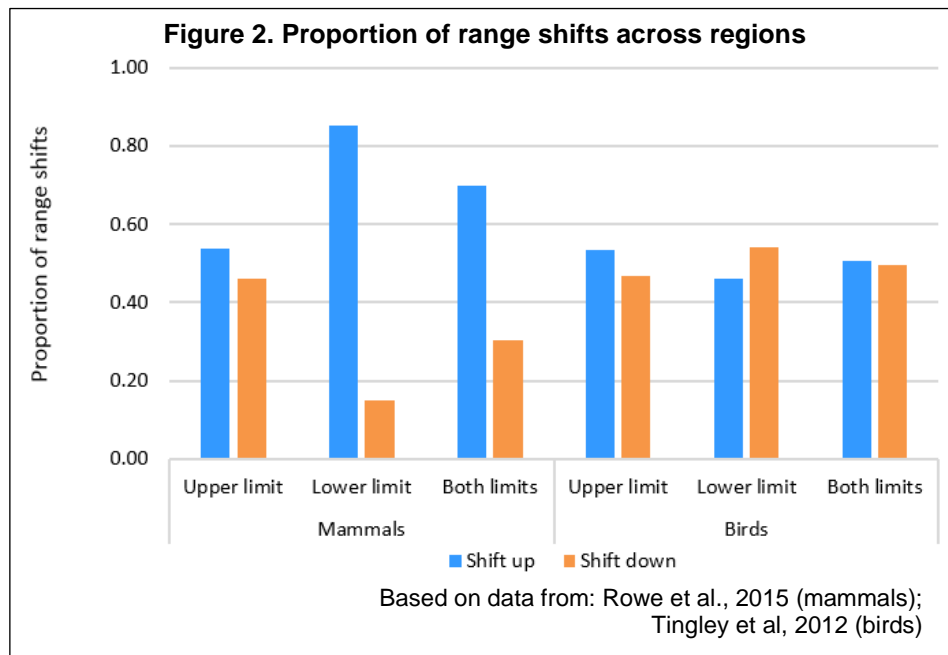
Certain birds and mammals are found at different elevations in the Sierra Nevada mountains today compared to a century earlier. Almost 75 percent of the small mammal species and over 80 percent of the bird species surveyed in this region have shifted ranges. While high-elevation mammals tended to shift their range upslope, birds and low-elevation mammals shifted downslope as frequently as upslope. Range responses of both taxa differed across montane portions of California.



What does the indicator show?

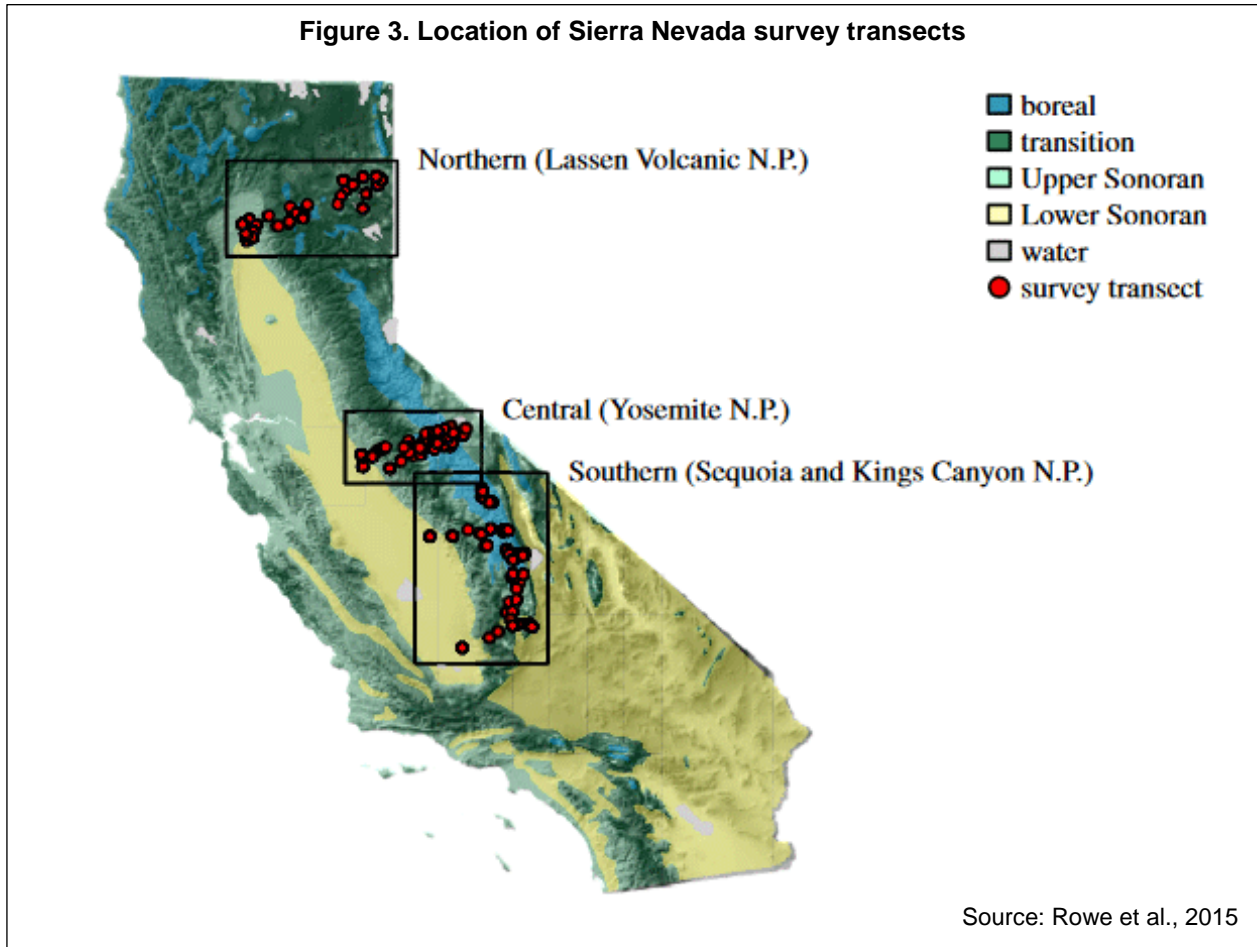
Significant changes have occurred in the elevational range of small mammals (Figure 1A) and birds (Figure 1B) in three study regions in the Sierra Nevada: the northern (Lassen), central (Yosemite) and southern (Sequoia and King's Canyon) regions (see map, Figure 2). The shifts reflect changes that have occurred since a survey conducted by Joseph Grinnell and a team of scientists in the early 20th century. Current ranges are based on resurveys of the same field sites conducted between 2003 and 2010. (See *Technical Considerations* for more information.)

Of the 34 mammalian species surveyed, 25 were found to have shifted their elevational ranges in at least one region (Figure 1A). A shift involves a contraction or expansion of the upper and/or lower limits of a species' elevational range. About two-thirds of the species ranges across the three regions remained unchanged at either or both the upper and lower elevational limits. Of the 22 species found in the three regions, none shifted both their upper and lower limits consistently in the same direction in all the regions (see Appendix, Figure A1). Across the three regions, elevational limits were more than twice as likely to have moved upslope as downslope (Figure 2). High-elevation species were more likely to contract their ranges (typically as a result of an upslope shift of their lower limits) than to expand them, whereas low-elevation species were just as likely to have contracted their limits as expanded them (Rowe et al., 2015).



Shifts in elevation among birds were more frequent than among mammals; 84 percent of bird species shifted their elevational distribution (Figure 1B). Upslope shifts occurred in 46 percent of lower elevation limits (resulting in range contraction), and 53 percent of upper limits (resulting in range expansion) (Figure 2). Downward shifts were as common as upward shifts (Tingley et al., 2012).





Why is this indicator important?

Animals reproduce, grow and survive within specific ranges of climatic and environmental conditions. Species may respond to changes in these conditions by, among other things, a shift in range boundaries. Globally, broad patterns of species shifts in response to warming temperatures have occurred over historical time scales ranging from years to millennia. Models project with high confidence that species movement will be a common phenomenon with continued warming (Settele et al., 2014).

Species respond uniquely to climatic and other environmental changes. This indicator shows both upslope and downslope shifts in elevation for small mammals and birds, demonstrating the idiosyncratic nature of species' responses to climate change. Range shifts can change community composition as the abundance of some species decreases or increases (Settele et al., 2014). Changes in species occurrence can lead to competitive displacement, intensification of predation or new predator-prey interactions and ultimately a decline in biodiversity (Blios et al., 2013). In general, climate change should favor species that are better able to tolerate warmer and more variable climatic conditions.



Certain species may not be able to shift their ranges fast enough to migrate to suitable environments, particularly where there has been loss or fragmentation of habitat or barriers to species movement (see *What factors influence this indicator?* below). Declines in population abundance can result. In extreme cases, extirpation (eradication) or extinction of species may occur (Settele et al., 2014). For example, the American pika, a small mammal adapted to high altitudes and cold temperatures, has disappeared from a 64-square-mile span of habitat from Mount Shasta to the southern Sierra Nevada (Stewart et al., 2015). Resurveys of historical pika locations over six years found they no longer occurred at 10 of 67 (15 percent) historical sites. The authors suggested that pikas have experienced climate-mediated range contraction over the past century tied to increasing summer temperatures.

The indicator presented here tracks changes in the elevation at which species are found today, compared to earlier in the century. This information will help in understanding and anticipating the long-term dynamics of the distribution of small mammals and birds in California, and examining the factors that influence them. This knowledge is crucial in efforts to identify which species are resilient or sensitive to climate change and, thus, to guide efforts to maintain species diversity in the face of regional warming. Models project with high confidence that species movement will be a common phenomenon with continued warming. The data from this indicator are useful in research to test the performance of model-based predictions of species' responses to changes in climate and land cover. Such research will improve predictions of future species' responses.

Changes in the composition of ecological communities, such as the loss of species, can change the ways in which ecosystems function (Hooper et al., 2005). Altered biodiversity has led to widespread concern for both economic (e.g., food sources) and non-economic (e.g., ethical, aesthetic) reasons. Wildlife and habitat conservation programs, government agencies and international scientific programs are taking steps to understand and minimize biodiversity loss and species invasions in an effort towards preserving ecosystems. This is important for our national parks, where scientists predict future warming will cause substantial turnover of species (Moritz et al., 2008).

What factors influence this indicator?

Range shifts are in part a response to the stresses of climate change (temperature and precipitation). Both the magnitude and the rate of climate change can impact a species' ability to adapt and survive. Recent research suggests that the picture is complex: temperature, precipitation and habitat may force range shifts in multiple directions and affect upper and lower range limits differently, with the relative contribution of different factors varying by elevation (Santos et al., 2017). The mixed or heterogeneous responses described here may reflect a species' intrinsic sensitivity to temperature, precipitation or other physical factors, as well as altered interactions with biological elements of the community (such as food sources, vegetation, and competitors) — all of which are changing in different ways in the three regions.

Changes in climate over the past century differed among the three study regions (Tingley et al., 2012; Rowe et al., 2015). The Central region reported the greatest and



the Northern region the least increase in mean annual temperature. Across all three regions, the maximum temperature of the warmest month was relatively constant, while the minimum temperature of the coldest month increased. The Yosemite Valley record indicates a substantial increase in monthly minimum temperatures of greater than 3 degrees centigrade ($^{\circ}\text{C}$). This temperature increase is also evident from tree ring data and analyses of vegetation change (Millar et al., 2004), snowmelt data, and retraction of the Mt. Lyell glacier. Precipitation increased most in the Northern region, which also cooled, and also in the Central region, but not in the Southern region. These kinds of spatially variable changes in climate over the past century in California can be seen in other ecosystem indicators, such as actual evapotranspiration and climatic water deficit (Rapacciolo et al., 2014).

Small mammals may respond differently to changes in minimum and maximum temperatures based on differences in species traits, such as lifespan, dietary breadth, and reproduction habitat (Moritz et al., 2008). Increased temperatures have been identified as a likely cause of the contractions of the high-elevation small mammal species and at least some of the upwards expansions of lower elevation species, although temperature effects on lower elevation species are less predictable. The effect of temperature is especially pronounced at higher elevations where changes in minimum temperature can affect thermoregulatory capacity, hibernation, behavior, and food-web structure (Santos et al., 2017). The average increase in elevation of about 500 meters for affected species in the Yosemite re-survey is consistent with what would be expected with the estimated temperature increase of 3°C , assuming that the species ranges are limited primarily by physiology (Moritz et al., 2008). The mechanisms explaining downslope shifts and the variable responses among related species are not well understood. Other factors also could be at play, including community structure and competitive interactions. The effects of changing precipitation on small mammals are not as clear but include challenges in finding water or cover (e.g., below the snow pack). Changes in moisture can also have metabolic impacts, such as difficulties in thermoregulation through transpiration when relative humidity is high (Santos et al., 2017). Moreover, some species may be able to persist in refugia (that is, areas in which individuals can survive through a period of unfavorable conditions) created by anthropogenic changes to the habitat, such as campgrounds where food and water are available (Morelli et al., 2012 and 2017).

Birds showed more heterogeneous elevational range shifts within species and among the three study regions over the past century (Tingley et al., 2012). In general, birds shifted upslope with increasing temperatures and shifted downslope with increased precipitation. Species-specific factors were also associated with the elevational changes: species were more likely to shift elevational ranges if they had small clutch sizes, defended all-purpose territories (i.e., where courtship, mating nesting, foraging all occur), and were non-migratory. The greatest changes to composition of montane bird communities occurred in the highest and lowest elevations (Tingley and Beissinger, 2013).



Birds have also been shown to respond to warming by breeding earlier to reduce the temperatures to which nests are exposed during breeding and to track shifting peaks in the availability of resources (Socolar et al., 2017). Using data from the Grinnell Resurvey Project, researchers found that breeding dates in the Sierra Nevada and the Coast Range (from the Oregon border to north of San Luis Obispo) shifted 5 to 12 days earlier over the last century. These findings suggest that earlier breeding might reduce both the need and the opportunity to shift geographically.

A group of researchers have studied biogeographic responses in birds, mammals and plants in California along with regional patterns of climate data during the 20th century to better understand species responses to a warming climate (Rapacciuolo et al., 2014). Although the expected response with warming is upward elevational shifts, they describe how downslope shifts are as common as upslope shifts. One common finding (noted above) was contractions of lower limits of high-elevation mammal species occurring primarily in response to warmer temperatures. They suggested that the substantial heterogeneity in response to warming with low elevation species may be due to influences such as interspecific competition and the spread of invasive species. In addition to temperature alone, species responses were also reportedly affected by the shifting seasonal balance of temperature and precipitation (water availability). They found that species-specific sensitivities to local-scale trophic interactions and habitat changes can also influence range shift dynamics, highlighting a need to adopt a more multifaceted and finer-scale understanding of climate change impacts.

The topography of a habitat can play a role in how an animal is impacted by climate change. Topographically complex areas provide potential climate change “refugia” whereas low-relief topography can exacerbate climate change impacts as organisms must travel further to remain in the same climate space (Maher et al., 2017). Mountains provide an extremely important climate refuge for many species because the rate of displacement required to track climate is low (i.e., they can disperse relatively short distances upslope to track favorable environmental conditions). However, species that already occur near mountaintops are among the most threatened by climate change because they cannot move upwards. The consequences of losing favorable climate space are not yet well understood (Settele et al., 2014).

In addition to topographic influences, research suggests that climate change effects on animals during the 20th century in California may have been largely affected by changes in vegetation rather than, or in addition to, direct physiological effects (Rapacciuolo et al., 2014), although warming winter temperatures are sometimes clearly important (Morelli et al., 2012). Substantial vegetation changes within the Central region (Yosemite National Park) have occurred since the early 1900’s due to a number of factors, including fires, fire suppression efforts, and temperature changes. Of the 23 small mammal species in Yosemite National Park, 11 shifted their elevational ranges in the same direction as shifts in vegetation, six species shifted in a different direction, and the rest showed no relationship (Santos et al., 2015). Species that shifted in the same direction as vegetation were mostly inhabitants of low to intermediate elevations, while species that shifted in different direction inhabited high elevations. Vegetation change



appears to directly affect some of the changes in the range of small mammals. For example, the expansion of the upper limit of the ranges of the California pocket mouse and the Piñon mouse (on the west slope) can be attributed to stand-replacing fires in the lower areas of the park. The large downwards shift in the elevation of the Montane shrew is probably related to its preference for wet meadows and the recovery of wet meadow systems in Yosemite Valley, following cessation of grazing and intense restoration efforts (Moritz et al., 2008).

Technical Considerations

Data Characteristics

Resurveys of small mammals and birds were conducted between 2003 through 2010 along three elevational transects in the Sierra Nevada Mountains that spanned four National Parks (see map above) and numerous other state, federal and private land holdings. The surveys revisited sites that were originally studied between 1911-1920 by Joseph Grinnell and staff of the Museum of Vertebrate Zoology (MVZ), University of California at Berkeley (Grinnell, 1930). The resurveys provide updated information on habitat and community changes at each site over the past century, while documenting the presence as well as ranges (geographic and habitat) of species of special concern to the lay and scientific communities. Detailed information on the Grinnell Resurvey Project can be found at: <http://mvz.berkeley.edu/Grinnell/index.html>.

Small mammal surveys were conducted at 166 locations: 38 in the Northern, 81 in the Central and 47 in the Southern region. Species were categorized as low elevation, high elevation or widespread for purposes of observing how species at different elevations respond. Statistical analyses of range shifts were restricted to 34 species that were detected at more than 10 percent of sites for at least one region in both eras. Details can be found in Rowe et al. (2014).

The resurvey of bird species for the three regions was conducted during breeding season. Observers collected data with temporal sampling as follows: Lassen, 2006-07; Yosemite, 2003-04; Southern Sierra, 2008-09. A total of 251 modern surveys were conducted at 84 sites, with each site surveyed a maximum of 5 times. Over 87 percent of the survey sites were located on permanently protected lands. All sites contained “west slope Sierran” vegetation communities. Habitat descriptions were matched to historic field notes wherever possible. The data from this resurvey can be found at: <http://arctos.database.museum>. Details can be found in Tingley et al. (2012).

Strengths and Limitations of the Data

Detailed maps and field notes from the Grinnell investigators facilitated the relocation of actual sites, transects and trap lines. The position of all generalized sites, based on documentation of the actual campsite, has been reasonably well established.

Substantial differences in small mammal survey methodologies between the two survey periods may result in biases in trapability. The Grinnell team used shotguns and snap traps for all mammal surveys, while the recent survey used live traps. To assess the comparability of survey success for each species across the time periods, statistical



("Occupancy") analyses were conducted. For the 34 species of small mammals considered above, detectability probabilities were sufficiently high across the survey periods to yield robust results. The analysis of changes in elevational range of mammals incorporates differences in detectability between study periods.

Natural year-to-year fluctuations in species' abundances may affect the detection of particularly rare species, and hence the comparisons between the study periods.

For purposes of examining possible climate change impacts on species shifts, field surveys were conducted in protected areas where other human influences (e.g., land use changes) were limited.

For more information, contact:



Steven R. Beissinger
130 Mulford Hall,
University of California, Berkeley, CA
94720-3110 (510) 643-3038
beis@berkeley.edu

References:

Blois JL, Zarnetske PL, Fitzpatrick MC and Finnegan S (2013). Climate change and the past, present and future of biotic interactions. *Science* **341**: 499-504.

Grinnell J (1930). *Vertebrate Natural History of a Section of Northern California Through the Lassen Peak Region*. Berkeley, CA: University of California Press.

Hooper DU, Chapin FS, Ewel JJ, Hector A, Inchausti P, et al. (2005). Effects of biodiversity on ecosystem functioning: a consensus of current knowledge. *Ecological Monographs* **75**(1): 3-35.

Maher SP, Morelli TL, Hershey M, Flint AL, Flint LE, et al. (2017). Erosion of refugia in the Sierra Nevada meadows network with climate change. *Ecosphere* **8**: e01673-n/a.

Millar CI, Westfall RD, Delany DL, King JC and Graumlich LJ (2004). Response of subalpine conifers in the Sierra Nevada, California, USA., to 20th century warming and decadal climate variability. *Arctic, Antarctic and Alpine Research* **36**(2): 181-200.

Morelli TL, Smith AB, Kastely CR, Mastroserio I, Moritz C, and Beissinger SR (2012). Anthropogenic refugia ameliorate the severe climate-related decline of a montane mammal along its trailing edge. *Proceedings of the Royal Society B-Biological Sciences* **279**: 4279-4286.

Morelli TL, Maher SP, Lim MCW, Kastely C, Eastman LM, et al. (2017). Climate change refugia and habitat connectivity promote species persistence. *Climate Change Responses* **4**: 8.

Moritz C, Patton JL, Conroy CJ, Parra JL, White GC and Beissinger SR (2008). Impact of a century of climate change on small-mammal communities in Yosemite National Park, USA. *Science* **322**(5899): 261-264.

Rapacciuolo G, Maher SP, Schneider AC, Hammomd TT, Jabis MD, et al. (2014). Beyond a warming fingerprint: individualistic biogeographic responses to heterogeneous climate change in California. *Global Change Biology* **20**: 2841-2855.



Rowe KC, Rowe KMC, Tingley MW, Koo MS, Patton JL, et al. (2015). Spatially heterogeneous impact of climate change on small mammals of montane California. *Proceedings of the Royal Society B* **282**: 20141857.

Santos MJ, Thorne JH, and Moritz C (2015). Synchronicity in elevation range shifts among small mammals and vegetation over the last century is stronger for omnivores. *Ecography* **38**: 556-568.

Santos MJ, Smith AB, Thorne JH and Moritz C (2017). The relative influence of change in habitat and climate on elevation range limits in small mammals in Yosemite National Park, California, U.S.A. *Climate Change Responses* **4**(7): 1-12.

Settele J, Scholes R, Betts R, Bunn S, Leadley P, et al. (2014). Terrestrial and inland water systems. In: *Climate Change 2014: Impacts, Adaptation, and Vulnerability. Part A: Global and Sectoral Aspects. Contribution of Working Group II to the Fifth Assessment Report of the Intergovernmental Panel on Climate Change*. Field CB, Barros VR, Dokken DJ, Mach KJ, Mastrandrea MD, et al. (Eds.). Cambridge, United Kingdom and New York, NY, USA: Cambridge University Press, pp. 271-359. Available at: http://www.ipcc.ch/pdf/assessment-report/ar5/wg2/WGIIAR5-Chap4_FINAL.pdf

Socular JB, Epanchin PN, Beissinger SR and Tingley MW (2017). Phenological shifts conserve thermal niches. *Proceedings of the National Academy of Sciences* **114**(49): 12976-12981.

Stewart JAE, Perrine JD, Nichols LB, Thorne JH, Millar CI, et al. (2015). Revisiting the past to foretell the future: summer temperature and habitat area predict pika extirpations in California. *Journal of Biogeography* **42**: 880-890.

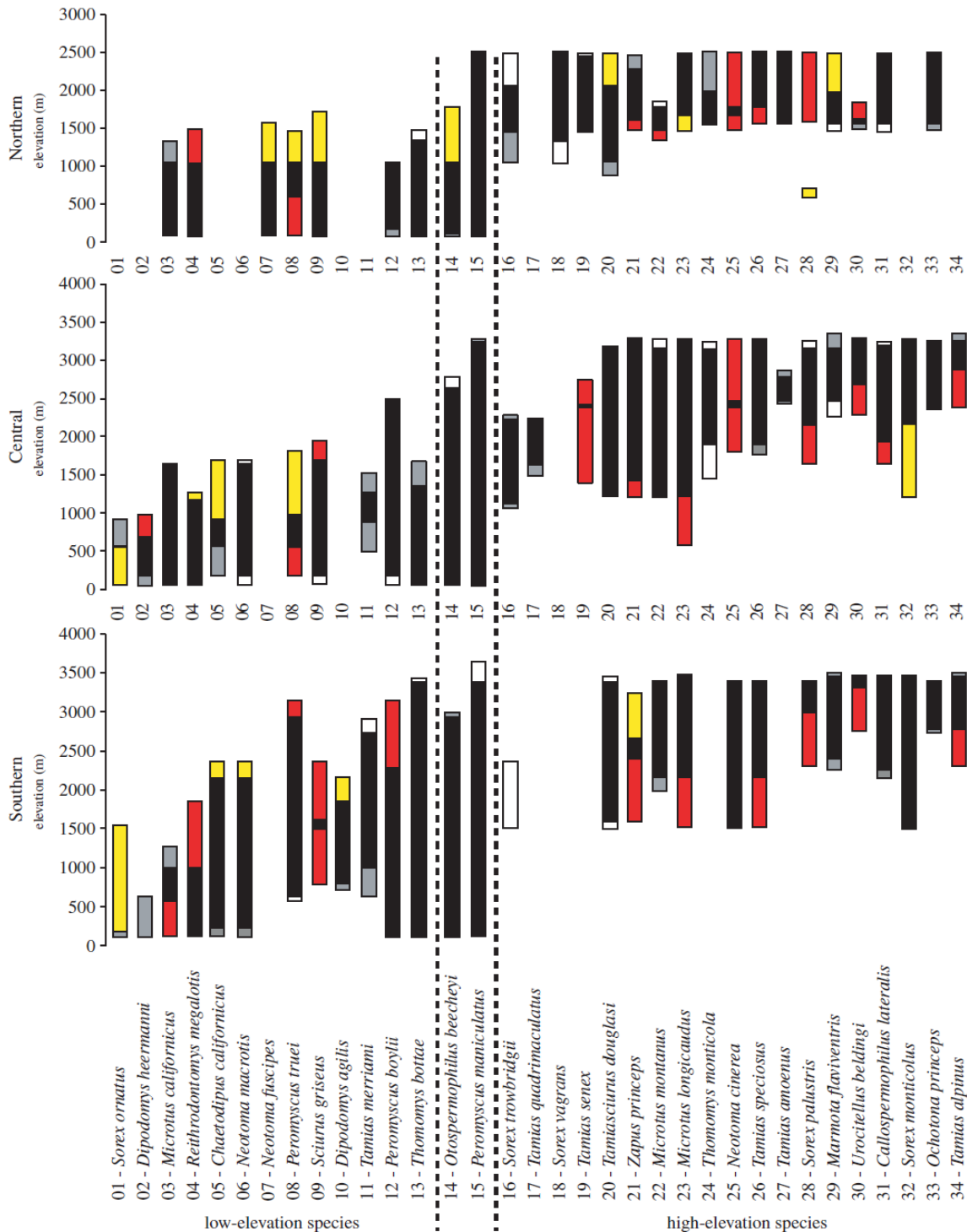
Tingley M and Beissinger SR (2013). Cryptic loss of montane avian richness and high community turnover over 100 years. *Ecology* **94**: 598-609.

Tingley MW, Koo MS, Moritz C, Rush, AC and Beissinger SR (2012). The push and pull of climate change causes heterogeneous shifts in avian elevational ranges. *Global Change Biology* **18**: 3279-3290.



APPENDIX

Figure A1. Small mammal range limit shifts, by species*



Red bars — range contractions; yellow bars — range expansions; gray bars — non-significant contractions; white bars — non-significant expansions (white); black bars — historic range. (Lack of a bar indicates that species is not found in that region.)

*List of common names follows.

Source: Modified from Rowe et al., 2015

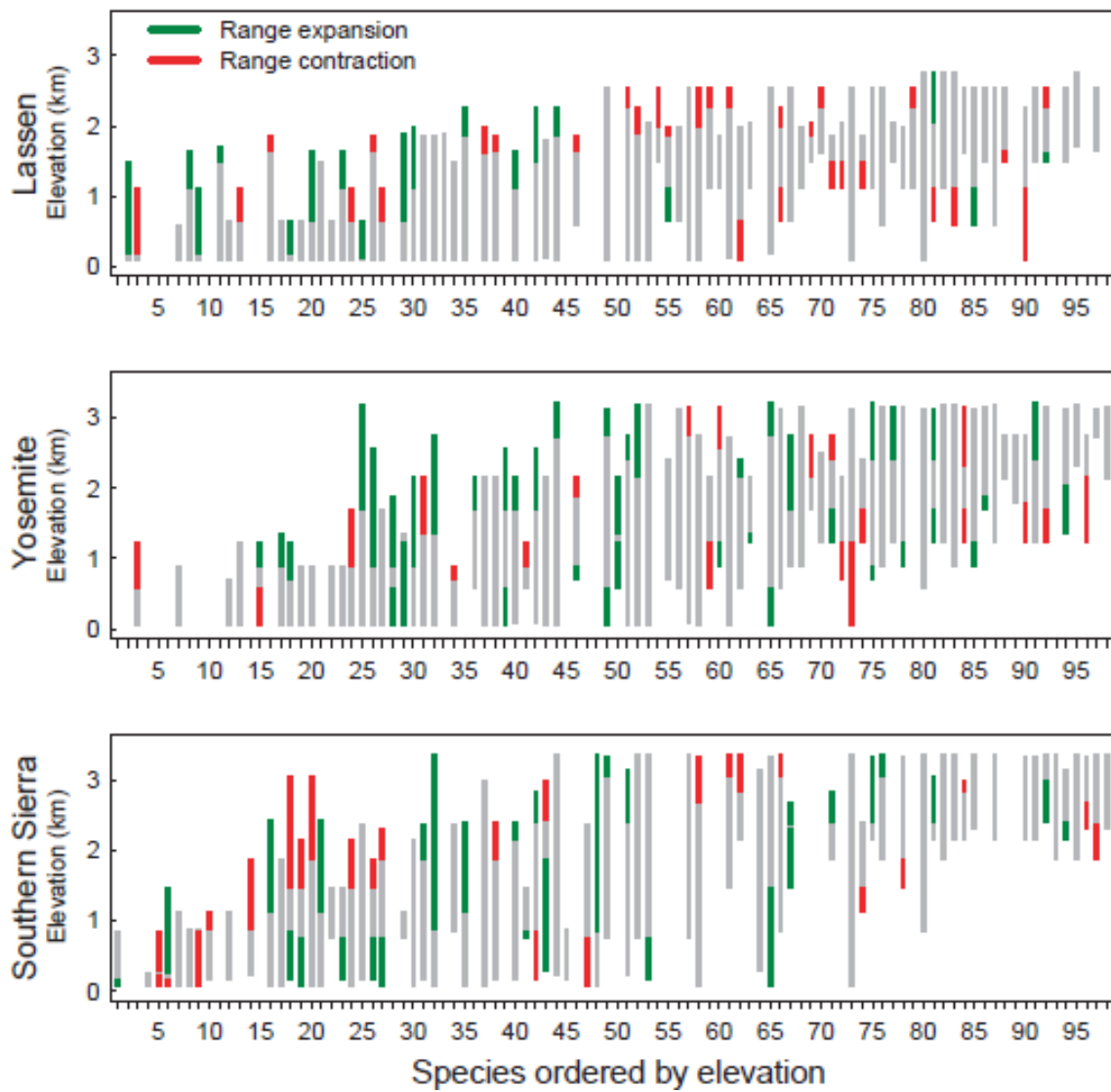


Common names for the species listed in Figure A-1 are as follows:

- 01 *Sorex ornatus* (Ornate shrew)
- 02 *Dipodomys heermanni* (Heermann's kangaroo rat)
- 03 *Microtus californicus* (Amargosa vole)
- 04 *Reithrodontomys megalotis* (Western harvest mouse)
- 05 *Chaetodipus californicus* (California pocket mouse)
- 06 *Neotoma macrotis* (Big-eared woodrat)
- 07 *Neotoma fuscipes* (Dusky-footed woodrat)
- 08 *Peromyscus truei* (Pinyon mouse)
- 09 *Sciurus griseus* (Western gray squirrel)
- 10 *Dipodomys agilis* (Agile kangaroo rat)
- 11 *Tamias merriami* (Merriam's chipmunk)
- 12 *Peromyscus boylii* (Brush mouse)
- 13 *Thomomys bottae* (Botta's pocket gopher)
- 14 *Otospermophilus beecheyi* (California ground squirrel)
- 15 *Peromyscus maniculatus* (Deer mouse)
- 16 *Sorex trowbridgii* (Trowbridge's shrew)
- 17 *Tamias quadrimaculatus* (Long-eared chipmunk)
- 18 *Sorex vagrans* (Vagrant shrew)
- 19 *Tamias senex* (Allen's chipmunk)
- 20 *Tamiasciurus douglasii* (Douglas' squirrel)
- 21 *Zapus princeps* (Western jumping mouse)
- 22 *Microtus montanus* (Montane vole)
- 23 *Microtus longicaudus* (Long-tailed vole)
- 24 *Thomomys monticola* (Mountain pocket gopher)
- 25 *Neotoma cinerea* (Bushy-tailed woodrat)
- 26 *Tamias speciosus* (Lodgepole chipmunk)
- 27 *Tamias amoenus* (Yellow-pine chipmunk)
- 28 *Sorex palustris* (American water shrew)
- 29 *Marmota flaviventris* (Yellow-bellied marmot)
- 30 *Urocitellus beldingi* (Belding's ground squirrel)
- 31 *Callospermophilus lateralis* (Golden-mantled ground squirrel)
- 32 *Sorex monticolus* (Dusky shrew)
- 33 *Ochotona princeps* (American pika)
- 34 *Tamias alpinus* (Alpine chipmunk)



Figure A2. Bird range limit shifts, by species*



Source: Tingley et al., 2012

Red bars — range contractions; green bars — range expansions; gray bars — historical range.
(Lack of a bar indicates that species is not found in that region.)

*Numbers along the x-axis correspond to the species list that follows.



Species are presented in Figure A-2 in the following order:

- 01 American Crow (*Corvus brachyrhynchos*)
- 02 American Goldfinch (*Spinus tristis*)
- 03 Yellow-breasted Chat (*Icteria virens*)
- 04 House Sparrow (*Passer domesticus*)
- 05 Horned Lark (*Eremophila alpestris*)
- 06 Northern Mockingbird (*Mimus polyglottos*)
- 07 Western Kingbird (*Tyrannus verticalis*)
- 08 Cliff Swallow (*Pterochelidon pyrrhonota*)
- 09 Common Yellowthroat (*Geothlypis trichas*)
- 10 Blue Grosbeak (*Passerina caerulea*)
- 11 Willow Flycatcher (*Empidonax traillii*)
- 12 Nuttall's Woodpecker (*Picoides nuttallii*)
- 13 Acorn Woodpecker (*Picus formicivora*)
- 14 Black-chinned Hummingbird (*Archilochus alexandri*)
- 15 Blue-gray Gnatcatcher (*Polioptila caerulea*)
- 16 Western Meadowlark (*Sturna neglectus*)
- 17 Bullock's Oriole (*Icterus bullockii*)
- 18 Bewick's Wren (*Thryomanes bewickii*)
- 19 California Towhee (*Melospiza crissalis*)
- 20 House Finch (*Haemorhous mexicanus*)
- 21 Lark Sparrow (*Chondestes grammacus*)
- 22 Oak Titmouse (*Baeolophus inornatus*)
- 23 California Quail (*Callipepla californica*)
- 24 Ash-throated Flycatcher (*Myiarchus cinerascens*)
- 25 Black Phoebe (*Sayornis nigricans*)
- 26 Bushtit (*Psaltiparus minimus*)
- 27 Western Scrub-Jay (now split into *Aphelocoma californica*, *Aphelocoma insularis*, and *Aphelocoma woodhouseii*)
- 28 Anna's Hummingbird (*Calypte anna*)
- 29 Downy Woodpecker (*Picoides pubescens*)
- 30 Mourning Dove (*Zenaidura macroura*)
- 31 Yellow Warbler (*Setophaga petechia*) *formerly *Dendroica petechia*
- 32 Red-winged Blackbird (*Agelaius phoeniceus*)
- 33 Tree Swallow (*Tachycineta bicolor*)
- 34 Western Bluebird (*Sialia mexicana*)
- 35 Song Sparrow (*Melospiza melodia*)
- 36 Pacific-slope Flycatcher (*Empidonax difficilis*)
- 37 Lesser Goldfinch (*Spinus psaltria*)
- 38 Black-headed Grosbeak (*Pheucticus melanocephalus*)
- 39 Canyon Wren (*Catherpes mexicanus*)
- 40 Spotted Towhee (*Pipilo maculatus*)
- 41 Wrentit (*Chamaea fasciata*)
- 42 Lazuli Bunting (*Passerina amoena*)
- 43 Violet-green Swallow (*Tachycineta thalassina*)
- 44 Brewer's Blackbird (*Euphagus cyanocephalus*)



- 45 Brown-headed Cowbird (*Molothrus ater*)
- 46 Black-throated Gray Warbler (*Setophaga nigrescens*)
- 47 Lawrence's Goldfinch (*Spinus lawrenci*)
- 48 Savannah Sparrow (*Passerculus sandwichensis*)
- 49 House Wren (*Troglodytes aedon*)
- 50 Band-tailed Pigeon (*Patagioenas fasciata*)
- 51 Warbling Vireo (*Vireo gilvus*)
- 52 White-breasted Nuthatch (*Sitta carolinensis*)
- 53 Northern Flicker (*Colaptes auratus*)
- 54 Red Crossbill (*Loxia curvirostra*)
- 55 Mountain Quail (*Oreortyx pictus*)
- 56 Orange-crowned Warbler (*Oreothlypis celata*)
- 57 Western Wood-Pewee (*Contopus sordidulus*)
- 58 Wilson's Warbler (*Cardellina pusilla*)
- 59 MacGillivray's Warbler (*Geothlypis tolmiei*)
- 60 Hermit Warbler (*Setophaga occidentalis*)
- 61 Western Tanager (*Piranga ludoviciana*)
- 62 Cassin's Vireo (*Vireo cassinii*)
- 63 Pileated Woodpecker (*Dryocopus pileatus*)
- 64 Common Raven (*Corvus corax*)
- 65 American Robin (*Turdus migratorius*)
- 66 Hairy Woodpecker (*Picoides villosus*)
- 67 Purple Finch (*Haemorhous purpureus*)
- 68 Nashville Warbler (*Oreothlypis ruficapilla*)
- 69 Hammond's Flycatcher (*Empidonax hammondi*)
- 70 Golden-crowned Kinglet (*Regulus satrapa*)
- 71 White-headed Woodpecker (*Picoides albolarvatus*)
- 72 Evening Grosbeak (*Coccothraustes vespertinus*)
- 73 Chipping Sparrow (*Spizella passerina*)
- 74 Red-breasted Sapsucker (*Sphyrapicus ruber*)
- 75 Olive-sided Flycatcher (*Contopus cooperi*)
- 76 Steller's Jay (*Cyanocitta stelleri*)
- 77 Calliope Hummingbird (*Selasphorus calliope*)
- 78 Brown Creeper (*Certhia americana*)
- 79 American Dipper (*Cinclus mexicanus*)
- 80 Rock Wren (*Salpinctes obsoletus*)
- 81 Fox Sparrow (*Passerella iliaca*)
- 82 Mountain Chickadee (*Poecile gambeli*)
- 83 Dark-Eyed Junco (*Junco hyemalis*)
- 84 Green-tailed Towhee (*Pipilo chlorurus*)
- 85 Red-breasted Nuthatch (*Sitta canadensis*)
- 86 Townsend's Solitaire (*Myadestes townsendi*)
- 87 Yellow-rumped Warbler (*Setophaga coronata*)
- 88 Lincoln's Sparrow (*Melospiza lincolni*)
- 89 Sooty Grouse (*Dedragapus fuliginosus*)
- 90 Pine Siskin (*Spinus pinus*)



- 91 Dusky Flycatcher (*Empidonax oberholseri*)
- 92 Hermit Thrush (*Catharus guttatus*)
- 93 Pygmy Nuthatch (*Sitta pygmaea*)
- 94 Cassin's Finch (*Haemorhous cassinii*)
- 95 Clark's Nutcracker (*Nucifraga columbiana*)
- 96 Ruby-crowned Kinglet (*Regulus calendula*)
- 97 Mountain Bluebird (*Sialia currucoides*)
- 98 Williamson's Sapsucker (*Sphyrapicus thyroideus*)
- 99 White-crowned Sparrow (*Zonotrichia leucophrys*)



EFFECTS OF OCEAN ACIDIFICATION ON MARINE ORGANISMS

TYPE III INDICATOR

Ocean chemistry is changing at an unprecedented rate due to anthropogenic carbon dioxide (CO₂) emissions to the atmosphere. When CO₂ is absorbed by seawater, chemical reactions occur that reduce seawater pH in a process known as “ocean acidification” (see *Acidification of coastal waters* indicator).

Several biological processes in marine organisms are sensitive to changes in seawater chemistry. The best-documented and mostly widely observed biological effects are due to a reduction in carbonate ion — a building block for shell forming organisms — under reduced pH conditions. Decreased calcification rates and/or shell dissolution has been observed in a wide range of shell-forming organisms, including plankton, mollusks, and corals. These processes have been elucidated in controlled laboratory experiments, including documentation of decreased shell size/thickness in shellfish. Through modeling, researchers have estimated that pteropod shell dissolution in response to increasingly acidic conditions experienced during seasonal upwelling events has increased ~19-26 percent along the US West Coast, including California, since the Industrial Revolution (Feely et al., 2016).

Impacts on the physiology and behavior of marine species can accrue as organisms face greater challenges in maintaining internal acid-base balance in ocean waters of lower pH (e.g., Munday et al., 2009; Somero et al., 2016; Jellison et al., 2016). Broader ecological consequences are additionally possible (Gaylord et al., 2015), including altered predator-prey relationships (e.g. Ferrari et al., 2011; Kroeker et al., 2014; Sanford et al. 2014), and degradation of habitat provisioning by structure-forming taxa like corals and mussels (e.g., Sunday et al., 2016). Current knowledge regarding changes to ocean chemistry and impacts on California species has been summarized by the West Coast Ocean Acidification & Hypoxia Panel (Chan et al., 2016). However, there is still much to learn about biological consequences of ocean acidification using ‘indicator species’ in the field.

The California Current Large Marine Ecosystem (CCLME) is the environment that spans from southern British Columbia to Baja California and includes US-controlled waters, the land-sea interface and adjacent wetlands. This ecosystem may provide early indication of the impacts of ocean acidification and decreasing dissolved oxygen due to its unique oceanography (Feely et al., 2008; Hauri et al., 2009). In particular, the wind-driven process of seasonal coastal upwelling brings deeper, high-CO₂ water to the surface where it bathes shoreline communities. In upwelled waters, elevated CO₂ conditions co-occur with low dissolved oxygen concentrations (hypoxia). As a result, California’s coastal waters may reach acidic and low oxygen conditions well before this is observed on a global scale (Feely et al., 2008). As such, California is positioned to provide for early examination of effects of ocean acidification and hypoxia.

Regional biological indicators can help improve the understanding of these impacts on California’s varied smaller-scale ocean ecosystems. A first step towards this goal was



accomplished by the Greater Farallones National Marine Sanctuary Advisory Council in the publication of *Ocean Climate Indicators: A Monitoring Inventory and Plan for Tracking Climate Change in the North-Central California Coast and Ocean Region* (Duncan et al., 2013). This plan recommends indicator species for processes such as climate change, ocean acidification, and hypoxia that include: primary producers, mid-trophic level species, habitat forming species, and seabirds. A comprehensive review and analysis of biological responses to ocean acidification provides additional possible indicator species and other guidance for indicators of ocean acidification (Kroeker et al., 2013). Results suggest that variables such as calcification and growth in key marine calcifiers are important to consider.

Other potential effects of ocean acidification on marine organisms that might be tracked include:

- Changes in ionic form of marine nutrients and potentially harmful substances (e.g., metals)
- Increased photosynthetic rates in carbon-fixing organisms
- Altered reproduction and survival in organisms
- Reduced olfaction (sensory function) in fish
- Changes in the strength or outcome of species interactions (including predation, herbivory, and competition)

In considering potential indicator species, the most successful target organisms are often those that are important community members and are present over a wide geographic extent, enabling their performance to operate as a metric of broader ecosystem function. Some potential species for tracking the biological impacts of ocean acidification in California waters are:

- The California mussel (*Mytilus californianus*) - a classic 'foundation species' that dramatically influences community structure both through its dominant status and because mussel beds provide habitat for hundreds of other species that reside within them (Suchanek, 1992). The distribution of *M. californianus* spans the entire west coast of the US (Morris et al., 1980), and the species is found in most of the state's shoreline Marine Protected Areas (MPAs). *M. californianus* has already been identified as an indicator species by two National Marine Sanctuaries in California. Research is ongoing to determine whether *M. californianus* can be utilized as an 'early warning' indicator of biological change due to ocean acidification and other stressors (Gaylord et al., 2011; California's Fourth Climate Change Assessment).
- Krill, a fundamental and important component of the marine food web. Krill have recently been shown to be sensitive to ocean acidification, with responses that include reductions in growth rates and increased mortality (e.g., Cooper et al., 2016; McLaskey et al., 2016). Krill therefore may provide an early indication of food web impacts from ocean acidification.



- Pelagic snails (pteropods) (see Figure 1), species which have delicate shells that are subject to severe dissolution when exposed to low pH seawater. Recent studies of the pteropod *Limacina helicina* within the California Current Large Marine Ecosystem indicate that 24 percent of offshore individuals and 53 percent of nearshore individuals exhibited signs of severe shell dissolution (Bednaršek et al., 2014). Continued acidification is expected to place these nearshore populations of pteropods at particular risk (Bednaršek et al., 2014; Feely et al., 2016; Bednaršek et al., 2017).



At the statewide level, excellent progress (albeit yet incomplete) has been made in identifying indicator species that can be monitored at local and regional scales to identify and track ocean acidification and other components of global environmental change. Specifically, for marine biological indicators for the state of California, there are over 490 publicly available data sets of observations or measurements of relevant parameters collected successively over a period of time (these data sets are referred to as “time series”). The majority of the longest running biological datasets in California are less than 10 years in length; however, a few extend beyond 20 years.

Broad-scale impacts of ocean acidification and climate change may be elucidated by integrated biological, chemical and physical oceanographic monitoring. Long-term ecological monitoring programs for intertidal and subtidal ecosystems (e.g., [LIMPETS](#), [MARINE](#), and [PISCO](#)), others associated with the Marine Protected Area Monitoring efforts (e.g., [Ocean Science Trust](#)), and oceanographic monitoring conducted by the Applied California Current Ecosystem Studies (ACCESS) (<http://www.accessoceans.org/>) provide essential data to better understand and interpret the impact of ocean acidification for California. Such data could be used by the scientific community to identify potential indicator species. For example, the longest biological dataset (64 years) for California quantifies zooplankton volume and diversity from quarterly cruises conducted by the California Cooperative Oceanic Fisheries Investigations (e.g., Bograd et al., 2003). To date, these biological data are paired with measurements of dissolved oxygen, but not other aspects of seawater chemistry (see *Dissolved oxygen in coastal waters* indicator). Another available dataset is based on surveys of *Macrocystis pyrifera* (giant kelp) and several fish species, which have been conducted by the Santa Barbara Coastal Long-Term Ecological Research program in the Santa Barbara Channel. However, these data are more limited in duration (12 years) and geographic extent (southern California only). Finally, the Partnership for



Interdisciplinary Studies of Coastal Oceans (PISCO) has generated a 12-year dataset on abundance, growth, and fecundity of several intertidal invertebrate and algal species. If these time series can be continued and extended, they may provide greater ability to detect the biological impacts of ocean acidification.

For more information, contact:



Tessa M. Hill, Ph.D.
University of California, Davis
Bodega Marine Laboratory
P.O. Box 247
Bodega Bay, CA 94923
(707) 875-1910
tmhill@ucdavis.edu

Brian Gaylord, Ph.D.
University of California, Davis
Bodega Marine Laboratory
P.O. Box 247
Bodega Bay, CA 94923
(707) 875-1940

Updates provided by UC Davis team: Rivest, Hill, Myhre, Gaylord, Sanford, Largier

References:

Bednaršek N, Feely RA, Reum JCP, Peterson B, Menkel J, et al. (2014). *Limacina helicina* shell dissolution as an indicator of declining habitat suitability owing to ocean acidification in the California Current Ecosystem. *Proceedings of the Royal Society B: Biological Sciences* **281**(1785): 20140123.

Bednaršek N, Klinger T, Harvey CJ, Weisberg S, McCabe RM, et al. (2017). New ocean, new needs: Application of pteropod dissolution as a biological indicator for marine resource management. *Ecological Indicators* **76**: 240-244.

Bograd SJ, Checkley Jr DA and Wooster WS (2003). CalCOFI: A half century of physical, chemical, and biological research in the California Current System. *Deep Sea Research Part II: Topical Studies in Oceanography* **50**: 2349-2353.

Chan F, Boehm AB, Barth JA, Chornesky EA, Dickson AG, et al. (2016, April). The West Coast Ocean Acidification and Hypoxia Science Panel: Major Findings, Recommendations, and Actions. California Ocean Science Trust, Oakland, California, USA. Available at www.westcoastoah.org.

Cooper HL, Potts DC and Paytan A. 2017. Effects of elevated pCO₂ on the survival, growth, and moulting of the Pacific krill species, *Euphausia pacifica*. *ICES Journal of Marine Science* **74**(4):1005-1012.

de Moel H, Ganssen GM, Peeters FJC, Jung SJA, Kroon D, Brummer GJA, Zeebe RE (2009). Planktic foraminiferal shell thinning in the Arabian Sea due to anthropogenic ocean acidification? *Biogeosciences* **6**: 1917-1925.

Duncan BE, Higgason KD, Suchanek TH, Largier J, Stachowicz J, et al. (2013). *Ocean Climate Indicators: A Monitoring Inventory and Plan for Tracking Climate Change in the North-central California Coast and Ocean Region*. Report of a Working Group of the Gulf of the Farallones National Marine Sanctuary Advisory Council.



Feely RA, Alin SR, Carter B, Bednaršek N, Hales B, et al. (2016). Chemical and biological impacts of ocean acidification along the west coast of North America. *Estuarine, Coastal and Shelf Science* **183** (Part A): 260-270.

Feely RA, Sabine CL, Hernandez-Ayon JM, Ianson D and Hales B (2008). Evidence for upwelling of corrosive 'acidified' water on the continental shelf. *Science* **320**: 1490-1492.

Ferrari MCO, McCormick MI, Munday PL, Meekan MG, Dixon DL, et al. (2011). Putting prey and predator into the CO₂ equation - qualitative and quantitative effects of ocean acidification on predator-prey interactions. *Ecology Letters* **14**: 1143-1148.

Gaylord B, Hill TM, Sanford E, Lenz EA, Jacobs LA, et al. (2011). Functional impacts of ocean acidification in an ecologically critical foundation species. *Journal of Experimental Biology* **214**: 2586-2594.

Gaylord B, Kroeker KJ, Sunday JM, Anderson KM, Barry JP et al. (2015). Ocean acidification through the lens of ecological theory. *Ecology* **96**: 3-15.

Hauri C, Gruber N, Plattner G-K, Alin S, Feely RA, Hales B, et al. (2009). Ocean acidification in the California Current System. *Oceanography* **22**(4): 60-71.

Jellison BM, Ninokawa AT, Hill TM, Sanford E and Gaylord B (2016). Ocean acidification alters the response of intertidal snails to a key sea star predator. *Proceedings of the Royal Society B* **283**(1833): 20160890.

Kroeker KJ, Kordas RL, Crim R, Hendriks IE, Ramajo L, et al. (2013). Impacts of ocean acidification on marine organisms: quantifying sensitivities and interaction with warming. *Global Change Biology* **19**: 1884-1896.

Kroeker KJ, Kordas RL, Crim RN, and Singh GG (2010). Meta-analysis reveals negative yet variable effects of ocean acidification on marine organisms. *Ecology Letters* **13**: 1419-1434.

Kroeker KJ, Sanford E, Jellison BM, and Gaylord B (2014). Predicting the effects of ocean acidification on predator-prey interactions: A conceptual framework based on coastal molluscs. *Biological Bulletin* **226**: 221-222.

McLaskey AK, Keister JE, McElhany P, Olson MB, Busch DS, et al. (2016). Development of *Euphausia pacifica* (krill) larvae is impaired under pCO₂ levels currently observed in the Northeast Pacific. *Marine Ecological Progress Series* **555**: 65-78.

Munday PL, Dixon DL, Donelson JM, Jones GP, Pratchett MS, et al. (2009). Ocean acidification impairs olfactory discrimination and homing ability of a marine fish. *Proceedings of the National Academy of Sciences* **106** (6): 1848 -1852.

Morris RH, Abbott DL, and Haderlie EC (1980). *Intertidal Invertebrates of California*. Stanford, CA: Stanford University Press.

NAS (2010). *Ocean Acidification: A National Strategy to Meet the Challenges of a Changing Ocean*. Committee on the Development of an Integrated Science Strategy for Ocean Acidification Monitoring, Research, and Impacts Assessment. National Academy of Sciences. Washington DC: National Academies Press. Available at: <https://www.nap.edu/catalog/12904/ocean-acidification-a-national-strategy-to-meet-the-challenges-of>

NOAA (2010). *NOAA Ocean and Great Lakes Acidification Research Plan*. NOAA Special Report. National Oceanic and Atmospheric Administration Ocean Acidification Steering Committee. Available at https://www.pmel.noaa.gov/co2/files/feel3500_without_budget_rfs.pdf



Sanford E, Gaylord B, Hettinger A, Lenz EA, Meyer K and Hill TM (2014). Ocean acidification increases the vulnerability of native oysters to predation by invasive snails. *Proceedings of the Royal Society B* **281**: 20132681.

Somero GN, Beers JM, Chan F, Hill TM, Klinger T and Litvin SY (2016). What changes in the carbonate system, oxygen, and temperature portend for the Northeastern Pacific Ocean: a physiological perspective. *BioScience* **66**: 14-26.

Suchanek TH (1992). Extreme biodiversity in the marine environment: mussel bed communities of *Mytilus californianus*. *Northwest Environmental Journal* **8**: 150-152.

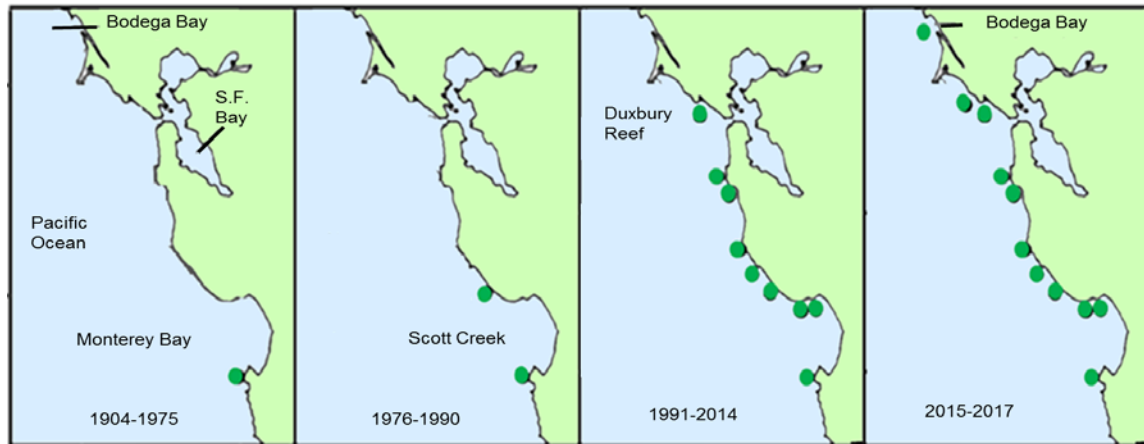
Sunday JM, Fabricious KE, Kroeker KJ, Anderson KM, Brown NE, et al. (2017). *Nature Climate Change* **7**: 81-85.



NUDIBRANCH RANGE SHIFTS

A species of nudibranch sea slug is expanding its range northward along the California coast in response to warming ocean conditions.

Figure 1. Northernmost locations of *Phidiana hiltoni* along the California coast (1904-2017)



Source: Adapted from Goddard et al., 2011, updated 2017

What does the indicator show?

Historical surveys of nudibranch populations along the California coast show a 210 kilometer (km) northward shift in the range for *Phidiana hiltoni* (*P. hiltoni*) since the mid-1970s (Goddard et al., 2011; 2016). Figure 1 shows locations where *P. hiltoni* had been observed (green dots) during four different periods, starting in 1904. Until 1975, *P. hiltoni*'s most northern location was on the Monterey Peninsula. Beginning in the late 1970s, its range expanded north across Monterey Bay to Santa Cruz County. By 1992, it had spread another 110 km up the coast into the San Francisco Bay area as far north as Duxbury Reef. By 2015, it had reached Bodega Bay. Following its initial spread, *P. hiltoni* has persisted at each of these sites to the present day.

Warm water conditions occur periodically in California's coastal waters, usually as part of the El Niño-Southern Oscillation. From late 2013 to 2016, the West Coast experienced unusually warm sea surface temperatures (Bond et al., 2015; Di Lorenzo and Mantua, 2016). Fish and other marine organisms, including many nudibranchs, shifted their distributions farther north during this unprecedented marine heat wave (Cavole et al., 2016). All told, 26 sea slug species were found at new northernmost locations (Goddard et al., 2016; Goddard, 2017). Among these was *P. hiltoni*, which after inhabiting Duxbury Reef for 13 years, was found for the first time in Bodega Bay in 2015. Warm ocean conditions ended in 2016, yet as of late 2017, *P. hiltoni* has persisted at this new northernmost location.

Why is this indicator important?

The habitats of nudibranchs overlap with commercially important organisms, including abalone, crab, and lingcod. Although changes in the ranges of small, short-lived marine organisms such as nudibranchs may seem inconsequential, the nudibranch's response



to ocean warming may foretell larger ecological changes that may already have been set in motion by climate change.

Species live in habitats defined by certain physical conditions, such as temperature and salinity. These conditions often show gradual change through space, creating an environmental gradient across latitudes, elevations, or depths. As conditions change, such as with warming ocean temperatures, species' distributions along an environmental gradient can provide important insights into how they will respond to climate change. For example, many species that can only survive within defined temperature ranges moved to higher elevations with long-term climate warming (IPCC, 2014). *P. hiltoni* has remained in its expanded range even after cooler temperatures have temporarily returned to coastal waters. With climate change driving a longer-term increase in global ocean temperature, scientists expect some of the other northward range shifts observed during the past few years in California to become permanent. Northern populations of these nudibranchs are being closely monitored.

The expansion of marine organisms into new territories can have negative biological impacts on resident organisms, similar to those of invasive species. Population declines in other nudibranch species have occurred at Duxbury Reef, where particularly high densities of *P. hiltoni* have been observed (Goddard et al., 2011). These declines appear to have resulted from *P. hiltoni* preying on other nudibranchs and competing for common prey species. Scientists suggest the range shift of this predatory species may therefore be disrupting food webs and altering community composition at sites along the California coast where its populations are dense.

What factors influence this indicator?

Nudibranchs inhabit the California Current System (CCS), which includes the span of coastline from Oregon to Baja California Sur. In this system, the El Niño-Southern Oscillation (ENSO), Pacific Decadal Oscillation (PDO) and North Pacific Gyre Oscillation (NPGO) influence sea surface temperatures (SSTs), coastal upwelling and strength of southerly currents. During certain phases of these oscillations, including El Niño events in which coastal waters shift from relatively cool to warm temperatures and poleward movement of ocean currents increases, researchers have found episodic northward range expansions of nudibranch species.

Local and basin-scale fluctuations in ocean climate can affect larval development, mortality, and transport, and these in turn can affect adult population dynamics. The



Photo Credit: Jeffrey Goddard

The nudibranch sea slug *Phidiana hiltoni* is a soft-bodied marine organism found on the California coast. Nudibranchs are recognized for their intricate shapes and striking colors. They are bottom-dwelling, specialized predators of aquatic invertebrates such as sponges, jellyfish, and in a few cases, other nudibranchs. Lifespans vary from weeks to about a year depending on species. Nudibranchs are not harvested by humans, and many are conspicuous and easy to count in the marine environment (Schultz et al., 2011).



transport of larval-stage nudibranchs, called *larval advection*, is hypothesized to explain the relationship between ocean climate conditions and changes in adult population abundance. For example, El Niño conditions appear to increase larval advection of nudibranchs from southern source populations, extending their ranges northward and increasing population sizes in shallow water (Schultz et al., 2011; Goddard et al., 2016).

The strong El Niños of 1982-83 and 1997-98 drove transient shifts of many nudibranchs from southern and central California to their northernmost sites (Engle and Richards, 2001; Goddard et al., 2016). In 1976-77 a shift from a cool to warm phase of the PDO and increased sea surface temperatures also corresponded with northward expansion of nudibranchs. When this warm phase ended in 2007 and cooler sea surface temperatures returned in 2008, *P. hiltoni* was the only nudibranch to remain in its expanded range. Interestingly, additional evidence presented by Goddard et al. (2011) suggests that *P. hiltoni* did not occur north of Monterey during the previous warm phase of the PDO, which lasted from 1925 to 1946 (Mantua and Hare, 2002).

Phidiana hiltoni and other nudibranchs are responding in a manner similar to other marine fishes and invertebrates, which have shifted their distributions to higher latitudes and/or into deeper depths in response to warmer conditions (Lluch-Belda et al., 2005; Cavole et al., 2016). A very strong El Niño contributed to an unprecedented multiyear marine heat wave along the Pacific Coast from late 2013 to 2016 and caused extensive biological impacts, including range shifts, at all trophic levels. Investigators documented range shifts for 48 species of sea slugs from 2014 through late 2017 along the California and Oregon coastline associated with the unusually warm ocean conditions (Goddard et al., 2016; Goddard, personal communication). Twenty-six species were found at new northernmost localities, while the remainder were located at or near northern range limits established during previous El Niños. It remains to be seen how many of these species will persist in their northern locations — as *P. hiltoni* has — when ocean conditions shift back to cooler temperatures.

Technical Considerations

Data Characteristics

Historical data (before 1969):

Qualitative searches for sea slugs, especially nudibranchs, were conducted from Monterey to Sonoma Counties by taxonomic specialists. Results are scattered in published papers and monographs, as well as the online database of the Invertebrate Collection at the California Academy of Sciences (http://researcharchive.calacademy.org/research/izg/iz_coll_db/index.asp). The counts of sea slugs in San Mateo County reported by Bertsch, et al. (1972) were conducted intermittently from 1966 to 1970 and were semi-quantitative in nature. The taxonomic results in Marcus (1961) were based largely on collections made in Marin and Sonoma Counties in 1958–9, and those in Steinberg (1963) on collections from Monterey to Sonoma Counties from 1948 to 1963.

Duxbury reef data:

Nudibranch population abundances prior to the arrival of *P. hiltoni* at Duxbury Reef were



estimated based on five timed counts conducted in June and July 1969, January and June 1970, and June 1972; and three more in December 1974 and May and December 1975. Since December 2007, 11 more timed counts of nudibranchs in the same area as the original counts were conducted. Data from all counts were standardized to number of individuals per hour per observer or number of species per hour per observer (Goddard, 2011).

Strengths and Limitations of the Data:

Historical data (before 1969):

Since the 1940s, coastal nudibranch counts by taxonomic specialists have had good geographic representation from Monterey to Sonoma County. Geographic coverage was more limited for the first half of the 20th century, when the only marine laboratory in the region was at Pacific Grove. However, collections of nudibranchs were made in the greater San Francisco Bay region in the early 20th century, and deposited in the Invertebrate Collection at the California Academy of Sciences (CAS), with the associated data now available via the CAS online database (Goddard et al., 2011).

Data since 1969:

The timed counts at Duxbury Reef in the 1960s-70s and again starting in 2007 were conducted by the same two taxonomic specialists in nudibranchs, assisted at times by experienced observers familiar with intertidal nudibranchs from California. This continuity ensures minimal effect of observer on those counts. Since 2011, additional timed counts, as well as qualitative surveys, have been conducted in Marin and Sonoma Counties, supplemented by observations of Bodega Marine Laboratory personnel and citizen scientists. Currently, three sites in Sonoma County, plus two in Mendocino County are being surveyed at least once a year for the presence of *P. hiltoni*.

For more information, contact:



Jeffrey Goddard
Marine Science Institute
University of California
Santa Barbara, CA 93106-6150
(805) 364-5114
jeff.goddard@lifesci.ucsb.edu

References:

- Bertsch H, Gosliner T, Wharton R and Williams G (1972). Natural history and occurrence of opisthobranch gastropods from the open coast of San Mateo County, California. *The Veliger* **14**:302–314.
- Bond NA, Cronin MF, Freeland H and Mantua N (2015). Causes and impacts of the 2014 warm anomaly in the NE Pacific. *Geophysical Research Letters* **42**(9): 3414-3420.
- Cavole LM, Demko AM, Diner RE, Giddings A, Koester I, et al. (2016). Biological impacts of the 2013–2015 warm-water anomaly in the Northeast Pacific: Winners, losers, and the future. *Oceanography* **29**: 273–285.



Di Lorenzo E and Mantua NJ (2016). Multi-year persistence of the 2014/15 North Pacific marine heatwave. *Nature Climate Change* **6**: 1042-1047.

Engle JM and Richards DV (2001). New and unusual marine invertebrates discovered at the California Channel Islands during the 1997-1998 El Niño. *Bulletin of the Southern California Academy of Sciences* **100**: 186–198.

Goddard JHR, Gosliner TM and Pearse JS (2011, updated 2017). Impacts associated with the recent range shift of the aeolid nudibranch *Phidiana hiltoni* (Mollusca: Opisthobranchia) in California. *Marine Biology* **158**: 1095–1109.

Goddard JHR, Treneman N, Pence WE, Mason DE, Dobry PM, et al. (2016). Nudibranch range shifts associated with the 2014 warm anomaly in the Northeast Pacific, *Bulletin of the Southern California Academy of Sciences* **115**: 15–40.

Lluch-Belda D, Lluch-Cota DB and Lluch-Cota SE (2005). Changes in marine faunal distributions and ENSO events in the California Current. *Fisheries Oceanography* **14**: 458–467.

Marcus E (1961). Opisthobranch mollusks from California. *The Veliger* **3** (Supplement): 1–85.

Mantua N and Hare SR (2002) The Pacific decadal oscillation. *Journal of Oceanography* **58**: 35–44.

Schultz ST, Goddard JHR, Gosliner TM, Mason DE, Pence WE, et al. (2011). Climate-index response profiling indicates larval transport is driving population fluctuations in nudibranch gastropods from the northeast Pacific Ocean. *Limnology and Oceanography* **56**: 749–763.

Steinberg JE (1963). Notes on the opisthobranchs of the west coast of North America. IV. A distributional list of opisthobranchs from Point Conception to Vancouver Island. *The Veliger* **6**: 68–75.



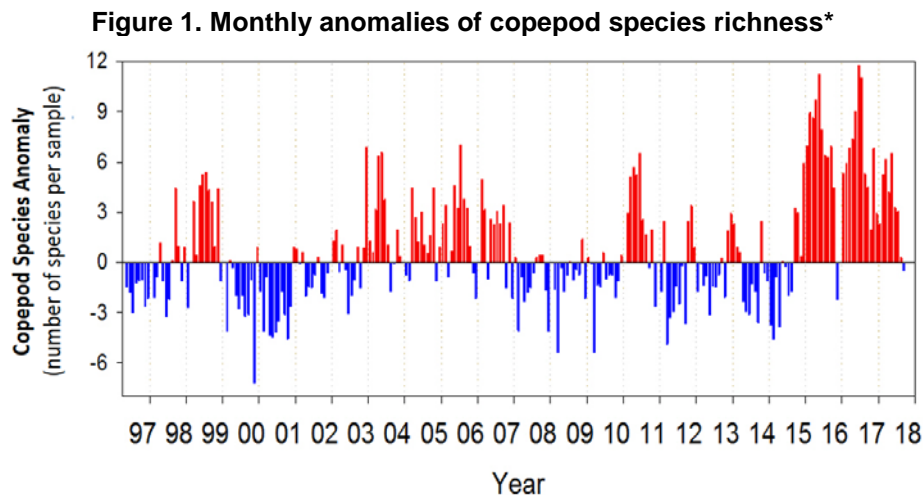
COPEPOD POPULATIONS

Variations in copepod populations in the Northern California Current Ecosystem reflect large-scale and regional changes in ocean circulation patterns.

Copepods are small marine crustaceans that comprise a large and diverse group of species that are a major food source for fish, whales, and seabirds. Copepods are planktonic, that is, they drift with the ocean currents.



Calanus marshallae



Source: NOAA/NWFSC, 2017a,b

***Copepod species richness** is the **number of copepod species** in a plankton sample. The **anomaly** is the difference between the monthly average and the long-term monthly average copepod species richness values.

Note: Blue bars indicate that copepods are being transported chiefly from northern, colder waters; red bars, from southern, warmer waters or offshore.

What does the indicator show?

As shown in Figure 1, copepod species richness has fluctuated throughout the last two decades with low anomalies from 1999 until 2002, generally high anomalies from 2003 until 2007, followed by a mixed pattern until a very high jump in species richness in much of 2015 through the summer of 2017. The data in Figure 1 are from a monitoring site off the coast of Newport, Oregon, which is about 300 kilometers north of Crescent City, California, in the northern portion of the California Current System (Figure 2).

Because copepods drift with ocean currents, they are good indicators of the type and sources of waters transported into the northern California Current. Thus, changes in copepod populations at this site are indicative of changes occurring off the California coast.

The copepod *species richness* index represents the average number of copepod species in monthly plankton samples (see *Data Characteristics* for more details). Figure 1 presents monthly anomalies — or departure from the long-term monthly



average — in copepod species richness values. These data are derived by subtracting the long term average (using the base period of 1996-2014) of species richness from the observed monthly average. Values are negative when the observed number of copepod species is less than the long-term monthly average, and positive when the observed number is greater.

Negative values in species richness anomalies generally indicate that the copepods are being transported to the monitoring location chiefly from the north, out of the coastal subarctic Pacific which is a region of low species diversity. Copepods from this cold-water region are referred to as northern species. Two of the northern species, *Calanus marshallae* and *Pseudocalanus mimus*, are lipid-rich, containing wax esters and fatty acids that appear to be essential for many pelagic fishes to grow and survive through the winter (Miller et al., 2017). Positive values in species richness anomalies generally indicate that the waters originate either from the south or from offshore, which are warmer, subtropical low-salinity waters containing a more species-rich planktonic fauna, referred to as southern species. These southern copepod species are generally smaller than northern species, and have low lipid reserves and nutritional quality.

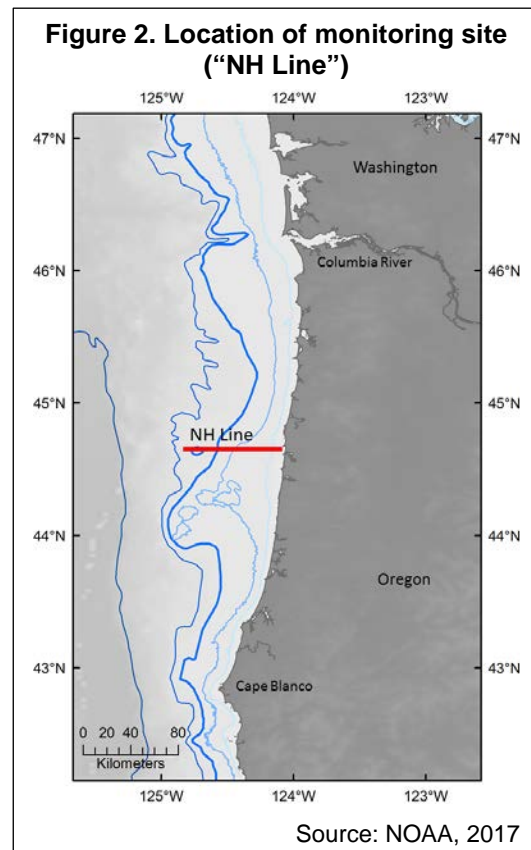
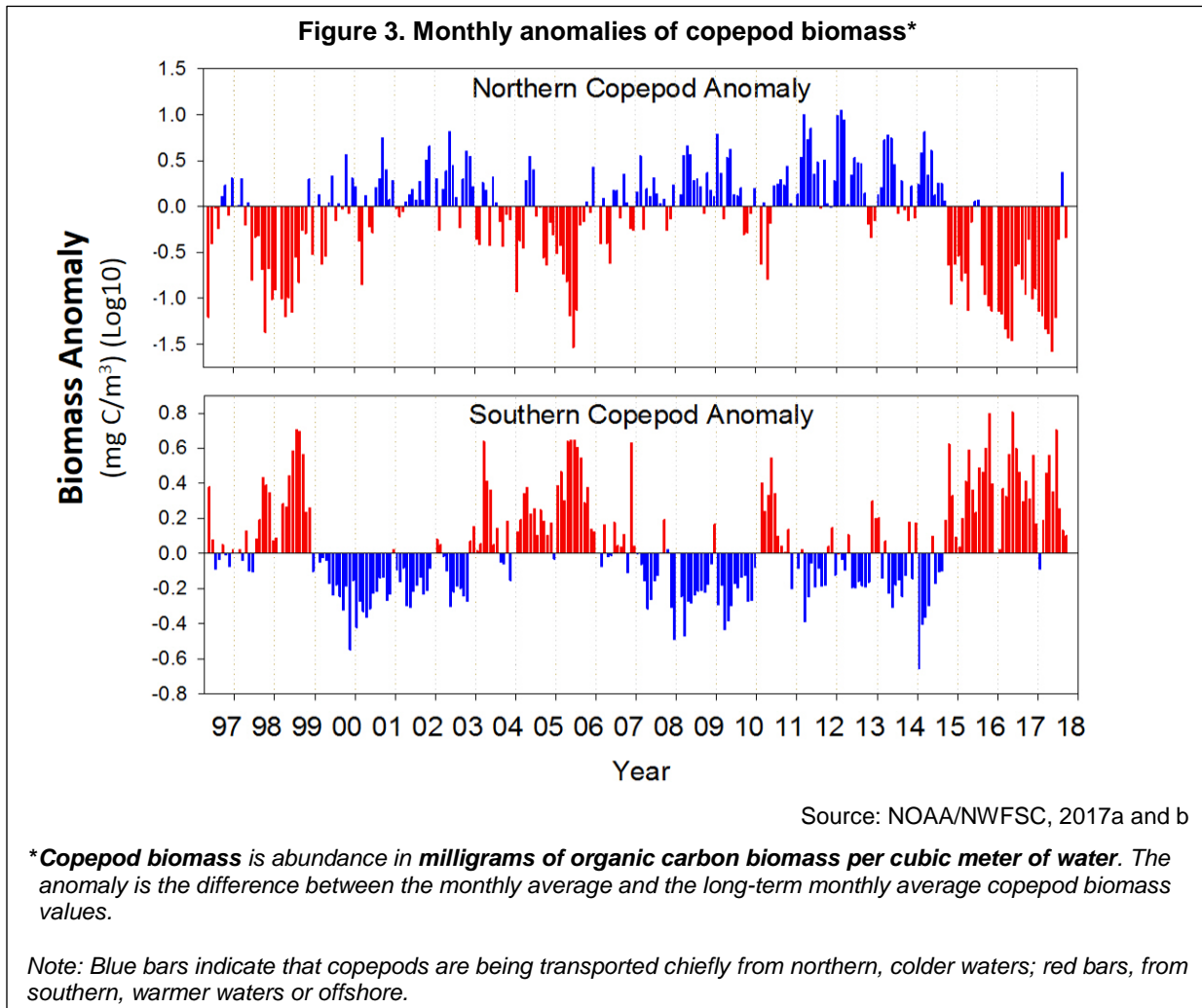


Figure 3 shows the abundance (in milligrams of organic carbon biomass per cubic meter of water) of two copepod groups (see also *Data Characteristics*) based on the affinities of copepods for different water types (i.e., temperature and salinity; Hooff and Peterson, 2006). The main species occurring at the monitoring site are classified into two groups: those with cold-water affinities (northern copepods) and those with warm-water affinities (southern copepods). The cold-water species usually dominate the coastal zooplankton community during the summer, while the warm-water species are usually dominant during the winter. Zooplankton anomalies are on a log₁₀ scale and represent a multiplicative (not additive) scaling relative to the average seasonal cycle: for example, an anomaly of +1 means that observations average 10 times the 1996–2014 monthly average.

Figures 1 and 3 show how the cycle of copepod richness and copepod biomass are related. Over the 22-year time series, during periods when the copepods are dominated by cold water northern species (positive biomass anomalies of northern copepods; Figure 3, top graph), there were usually negative anomalies of southern copepod species (Figure 3, bottom graph) and lower than average species richness (Figure 1). These low frequency changes are independent of the seasonal pattern of low species



richness in the summer and high richness in the winter. Throughout much of 2015 and into the summer of 2017, large populations of southern copepod species dominated the coastal waters, and species richness was the highest observed in the 22-year time series as a result of warming ocean temperatures (described below).



While copepod population metrics predominantly describe interannual to decadal climate variability, it is likely to indicate long-term climate change, since changes in ocean transport and water mass source are responsive to variations in global climate. Over time, these indices may reveal a clear trend toward one dominant group of copepod species due to climate change.

Why is this indicator important?

Copepods are the base of the food chain, eaten by many fish (especially anchovies, sardines, herring, smelt and sand lance), which in turn are consumed by larger fish, sea mammals and seabirds. Because they are planktonic, copepods drift with the ocean currents and therefore are good indicators of the type of water being transported into the northern California Current. Tracking copepods provides information about changes



occurring in the food chain that fuels upper trophic-level marine fishes, birds, and mammals. Knowledge of year-to-year variations in their abundance and species composition predict the abundance of small fishes, as well as species that feed on these fish (Peterson et al., 2014). As noted above, “northern species” are larger and bioenergetically richer than the “southern species.” When copepods largely consist of northern species, the pelagic (water column) ecosystem is far more productive than when southern species dominate.

It is noteworthy that the four years of positive anomalies of northern copepod species from 1999-2002 are correlated with extraordinarily high returns of Coho and Chinook salmon to the rivers of California and Oregon. Conversely, during the years 2003-2007 and 2014-2016, when salmon returns began to decline dramatically, positive anomalies of southern copepod species were occurring. These observations reflect a rich food chain from 1999-2002 and an impoverished food chain from 2003-2007 and 2014-2017.

Like other zooplankton, copepods are useful in the study of ecosystem response to climate variability. Due to their short life cycles (on the order of weeks), their populations respond to and reflect short-term and seasonal changes in environmental conditions and are sensitive to the magnitude of environmental change (Fisher et al., 2015). Moreover, many zooplankton taxa are indicator species whose presence or absence may represent the relative influence of different water types on ecosystem structure.

Copepod species reflect ocean transport processes in the northern California Current. For instance, in both 2015 and 2016, the seasonal springtime shift from a warm southern copepod community to a cold summer northern community did not occur. The copepod community remained with the lowest biomass of lipid-rich northern copepods and the highest biomass of small tropical and sub-tropical southern copepods in the 22-year time series. Anomalously low numbers of copepod species (i.e., a “negative species enrichment anomaly”) indicate the transport of coastal subarctic water into the coastal waters of the northern California Current (1999-2002; 2011 to 2014). Anomalously high species numbers are associated with either a greater amount of onshore transport of warm, offshore, subtropical water, or northward transport of subtropical coastal water along the coastal corridor (as happened in late 2002 to early 2006, and during 2014-15). The species richness remained high throughout 2016, peaking during the summer months when species richness is generally the lowest (Figure 1; Peterson et al., 2017).

Finally, copepod populations may give an advance warning of major changes in ocean conditions. Copepod indices have proven useful for the prediction of the returns of Chinook and Coho salmon (Peterson and Schwing, 2003; Peterson et al., 2014), and forecasts of salmon survival have been developed for the Coho and Chinook salmon runs along the Washington/Oregon coasts based on copepod indices (NOAA, 2018) (see *Sacramento fall-run Chinook salmon abundance* indicator). These same copepod indices have been correlated with the recruitment, that is the addition of young to a population, of the invasive green crab along the west coast of the US (Yamada et al., 2015); anchovy (Emmett, personal communication); and sablefish, rockfish, and sardine



(Peterson et al., 2014). They have also correlated with seabird nesting success in Central California (Jahncke et al., 2008; Wolf et al., 2009; Manugian et al., 2015; also see *Cassin's Auklet breeding success* indicator) and seabird mortality off northern Washington (Parrish, personal communication).

What factors influence this indicator?

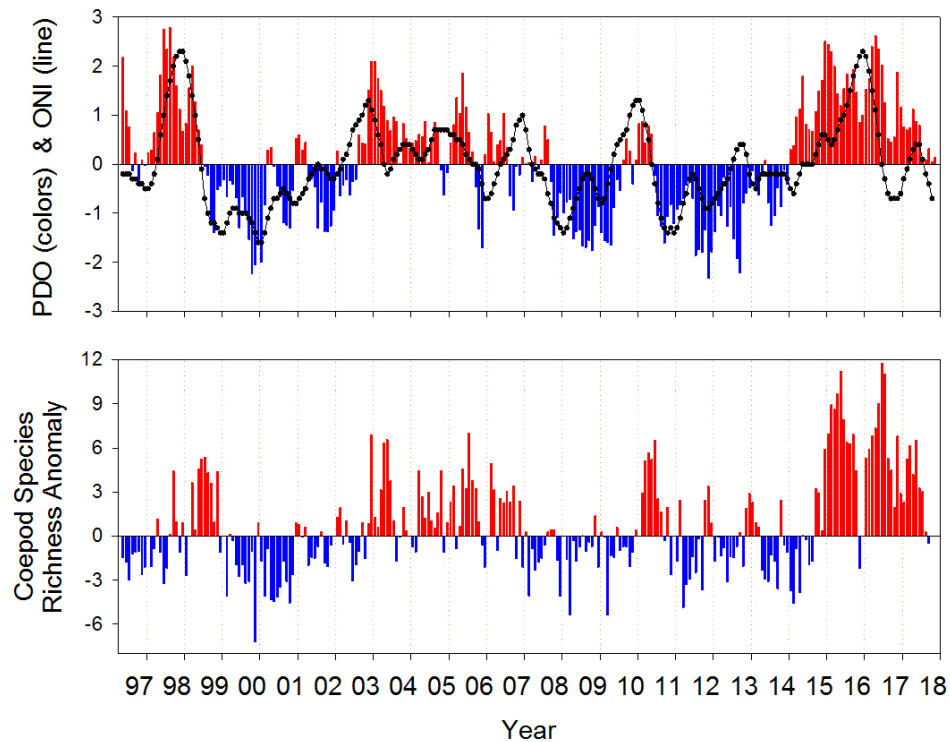
Copepod dynamics in this region of the California Current display strong seasonal patterns, influenced by circulation patterns of local winds and coastal currents. The copepod community tends to be dominated by cold-water species during the upwelling season, typically from May through September, as winds blow toward the equator and subarctic waters are transported southward from the Gulf of Alaska. As noted above, the cold-water copepod species are characterized by low species diversity. During winter, offshore warmer waters from the south carry more zooplankton species-rich water to the Oregon continental shelf. During the spring, there is a shift back to the upwelling season with increased northern copepod species and decreased species richness.

The interannual patterns of species richness and biomass anomalies of copepods with different water-type affinities are found to track measures of ocean climate variability (Fisher et al., 2015). The Pacific Decadal Oscillation (PDO) is a climate index based on sea surface temperatures across the entire North Pacific Ocean. When the ocean is cold in the eastern Pacific, the PDO has a negative value; when the ocean is warm in the California Current, the PDO has a positive value. In addition to atmospheric conditions in the North Pacific Ocean (as indexed by the PDO), coastal waters off the Pacific Northwest are also influenced by equatorial Pacific conditions, especially during El Niño events. The presence or absence of conditions resulting from the El Niño Southern Oscillation is gauged using the Oceanic Niño Index (ONI). Positive ONI values indicate warming (El Niño) conditions at the equator, while negative values indicate cooling in the eastern equatorial Pacific.

In Figure 4, the upper panel shows two time series: monthly values of the PDO (red and blue bars) and the ONI (black dotted line). The lower panel is the same graph as Figure 1 (monthly anomalies in copepod species richness). There are clear relationships between interannual variability in the physical climate indicators (PDO and ONI) and copepod species richness anomalies. The switch to a positive PDO in 2014 corresponded with high species richness in 2014 through the summer of 2017. The biomass anomalies of the southern and northern copepod species also ocean climate variability. When the PDO is negative, the biomass of northern copepods is high (positive) and the biomass of southern copepods is low (negative), and vice versa (not shown).



Figure 4. PDO and ONI ocean indices (upper) and copepod species richness (lower) anomalies



Source: NOAA/NWFSC, 2017b

Top graph: Blue bars indicate colder waters; red bars warmer waters.

Lower graph: Blue bars indicate that copepods are being transported chiefly from northern, colder waters; red bars, from southern, warmer waters or offshore.

The shift to high richness anomalies observed in 2014 and persisting through summer 2017 originated from an intrusion of warm water (dubbed the “warm blob”) into the Oregon shelf due to the North Pacific marine heat wave originated in late 2013. Subsequently, the North Pacific heat wave interacted with an El Niño developing in the equatorial Pacific in 2015 resulting in an unusually long period of strong warm anomalies (Peterson et al., 2017). Because of the anomalously warm ocean conditions throughout much of 2015 and 2016, the copepod community was dominated by warm-water species while the biomass of northern species was lower than usual. These conditions lead to poor feeding conditions for small fish, that in turn are prey for juvenile salmon, affecting the local hydrography and pelagic communities. As previously stated, the seasonal shift from a winter warm copepod community to a cold summer community did not occur in 2015 or 2016. However, in July 2017, the copepod community did shift to a community dominated by cold water species and the species richness also dropped to average levels. This is the first indication that the pelagic ecosystem might be returning to normal following 3 years of anomalous conditions that far exceeded previous perturbations the past 22 years (Wells et al., 2017).



Technical Considerations

Data Characteristics

The copepod data are based on biweekly sampling off Newport, Oregon, and are usually available by the end of each month. The sampling station is a coastal shelf station located 9 kilometers offshore, at a water depth of 62 meters. Samples are generally collected during daylight hours, using nets hauled from 5 meters off the bottom to the surface. One milliliter subsamples containing 300-500 copepods were used to enumerate copepods by species, developmental stage, and taxa-specific biomass estimated from literature values or the investigators' unpublished data of carbon weights. Samples collected from 1996 through May 2017 were counted by the same person, thereby limiting taxonomic inconsistencies or bias among plankton counters.

Northern and southern biomass anomalies are derived by converting counts to biomass using length-to-mass regressions and standardized to units of mg Carbon m⁻³. The copepod biomass data (mg C m⁻³) are averaged monthly and transformed by taking the base 10 logarithm, specifically log₁₀(x + 0.01). Monthly biomass anomalies are calculated for each species using 1996–2014 as the base period. Species are grouped based on their water mass affinities (southern or northern), and the individual biomass anomalies are averaged within each group (southern and northern) (Fisher et al., 2015).

Values are posted on two websites (<https://www.nwfsc.noaa.gov/oceanconditions> and <https://www.integratedecosystemassessment.noaa.gov/regions/california-current-region/indicators/climate-and-ocean-drivers.html>) and updated annually. Monthly values are available to anyone who requests them. Details of the sampling program and data analysis can be found in Peterson and Schwing, 2003; Peterson and Keister, 2003; and Fisher et al., 2015.

Strengths and Limitations of the Data

This 22-year time series represents the longest biological monitoring of lower trophic levels in the northern California Current. While longer time series of physical variables (e.g., PDO) provide important context for understanding variability over decadal scales, these monitoring efforts provide the foundation for examining relationships between copepod populations and fish, birds, and mammals.

For more information, contact:



Kym Jacobson
NOAA Fisheries, Hatfield Marine Science Center
Newport, OR 97365
(541) 867-0375



Jennifer Fisher
Cooperative Institute for Marine Resources Studies
Oregon State University
Newport, OR 97365
(541) 867-0109



References:

- Emmett R (personal communication). NOAA Fisheries Service, Hammond, OR.
- Fisher JL, Peterson WT, and Rykaczewski RR (2015). The impact of El Niño events on the pelagic food chain in the northern California Current. *Global Change Biology* **21**(12): 4401–4414.
- Hooff R and Peterson WT (2006). Copepod biodiversity as an indicator of changes in ocean and climate conditions in the northern California current ecosystem. *Limnology Oceanography* **51**(6): 2607-2620.
- Jahncke J, Saenz BL, Abraham CL, Rintoul C, Bradley RW, and Sydeman WJ (2008). Ecosystem responses to short-term climate variability in the Gulf of the Farallones, California. *Progress in Oceanography* **77**(2-3): 182-193.
- Manugian S, Elliott ML, Bradley R, Howar J, Karnovsky N, et al. (2015) Spatial Distribution and Temporal Patterns of Cassin's Auklet Foraging and Their Euphausiid Prey in a Variable Ocean Environment. *PLoS ONE* **10**(12): e0144232.
- Miller, JA, Peterson WT, Copeman LA, Du X, Morgan CA, and Litz MNC (2017). Temporal variation in the biochemical ecology of lower trophic levels in the Northern California Current. *Progress in Oceanography* **55**:1–12.
- NOAA/NWFSC (2017a). National Oceanic and Atmospheric Administration Northwest Fisheries Science Center. Northern and southern copepod anomalies. Retrieved December 11, 2017 from <https://www.nwfsc.noaa.gov/research/divisions/fe/estuarine/oeip/eb-copepod-anomalies.cfm>
- NOAA/NWFSC (2017b). National Oceanic and Atmospheric Administration Northwest Fisheries Science Center. Copepod biodiversity. Retrieved December 11, 2017 from <https://www.nwfsc.noaa.gov/research/divisions/fe/estuarine/oeip/ea-copepod-biodiversity.cfm>
- NOAA (2018). National Oceanic and Atmospheric Administration Northwest Fisheries Science Center. Forecast of adult returns for coho salmon and chinook salmon. Retrieved December 10, 2017 from <https://www.nwfsc.noaa.gov/research/divisions/fe/estuarine/oeip/g-forecast.cfm>
- Parrish J (Personal communication). University of Washington, School of Aquatic and Fishery Science, Seattle, WA.
- Peterson WT and Keister JE (2003). Interannual variability in copepod community composition at a coastal station in the northern California Current: a multivariate approach. *Deep Sea Research Part II: Topical Studies in Oceanography* **50**(14–16): 2499-2517.
- Peterson WT and Schwing F (2003). A new climate regime in Northeast Pacific ecosystems. *Geophysical Research Letters*. **30**(17): 1896.
- Peterson WT (2009). Copepod species richness as an indicator of long term changes in the coastal ecosystem of the northern California Current. *California Cooperative Oceanic Fisheries Investigations Reports* **50**: 73-81.
- Peterson WT, Morgan CA, Casillas E, Fisher J, and Ferguson JW (2011). *Ocean Ecosystem Indicators of Salmon Marine Survival in the Northern California Current*. National Oceanic and Atmospheric Administration Northwest Fisheries Science Center. Available at http://www.nwfsc.noaa.gov/research/divisions/fed/oeip/documents/peterson_et_al_2010.pdf
- Peterson WT, Fisher JL, Peterson JO, Morgan CA, Burke BJ, et al. (2014) Applied fisheries oceanography: Ecosystem indicators of ocean conditions inform fisheries management in the California Current. *Oceanography* **27**(4): 80–89.



Peterson WT, Fisher JL, Strub PT., Du X, Risien C, et al. (2017). The pelagic ecosystem in the Northern California Current off Oregon during the 2014-2016 warm anomalies within the context of the past 20 years. *Journal of Geophysical Research Oceans* **122**(9): 7267–7290.

Wells B, Schroeder I, Bograd S, Hazen E, Jacox M, et al. (2017). State of the California Current 2016-17: still anything but "normal" in the north. *California Cooperative Oceanic Fisheries Investigations Report* **58**.

Wolf SG, Sydeman WJ, Hipfner JM, Abraham CL, Tershy BR, and Croll DA (2009). Range-wide reproductive consequences of ocean climate variability for the seabird Cassin's Auklet. *Ecology* **90**(3): 742-753.

Yamada SB, Peterson WT, and Kosro PM (2015). Biological and physical ocean indicators predict the success of an invasive crab, *Carcinus maenas*, in the northern California Current. *Marine Ecology Progress Series* **537**:175-89.



SACRAMENTO FALL-RUN CHINOOK SALMON ABUNDANCE

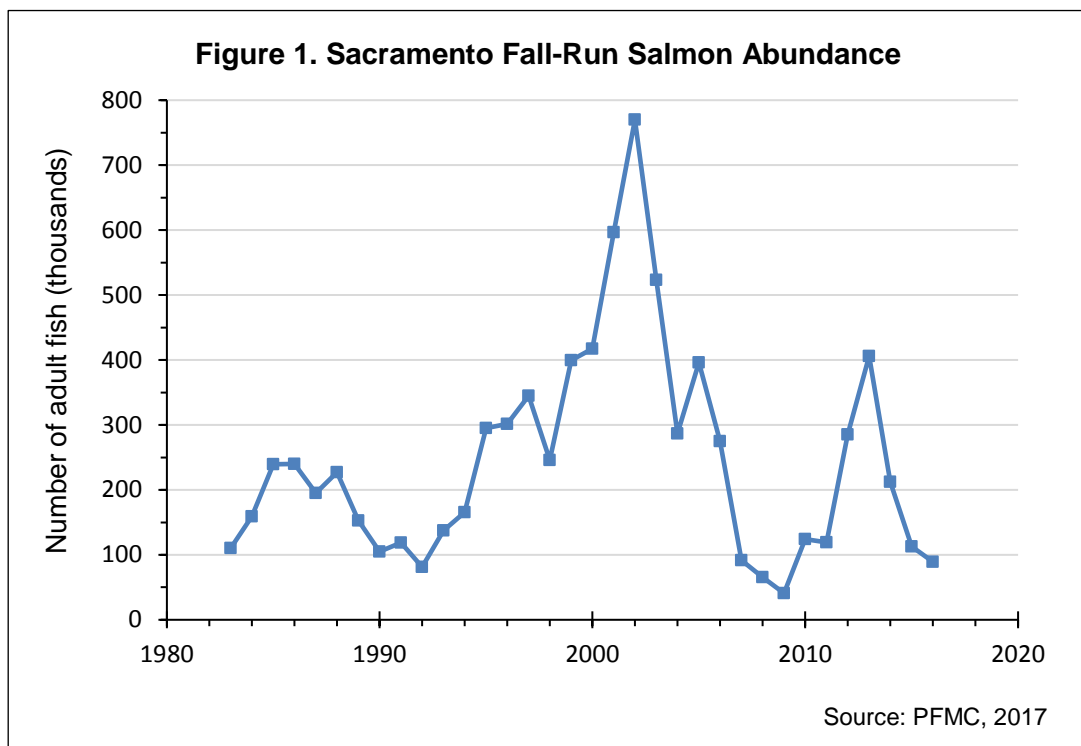
Salmon juvenile survival — and resultant adult abundance — has become more variable, with extreme juvenile mortality events occurring in the last two decades.



Photo: Allen Harthorn

Central Valley Chinook salmon (*Oncorhynchus tshawytscha*) rear in the fresh water of interior California, migrate as juveniles to feeding grounds in the Pacific Ocean, and return to fresh water from July to December to spawn. Four distinct runs of Chinook salmon spawn in the Sacramento-San Joaquin River system, named for the season when the majority of the run enters freshwater as adults.

The Sacramento River fall/late fall-run salmon comprise a large proportion of Chinook salmon spawners returning to Central Valley streams and hatcheries. This subpopulation is designated as the “indicator stock” for the Central Valley fall Chinook runs, and as a Species of Concern under the federal Endangered Species Act.



What does the indicator show?

Figure 1 shows annual escapement — the number of adult salmon returning to their freshwater spawning habitat — of Sacramento fall-run Chinook salmon, in thousands of fish. Fall-run Chinook salmon abundance fluctuated from 1983 to 2016. Relatively constant prior to 1995, the numbers peaked in 2002 before declining to near normal



levels in 2006. The sudden drop in 2007 was followed by two years of record lows — 2008 and 2009, when only about 65,000 and 41,000 adults, respectively, returned to spawn. Extremely low escapement led to the closure of commercial and recreational fisheries in 2008 and 2009 and opened for only a few days in 2010.

Salmon abundance increased to levels above the long-term average in 2012 and 2013 before declining again in 2014 and 2015. In 2016 the number of returning fall-run dropped to values similar to those witnessed in 2007.

Why is the indicator important?

Salmon are among California's most valued natural resources (CDFW, 2013). The Chinook salmon is the largest of the salmon species. This iconic fish is legendary for its migration from the streams in which it is hatched to the Pacific Ocean, where it can travel as far as a thousand miles, only to return to its natal stream to spawn and die. California marks the southern end of the range of all salmon on the Pacific coast (Moyle et al., 2017; UC Davis, 2017). In addition to their important role in the aquatic ecosystem, Sacramento fall-run Chinook salmon have been the largest contributor to ocean salmon harvest off California and Oregon for decades (O'Farrell et al., 2008). They provide a highly nutritious food source and an important source of income for the commercial salmon industry. Salmon fishing also supports a large recreational fishing community and Native Americans depend on and celebrate them in many aspects of their culture.

Salmon play a key role in marine and inland ecosystems and thus can serve as an indicator of the health of both ecosystems. They are both top predator and prey, and their carcasses contribute to nutrient cycling of riparian systems (CDFW, 2013). In combination with an understanding of the processes underlying salmon abundance, scientists can use the conditions of the ocean ecosystem to allow for rough estimates of the future abundance of adult Chinook salmon.

Both climate change and other factors described below will likely put the salmon population at risk of extirpation and/or extinction. Experts suggest that nearly all of California's salmon face extinction within 50 to 100 years, with about 45 percent of the population at risk of extinction within 50 years, if current trends in climate change and other anthropogenic stressors persist. Management strategies that protect and restore habitats and promote salmon diversity and abundance will greatly help salmon in the years to come (Moyle et al., 2017; UC Davis, 2017).

What factors influence this indicator?

California salmon abundance is influenced by dynamic interactions between natural landscape features (such as climate and topography) and commercial activities. Much of the information concerning anthropogenic impacts on salmon populations has focused on activities such as urban and agricultural runoff as well as mining. Scientists have recently started to look more critically at climate change influences on the health and survival of salmon (Moyle et al., 2013; Wells et al., 2014).



Climate change can alter freshwater, estuarine, and marine habitats, putting salmon populations at risk (Wells et al., 2014). As air temperatures rise, river and stream temperatures have increased in California and will likely continue to increase. With warming temperatures, more precipitation falls as rain instead of snow in the mountains (see *Precipitation* indicator), reducing the amount of snowmelt that provides cold water year-round to rivers and streams. Significant reductions in cold-water river and stream flows in summer will likely affect juvenile and adult migration, spawning, egg viability, and rearing conditions.

For fall-run Chinook salmon, warming freshwater temperatures delay adults' migration to streams later in the season and could cause juveniles to leave freshwater earlier in the spring, narrowing the window of time for successful reproduction and rearing. Snowpack losses are expected to be increasingly significant, especially at elevations below 3,000 meters. The lower abundance of fall-run salmon in the years 2014 and 2015 were likely influenced by a significant reduction in snowpack during those years (see *Snow-water content* indicator). Future changes in stream flow and temperature are expected to be much greater in the Sacramento River and its tributaries, which are fed by the relatively lower northern Sierra Nevada. The practice of maintaining a large pool of cold water behind reservoirs allows for controlled releases to compensate for the warmer water temperatures in the fall. A decline in snowmelt volume could threaten this pool of cold water, thus threatening successful spawning (Moyle et al., 2017).

Winter- and spring-run Chinook salmon also inhabit the complex Sacramento-San Joaquin River system. These subpopulations may respond differently to changing climate conditions due to differing life history patterns and area-specific environmental conditions. For example, while fall-run Sacramento River Chinook migrate upstream and spawn in the river during the cooler months, spring- and winter-run Sacramento River Chinook enter the river and spawn during the warmer months and for longer periods of time (CDFW, 2013), making them more vulnerable to warming freshwater temperatures associated with climate change.

Changes in physical, chemical and biological components and processes in the marine environment also affect salmon (Wells et al., 2014). Water temperature affects fish metabolism, development, behavior, and distribution. Salmon survival during the initial months of ocean life depends on available prey (largely krill, forage fish and crab larvae). Increasing ocean temperatures can negatively alter the food web on which salmon depend, changing the range of predators, competitors, and prey species. Overall, warming ocean temperatures are expected to result in range changes for California salmon, a phenomenon that is already occurring with other fishes.

In 2014-2015, the west coast of North America experienced unusually warm sea surface temperatures (see *Coastal ocean temperature* indicator). This marine heat wave first appeared as a large area of exceptionally high sea surface temperatures, informally known as the "warm blob", in the Gulf of Alaska in November 2013. It later extended southward along the entire Pacific coast of the contiguous US, where surface temperatures reached unprecedented levels in many locations. Although not yet well



understood, these unusually warm conditions were influenced by periods of weaker upwelling, the absence of winter storms, and El Niño-Southern Oscillation (ENSO) conditions.

The timing and intensity of coastal upwelling — a wind-driven motion of dense, cooler, and usually nutrient-rich water towards the surface — also impacts salmon. Salmon feed on krill and other phytoplankton in upwelled waters and have suffered population declines during years of weak upwelling conditions. As surface waters warm, an increase in water column thermal stratification is expected to increase, reducing upwelling of cold nutrient-rich water. For example, the rapid decline in krill in the juvenile salmon feeding area between 2001 and 2007 paralleled a sharp decline in salmon abundance in the Gulf of Farallones and in the central northern California region (Lindley et al., 2009). Another coastal phenomenon, rising sea levels, can lead to inundation of low-lying lands and increases in salinity, transforming estuary habitats for migrating salmon.

Another factor that may threaten salmon is the acidification of coastal waters as a consequence of increasing atmospheric carbon dioxide (Wells et al., 2014). Although acidification will likely have little direct effect on salmon, it may have a significant impact on invertebrate species that are important to the salmon diet.

Taken together, threats from climate change and historical stressors such as habitat loss and urban/agricultural runoff place salmon in a precarious condition.

Technical Considerations

Data Characteristics

Total spawning escapement values were taken from Table II-1 of the Pacific Fisheries Management Council's Preseason Report (PFMC, 2017). Natural-area escapement estimates are made using methods such as carcass surveys, aerial red counts, ladder counts, weir counts and video monitoring (O'Farrell et al., 2013).

Strengths and Limitations of the Data

Estimates of spawning escapement are extremely important to salmon management as an indication of the actual reproductive population size. The number of reproducing adults is important in defining population viability, as a measure of both demographic and genetic risks. It is equally important to harvest management, which typically aims at meeting escapement goals such that the population remains viable (for Endangered Species Act-listed populations) or near the biomass that produces maximum recruitment (for stocks covered by a fisheries management plan). Spawning escapement is the most widely available measure of abundance for West Coast salmon, although these data are often limited to the most commercially important stocks.

Spawning escapement, as an indicator of salmon abundance, differs from metrics used by fishery managers (such as the Sacramento Index). The former focuses on trends relevant for evaluating salmon populations from an ecosystem perspective.



Estimates of the number of Chinook salmon returning to spawn have been made since the early 1950s, and in some cases since the 1940s. Programs have evolved over the years, and vary in methods used, intensity of sampling effort, and reliability of estimates. Mark-recapture carcass surveys are now widely used as the standard method to estimate in-river spawning escapement. Despite their widespread use in the Central Valley, models to estimate in-river spawning escapement based on mark-recapture carcass survey data require a number of assumptions which may not be met in the surveys. Field and data analysis methods used in the existing escapement surveys have not been reviewed for adequacy of statistical power or potential bias. In addition, data management and reporting in the Central Valley is not standardized; escapement data and reports are not readily accessible in a timely way by other researchers, stakeholders, or the public.

For more information, contact:



Brian Wells
Southwest Fisheries Science Center
NOAA Fisheries Service
1352 Lighthouse Avenue
Pacific Grove, CA 93950-2097
(831) 420-3969
Brian.Wells@noaa.gov

References:

CDFW (2013). *Status of the Fisheries Report: An Update through 2011. Report to the California Fish and Game Commission as directed by the Marine Life Management Act of 1998*. California Department of Fish and Wildlife Marine Region. Available at <https://nrm.dfg.ca.gov/FileHandler.ashx?DocumentID=65489&inline>

Lindley ST, Grimes CB, Mohr MS, Peterson WT, Stein J, et al. (2009). *What caused the Sacramento River fall Chinook stock collapse? Technical memorandum* (NOAA-TM-NMFS-SWFSC-447). National Marine Fisheries Service/Southwest Fisheries Science Center. National Oceanic and Atmospheric Administration. Available at <https://s3.amazonaws.com/newsdeeply/waterdeeply/public/NOAA+2009+Report+on+Salmon+Crash.pdf>

Moyle P, Kiernan JD, Crain PK and Quinones R (2013). Climate change vulnerability of native and alien freshwater fishes of California: A systematic assessment approach. *PLoS One* **8**(5): e63883.

Moyle P, Lusardi R, Samuel P and Katz J (2017). *State of the Salmonids: Status of California's Emblematic Fishes 2017*. Center for Watershed Sciences, University of California, Davis and California Trout. San Francisco, CA. Available at <https://watershed.ucdavis.edu/news/2017/08/24/state-salmonids-status-californias-emblematic-fishes-2017-scientific-report-released>

O'Farrell MR, Mohr MS, Palmer-Zwahlen ML and Grover AM (2008). *The Sacramento Index*. Available at http://cahatcheryreview.com/wp-content/uploads/2012/08/Sacramento-Index-11_08.pdf

O'Farrell MR, Mohr MS, Palmer-Zwahlen ML and Grover AM (2013). *The Sacramento Index. National Marine Fisheries Service Technical Memorandum, June 2013* (NOAA-TM-NMFS-SWFSC-512). National Oceanic and Atmospheric Administration. Available at <https://swfsc.noaa.gov/publications/TM/SWFSC/NOAA-TM-NMFS-SWFSC-512.pdf>



PFMC (2017). *Preseason Report I: Stock Abundance Analysis and Environmental Assessment Part 1 for 2017 Ocean Salmon Fishery Regulations, March 2017* (Regulation Identifier Number 0648-BG59). Pacific Fishery Management Council. Available at http://www.pcouncil.org/wp-content/uploads/2017/03/2017_Preseason_Report_I_03MAR17_final2.pdf

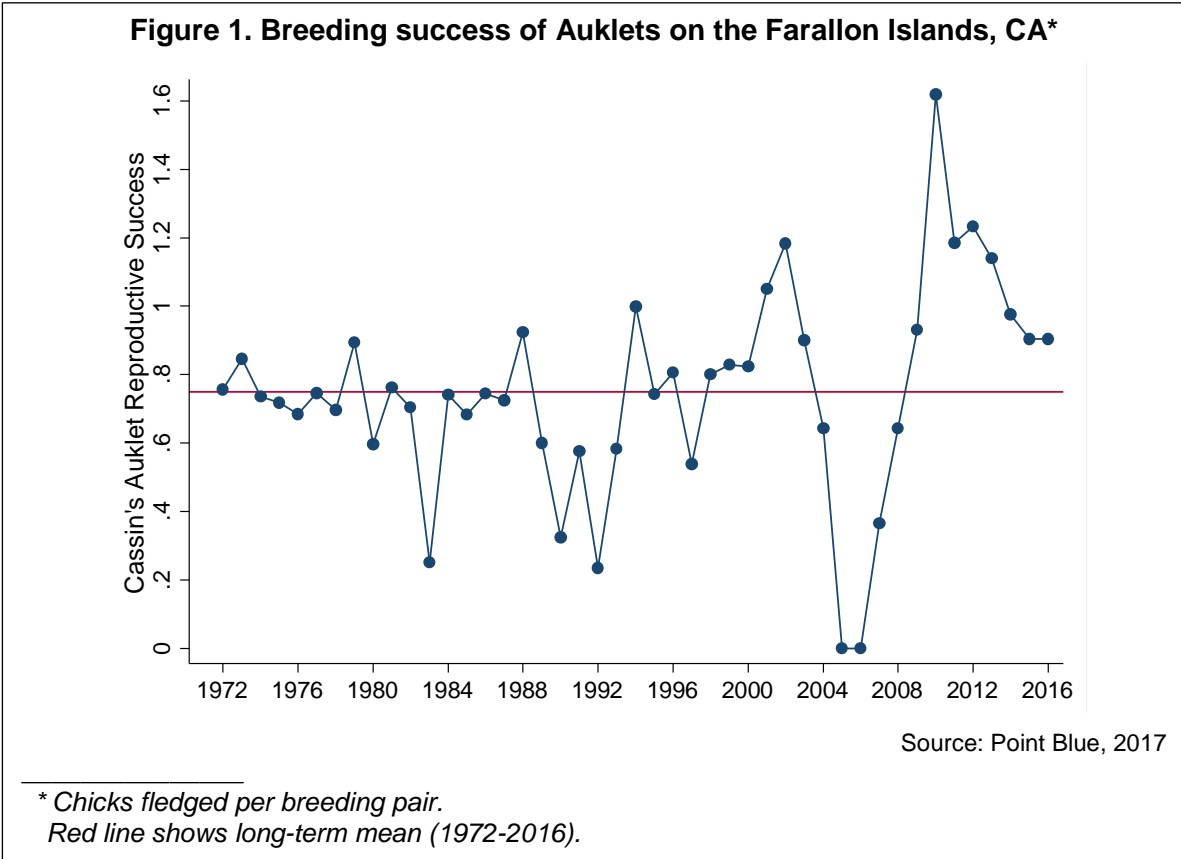
UC Davis (2017). *State of the Salmonids II: Fish in Hot Water. State of the Salmonids II: Fish in hot water Status, threats and solutions for California salmon, steelhead, and trout*. Based on a report by Dr. Peter B. Moyle, Dr. Rob Lusardi, and Patrick Samuel, University of California, Davis and California Trout. Available at https://www.waterboards.ca.gov/northcoast/board_info/board_meetings/02_2018/pdf/8/jwSOS%20II%20-%20Fish-in-hot-water.pdf

Wells B, Wainwright T, Thomson C, Williams T, Mantua N, et al. (2014). *CCIEA Phase III Report 2013: Ecosystem Components, Protected Species- Pacific Salmon*. California Current Integrated Ecosystem Assessment. Available at https://www.integratedecosystemassessment.noaa.gov/Assets/iea/california/Report/pdf/8.Salmon_2013.pdf



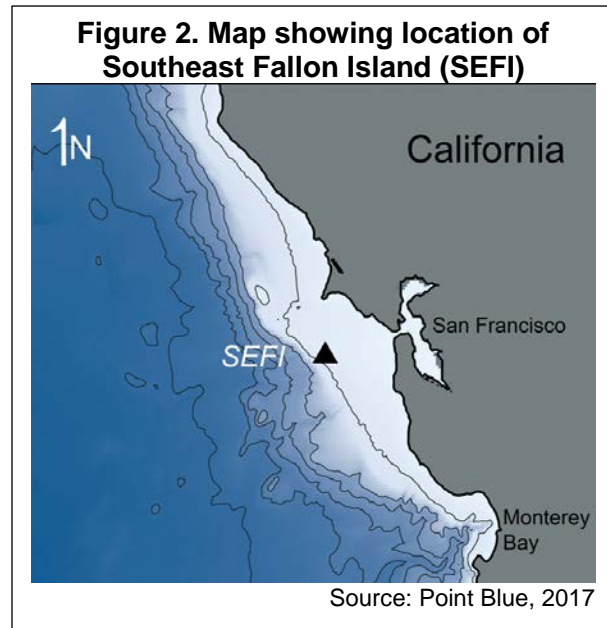
CASSIN'S AUKLET BREEDING SUCCESS

Over a 45-year period, the reproductive success of the Cassin's auklet has exhibited increasing variability (extremely low and extremely high reproductive success) with time, while showing an overall increase in reproductive success over the past 25 years.



What does the indicator show?

Figure 1 shows the variable year-to-year reproductive success of Cassin's auklets over the period 1972-2016 in study sites on Southeast Farallon Island (see map, Figure 2). Reproductive success, measured as the mean number of offspring produced per year per breeding pair declined slightly until about 1992 but since then has exhibited a significantly increasing trend. In the last 15 years, reproductive success has averaged 0.842 chicks produced ("fledged") per pair, above the previous 15-year average of 0.704 (see Table 1); the 45-year mean value is 0.75 chicks per pair.



Notable is the increase in year-to-year variability: reproductive success during the last 15 years was three times more variable than during the first 15 years (see Table 1). The two years with the lowest values and the five with the highest also occurred during the last 15 years.

Table 1. Annual variability in Cassin's Auklet breeding success, divided into three 15-year intervals

Time period	Reproductive success, Mean (Standard deviation)	Proportion of double-brooding	Rate of abandonment
1972-1986	0.704 (0.143)	0.137	0.215
1987-2001	0.704 (0.230)	0.234	0.251
2002-2016	0.842 (0.451)	0.334	0.239



The Cassin's auklet (*Ptychoramphus aleuticus*) is a small, diving seabird. Its breeding range extends from the Aleutian Islands, Alaska to islands off the middle Baja California peninsula. Its center of distribution is located off British Columbia, on Triangle Island (Rodway, 1991). Important colonies in California occur on Southeast Farallon Island (part of the Farallon Islands National Wildlife Refuge, located 30 miles west of San Francisco) and on the Channel Islands off southern California.

Cassin's auklets lay one egg per breeding attempt, and are the only species in the Alcidae family which show regular behavior of "double-brooding," that is, rearing a second chick after successfully fledging their first chick (Johns et al., 2017). Double-brooding allows productivity of the population to exceed 1.0 chick per pair in exceptionally good years. There have only been six years when mean reproductive success for the population exceeded this threshold, all since 2000. The rate of double-brooding varies among years, and as shown in Table 1, has increased over time ($P = 0.043$).

Double-brooding and the rate of abandonment of eggs during incubation are two components that account for much, but not all, of the annual variation in reproductive success. While double-brooding has increased over time, the abandonment rate has shown no such trend (Table 1). Two recent years (2005 and 2006) were unusual in that reproductive success was zero and the abandonment rate was also extremely high (100 percent and 86 percent, respectively). Neither of these years were El Niño years, but they were years in which krill were absent from the diet fed to chicks (see below). In the other 43 years, the relationship between abandonment and reproductive success was more variable. Some years with low reproductive success also had high abandonment (67 percent in 1983 and 65 percent in 1992); in 1990 reproductive success was low but abandonment was also low (17.5 percent compared to the 45-year mean of 24 percent).



Why is this indicator important?

Seabirds such as the Cassin's auklet respond to changes in prey availability and prey quality, which in turn are influenced by climate (Lee et al., 2007; Wolf et al., 2009). Hence, seabirds can be, and have been, used as reliable indicators of food web changes in marine ecosystems (Piatt et al., 2007). Seabirds are among the most conspicuous of all marine organisms and changes in their populations or vital rates may reflect changes in their prey base, such as krill, that are more difficult to study (Ainley et al., 1995; Piatt et al., 2007; Manugian et al., 2015).

Studies of seabirds suggest that ocean warming and other forms of marine climate change are affecting the coastal food web, particularly krill. Krill is a major food resource not only for seabirds, but also for salmon, other fish, and marine mammals, including whales (Dransfield et al., 2014, Sydeman et al. 2014). Ocean warming may reduce the efficacy of upwelling — the upward movement of deep, cold, nutrient-rich waters to the surface, where plankton growth occurs (Snyder et al., 2003; Manugian et al., 2015). Reduced upwelling decreases nutrient availability and photosynthesis by phytoplankton, ultimately leading to a reduction in krill and other zooplankton. Hence, upwelling is key for many seabirds in the California Current.

Measurements of auklet reproductive success provide a strong signal of changes in ocean conditions — as reflected in prey availability — in the ecosystem over the period of time when the birds are reproductively active each year (March through August). Recent years of record-high auklet productivity on the Farallones have been associated with large local increases in krill, as documented below. In addition, seabird reproductive success has been shown to correlate with salmon abundance (Roth et al., 2007), suggesting that the reduction of krill abundance may be affecting salmon as well. Thus, the auklet reproductive success indicator reflects bio-physical processes occurring in the marine ecosystem. The recent increase in both overall reproductive success and annual variability of this indicator provide insights into temporal patterns of variation in the local marine ecosystem.

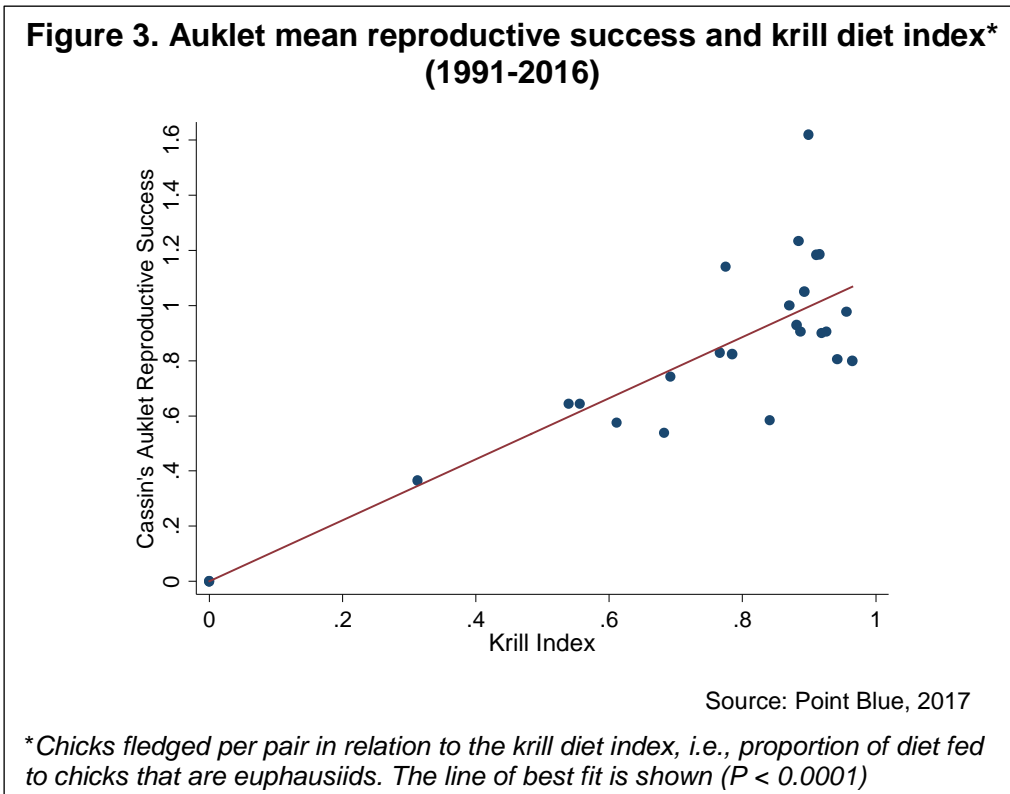
What factors influence this indicator?

Cassin's auklet breeding success on Southeast Farallon Island is most closely associated with variation in the availability of their prey, particularly krill. Krill are the main prey consumed by auklet chicks on Southeast Farallon Island, accounting for about 80 percent of their diet in typical years (Abraham and Sydeman, 2004). Auklets feed primarily on two krill species — *Euphausia pacifica* and *Thysanoessa spinifera* — as well as mysids and some larval fishes (sanddabs, rockfish, etc.). Years characterized by low krill biomass in the auklet's foraging grounds in the Gulf of the Farallones (e.g., 2005 and 2006) were associated with low reproductive success (Sydeman et al., 2006; Jahncke et al., 2008; Manugian et al., 2015). Conversely, during years when krill was abundant in the region (e.g., 2010 and 2011), auklets exhibited high productivity, more specifically high rates of double-brooding, as described below.

Auklet reproductive success is strongly related to measures of krill abundance and/or availability. There was a strong, linear relationship between the "krill diet index" for



Cassin’s auklets and their reproductive success (see Figure 3 below). The krill diet index is the proportion of prey fed to Cassin’s auklet chicks that consists of the two krill species listed above. The median value of the krill diet index was 87 percent (n = 25 years). However, in years when the krill diet index was less than 75 percent, reproductive success was in every case (n = 8 years) below the mean (and median) value for the entire time series. The krill index in 2005 and 2006 was zero. Conversely, high krill index values are associated with moderate to high reproductive success, though, even then, auklets exhibit considerable variability in outcome.



In addition, measures of krill abundance or biomass (to 30 meters deep, estimated by acoustic surveys conducted by Point Blue’s ACCESS Project) (Manugian et al., 2015) were more closely related to reproductive success than the krill diet index alone. In particular, the frequency of double-brooding is more closely related to krill biomass than the krill diet index. These results make clear that krill abundance and/or availability determines both high values of reproductive success (when double-brooding is common) and low values.

The influence of seasonal, wind-driven upwelling processes off the California coast on the productivity of the marine food web is well established (Garcia-Reyes et al., 2015). Upwelling brings deep, nutrient-rich waters to the surface. These nutrients are vital to the growth of plankton, which form the base of the marine food chain. Upwelling is driven by oceanographic conditions, especially wind patterns, which in turn reflect large-scale climate signals associated with the tropical Pacific Ocean – El Niño-Southern Oscillation (ENSO) (WRCC, 1998) — as well as with the North Pacific (Pacific Decadal



Oscillation and the North Pacific Gyre Oscillation (NPGO) (Di Lorenzo et al. 2008)). ENSO is a cyclic interaction between the atmosphere and ocean in the tropical Pacific that has manifold effects, including the periodic variation between below-normal and above-normal sea surface temperatures. NPGO is part of a large-scale pattern of climate variability in the North Pacific that affects sea surface height and sea surface temperature; it also influences the strength of ocean circulation in the North Pacific Gyre, which includes waters transported into the California Current Ecosystem.

Cassin's auklet reproductive success, in turn, has been associated with these underlying patterns of climate variability (Abraham and Sydeman, 2004; Sydeman et al., 2006; Jahncke et al., 2008; Wells et al., 2008). During two of the strongest El Niño periods in the last four decades (1982-83 and 1991-1992), there was a substantial decrease in auklet breeding success. In contrast, recent years have shown auklet reproductive success to be less linked to ENSO signals and more strongly associated with the NPGO (Di Lorenzo et al. 2008, Schmidt et al., 2014). Changes in both the characteristics of the El Niño Southern Oscillation (such as a shift in the center of the warm water anomaly from the eastern Pacific to central Pacific) and a shift to greater positive values of the NPGO (which is associated with the earlier onset of upwelling favorable conditions) are likely playing a role in the shift in the auklet response (Schmidt et al., 2014). It is hypothesized that local changes in upwelling winds in the California Current are more consistent with changes in the NPGO index than indices of ENSO.

Technical Considerations

Reproductive success of Cassin's Auklets is measured by monitoring breeding birds in 44 nest boxes on Southeast Farallon Island (Abraham and Sydeman, 2004; Lee et al., 2007). Greater than 90 percent of the boxes are occupied by breeding birds each year, although fewer pairs attempt reproduction in years of poor food availability. Each nest box is checked every 5 days for nesting activity. Parent birds are uniquely banded for future identification. The date of egg-laying, number of eggs laid and hatched, and the number of chicks raised to independence by each breeding pair is counted. For this indicator, the overall annual reproductive success is assessed as the average number of offspring fledged per breeding pair per year. "Double brooding" rate, as discussed here, is defined as the proportion of birds that initiate a second reproductive effort (i.e., lay an egg) after fledging a chick successfully in their first attempt. "Abandonment rate" is defined as the proportion of breeding pairs which permanently left eggs unattended during incubation, leading to egg failure.

Strengths and Limitations of the Data

Cassin's Auklets and other breeding seabirds have been monitored on the Farallon Islands using standardized methods since 1972 (Boekelheide et al., 1990; Johns et al., 2017). During the 45-year period, great care was taken to keep the methodology as comparable as possible. Field biologists are intensively trained by professional biologists from Point Blue Conservation Science. Thus, methodology has remained highly consistent over the past 45 years.



Seabirds have demonstrated that they are excellent indicators of ecological conditions (Parsons et al., 2008). One strength of the indicator is the ability to correlate reproductive success directly with a key determinant of this ecological variable, the availability and/or abundance of two key prey species. The time series reflecting krill in the chick diet is now 25 years. The time series based on direct measures of krill biomass in the areas near the breeding colony is now 13 years. The longer time series has provided a better understanding of determinants of krill abundance (Manugian et al., 2015).

Their ability to initiate a second clutch after a successful first breeding make Cassin's auklets particularly valuable as an ecosystem indicator among seabirds. Their flexible reproductive strategy allows for tracking both positive deviations (when double-brooding is more common) and negative deviations (when mortality of eggs and/or chicks is high). Thus, the range of outcomes for Cassin's auklets is greater than that of species that lay only one clutch of a single egg.

A limitation of the indicator is that identifying a climate change signal due to anthropogenic influences is difficult to discern, compared to the effect of natural climate variability (e.g., impacts of the El Niño Southern Oscillation). In this regard, the increased variability of the indicator in recent years is a finding of note; it improves the understanding of what may be underlying both the especially low and especially high values of auklet reproductive success.

For more information, contact:



Point Blue
Conservation
Science

Nadav Nur, Ph.D.
Point Blue Conservation Science
3820 Cypress Dr. #11
Petaluma, CA 94954
(707) 781-2555 ext. 301
nnur@pointblue.org

Russell W. Bradley
Point Blue Conservation Science
3820 Cypress Dr. #11
Petaluma, CA 94954
(707) 781-2555 ext. 314
rbradley@pointblue.org

Jaime Jahncke, Ph.D.
Point Blue Conservation Science
3820 Cypress Dr. #11
Petaluma, CA 94954
(707) 781-2555 ext. 335
jjahncke@pointblue.org



References:

- Abraham CL and Sydeman WJ (2004). Ocean climate, euphausiids and auklet nesting: inter-annual trends and variation in phenology, diet and growth of a planktivorous seabird, *Ptychoramphus aleuticus*. *Marine Ecology Progress Series* **274**: 235-250.
- Adams J, Mazurkiewicz D, and Harvey AL (2014). Population monitoring and habitat restoration for Cassin's auklets at Scorpion Rock and Prince Island, Channel Islands National Park, California: 2009–2011. Interim data summary report.
- Ainley DG, Sydeman WJ and Norton J (1995). Upper trophic level predators indicate interannual negative and positive anomalies in the California Current food web. *Marine Ecology Progress Series* **118**: 69 - 79.
- Di Lorenzo E, Schneider N, Cobb KM, Franks PJS, Chhak K, Miller AJ, et al. (2008). North Pacific Gyre Oscillation links ocean climate and ecosystem change. *Geophysical Research Letters* **35**(8).
- Dransfield A, Hines E, McGowan J, Holzman B, Nur N, et al. (2014). Where the whales are: Using habitat modeling to support changes in shipping regulations within National Marine Sanctuaries in Central California. *Endangered Species Research* **26**, 39-57.
- García-Reyes M, Sydeman W, Schoeman D, Rykaczewski R, Black B, et al. (2015). Under pressure: Climate change, upwelling, and eastern boundary upwelling ecosystems. *Frontiers of Marine Science* **2**:109.
- Jahncke J, Saenz BL, Abraham CL, Rintoul C, Bradley RW and Sydeman WJ (2008). Ecosystem responses to short-term climate variability in the Gulf of the Farallones, California. *Progress In Oceanography* **77**(2–3): 182-193.
- Johns ME, Warzybok P, Bradley RW, Jahncke J, Lindberg M, and Breed G (2017). Age, timing, and a variable environment affect double brooding of a long-lived seabird. *Marine Ecology Progress Series* **564**: 187-197.
- Lee DE, Nur N and Sydeman WJ (2007). Climate and demography of the planktivorous Cassin's auklet off northern California: implications for population change. *Journal of Animal Ecology* **76**(2): 337-347.
- Levitus S, Antonov JI, Wang J, Delworth TL, Dixon KW and Broccoli AJ (2001). Anthropogenic warming of Earth's climate system. *Science* **292**(5515): 267-270.
- Manugian S, Elliot M, Bradley R, Howar J, Karnovsky N, et al. (2015). Spatial distribution and temporal patterns of Cassin's auklet foraging and their euphausiid prey in a variable ocean environment. *PLoS ONE* **10**(12): e0144232.
- Manuwal DA and Thoresen AC (1993). *Cassin's Auklet (Ptychoramphus aleuticus)*. In: The Birds of North America (no. 50). Poole A and Gill F (Eds.), Philadelphia: The Academy of Natural Sciences.
- McGowan JA, Cayan DR and Dorman LM (1998). Climate-ocean variability and ecosystem response in the northeast Pacific. *Science* **281**(5374): 210-217.
- Parsons M, Mitchell I, Butler A, Ratcliffe N, Frederiksen M, et al. (2008). Seabirds as indicators of the marine environment. *ICES Journal of Marine Science* **65**: 1520–1526.
- Piatt IJ, Sydeman WJ and Wiese F (2007). Introduction: Seabirds as indicators of marine ecosystems. *Marine Ecology Progress Series* **352**: 199-204.
- Point Blue Conservation Science (2017). Unpublished data on Cassin's auklet reproductive success. For more information: contact Dr. Jaime Jahncke (see contact information below.)



Rodway MS (1991). Status and conservation of breeding seabirds of British Columbia. Croxall JP (Eds.), *Supplement to status and conservation of the world's seabirds*. (11): 43-102.

Roth JE, Mills KL and Sydeman WJ (2007). Chinook salmon (*Oncorhynchus tshawytscha*) - seabird co-variation off central California and possible forecasting applications. *Canadian Journal of Fisheries and Aquatic Sciences* **64**(8): 1080-1090.

Schmidt AE, Botsford LW, Eadie JM, Bradley RW, Di Lorenzo E, and Jahncke J. (2014). Non-stationary seabird responses reveal shifting ENSO dynamics in the northeast Pacific. *Marine Ecology Progress Series* **499**:249-58.

Snyder MA, Sloan LC, Diffenbaugh NS and Bell JL (2003). Future climate change and upwelling in the California Current. *Geophysical Research Letters* **30**(15): 1823.

Sydeman WJ, Bradley RW, Warzybok P, Abraham CL, Jahncke J, Hyrenbach KD, et al. (2006). Planktivorous auklet *Ptychoramphus aleuticus* responses to ocean climate, 2005: Unusual atmospheric blocking? *Geophysical Research Letters* **33**(22): L22S09.

Sydeman W, García-Reyes M, Schoeman D, Rykaczewski R, Thompson S, et al. (2014a). Climate change and wind intensification in coastal upwelling ecosystems. *Science* **345**: 77–80.

Wells BK, Field JC, Thayer JA, Grimes CB, Bograd SJ, Sydeman WJ, et al. (2008). Untangling the relationships among climate, prey and top predators in an ocean ecosystem. *Marine Ecology Progress Series* **364**: 15-29.

Wolf SG, Sydeman WJ, Hipfner JM, Abraham CL, Tershy BR and Croll DA (2009). Range-wide reproductive consequences of ocean climate variability for the seabird Cassin's Auklet. *Ecology* **90**(3): 742-753.

WRCC (1998). Western Regional Climate Center. El Niño, La Niña, and the Western U.S. Frequently Asked Questions. Retrieved from https://wrcc.dri.edu/Climate/enso_faq.php



CALIFORNIA SEA LION PUP DEMOGRAPHY

Unusually warm sea surface temperatures have been associated with declines in pup births, increased pup mortality and poor pup condition among California sea lions.

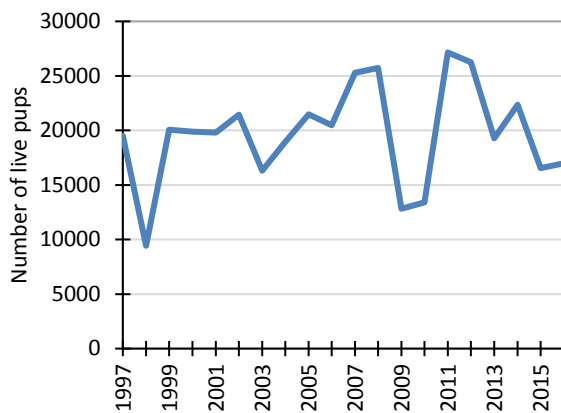
The California sea lion (*Zalophus californianus*) is a permanent resident of the California Current System. Females give birth to a single pup between May and June. For about 11 months, lactating females travel to sea for 2-5 days to feed and return to nurse their pup.

The Point Bennett Study Area at San Miguel Island (off Santa Barbara) is a large sea lion breeding area used as a long-term index colony for monitoring pup production and mortality.



Photo: Eric Boerner, NOAA

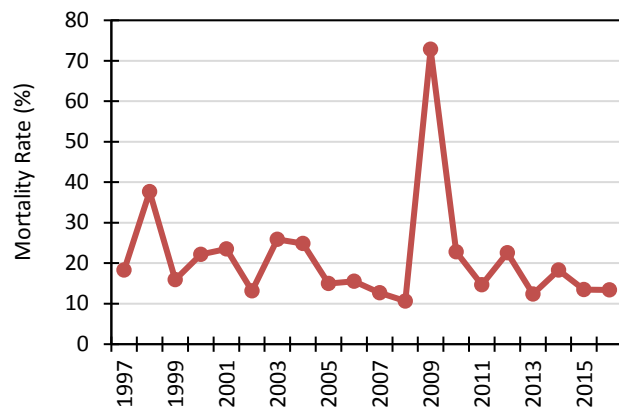
Figure 1. Sea Lion Live Pup Count*



* Based on live pups counts conducted July 20-30 annually

Source: Harvey et al., 2017

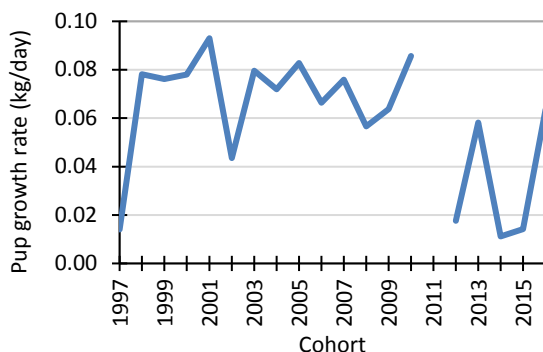
Figure 2. Sea Lion Pup Mortality Rate*



* At 5 weeks of age in the Point Bennett Study area

Source: NMFS, unpublished data

Figure 3. Female Sea Lion Pup Growth Rate*



* Estimated mean daily growth rate of female pups between 4 and 7 months of age; no count was conducted in 2011.

Source: Harvey et al., 2017

What does the indicator show?

Sea lion demographic parameters fluctuate with oceanographic conditions, particularly warm surface water temperatures. The indicator consists of three metrics based on monitoring of California sea lion population indices (pup births, pup mortality, and pup growth) and oceanic conditions between 1997 and 2016 at San Miguel Island's Point Bennett Study Area (see map, Figure 4). (Melin et al., 2010).

Annual pup counts at San Miguel Island between 1997 and 2016 ranged from a low of 9,428 to a high of 27,146 (Figure 1). The



greatest declines occurred in 1998, 2009, and 2010, all years characterized by warm ocean conditions (Wells et al., 2017).

Pup production is a result of successful pregnancies and is an indicator of fish and cephalopods that serve as prey for sea lions. The high pup counts in 2011 and 2012 suggest that pregnant females experienced good foraging conditions in these years when cooler ocean conditions prevailed. The number of births declined again in 2015 and 2016 in response to warmer ocean waters due to a marine heat wave and El Niño conditions in 2015 (McClatchie, 2016; Wells et al., 2017).

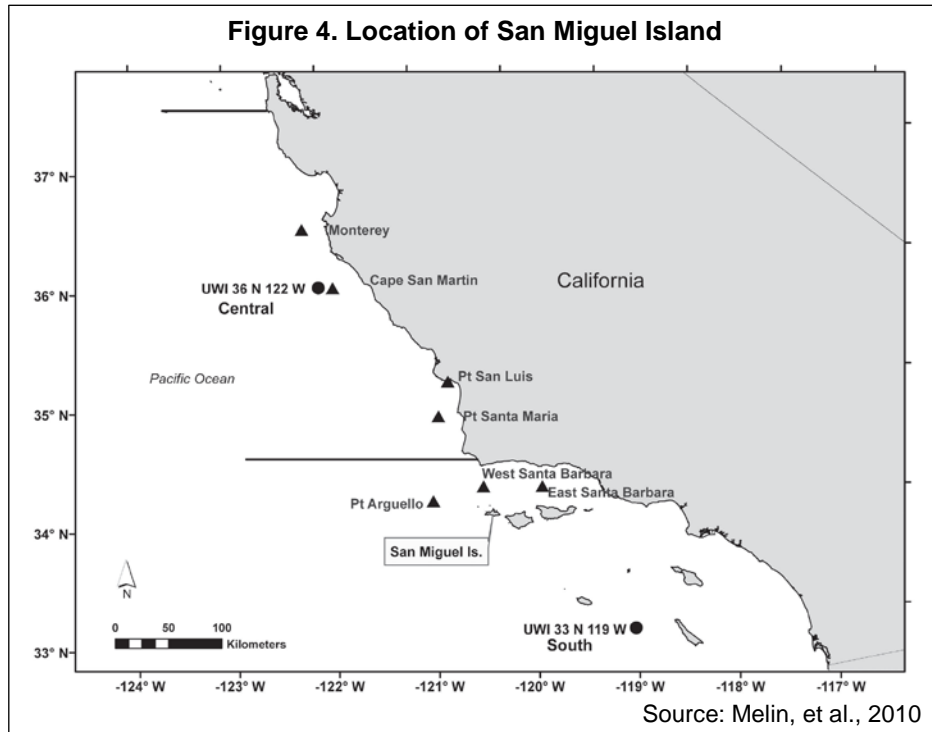


Figure 2 shows that in 2009, early pup mortality among sea lions during the first 5 weeks of life was exceptionally high, almost four times greater than the long-term average (73 percent in 2009, compared to about 20 percent long-term). The high pup mortality rates in 1998 and especially 2009 were associated with anomalously high sea surface temperatures (SSTs). However, during more recent warm ocean events in 2014-2015, pup mortality was near average, while pup growth rate during this period was low. This suggests that lactating females were able to support their pups for the short-term (first 5 weeks) but that females could not provide enough energy for long-term growth of their pups.

Pup growth from birth to 7 months of age is an indicator of the transfer of energy from the mother to the pup through lactation, which is related to prey availability during this time period. The lowest female pup growth rates occurred in 1997, 2014, and 2015 (Figure 3). (No data are available for 2011; researchers were unable to conduct a count that year.) These years were characterized by unusually warm ocean temperatures that were associated with El Niño conditions (1997, 2015) and a marine heat wave (2014-



2015) (Wells et al., 2017). Pup growth for the 2014 cohort was the lowest observed over the time series. As ocean conditions returned to near-normal in 2016, pup growth improved, returning to the long-term average (Wells et al., 2017). The very low growth rate for the 2012 cohort occurred during an unusually cold period of ocean conditions during winter 2012/2013 that normally would have resulted in good growth rates; the causes of the low growth rates for the 2012 cohort remain unexplained.

Why is this indicator important?

Sea lions and other marine mammals are prominent animals that reflect ecosystem variability and degradation in the ocean environment. Animals at higher levels in the food chain provide insights into relationships among marine community structure and oceanographic conditions (Weise, 2008). Scientists use marine mammals as sentinels of ocean production and changes in food webs, and increasingly include them in studies of changing oceanographic conditions (Moore, 2008).

Sea lions are among the most abundant top predators of the food chain in the coastal and offshore California waters. They are vulnerable to the seasonal, annual and multiyear fluctuations in the productivity of the ocean. Sea lion prey such as fish and cephalopods are also influenced by particular sets of environmental conditions along the California coast.

One of the greatest threats to the California sea lion comes from changes in their food resources due to climate and other influences (Learmonth et al., 2006). Air and ocean temperatures are warming and projected to continue to warm, especially in the summer. The biological impacts of these changes may be a lower rate of ocean productivity and thus less food for many species. This can lead to shifts in the geographical distributions of marine species (for example to higher latitudes or deeper waters), and cause changes in community composition and interactions (IPCC, 2014). More resilient species may gain predominance and abundance while others become less competitive or easier prey. Shifts in the abundance and distribution of prey have had serious consequences for sea lion reproduction and survival.

Tracking pup population indices provides insight into how the California sea lion population is responding to environmental and anthropogenic changes. Although the population of California sea lions in coastal waters from the United States-Mexico border to southeast Alaska has steadily increased since the early 1970s, recent declines in pup production and survival in this area suggest that the population may have stopped growing (Laake et al., 2018).

What factors influence this indicator?

The California Current System (CCS) has a large impact on the food supply and survival of sea lion pups along the coast. A regional process known as “upwelling” carries the deep, cooler waters transported by the current upward, closer to the surface where photosynthesis by phytoplankton occurs. This productive zone supports important commercial fisheries as well as marine mammal and sea bird populations. CCS waters are influenced by large-scale processes resulting from the



El Niño-Southern Oscillation (ENSO). El Niño conditions associated with the warm phase of ENSO occur irregularly at intervals of two to seven years, often leading to a weakened upwelling, low-nutrient waters and higher SSTs. Increased summertime SSTs due to decreased upwelling strength of ocean currents is reported to reduce availability of prey in the sea lion foraging zone.

Sea lion pups are solely nutritionally dependent on their mother's milk for the first six months of their lives. Sea lion pup survival is highly dependent on the lactating mother's ability to find food in coastal waters near the colony. While their mothers are at sea on feeding trips, the pups are fasting at the colony. When prey availability is reduced near the colony, lactating females must travel farther to obtain food, resulting in longer periods away from their pups. Consequently their fasting pups are more vulnerable to starvation. Further, if the female does not obtain enough prey for her own nutritional and energy needs, she may not be able to provide sufficient energy for her pup to grow. Newly weaned pups just learning to forage on their own may also be vulnerable when prey availability is low because they have less fat to sustain periods of poor feeding conditions and fewer behavioral options to acquire food (e.g., limited diving ability). During periods of reduced prey conditions, increased numbers of malnourished sea lion pups are found stranded along the coast.

The low pup count, highest pup mortality rate and record number of strandings in 2009 were associated with anomalous oceanographic conditions along the California coast between May and August. During that year, upwelling was the weakest in the past 40 years; this was accompanied by uncharacteristically warm June SSTs. Negative upwelling patterns and warmer SSTs during the summer required lactating females to take longer than average foraging trips (averaging 7 days, approaching the maximum duration for which pups survive without nursing, 9 days). Additionally, the diet of California sea lions in 2009 varied significantly from other years, with cephalopods and rockfish occurring more frequently. The combination of longer foraging trips and a diet principally of rockfish and cephalopods did not provide adequate energy for lactating females to support their pups.

Since 2013, fisheries surveys confirm that the primary prey fish of sea lions (e.g., anchovy, sardine, hake) have not been abundant in the foraging area, probably in response to warmer ocean conditions (McClatchie, 2016; Wells et al., 2017). This was especially evident in 2014-2015, when the Pacific Coast experienced unusually warm SSTs due to the marine heat wave and El Niño conditions (Leising et al., 2015). Consequently, nursing females were not able to provide enough energy for their pups to grow, pups weaned too early or weaned in poor condition, and large numbers of pups stranded along the California coast in 2015 (McClatchie, 2016). When ocean conditions began returning to neutral conditions in 2016, sea lions responded fairly quickly with higher numbers of pup births, reduced pup mortality and improved pup condition and growth, further supporting their utility as an indicator of CCS conditions.

Harmful algal blooms periodically occur along the California coast, especially during years when water temperatures are unusually warm. During the 2014-2015 marine



heatwave, a record-breaking algal bloom extended across the entire west coast, and included the phytoplankton *Pseudo-nitzschia*, which produces the neurotoxin domoic acid. This toxin can enter the marine food web, contaminate sea lion prey species and pose a threat to foraging sea lions and their offspring. Although incidents of sea lion poisoning from domoic acid have been reported, scientists have not quantified the effects of this toxin on sea lion pup births and growth. However, in a warming marine environment, harmful algal blooms and related toxins may become an increasingly important threat to the coastal food web, including the sea lion population.

Technical considerations

Data characteristics

San Miguel Island, California (34.03°N, 120.4°W), contains one of the largest colonies of California sea lions. The Point Bennett Study Area contains about 50 percent of the births that occur on San Miguel Island and provides a good index of trends for the entire colony. This site has been used as a long-term index site since the 1970s for measuring population parameters.

Population indices (live pups, pup mortality, pup growth) were measured by observers at San Miguel Island. Because of the large size of the colony, index sites were used to estimate population parameters.

Live pups were counted after all pups were born (between 20–30 July) each year. Observers walked through the study area, moved adults away from pups, and then counted individual pups. A mean of the number of live pups was calculated from the total number of live pups counted by each observer. The total number of births was the sum of the mean number of live pups and the cumulative number of dead pups counted up to the time of the live pup survey.

Pup mortality was assessed to calculate mortality at 5 weeks of age, 14 weeks of age, and the total number of pups born. Pup mortality surveys conducted every 2 weeks from late June to the end of July were used as an index of pup mortality at 5 weeks of age and to calculate total births for the study area. A final survey was conducted the last week of September to estimate pup mortality at 14 weeks of age. On each survey, dead pups were removed from the breeding areas as they were counted. The total number of observed dead pups for each survey described the temporal trend in pup mortality and was an estimate of the cumulative mortality of pups at 5 weeks or 14 weeks of age. Cumulative pup mortality rate was calculated as the proportion of the number of pups born in each year that died by 5 weeks of age or 14 weeks of age of the total number of pups born in each year.

Female sea lion **pup growth rates** are shown in Figure 3. Data for male pup growth rates (not presented) show the same trend over this 18-year period. To estimate sea lion pup growth rate, between 310 and 702 pups were selected from large groups of California sea lions hauled out in Adams Cove (part of the Point Bennett Study Area) over 4–5 days in September or October in each year (pups about 14 weeks old). Pups were sexed, weighed, tagged, branded, and released. Because the weighing dates



were not the same in each year, the weights were standardized to an October 1 weighing date. A mean daily weight gain rate multiplied by the number of days from the weighing date to October 1 was added or subtracted from the pup weight based on the number of days before (–) or after (+) October 1 when the pup was weighed. The number of days between October 1 and the actual weighing day was included as a parameter (days) in models to describe the annual variability in pup weights. Similarly, pups were recaptured in February a second time and weights were adjusted to a February 1 date to determine growth rate between October 1 and February 1. Growth rate data are missing in 2011 because the investigators were unable to conduct field sampling in February of that year.

The response of sea lions to warmer ocean conditions was determined from models of SST and the sea lion population indices (Melin et al., 2012). Sea surface temperature anomalies were calculated from seven buoys along the central coast (from San Luis Obispo to the San Miguel Island area). This length of coastline represents the foraging range of the juvenile and lactating female sea lions. The buoy data were obtained from the NOAA National Data Buoy Center (<http://ndbc.noaa.gov/rmd.shtml>). The mean daily SSTs from the seven buoys were used to calculate mean monthly SSTs and averaged to create monthly sea surface temperature anomaly indices for the years 1997 to 2016 used in the analysis.

Strengths and limitations of the data

The study area represents about 45 percent of the US sea lion breeding population (Melin et al., 2010), thus providing a representative measure of trends in population responses to changes in the ocean environment. Because the area is large, index sites across the colony were used to measure population parameters. Instead of using total counts for pup production and mortality, mean values were used to estimate these parameters.

The use of SST from buoys represents a very localized view of ocean conditions at the surface but does not reflect more complex oceanographic processes occurring offshore or deeper in the water column that also may influence prey availability and the resulting population responses.

For more information, contact:



Sharon Melin
NOAA, National Marine Fisheries Service
Alaska Fisheries Science Center
National Marine Mammal Laboratory
7600 Sand Point Way N.E.
Seattle, WA 98115
(206) 526-4028
Sharon.Melin@noaa.gov



References:

Gentemann C, Fewings M and Garcia-Reyes M (2017). Satellite sea surface temperature along the West Coast of the United States during the 2014-2016 northeast Pacific marine heat wave. *Geophysical Research Letters* **44**: 312-310.

Harvey C, Garfield N, Williams G, Andrews K, Barceló C, et al. (2017). *Ecosystem Status Report of the California Current for 2017: A Summary of Ecosystem Indicators Compiled by the California Current Integrated Ecosystem Assessment Team (CCIEA)*. (NOAA Technical Memorandum NMFS-NWFSC-139). Seattle, WA: Northwest Fisheries Science Center, U.S. Department of Commerce. Available at <https://doi.org/10.7289/V5/TM-NWFSC-139>

Laake JL, Lowry MS, DeLong RL, Melin SR and Carretta JV (2018). Population growth and status of California sea lions. *Journal of Wildlife Management* **82**(3): 583-595.

Learmonth JA, Macleod CD, Santos MB, Pierce GJ, Crick HQP and Robinson RA (2006). Potential effects of climate change on marine mammals. *Oceanography and Marine Biology: An Annual Review* **44**: 431-464.

Leising AW, Schroeder ID, Bograd SJ, Abell J, Durazo R, et al. (2015). State of the California Current 2014-15: Impacts of the warm water “blob”. *CalCOFI Report* **56**:31-68. Available at <http://www.calcofi.org/publications/calcofireports/v56/Vol56-CalCofi.Journal.2015.pdf>

McClatchie S (2016). State of the California Current 2015-16: Comparisons with the 1997–98 El Niño. *CalCOFI Report* **57**:5-108. Available at http://calcofi.org/publications/calcofireports/v57/Vol57-CalCofi_pages.2016.pdf

McClatchie SI, Hendy L, Thompson AR, and Watson W (2017). Collapse and recovery of forage fish populations prior to commercial exploitation. *Geophysical Research Letters* **44**: 1-9.

Melin SR, Orr AJ, Harris JD, Laake JL, DeLong RL, et al. (2010). Unprecedented mortality of California sea lion pups associated with anomalous oceanographic conditions along the central California coast in 2009. *CalCOFI Reports* **51**: 182-194. Available at http://calcofi.org/publications/calcofireports/v51/Vol51_Melin_pg182-194.pdf

Melin SR, Orr AJ, Harris JD, Laake JL and DeLong RL (2012). California sea lions: An indicator for integrated ecosystem assessment of the California Current System. *CalCOFI Report* **53**:140–152.

Moore SE (2008). Marine mammals as ecosystem sentinels. *Journal of Mammalogy* **89**(3): 534-540. Available at <http://www.mammalsociety.org/articles/marine-mammals-ecosystem-sentinels>

NMFS (2017). *Sea lion pup mortality survey results*. National Marine Fisheries Service. Unpublished data.

Portner H-O, Karl DM, Boyd PW, Cheung WWL, Lluich-Cota SE, et al. (2014): Ocean systems. In: *Climate Change 2014: Impacts, Adaptation, and Vulnerability. Part A: Global and Sectoral Aspects. Contribution of Working Group II to the Fifth Assessment Report of the Intergovernmental Panel on Climate Change*. Field CB, Barros VR, Dokken DJ, Mach KJ, Mastrandrea MD, et al. (Eds.]. Cambridge, United Kingdom and New York, NY, USA: Cambridge University Press. pp. 411-484. Available at http://ipcc.ch/pdf/assessment-report/ar5/wg2/WGIIAR5-Chap6_FINAL.pdf

Weise MJ and Harvey JT (2008). Temporal variability in ocean climate and California sea lion diet and biomass consumption: implications for fisheries management. *Marine Ecology Progress Series* **373**: 157-172. Available at <http://www.int-res.com/abstracts/meps/v373/p157-172/>



Wells BK, Schroeder ID, Bograd SJ, Hazen EL, Jacox MG, et al. (2017). State of the California Current 2016-17: Still anything but "normal" in the north. *CalCOFI Report* **58**: 1-55. Available at http://calcofi.org/publications/calcofireports/v58/Vol58-CalCOFI_2017.pdf



EMERGING CLIMATE CHANGE ISSUES

Scientists are reporting changes in California's environment that are plausibly — but not yet established to be — influenced by climate change. The link to climate change is supported by scientifically defensible hypotheses, models and/or limited data. However, deciphering the influence of climate among other factors presents a challenge. Factors such as land use and environmental pollution, as well as the inherent variability of the climate system, make it difficult to attribute some of these changes and impacts to climate change. Environmental changes and trends for which the influence of climate change remains uncertain are discussed in this section as **emerging issues**. Additional data or further analyses are needed to determine the extent by which climate change plays a role.

COASTAL FOG

Fog is a cloud layer at ground level. Fog droplets are 100 times smaller than raindrops and stay suspended in air, sometimes coalescing into drizzle or impacting on surface to form fog drip. In hilly terrain along the California coast, the low cloud layer only touches the ground at higher elevation. Coastal fog is a result of a delicate balance between moist marine air cooled by the ocean and an upper layer of drier, warmer air capping the fog layer, forming an inversion.

Globally, observations of fog from ships since 1800 are available, as well as observations from airports since 1950, and from satellites since 1980. Each of these vantage points gives a different perspective on long-term trends. Ship-based observations show an increasing trend in fog since 1950 off the California coast (Dorman, 2017). Researchers have used hourly airport measurements of cloud ceiling heights from 1951-2008 and a temperature-based statistical method to model fog frequencies along California's coastal redwood region (Johnstone and Dawson, 2010). The backcast analysis inferred that there has been a 33 percent reduction in summertime coastal fog. The only dynamic simulation model for California coastal fog to date estimated a 12 to 20 percent reduction from the period 1900-2070 (O'Brien et al., 2013). However, because the model was limited in its ability to incorporate certain processes and feedbacks, the results are uncertain. Reductions in summertime coastal fog due to shifts in coupled ocean-atmospheric process have also been observed globally, including Hokkaido, Japan (Sugimoto et al., 2013); the Kiril Islands, Russia (Zhang et al., 2015); and in Europe (Egli et al., 2017).

Coastal fog formation is driven by many climate processes and physical influences (Koračin et al., 2014; Clemesha et al., 2017). High pressures zones over the Pacific, which help to produce inversions, can change position leading to changes in fog frequency. Strong coastal winds can increase colder ocean water upwelling, leading to a thicker fog layer (Dorman, 2017). Turbulence between layers of moist air and dry air can carry moisture out of the fog layer as it mixes into the drier air layer above it, dissipating the fog. In addition, highly localized offshore and onshore movements of fog are affected by complex topographical features such as mountains and other geological barriers (Torregrosa et al., 2016; Wang and Ullrich, 2017).

Warming temperatures can have a strong influence on some of the processes affecting fog formation. Periodic increases of coastal fog have been associated with the warm phase of the Pacific Decadal Oscillation, an ocean temperature index (Witiw and LaDochy, 2015). Changes in global air patterns can also cause strong changes in fog at the local level. For example, the resilient atmospheric ridge that parked warm dry air over California in August 2017 shut down the usual pattern of onshore coastal fog advection into coastal ecosystems (see also September 2010 event, Kaplan et al., 2017). How these climate processes work together under the influence of changing climate conditions is not well understood.

In addition to large-scale climate forces, fog formation is influenced by local conditions. Studies of coastal fog in Southern California report reductions in fog near densely populated urban areas (Williams et al., 2015; LaDochy and Witiw, 2012). Urban surfaces warm during the day, causing warmer nighttime air temperatures that prevent fog droplets from forming. Declining atmospheric particulate levels are also associated with reductions in coastal fog in Southern California. Similarly, a decrease in airborne particulates appears to be a major factor in the decline of fog formation in California's Central Valley (see *Central Valley fog*, emerging indicator).

Fog plays a vital role in coastal ecosystems. Species restricted to the coastal zone such as coast redwood trees can get up to a third of their water from fog (Burgess and Dawson, 2004). Plants in fog-filled forests can take in water through their leaves, supplying lifesaving "fog drip" to salmon and trout in low flow coastal streams that would otherwise dry out during the late summer dry season (Dawson, 1998; Sawaske and Freyberg, 2015). Shade from summertime fog and low clouds cools coastal systems, reducing the rate of plant evapotranspiration and plant uptake of subsurface water reserves, leaving more water in the system (Chung et al., 2017). Summertime fog and low clouds carried by winds move deep into California's northwestern oriented valleys that are some of the states' most productive agricultural regions, including the Salinas Valley and the wine grape growing regions of Sonoma and Napa counties (Torregrosa et al., 2016).

The disappearance of fog in late summer can exacerbate the climatic water deficit for entire watersheds, leading to fire-ready tinder conditions. In urban areas, the disappearance of summertime fog leads to warmer summertime temperatures that result in greater electrical demand for cooling. The importance of fog to California's water and energy balance and to human and ecosystem wellbeing is receiving increased attention and study (Torregrosa et al., 2014; Burns, 2017; McLaughlin et al., 2017). Researchers are even exploring the use of geoengineering to increase marine clouds to cool the planet (Ahlm et al., 2017). Research on climate change impacts on fog formation will help to improve forecasts of future trends and understanding of coastal fog impacts on California.

CENTRAL VALLEY FOG

Both anecdotal evidence and field measurements indicate that California's Central Valley winters are less foggy than they were several decades ago. Scientists have collected data from satellite imagery and weather stations to analyze weather conditions and occurrences, spatial extent and long-term trends in "tule fog" — a thick winter ground fog that blankets the valley (Baldocchi and Waller, 2014). The researchers paired National Aeronautics and Space Administration and National Oceanic and Atmospheric Administration satellite records with data from a network of valley weather stations and counted the number of days each year when fog occurred during the winter from 1981-2014. Over the 32-year timespan, the number of winter fog events decreased 46 percent, on average, with much year-to-year variability.

The optimal meteorology for Central Valley fog formation occurs during winters with periodic storms followed by periods of high pressure across California. This allows ample humidity from evaporating soil moisture to condense and form fog during the cold, clear nights (Baldocchi and Waller, 2014). Valley fog promotes colder temperatures during the winter, a critical factor for achieving a period of soil dormancy in agricultural regions. Tree crops such as almonds, walnuts, cherries and peaches go through a necessary dormant period brought on and maintained by colder temperatures, or "winter chill." Fog is important in shielding plant buds from the sun and helping them accumulate winter chill. Analyses of wintertime temperatures show that the accumulation of winter chill is showing regional changes in the Central Valley (see *Winter chill* indicator). Declines in winter chill can have both adverse consequences — decreased yields in California's fruit and nut-growing regions — as well as benefits resulting from reduced energy use for heating in the Central Valley.

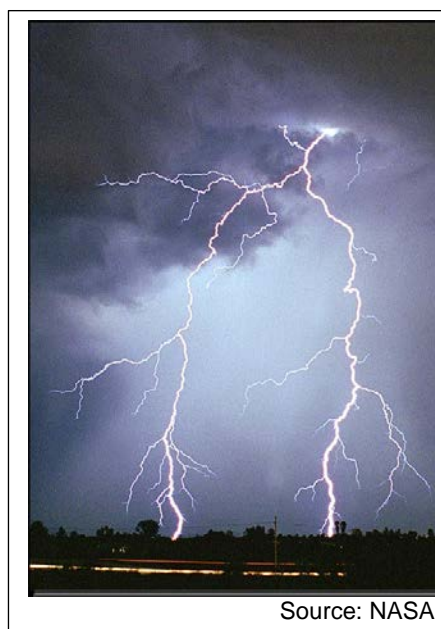
Scientists have hypothesized that rising temperatures in densely populated areas (the "urban heat island effect") are associated with a decline in the number of days and spatial extent of valley fog (Klemm and Neng-Huei, 2016). Increasing temperatures make it more difficult for atmospheric water vapor to condense and less likely for fog to form. Further, higher temperatures can evaporate fog that forms (hence, why fog evaporates in the morning when the sun rises). In addition to air temperature, drought years tend to be associated with lower numbers of fog days because there is not enough evaporating soil moisture to form fog (Baldocchi and Waller, 2014).

Recent studies report that the observed reduction in fog in the Central Valley and in other areas worldwide correlates more with a decline in air pollution (Klemm and Neng-Huei, 2016; Gray et al., 2016). Fog forms when water vapor condenses around solid particles, including dust and other types of air pollution. From 1930-1970, valley fog significantly increased due to high levels of nitrogen oxide (NO_x) emissions attributed to a surge in use of motor vehicles. The downward trend in fog frequency since 1980 is consistent with the trend of decreasing air pollution due to statewide vehicular emissions regulations over the past decades. While air pollution appears to be a major factor in the decline of fog formation, scientists recognize that rising temperatures also play a role (discussed above) and will likely have a significant impact as temperatures continue to rise in the future. The concurrent roles of changes in air pollution (including

agricultural burning) and climate on changing fog trends in the Central Valley remain an area of ongoing research.

LIGHTNING

Lightning is a transient, high-current electric discharge in the atmosphere. Air movements and collisions between particles of liquid water, ice crystals and hail in clouds cause these particles to become charged. Air acts as an insulator between the positive and negative charges in the cloud and between the cloud and the ground. When the opposite charges build up above a certain threshold, the insulating capacity of air breaks down, resulting in a rapid discharge of electricity known as lightning. The flash of lightning temporarily equalizes the charged regions in the atmosphere until the opposite charges build up again (NSSL, 2018, Schumann and Huntrieser, 2007).



A number of studies have shown that lightning activity is sensitive to surface air temperature changes (Price, 2013). An analysis of observational data for the contiguous United States found precipitation and convective available potential energy (CAPE), a measure of atmospheric instability, to be highly correlated with lightning frequency (Romps et al., 2014). Using climate models that predict an increase in CAPE and variable changes in precipitation over the 21st century, the researchers estimated an increase in annual mean lightning strike frequency of 12 percent per degree Centigrade (°C) increase in global average temperature (an increase of about 50 percent over this century, based on a projected 3.6°C increase in temperature). However, other studies that account for the effect of warming temperatures on the formation of ice particles in clouds projected decreases in lightning activity globally (Finney, et al., 2018; Jacobson and Street, 2009). These conflicting findings suggest the need for further research, particularly in light of the role that lightning plays in climate change.

Lightning strongly influences chemical processes that affect the formation of greenhouse gases in the atmosphere (Schumann and Huntrieser, 2007). Lightning produces nitrogen oxides that lead to the production of tropospheric ozone, a potent greenhouse gas. In addition, lightning can initiate wildfires, igniting vegetation that will be drier and easier to burn in a warming climate (although a greater number of lightning strikes does not necessarily lead to more or larger wildfires).

FOREST DISEASE AND PEST INFESTATIONS

Climate change is projected to affect forest ecosystems in the Western United States by influencing the survival and spread of disease-causing pathogens (fungi, bacteria) and pests (bark beetles) as well as changing the susceptibility of host trees (USFS, 2012; USFS, 2011). Climate-related diseases in forests can be due to direct climate effects on trees, or climate effects on the life cycle of pathogens and pests; increases in temperature and changes in precipitation can alter stages and rates of development of a pathogen or pest, modify host resistance, and lead to changes in their interactions (Anderegg, 2015). Increased populations and greater dispersal of pathogens and pests can lead to dramatic increases in the rates of forest diseases or infestations, or tree mortality, ultimately affecting the geographical distribution and abundance of forest tree species.



Sudden oak death of tanoak on Mount Tamalpais, California

Credit: US Forest Service

Climate change has had a significant impact on forest insect population outbreaks. In recent decades, a record number of coniferous trees have been killed by native bark beetles in Western US forests; several of the recent outbreaks are among the largest in history (Bentz et al., 2014a). Changing climatic conditions appear to be a major factor driving at least some of the recent bark beetle outbreaks. In particular, temperature is a major factor that directly influences the development rate and other physiological processes of bark beetles, such as the number of eggs laid by a female, the ability to disperse to new host trees, over-winter survival, and developmental timing — all of which drive population success (Bentz et al., 2014b).

Extreme weather events will likely have long-term effects on bark beetle population growth and outbreaks. Shifts in precipitation patterns and associated drought can additionally stress host trees (which alone may not be lethal), making them more vulnerable to bark beetle attacks and latent pathogens (Das, 2016). Fire, an important forest disturbance that is influenced by climate change (see *Wildfires* indicator), can also reduce the resistance of surviving trees to bark beetle attacks. In certain areas, stressed vegetation can provide more resources and prime breeding habitats for bark beetle species, accelerating their population growth and creating the potential for localized outbreaks (Gandhi et al., 2007). These more extreme events can be considered megadisturbances which call for new approaches to forest management strategies (Millar and Stephenson 2015).

Pathogens associated with forest disease include fungi, bacteria, viruses, parasitic plants, and nematodes. Warmer winters will contribute to greater overwintering success of pathogens and associated insects. Some diseases are spread by insects that

damage tree tissue, leaving them vulnerable to pathogen attack. In California, sudden oak death mortality rates are driven by extreme weather events such as heavy rains that initiate optimal infection conditions. High temperatures and periods of dry weather following these events can lead to tree deaths due to their reduced capacity to manage water, which lowers their resistance to infection (Frankel et al., 2012).

The relationship among climate, forest pathogens and pests, and their tree hosts, is complex. Pathogen and pest outbreaks and climate change are overlapping and integrated. Climate change can affect pathogens and pest infestations, while tree deaths due to infestations can reduce carbon storage in forests. Understanding how the severity and distribution of forest diseases are affected by climate change (extreme temperatures, precipitation, water availability) can assist in forecasting the direction of change expected in future scenarios (Frankel et al., 2012).

INVASIVE AGRICULTURAL PESTS

Current warming has already enabled many invasive species worldwide, including insects, to extend their distributions into new areas (IPCC, 2014). Generally, the establishment and spread of an introduced species will be most successful when it has characteristics favored by the changing climate, such as being drought tolerant. While climate change increases the likelihood of the establishment, growth, spread, and survival of invasive populations, human factors such as the movement of goods and people and habitat disturbance are overwhelmingly more important (Porter, 2014).

Temperature is probably the single most important environmental factor influencing insect behavior, distribution, development, survival and reproduction (Das et al., 2011). Generally, increasing air temperature is beneficial to insect pests. For those insects that breed continuously, as long as upper critical limits are not exceeded, rising temperatures accelerate every stage of an insect's life cycle. The reduced time between generations leads to larger insect populations. In addition, warming temperatures can cause host crops to ripen early and prompt an earlier invasion by insect pests; at the same time, warming also lengthens the growing season, providing more opportunities for insects to inflict more damage on crops. During the winter, warmer temperatures will reduce insect death, allowing greater numbers to survive and reproduce in subsequent growing seasons (USDA, 2013).

In California, new insect species arrive frequently. Warmer temperatures can allow such species to thrive where they previously could not survive. Invasive species include insects destructive to a wide variety of crops grown in the state, such as the *Bactrocera dorsalis*, also known as the Oriental fruit fly (OFF). OFF is endemic to Southern Asia and established in the Hawaiian Islands. These flies were first found in California in 1960 and have been reintroduced every year since 1966 through the movement of infested goods into the state. Economic impacts from establishment of this fly include damaged fruit and adverse impacts on native plants, increased pesticide use statewide by commercial and residential growers and loss of revenue due to export restrictions on fruit. It has been estimated that the cost of not eradicating OFF in California would

range from \$44 to \$176 million in crop losses, additional pesticide use, and quarantine requirements (CDFA, 2008).

Climate change may be influencing OFF populations in California. Records from the California Department of Food and Agriculture (CDFA) and County Agricultural Commissioners of over 63,000 detection traps statewide for exotic fruit flies (CDFA- exotic fruit fly page), show that historical trappings of OFF were reported primarily between the months of June through December. In recent years, detections have continued into January and February (2011 and 2015), suggesting that winter temperatures may be becoming more favorable for the insects (CDFA, 2016). Furthermore, earlier detections in April and May have become a common occurrence.

These changes may be due to the earlier importation of infested fruit into the state (as fruit ripen earlier at their location of origin with warming temperatures). Likewise, warmer temperatures in California are likely to cause earlier ripening of host fruits, increase fly populations, and reduce temperature-related mortality. Scientists caution that biological responses are complex and cannot be predicted by single variables (e.g., increase in temperature or rainfall) (CDFA, 2013). Attributing changes in invasive pest populations to climate change is difficult without accounting for dynamic interactions between multiple species and climate variables as well as human influences.



Adult female oriental fruit fly, *Bactrocera dorsalis*, laying eggs by inserting her ovipositor in a papaya.

Credit: Scott Bauer. USDA

Eradication actions undertaken by CDFA and the US Department of Agriculture over the years have prevented invasive pest introductions from becoming permanently established. CDFA has initiated efforts to evaluate pest and invasive species movement with climate change using internal pest detection databases. This information will be used to develop predictive models that assist CDFA's invasive species programs to effectively control invasive species and mitigate food crop loss (California Natural Resources Agency, 2016).

BLUETONGUE IN LIVESTOCK

A warming climate can impact livestock directly by causing heat stress and indirectly by affecting vector-borne disease occurrence (IPCC, 2014). Bluetongue (BT) is a vector-borne viral disease of sheep, goats and cattle transmitted by biting midges of the arthropod genus *Culicoides*. Bluetongue infections cause high morbidity and mortality primarily in sheep. Disease outbreaks can have major economic consequences; for example, in Ontario, Canada the detection of infected cattle in 2015 caused the immediate suspension of exports of live animals, semen, and embryos, valued at nearly 300 million Canadian dollars (Mann, 2015).

Bluetongue disease occurs globally and is common throughout California, primarily in the San Joaquin and Sacramento River valleys (Moeller, 2016). Although BT is endemic

in the US, climate change may alter the transmission of the virus and increase the threat to both domestic and wild ruminants.

As discussed above, insects are sensitive to changes in temperature, suggesting they are likely to respond to climate change. Warming temperatures can alter the distribution of vectors and accelerate disease transmission (see *Vector-borne diseases* indicator). For example, BT incidents have expanded northward and persisted in Europe and Canada; in addition, ten new (exotic) BT virus strains have been detected in the US since 1998 (Mellor et al., 2008; MacLachlan, 2010; Jimenez-Clavero, 2012). Researchers suggest the *Culicoides* vector is especially responsive to climate change (Purse et al., 2005, 2008). In general, warm temperatures enhance the recruitment, development, activity and survival rates of *Culicoides* vectors. Scientists expect increases in temperature (particularly at night-time and in winter) — as well as precipitation (particularly in dry areas) — to lead to an increased geographical and seasonal incidence of BT virus transmission.

Investigators modeling the distribution of *Culicoides* in North America using future climate scenarios predict expansion of the vector beyond the current northern limit and increased risk of *Culicoides*-borne disease over the next several decades, particularly at the US-Canada border (Zuliani et al., 2015). The northward expansion of BT outbreaks in Europe in recent decades has been examined with climate-driven models that show increasing temperatures may explain aspects of this expansion (Guis et al., 2012) and predict a trend of increasing risk globally using future climate scenarios (Samy and Peterson, 2016). However, BT incidence is influenced by many factors, including vector ecology and transmission cycles, water availability, land use, and agricultural management, which hampers the ability to link climate change with disease outcome.

Research was recently conducted to better understand the ecology of the vector, and what climatic, environmental, and anthropogenic factors may affect disease transmission in California (Mayo et al., 2016). This information will help direct risk assessment and targeted surveillance for presence of the virus. Bluetongue occurrence in livestock is currently reportable to and monitored by the California Department of Food and Agriculture's Animal Health Branch (<https://www.cdffa.ca.gov/ah/>).

HARMFUL ALGAL BLOOMS

Harmful algal blooms (HABs) are colonies of algae and/or plant-like bacteria (cyanobacteria) that grow out of control, threatening fisheries, marine and freshwater ecosystems, public health and economies. HABs can produce natural toxins that contaminate seafood and waterbodies used for recreation or drinking water sources. Even without producing toxins, HABs can damage aquatic environments by suffocating fish, blocking sunlight, or depleting oxygen in the water (COST, 2016; WHO 1999). Scientific data indicates that HABs are expanding globally in distribution, frequency, and abundance. Scientists hypothesize that climate change is a driving influence in HAB expansion due to increased temperatures, nutrients, and carbon dioxide levels in water, and decreased water mixing (Hallegraeff 1993; Paerl and Paul 2012; Gobler et al., 2017).

Climate change may be influencing the occurrence of HABs in California, but scientists need more data in order to clarify this relationship. An unprecedented marine HAB stretched from Santa Barbara to southeastern Alaska during 2015. This resulted in very high levels of the neurotoxin domoic acid in California seafood, affecting major commercial and recreational fisheries for Dungeness crab, rock crab and other species in 2015 and 2016 (COST, 2016). The bloom was unusual in its geographic range, longevity, and severity of impacts (McCabe et al., 2016). A driving factor of this HAB was the unusual formation of a massive pool of warm water in the Northeast Pacific Ocean during 2013-2014. Natural variability appears to be the primary cause of the warm ocean pool (Kintisch, 2015), although some climate models detected an anthropogenic influence (Swain et al., 2014; Wang et al., 2014).

Observational data show an increase in the number of California inland waterbodies affected by HABs between 2016 and 2017 (CWQMC 2017; earlier data is not available). Public health warnings at inland waterbodies increased by 75 percent in 2017 (from 80 to 141). Scientists have linked drought conditions (flow, temperature and stratification) to the occurrence of HABs in freshwater and estuarine waterbodies in California (Lehman et al., 2017; Power et al., 2015). Additionally, animal deaths in California due to toxins from freshwater and estuarine HABs may have increased in recent years or, alternatively, the recognition of these poisonings may have increased (Backer et al., 2013).

Climate change affects the factors that drive HAB formation worldwide (US EPA, 2017). Warmer water temperatures, drought conditions, increased carbon dioxide, changes in coastal upwelling, and alternating periods of storms and drought are all known to promote HAB formation by enhancing the growth of HAB-forming algae and cyanobacteria, increasing nutrients to excess levels (eutrophication) and preventing water from mixing. However, factors unrelated to climate are also likely involved in the apparent global expansion of HABs, such as the increased monitoring of HABs and land uses that increase nutrient loading. This issue is complex; however, future data may support a HAB-related indicator of climate change in California.

References:

Ahlm L, Jones A, Stjern C, Muri H, Kravitz BS, et al. (2017). Marine cloud brightening-as effective without clouds. *Atmospheric Chemistry Physics* **17**: 13071-13087.

Anderegg WRL, Hicke JA, Fisher RA, Allen CD, Aukema J, et al. (2015). Tree mortality from drought, insects, and their interactions in a changing climate. *New Phytologist* **208**(3): 674–683.

Backer LC, Landsberg JH, Miller M, et al (2013). Canine cyanotoxin poisonings in the United States (1920s–2012): Review of suspected and confirmed cases from three data sources. *Toxins* **5**(9):1597-1628.

Baldocchi D and Waller E (2014). Winter fog is decreasing in the fruit growing region of the Central Valley of California. *Geophysical Research Letters* **41**(9): 3251-3256.

Bentz BJ and Klepzig K (2014a). Bark Beetles and Climate Change in the United States. U.S. Department of Agriculture, Forest Service, Climate Change Resource Center. Retrieved March 8, 2018 from: www.fs.usda.gov/ccrc/topics/insect-disturbance/bark-beetles

- Bentz BJ, Vandygriff J, Jensen C, Coleman T, Maloney P, Smith S, Grady A, Schen-Langenheim G (2014b). Mountain Pine Beetle Voltinism and Life History Characteristics across Latitudinal and Elevational Gradients in the Western United States. *Forest Science* **60**(3): 434–449.
- Burgess SSO and Dawson TE (2004). The contribution of fog to the water relations of *Sequoia sempervirens* (D. Don): foliar uptake and prevention of dehydration. *Plant, Cell & Environment* **27**(8): 1023–1034.
- Burns EE (2017). Understanding *Sequoia sempervirens*. Gen. Tech. Rep. PSW-GTR-258. Albany, CA: US Department of Agriculture, Forest Service, Pacific Southwest Research Station: 9-13, 258, 9-13.
- California Natural Resources Agency (2016). Safeguarding California, Implementation and Action Plans: Agricultural Sector Plan. California's Climate Adaptation Strategy. Available at: <http://resources.ca.gov/docs/climate/safeguarding/Agricultural%20Sector%20Plan.pdf>
- CDFA (2008). Oriental Fruit Fly Fact Sheet. California Department of Food and Agriculture. Retrieved March 12, 2018, from: https://www.cdfa.ca.gov/plant/factsheets/OFF_FactSheet.pdf
- CDFA (2013). Climate Change Consortium for Specialty Crops: Impacts and Strategies for Resilience. California Department of Food and Agriculture. Available at: <https://www.cdfa.ca.gov/environmentalstewardship/pdfs/ccc-report.pdf>
- Chung M, Dufour A, Pluche R, and Thompson S (2017). How much does dry-season fog matter? Quantifying fog contributions to water balance in a coastal California watershed. *Hydrological Processes* **31**(22): 3948-3961.
- Clemesha RE, Gershunov A, Iacobellis SF, and Cayan DR (2017). Daily variability of California coastal low cloudiness: A balancing act between stability and subsidence. *Geophysical Research Letters* **44**(7), 3330-3338.
- COST (2016). Frequently Asked Questions: Harmful Algal Blooms and California Fisheries, Developed in Response to the 2015-2016 Domoic Acid Event. California Ocean Science Trust. Oakland, CA. Available at: <http://www.oceansciencetrust.org/wp-content/uploads/2016/08/HABs-and-CA-Fisheries-FAQ-8.5.16.pdf>
- CWQMC (2017). California Water Quality Monitoring Council: Where are freshwater harmful algal blooms occurring in California? Retrieved December 21, 2017, from https://public.tableau.com/profile/swamp.oima#!/vizhome/FullHABSList_0/Dashboard3
- Das DK, Singh J, and Vennila S (2011). Emerging crop pest scenario under the impact of climate change. *Journal of Agricultural Physics* **11**: 13-20.
- Das AJ, Stephenson NL, and Davis KP (2016). Why do trees die? Characterizing the drivers of background tree mortality. *Ecology* **97**(10): 2616–2627.
- Dawson TE (1998). Fog in the California redwood forest: Ecosystem inputs and use by plants. *Oecologia* **117**(4): 476-485.
- Dorman CE, Mejia J, Koračin D, and McEvoy D (2017). Worldwide Marine Fog Occurrence and Climatology. In *Marine Fog: Challenges and Advancements in Observations, Modeling, and Forecasting* (pp. 7-152). Koračin D, Dorman C (Eds.). Springer International Publishing.
- Egli S, Thies B, Drönner J, Cermak J, and Bendix J (2017). A 10 year fog and low stratus climatology for Europe based on Meteosat Second Generation data. *Quarterly Journal of the Royal Meteorological Society* **143**(702): 530-541.

Frankel S, Juzwik J, Koch F (2012). Forest Tree Diseases and Climate Change. U.S. Department of Agriculture, Forest Service, Climate Change Resource Center. Retrieved March 8, 2018 from <https://www.fs.usda.gov/ccrc/topics/forest-tree-diseases-and-climate-change>

Finney D, Doherty R, Wild O, Stevenson DS, MacKenzie IA, Blyth AM (2018). A projected decrease in lightning under climate change. *Nature Climate Change* **8**: 210-213.

Gandhi KJK, Gilmore DW, Katovich SA, Mattson WJ, Spence JR and Seybold SJ (2007). Physical effects of weather events on the abundance and diversity of insects in North American forests. *Environmental Reviews* **15**(1): 113-152.

Gobler CJ, Doherty OM, Hattenrath-Lehmann TK, Griffith AW, Kang Y, et al. (2017) Ocean warming since 1982 has expanded the niche of toxic algal blooms in the North Atlantic and North Pacific oceans. *Proceedings of the National Academy of Sciences* **114**(19): 4975-4980.

Gray E, Baldocchi D and Goldstein A (2016, December). Influence of NO_x emissions on Central Valley fog frequency and persistence. International Global Atmospheric Chemistry Conference. Breckenridge, Colorado.

Guis H, Caminade C, Calvete C, Morse AP, Tran A, et al. (2012). Modelling the effects of past and future climate on the risk of bluetongue emergence in Europe. *Journal of the Royal Society Interface* **9**(67): 339-350.

Hallegraeff GM (1993). A review of harmful algal blooms and their apparent global increase. *Phycologia* **32**(2):79-99.

IPCC (2014). Climate Change 2014 Synthesis Report. Contribution of Working Groups I, II and III to the Fifth Assessment Report of the Intergovernmental Panel on Climate Change [The Core Writing Team, Pachauri RK, and Meyer L (eds.)]. Intergovernmental Panel on Climate Change, Geneva, Switzerland. Available at: http://www.ipcc.ch/pdf/assessment-report/ar5/syr/SYR_AR5_FINAL_full_wcover.pdf

Jacobson MZ and Streets DG (2009). Influence of future anthropogenic emissions on climate, natural emissions, and air quality. *Journal of Geophysical Research* **114**(D8).

Jimenez-Clavero MA (2012). Animal viral diseases and global change: Bluetongue and West Nile fever as paradigms. *Frontiers in Genetics* **3**:105.

Johnstone JA and Dawson TE (2010). Climatic context and ecological implications of summer fog decline in the coast redwood region. *Proceedings of the National Academy of Sciences* **107**(10): 4533-4538.

Kaplan ML, Tilley JS, Hatchett BJ, Smith CM, Walston JM, et al. (2017). The Record Los Angeles Heat Event of September 2010: 1. Synoptic-Scale-Meso- β -Scale Analyses of Interactive Planetary Wave Breaking, Terrain-and Coastal-Induced Circulations. *Journal of Geophysical Research: Atmospheres* **122**(20): 10, 729-10, 750.

Kintisch E (2015). Marine science. 'The Blob' invades Pacific, flummoxing climate experts. *Science* **348**(6230): 17-18.

Klemm O and Neng-Huei L (2016). What causes observed fog trends: Air quality or climate change? *Aerosol and Air Quality Research* **16**: 1131–1142.

Koraćin D, Dorman CE, Lewis JM, Hudson JG, Wilcox EM, et al. (2014). Marine fog: A review. *Atmospheric Research* **143**: 142-175.

LaDochy S and Witiw M (2012). The continued reduction in dense fog in the southern California region: Possible causes. *Pure and Applied Geophysics* **169**(5-6): 1157-1163.

- Lehman PW, Kurobe T, Lesmeister S, Baxa D, Tung A, Ten SJ (2017). Impacts of the 2014 severe drought on the Microcystis bloom in San Francisco Estuary. *Harmful Algae* **63**:94-108.
- MacLachlan NJ (2010). Global implications of the recent emergence of bluetongue virus in Europe. *Veterinary Clinics of North America: Food Animal Practice* **26**(1), 163-171.
- Mann S (2015). "International markets react to bluetongue presence in Ontario". Better Farming. Retrieved March 30, 2017, from <http://www.betterfarming.com/online-news/international-markets-react-bluetongue-presence-ontario-61013>
- Mayo C, Shelley C, MacLachlan NJ, Gardner I, Hartley D and Barker C (2016). A deterministic model to quantify risk and guide mitigation strategies to reduce bluetongue virus transmission in California dairy cattle. *PLoS One* **11**(11): e0165806.
- McCabe RM, Hickey BM, Kudela RM, Lefebvre KA, Adams NG, et al. (2016). An unprecedented coastwide toxic algal bloom linked to anomalous ocean conditions. *Geophysical Research Letters* **43**(19): 10,366-310,376.
- McLaughlin BC, Ackerly DD, Klos PZ, Natali J, Dawson TE, and Thompson SE (2017). Hydrologic refugia, plants, and climate change. *Global change biology* **23**(8): 2941-1961.
- Mellor PS, Carpenter S, Harrup L, Baylis M, and Mertens PP (2008). Bluetongue in Europe and the Mediterranean Basin: History of occurrence prior to 2006. *Preventive Veterinary Medicine* **87**(1-2): 4-20.
- Millar CI and Stephenson NL (2015). Temperate forest health in an era of emerging megadisturbance. *Science* **349**(6250): 823-826.
- Moeller RB (2016). Factsheet: Bluetongue virus. University of California at Davis, Veterinary Medicine. Available at: http://www.vetmed.ucdavis.edu/cahfs/local_resources/pdfs/fact%20sheets/BT_fact_sheet_2016.pdf
- NSSL (2018). National Severe Storms Laboratory. Severe Weather 101: Lightning Basics. Retrieved February 16, 2018, from <https://www.nssl.noaa.gov/education/svrwx101/lightning/>
- O'Brien TA, Sloan LC, Chuang PY, Faloona IC, and Johnstone JA (2013). Multidecadal simulation of coastal fog with a regional climate model. *Climate Dynamics* **40**(11-12): 2801-2812.
- Paerl HW and Paul VJ (2012). Climate change: Links to global expansion of harmful Cyanobacteria. *Water Research* **46**: 1349-1363.
- Porter JR, Xie L, Challinor, AJ, Cochrane, K, Howden SM, et al. (2014). Food security and food production systems. In: *Climate Change 2014: Impacts, Adaptation, and Vulnerability. Part A: Global and Sectoral Aspects. Contribution of Working Group II to the Fifth Assessment Report of the Intergovernmental Panel on Climate Change* [Field, CB, Barros VR, Dokken, DJ, Mach, KJ, Mastrandrea MD, et al. (eds.)]. Cambridge, United Kingdom and New York, NY, USA: Cambridge University Press, pp. 485-533. Available at: https://ipcc.ch/pdf/assessment-report/ar5/wg2/WGIIAR5-Chap7_FINAL.pdf
- Power ME, Bouma-Gregson K, Higgins P, et al. (2015). The Thirsty Eel: Summer and Winter Flow Thresholds that Tilt the Eel River of Northwestern California from Salmon-Supporting to Cyanobacterially Degraded States. *Copeia* **103**(1): 200-211.
- Price CG (2013). Lightning Applications in Weather and Climate Research. *Surveys in Geophysics* **34**(6): 755-767.
- Purse BV, Mellor PS, Rogers DJ, Samuel AR, Mertens PP, et al. (2005). Climate change and the recent emergence of bluetongue in Europe. *Nature Reviews Microbiology* **3**(2): 171-181.

Purse BV, Brown HE, Harrup L, Mertens PP, and Rogers DJ (2008). Invasion of bluetongue and other orbivirus infections into Europe: The role of biological and climatic processes. *Revue Scientifique et Technique*, **27**(2): 427-442.

Romps DM, Seeley JT, Vollaro D, and Molinari J (2014). Projected increase in lightning strikes in the United States due to global warming. *Science* **346**(6211): 851-854.

Samy AM and Peterson AT (2016). Climate change influences on the global potential distribution of bluetongue virus. *PLoS ONE* **11**(3): e0150489.

Sawaske SR and Freyberg DL (2015). Fog, fog drip, and streamflow in the Santa Cruz Mountains of the California Coast Range. *Ecohydrology* **8**(4): 695-713.

Schumann U and Huntrieser H (2007). The global lightning-induced nitrogen oxides source. *Atmospheric Chemistry and Physics* **7**: 3823-3907.

Sugimoto S, Sato T, and Nakamura K (2013). Effects of synoptic-scale control on long-term declining trends of summer fog frequency over the Pacific side of Hokkaido Island. *Journal of Applied Meteorology and Climatology* **52**(10): 2226-2242.

Swain DL, Tsiang M, Haugen M, Singh D, Charland A, et al. (2014). The extraordinary California drought of 2013/2014: Character, context, and the role of climate change. *Bulletin of American Meteorological Society* **95**(9): S3-S7.

Torregrosa A, O'Brien TA, and Faloona IC (2014). Coastal fog, climate change, and the environment. *Eos, Transactions American Geophysical Union* **95**(50): 473-474.

Torregrosa A, Combs C, and Peters J (2016). GOES-derived fog and low cloud indices for coastal north and central California ecological analyses. *Earth and Space Science* **3**(2): 46-67.

USDA (2013). Climate Change and Agriculture: Effects and Adaption. United States Department of Agriculture. Washington, DC: Technical Bulletin 1935. Available at: [https://www.usda.gov/oce/climate_change/effects_2012/CC%20and%20Agriculture%20Report%20\(02-04-2013\)b.pdf](https://www.usda.gov/oce/climate_change/effects_2012/CC%20and%20Agriculture%20Report%20(02-04-2013)b.pdf)

US EPA (2017). Nutrient Pollution: Climate Change and Harmful Algal Blooms. United States Environmental Protection Agency. Retrieved December 18, 2017, from <https://www.epa.gov/nutrientpollution/climate-change-and-harmful-algal-blooms>

USFS (2011). A Risk Assessment of Climate Change and the Impact of Forest Diseases on Forest Ecosystems in the Western United States and Canada. United States Department of Agriculture, Forest Service, Pacific Southwest Research Station. Available at: http://www.fs.fed.us/psw/publications/documents/psw_gtr236/psw_gtr236.pdf

USFS (2012). Major Forest Insect and Disease Conditions in the United States: 2011. United States Department of Agriculture, Forest Service. Forest Health Protection, FS-1000. Available at: https://www.fs.fed.us/foresthealth/publications/ConditionsReport_2011.pdf

Wang M and Ullrich P (2017). Marine air penetration in California's Central Valley: Meteorological drivers and the impact of climate change. *Journal of Applied Meteorology and Climatology* **57**(1).

Wang SY, Hipps L, Gilles RR, and Yoon JH (2014). Probable causes of the abnormal ridge accompanying the 2013-2014 California drought: ENSO precursor and anthropogenic warming footprint. *Geophysical Research Letters* **41**(9): 3220-3226.

Williams AP, Schwartz RE, Iacobellis S, Seager R, Cook BI, et al. (2015). Urbanization causes increased cloud base height and increased fog in coastal Southern California. *Geophysical Research Letters* **42**(5): 1527-1536.

Witiw MR and LaDochy S (2015). Cool PDO phase leads to recent rebound in coastal southern California fog. *Journal of the Geographical Society of Berlin* **146**(4): 232-244.

WHO (1999). Toxic Cyanobacteria in Water: A guide to their public health consequences, monitoring and management. World Health Organization. London and New York: E & FN Spon.

Zhang S, Chen Y, Long J, and Han G (2015). Interannual variability of sea fog frequency in the Northwestern Pacific in July. *Atmospheric Research* **151**: 189-199.

Zuliani A, Massolo A, Lysyk T, Johnson G, Marshall S, et al. (2015). Modelling the northward expansion of *Culicoides sonorensis* (Diptera: Ceratopogonidae) under future climate scenarios. *PLoS ONE* **10**(8): e0130294.



For more information contact:

Office of Environmental Health Hazard Assessment

P. O. Box 4010, Mail Stop 12-B

Sacramento, California 95812-4010

(916) 324-7572

www.oehha.ca.gov



Printed on recycled paper